

# Preface

Modern fastening technology is becoming increasingly important in civil and structural engineering worldwide. Cast-in-place fastenings, which are placed in the formwork before the concrete is poured, as well as post-installed fastening systems, which are installed in hardened concrete or masonry, have found widespread use in construction practice.

Anchor bolts transfer applied tension loads to the anchorage material through mechanical interlock, friction, bond, or a combination of these mechanisms. Regardless of the load-transfer mechanism, however, fastening systems rely on the tension strength of the concrete or masonry. This fact must be accounted for both in the design of the fastening and the design of the supporting (or supported) concrete or masonry member.

Every fastening element is designed for optimal performance for a specific application. When a fastening element is used for an application for which it was not intended, its performance can be negatively affected. Knowledge of the behaviour of different fastenings is therefore necessary to select the proper fastening system for a given application and to implement the design of the fastening correctly. Fastening behaviour may be influenced by many parameters. Environmental conditions such as chemical attack, temperature fluctuation, and fire exposure must also be considered.

Although each year millions of anchors are installed in concrete and masonry elements on construction sites around the world, the state of knowledge about this technology in the practice is often very poor. It is therefore the goal of this book to present the state of the art relative to fastening technology for concrete. Fastening products currently available on the market, as well as their intended areas of application, are discussed. The fundamentals of their load-bearing behaviour under short- and long-term loading, dynamic loading including seismic loading,

and the dependence of the behaviour on the loading direction and failure mode are presented. The influence of the condition of the concrete, non-cracked versus cracked, as well as the behaviour of fastenings under fire loading and the corrosion behaviour of fasteners is examined. Additionally, a detailed discussion of the design of fastenings is provided.

This book builds on the volume '*Befestigungstechnik in Beton- and Mauerwerk*' by Eligehausen, Mallée (2000) and translated into the English by Philip Thrift (Hannover). Extensive editing of the translated text was performed by John Silva. The content in this book, however, has been significantly extended and updated.

Research in the field of fastening technique from around the world is brought together in this book. Much of this research was conducted at the Department of Fastening Technology at the University of Stuttgart. The department was founded in the 1970's by Professor Emeritus Dr.-Ing. Dr.-Ing. E.h. (mult) Gallus Rehm and flourished under his oversight until his retirement in 1989. The authors owe him a great deal of gratitude.

This book would not have been possible without the support of many individuals. We would like to thank Mr. M. Hoehler, M.Sc., who contributed to section 10 on seismic loading, and edited the completed manuscript as well as Dr.-Ing. J. Asmus and Dr.-Ing. T. Sippel for supplying numerous figures. Furthermore we would like to thank Ms. Dipl.-Ing. A. Clauss, Ms. Dipl.-Ing. Y. Grewin, Ms. Dipl.-Ing. I. Simons, Dipl.-Ing. J. Appl, Dipl.-Ing. L. Bezecny, Dipl.-Ing. J. Hofmann, Dipl.-Ing. T. Huer, Dipl.-Ing. M. Potthoff, Dipl.-Ing. K. Schmid, for their tireless effort preparing and editing figures.

Rolf Eligehausen  
Rainer Mallée  
John Silva

# Contents

<b>1</b>	<b>Introduction</b> .....	<b>1</b>
1.1	A historical review .....	1
1.2	Requirements for fastenings .....	2
1.3	Nature and direction of actions .....	2
<b>2</b>	<b>Fastening systems</b> .....	<b>5</b>
2.1	General .....	5
2.2	Cast-in-place systems .....	5
2.2.1	Lifting inserts .....	6
2.2.2	Anchor channels .....	7
2.2.3	Headed studs .....	9
2.2.4	Threaded sleeves .....	9
2.3	Drilled-in systems .....	10
2.3.1	Drilling techniques .....	10
2.3.2	Installation configurations .....	10
2.3.3	Drilled-in anchor types .....	11
2.3.3.1	Mechanical expansion anchors .....	11
2.3.3.2	Undercut anchors .....	16
2.3.3.3	Bonded anchors .....	19
2.3.3.4	Screw anchors .....	25
2.3.3.5	Ceiling hangers .....	25
2.3.3.6	Plastic anchors .....	27
2.4	Direct installation .....	29
<b>3</b>	<b>Principles</b> .....	<b>33</b>
3.1	General .....	33
3.2	Behaviour of concrete in tension .....	34
3.3	Failure mechanisms of fastenings .....	37
3.3.1	Theoretical studies .....	37
3.3.2	Experimental studies .....	45
3.3.3	Conclusions drawn from theoretical and experimental studies .....	50
3.4	Cracked concrete .....	51
3.5	Why anchors may use the tensile strength of concrete .....	54
3.6	Prestressing of anchors .....	55
3.7	Loads on anchors .....	58
3.7.1	Calculation according to elastic theory .....	58
3.7.1.1	Tension load .....	58
3.7.1.2	Shear loads .....	59
3.7.2	Calculation according to non-linear methods .....	61
3.7.3	Calculation of loads on anchors of anchor channels .....	61
3.7.3.1	Tension loads .....	61
3.7.3.2	Shear loads .....	63

<b>4</b>	<b>Behaviour of headed studs, undercut anchors and metal expansion anchors in non-cracked and cracked concrete</b> .....	<b>65</b>
4.1	Non-cracked concrete .....	65
4.1.1	Tension load .....	65
4.1.1.1	Load-displacement behaviour and modes of failure .....	65
4.1.1.2	Failure load associated with steel rupture .....	68
4.1.1.3	Failure load associated with concrete cone breakout .....	69
4.1.1.4	Failure load for local concrete side blow-out failure .....	93
4.1.1.5	Failure loads associated with pull-out and pull-through failures .....	97
4.1.1.6	Failure load associated with splitting of the concrete .....	100
4.1.2	Shear .....	103
4.1.2.1	Load-displacement behaviour and modes of failure .....	103
4.1.2.2	Failure load associated with steel rupture .....	105
4.1.2.3	Failure load associated with pry-out .....	109
4.1.2.4	Concrete edge failure for a shear load perpendicular to the edge .....	112
4.1.2.5	Concrete edge breakout load associated with shear loads oriented at an angle $\alpha < 90^\circ$ to the edge .....	125
4.1.3	Combined tension and shear (oblique loading) .....	128
4.1.3.1	Load-displacement behaviour and modes of failure .....	128
4.1.3.2	Failure load .....	132
4.1.4	Bending of the baseplate .....	137
4.1.5	Sustained loads .....	138
4.1.6	Fatigue loading .....	139
4.2	Cracked concrete .....	142
4.2.1	Tension .....	143
4.2.1.1	Load-displacement behaviour and modes of failure .....	143
4.2.1.2	Failure load corresponding to steel failure .....	146
4.2.1.3	Failure load associated with concrete cone breakout .....	146
4.2.1.4	Failure load associated with local blow-out failure .....	154
4.2.1.5	Failure load associated with pull-out/pull-through failure .....	155
4.2.1.6	Failure load associated with splitting of the concrete .....	157
4.2.2	Shear .....	157
4.2.2.1	Load-displacement behaviour and modes of failure .....	157
4.2.2.2	Failure load associated with steel failure .....	157
4.2.2.3	Failure load associated with pry-out failure .....	158
4.2.2.4	Failure load associated with concrete edge breakout .....	158
4.2.3	Combined tension and shear .....	159
4.2.3.1	Load-displacement behaviour and modes of failure .....	159
4.2.3.2	Failure load .....	159
4.2.4	Sustained loads .....	160
4.2.5	Fatigue loading .....	162
<b>5</b>	<b>Behaviour of cast-in anchor channels in non-cracked and cracked concrete</b> .....	<b>163</b>
5.1	Non-cracked concrete .....	163
5.1.1	Tension .....	163
5.1.1.1	Load-displacement behaviour and modes of failure .....	163
5.1.1.2	Failure load associated with steel failure .....	164
5.1.1.3	Failure load associated with concrete cone breakout .....	165
5.1.1.4	Failure load associated with local concrete side blow-out failure .....	168
5.1.1.5	Failure load associated with pull-out failure .....	168

5.1.1.6	Failure load associated with splitting of the concrete .....	169
5.1.2	Shear .....	170
5.1.2.1	Load-displacement behaviour and modes of failure .....	170
5.1.2.2	Failure load associated with steel failure .....	170
5.1.2.3	Failure load associated with pry-out failure .....	170
5.1.2.4	Failure load associated with concrete edge failure .....	170
5.1.3	Combined tension and shear .....	178
5.1.4	Sustained and fatigue loading .....	179
5.2	Cracked concrete .....	179
<b>6</b>	<b>Behaviour of bonded anchors in non-cracked and cracked concrete .....</b>	<b>181</b>
6.1	Non-cracked concrete .....	181
6.1.1	Tension load .....	181
6.1.1.1	Load-displacement behaviour and modes of failure .....	181
6.1.1.2	Failure load associated with steel failure .....	184
6.1.1.3	Failure load associated with concrete breakout/pull-out failure .....	184
6.1.1.4	Failure load associated with splitting .....	200
6.1.2	Shear load .....	200
6.1.2.1	Load-displacement behaviour and modes of failure .....	200
6.1.2.2	Failure load associated with steel failure .....	200
6.1.2.3	Failure load associated with pry-out failure .....	200
6.1.2.4	Failure load associated with concrete edge breakout .....	200
6.1.3	Combined tension and shear load .....	200
6.1.4	Sustained and fatigue loading .....	200
6.1.5	Environmental factors .....	202
6.2	Cracked concrete .....	204
6.2.1	Tension load .....	204
6.2.1.1	Load-displacement behaviour and modes of failure .....	204
6.2.1.2	Failure load corresponding to steel failure .....	205
6.2.1.3	Failure load corresponding to pull-out failure .....	205
6.2.1.4	Failure loads corresponding to concrete cone failure and splitting of the concrete .....	206
6.2.2	Shear load .....	207
6.2.3	Combined tension and shear load .....	207
6.2.4	Sustained and fatigue loads .....	208
6.2.5	Environmental factors .....	208
6.3	Bonded undercut anchors and bonded expansion anchors .....	208
6.3.1	Non-cracked concrete .....	208
6.3.2	Cracked concrete .....	208
6.3.2.1	Tension load .....	208
6.3.2.2	Shear and combined tension and shear load .....	210
<b>7</b>	<b>Behaviour of plastic anchors in non-cracked and cracked concrete .....</b>	<b>211</b>
7.1	Non-cracked concrete .....	211
7.1.1	Tension load .....	211
7.1.2	Shear and combined tension and shear load .....	215
7.1.3	Long-term behaviour .....	215
7.2	Cracked concrete .....	220
7.2.1	Tension load .....	220
7.2.2	Shear and combined tension and shear load .....	222
7.2.3	Long-term behaviour .....	222

<b>8</b>	<b>Behaviour of power actuated fasteners in non-cracked and cracked concrete</b> .....	223
8.1	Non-cracked concrete .....	223
8.1.1	Tension load .....	223
8.1.2	Shear and combined tension and shear load .....	224
8.1.3	Sustained and repetitive loading .....	224
8.2	Cracked concrete .....	225
8.2.1	Tension load .....	225
8.2.2	Shear and combined tension and shear load .....	226
<b>9</b>	<b>Behaviour of screw anchors in non-cracked and cracked concrete</b> .....	227
9.1	Installation .....	227
9.2	Non-cracked concrete .....	231
9.2.1	Tension load .....	231
9.2.1.1	Load-displacement behaviour and failure modes .....	231
9.2.1.2	Failure loads associated with steel failure .....	231
9.2.1.3	Failure loads associated with pull-out failure .....	231
9.2.1.4	Failure loads associated with concrete cone failure .....	231
9.2.2	Shear load .....	233
9.2.2.1	Load-displacement behaviour and modes of failure .....	233
9.2.2.2	Failure load associated with steel failure .....	233
9.2.2.3	Failure load associated with pry-out failure .....	233
9.2.2.4	Failure load associated with concrete edge breakout .....	233
9.2.3	Combined tension and shear load .....	234
9.2.4	Sustained and fatigue loads .....	234
9.3	Cracked concrete .....	234
9.3.1	Tension load .....	234
9.3.2	Shear load and combined tension and shear load .....	235
9.3.3	Sustained and fatigue loads .....	235
10	Behaviour of anchors under seismic loading .....	237
10.1	Anchor applications .....	237
10.2	Seismic actions .....	238
10.3	Assumptions regarding the condition of the concrete .....	239
10.4	Behaviour of anchors under seismic conditions .....	240
10.4.1	Tension cycling .....	241
10.4.2	Shear cycling .....	242
10.4.3	Combined tension and shear cycling .....	245
10.4.4	Loading rate .....	245
10.4.5	Load cycle sequence .....	246
10.4.6	Crack cycling .....	247
<b>11</b>	<b>Behaviour of anchors in fire</b> .....	249
<b>12</b>	<b>Corrosion of anchors</b> .....	255

<b>13</b>	<b>Influence of fastenings on the capacity of components in which they are installed</b> .....	259
<b>14</b>	<b>Design of fastenings</b> .....	265
14.1	General .....	265
14.2	Verifying the suitability of an anchor system .....	266
14.3	Design of fastenings with post-installed metal expansion, undercut and bonded expansion anchors according to the EOTA Guideline .....	267
14.3.1	General .....	267
14.3.2	Scope .....	268
14.3.3	Design concept .....	269
14.3.3.1	Analysis for the ultimate limit state .....	269
14.3.3.2	Analysis for the serviceability limit state .....	270
14.3.4	Forces on anchors .....	271
14.3.5	Characteristic resistances .....	274
14.3.5.1	Tension resistances .....	275
14.3.5.2	Shear resistances .....	277
14.3.5.3	Combined tension and shear .....	280
14.3.6	Serviceability limit state .....	281
14.3.6.1	Anchor displacements .....	281
14.3.6.2	Shear load with changing sign .....	281
14.3.7	Additional analyses for ensuring the characteristic resistance of concrete member .....	281
14.3.7.1	General .....	281
14.3.7.2	Shear resistance of the concrete member .....	281
14.3.7.3	Resistance to splitting forces .....	283
14.4	Design of fastenings according to the CEN Technical Specification .....	283
14.4.1	General .....	283
14.4.2	Scope .....	283
14.4.3	Basis of design .....	285
14.4.4	Partial safety factors .....	286
14.4.4.1	Static actions, indirect actions and fatigue actions .....	286
14.4.4.2	Resistances .....	286
14.4.4.2.1	Ultimate limit state (static loading) and seismic loading .....	286
14.4.4.2.2	Limit state of fatigue .....	287
14.4.4.2.3	Serviceability limit state .....	287
14.4.5	Forces acting on fasteners .....	287
14.4.5.1	Tension loads .....	287
14.4.5.2	Shear loads .....	287
14.4.5.2.1	Distribution of loads .....	287
14.4.5.2.2	Shear loads without lever arm .....	288
14.4.5.2.3	Shear loads with lever arm .....	289
14.4.6	Design of headed fasteners .....	289
14.4.6.1	Determination of action effects .....	289
14.4.6.2	Verification of ultimate limit state by elastic analysis .....	290
14.4.6.2.1	Tension loads .....	290
14.4.6.2.2	Shear loads .....	293
14.4.6.2.3	Combined tension and shear loads .....	302
14.4.7	Design of anchor channels .....	302
14.4.7.1	Derivation of forces acting on the anchors of the anchor channel .....	303
14.4.7.1.1	Tension loads .....	303

14.4.7.1.2	Shear loads .....	304
14.4.7.2	Tension forces in the supplementary reinforcement .....	304
14.4.7.2.1	Tension loads .....	304
14.4.7.2.2	Shear loads .....	304
14.4.7.3	Verification of ultimate limit state by elastic analysis .....	305
14.4.7.3.1	Tension loads .....	305
14.4.7.3.2	Shear loads .....	309
14.4.7.3.3	Combined tension and shear loads .....	313
14.4.7.3.3.1	Anchor channels without supplementary reinforcement .....	313
14.4.7.3.3.2	Anchor channels with supplementary reinforcement .....	313
14.4.8	Design of post-installed fasteners – mechanical systems .....	313
14.4.8.1	Scope .....	313
14.4.8.2	Determination of action effects .....	313
14.4.8.3	Verification of ultimate limit state by elastic analysis .....	313
14.4.8.3.1	General .....	313
14.4.8.3.2	Tension loads .....	314
14.4.8.3.3	Shear loads .....	314
14.4.8.3.4	Combined tension and shear loads .....	315
14.4.9	Design of post-installed fasteners – chemical systems .....	315
14.4.9.1	Tension resistances .....	315
14.4.9.2	Shear loads .....	316
14.4.9.3	Combined tension and shear loads .....	316
14.4.10	Fatigue loads .....	316
14.4.11	Seismic loads .....	319
14.4.11.1	General .....	319
14.4.11.2	Actions .....	320
14.4.11.3	Resistances .....	322
14.4.12	Verification of serviceability limit state .....	322
14.4.13	Fire .....	323
14.4.13.1	General .....	323
14.4.13.2	Partial safety factors .....	323
14.4.13.3	Resistance .....	323
14.4.13.3.1	Tension loading .....	323
14.4.13.3.2	Shear loading .....	324
14.4.13.3.3	Combined tension and shear loading .....	325
14.4.14	Plastic design of fastenings with headed fasteners and post-installed fasteners .....	325
14.4.14.1	Field of application .....	325
14.4.14.2	Loads on fastenings .....	326
14.4.14.3	Design of fastenings .....	328
14.4.14.3.1	Partial safety factors .....	328
14.4.14.3.2	Resistance to tension load .....	328
14.4.14.3.3	Resistance to shear load .....	329
14.4.14.3.4	Resistance to combined tension and shear load .....	329
14.5	Design of fastenings with cast-in and post-installed metal anchors according to ACI 318-05 Appendix D .....	330
14.5.1	General .....	330
14.5.2	Scope .....	330
14.5.3	Design concept .....	331
14.5.3.1	Analysis for the ultimate limit state .....	331
14.5.3.2	Serviceability limit state .....	333
14.5.4	Forces on anchors .....	333

---

14.5.5	Characteristic resistances .....	333
14.5.5.1	General .....	333
14.5.5.2	Tension resistance .....	333
14.5.5.3	Shear resistance .....	336
14.5.5.4	Combined tension and shear .....	339
14.5.6	Required edge distances, spacings and member thicknesses to preclude splitting failure .....	339
14.5.7	Resistance where load cases include seismic forces .....	340
14.5.8	Provisions of ACI 349-01 Appendix B .....	340
14.5.8.1	Scope .....	340
14.5.8.2	Ductile design requirements .....	340
14.5.8.3	Baseplate design .....	341
<b>References</b>	.....	<b>343</b>
<b>Subject Index</b>	.....	<b>371</b>



# 1 Introduction

## 1.1 A historical review

The task of connecting building components is as old as building itself. Throughout history, the job has been handled in different ways depending on the building material, the structural system and the particular requirements of the construction.

In wood construction traditional joinery began with timbers bound with tough natural fibres and developed into various types of interlocking, screwed and doweled joints, glued and finger joints as well as embedded steel plates and ring connectors.

Steel construction, a comparatively 'young' discipline, employs connection techniques ranging from cast-iron fittings to rivets, bolts and welding, whereby only bolting and welding are in common use today.

In concrete and masonry construction, various means of anchoring are in regular use (Fig. 1.1).

The mortar used in masonry assemblies can be regarded as the oldest type of connection material. In fact, the hewn dovetails, cast metal joints and embedded metal studs or sleeves historically employed in stone masonry may be considered to be the predecessors of today's modern fastening technology. Today, these methods have been largely replaced by plastic and/or metal elements of sophisticated design inserted into pre-drilled holes and secured via friction, mechanical interlock, chemical bond, or a combination thereof. Today there are systems available that are suitable for practically any type of masonry.

Concrete and reinforced concrete construction initially borrowed fastening techniques from other building trades, either unchanged or only slightly modified. Wood lathe placed in the formwork was anchored in the concrete via pre-driven nails and served as an attachment point for the entire range of building systems, as well as for suspended ceilings. Later, threaded

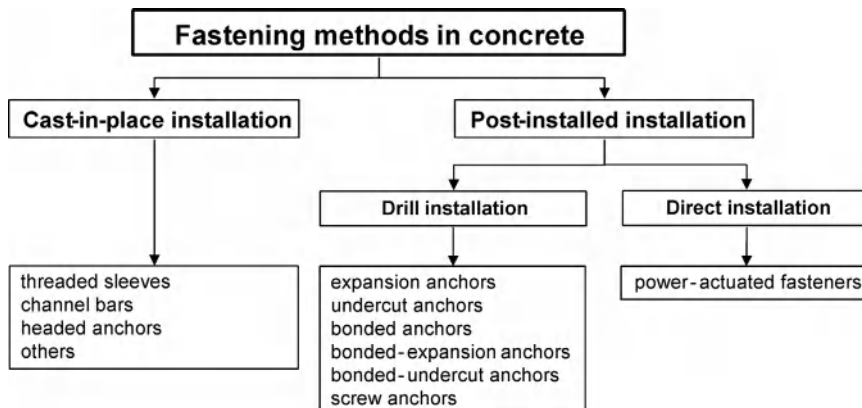


Fig. 1.1 Fastening methods in concrete

sleeves, anchor channels and headed studs welded to steel plates were employed, these being secured inside the formwork and cast into the concrete.

These so-called “cast-in-place” techniques were later rivalled by systems designed to be installed after the concrete had cured. The evolution of drilling technology from chisels to rotary-percussion tools and the more recent development of diamond core drilling has opened up new opportunities for the field of post-installed anchoring technology.

For minor loads, the ubiquitous plastic anchor, successor to hemp and lead plugs, has all but replaced other techniques. To cope with higher loads, various types of metal expansion anchors have been developed that employ, in principle, the same functional principles but with varying construction details and attendant variations in installation and application conditions.

Bonded anchors, in which a steel rod is grouted into a pre-drilled hole, continue to be frequently used. Representing the latest stages in this chain of development are undercut anchors, hybrid systems employing bond, friction and/or mechanical interlock, and second-generation self-tapping screws.

Parallel with the development of anchors for pre-drilled holes, the technology of high-strength steel nails or studs driven into steel and concrete by an explosive or pneumatic energy source (so-called power-actuated fastening) has seen growing use over the past four decades. These systems serve to simplify the attachment of piping systems, lightweight suspended ceilings, etc., and are also widely employed for the attachment of metal deck to steel framing.

Clearly, post-installed fastening in concrete and masonry is a relatively young discipline, meaning that the state of the art is generally in a state of flux. Consequently, these systems typically cannot be regulated via prescriptive standards, as is done, say, with high-strength structural bolts. Consequently, in the member states of the European Community, the U.S. and other countries the design and installation of post-installed fastenings is usually carried out in accordance with product-specific approvals.

## 1.2 Requirements for fastenings

Fastenings must be designed in such a way that they do the job for which they are intended, are durable and robust, and exhibit sufficient load-carrying and deformation capacity. Fastenings for less critical applications, e.g. securing lightweight duct, lighting, and wiring, can be selected on the basis of the user’s experience and do not usually require analysis or structural review (outside areas of seismic hazard). On the other hand, fastenings that are relevant to life safety, i.e. whose failure could pose a hazard to life or result in significant economic loss, must generally be selected on the basis of structural considerations and are typically designed and detailed by a structural engineer. The design establishes whether the requirements of the serviceability and ultimate limit states are met. The serviceability limit state includes requirements for limiting deformation, and requirements on durability (corrosion, chemical resistance). At the ultimate limit state it must be proven that the design value of the actions does not exceed the design value of the fastening resistance. Analyses of the serviceability and ultimate limit states generally make a distinction between the type and direction of the load. Section 1.3 deals with loads acting on connections and section 3.7 with the distribution of these loads to the fasteners. The capacities of the fastenings are explained in relation to the type of fastener and type of base material as well as failure mode in sections 4 to 9. The behaviour of fasteners under seismic excitations and under fire is dealt with in sections 10 and 11 respectively. Corrosion and corrosion protection is discussed in section 12 and the influence of fastenings on the capacity of concrete members in which they are installed is explained in section 13. Requirements on the suitability of fasteners for the application in question and the design of fastenings are discussed in section 14.

## 1.3 Nature and direction of actions

Actions (loads) can be classified according to the frequency of their occurrence and their duration. In addition, we can make a distinction as to whether or not inertial forces are involved. Table 1.1 provides an overview of various actions. Dynamic forces arise in cases of

**Table 1.1** Classification of actions

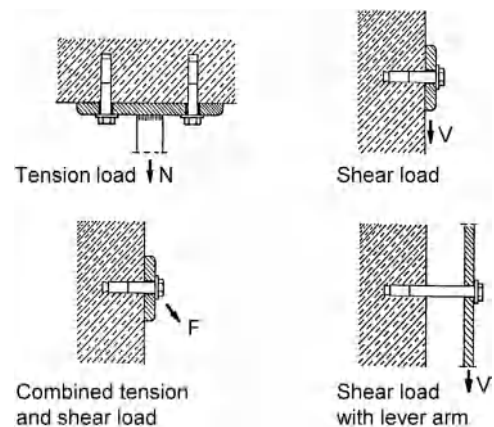
None (constant)	Number of load cycles			
	Low		High	
	Without inertial forces	With inertial forces	Without inertial forces	With inertial forces
<ul style="list-style-type: none"> <li>● Self-weight</li> <li>● Partitions</li> <li>● People</li> <li>● Fixtures and fittings</li> <li>● Stored materials</li> <li>● Snow</li> <li>● Water</li> <li>● Wind</li> <li>● Restraint of deformations</li> </ul>	<ul style="list-style-type: none"> <li>● Restraint of deformations</li> </ul>	<ul style="list-style-type: none"> <li>● Impact</li> <li>● Earthquake</li> <li>● Explosion</li> </ul>	<ul style="list-style-type: none"> <li>● Traffic loads on bridges and basement roofs</li> <li>● Crane rails</li> <li>● Lifts</li> <li>● Machines without inertial acceleration</li> </ul>	<ul style="list-style-type: none"> <li>● Machines generating high inertial accelerations (punches, presses, rams, forges)</li> </ul>
	<ul style="list-style-type: none"> <li>● Primarily static actions</li> </ul>	<ul style="list-style-type: none"> <li>● Dynamic actions</li> </ul>	<ul style="list-style-type: none"> <li>● Frequently alternating actions</li> </ul>	<ul style="list-style-type: none"> <li>● Dynamic actions</li> </ul>

impact, earthquake, explosion or machines that generate large inertial loads. If the load is permanent or occurs only a few times and does not include inertial forces, then the action is considered to be static. If the number of load cycles is large but, again, inertial loads are not present, then we refer to fatigue loading. If inertial forces are involved, then the action is dynamic, regardless of the number of load cycles.

Static actions are the sum of permanent and semi-permanent (slowly changing) actions. These actions are sometimes referred to as dead and live loads. The permanent actions result from the weight of the structural components to be anchored and any other constant loads that the attached components must carry, e.g. back-fill, floor coverings, and plaster. Semi-permanent actions include, for example, foot traffic, fixtures and fittings, non-load-bearing light-weight partitions, stored materials, wind and snow. Given values for the applicable permanent and semi-permanent actions can be found in the relevant national and international standards (e. g. DIN 1055, Eurocode 1: EN 1990: 2002 (2002), ASCE 7 (*American Society of Civil Engineers* (2002)) ).

Deformations can occur in anchored components, e.g. due to temperature fluctuations or due to shrinkage and creep of the concrete components. Temperature fluctuations may be due to weather conditions, as with building facades,

or may simply be a result of the component function, as in the case of chimneys, silos, boiler rooms and cold storage rooms. Restraint of these deformations gives rise to stresses in the fasteners, the magnitude of which depends on the geometry and position of the fastenings as well as the mechanical properties of the materials involved. These stresses may be relevant to the fatigue-resistance of the fastener, depending on the number of temperature-induced strain cycles. For example, in the case of facade support structures, assumptions of  $10^4$  to  $2 \cdot 10^4$  load cycles are often used in design.

**Fig. 1.2** Actions on fasteners

Frequently alternating actions (fatigue loads) are caused by, for example, traffic loads, crane rails, lift and machines. The magnitude of the changing action required for design is again to be found in the relevant national and international standards. These standards also define whether a changing action should be viewed as a static action or as a fatigue load. For example, a wind load frequently changes in magnitude and direction but is often regarded as a static load for design purposes.

The essential difference between dynamic and static actions lies in the presence of inertial and

attenuation forces. These forces arise from the induced accelerations and must be taken into account when determining the forces on the fastening. Dynamic forces are brought about by earthquakes, sudden actions such as impacts and explosions, and by machines with high inertial acceleration, e.g. printing presses. Dynamic actions generated by machines are also regarded as relevant for fatigue.

Loads can occur as tension, shear or a combination of tension and shear. In the case of shear, we distinguish between loading with or without bending of the fastener (Fig. 1.2).

## 2 Fastening systems

### 2.1 General

Fasteners transfer applied tension loads to the base material in various ways. Load-transfer mechanisms are typically identified as mechanical interlock, friction or bond (Fig. 2.1).

Mechanical interlock involves transfer of load by means of a bearing interlock between the fastener and the base material. Mechanical interlock is the load-transfer mechanism employed by headed anchors, anchor channels, screw anchors, and undercut anchors.

Friction is the load-transfer mechanism employed by expansion anchors. During the installation process, an expansion force is generated which gives rise to a friction force between the anchor and the sides of the drilled hole. This friction force is in equilibrium with the external tensile force.

In the case of chemical interlock, the tension load is transferred to the base material by means of bond, i.e. some combination of adhesion and

micro-keying. Chemical interlock is the load-transfer mechanism employed by bonded anchors.

The majority of commercially available fasteners resist tension loads via one or more of the above described mechanisms.

Another way of differentiating anchor systems is by the way they are installed. A distinction is made between cast-in-place, drilled-in and direct installation. Cast-in-place components are secured in the formwork prior to casting. Drilled-in anchors are installed in holes drilled into the hardened base material. Direct installation refers to studs or nails driven into the base material with powder cartridges or pneumatic action.

The following sections describe anchors commonly used in plain and reinforced concrete.

### 2.2 Cast-in-place systems

A variety of inserts are used for cast-in-place installations. These include lifting inserts for the transportation of precast concrete components, anchor channels, embedded plates with headed studs, bent reinforcing bars equipped with internally threaded unions, as well as custom components for hanging heavy facade panels and for securing masonry. Sections 2.2.1 to 2.2.4 describe the more common cast-in-place systems listed above. Design procedures for cast-in-place headed anchors and anchor channels are outlined in section 14.

As previously discussed, cast-in-place systems transfer external tension loads into the base material by means of a mechanical interlock between the embedded component and the concrete. Their positions must be coordinated with the reinforcement layout. They can also be installed in heavily reinforced elements without

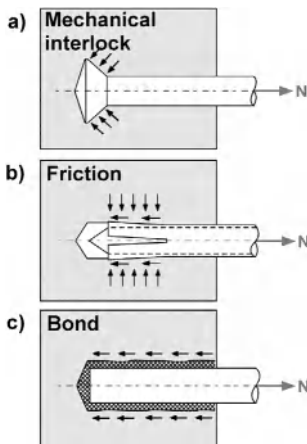


Fig. 2.1 Anchor load-transfer mechanisms

difficulty. The advantage of cast-in-place systems lies in the fact that the location of the anticipated external loads is known and so can be accommodated in the design of the reinforced concrete member through appropriately placed reinforcement. The disadvantage lies in the extra layout and planning required for these systems, as well as in the potential for erroneous placement.

### 2.2.1 Lifting inserts

Lifting inserts used for the transport of plain and reinforced concrete precast elements must often conform to applicable local specifications regulating their design. Examples include the safety guidelines of Germany's *Hauptverband der gewerblichen Berufsgenossenschaften* (1992) and the U.S. *Occupational Safety and Health Administration (OSHA)* (1989) which specifies capacity requirements for inserts and lifting hardware.

In the case of cast-in cable loops, the crane hook or lifting tackle is simply attached to a loop of cable projecting from the concrete (Fig. 2.2).

A wide variety of commercially available lifting inserts are equipped with flush-set internally threaded sleeves to accommodate lifting tackle (Fig. 2.3). These are anchored in the concrete by various means including deformations, transverse dowels, and hairpins. Lifting inserts may also be constructed by swaging an internally threaded insert directly onto the end of a piece of reinforcing bar (Fig. 2.4).

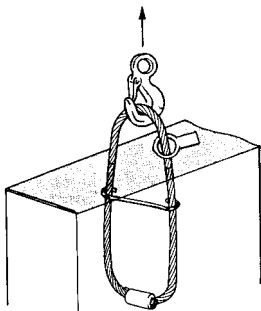
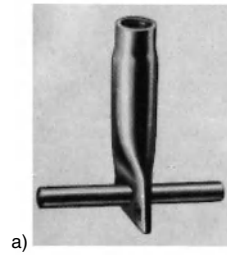


**Fig. 2.2** Cast-in cable loop for crane hook (Bertram (1997))



a)



b)



c)

**Fig. 2.3** Typical threaded sleeves (Bertram (1997))

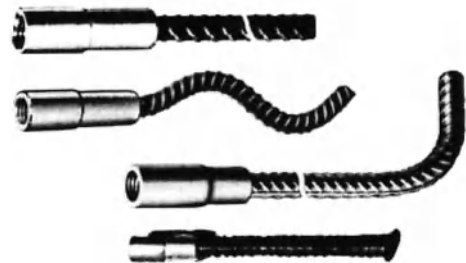


**Fig. 2.4** Transport anchors with swaged threaded sleeves (Bertram (1997))

A simple form of transport anchor is constructed from bar stock, one end of which has been sheared and bent to form a 'swallow tail'. A hole drilled into the opposite end serves to accommodate the lifting hardware attachment (Fig. 2.5).

Headed anchors with cold-formed heads (Fig. 2.6) at each end are designed to accommodate special lifting hardware that engages the larger head.

There are also systems available in which the lifting tackle can be remotely disconnected (Fig. 2.7).

The installation instructions of the manufacturer must be adhered to when using lifting inserts. These specify permissible load, minimum concrete strength, minimum component



**Fig. 2.5** Steel flatbar with "fishtail"



**Fig. 2.6** Round-headed transport anchor



**Fig. 2.7** Lifting tackle with remote release

thickness, minimum spacing, and edge distance, as well as the necessary reinforcement. As a rule, specific additional reinforcement is required since lifting inserts are often positioned close to edges or in narrow components.

Lifting inserts used to carry permanent loads as part of the finished structure must satisfy additional requirements for such installations (e.g. as per the constraints of the relevant approval).

**2.2.2 Anchor channels**

Anchor channels (Figs. 2.8 and 2.9) consist of a cold-formed or hot-rolled steel channel

equipped with special anchor fittings. These channels, filled with rigid urethane foam to prevent concrete intrusion, are attached directly to

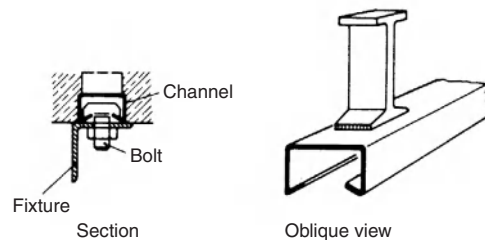


**Fig. 2.8** Cast-in-place channel anchor (Eligehausen, Mallee, Rehm (1997))

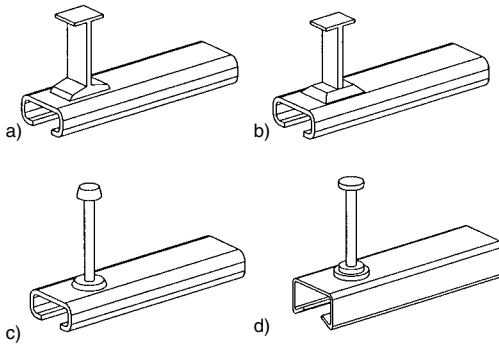


**Fig. 2.9** Variants for cast-in-place anchor channels (Wohlfahrt (1996))

- a) Welded profile
- b) Swaged profile
- c) Swaged headed stud
- d) Welded headed stud
- d) Welded special nut with screw

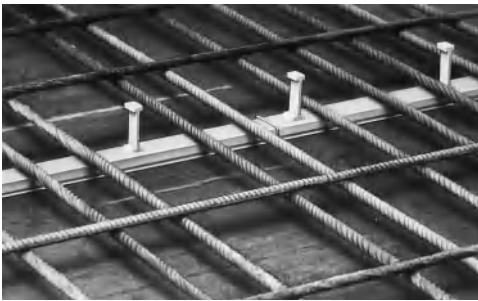


**Fig. 2.10** Anchor channel placed in the formwork

the inside of the formwork (Fig. 2.10). Following removal of the formwork and of the rigid foam, a variety of components can be attached with the aid of special T-headed bolts (Fig. 2.11).

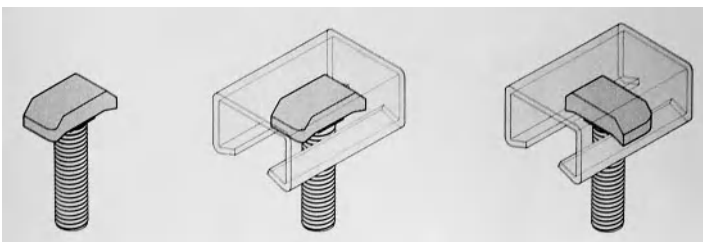


**Fig. 2.11** Installing a T-head bolt in a cast-in-place channel

Transfer of the load back into the concrete in the case of anchor channels is generally achieved by way of T-, I-shaped or headed anchors welded (Fig. 2.9a) or forged to the channel (Fig. 2.9b, c) or special nuts welded to the channel into which a bolt is screwed (Fig. 2.9d). However, there are also anchor channels available in which the load is transferred into the base material by way of loops of steel with tabs that are passed through the back of the channel and bent. This type of anchorage presents a problem because the anchorage may become effective only after a certain degree of slip of the channel. In addition, it cannot be guaranteed that the steel tabs are bent properly on site. In Germany such anchor channels are not approved for use in safety relevant applications.

The anchor channels described above may only be loaded perpendicular to the axis of the channel because transferring forces along the length of the channel is only achieved by way of friction between the T-headed bolt and the lip of the rail, and the magnitude of this friction force is uncertain. To transfer loads along the length of the channel there are special channels with serrated lips. The matching T-headed bolts also exhibit serrations which engage with those of the channel (Fig. 2.12). To guarantee an interlocking connection which transfers the loads, these bolts have to be prestressed with a defined torque.



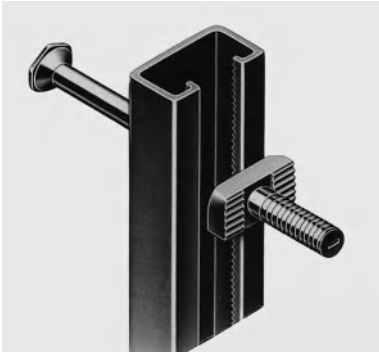


**Fig. 2.12** Cast-in-place channel with serrated edges for resisting shear loads along the length of the rail

**2.2.3 Headed studs**

Headed stud anchorages (Fig. 2.13) consist of a steel plate with headed studs butt-welded on. Long headed studs can be produced by welding short studs together (Fig. 2.13). In such cases a soft pad should be placed under the intermediate heads in order to prevent a mechanical interlock (Fig. 2.14). However, instead of welding short headed studs together, it is recommended to use longer studs.

Headed studs with smooth shanks are usually welded on using drawn arc stud welding.



**Fig. 2.13** Steel embed plate with welded headed studs

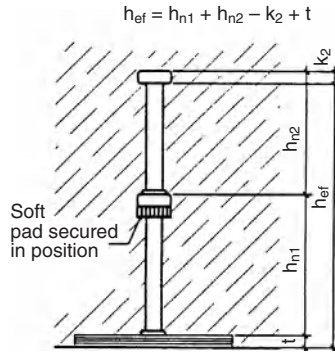


**Fig. 2.14** Two headed studs welded together with a soft pad placed beneath the head nearest the surface

Headed studs can also be made from ribbed reinforcing bars and welded to the steel plate by means of metal arc welding. The welding is not usually carried out on site but rather under controlled factory conditions. The fixture is normally welded to the cast-in steel plate.

**2.2.4 Threaded sleeves**

Threaded sleeves consist of a tube with an internal thread which is anchored back into the concrete. We distinguish between sockets for lifting eyes and sleeve anchors (Fig. 2.3). Sockets for lifting eyes have a flat section with a hole at one end (Fig. 2.3a,b). They are anchored back into the concrete by passing a steel rod or reinforcing bar through the hole. In the case of sleeve anchors, the flat section at one end includes a hook (Fig. 2.3c). Curved anchors (Fig. 2.15) comprise a bent ribbed reinforcing bar with a threaded sleeve pressed on.

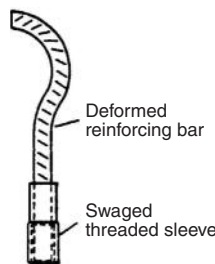


**Fig. 2.15** Hooked reinforcing bar with swaged threaded sleeve (Eligehausen, Mallée, Rehm (1997))

## 2.3 Drilled-in systems

### 2.3.1 Drilling techniques

Advances in drilling technology have contributed significantly to the widespread use of post-installed anchors. Rotary-impact drills (rotary hammers) are most often used for anchoring applications. Diamond core drills are used less frequently, although recent advances in weight reduction, slurry-capture, and dry coring have made these systems more attractive for anchoring applications where existing reinforcement is expendable. In some cases, rock drills are used for large anchorages.

An electro-pneumatic rotary-impact drill employs a piston to generate the percussive action of the drill bit. These drills operate at low rotational speeds but with high impact energy. The speed at which the drill advances is generally not dependent on the applied pressure. Depending on the power rating of the drill, holes with diameters up to 40 mm can be produced easily and economically with carbide tipped bits. Drilling through reinforcing bars of small diameter is possible, although bit life is significantly reduced. Newer models have built-in vacuum systems to capture the dust generated during drilling, thus mitigating the contamination and inconvenience caused by the dust, reducing the drilling time and extending the bit life. Dust capture can also reduce health risks for the drill operator.

Diamond core drills are employed for a variety of applications. The cutting edges of the hollow cylindrical bit are tipped with a diamond matrix. The concrete is removed not through chiselling action, but rather by abrasion. Diamond drilling equipment is often secured to the component being drilled and water is typically used to both cool the bit and transport drilling slurry to the surface. The rate of diamond grit loss during drilling is crucial for proper functioning of the bit and requires the correct pairing of bit type and concrete aggregate hardness. Recently, hand-held core drill rigs more suited to anchoring applications and “dry” bits that do not require water cooling have become widely available. It should be remembered when employing diamond core drilling that reinforcing bars of any diameter can be severed without difficulty

or noticeable changes in drill operation. Therefore, particular attention should be paid to coordinating the position of the drilled holes with respect to the reinforcing steel in order to avoid damaging structural reinforcement.

Many anchor systems are sensitive to deviations of the as-drilled hole diameter outside of specified tolerances, and in turn on the dimension of the carbide-tipped drill bit as measured across the tip. Carbide drill bits used for anchoring applications should be checked that their dimensional tolerances, particularly those relating to tip dimensions and concentricity, conform to anchor manufacturer requirements. Typically, national standards such as those of the *Deutsches Institut für Bautechnik* (2002) or the *American National Standards Institute* (1994) are referenced and can be used to confirm drill bit suitability. Drill bits conforming to *Deutsches Institut für Bautechnik* (2002) are marked with a special sign (Fig. 2.16).



**Fig. 2.16** Special mark for drill bits conforming to *Deutsches Institut für Bautechnik* (2002)

Use of diamond core drill bits for anchoring applications should be verified with the anchor manufacturer, since the actual hole diameter associated with a core drill bit of correct nominal diameter may not be within the tolerances necessary for the anchor to function properly. Additionally, some anchor systems, notably bonded anchors, may be sensitive to hole roughness. “Matched tolerance” core bits are tested to verify correct functioning of the anchor in holes drilled with these bits.

### 2.3.2 Installation configurations

Three types of installation configuration may be distinguished (Fig. 2.17):

- pre-positioned
- in-place
- stand-off

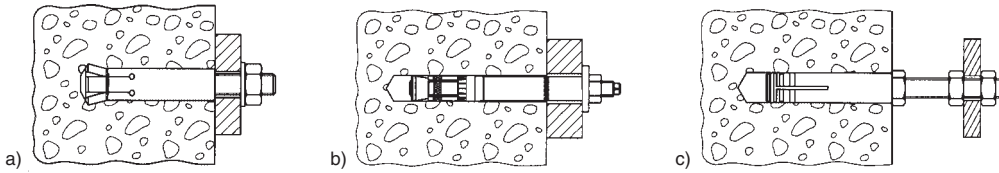


**Fig. 2.17** Anchor installation configurations

- a) Pre-positioned installation  
 b) In-place installation  
 c) Stand-off installation

A pre-positioned installation (Fig. 2.17a) involves drilling a hole, inserting the anchor and subsequently placing and securing the item to be fastened. The drilled hole in the base material is typically larger than the clearance hole in the component being fastened.

An in-place installation uses the element to be fastened as a template for drilling the anchor hole(s). Therefore, the diameter of the hole in the component to be fastened must be at least as large as the required diameter of the drilled hole (Fig. 2.17b).

In a stand-off installation, the item to be fastened is mounted at a distance from the surface of the base material (Fig. 2.17c). It is necessary in this type of installation to ensure that the fastener is capable of delivering both tension and compression loads to the base material. In the case of post-installed mechanical anchors, it is necessary to provide a bearing washer and nut at the surface of the base material to receive compression loads. This is also advisable, although not required, for bonded anchors.

Pre-positioned or in-place installations require that the useable fixing length  $l_{fix}$  is at least equal

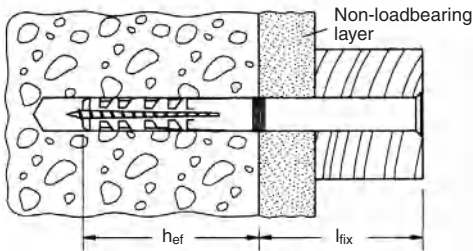


**Fig. 2.18** Accounting for non-load-bearing layer in determining the useable fastening length

to the thickness  $t_{fix}$  of the item to be fastened. If the base material is covered with a non-load-bearing layer (e.g. plaster or insulation), then the fixing length  $l_{fix}$  must be selected so that it is at least equal to the thickness of the non-load-bearing layer plus the thickness of the item to be fastened (Fig. 2.18).

Although the useable fixing length of an anchor equipped with internal threads can be varied by simply selecting a bolt of suitable length, it is a set dimension for most other types of mechanical anchors. The manufacturer's specification should be consulted to determine the maximum possible useable fixing length of an individual anchor. Note also that with in-place installation the actual embedment length of fasteners with a defined useable fixing length will be equal to the minimum embedment plus the balance of the fixing length not used by the thickness of the item to be fastened and any surface coatings, pads, etc.

### 2.3.3 Drilled-in anchor types

#### 2.3.3.1 Mechanical expansion anchors

Mechanical expansion anchors can be divided into two groups (Fig. 2.19):

- torque-controlled (Fig. 2.19a)
- displacement-controlled (Fig. 2.19b)

Torque-controlled expansion anchors may be further classified as either sleeve- or bolt-type. Sleeve-type anchors generally consist of a bolt or threaded rod with nut, washer, spacer and expansion sleeve, deformations to prevent spinning of the anchor in the hole, and either one expansion cone (Fig. 19a<sub>1</sub>) or two cones (Fig. 2.19a<sub>2</sub>). Bolt-type anchors typically consist of a bolt, the end of which has been swaged or

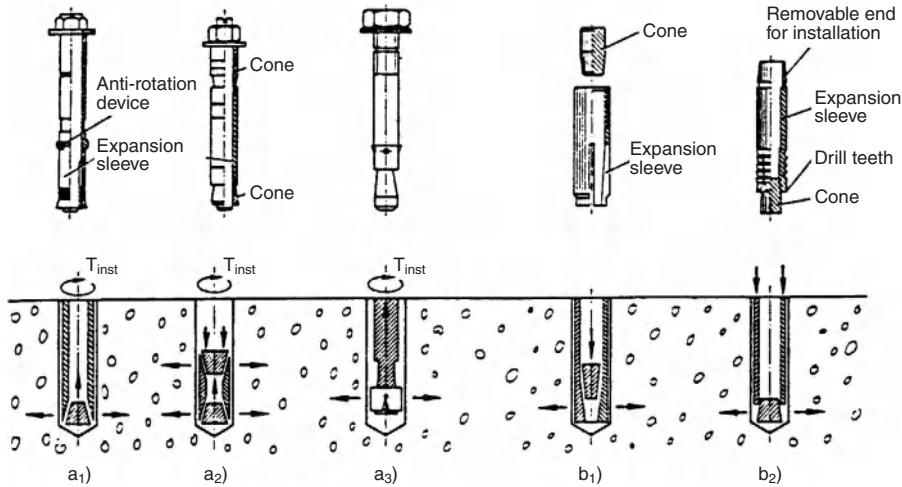


**Fig. 2.19** Details and working principles of metal expansion anchors (Eligehausen, Mallée, Rehm (1997))  
 a) Torque-controlled expansion anchor  
 b) Displacement-controlled expansion anchor

machined into a conical shape, expansion segments nested in the recessed conical end of the bolt, and a nut and washer (Fig. 2.19a<sub>3</sub>).

Torque-controlled expansion anchors are installed by drilling a hole, removing drilling dust and debris, inserting the anchor into the hole and securing it by applying a specified torque to the bolt head or nut with a torque wrench (Fig. 2.20). Once the bolt or nut achieves bearing against the base material, the further application of torque draws the cone at the embedded end of the anchor up into the expansion sleeve (or expansion segments), thereby expanding the expansion element(s) against the sides of the drilled hole. The ensuing frictional resistance places the bolt in tension. The compression forces acting on the concrete due to the dilation of the expansion elements are

known as expansion forces. If the concrete around the anchor is continuous and undisturbed by cracking or a proximate edge, the resulting stresses are distributed roughly symmetrically around the anchor perimeter. In the past, torque-controlled anchors were occasionally referred to as “force-controlled” expansion anchors because the torque generates a tensile force in the anchor. However, “torque-controlled” is a better descriptor for the working principle of the anchor since a prescribed torque is used to set the anchor. Torque also serves as a way of checking the installation of torque-controlled expansion anchors. An anchor that was not set correctly will rotate before achieving the prescribed torque. Rotation is nominally prevented by deformations in the anchor elements contacting the sides of the hole. Oversized holes or local defects in the concrete may reduce their

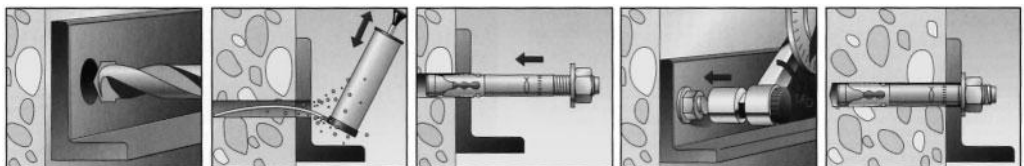


**Fig. 2.20** Installation of a torque-controlled stud-type expansion anchor

effectiveness and allow the anchor to spin, thereby preventing attainment of the required expansion force. Alternatively, the anchor may attain the required torque but only after the anchor has been drawn out of the hole to an excessive degree. Either of these conditions is an indication of improper set and could lead to reduced anchor capacity.

Torque-controlled expansion anchors compensate for minor deviations in the diameter and roundness of the drilled hole by variations in the extent to which the cone is drawn into the expansion element (Fig. 2.21). This is known as expansion reserve; it is determined by the geometry of the anchor and is necessarily limited. For this reason, torque-controlled expansion anchors should be installed with drill bits conforming to the tolerances of recognised national standards as discussed above. When this condition is satisfied, normal deviations of drilled hole geometry as caused by e.g., operator position, base material hardness, etc., should have little effect on anchor function.

In the system shown in Fig. 2.19a<sub>2</sub>, the expansion sleeve is expanded by cones both the top and bottom of the sleeve. However, although double-cone anchors can exhibit a higher load-carrying capacity than single-cone anchors, they require greater minimum edge distances owing to the greater expansion forces.

The setting process of a torque-controlled expansion anchor results in expansion forces which in turn generate high stresses (Fig. 2.22) and localised deformations in the concrete. The degree of expansion and the magnitude of the



**Fig. 2.22** Stress contours in the anchorage zone of a torque-controlled expansion anchor (Seghezzi (1983))

deformation of the hole wall both depend on the force with which the cone is drawn into the sleeve (or expansion segments) as well as on the resistance of the concrete to deformation. The deformation of the hole wall may be critical for proper functioning of the anchor. Expansion anchors set in high-strength concrete (concrete compressive strengths  $\geq 65 \text{ N/mm}^2$ ) typically produce deformations of negligible magnitude. Therefore, torque-controlled expansion anchors developed for use in concrete of normal strength may be unsuitable for applications in high-strength concrete.

Torque-controlled expansion anchors transfer external tensile forces to the base material via friction and, to a limited extent, via mechanical interlock in the region of the deformed concrete. As the torque is introduced, it generates a prestressing force in the bolt or stud which at the same time clamps the item being fastened against the surface of the base material. This prestressing force diminishes after installing the anchor as a result of several factors, including localised relaxation of the concrete. If cracks occur in the base material in the vicinity of the installed anchor, then the prestressing force drops further. As the anchor is loaded externally, most of the load acts to relieve the prestressing, or clamping, force in the anchorage. Loading beyond the point where the residual prestressing force is completely balanced by the external load produces a proportional increase in the force in the bolt, with the result that the cone is drawn further into the

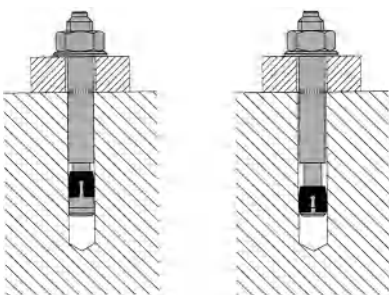


**Fig. 2.21** Torque-controlled expansion anchors in drilled holes with different diameters



sleeve (or segments) and the anchor is expanded further (follow-up expansion). This follow-up expansion generates the necessary additional friction to resist an increasing imposed external load. Follow-up expansion is only possible when the frictional resistance between cone and expansion sleeve (or segments) is less than the friction force generated between the sleeve (or segments) and the sides of the drilled hole. If this is not the case, then the anchor exhibits uncontrolled slip under tension loading, i.e. it is pulled partially or completely out of the hole without any increase in load beyond the onset of noticeable slip. To increase the friction potential between the expansion sleeve and the concrete, some expansion anchors utilise ribs, knurling or other deformations.

Torque-controlled expansion anchors are typically available in a wide range of diameters, from 6 mm to 24 mm. They are typically provided with zinc electroplating (coating thickness  $\geq 5 \mu\text{m}$ ) in order to prevent corrosion during storage and transport. Sheradising or hot-dip galvanising may be used to achieve a more robust zinc coating thickness (in the range of  $50\mu\text{m}$ ). However care must be taken to prevent uneven coating thickness on friction surfaces and threaded parts. Where additional corrosion protection is required, torque-controlled expansion anchors may also be fabricated in stainless steel, although care must be taken to avoid jamming of threads and friction surfaces. Studs and bolts may be fabricated from a variety of steels depending on the production method used and the desired mechanical properties after fabrication. In Europe, carbon steel anchor bolts are typically fabricated to conform to the requirements of a Grade 8.8 steel according to *ISO 898, Part 1* (1988). Stainless steel bolts generally reference to A4-70 (austenitic steel) as per *ISO 3506* (1979). For anchors fabricated in the U.S., no single standard is universally specified.

Reference is often made, however, to *ASTM A510-03* (2003) or *ASTM A108-03* (2003) for the mechanical properties of carbon steel anchor bolts. Stainless steels typically conform to either *AISI 303* (1995), *AISI 304* (1995) or *AISI 316* (1995) with respect to chemical composition, whereby *ASTM A276-04* (2004) or *ASTM A493-95* (2004) may be referenced for the mechanical properties. When a thorough understanding of the bolt properties is required, the manufacturer should be consulted for detailed information. Commercially available torque-controlled expansion anchors are offered in a wide array of configurations and designs that vary with respect to the number of cones as well as the shape, dimensions and number of expansion sleeves and expansion segments. Additionally, newer designs specifically authorised for applications in cracked concrete may employ special features, e.g. friction-reducing coatings, to improve the follow-up expansion behaviour of the anchor.

Displacement-controlled expansion anchors usually consist of an expansion sleeve and a conical expansion plug, whereby the sleeve is internally threaded to accept a threaded element (bolt, rod, etc.). They are set via the expansion of the sleeve as controlled by the axial displacement of the expansion plug within the sleeve. In the common displacement controlled anchor type as depicted in Fig. 2.19b<sub>1</sub>, known as a drop-in anchor, this is achieved by driving the expansion plug into the sleeve with a setting tool and a hammer (Fig. 2.23). Alternatively, in the type of displacement-controlled anchor shown in Fig. 2.19b<sub>2</sub>, setting is achieved by driving the sleeve over the cone. Like torque-controlled expansion anchors, displacement-controlled expansion anchors transfer external tension loads into the base material via friction and, in the zone of the localised deformation, some degree of mechanical interlock.

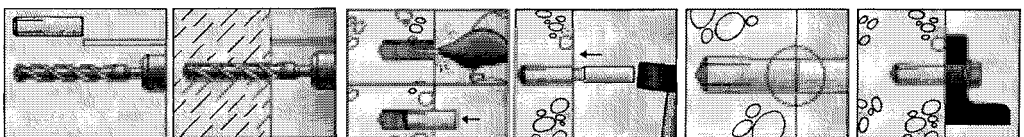


**Fig. 2.23** Installation of a drop-in anchor of the type shown in Fig. 2.19b<sub>1</sub>

In the anchor shown in Fig. 2.19b<sub>1</sub>, the magnitude of the expansion force depends on the degree of sleeve expansion, the gap between the anchor and the sides of the drilled hole, and the deformation resistance of the concrete. The initial expansion force generated by a fully-installed displacement-controlled anchor of this type is typically considerably greater than that created by a torque-controlled expansion anchor of similar size. This high initial expansion force is substantially reduced through relaxation of the concrete, however, and cannot be renewed except by re-setting of the anchor. In particular, the expansion force does not increase with the introduction of an external load, since the anchor has no follow-up expansion capability. As such, its tension load-bearing behaviour depends substantially on the depth of the localised deformation into the concrete and therefore significantly on the drilled hole tolerance. If the hole diameter is too small, the expansion force generated during setting may be so high that the concrete spalls or is split. Additionally, if the concrete has a high compressive strength (e.g.  $\geq 50 \text{ N/mm}^2$ ), it may be physically impossible to expand the anchor to the required degree. Conversely, if the hole is oversized, the expansion sleeve does not engage the hole wall sufficiently (Fig. 2.24) and the load-carrying capacity of the anchor is correspondingly diminished.

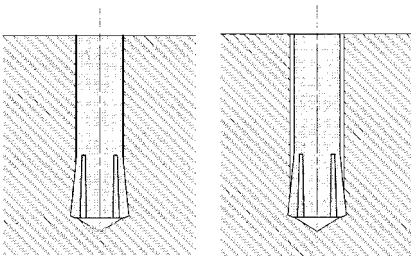


**Fig. 2.24** Drop-in anchors in drilled holes with different diameters

Owing to their sensitivity with respect to hole and installation tolerances, displacement-controlled anchors require strict adherence to correct drill bit tolerances, as discussed previously as well as on-site installation checks. For drop-in anchors as depicted in Fig. 2.19b<sub>1</sub>, proper

installation is verified visually when the collar of the setting tool contacts the sleeve of the anchor, as shown in Fig. 2.23. Only in this way can full expansion of the anchor be assured.

A significant amount of driving energy is required to ensure complete expansion of drop-in anchors. According to studies by *Eligehausen, Graf, Meszaros, Lee* (1995), full expansion requires anywhere from 5 to 30 hammer blows (using a representative hammer size and weight), depending on type and size of the anchor, hole diameter and concrete strength. In overhead installations, (e.g. in a slab soffit), the required number of hammer blows increases roughly 2 to 3 times. In many cases, this level of effort is not achieved in practice. *Eligehausen, Meszaros* (1992) investigated the *in-situ* condition of roughly 220 drop-in anchors (M8-M12) of various manufactures installed on several different building sites. The degree of expansion was found to be approximately 30 % to 70 % (on average 50 %) of full expansion, which is relatively low. Inadequate expansion has roughly the same effect as an oversized hole (see Fig. 2.24) on drop-in anchor tension load capacity.

In anchors of the type depicted in Fig. 2.19b<sub>2</sub>, the maximum expansion occurs at the extreme end of the sleeve and decreases along the anchor length. The primary action of the setting process is to chip away at the concrete and the expansion force generated is less than that associated with anchors of the type shown in Fig. 2.19b<sub>1</sub>.

One representative of the anchor type shown in Fig. 2.19b<sub>2</sub> is the so-called self-drilling anchor. Its anchor body is designed to serve as a drill bit (it has a removable end for insertion into the drill chuck adapter with the intent that hole tolerance is eliminated as a factor in the load-carrying capacity of the anchor. Furthermore the required hole depth is automatically ensured. After the anchor has been used to drill the hole, it is removed, the expansion plug is inserted into the end of the sleeve, and the anchor placed back into the hole and hammered over the expansion plug with the rotary-impact drill set to hammer-only mode until the drill chuck adapter touches the concrete surface. This design places high demands on the anchor materials and the manufacturing process. The anchor body must, on the

one hand, possess sufficient hardness to facilitate drilling, while at the same time remaining sufficiently ductile to permit expansion.

With sleeve-down type anchors similar to the one shown in Fig. 2.19b<sub>2</sub> the hole is drilled by means of a rotary impact drill. During installation the sleeve is hammered onto the cone until the upper rim of the sleeve sits flush with the concrete surface. To ensure full anchor expansion the proper drill hole depth is essential which should be ensured by using a drill that stops at the required depth (stop-drill).

The load-carrying capacity of deformation-controlled self-drilling or sleeve-down type anchors depends on achieving the required expansion. As this cannot be verified visually after installation, it is essential to check the distance between the rim of anchor sleeve and the top of the expansion plug.

Displacement-controlled expansion anchors are produced in the size range M6 to M20 and are typically provided with zinc electroplating ( $\geq 5 \mu\text{m}$ ). Drop-in anchors manufactured from stainless steel are available as well. The manufacturer information or approval documentation should be consulted for details of the grade of steel used in a particular anchor.

### 2.3.3.2 Undercut anchors

As with cast-in-place systems, undercut anchors develop a mechanical interlock between anchor and base material. To do this, a cylindrically drilled hole is modified to create a notch, or undercut, of a specific dimension at a defined location either by means of a special drilling apparatus (Fig. 2.25a, b), or by the undercutting action of the anchor itself (Fig. 2.25c, d). Fig.

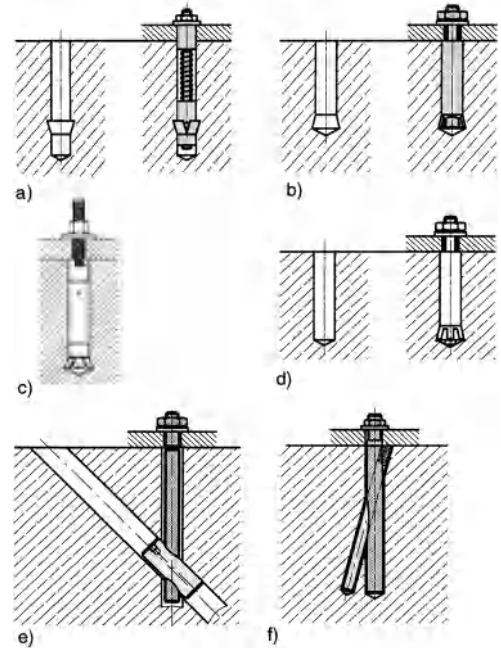


**Fig. 2.25** Undercut anchors  
 a) Reverse undercut  
 b) to d) Forward undercut  
 e) and f) Other interlocking systems

2.25 e and f illustrate two further variations of undercut anchors. In terms of the shape of the undercut, a distinction is made between those that widen towards the surface (Fig. 2.25a) and those that widen towards the bottom of the hole (Fig. 2.25 b–d).

The anchor depicted in Fig. 2.25a consists of a threaded rod with hex nut and washer, a cylindrical nut, three curved bearing segments, cone, spacer sleeve, helical spring and a plastic ring

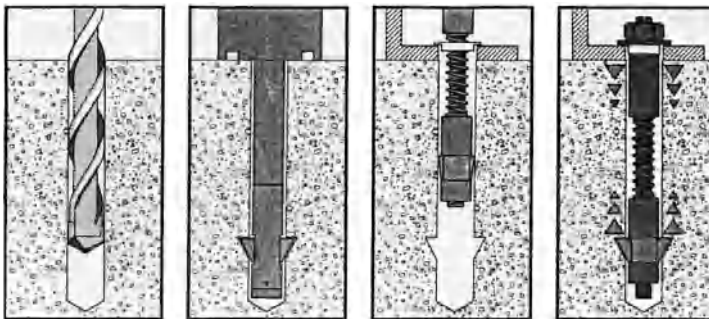


**Fig. 2.26** Installation of an undercut anchor of the type shown in Fig. 2.25a (hole cleaning step not shown)



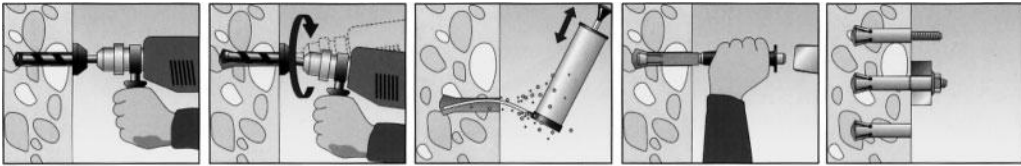


**Fig. 2.27** Installation of an undercut anchor of the type shown in Fig. 2.25b

which secures the bearing segments prior to installing the anchor. The installation sequence is shown in Fig. 2.26. After drilling a cylindrical hole, the undercut is created with the help of a water-cooled undercutting tool with diamond grit blades. Afterwards the anchor is inserted into the hole and the bearing elements are allowed to unfold into position at the level of the undercut. Torquing the anchor brings the bearing segments into contact with the undercut surfaces. The tension load-bearing behaviour depends largely on achieving the necessary undercut. This has to be ensured through appropriate checks during the undercutting process. In order to prevent over-torquing and consequent shearing of the undercut surfaces, the number of turns of the nut permitted to achieve the required torque is limited.

The undercut anchor represented in Fig. 2.25b typically consist of a threaded stud with a conical end (cone bolt), expansion sleeve, nut, and washer. Internally threaded versions (not illustrated) accept bolts or threaded rods. One such anchor employs the installation procedure depicted in Fig. 2.27. First, the cylindrical hole is drilled with a special stop-drill bit. When the stop-drill bit limit has been reached, the undercut is created by gyroscopic rotation of the hammer drill. The unique design of the stop-drill bit defines the extent of the gyroscopic rotation and thereby the resultant undercut. After cleaning out the hole, the expansion sleeve is hammered over the cone bolt with a setting tool.

The anchor systems represented by Fig. 2.25c typically consist of a cone bolt, an expansion sleeve designed for undercutting, and either a nut and washer or an internal thread in the sleeve to accept bolts and threaded rods. Fig. 2.28 shows how such an anchor is installed. The cylindrical hole is drilled using a stop-drill. The undercut is generated using the expansion ele-

ments of the anchor, which are typically equipped with hardened drilling points. The anchor is mounted in a rotary-impact drill and

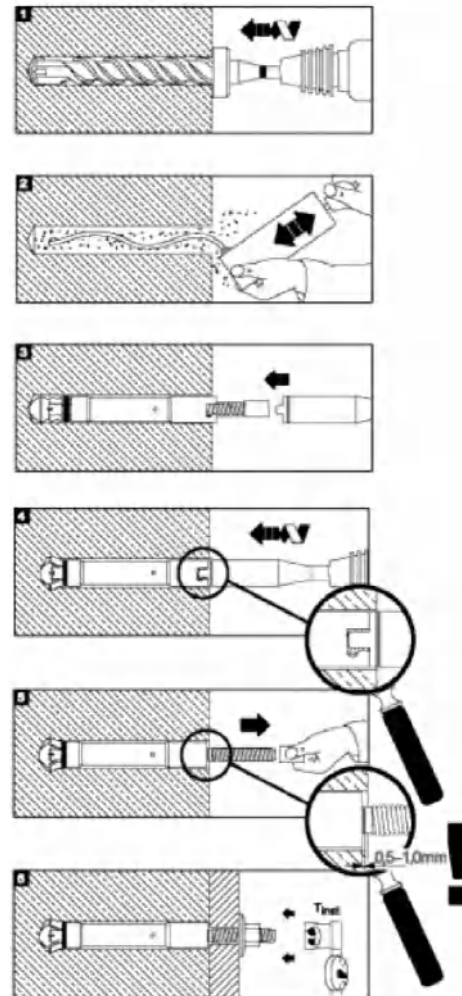


**Fig. 2.28** Installation of an undercut anchor of the type shown in Fig. 2.25c

inserted into the pre-drilled hole. Use of rotary-impact action permits the expansion elements to simultaneously undercut the concrete and widen to their fully-installed position. The cone bolt provides at its end space for the drilling dust which accumulates during formation of the undercut. This process results in a precise match between the undercut form and anchor geometry.

Undercut anchors of the type described in Fig. 2.25d are similar to those of Fig. 2.25c with the exception that the undercutting process is accomplished with hammering action only (Fig. 2.29). Typically, the degree of undercutting associated with these systems is smaller than that achieved with the systems utilising both rotary and hammering action to produce the undercut.

The undercut anchors described in Fig. 2.25 b–d all require that the vertical hole depth be controlled with a stop-drill bit. For all anchors with a continuous sleeve (Fig. 2.25 b–d), it is important to check that clearance exists over the top of the sleeve in its final set position to ensure that the sleeve is not placed in compres-

sion as the anchor is torqued or loaded in tension. The value of the clearance depends on the anchor system and is on the order of a few millimeters. Note also that if this gap is too large, it could lead to diminished shear capacity. Typically, correct set of undercut anchors utilising a cone bolt is checked by means of a mark on the rod that becomes visible when the anchor is fully expanded. Internally threaded anchor systems are checked via the position of the sleeve relative to the surface of the concrete (Fig. 2.29).

The anchor shown in Fig. 2.25e consists of a threaded bar equipped with an oblique barrel nut, as well as a conventional hex nut and washer. The installation process is depicted in Fig. 2.30. First, a hole is drilled perpendicular to the surface of the concrete with a special diamond core drill. The same drill is then used to drill a second hole at an angle of 45° to the first. The drilling equipment is designed to ensure that the two holes intersect. A special tool is used to position the oblique barrel nut in the 45° hole at the intersection with the vertical hole. The anchor rod is then threaded into the barrel nut.

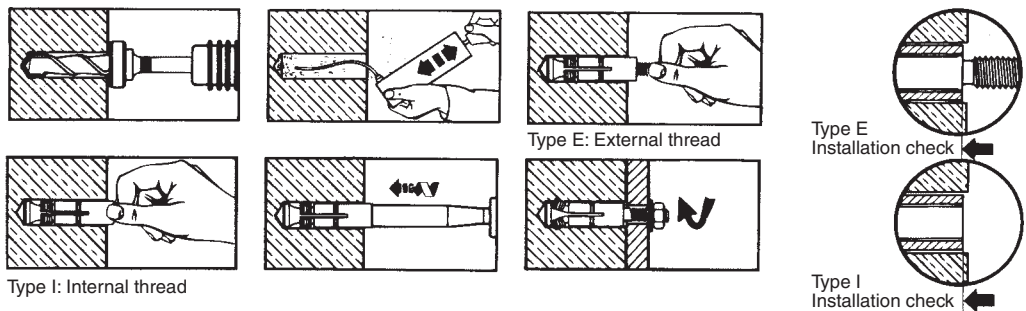


**Fig. 2.29** Installation of an undercut anchor of the type shown in Fig. 2.25d

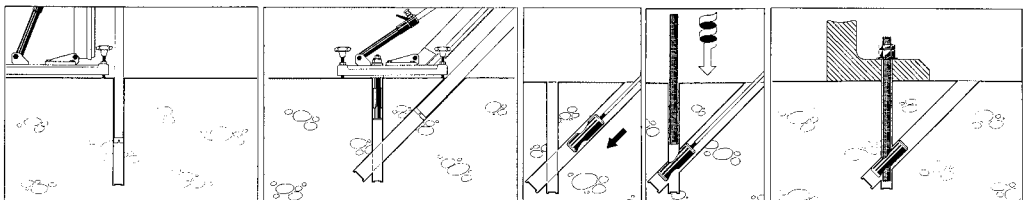


**Fig. 2.30** Installation of an undercut anchor of the type shown in Fig. 2.25e (water removal step not shown)

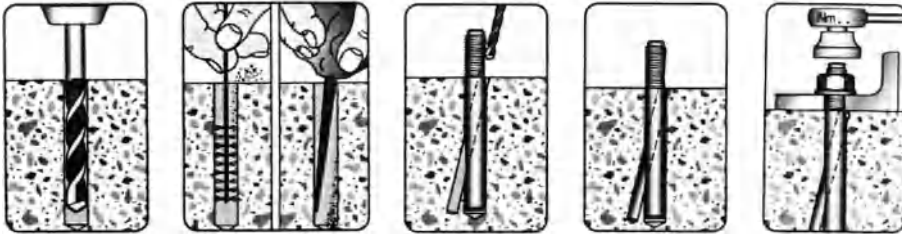


**Fig. 2.31** Installation of an undercut anchor of the type shown in Fig. 2.25f

A variant on this concept is shown in Fig. 2.25f, whereby the anchor consists of a rod provided with an inclined hole and threaded at one end, a second (unthreaded) rod of smaller diameter, and a nut and washer. The threaded rod is inserted into a vertically drilled hole having a defined depth. A second, inclined hole is then drilled using the inclined hole in the threaded rod as a guide (Fig. 2.31). The second rod is then inserted into the inclined hole until it is flush with the surface of the concrete, locking the vertical rod in place.

Fig. 2.32 shows an undercut-type of anchor (installed) designed for use in autoclaved aerated concrete. It consists of a threaded bar with conical nut, expansion sleeve, nut and washer. The expansion sleeve is driven over the cone with a special setting tool. In doing so, the sleeve is expanded and penetrates into the soft autoclaved aerated concrete.

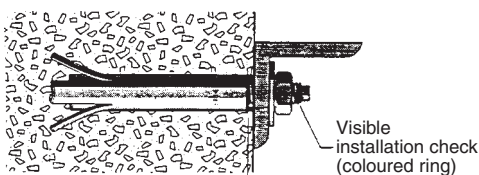


**Fig. 2.32** Undercut expansion anchor for autoclaved aerated concrete

Note that in each case, the anchor components, stop-drills and, if required, undercut drills are coordinated with each other and form a system. Typically, the drills of the various manufacturers cannot be used interchangeably.

These undercut anchors are available in a wide range of diameters and embedment depths. Anchors according to Fig. 2.25e are supplied

with an embedment depth up to 60 mm. All anchors are typically provided with electroplate galvanising and some are also available in stainless steels of various grades, with hot-dip galvanising or sheradised zinc coating.

Unlike expansion anchors, undercut anchors typically generate minimal or no expansion forces during installation. As with all anchors, prestressing (torquing) and loading do induce hoop stresses in the concrete. Nevertheless, these splitting forces are markedly less than those associated with mechanical expansion anchors.

### 2.3.3.3 Bonded anchors

A wide spectrum of bonded anchor systems are currently available (Fig. 2.33). A distinction can be made between so-called capsule anchors, in which the constituent bonding materials are contained in glass capsules or foil pouches, and injection systems. The bonding materials may consist of polymer resins, cementitious materials, or a combination of the two.

#### a) Capsule anchor systems

Capsule anchor systems employ a threaded rod equipped with a 45° chisel or wedge-shaped tip and a hexagonal nut and washer in conjunction with the glass capsule or foil pouch filled with the constituent bonding materials. The required embedment depth is marked on the threaded bar. The capsule contains polymer resin, hardener and quartz aggregate in a defined mix ratio. Resins employed in capsule anchor systems include unsaturated polyester, vinyl ester with and without styrene, and epoxy.

The capsule or pouch is placed in a hole from which all drilling dust has been removed. Mul-

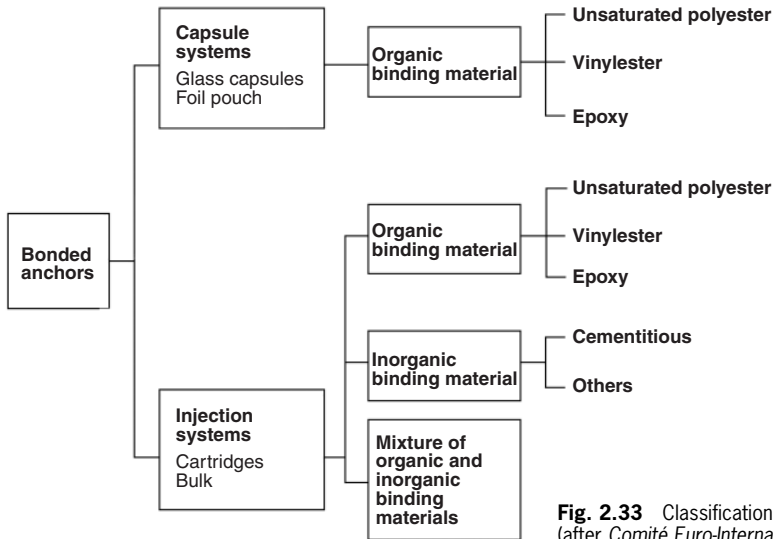


**Fig. 2.33** Classification of bonded anchors  
(after Comité Euro-International du Béton (CEB) (1994))

multiple capsules may be used for longer embedments. The threaded rod is driven through the capsules until the embedment depth mark is level with the surface of the base material using both percussive and rotary action (Fig. 2.34). This may be done either using a special installation tool or by locking a washer between two hexagonal nuts, which are mounted in a rotary-impact drill equipped with a chuck designed to accept the hex nut assembly. When driving the threaded rod into the hole, the glass capsule is broken and fragmented, the resin, hardener, aggregates and capsule fragments are mixed with sufficient energy input to induce rapid curing, and the annular gap around the threaded rod is filled with the polymer matrix. When a foil pouch is used, the foil is likewise shredded into small fragments which become part of the hardened polymer matrix. If the anchor bar is driven with hammering action alone, proper mixing of the mortar is not ensured. Likewise, the use of rock drills and impact wrenches to set

these anchors may result in incomplete bonding. The quantity of polymer materials contained in the capsule or pouch is such that, taking into account possible hole tolerances, a small excess of bonding material will be expelled from the top of the hole when the required embedment depth has been reached (Fig. 2.34). This visual check ensures that complete bonding of the threaded bar has been achieved.

Glass capsule systems are also available in which the anchor rod is driven with hammering action alone (so-called hammer-in capsules). The installation of such a capsule is shown in Fig. 2.35. However, the tension load-carrying capacity is generally inferior to that achieved with capsule anchor systems designed for installation with a rotary-impact drill action. In addition, the degree of hole cleanliness has a great influence on the bond strength of hammer-in capsule anchors (see section 6.1.1.3).

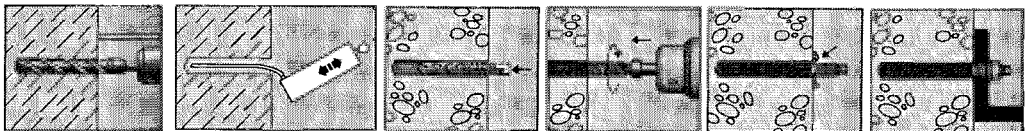


**Fig. 2.34** Installation of a bonded anchor (standard glass capsule or foil pouch)

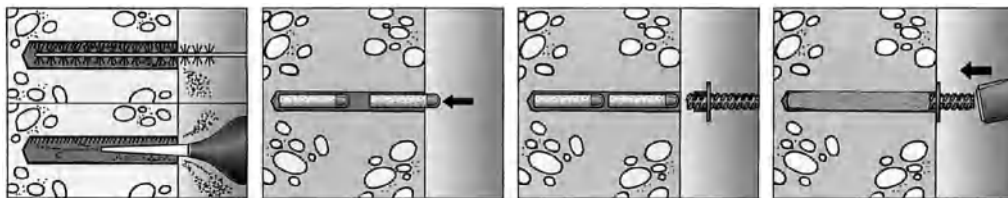


**Fig. 2.35** Installation of a bonded anchor (hammer-in capsule)

The rate of cure of the polymer resin depends on the resin type as well as the ambient temperature of the resin, the air, and the base material. Therefore, the delay, or cure time, to be observed between installing and loading the anchor is temperature dependent. Under dry conditions, the nominal cure time for unsaturated polyester and vinyl ester resins at normal temperatures (10–20°C) is 30 minutes. At a temperature of –5°C, the time required to assure full cure increases to five hours. These cure times should be doubled when the drilled hole is damp. For capsule anchor systems based on these resins, the temperature of the base material should generally not be lower than –5°C at the time of installation. Note that an initial gel time must also be observed for capsule anchors, during which time the anchor rod should not be manipulated, jarred, or otherwise disturbed. Failure to adhere to the gel time may prevent the bonding material from reaching full strength.

Resin-containing capsules should be protected against direct sunlight (UV) exposure and should be stored in a cool place to prevent premature curing, as indicated by thickening, or gelling, of the liquid resin. Capsules in which the resin has gelled should not be used. A visual check that the resin flows freely within the glass capsule when warmed in the hand is sufficient in most cases. For systems employing foil pouches, the possible onset of gelling can usually be detected by manipulation of the pouch. Some manufacturers provide expiration date labelling on their products which is intended to indicate a minimum shelf life for the product assuming adherence to the storage conditions printed on the product packaging.

Bonded anchors resist tension loads by adhesion and micro-keying of the resin to the anchor

rod or dowel and to the sides of the drilled hole. Therefore, the tension load capacity of the installed anchor depends significantly on the condition of the drilled hole wall prior to installation. When capsule anchors are installed with rotary and percussive action, adhered concrete dust is generally scoured away by the quartz aggregate and, in the case of glass capsules, by glass fragments. This material is subsequently mixed into the resin matrix. In hammer-in systems, the scouring action is less efficient, and the retained dust layer can considerably reduce the bond strength of the anchor. Therefore, when hammer-in capsules are employed, special care should be taken to clean the drilled hole by means of brushing and air jetting (Fig. 2.35). For other systems, it is generally sufficient to air-jet the hole (Fig. 2.34).

While expansion forces are not generated upon installation of capsule anchors, splitting tensile stresses do occur – as with all anchorages – upon prestressing and loading of the anchor. These splitting tensile stresses are, however, much lower than those associated with mechanical expansion anchors.

Capsule anchors are commonly available for anchor rod diameters M8 to M30 (1/4" to 1-1/4") in carbon (zinc-plated) and stainless steels. Hammer capsules are mainly used for bonding-in starter bars.

Many commercially available adhesives contain styrene, which in some countries is regarded as hazardous to both humans and the environment. Systems based on styrene-free resin formulations are available.

### **b) Injection systems**

Polymer resins for injection systems are typically supplied in either disposable cartridges or in bulk form. In cartridge systems the resin and



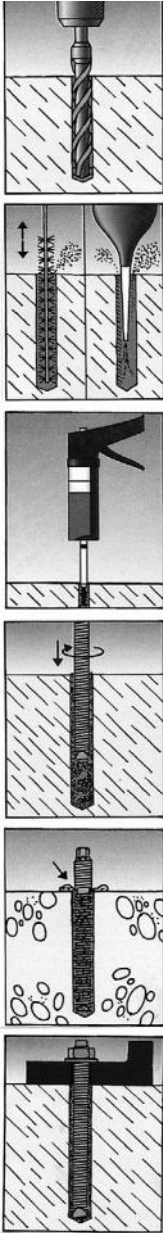


**Fig. 2.36** Installation of a bonded anchor with an injection nozzle equipped with a mixing element (adhesive mixed in injection nozzle)

hardener are contained in separate chambers. They are based on similar formulations as capsule systems. In addition hybrid systems are used which contain resin and cement as binding materials. The injection of the components into the drilled hole is accomplished with the aid of

a mechanical or pneumatic dispenser. Some systems mix the resin and hardener in the cartridge before being injected. The disadvantage of this method is that the contents of the cartridge must be used within a fraction of the cure time of the reacted resin. Other systems are designed to dispense resin and hardener in a fixed mix ratio and these components are mixed together in the mixing nozzle of the dispensing system. This permits the contents of the cartridge to remain useable over a longer period of time. The initial quantity of mixed resin delivered by the dispenser usually must be discarded to ensure attainment of the proper mix ratio. If the resin hardens in the nozzle (e.g. during a pause in the work), then the cartridge can often continue to be used following attachment of a new mixing nozzle. The hole is typically filled one-half to two-thirds with resin. When the anchor rod is inserted into the hole, a small amount of excess resin expelled from the hole indicates that the annular space around the rod has been completely filled.

It is important to ensure that the bonding material is injected from the back of the hole to prevent the entrainment of air bubbles. To ensure this for deeper holes special injection equipment might be needed. Cure time is typically extended slightly compared to capsule systems with the same resin in order to ensure sufficient working time for injection. Epoxy resins require considerably longer cure times than unsaturated polyesters, vinyl ester resins with and without styrene, and hybrid systems.

Bulk adhesives are typically mixed and delivered using a bulk adhesive mixer in accordance with the specified mix ratio. Bulk mixers require calibration and close monitoring to ensure that the mix ratio is correctly maintained. While a mix ratio that is outside of specified tolerances may still result in hardening of the adhesive components, the final bond strength in-situ will likely be affected. As such, an additional degree of uncertainty is associated with the use of bulk mixers for anchoring applications. Bulk adhesives may also be mixed in an open container, such as a bucket, with an industrial paddle mixer. It may then be simply poured into a drilled hole, or injected with a hand dispenser. Owing to the uncertainties asso-

ciated with the mix ratio and the introduction of the adhesive into the drilled hole, this type of installation is not suitable for many applications.

Cementitious mortars are delivered in bulk form, mixed on the building site with a defined quantity of water and usually poured into the cleaned and wetted drill hole. The diameter of the hole is larger than with resin based injection systems. With respect to uncertainties in connection with mixing and injection the above remarks for bulk adhesives apply.

The tension load transfer mechanisms associated with injection anchors is, as for capsule anchors, adhesion and micro-keying. However, as in the case of hammer-in capsules, the bond strength depends significantly on the degree to which drilling dust has been removed from the hole. Therefore, drilled holes for injection anchors should be thoroughly cleaned out using vacuum, air-jet blowing and wire brushing or other methods. In the case of cementitious materials, the hole must be wetted.

Injection systems are also employed for post-installing reinforcing bars.

### c) Bonded anchors for cracked concrete

Conventional bonded anchors are less than ideal for resisting tension loads in concrete that is subject to cracking (see section 6). Special bonded anchor systems have been developed, however, that are particularly suited to these conditions.

In the bonded undercut anchor system depicted in Fig. 2.37, a hole is first drilled with a conventional diamond core drill. The undercut is produced in a second operation using a special diamond-tipped, water-cooled drill bit (Fig.

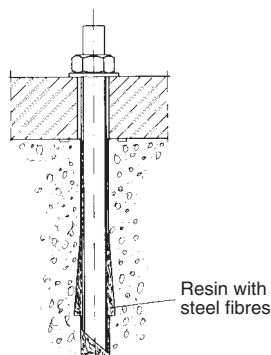


**Fig. 2.37** Bonded undercut anchor (Elgehausen, Mallée, Rehm (1997))

2.38). After flushing the hole with water, a glass capsule containing polymer resin is inserted into the hole and the anchor rod is driven through the capsule using rotary action. The capsule contains unsaturated polyester resin, hardener, quartz aggregate and short steel fibres for increasing the shear strength of the polymer matrix in the region of the undercut.

The load-bearing behaviour and failure mode exhibited by bonded undercut anchors in non-cracked concrete are essentially the same as for conventional bonded anchors, albeit with the additional benefit of the undercut. However, when a crack in the concrete intersects the anchor location, the bond (adhesion, micro-keying) between the concrete and the adhesive is largely lost, although the bond between the adhesive and the anchor rod is maintained. External tensile loads are therefore mainly transferred into the adhesive by bond in the region of the undercut and subsequently into the concrete via mechanical interlock.

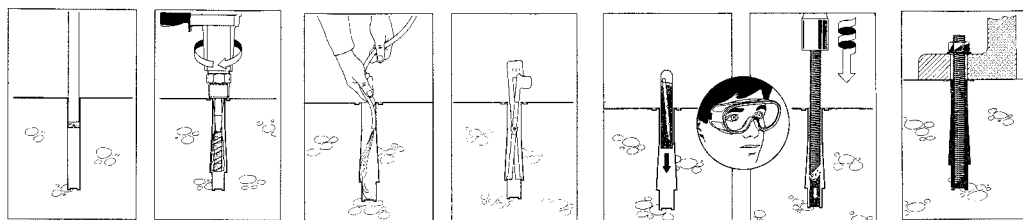


**Fig. 2.38** Installation of a bonded undercut anchor shown in Fig. 2.37

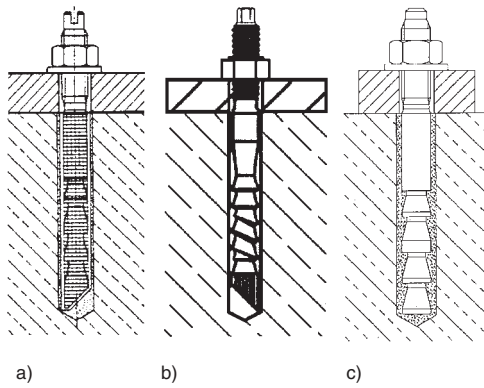


**Fig. 2.39** Bonded expansion anchors

The load-bearing behaviour of this anchor system depends to a substantial degree on the proper formation of the undercut in the concrete. To confirm that the undercut has been correctly formed, the undercutting tool scribes a mark on the surface of the concrete. The anchor should be loaded only after the check for this mark has been made.

The bonded expansion anchor system described in Fig. 2.39a employs a unique anchor rod geometry with multiple conical surfaces. These surfaces are coated with a bond-breaker coating to prevent adhesion between the anchor rod and the bonding material. In the system pictured here, a screen tube is used to prevent damage to the bond-breaker coating during the setting process. In the systems shown in Fig. 2.39b, c the surface of the multi-cone anchor rod is smooth and hard and the bond-breaker consists of a thin coating.

The anchors illustrated in Fig. 2.39a and b are designed for use with adhesive capsules and they are installed with rotary and percussive drill action (Fig. 2.40). The system in Fig. 2.39b is also designed for use with a cartridge injection adhesive. The system in Fig. 2.39c is only used for injection. With injection systems the multi-cone anchor rod is installed by simply pushing it into the adhesive-filled hole (Fig. 2.41). The rod is designed to permit the flow of bonding material up and around the conical bearing surfaces.

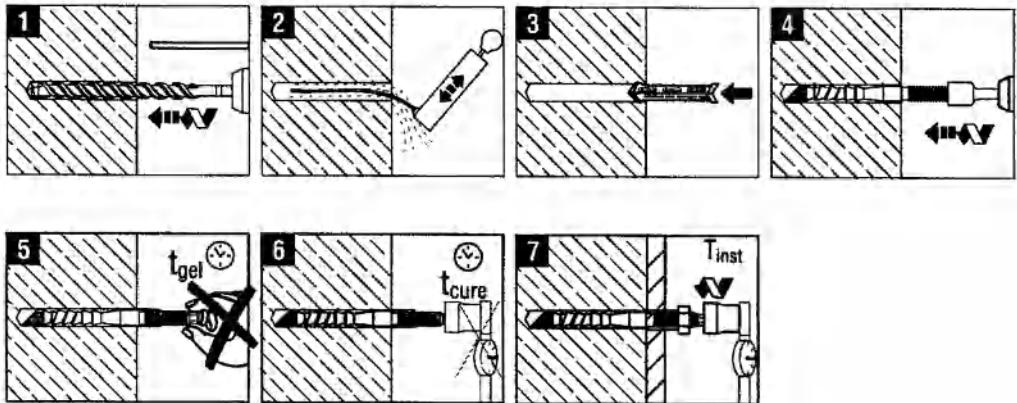


**Fig. 2.40** Installation of a bonded expansion anchor (capsule type)

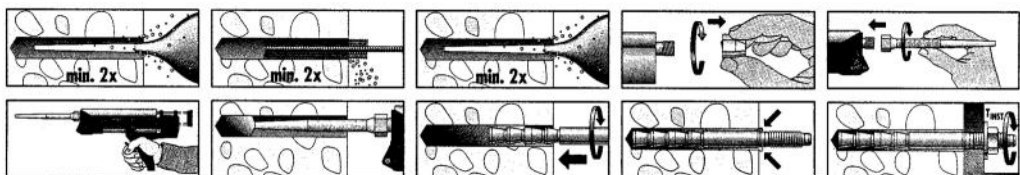


**Fig. 2.41** Installation of a bonded expansion anchor (injection type)



When a tensile force is applied to the anchor, the cones are displaced upward relative to the position of the hardened bonding material matrix, which in turn behaves like an expansion sleeve. This action generates expansion forces, and the attendant frictional resistance between the polymer matrix and the sides of the hole is typically sufficient to transfer the external load into the base material without relying on adhesion. Nevertheless, the expansion forces generated by these systems are lower than those produced by conventional mechanical expansion anchors.

#### 2.3.3.4 Screw anchors

Screw anchors (Fig. 2.42) are typically hardened to permit the thread to engage the base material during installation. They are installed in drilled holes. The thread pitches at the tip may be provided with special cutting surfaces in order to assist the process of cutting threads in the wall of the drilled hole. They may be driven by means of a special impact driver (Fig. 2.43) or, in other systems, with a conventional drill equipped with an adapter. The hole depth is typically set slightly longer than the screw embed-

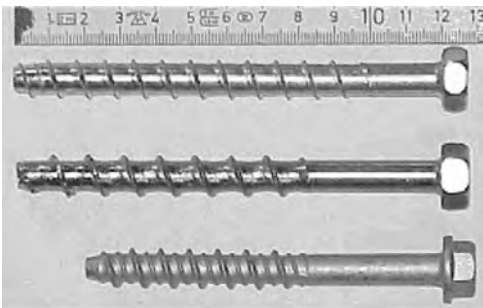


**Fig. 2.42** Different types of screw anchors (Eligehausen, Küenzlen (2002))

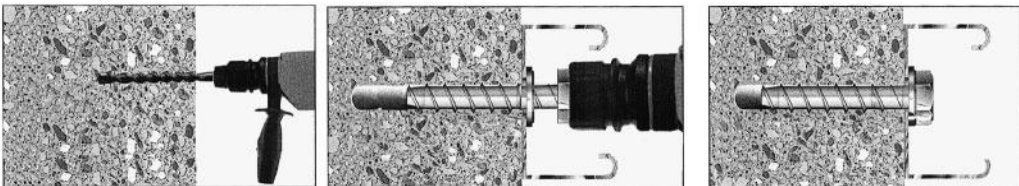


**Fig. 2.43** Installation of a screw anchor (hole cleaning step not shown)

ment to provide space for the products of the thread-cutting process. The diameter of the drilled hole is matched to the geometry of the screw so that the thread cuts into the concrete and an external force can be transferred to the concrete through this positive interlocking connection. By requiring a minimum embedment for each diameter, it can be ensured that the failure mode associated with over-driving of the screw is twisting-off of the screw head, and not partial or full stripping of the concrete threads.

The tension load-bearing behaviour of screw anchors essentially depends on the tolerance of the drilled hole. Therefore, the use of matched tolerance drill bits is essential. This is typically regulated in the approval for the product.

Concrete screws are available in an increasingly wide range of diameters and are generally suitable for applications in non-cracked and cracked concrete. In Germany, for example, they are approved for ceiling hangers, as well as for general applications in cracked concrete.

The heat treatment of steel as required to facilitate installation of screw anchors in concrete may result in hydrogen embrittlement. This can lead to premature fatigue or stress corrosion failure. Consequently, some screw anchors are manufactured using procedures to limit the zone of hardened steel to the cutting tip of the screw.

#### 2.3.3.5 Ceiling hangers

There are many anchoring systems available on the market today for suspended lightweight ceilings. Many of the anchors used for this purpose are conventional torque- or displacement-controlled mechanical expansion anchors in the sizes M6 and M8 (1/4" and 3/8"); these have already been discussed in section 2.3.3.1. Screw anchors may also be used (see section 2.3.3.4).

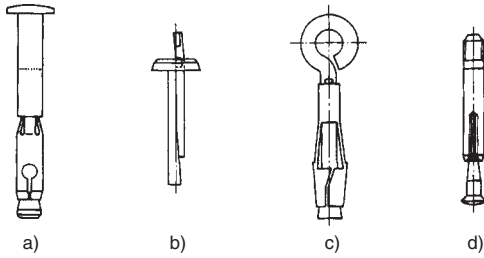


**Fig. 2.44** Typical ceiling hangers (Eligehausen, Mallée, Rehm (1997))

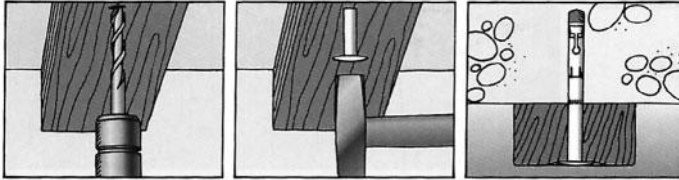


**Fig. 2.45** Installation of a ceiling hanger of the type shown in Fig. 2.44a

Only those systems which are designed expressly for hanging ceilings will be described in the following section.

Some typical ceiling hangers are depicted in Fig. 2.44. The hanger shown in Fig. 2.44a consists of a stud with a nail head at one end and a cone at the other, as well as an expansion element. This anchor as shown must be driven into the drilled hole through the element being anchored (Fig. 2.45). The expansion element, which is made from spring steel, has a diameter slightly larger than the diameter of the drilled hole. It is compressed when driven into the hole and generates an expansion force by spring action. Loading the anchor causes follow-up expansion. Other versions of this anchor are equipped with either a threaded stud or an eye.

The system shown in Fig. 2.44b consists of two opposing tapered wedges with an attached bear-

ing plate. This hanger is inserted into a drilled hole through the fixture as far as the bearing plate and subsequently expanded by driving in the projecting wedge with a hammer (Fig. 2.46). Correct set is checked via the position of the wedge after driving.

The anchor type represented in Fig. 2.44c consists of an anchor rod with a swaged cone on one end and an eye at the other wrapped with a sheet metal expansion element. The hanger is driven into a drilled hole until the base of the eye, typically a flattened surface, bears on the concrete. The anchor is expanded by pulling the eye, either with a hammer claw or by hand (Fig. 2.47).

Ceiling hangers of the type depicted in Fig. 2.44d comprise a nail-like shaft sleeved and slotted at one end and equipped with a conical plug. They are expanded by driving the shank

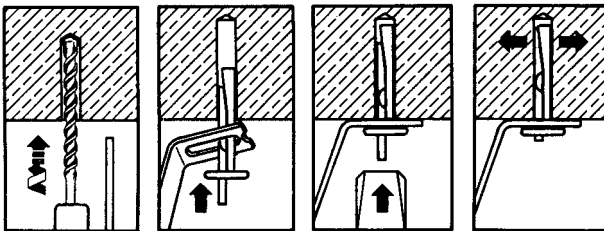


**Fig. 2.46** Installation of a ceiling hanger of the type shown in Fig. 2.44b

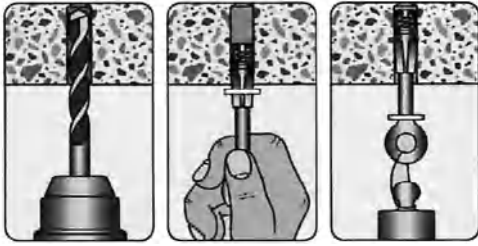


**Fig. 2.47** Installation of a ceiling hanger of the type shown in Fig. 2.44c

over the conical plug, whereby the plug bears against the base of the drilled hole (Fig. 2.48). Correct installation is verified by the final position of the anchor relative to the concrete surface. Consequently, proper expansion depends on maintaining the prescribed hole depth. This is assured by using a stop-drill bit.

The degree of expansion associated with these ceiling hangers is relatively small due to the small diameters of the anchors themselves. Inasmuch as their load-carrying capacity is clearly influenced by the drilled hole tolerances, it is particularly important that the holes are drilled with matched-tolerance drill bits as discussed in section 2.3.1.

### 2.3.3.6 Plastic anchors

Plastic anchors can be classified according to their suitability for normal-weight or autoclaved aerated concrete applications.

Plastic anchors for use in normal-weight concrete consist of cylindrical sleeves moulded from tough polymer materials (e.g. Nylon) and matched-geometry screws. The plastic anchors available commercially are distinguished not only by the external geometry of the sleeve, particularly the expansion part, but also by the internal profile. Accordingly, the threads of the matching screw are equipped with a specific profile to match that of the anchor. The expansion part of the sleeve is split and includes lugs or other deformations to prevent it from rotating during the screw installation. Fig. 2.49 shows typical examples of plastic anchors approved in Germany for anchoring light facade cladding.

As already mentioned, these approved systems may only be used together with their associated

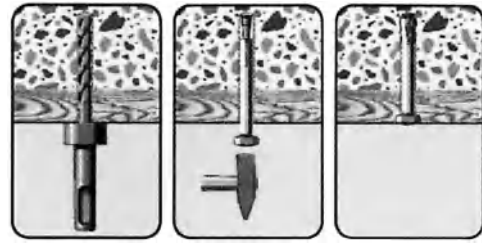


**Fig. 2.48** Installation of a ceiling hanger of the type shown in Fig. 2.44d

special screws (supplied together with the plastic sleeve) in order to assure the necessary thread reach and adequate contact pressure between the anchor sleeve and the sides of the hole. Owing to their different thread profiles and relatively large dimensional tolerances (*Plank (1977)*), conventional wood screws may not be used with these anchors.

The anchor sleeve is expanded by inserting the screw (Fig. 2.50). As torque is applied to the screw, it impresses and cuts a thread into the plastic and at the same time expands the sleeve against the sides of the hole. In concrete, such anchors function by way of friction between the sleeve and the sides of the hole. Because the plastic is too soft to deform or interlock with the base material, these anchors are sensitive to all parameters that can act to reduce the contact pressure, such as drilling the hole with an out of tolerance drill bit.

To avoid brittle fracture of the plastic anchor sleeve, it should not be subjected to temperatures below 0°C during installation of the screw. The screw should be installed to the edge of the

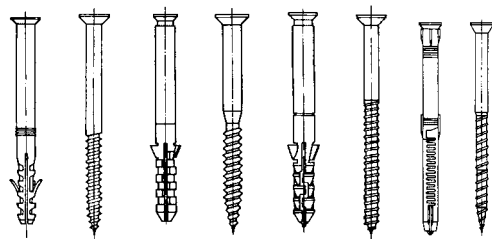


**Fig. 2.49** Typical plastic anchors (screw as expansion element)

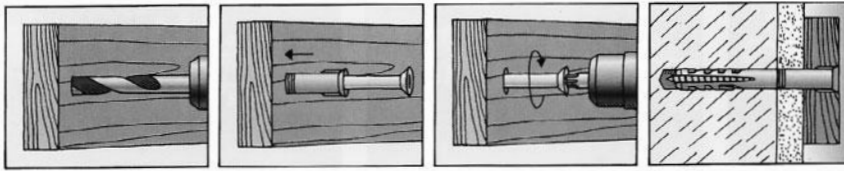


**Fig. 2.50** Installation of a screw type plastic anchor

sleeve so that the tip of the screw just penetrates the base of the sleeve (Fig. 2.50). As a guide to assessing the quality of the anchorage, after the screw has been fully inserted, neither the anchor body nor the screw should rotate with the application of normal screwdriver force.

A plastic anchor that has been removed from a hole should not be re-used under any circumstances.

Some plastic anchors are designed to accept a profiled nail instead of a screw. As these anchors generate relatively small expansion forces, their behaviour under load is particularly influenced by inaccuracies during installation. As a consequence, they are generally not permitted in Germany for the anchorage of facade support systems.

Plastic anchors are permitted in many countries for the anchorage of facades and comparable

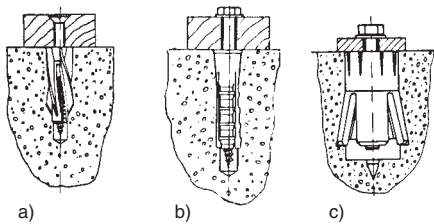


**Fig. 2.51** Plastic anchors for fastenings in autoclaved aerated concrete (Eligehausen, Mallée, Rehm (1997))

structural systems provided the anchors are used in a redundant fashion. They are also used for attaching thermal insulation composite systems.

Special anchors have been developed for anchorages in autoclaved aerated concrete (Fig. 2.51).

Fig. 2.51a shows an anchor for autoclaved aerated concrete consisting of a sleeve with helical ribs plus a screw. The anchor is hammered into a cylindrical hole (drilled without hammer action) whose diameter matches that of the cylindrical anchor shank. The sleeve is subsequently expanded by installing the screw (Fig. 2.52). The ribs serve to prevent the sleeve from turning as it expands as well as to distribute the load over a larger area of the substrate.

The anchor shown in Fig. 2.51b consists of a plastic sleeve with guide ridges and external ribs and a matching screw. This anchor is hammered into a conventionally drilled hole and the matching screw is installed (Fig. 2.53). It is designed to develop a greater degree of expansion than the conventional plastic anchors shown in Fig. 2.49.

Correct installation of the autoclaved aerated concrete anchors shown in Fig. 2.51a and b requires that the length of the screw is matched to the thickness of the fixture. The overall length of the screw must be at least equal to the

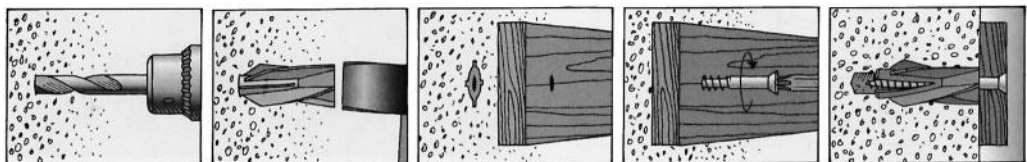


**Fig. 2.52** Installation of an anchor for autoclaved aerated concrete of the type shown in Fig. 2.51a

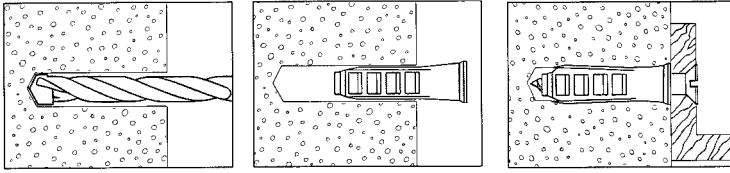


**Fig. 2.53** Installation of an anchor for autoclaved aerated concrete of the type shown in Fig. 2.51b

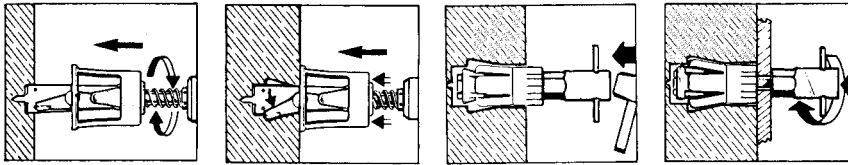


**Fig. 2.54** Installation of an anchor for autoclaved aerated concrete of the type shown in Fig. 2.51c

length of the anchor sleeve plus the diameter of the screw plus the thickness of the fixture.

The anchor shown in Fig. 2.51c consists of a cone, an expansion sleeve, and a nut and washer. A cylindrical hole is drilled and undercut with the help of a special drill operating without percussive action (Fig. 2.54). Afterwards, the anchor is inserted and expanded by tightening the nut, whereby the expansion sleeve expands into the undercut.

The anchors depicted in Fig. 2.51 can generally be used only for pre-positioned applications,

since the diameter of the anchor body is greater than the hole in the part to be fastened. This is disadvantageous for many applications. Systems have been developed for in-place installations in autoclaved aerated concrete. Tension loads are transferred to the base material via a combination of undercut and friction.

One system which is approved for use in Germany employs a conventional plastic anchor geometry as shown in Fig. 2.49. The hole in the autoclaved aerated concrete is, however, not produced with a standard drill but instead with a special punch (Fig. 2.55a). This ensures a close-tolerance hole and generally eliminates inaccuracies in the geometry of the hole resulting, for instance, from unintended movement of the drill.

Other systems make use of special plastic sleeves. The anchors are installed in the conventional manner as shown in Fig. 2.50. However, installation of the screw produces a greater than normal expansion of the sleeve as shown in Fig. 2.55b. The hole may therefore be drilled with a standard rotary-impact drill set to rotary-only action.

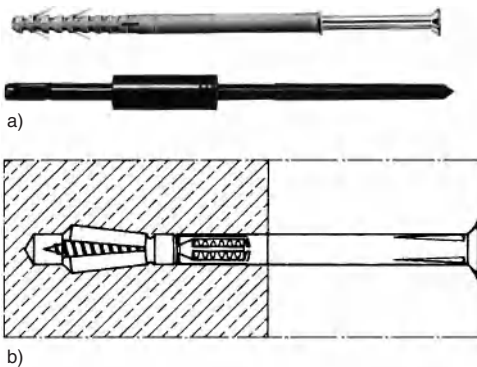


**Fig. 2.55** Plastic anchor for in-place installation in autoclaved aerated concrete (Eligehausen, Mallée, Rehm (1997))

- a) Plastic anchor and punch for forming hole  
b) Installed plastic anchor, hole formed with hammer drill

## 2.4 Direct installation

The term direct installation refers to driving high strength steel fasteners (pins and studs) directly into steel or concrete by means of an explosive charge or compressed air. Complete



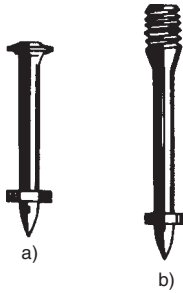


**Fig. 2.56** Direct installation fasteners (Eligehausen, Mällée, Rehm (1997))  
 a) Pin  
 b) Stud with thread

systems are available consisting of setting tools, powder cartridges (for non-pneumatic or gas systems) and pins for a variety of application-specific configurations. The setting tools are often referred to as powder- or, more generically, power-actuated tools.

Steel pins (Fig. 2.56a) are driven through the component to be fastened. Fasteners configured as studs (Fig. 2.56b) provide a projecting thread onto which the component can be secured with a nut. Both pins and studs are fabricated using processes that result in a high-strength but at the same time resilient steel.

Power-actuated fasteners find applications in both concrete and steel base materials. Direct installation applications in steel substrates are not dealt with further in this volume.

In powder-actuated systems, pins and studs are driven into the concrete with the energy released by a black powder charge. Older direct-acting tools operate much like a gun (Fig. 2.57a), with the energy from the explosive charge imparted directly to the fastener as kinetic energy. Owing to its relatively small mass, the fastener achieves bullet-like velocities at the point of impact with the base material. These types of systems can present a hazard to both the operator and surroundings if the pin is not captured in the target base material. In contrast, modern indirect-acting tools are based on the piston system (Fig. 2.57b) in which the energy from the powder charge is transmitted to a piston which then drives the fastener into the base material. In these systems, the piston retains approximately 95% of the total driving energy (with its larger mass, the associated piston velocity is relatively low) and the kinetic energy imparted to the pin is small. Since the

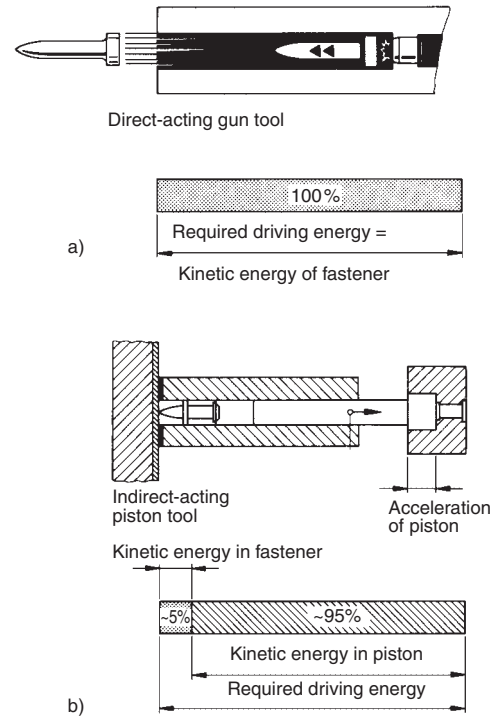


**Fig. 2.57** Operating principles of tools used for direct installation (Seghezzi, 1984)  
 a) Direct-acting principle  
 b) Indirect-acting principle

piston is captured in the tool, driving of the pin is displacement-controlled and therefore presents a greatly reduced hazard on the job site. Gas tools function in a similar manner to powder-actuated systems, whereby combustible gas is substituted for the black powder charge. The maximum energy output of these tools is less than that associated with powder-actuated tools, however, they offer some advantages for large scale applications.

The capacity of power-actuated fasteners to resist tension forces stems largely from friction. Rapid driving of the fastener and the resulting displacement of the base material gives rise not only to high compressive stresses in the immediate vicinity of the fastener, but compaction of the concrete and to some extent destruction of the concrete microstructure. Owing to the high penetration speed of the fastener, a localised temperature increase occurs at the friction face

during driving, which results in improved adhesion between the fastener and concrete.

Optimally, aggregates in the concrete are penetrated by the power-actuated fastener. However, if the angle of incidence between aggregate and fastener is unfavourable, harder aggregates may cause the fastener to be deflected and/or bent (Fig. 2.58a). In these cases the load-carrying capacity of the fastener is reduced and may be negligible (setting failure).

This disadvantage may be overcome by installing the fasteners in pre-drilled pilot holes, whereby the diameter of the hole is slightly larger than the diameter of the fastener (Fig. 2.59). The shaft of the pin is lengthened to compensate for the length of the drilled hole such that the actual penetration of the fastener into the base material remains unchanged. Installation failures are virtually eliminated with this method, even in high strength concrete or concrete containing harder aggregates. Likewise, damage to the concrete surface in the form of spalling is avoided, even in cases where the fastener bends during installation (Fig. 2.58b). In addition, the increased embedment results in increased pull-out values compared to conventionally installed fasteners. Scatter of the failure loads is similarly reduced. With pins and studs with a diameter of about 4 mm a pre-drilled hole depth of approximately 20 mm is adequate to rule out installation failure (Bereiter (1986)).

Because power- and gas-actuated tools are not dependent on an external power source, they offer economy and flexibility combined with relatively low environmental impact. Conventional power-actuated fasteners (i.e. *without* pre-drilling) are commonly used in the U.S. for hanging lightweight suspended ceilings, whereby care must be taken to ensure that setting failures are detected. They may also be used to attach thermal composite insulation systems to concrete walls. In these systems, the set-

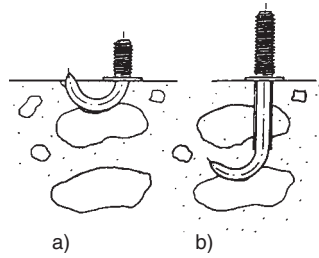


**Fig. 2.58** Bending of power-actuated fasteners due to hard aggregate (Eligehausen, Mallée, Rehm (1997))  
a) Without pilot hole  
b) With pilot hole

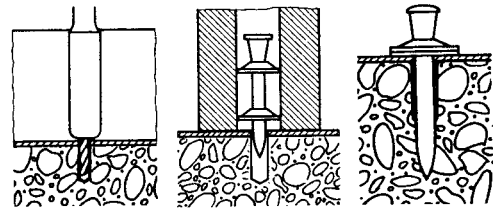


**Fig. 2.59** Installation of a power-actuated fastener in a pilot hole

ting adapter on the tool engages the specially designed insulation retainer. Withdrawal of the tool from the retainer serves to proof load the fastener sufficiently to detect setting failures. In the U.S., conventional power-actuated fasteners are often used to hang sprinkler branch lines. In Germany, power-actuated fasteners *installed in pre-drilled pilot holes* are deemed suitable for a variety of applications, including the suspension of lightweight ceilings. Stainless steel fasteners may be used as ceiling hangers in damp interior environments and for anchoring facade claddings to concrete walls. In addition, they are approved for the attachment of metal decking to non-cantilever single-span reinforced concrete beams.

## 3 Principles

### 3.1 General

Fasteners transfer external loads into the base material by means of mechanical interlock, friction, chemical bond (see Fig. 2.1), or some combination of these mechanisms. In all cases, application of external load induces tensile stresses in the concrete. In many cases the anchor fails because the tensile capacity of the concrete is exceeded. Fig. 3.1 provides a characteristic representation of concrete cone failure associated with an undercut anchor loaded in tension, while Fig. 3.2 shows the concrete failure associated with a near-edge anchor loaded in shear towards the free edge. To understand these failure modes better, an understanding of the behaviour of concrete in tension and the concrete fracture process is required. These subjects are therefore presented in sections 3.2 and 3.3.

Both the load-displacement behaviour and ultimate capacity of an anchor in concrete depend greatly on whether the concrete in the vicinity of the anchor is cracked or non-cracked. Causes and types of cracks and the influence of anchors on the formation of cracks in concrete are dealt with in section 3.4. Section 3.5 provides a rationale for the utilisation of the local tensile strength of the concrete in anchor design.



**Fig. 3.1** Concrete cone failure of an undercut anchor loaded in tension (Eligehausen (1984))



**Fig. 3.2** Concrete cone failure of an anchor located close to an edge and loaded in shear towards the edge

Load-displacement behaviour is also influenced by the prestress in the anchor; this is covered in section 3.6. Section 3.7 deals with the distribution of loads acting on a baseplate of a group of anchors to the individual anchors of the group.

Each type of anchor described in section 2 has an optimum range of application and may be less suitable or in fact inappropriate for applications outside of that range. Therefore, in order to choose the correct anchor for a given task and to be able to design the anchor, detailed knowledge regarding the load-bearing behaviour of the various anchor systems is required. This behaviour is influenced by a multitude of parameters, including the condition of the base material (cracked or non-cracked), the direction of the action (tension, shear, combined tension and shear, or shear with lever arm – see Fig. 1.2), concrete strength, embedment depth, distance to neighbouring fasteners and to edges, nature of the action (transitory, sustained or fatigue load, seismic or shock load, see Table



1.1) and amount and configuration of proximate reinforcement. In addition, environmental factors such as corrosion, temperature extremes and fire can affect anchor performance and must be properly considered in anchor design. The behaviour of the different types of fasteners is discussed in section 4 to 9.

### 3.2 Behaviour of concrete in tension

Fig. 3.3b illustrates a typical load-deformation curve for a concrete element subjected to axial tension (Fig. 3.3a), measured in a deformation-controlled test. The horizontal axis represents the total deformation, measured over the gauge

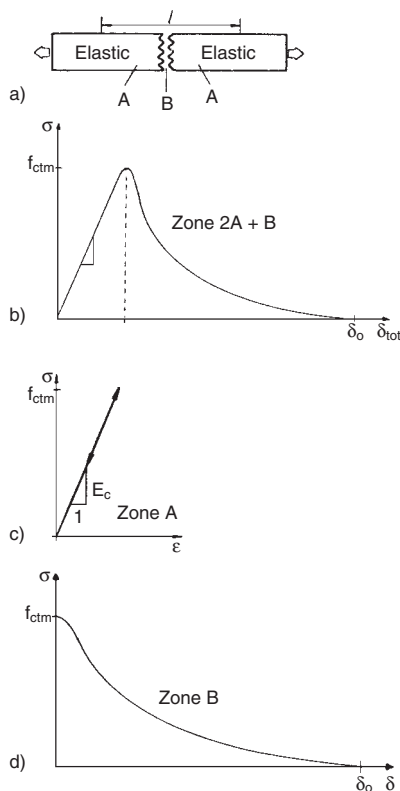


**Fig. 3.3** Stress-strain curves for concrete loaded in uni-axial tension, measured in a displacement-controlled test (Reinhardt (1997))

- Concrete member subjected to uni-axial tension
- Stress-deformation curve measured over gauge length  $l$
- Stress-strain curve preceding the crack process zone
- Relationship between stress and crack opening

length  $l$ . The behaviour is virtually linear-elastic up to ultimate load. However, just prior to reaching the ultimate load a single crack forms at the point where the concrete exhibits minimum tensile strength. The crack continues to widen until the element is completely transected by the crack at deformation  $\delta_o$ , thereafter the load that can be carried decreases continuously. A great number of experimental studies have shown that this non-linear behaviour of concrete (post-cracking behaviour) can be attributed to the formation of microcracks. While Hillerborg (1983) assumes one discrete crack, Bazant, Oh (1983) assume a system of hairline cracks (the so-called crack process zone). The deformations measured across the crack are composed of a component in zone A outside the crack process zone, together with the crack opening in zone B. The deformation component outside the crack process zone can be assumed to be approximately linear elastic, and the stress that can be accommodated depends on the strain in the concrete (Fig. 3.3c). The stress that can be transferred across the crack depends solely on the width of the crack (Fig. 3.3d).

The transfer of stress across a narrow crack can be attributed to interlocking of the rough surfaces of the crack. For this reason, post-crack behaviour is "more ductile" when the crack trajectory is not straight but rather as irregular as possible. This is shown in Fig. 3.4. In lightweight concrete subjected to tensile stress the aggregate fractures and the surface of the crack is, compared to the fracture process in concrete containing normal weight aggregate, relatively

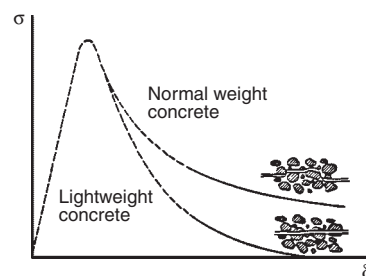


**Fig. 3.4** Influence of crack path on the stress-deformation behaviour of concrete (Hordijk, Van Mier, Reinhardt (1989))

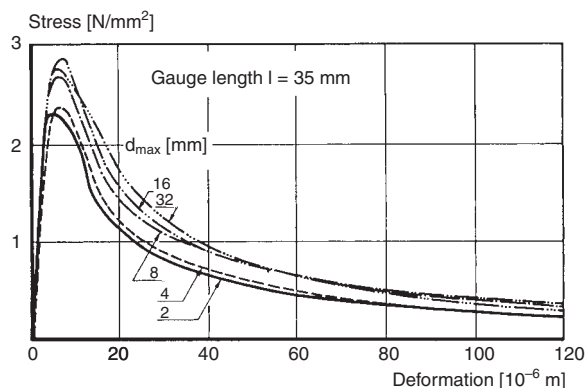


**Fig. 3.5** Influence of maximum aggregate size on the stress-deformation behaviour of concrete subjected to uni-axial tension (Hordijk (1991))

smooth. Therefore, the descending (strain softening) part of the load-deformation curve for normal weight concrete is less steep than in the case of lightweight concrete. Assuming that the aggregate does not fracture, as the maximum aggregate size increases the crack trajectory becomes more irregular. Therefore, the stress-deformation behaviour is also influenced by the maximum aggregate size (Fig. 3.5).

The stress-deformation behaviour can be characterised by the following parameters: the modulus of elasticity of the concrete  $E_c$ , the concrete tensile strength  $f_{ct}$ , the shape of the strain softening portion of the load-deformation curve, the displacement  $\delta_o$  at which no more load can be transferred across the crack, and the fracture energy  $G_f$ . The fracture energy is defined as the energy required to form a single crack.

The modulus of elasticity  $E_c$  of concrete in tension corresponds roughly to the value measured for concrete in uni-axial compression. The ascending branch of the load-deformation curve is straight until just before reaching the ultimate load. Therefore, an assumption of ideal elastic behaviour is justified, and Hooke's law applies up to ultimate load. It should be noted that, for concrete having a constant concrete compressive strength, the modulus of elasticity may vary as a function of the concrete mix design. The modulus increases with increasing modulus of elasticity of the aggregate, decreasing volume of hydrated cement and decreasing water/cement ratio. Further information on this subject can be found in Wesche (1993).

The axial tensile strength of concrete at 28 days after storage in water or moist conditions can be determined according to Heilmann (1969) as follows:

$$f_{ct} = k \cdot f_{cc,200}^{2/3} \quad (3.1)$$

where:

$k = 0.17$  to  $0.35$ , on average approximately  $0.25$

However, equation (3.1) overestimates the tensile strength for concrete compressive strengths  $f_{cc} > 60 \text{ N/mm}^2$  (Remmel (1994)). In order to describe the tensile strength of concrete with sufficient accuracy throughout the whole range of concrete compressive strengths, it is frequently assumed that  $f_{ct}$  is proportional to  $\sqrt{f_{cc}}$  or  $\sqrt{f_c}$ .

The concrete tensile strength is primarily influenced by the adhesion between the hydrated cement paste and the aggregate. Therefore, the volume, shape, surface properties and maximum size of the aggregate all have an effect on the tensile strength of the concrete. For the same concrete mix, concretes with aggregate of broken natural stone generally exhibit a tensile strength approximately 20% higher than those containing round gravel and sand. Within a limited range, the tensile strength increases with the maximum aggregate size (Fig. 3.6).

The behaviour of concrete in the presence of a tension strain gradient is mainly influenced by the shape of the strain softening branch of the load-deformation curve (Fig. 3.3b) or the stress-crack width curve (Fig. 3.3d). A strain gradient is present, for example, in a beam subjected to

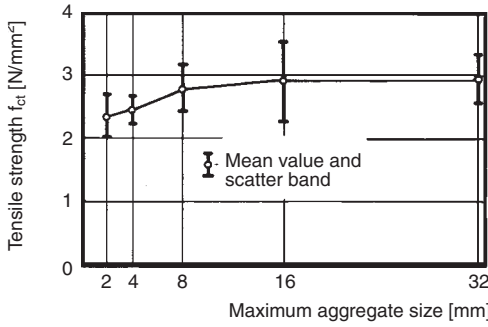


**Fig. 3.6** Influence of maximum aggregate size on the uni-axial tensile strength of concrete (Wolinski, Hordijk, Reinhardt, Cornelissen (1987))

bending and also in the load transfer zone of an anchor. In the latter case the gradient can be extreme. The form of the tensile stress-crack width relationship depends on the concrete mix and the geometry of the test specimen. The tensile stress-crack width ratios measured by various authors in axial tensile tests on concrete with a compressive strength of approximately 30 N/mm<sup>2</sup> produced from natural aggregates with a maximum aggregate size of 8 or 16 mm, are shown in Fig. 3.7. They can be approximated by the following equation:

$$\sigma(w) / f_{ct} = e^{-(f_{ct}/G_f) \cdot w} \tag{3.2}$$

where:

- $w$  = crack width [mm]
- $f_{ct}$  = tensile strength [N/mm<sup>2</sup>]
- $G_f$  = fracture energy [N/mm<sup>2</sup>]

The displacement  $\delta_o$  at which load can no longer be transferred across the crack is a material constant. It ranges from 0.14 to 0.20 mm depending on the concrete mix (Reinhardt (1997)).

Crack propagation in concrete members depends essentially on the fracture energy. This lies roughly between 80 and 200 J/m<sup>2</sup> (N/m) depending on concrete strength, maximum aggregate size, and type of aggregate. It is influenced by the same parameters that determine the tensile strength. Fig. 3.8 applies to rounded gravel concrete and illustrates the relationship between the fracture energy and maximum aggregate size (Fig. 3.8a) or concrete compressive strength (Fig. 3.8b). In concrete with bro-

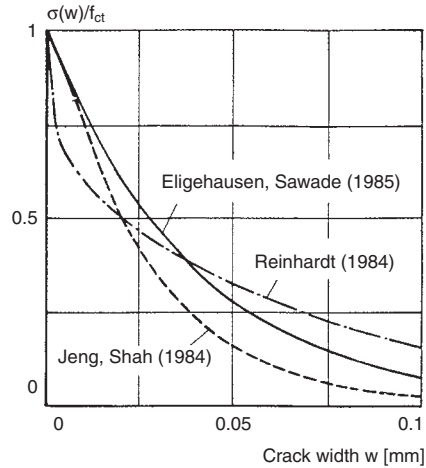


**Fig. 3.7** Tensile stress transferable across the crack as a function of crack width (Eligehausen, Sawade (1985))

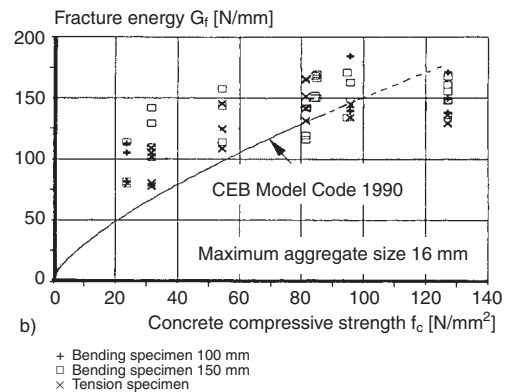
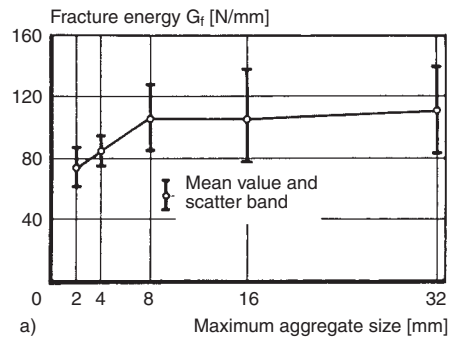


**Fig. 3.8** Fracture energy of concrete containing gravel aggregate in relation to:  
 a) maximum aggregate size (Wolinski, Hordijk, Reinhardt, Cornelissen (1987))  
 b) concrete compressive strength (Remmel (1994))

ken aggregate (crushed rock) the fracture energy for concrete strengths  $f_{cc} < 60 \text{ N/mm}^2$  can be up to 50% higher because the irregular shape of the crushed rock brings about a mechanical interlock between the sides of the crack that is significantly stronger than that associated with round gravel aggregate. In high strength concrete the type of aggregate (crushed or round) has less influence on the fracture energy because the tensile strength of the cement paste is sufficient to fracture the aggregate.

The behaviour of concrete subjected to tension in connection with a strain gradient which is present in the load transfer zone of an anchor can be described by the model of a fictitious crack after *Hillerborg* (1983), modified by *Ingraffea, Gerstle* (1984) (Fig. 3.9). At a critical crack width  $w_c$ , the crack boundary is stress free, i.e. a discrete crack exists. This is followed by a crack process zone exhibiting non-linear material behaviour in which the tensile stress depends on the width of the crack. Outside this zone the concrete behaves linear-elastically and the tensile stress depends on the strain in the concrete. At maximum it is equal to the uniaxial tensile strength. In observations with the naked eye, the visible crack ends in the crack process zone.

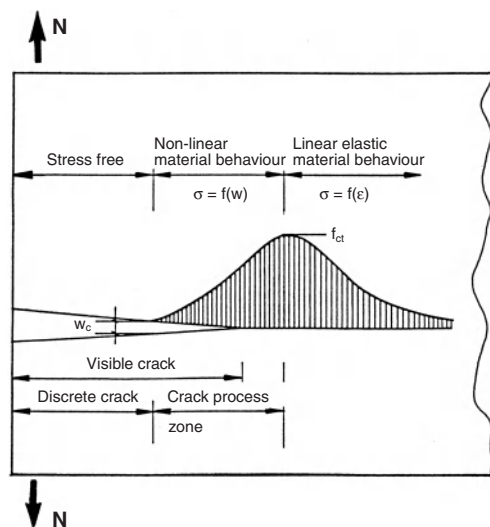


**Fig. 3.9** Stress distribution in concrete at the crack tip in the case of tension loading with a strain gradient (after *Hillerborg* (1983) and *Ingraffea, Gerstle* (1984))

A similar model which assumes a crack band of a certain width instead of one discrete crack has been proposed by *Bazant, Oh* (1983).

The stress distribution in the crack process zone depends on the relationship between transferable tensile stress and crack width (Fig. 3.7), as well as the distribution of the crack width over the length of the crack process zone. In the case of tension loading with a strain gradient, this non-linear behaviour of the concrete at the crack enables the redistribution of stress from highly stressed to less highly stressed zones. The ability of concrete to redistribute stress in this way has positive implications for the load-bearing behaviour of anchors in concrete.

### 3.3 Failure mechanisms of fastenings

#### 3.3.1 Theoretical studies

*Ballarini, Shah, Keer* (1986) described in detail the analytical and numerical studies carried out before 1985, while those performed up to 1989 are outlined in *Eligehausen, Sawade* (1989). Further information on this subject can be found in *Comité Euro-International du Béton (CEB)* (1994). The current state of findings is summarised in this section.

Theoretical studies concerning the load-bearing behaviour of fastenings were initially performed under the assumption that the concrete behaves elastically in compression and tension. However, with this approach the principal compressive and tensile stresses are, even under service loads, considerably higher than the uni-axial compressive and tensile strength of the concrete (*Weyershäuser* (1977), *Pusill-Wachtsmuth* (1982)). The reason for this is that owing to the relatively small load transfer area, high deformation gradients and stresses occur locally and these lead to microcracks in the concrete. Therefore, the load-bearing behaviour of fastenings can only be described with sufficient accuracy by taking into account the non-linear behaviour of concrete.

*Eligehausen, Clausnitzer* (1983) investigated the behaviour of expansion anchors with the help of the finite element method. They assumed a non-linear material behaviour for the concrete and smeared cracks occurring in the concrete over the width of the element. They studied the influence of the assumption for the

behaviour of concrete in tension as well as the size of the element and the number of loading increments to ultimate load.

Fig. 3.10 shows the calculated load-displacement curves for an expansion anchor in tension with 80 mm embedment depth. For comparison, the curve measured in the test is also drawn. Only the assumption for the behaviour of concrete in tension was varied, all other conditions were kept constant. A cone-shaped failure of the concrete occurred in both the test and the calculations. The calculated displacements are much smaller than the measured values. This is probably due to the anchor slipping in the drilled hole – an aspect that was ignored in the calculations. If we assume elastic – perfectly plastic behaviour of the concrete in tension (curve 1), then the calculated failure load is approximately 4.5 times the value applicable for elastic-brittle concrete behaviour (curve 2). The failure load observed in the test (curve 3) lies between these values. The result shows that the concrete cone

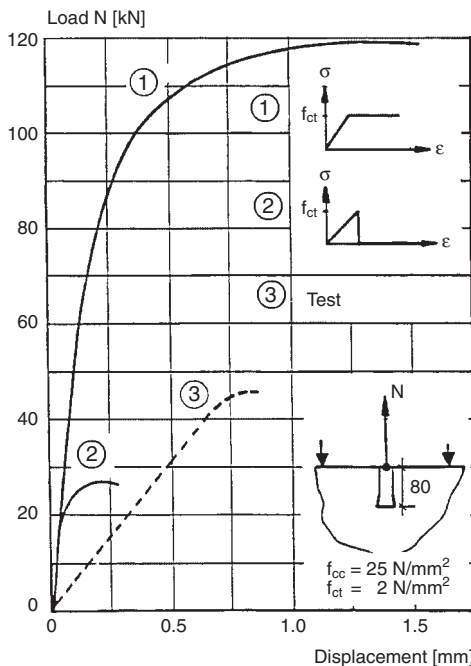


**Fig. 3.10** Load-displacement curves for an anchor loaded in tension – results from numerical analysis and tests (Eligehausen, Clausnitzer (1983))

failure loads can only be calculated with sufficient accuracy when the material behaviour of concrete in tension is described realistically.

Eligehausen, Clausnitzer (1983) also discovered that the size of the elements and the number of load increments had a considerable influence on the ultimate load. The ultimate load increased as the elements became larger and the number of load increments was reduced. This outcome is not surprising. Cedolin, Bazant (1980) showed that the use of so-called smeared cracks in conjunction with a strength limit failure criterion in the finite element method can lead to incorrect results. According to Cedolin, Bazant (1980) realistic results that are independent of the mesh geometry can only be expected when the crack propagation is described on the basis of non-linear fracture mechanics.

Peier (1983) investigated the behaviour of headed studs as well as expansion and bonded anchors subjected to tension with the help of a non-linear FEM program. Simulated was a pull-out test with large spacing between fastener and support. The behaviour of the concrete was represented with a 3D material model based on that proposed by Ottosen (1981), whereby brittle failure of concrete in tension was assumed. When the tensile strength in a given element was exceeded, a zero stress crack was initiated in that element, smeared across the width of the element. The assumed behaviour of concrete in tension matched assumption 2 in Fig. 3.10. Based on these investigations, Seghezzi (1986) described the failure of torque-controlled expansion anchors as follows (Fig. 3.11). A hydrostatic pressure condition in the concrete is established in a very small zone around the expansion shell of the anchor. In this region the concrete is severely crushed. A system of circumferential tension cracks runs from the load transfer zone to the surface of the concrete. In addition, radial cracks occur starting at the surface. If the expansion sleeve is sufficiently large and thick, then a concrete cone failure is the result – when the circumferential tension cracks reach almost to the surface of the concrete. But if the expansion shell is too small and/or too thin, then the concrete outside the pulverised zone fails in compression and the anchor is pulled out.

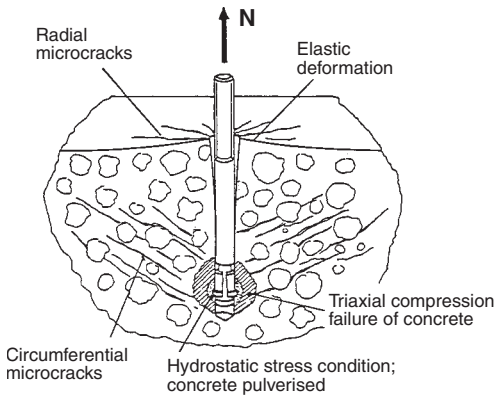


**Fig. 3.11** Failure mechanism of an expansion anchor, derived from the numerical analysis of Peier (1983) (Seghezzi (1986))

The failure mechanisms obtained numerically correspond well with the behaviour observed in tests. However in tests only a single conical circumferential crack is observed at failure. The concrete cone failure loads calculated for headed studs with large heads and expansion anchors with sufficiently large expansion shells correlate well with test results. However, it should be noted that the calculated results are mesh dependent and therefore cannot be generalised.

The studies described below make use of material models which are based on non-linear or linear fracture mechanics. Only those studies in which the support spacing was taken as sufficiently large to permit unrestrained formation of the fracture surface are considered. The load-bearing behaviour of headed studs with close support spacing (e.g. as in the Lok Test) is not described.

*Elfgren, Broms, Cederwall, Gylltoft* (1982) performed numerical investigations into the behaviour of a headed stud with an embedment depth  $h_{ef} = 300$  mm subjected to tension loading in a large concrete block. The load was applied in a manner simulating displacement control. In the study a discrete crack was assumed with the crack direction pre-defined. Fig. 3.12 shows details of the test specimen, the material model selected for concrete in tension, as well as some results. These calculations lead to the following description of the failure mechanism. At low

loads circumferential tension cracks form in the concrete starting at the head of the stud. The lengths of microcracks (dotted line) and wider discrete cracks (solid line) grow as the load increases. Since the crack formation is conical, incremental crack growth transects an ever larger area as the length increases. For this reason crack growth remains stable up to ultimate load. As the load is increased until failure there is a constant redistribution of the stresses in the concrete, whereby the location of maximum tensile stress at the crack tip is driven towards the surface of the concrete. At ultimate load the length of the crack is approximately 50% of the total length of the final concrete cone. As the deformation at ultimate load is exceeded, crack formation becomes unstable and the final concrete cone forms. The ultimate load is determined by the capacity of the concrete to carry tension stress. For a constant tensile strength (as measured in a uni-axial test), the ultimate load rises with increasing fracture energy  $G_f$  (*Elfgren, Ohlsson* (1986)). The behaviour of the anchorage does not alter significantly if instead of a straight crack trajectory a curved one is assumed (*Elfgren, Ohlsson, Gylltoft* (1989)).

The crack propagation behaviour and failure mechanisms derived numerically in these investigations correlate well with the behaviour observed in tests (see section 3.3.2). However, the calculated failure load is approximately 50% higher than the value obtained from testing of physical specimens. This might be due to the fact that in the numerical studies a significant portion of the resistance is obtained shear stresses transmitted across the fracture surface. In contrast, tests by *Eligehausen, Sawade* (1989) indicate that these shear stresses have a small influence on the ultimate load.

*Sawade* (1994) developed a model for describing the cracking process in concrete subjected to tension in which crack propagation and crack widening are considered as time-dependent processes associated with energy dissipation. In this formulation the specific surface energy is considered as a function of the crack width. Deformation zone, crack trajectory, crack width and plastic deformation are regarded as mechanical variables. Under monotonic loading, crack propagation is conditioned on the lib-

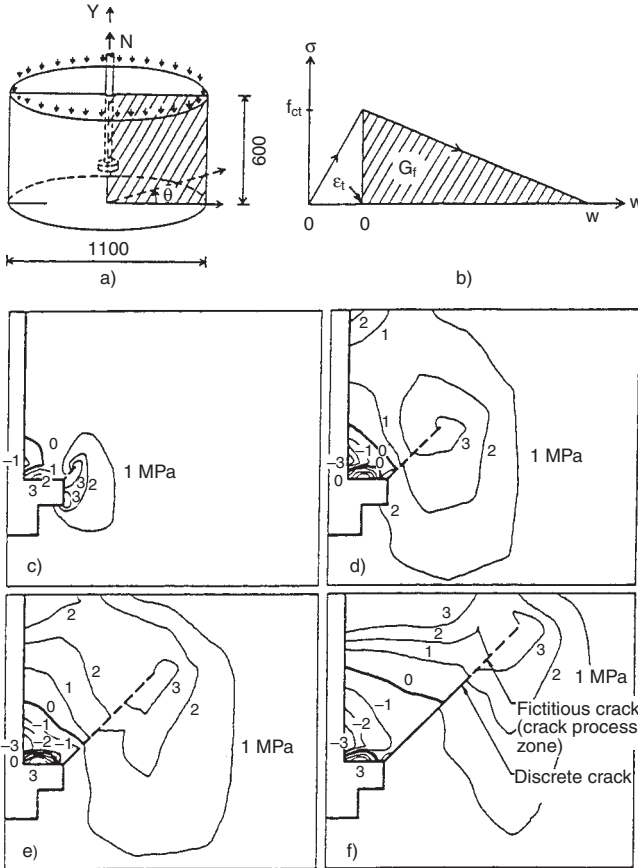


**Fig. 3.12** Fracture mechanics model for studying the crack propagation around a headed stud (Elfgren, Broms, Cederwall, Gylltoft (1982))  
 a) Dimensions of finite element model  
 b) Material model for loading and unloading a crack element ( $\epsilon_t$  = tensile strain,  $w$  = crack width)  
 c)–f) Lines of equal tensile stress; hairline cracks are shown as dotted lines and “real” cracks as solid lines;  
 (c)  $N = 0.35 N_u$ , (d)  $N = 0.9 N_u$ , (e)  $N = N_u$ , (f)  $N = 0.92 N_u$  (post-ultimate load)

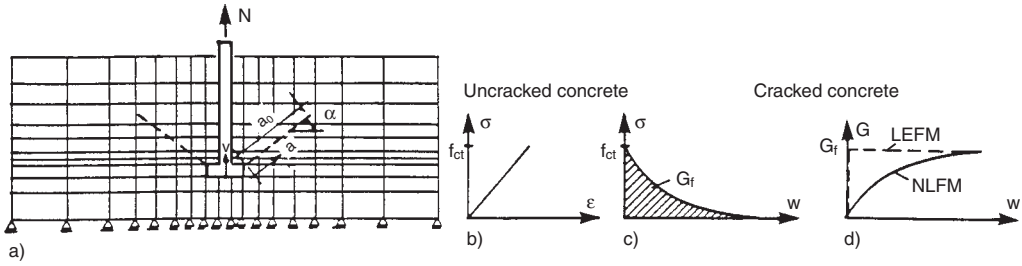
erated energy (sum of elastic deformation energy and surface energy) assuming a minimum.

Fig. 3.13 depicts this model as applied to a headed stud loaded in tension in a large concrete block (Eligehausen, Sawade (1989)). Only the formation of a circumferential tension crack is considered (Fig. 3.13a). The concrete in the direct vicinity of the crack is presumed to act linear-elastically (Fig. 3.13b). Non-linear material behaviour is assumed in the crack (Fig. 3.13c). The calculations according to non-

linear fracture mechanics take the specific crack formation energy to be a function of the crack width (Fig. 3.13d). The length and shape of the crack are determined iteratively as a function of the applied load.

Linear fracture mechanics can be applied for fasteners with large embedment depths. Here, the crack widening energy corresponds to the fracture energy  $G_f$  irrespective of the width of the crack (Fig. 3.13d). The resulting crack length  $a$  related to the side length  $l_c$  of the cone envelope is illustrated in Fig. 3.14 as a function





**Fig. 3.13** Sawade fracture mechanics model applied to a headed stud anchorage (Eligehausen, Sawade (1989))  
 a) Model  
 b) Stress-strain relationship for non-cracked concrete  
 c) Stress-crack width relationship for cracked concrete  
 d) Relationship between fracture energy and crack width

of the specific load. According to this figure, crack growth remains stable up to ultimate load and crack length at ultimate load is approximately 0.45 times the side length of the final cone. According to Sawade (1994) the ultimate load is given by:

$$N_u = 2.1 \cdot (E_c \cdot G_f)^{0.5} \cdot h_{ef}^{1.5} \tag{3.3}$$

According to equation (3.3) the ultimate load depends not on the concrete tensile strength but rather on the value  $(E_c \cdot G_f)^{0.5}$ , which describes

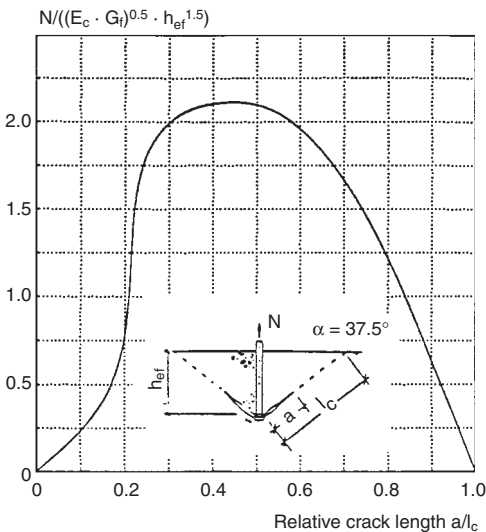


**Fig. 3.14** Relative tension load as a function of relative crack length (Eligehausen, Sawade (1989))

realistically the influence of the concrete mix design on the ultimate load (Sawade (1994)).

If a constant angle between the crack and concrete surface is assumed, the cone envelope area enlarges in proportion to the square of the embedment depth. In contrast, the ultimate load according to equation (3.3) is proportional to  $h_{ef}^{1.5}$ . This so-called size effect can be attributed to the fact that at ultimate load the tensile stress taken as an average over the fracture surface is not constant but instead decreases as the size of the fracture area increases. The size effect applies not only to concrete cone failures but more generally to concrete subjected to tensile strain gradients (e.g. for the bending strength of non-reinforced concrete specimens and the shear strength of slabs without shear reinforcement.) The size effect was found by theoretical arguments by Bazant (1984).

Ozbolt, Eligehausen (1990) conducted numerical investigations of the behaviour of headed bolts in tension with embedment depth  $h_{ef} = 130$  mm and diameter  $d = 22$  mm in a large radially symmetric concrete block. A so-called non-local microplane model was employed as the material model for the concrete. This model is explained in Bazant, Ozbolt (1990) and is very well suited to describing the behaviour of concrete under any strain conditions. In the numerical experiment, the displacement of the anchor head is progressively increased. Headed stud and concrete are connected solely via the bearing surface of the head. At the surface of the concrete only the nodes in the region of the support are fixed for all degrees of freedom.

Fig. 3.15 shows the calculated load-displacement curve. The curve measured in the test by Eligehausen, Sawade (1989) is included for comparison. Although measured and calculated

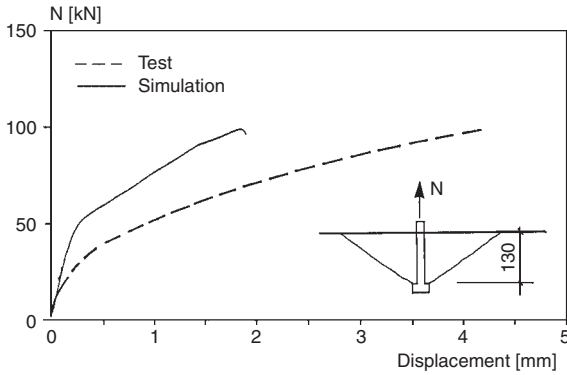


**Fig. 3.15** Measured and numerically obtained load-displacement relationship for a headed stud loaded in tension (Ozbolt, Eligehausen (1990))

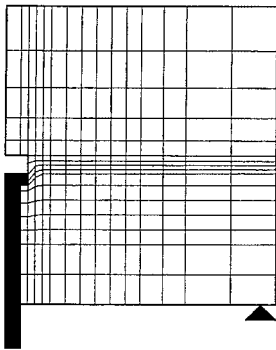


**Fig. 3.16** Deformed finite element mesh at ultimate load (Ozbolt, Eligehausen (1990))

ultimate loads coincide well, the measured displacement at failure is considerably larger than the calculated value. The major part of the deformation is caused by the crushing of the concrete below the head (Fig. 3.16) because the small head diameter ( $d_h = 35$  mm) leads to very high bearing stresses; at ultimate load about 10 times the uni-axial concrete compressive strength. Apparently the stiffness response of the concrete in the tri-axially stressed region of the head is too high in the calculations.

According to the simulation, a circumferential tension crack forms at the head of the stud at a low load and extends towards the surface of the concrete as the load increases. Radial cracks occur at the concrete surface at relatively high loads. Failure is brought about by the formation of a concrete cone. The average angle between the cone envelope and concrete surface is approximately  $35^\circ$ .

Fig. 3.17 shows the relationship between the crack and fracture cone area depending on the load related to the ultimate load according to the calculation and the tests by Eligehausen, Sawade (1989). The circumferential tension crack forms at about 30% of the ultimate load and crack growth remains stable up to ultimate load. As the deformation at ultimate load is exceeded, we see unstable crack growth with increasing deformations.

Ozbolt (1995) also undertook a numerical investigation of the load-bearing behaviour of

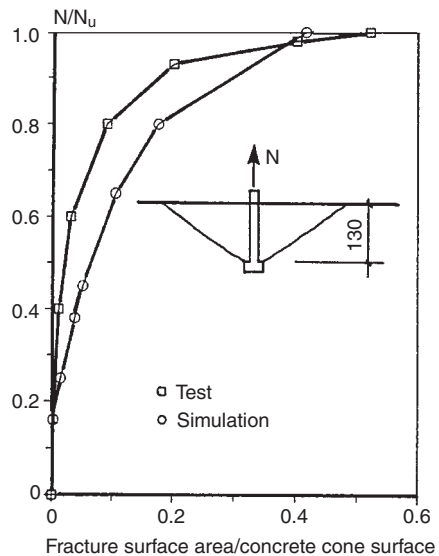


**Fig. 3.17** Test result and simulation for the normalised axial load as a function of relative crack area (Ozbolt, Eligehausen (1990))

headed studs subjected to tension load in a large concrete block, whereby he employed an improved “non-local microplane model”. Only material parameters and embedment depth were varied. Fig. 3.18 illustrates the influence of the concrete tensile strength as well as the fracture energy on the concrete cone failure load. According to the figures, the concrete tensile strength – at constant fracture energy – has only a minimal influence on the concrete cone failure load. In contrast, the concrete cone failure load for a constant concrete tensile strength increases roughly proportional to the square root of the fracture energy. These results agree with those obtained by *Sawade (1994)*.

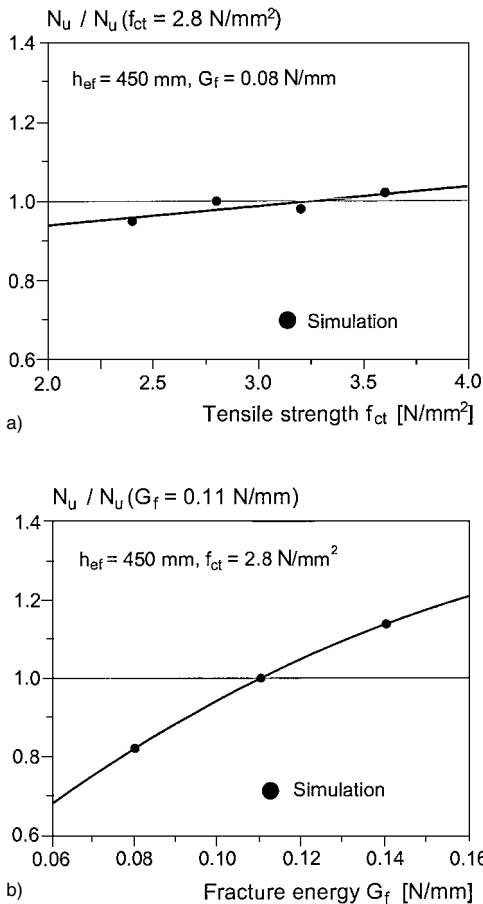


**Fig. 3.18** Normalised failure load as a function of (a) concrete tensile strength and (b) concrete fracture energy (*Ozbolt (1995)*)

The embedment depth was varied from  $h_{ef} = 50$  mm to  $h_{ef} = 2700$  mm. The calculated concrete cone failure loads are plotted against embedment depth in Fig. 3.19. The test results are shown for comparison. Also drawn are the failure loads to be expected according to *American Concrete Institute 349 (1990)*, the size effect law after *Bazant (1984)* and equation (3.6).

According to *American Concrete Institute 349 (1990)* the concrete cone failure load is given by equation (3.4). It increases in proportion to  $h_{ef}^2$  for  $d_h/h_{ef} = \text{constant}$  and thus ignores the size effect.

$$N_u = 0.96 \cdot f_{cc,200}^{0.5} \cdot h_{ef}^2 \cdot (1 + d_h / h_{ef}) \quad (3.4)$$

*Bazant (1984)* assumes that the failure load can be calculated according to plastic theory for small component thicknesses and according to linear fracture mechanics for thick components. A continual transition is assumed between these two limits. If we transfer this approach to the concrete cone failure load of headed studs, then the component thicknesses corresponds to the embedment depth and we obtain equation (3.5):

$$N_u = k_1 \cdot f_{cc,200}^{0.5} \cdot h_{ef}^2 / (1 + h_{ef} / h_{ef}^0)^{0.5} \quad (3.5)$$

where  $k_1$  and  $h_{ef}^0$  are constants

Evaluations of tests have produced values of  $k_1 = 2.7$  and  $h_{ef}^0 = 50$  mm. According to equation (3.5) the failure load for large embedment depths is roughly proportional to  $h_{ef}^{1.5}$ .

The following equation for calculating the concrete cone failure load, which can be regarded as a simplification of equation (3.5), is proposed in section 4.1.1.3:

$$N_u = 15.5 \cdot f_{cc,200}^{0.5} \cdot h_{ef}^{1.5} \quad (3.6)$$

In equations (3.4) to (3.6)  $f_{cc,200}^{0.5}$  corresponds to the factor  $(E_c \cdot G_f)^{0.5}$  in equation (3.3). While the latter factor describes the influence of the concrete mix well, the factor  $f_{cc,200}$  is better suited to a design equation.

Fig. 3.19 shows that equation (3.5) provides the best description of the numerical results but the difference between equation (3.5) and equation (3.6) is small. Both equations correlate with the test results sufficiently accurately. In contrast,

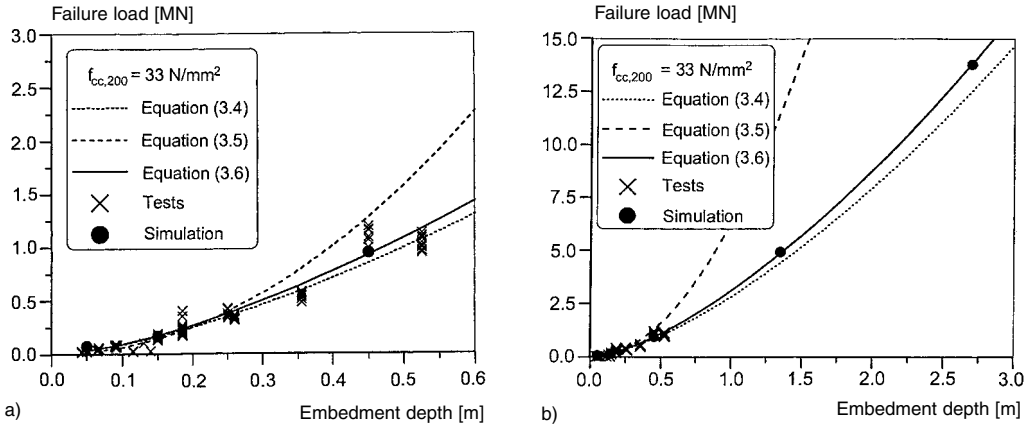


**Fig. 3.19** Concrete cone failure load as a function of embedment depth – comparison of various predictive equations with experiment and numerical simulation results (Ozbolt (1995))  
 a)  $h_{ef} \leq 600$  mm  
 b)  $h_{ef} \leq 3000$  mm

equation (3.4) clearly overestimates the failure loads as the embedment depth increases. The principal strains calculated at ultimate load and at the final load step for small embedment ( $h_{ef} = 150$  mm) and large embedment ( $h_{ef} = 1350$  mm) are illustrated in Fig. 3.20. The dark

regions indicate zones of damage or circumferential tension cracks. The crack length at ultimate load is approximately 40% of the side length of the cone envelope for the small embedment depth and approximately 25% for the large embedment depth. The slope of the

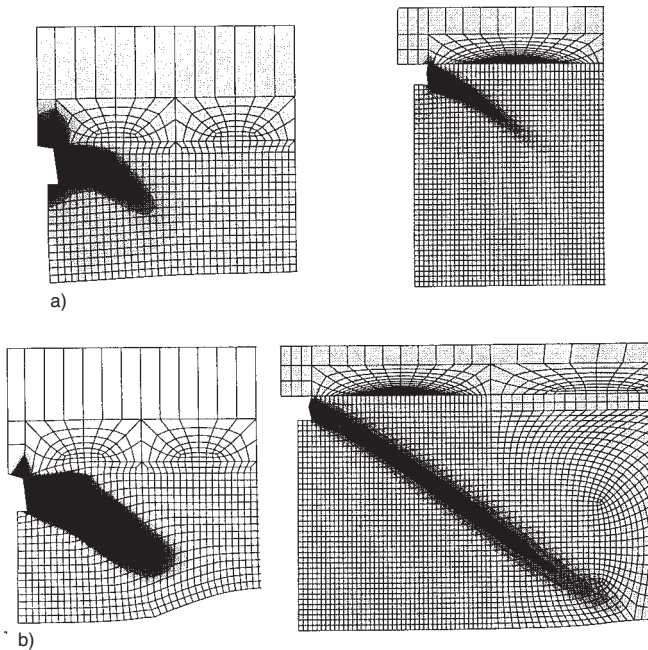


**Fig. 3.20** Areas of equal principle strain in concrete – headed studs with  $h_{ef} = 150$  mm (left) and  $h_{ef} = 1350$  mm (right) (Ozbolt (1995))  
 a) Ultimate load  
 b) Last step of numerical simulation

concrete cone is virtually independent of the embedment depth and measures approximately  $35^\circ$  from the horizontal. The size effect can thus be attributed to a change in the distribution of tensile stresses over the surface of the failure cone and the reduction in the average tensile stresses over the fracture surface as the embedment depth increases.

The results obtained from studies by various authors applying the principles of fracture mechanics with different material models can be summarised as follows. At service loads, circumferential tension cracks form in the concrete. These cracks propagate with increasing load from the anchorage region towards the surface of the concrete. Crack propagation remains stable up to ultimate load. The length of the crack at ultimate load for small embedment depths is approximately 40 to 50 % of the side length of the final cone and approaches a constant value of approximately 25 % of the side length for very large embedment depths. When deformations exceed that at ultimate load, the concrete failure cone forms completely as deformations increase and pull-out resistance decreases. The concrete cone failure load is proportional to  $h_{ef}^{1.5}$ . The very marked size effect can be attributed to the high strain gradient in the load transfer zone. The concrete cone failure load is not influenced significantly by the concrete tensile strength but rather by the factor

$(E_c \cdot G_f)^{0.5}$ . This factor can be replaced by  $f_{cc}^{0.5}$  with sufficient accuracy because both  $E_c$  and  $G_f$  are approximately proportional to  $f_{cc}^{0.5}$ .

### 3.3.2 Experimental studies

Experimental studies are divided between tests to clarify failure mechanisms and tests to determine the ultimate load of headed anchors embedded in large concrete blocks in which the formation of the concrete failure cone is unrestrained.

*Eligehausen, Sawade (1985)* describe tests on headed anchors with embedment depth  $h_{ef} = 80$  mm. Test specimens are depicted in Fig. 3.21. The test specimen shown in Fig. 3.21a was conceived to permit direct observation of the crack formation process during anchor loading. A restraining bar placed at the location of the anchor head (not shown) prevented horizontal translation of the anchor during loading. All loading was displacement controlled. A fluorescent penetrating fluid of the type used to inspect welds was sprayed on the exposed surface at periodic intervals, rendering visible cracks with a width  $> 0.001$  mm under ultraviolet light and magnification. In later tests the strains at the surface of the concrete were measured with strain gauges (gauge length = 20 mm). In addition, tests using acoustic emission analysis to detect the onset of cracking were conducted with the specimen shown in Fig. 3.21b.

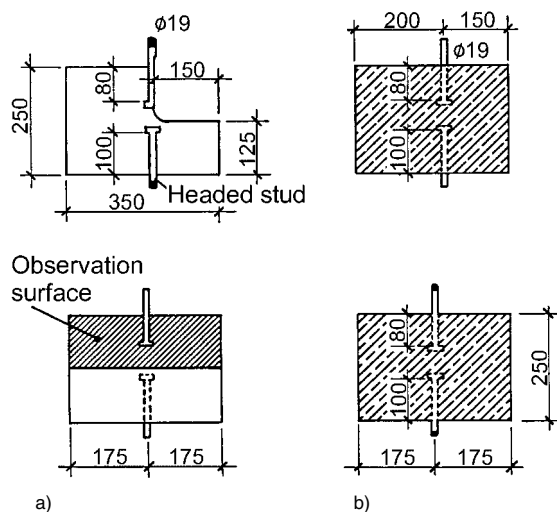


**Fig. 3.21** Geometry of test specimens developed for investigating crack propagation around a headed stud anchorage (dimensions in [mm]) (*Eligehausen, Sawade (1985)*)  
a) Crack observation specimen  
b) Tension test specimen

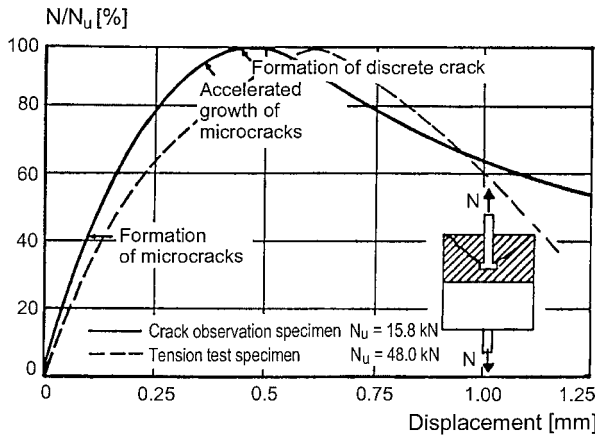


**Fig. 3.22** Normalised load as a function of anchor displacement; the various stages of crack formation are indicated on the load-displacement curve of the crack observation specimen (Eligehausen, Sawade (1985)).

All test specimens exhibited concrete cone fractures at failure. Accounting for the diminished fracture surface area, measured ultimate loads obtained with the specimen shown in Fig. 3.21a were approximately 65% of those measured with the specimen shown in Fig. 3.21b. This difference can be attributed, however, to the disruption of the rotationally-symmetric stress field in the stepped specimen, a condition analogous to that of an anchor positioned in a full-depth crack (see section 4.2.1.3).

Fig. 3.22 shows typical load-displacement curves for the specimens shown in Fig. 3.21. The displacement of the stud increases in nearly linear fashion up to about 40% of the ultimate load and thereafter non-linearly. Following the peak load, the load gradually drops. There is no significant difference in the load-displacement behaviour of the two different test specimens. At approximately 40% of ultimate load, a short initial crack forms in the region of the head of

the stud. This crack increases in length slowly and regularly as the load rises. Crack growth accelerates at approximately 90% to 95% of the ultimate load. At ultimate load, the crack has not reached the surface of the specimen, and the origin of the primary fracture at the head of the stud is clearly visible without magnification. Further displacement causes the crack to propagate until the failure surface is fully formed.

In further tests, concrete strains measured perpendicular to the fracture plane (Fig. 3.23) confirm the visual observations. The concrete strains increase in proportion to the load up to a strain of approximately 0.01%; afterwards they increase very rapidly. This confirms the formation of microcracks which increase in length as the load increases. The microcracks intersect the first strain gauge, positioned 15 mm from the head of the stud along the fracture plane, at approximately 50% of ultimate load. The second strain gauge, positioned 35 mm from the

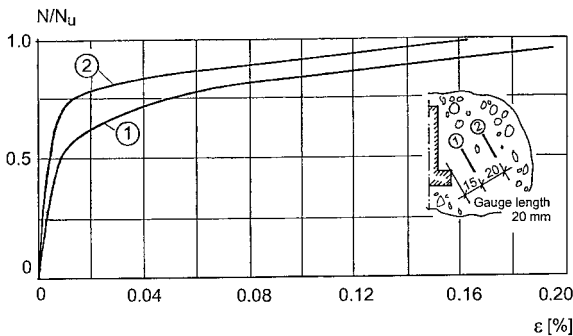


**Fig. 3.23** Normalised load as a function of concrete strain perpendicular to crack (Eligehausen, Sawade (1985))

head of the stud, is reached at roughly 70% of the ultimate load.

The applied load, the sum of recorded acoustic emission events and the amplitude of the acoustic emissions are plotted against time in Fig. 3.24 for loading cycles in the region of the ultimate load. The first acoustic emission events are registered at about 45% of the ultimate load. In the subsequent loading cycles, acoustic emission events are first recorded again as the peak load of the previous loading cycle is exceeded. This suggests the formation of new micro-cracks. At approximately 95% of ultimate, the sum of acoustic emission events and the amplitude of the acoustic emission events increase rapidly. This clearly indicates the formation of a discrete crack.

Further pull-out tests with headed studs having embedment depths  $h_{ef} = 130 \text{ mm}$  to  $520 \text{ mm}$  have been described by *Eligehausen, Sawade* (1989). The displacement of the headed bolts was increased continuously. The concrete strains were measured with the aid of strain gauges placed in three positions: vertical, circumferential, and parallel to the surface of the anticipated failure cone. The strain gauges were positioned in such a way that they lay either parallel and adjacent to or perpendicular and directly across the anticipated fracture surface, which was known from prior tests. Fig. 3.25

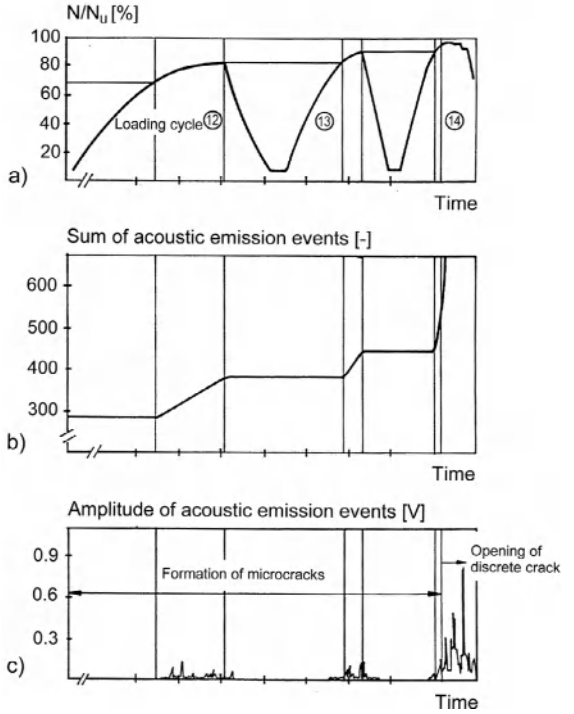


**Fig. 3.24** Results of acoustic emission analysis at near maximum load, plotted against time (*Eligehausen, Sawade* (1985))

- a) Applied load as a function of the ultimate load  $N_u$
- b) Sum of acoustic emission events
- c) Amplitude of acoustic emission events

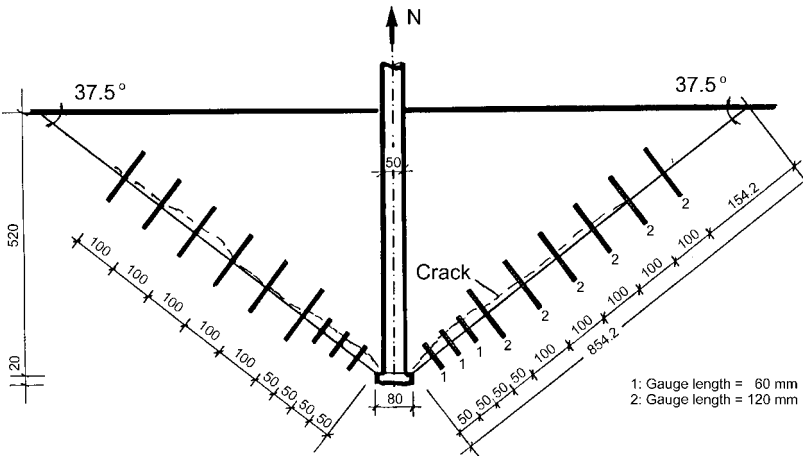


**Fig. 3.25** Positions of strain gauges for measuring strains perpendicular to the crack (dimensions in [mm]) (*Eligehausen, Sawade* (1989))



shows the positioning of strain gauges perpendicular to the anticipated fracture surface for a headed anchor with an embedment depth  $h_{ef} = 520$  mm.

Fig. 3.26 illustrates the strains measured along the fracture crack perpendicular to its average

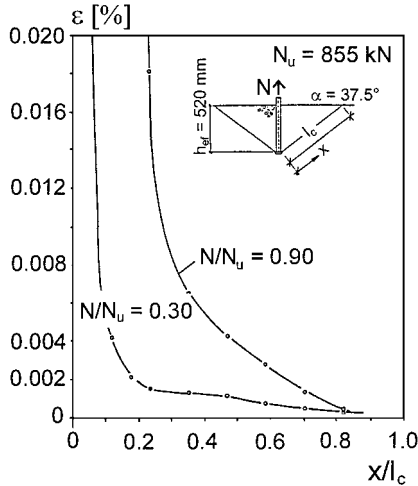


**Fig. 3.26** Strain distribution perpendicular to the failure cone surface along the cone envelope for two loading stages (Eligehausen, Sawade (1989))

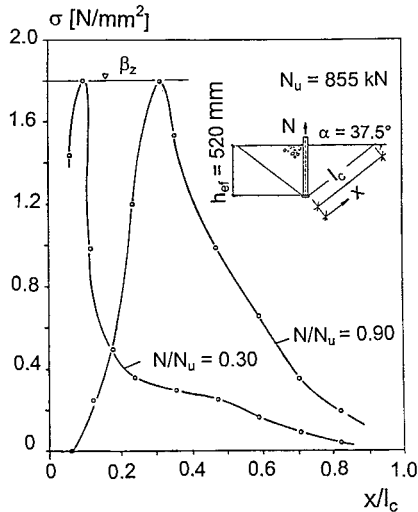


**Fig. 3.27** Tensile stress distribution perpendicular to the failure cone surface, calculated from the strains shown in Fig. 3.26 (Eligehausen, Sawade (1989))

slope for a loading at service and at ultimate load level ( $N/N_u = 0.3$  and  $N/N_u = 0.9$ ). The diagram applies to embedment depth  $h_{ef} = 520$  mm. It can be seen that the areas with high strains and high strain gradient moves from the load transfer point to the surface of the concrete as the load increases. This can be attributed to microcrack formation.

The tensile stresses perpendicular to the surface of the crack are calculated from the measured strains. It is assumed that the measured strains are the sum of the elastic strain in the concrete and the strain resulting from crack width (see equation (3.7)).

$$\epsilon = \epsilon_{el} + (w/l_m) \tag{3.7}$$

$$\sigma(w)/E_c + w/l_m$$

where:

- $\epsilon$  = measured strain
- $\epsilon_{el}$  = elastic concrete strain
- $w$  = crack width
- $l_m$  = gauge length

The crack width  $w$  and the stress  $\sigma(w)$  may be derived using the crack opening function  $\sigma(w)$  given in equation (3.2).

Results for the example shown in Fig. 3.26 are illustrated in Fig. 3.27. Plotted is the calculated distribution of tensile stresses perpendicular to the fracture plane along the envelope of the failure cone. The redistribution of tensile stresses, a result of the formation of microcracks as the load increases, is clearly shown. The crack width equation applies to the ascending branch of both curves in Fig. 3.27. The descending branch is valid assuming elastic behaviour. The length of the crack corresponds to the distance between the head of the stud and the point at which the concrete tensile strength is reached. At 90% of ultimate load, the length of the crack corresponds to about 30% of the side length of the cone envelope.

Eligehausen, Sawade (1989) integrated the vertical component of the tensile stresses acting perpendicular to the fracture plane over the fracture surface. At ultimate load the calculated force deviates by a maximum of 15% from the actual applied tension load. From this it is concluded that shear stresses acting along the fracture surface play a relatively minor role in

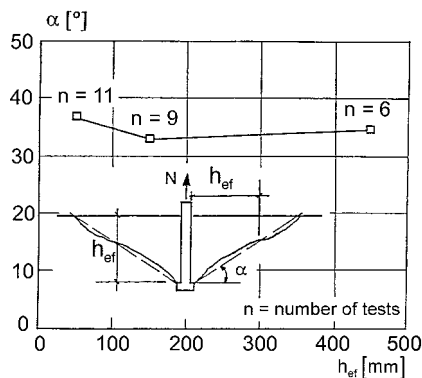


**Fig. 3.28** Average angle of failure cone measured with respect to the surface of the member as a function of embedment depth – tests by *Eligehausen, Bouska, Cervenka, Pukl* (1992) (taken from *Fuchs, Eligehausen, Breen* (1995/2))

determining the ultimate capacity. Only a small part of the applied tension load is transferred in the crack process zone at greater embedment depths. However, this component is quite large at small embedment depths. This implies that the behaviour of fasteners with small embedment depths can be described using non-linear fracture mechanics, whereas the behaviour of fasteners with large embedment depths may be approximated using linear fracture mechanics.

*Eligehausen, Bouska, Cervenka, Pukl* (1992) carried out pull-out tests on headed studs with embedment depths  $h_{ef} = 50$  mm, 150 mm, and 450 mm. The dimensions of the test specimens were chosen in proportion to the embedment depth. In the tests evaluated in Fig. 3.28 the bearing area of the head was established such that the bearing pressure beneath the head at ultimate load was independent of the embedment depth  $\sigma \approx 14 \cdot f_c$ . After the tests the dimensions of the concrete cones were measured along eight sections. The angle of the failure cone measured with respect to the horizontal varied around the circumference and scattered considerably.

Fig. 3.28 shows the average value of the measured angle in relation to the embedment depth. It can be seen that this angle, which is approximately  $35^\circ$  on average, is only somewhat dependent on the embedment depth. However, according to the studies by *Zhao* (1993), the

embedment depth does have an influence on the slope of the concrete failure cone, whereby the angle increases with increasing embedment depth.

The influence of the embedment depth on the concrete failure load of headed studs was investigated systematically by *Bode, Hanenkamp* (1985), *Eligehausen, Sawade* (1989) and *Eligehausen, Bouska, Cervenka, Pukl* (1992). The results indicate – with sufficient accuracy – that the failure loads increase in proportion to  $h_{ef}^{1.5}$  (see section 4.1.1.3).

*Sawade* (1994) performed pull-out tests on headed studs with an embedment depth  $h_{ef} = 250$  mm. Maximum aggregate size ( $d_{max} = 2$  mm to 32 mm) and concrete compressive strength ( $f_{cc,200} = 22$  N/mm<sup>2</sup> to 72 N/mm<sup>2</sup>) were varied. The modulus of elasticity of the concrete fluctuated between  $E_c = 20,500$  N/mm<sup>2</sup> and 37,000 N/mm<sup>2</sup>, and the fracture energy between  $G_f = 0.03$  N/mm and 0.15 N/mm. The measured concrete cone failure loads are shown in Fig. 3.29 as a function of the factor  $(E_c \cdot G_f)^{0.5}$ . The failure loads according to equation (3.3) are included for comparison. It can be seen that the measured failure loads coincide reasonably well with the calculated values.

*Sawade* (1994) describes a pull-out test on a headed stud anchored in optical glass ( $h_{ef} = 50$  mm). The tensile strength of the glass is approximately 25 times higher than that of concrete but the product of  $E_c \cdot G_f$  corresponds

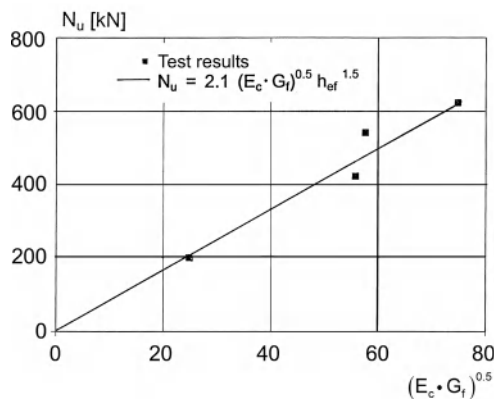


**Fig. 3.29** Measured and calculated failure loads as a function of the factor  $(E_c \cdot G_f)^{0.5}$  (after *Sawade* (1994))

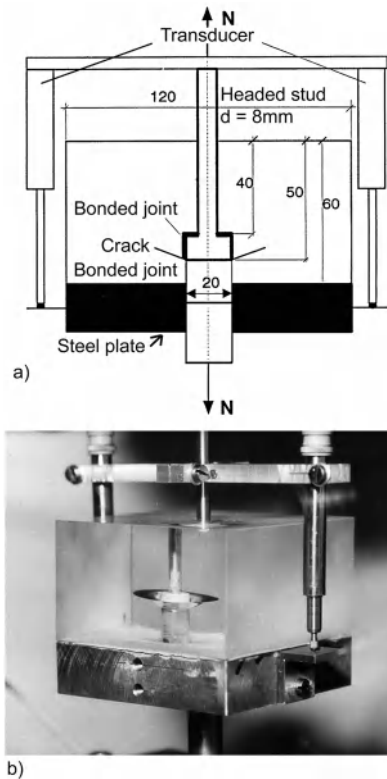


**Fig. 3.30** Circumferential tension crack in optical glass in the load transfer zone of a headed stud (Sawade (1994))

a) Test set-up (dimensions in [mm])

b) Photograph of test specimen at  $N = 0.93 N_u$

roughly to the value for concrete. A circumferential tension crack is observed which occurs well before the ultimate load is reached. Its length grows steadily and at ultimate load is only a fraction of the length of the failure cone (Fig. 3.30). If the failure load is assumed to be proportional to the tensile strength of the glass, the failure load would be on the order of  $N_u \approx 770$  kN. The actual failure load of  $N_u = 19$  kN corresponds roughly to the value given by equation (3.3).

### 3.3.3 Conclusions drawn from theoretical and experimental studies

According to the results of the theoretical and experimental studies described above, the load-bearing behaviour of a headed anchor embed-

ded in a large concrete block and subjected to tension loading can be described as follows:

High circumferential tensile stresses (hoop stresses) develop in the concrete in the load transfer zone. These stresses result in microcrack formation at service load levels. With increasing load, the microcracks propagate at a stable rate up to ultimate load. This is attributable to the disproportionate increase in the volume of concrete mobilised in the fracture process zone as the fracture crack lengthens, and the redistribution of tensile stress across the microcracks. Beyond peak load, crack growth becomes unstable and the final failure cone forms with rapidly increasing displacements and decreasing tension capacity.

The angle of the failure cone varies around the circumference and from test to test. It is on average approximately  $35^\circ$  measured with respect to a plane perpendicular to the anchor axis. It tends to increase with increasing embedment depth.

The concrete cone failure load can be predicted using the size effect law of *Bazant* (1984) (see equation (3.5)). Accordingly, the tensile stress averaged over the fracture surface at ultimate load decreases as the embedment depth increases. This implies that the increase in failure load is less than proportional to the increase in the failure surface, which varies with the square of the embedment depth. We can assume – with sufficient accuracy – that the concrete cone failure load is proportional to  $h_{ef}^{1.5}$  (equation (3.6)). This corresponds to the maximum possible size effect as given by linear fracture mechanics.

The concrete cone failure load is influenced by the concrete mechanical properties  $E_c$  (modulus of elasticity) and  $G_f$  (fracture energy). In contrast, the influence of the concrete tensile strength  $f_{ct}$  is negligible. Given that modulus of elasticity and fracture energy are related to the compressive strength of concrete, it is assumed in design equations that the failure load is proportional to  $f_{cc}^{0.5}$  or  $f_c^{0.5}$  respectively. However, it should be noted that for the same compressive strength, modulus of elasticity and fracture energy may also be influenced by the concrete mix, in particular the type and maximum size of

aggregate. This may explain why anchors tested in concrete specimens having the same compressive strength but varying mix designs sometimes exhibit varying concrete cone failure loads. Failure loads corresponding to concrete cone fracture are seen to be clearly higher with concrete containing large crushed coarse aggregate than for concrete containing smooth aggregate of smaller maximum aggregate size.

### 3.4 Cracked concrete

In the design of reinforced concrete flexural or tension components, a cracked tension zone is assumed because concrete possesses relatively low tensile strength, which may be fully or partly used by internal or restraint tensile stresses not taken into account in the design. Experience has shown that crack widths resulting from primarily quasi-permanent loads (dead load plus a fraction of the live load) do not exceed the value of  $w_{95\%} \sim 0.3$  mm to 0.4 mm (Schießl (1986), Bergmeister (1988), Elgehausen, Bozenhardt (1989)). These crack widths are generally acknowledged as permissible. Wider cracks are to be expected under maximum permissible service loads, which according to Elgehausen, Bozenhardt (1989) reach  $w_{95\%} \sim 0.5$  mm to 0.6 mm. Even wider individ-

ual cracks can occur under conditions of restraint if no additional reinforcement has been included to limit crack widths (Schießl (1986)).

The causes of cracking, as well as type, appearance and features of the various types of cracks are described in detail in *Comité Euro-International du Béton (CEB) (1981)* and *Deutscher Betonverein (1991)*. Cracks can occur in one direction (e.g. in beams, one-way-spanning slabs or tension members, Fig. 3.31a, b), or in two orthogonal directions (e.g. in two-way-spanning slabs and flat slabs, Fig. 3.31c). They may taper in width (flexural cracks, Fig. 3.31b) or transect the section with more or less constant width (cracks in tension members, Fig. 3.31a). Cracks may run inclined to the axis of the component (shear or torsion cracks); they may also occur parallel to reinforcement as a result of transverse splitting stresses. Fasteners can lie adjacent to or in cracks and in the most unfavourable case may be positioned at the junction of two intersecting cracks.

It has been observed that when cracks form in a concrete member, there is a relatively high likelihood that they will intersect the anchor location either directly or tangentially. This occurs because higher tensile stresses exist around the anchor as a result of (a) hoop stresses associated

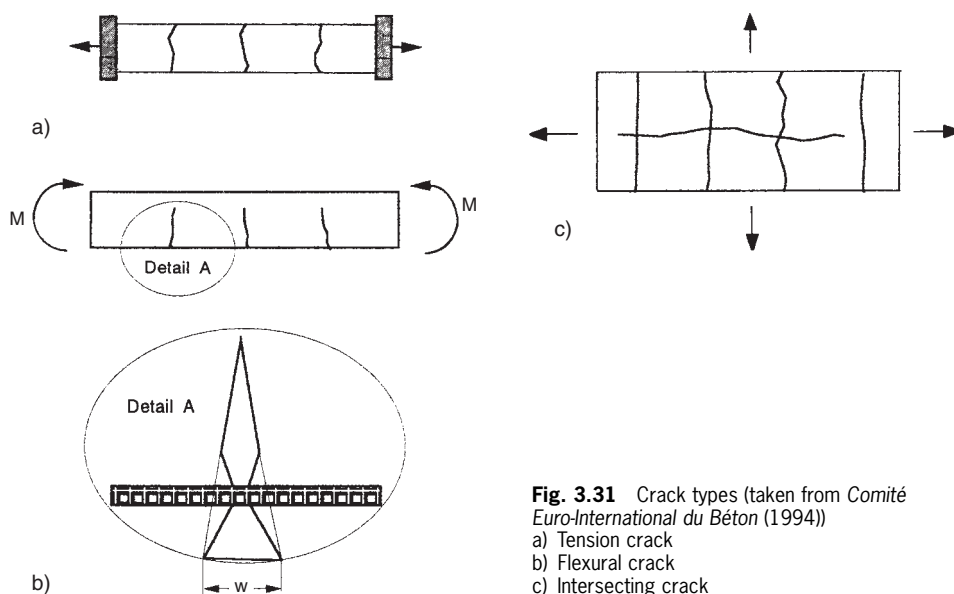


**Fig. 3.31** Crack types (taken from *Comité Euro-International du Béton (1994)*)

- a) Tension crack
- b) Flexural crack
- c) Intersecting crack

with the prestressing and loading of the anchor, (b) possible local flexural stresses resulting from the concentrated load introduced by the anchor, and (c) the stress concentrations caused by the presence of the anchor hole (i.e. the discontinuity in the concrete continuum, notch effect).

Tests have been performed to confirm these observations experimentally (Eligehausen, Lotze, Sawade (1986), Lotze (1987/2)). The tests were carried out on slabs with a depth of 250 mm reinforced with ribbed reinforcing bars or welded wire fabric. Transverse reinforcement was placed at 250 mm centres. Torque-controlled expansion and undercut anchors were installed in the slab. The thread size was 12 mm and the embedment depth  $h_{ef} = 80$  mm. The loads on the anchors (prestressed only or loaded with 1.3 times the permissible load) and the distance of the anchors from the transverse reinforcement (40 and 80 mm) were varied in the tests. In addition some drilled holes were left open without anchors. The anchors were installed in the concrete and loaded prior to loading of the slab. The slab was then loaded in increments up to its permissible service load calculated according to *DIN 1045* (1988).

At roughly 40% of the slab permissible load, flexural cracks began to form in the slab. As a rule the cracks followed the transverse reinforcing bars, however, they deviated from this path sufficiently to intersect the anchor locations. At 100% of the slab permissible load, nearly all of the anchors and a majority of the drilled hole locations were intersected by cracks, regardless of the distance of the anchor from the transverse reinforcement and the way in which they were loaded (Fig. 3.32). The cracks ran vertically through the anchorage zone of the anchors (Fig. 3.33). The load-displacement curves recorded for the anchors confirmed that the anchors were located in the crack even as the crack began to form. Similar results were recorded by Cannon (1981), Bergmeister (1988) and Bensimhon, Lugez, Combette (1989).

Anchors can also cause cracking in otherwise non-cracked concrete (Mayer (1988)).

The load-bearing behaviour of an anchor can be significantly influenced by the presence of a crack passing through the anchor location (see sections 4.2, 5.2, 6.2, 7.2, 8.2 and 9.3). As such, cracking should be explicitly taken into account when designing anchors. It should only be

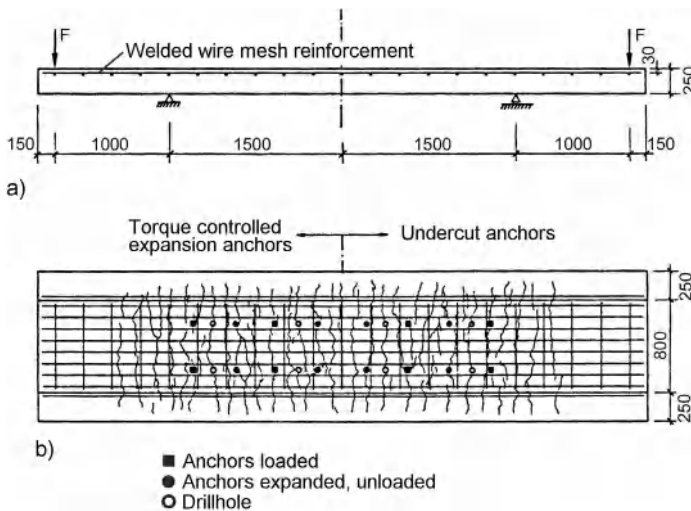


**Fig. 3.32** Crack pattern in a flexurally loaded slab at service load (dimensions in [mm]) (Lotze (1987/2))

- a) Test set-up  
b) Crack pattern and position of anchors and drill holes

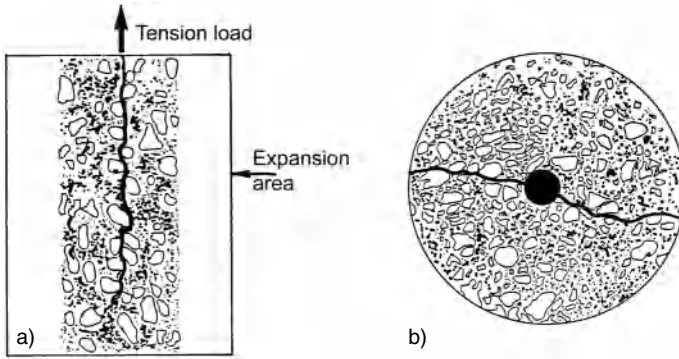


**Fig. 3.33** Path of a crack passing near an anchor (Lotze (1987/2))  
 a) Longitudinal section over member depth  
 b) Cross-section through anchor location

neglected when no cracks are expected in the concrete.

As a practical matter cracked concrete should be assumed for design in most cases because in practice it is difficult to differentiate between locations where the concrete will crack and where it will not crack over the life of the anchorage. Only through a careful statical analysis can a determination of the theoretical zones of cracking be made. Such an analysis would recognise that components subjected mainly to bending exhibit large zones of tensile stress under various loading cases (Fig. 3.34), and hence could be expected to develop flexural cracking. However, even in vertical load-bearing elements such as walls, the anchorages themselves may introduce loads of sufficient

magnitude to introduce local tensile stresses in the concrete which may cause cracks, at least transverse to the main load-bearing direction (Fig. 3.35). Such an analysis must also account for tensile stresses corresponding to restraint of deformations as caused by shrinkage, temperature fluctuation, support settlement, etc., the magnitude of which may be very difficult to estimate. In such cases the estimation of cracking potential is made more complex. If it is only shown that no tensile stresses from *external* loads occur in the *primary* load-bearing direction of the component serving as base material, i.e. tensile stresses resulting from *restraint* are ignored (and in planar structures tensile stresses from loads in the *secondary* load-bearing direction), then cracking cannot be ruled out.

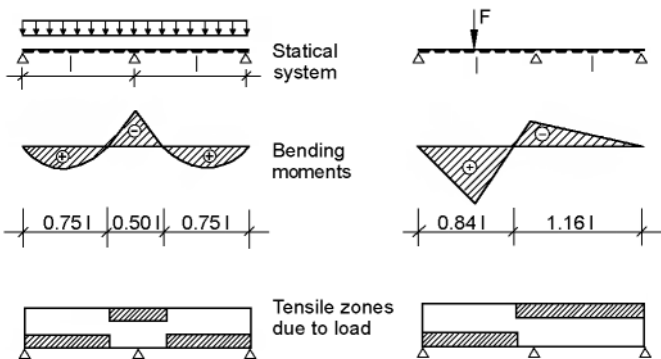


**Fig. 3.34** Position of compression and tension zone in a two-span beam for different load cases (Eligehausen, Mallée, Rehm (1997))



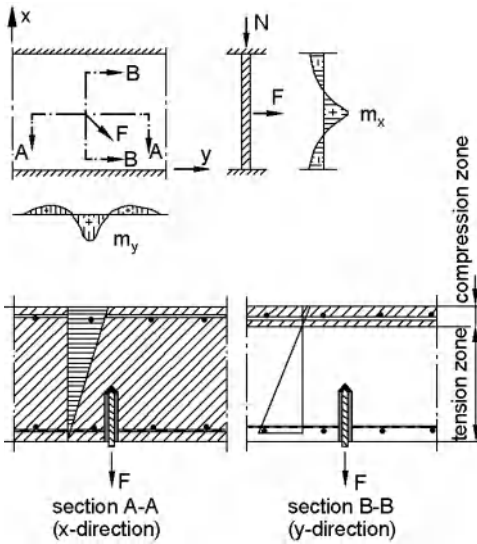


**Fig. 3.35** Tension and compression zones in a wall due to a point load (Riemann (1981))

### 3.5 Why anchors may use the tensile strength of concrete

Anchors designed for use in concrete employ the local capacity of the concrete to carry tensile stresses. In contrast, concrete tensile strength is generally neglected in the flexural and tension design of reinforced concrete elements, whereby the tension forces are assumed to be carried entirely by the reinforcement. This is in part justified because tensile stresses in the concrete can also be induced by restraint of deformations resulting from creep, shrinkage, thermal movements and settlement of supports. These stresses, the magnitude of which can

exceed the tension capacity of the concrete, generally act parallel to the stresses caused by external loads (Fig. 3.36a), and they can in fact result in component failure if reinforcement is not provided to carry external loads.

A different geometry is present for anchorages to concrete. The failure surface is inclined relative to the surface of the concrete and is generally rotationally symmetric about the anchor axis (Fig. 3.36b). Thus the overlap of longitudinal tensile stresses due to external restraint with the parallel component of those generated along the anchor failure plane occurs only over a small part of the total failure surface. Based on this simple geometric consideration, a maximum reduction in the anchor concrete cone failure load of 20% can be predicted when tensile stresses in the region of the anchorage due to restraint of deformations approach the concrete tensile capacity (Eligehausen (1984)). This reduction is in fact less than the decrease in tension capacity associated with an anchor suitable for use in cracks (e.g. headed stud, undercut anchor, specially designed expansion anchor or bonded expansion anchor) situated in a crack. If we therefore assume a cracked concrete section when designing such an anchor, the influence of tensile restraint stresses on the concrete cone failure load is adequately accounted for.

In the design of reinforced concrete members the capacity of the concrete to resist tensile stresses is also explicitly taken into account in situations where tensile restraint stresses are not expected to exert a significant influence on the load-bearing behaviour of the component. For example, slabs and walls may be designed without shear reinforcement if the shear stresses are

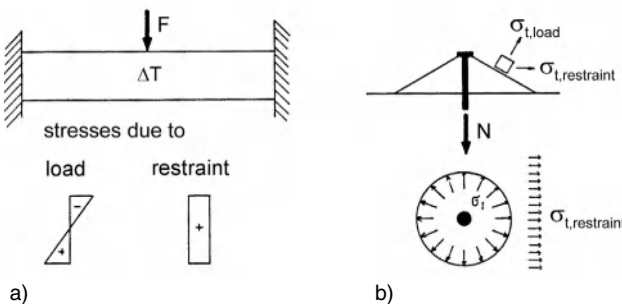


**Fig. 3.36** Superimposition of stresses due to load and restraint (Eligehausen, Ozbolt (1991))  
 a) Beam  
 b) Anchorage



low, and transverse reinforcement may often be omitted in the vicinity of anchorages and at reinforcing bar splices.

Such considerations indicate that it is possible to safely exploit the tensile capacity of the concrete when designing anchors, given that a sufficiently conservative factor of safety is used.

### 3.6 Prestressing of anchors

Connections employing anchors are typically prestressed, i.e. a clamping force is developed in the connection which is balanced by a tension force in the anchor bolt. Note that this does not apply to cast-in-place embed plates equipped with welded studs, nor does it generally apply to cast-in-place anchor channels. In these cases, the clamping force is developed between the fixture and the embedded channel or plate unless the channel or plate, is recessed below the concrete surface. Cast-in-place headed studs that are threaded to provide a bolted connection may likewise be prestressed.

A pre-defined torque is typically applied to anchor connections to induce the requisite clamping or prestressing force. The amount of prestressing force  $F_{S,V}$  induced in the bolt or stud for a given level of applied torque essentially depends on the thread friction as well as the friction between nut and washer or washer and adjoining component (fixture), and can vary over a wide range. Provided the corresponding friction parameters are known, the prestressing force associated with a given torque  $T$  can be calculated using equation (3.8) (Kellermann, Klein (1955), VDI (1983)). The prestressing force simultaneously induces a clamping force between the fixture and the base material.

$$F_{S,V} = \frac{T}{0.5 \cdot d_2 \cdot \tan(\delta_g + \alpha) + 0.5 \cdot d_k \cdot \tan(\delta_k)} \quad (3.8)$$

where:

- $T$  = torque
- $d_2$  = flank diameter
- $d$  = head friction diameter
- $\delta$  = thread friction angle
- $\delta_k$  = head friction angle
- $\alpha$  = thread flank angle

The first term in the denominator of equation (3.8) describes the thread friction whereas the

**Table 3.1** Friction coefficients for bolted connections (VDI (1983))

Surface	$\tan(\delta_g)$	$\tan(\delta_k)$
Electrogalvanised, dry	0.12 – 0.20	0.16 – 0.20
Electrogalvanised, oiled	0.10 – 0.18	0.10 – 0.18
Stainless steel A2	0.26 – 0.50	0.35 – 0.50
Stainless steel A2, lubricated	0.12 – 0.23	0.08 – 0.12

second term defines the friction under the bolt head or nut. Recommended values for thread and bolt head friction are given in VDI (1983) (Table 3.1).

Equation (3.8) can be simplified as follows:

$$F_{S,V} = \frac{T}{k \cdot d} \quad (3.9)$$

In equation (3.9)  $k$  is a constant which is more or less independent of the thread diameter for the same form and surface roughness of bolt head and thread.

If the clamping action between the washer or base plate and the base material is not impeded, then the contact or clamping force  $F_K$  corresponds to the force in the bolt  $F_{S,V}$ . The introduction of an external tension force  $N$  acts both to relieve the clamping force and increase the bolt tension force, each according to the relative stiffness of the corresponding load path (Fig. 3.37). As the stiffness of the base material in compression is considerably greater than that of the bolt, the degree to which the bolt tension

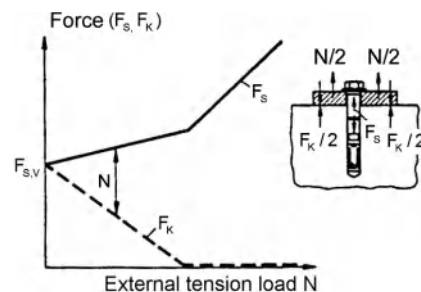


**Fig. 3.37** Bolt- and clamping forces in an anchorage as a function of the externally applied tension load (Rehm, Eligehausen, Mallee (1988))

force is increased is minimal as long as some clamping force remains in the connection. If the load increases beyond the clamping force, then the fixture becomes loose and the tensile force in the bolt increases in proportion to the external tension force.

Note that in the case of sleeve-type expansion anchors, clamping action may not occur if the sleeve is allowed to come in contact with the base plate or washer. This condition may arise if the anchor sleeve projects beyond the concrete surface and the hole in the fixture is not dimensioned accordingly, or if the anchor is drawn up and into contact with the fixture or the washer respectively during application of the setting torque. In these cases, the prestressing force will be absorbed by the anchor internally, and no clamping force will be induced in the connection. Note that in this case, the application of external load will result in immediate lift-off of the connection and a larger increase in the bolt tension force, since the stiffness of the compression and tension load paths are nearly equal. In cases where the fixture contacts both the anchor sleeve and the base material, the degree of clamping force induced depends on the relative stiffness of the two load paths. Some sleeve anchors are equipped with a collapsible or otherwise compressible sleeve ele-

ment between the steel sleeve and the expansion sleeve in order to mitigate this condition.

The prestressing force and hence the clamping force induced in the concrete decrease as a result of levelling of irregularities in the stressed thread pitches as well as creep and relaxation of the highly stressed concrete adjacent to the expansion zone of the anchor. The reduction in prestressing force in expansion and undercut anchors is marginally influenced by its initial value and the anchor load transfer mechanism, and depends largely on the free bolt length (i.e. embedment depth) over which strain is developed. While the greatest reduction in prestress takes place within the first few minutes and hours, continuing relaxation over time will cause the residual prestress in typical expansion and undercut anchors in *non-cracked* concrete to fall to about 40 to 50% of the original value (Fig. 3.38). Re-torquing of the anchor will precipitate a repetition of the relaxation process, but the percentage loss of prestress after each re-torquing is diminished (Fig. 3.39), and therefore re-torquing can be used to raise the level of residual prestressing force. Re-torquing after a few hours, or preferably after a few days, is very effective (*Wagner-Grey (1977/2) and Seghezzi (1986)*). A torque-controlled expansion anchor subjected to cracked

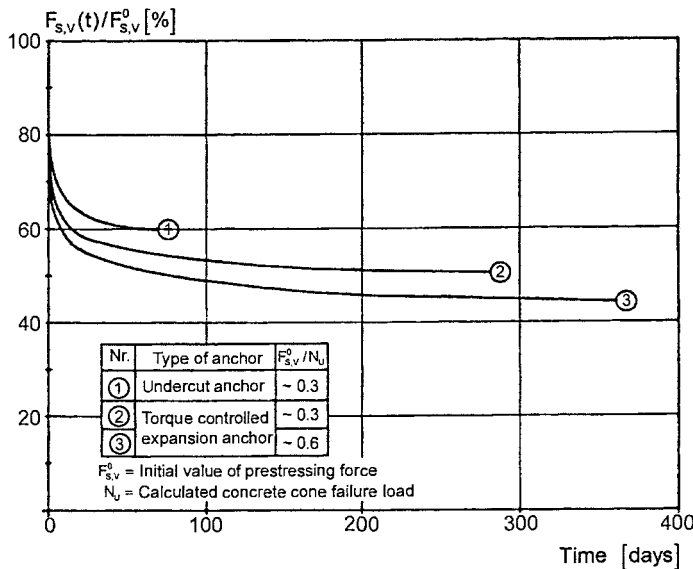


**Fig. 3.38** Decrease of prestressing force in anchors, plotted against time (after *Seghezzi (1986) and Burdette, Perry, Runk (1987)*)

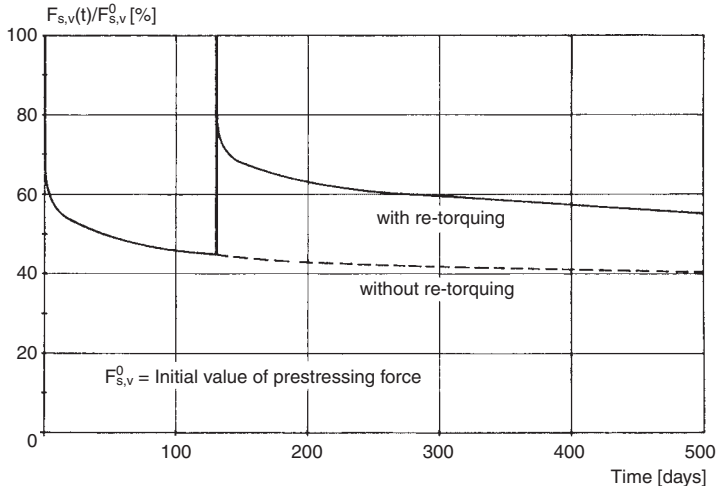


**Fig. 3.39** Influence of re-torquing on the prestressing force in anchors (after Seghezzi (1986))

concrete conditions can generally be assumed to lose any residual prestress as the anchor re-expands to accommodate the crack. Similarly the prestressing force of other anchor types (e.g. undercut anchors, displacement-controlled anchors and screw anchors) will be reduced significantly by cracks because of displacement increase to bridge the crack.

The prestressing force associated with an applied torque can be calculated for bonded anchors using equation (3.8) as well. Nevertheless, while the bolt prestress in expansion, undercut and cast-in-place headed anchors is constant between the nut and the expansion or bearing surface, bonded anchors with  $h_{ef} \sim 10d$  exhibit a variation in prestress force from a maximum at the surface of the concrete to zero at the end of the anchorage length. The distribution of the prestressing force is a function of the bond stresses developed between the mortar and the concrete. Therefore, for the same embedment, bolt diameter and applied torque, the effective elongation or strain induced in a bonded anchor is less than that developed by the anchor types mentioned above during setting. At high stress levels, creep of the bonding material must be expected as well. For these reasons, the prestressing force in bonded anchors drops faster, the percentage reduction is greater, and

the residual prestress level is less predictable than in the case of expansion, undercut, and cast-in-place anchors.

Plastic anchors are typically not prestressed with a defined torque, but are rather tightened to a snug fit condition. Therefore, the actual prestressing force generated can vary widely. Owing more to creep of the plastic parts than the base material, this prestress also decreases significantly over time.

In connections utilising anchors, serviceability considerations stipulate that contact be maintained between the fixture and the base material at service load levels. This is achieved only if the applied installation torque is translated into a clamping force in the connection and not in the anchor sleeve as discussed above. In addition, the clamping force is directly dependent on the magnitude of the applied torque. Therefore, the installation should be checked for the necessary clearances and the prescribed torque must be applied with a calibrated torque wrench in order to ensure the desired level of prestress. Re-torquing of anchors is recommended to increase the level of residual prestress force. In general, for anchors located in cracked concrete, defined prestress levels can only be assured by incorporating spring elements with sufficient working range to accommodate the

anchor displacement associated with crack opening.

### 3.7 Loads on anchors

The forces acting on an anchor can generally be determined using general principles of structural mechanics. In doing so, the displacement of the anchor is usually assumed to be small (i.e. negligible). The distribution of forces acting on a fixture of an anchor group to the individual anchors of the group can be calculated either with elastic theory or with non-linear methods.

#### 3.7.1 Calculation according to elastic theory

##### 3.7.1.1 Tension load

Calculation of anchor loads induced by tension loads and bending moments acting on the fixture per elastic theory involves the following assumptions (Fig. 3.40b):

- The fixture remains plane (flat) under the influence of internal forces. In order to warrant this supposition, the fixture must be sufficiently stiff and must be in contact with the base material or grout bed over its full area

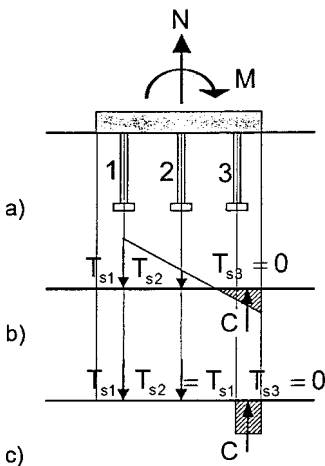


**Fig. 3.40** Distribution of forces in an anchor group subjected to tension force and bending moment  
a) Anchor group  
b) Anchor force distribution as predicted by elastic theory  
c) Anchor force distribution as predicted by plastic theory

before loading unless the anchors are configured for a stand-off installation (i.e. equipped with levelling nuts). A stiff fixture may be assumed if under the design actions the stresses in the fixture are smaller than the design resistance of the fixture material. For the definition of design actions and design resistances see section 14.3.3.1. The stiff fixture assumption corresponds to the Bernoulli hypothesis in reinforced concrete design, wherein plane cross-sections are assumed to remain plane.

- In the part of the fixture subjected to compression, anchors do not act in either tension or compression, unless they are configured for a stand-off installation.
- The stiffness of all anchors in a group are identical. The anchor stiffness is directly proportional to the area of the stressed cross-section and the modulus of elasticity of the steel. The stiffness of the concrete is characterised by its elastic modulus and the stressed area.

Consequently, the calculation of the tension forces in the anchors corresponds to how one determines the tension resultant in the reinforcing bars of a reinforced concrete member. However, in contrast to strength design of reinforced concrete members, we assume here that the response of the concrete and steel elements remains linear elastic.

The assumption of a rigid fixture is not always assured with the thicknesses of fixtures often encountered in practice. A non-rigid fixture, depending on the anchor stiffness, leads to a reduction in the lever arm of the internal forces. However, the assumptions of negligible anchor displacement and a triangular compressive stresses block in the concrete below the fixture are both conservative. Deformations in the concrete lead to larger rotations of the fixture. Furthermore, the compression capacity of the concrete below the fixture exceeds the uni-axial concrete compressive strength owing to the localised tri-axial stress state. Both effects lead to a reduced depth of the compression block and hence to an increased internal lever arm. For these reasons, elastic theory delivers sufficiently accurate results in most practical cases.

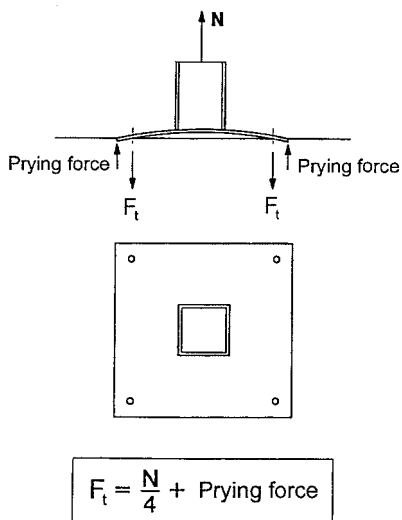


**Fig. 3.41** Increase in anchor forces associated with a flexible fixture

This is confirmed by non-linear calculations using finite elements (Mallée, Burkhardt (1999)). In these investigations, realistic assumptions were made about the displacement behaviour of the anchors, the stress-strain behaviour of the compressed concrete and the flexural stiffness of the fixture.

In practice it is frequently assumed that the internal lever arm corresponds to the centre-to-centre spacing of the anchors even though the anchors are not equipped with levelling nuts. This assumption is generally conservative for a uni-directional moment combined with tension loading and for typical fixture toe dimensions (one to two times the diameter of the hole in fixture). Where larger fixture toe projections are used in conjunction with predominantly tension loading and a relatively flexible fixture, prying of the fixture can occur, resulting in a significant increase in the anchor tension forces (Fig. 3.41). In cases with an applied moment and compression load with eccentricity  $e = M/N > -1$  (primarily compressive loading), the assumption of an internal lever arm corresponding to the centre-to-centre anchor spacing may result in underestimation of the anchor tension forces since the actual lever arm is smaller (Mallée, Burkhardt (1999)).

### 3.7.1.2 Shear loads

In calculating the distribution of shear loads through a fixture to the anchors of a group positioned away from an edge, it is assumed that all anchors exhibit the same shear stiffness. Additionally, it is generally assumed that all anchors participate in accommodating the shear loads (Fig. 3.42a). To comply with this condition, however, the anchor holes cannot be oversized. *Deutsches Institut für Bautechnik* (1993) and *European Organisation for Technical Approvals (EOTA)* (1997) provide permissible diameters for clearance holes in components to be connected with anchor bolts as given in Table 3.2. In *Comité Euro-International du Béton* (1997) permissible diameters for clearance holes is  $d_c \leq 1.2 d$  (bolt is assumed to bear against fixture, pre-positioned installation) or  $d_c \leq 1.2 d_{nom}$  (sleeve is assumed to bear against fixture, in-place installation).

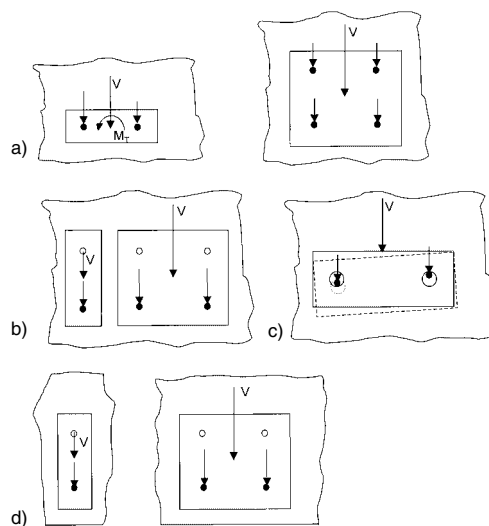


**Fig. 3.42** Distribution of shear forces in an anchor group

- Examples of connections in which all anchors participate in resisting the shear load
- Examples of shear load distributions associated with oversized clearance holes
- Distribution of the shear load to a group of two anchors where the fixture is free to rotate
- Examples of shear load distribution for anchor groups with clearance holes in the fixture near a free edge

**Table 3.2** Permissible diameter of clearance hole in fixture (after *Deutsches Institut für Bautechnik* (1993) and *European Organisation for Technical Approvals (EOTA)* (1997))

	Anchor diameter in region of fixture [mm] <sup>1)</sup>											
	6	8	10	12	14	16	18	20	22	24	27	30
Maximum permissible diameter $d_c$ of clearance hole in fixture [mm]	7	9	12	14	16	18	20	22	24	26	30	33

1) Corresponds to nominal diameter of anchor sleeve for in-place installation or nominal diameter of stud for pre-positioned installation.

If the clearance holes are larger than the values given in Table 3.2 or recommended by *Comité Euro-International du Béton* (1997) and if the anchors are positioned linearly and parallel to the load direction, then the distribution of the forces to the individual anchors is not uniform. The distribution of the shear load depends on the diameter of the clearance hole, the initial position of the anchor in the hole (with or without contact) and the deformation response of the anchor. The distribution of the load under these circumstances is difficult to estimate. For this reason, the *European Organisation for Technical Approvals (EOTA)* (1997) proposes that the total shear load in groups should be taken by the most unfavourable anchors (e.g. anchors having the least calculated resistance due to combined loading). According to this proposal, for the examples shown in Fig. 3.42b in a group of two anchors the shear load is carried by one anchor only, and in groups of four anchors by just two anchors. This assumption simplifies the calculation but can lead to a very conservative design.

If a shear load applied to a group of two anchors acts perpendicular to a line joining the two anchors and the fixture is free to rotate, then the shear load is resisted by both anchors (Fig. 3.42c). If the fixture is prevented from rotating, then the anchor in contact with the fixture resists the entire shear load. Note that in this case the connecting element must be proportioned to accommodate the resulting eccentric moment (torsion).

According to the *Deutsches Institut für Bautechnik* (1993) and *European Committee for Standardisation (CEN)* (2004), when the holes in the fixture are oversized, it may be assumed that *all* anchors in the group participate in

resisting the load, whereby it must *also* be assumed that the anchors are subjected to cantilever bending as a function of the rotational freedom of the anchor in the fixture. This in turn leads to a considerable reduction in the design shear load that the anchor can resist.

The proposal according to *European Organisation for Technical Approvals (EOTA)* (1997) is easy to handle in the applications shown in Fig. 3.42b. However, in more complicated cases, e.g. groups with four anchors loaded by a shear load acting not parallel to the lines connecting the anchors with or without an additional torsion moment or groups with more than four anchors, it may be difficult to judge which anchors are most unfavourable. Therefore the authors recommend to use for all applications the proposal of *Deutsches Institut für Bautechnik* (1993) and *European Committee for Standardisation (CEN)* (2004).

Fastenings near the edge of a component, with a clearance hole in the fixture, which are subjected to a shear load in the direction of the edge, can give rise to a brittle fracture of the concrete edge before all anchors participate in resisting the shear load. Depending on the ratio of the distance between the front and rear anchors to the edge distance of the front anchors the failure load is governed either by the front or the rear anchors. This is discussed in detail in section 4.1.2.4(b). For small ratios the front anchors are decisive. This case is shown in Fig. 3.42d where it is assumed that the shear load is carried only by those anchors nearest the edge.

In Fig. 3.42 it is assumed that the shear load acts at the centre of gravity of the group of anchors. When the shear load acts eccentrically, the forces in the anchors should be calculated tak-

ing into account equilibrium conditions based on steel design principles.

### 3.7.2 Calculation according to non-linear methods

A non-linear analysis of anchor load distribution requires realistic assumptions to be made about the stress-strain behaviour of the concrete, the stiffness of the fixture and the load-displacement behaviour of the anchors subjected to tension and shear loads. Equilibrium and compatibility conditions should be considered in the analysis. Such analyses are elaborate and time-consuming and can only be carried out with the help of numerical analysis techniques. One such analysis procedure is described in *Li, Eligehausen* (1994).

Plastic theory represents a simpler variant of non-linear analysis. Plastic theory dictates that only equilibrium conditions need be satisfied whereas compatibility conditions are neglected. The distribution of tension and shear loads to the individual anchors of a group is therefore arbitrary if equilibrium conditions are satisfied. Combined bending and tension usually leads to the assumption that all tension loaded anchors resist equal loads and a rectangular compressive stress block forms beneath the fixture (Fig. 3.40c). According to *Cook, Klinger* (1989) the shear loads are initially assigned to the anchors in the compression zone beneath the fixture. If the load-carrying capacity of these anchors is exceeded, then the tension loaded anchors are engaged to share the shear load as well.

Plastic theory assumes that the fasteners exhibit sufficient ductility under tension and shear loads to enable load redistribution. This condition is met assuming the following holds true: failure is controlled by ductile rupture of the steel, small clearances between the anchors and the fixture holes exist, and a constant anchor bolt cross-section is present over the full embedment depth. The requirements for an anchor to be regarded as 'sufficiently ductile' are dealt with in section 14.4.13.

Detailed experimental and numerical investigations of the load-bearing behaviour of groups of post-installed anchors subjected to combined tension and shear and exhibiting steel failure

were conducted by *Lotze, Klinger* (1997). A model described by *Li, Eligehausen* (1994) was used for numerical analysis to determine the load-carrying capacity with the influence of hole clearance explicitly considered. Representative load-displacement curves for the individual anchors were employed for this analysis. The calculated capacities show good agreement with the measured values. For higher shear loads and concrete grades above C20/25, the plastic model of *Cook, Klinger* (1989) outlined above predicted capacities approximately 10% higher than those measured in the tests. While no experimental investigations were conducted with anchor groups in low-strength concrete (C12/15), numerical analyses were performed. The capacities predicted by the *Cook, Klinger* (1989) model were approximately 25% higher than the values predicted by the more detailed *Li, Eligehausen* (1994) numerical model. This apparent overestimation of the capacity when using plastic theory can be attributed to the fact that failure of the group is initiated via shear fracture of the anchors on the compression side of the connection. The deformation capability of these anchors is less than that of the tensioned anchors. Therefore at ultimate load of the group the deformation capability of the tensioned anchors cannot be fully exploited and the shear load taken up by these anchors is less than their capacity predicted by the usual interaction equation. The authors therefore recommend that elastic theory be used for the distribution of shear loads to the anchors in the group, even where failure of an individual anchor is governed by steel rupture. This approach is conservative.

### 3.7.3 Calculation of loads on anchors of anchor channels

#### 3.7.3.1 Tension loads

The load transfer of anchor channels is different from that of fastenings with cast-in-place or post-installed anchors, because in general the stiffness of a channel is less than that of a stiff fixture assumed in section 3.7.1.1. The distribution of tension loads acting on the channel to the anchors may be calculated using a beam on elastic supports with a partial restraint of the channel ends. The stiffness of the elastic sup-



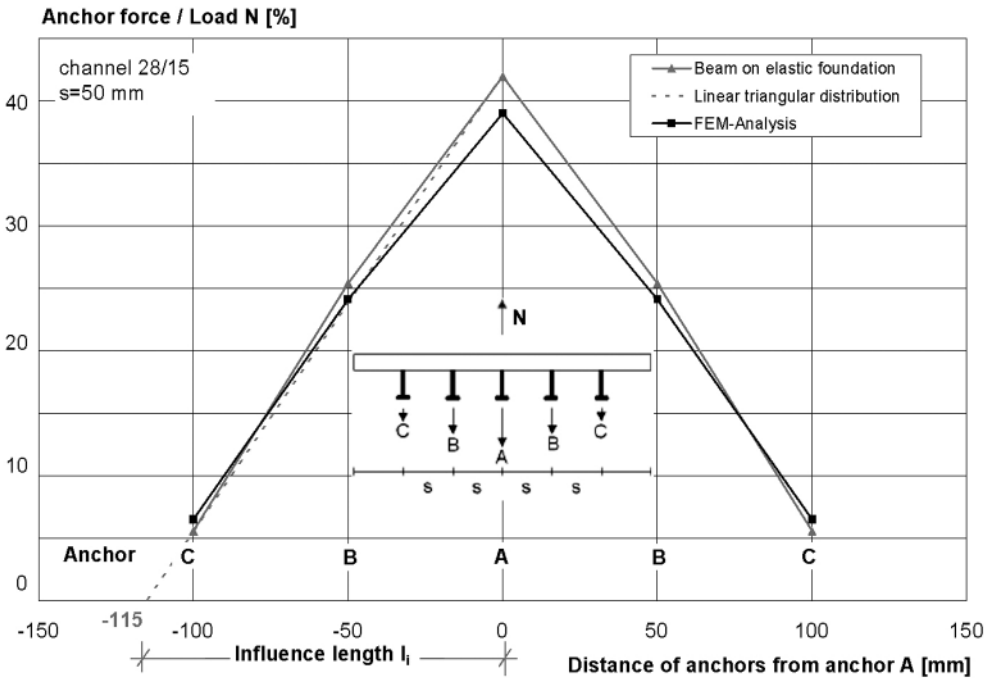


**Fig. 3.43** Distribution of tension loads on anchors for an anchor channel with five anchors (Grewin, Eligehausen (2003))

ports corresponds to the displacement of the anchors which includes the displacements of channel lips, anchors, and concrete. In Fig. 3.43 the calculated distribution of anchor forces is shown for an anchor channel with 5 anchors loaded over the middle anchor. The distribution of anchor forces can be approximated by a triangle with a peak at the applied load and an influence length  $l_i$  (Kraus (2003)). The influence length depends mainly on the anchor spacing, the moment of inertia of the channel and on the head size. Further minor influencing factors are the concrete compression strength, the type of steel (galvanised or stainless steel) and the state of concrete (cracked or non-cracked) (Grewin, Eligehausen (2003)). For sufficiently large head sizes (head pressure  $p_u < 6 \cdot f_c$ ) the influence length can be taken as:

$$l_i = 11 \cdot I^{0.05} \cdot s^{0.5} \geq s \quad [\text{mm}] \quad (3.10)$$

where:

- $I$  = moment of inertia of the channel [mm<sup>4</sup>]
- $s$  = anchor spacing [mm]

Fig. 3.44 shows the influence length as a function of the anchor spacing for three different sizes of channels. The influence length was evaluated from the results of calculations using a beam on elastic supports (Grewin, Eligehausen (2003)). Similar results were obtained in non-linear finite element calculations on anchor channels where failure was caused by concrete cone break-out (Kraus (2003)). For comparison the influence length according to equation (3.10) is plotted as well. It can be seen that equation (3.10) predicts the influence length found in numerical analysis quite well. Equation (3.10) may also be used if failure is caused by rupture of the anchors (Wüstner (2002)).

For an arbitrary position of the load  $N$  the forces on the anchors can be calculated in accordance with equation (3.11) (see example in Fig. 3.45).

$$N_{\text{anchor } i} = k \cdot A_i' \cdot N \quad (3.11)$$

where:

$$k = 1 / \sum A_i' \quad (3.11a)$$

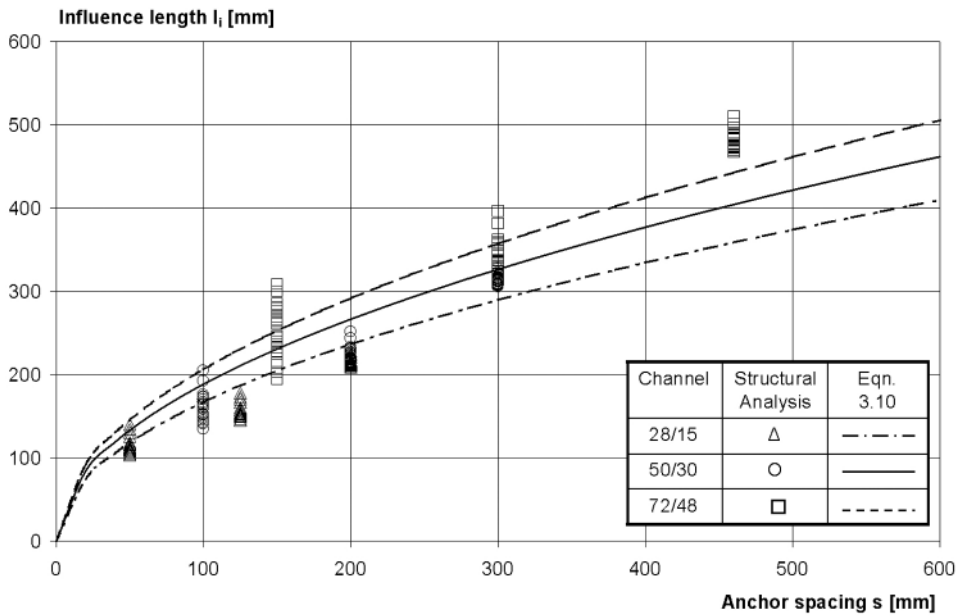


**Fig. 3.44** Influence length as a function of anchor spacing (Grewin, Eligehausen (2003))

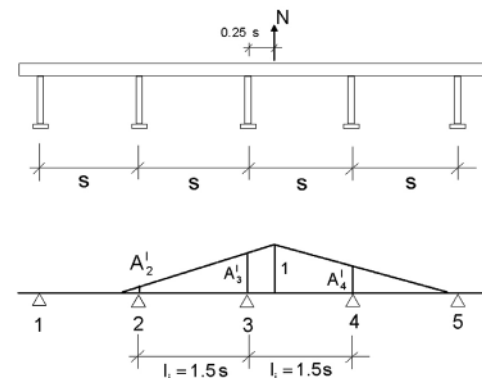
$A'_i$  ordinate of a triangle with a height  $l$  at the position of the load  $N$  and the base length  $2 \cdot l_i$  ( $l_i$  according to equation (3.10)) at the position of the anchor  $i$

If several tension loads are acting on the channel a linear superimposition of the anchor forces for all loads should be assumed. This approach is supported by the results of more than 200 finite element calculations on anchor channels with the failure mode concrete break-out (Kraus (2003)).

If in the design the exact position of the load on the channel is unknown the most unfavourable loading position should be assumed for each failure mode (e.g. load acting over an anchor for the case of failure of an anchor by steel rupture or concrete break-out and load acting between anchors in case of bending failure of the channel).

**3.7.3.2 Shear loads**

According to Eligehausen, Potthoff, Grewin, Lotze (2004) shear loads acting on the channel are mainly transferred by compression stresses



$$A'_2 = \frac{l - 1.25s}{l} = \frac{1}{6} \quad N_{\text{anchor},1} = N_{\text{anchor},5} = 0$$

$$A'_3 = \frac{l - 0.25s}{l} = \frac{5}{6} \quad N_{\text{anchor},2} = \frac{1}{6} \cdot \frac{2}{3} \cdot N = \frac{1}{9} N$$

$$A'_4 = \frac{l - 0.75s}{l} = \frac{1}{2} \quad N_{\text{anchor},3} = \frac{5}{6} \cdot \frac{2}{3} \cdot N = \frac{5}{9} N$$

$$k = \frac{1}{A'_2 + A'_3 + A'_4} = \frac{2}{3} \quad N_{\text{anchor},4} = \frac{1}{2} \cdot \frac{2}{3} \cdot N = \frac{1}{3} N$$

**Fig. 3.45** Example for the calculation of anchor tension forces according to the influence method for an anchor channel with five anchors. The influence length is assumed as  $l_i = 1.5 \cdot s$  (Kraus (2003))

between channel and concrete and to a smaller extent by the anchors. However, the anchors are stressed by tension forces due to the eccentricity between the acting shear load and the resultant of the stresses in the concrete. The anchor tension forces are much higher than the anchor shear forces.

In section 5.1.2.4 a model is described to calculate the concrete edge capacity of channel bars under shear loading towards the edge. It

assumes that shear forces acting on the channel are transferred by bending of the channel to the anchors and by the anchors into the concrete. This approach simplifies the real behaviour.

It has been chosen to allow for a simple interaction between tension and shear forces acting on the channel. For reasons of simplicity it is proposed to calculate the (fictitious) shear forces on anchors using the same approach and the same influence length as for tension loads.

## 4 Behaviour of headed studs, undercut anchors and metal expansion anchors in non-cracked and cracked concrete

Headed studs, undercut anchors and metal expansion anchors, regardless of their functional differences (see section 2), exhibit many similarities in load-bearing behaviour and they are therefore addressed jointly in this section.

The equations given in this section describe the mean failure load.

### 4.1 Non-cracked concrete

#### 4.1.1 Tension load

To assess the load-bearing behaviour of an anchor, we need to look at its load-displacement behaviour, failure modes, and ultimate capacity.

##### 4.1.1.1 Load-displacement behaviour and modes of failure

Anchors typically exhibit four possible failure modes when loaded in tension (Fig. 4.1). Each of these four failure modes is characterised by a unique load-displacement behaviour (Fig. 4.2). The total displacement measured at the surface of the concrete is made up of the displacement of the anchor with respect to the surrounding concrete (slip) plus the deformations in the base material and the steel components of the anchor.

##### a) Pull-out and pull-through failure

Pull-out failure is characterised by the anchor being pulled out of the drilled hole, whereby the concrete in the immediate vicinity of the anchor may or may not be damaged as well (Fig. 4.1a<sub>1</sub>). For a displacement-controlled expansion anchor this type of failure occurs when the expansion force is insufficient to hold the anchor at the installed embedment depth for the load corresponding to concrete cone failure. Curve a<sub>1,1</sub> in Fig. 4.2 depicts representative load-displacement relationship for a drop-in anchor exhibiting pull-out failure. At the first peak the static friction is exceeded, whereupon

the resistance drops and subsequent behaviour is governed by sliding friction. Since the surface of the drilled hole is typically uneven, the load-displacement curve is also irregular. Pull-out failure can also occur with torque-controlled expansion anchors when follow-up expansion of the anchor does not develop properly (see Fig. 4.2, curves a<sub>1,2</sub> and a<sub>1,3</sub>). The ultimate resistance that can be developed in these cases depends on the degree of irregularity in the surface of the drilled hole and cannot be predicted. As a consequence, this failure mode is not permitted for torque-controlled expansion anchors in some countries. In Europe, for example, approval tests on such anchors must verify that this failure mode will not occur (see section

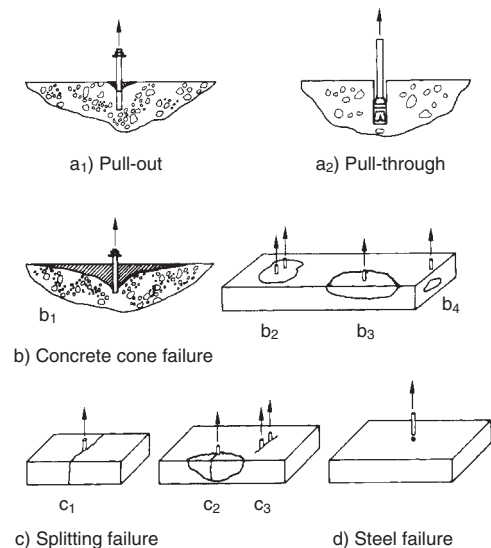


**Fig. 4.1** Failure modes associated with tension loading  
a) Pull-out and pull-through failure  
b) Concrete cone failure  
c) Splitting failure  
d) Steel failure

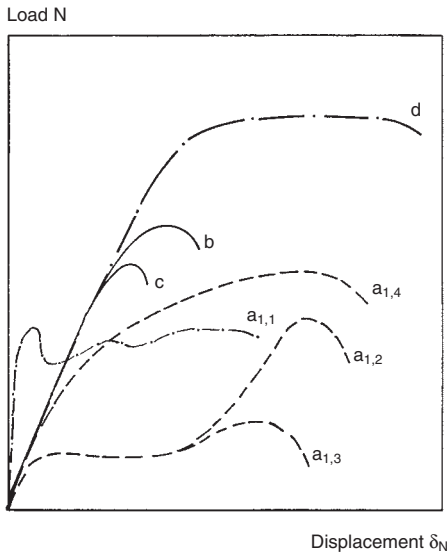


**Fig. 4.2** Idealised load-displacement curves for tension-loaded anchors exhibiting various failure modes (after Fuchs, Eligehausen, Breen (1995))

14.2). Pull-out failure can occur with undercut anchors and headed studs if the mechanical interlock (bearing surface) is inadequate. The load-displacement behaviour associated with this case is represented by curve  $a_{1,4}$  in Fig. 4.2.

Pull-through (Fig. 4.1a<sub>2</sub>), whereby the cone is pulled through the expansion sleeve, is a failure mode unique to torque-controlled expansion anchors that exhibit follow-up expansion. It is a failure mode that is consistent with the correct function of the anchor. The load-displacement behaviour is similar to that exhibited by undercut anchors and headed studs failing by pull-out (Fig. 4.2, curve  $a_{1,4}$ ). The initial stiffness, ultimate capacity, and displacement at ultimate load depend substantially on the geometry and construction of the anchor. The ultimate capacity is, however, reduced compared with an anchor of equal embedment failing by concrete cone breakout.

#### **b) Concrete cone failure**

The concrete cone breakout failure mode is characterised by the formation of a cone-shaped fracture surface in the concrete (Fig. 4.1b<sub>1</sub>). The full tensile capacity of the concrete is utilised. Expansion anchors that develop sufficient

expansion force exhibit concrete cone breakout provided they do not fail by pull-through or steel rupture. Likewise, headed studs and undercut anchors with an adequately large bearing surface will generate concrete cone breakout failures if the steel capacity is not exceeded. A load-displacement curve characteristic of concrete cone breakout failure is shown in Fig. 4.2, curve b. The load-displacement behaviour is relatively non-ductile, but the deformations at service load and at failure depend largely on the anchor type (Fig. 4.3). In the tests represented in Fig. 4.3, the installation prestressing force was relaxed by loosening the nut or bolt prior to loading. Fully expanded drop-in anchors exhibit the smallest displacement of any expansion anchor failing by concrete cone breakout (Fig. 4.3a) because the high expansion forces associated with these anchors prevent anchor slip. Conversely, self-drilling anchors exhibit relatively large displacements because the concrete bearing pressures in the expansion zone are very high. The displacement of torque-controlled expansion anchors is increased by the relative movement between the expansion cone and anchor sleeve associated with follow-up expansion. Undercut anchors and headed studs transfer the tensile force into the base material through bearing (mechanical interlock). Consequently, for the same load, the amount of displacement depends on the bearing contact area and the initial fit between anchor and undercut geometry (Fig. 4.3b).

If several closely spaced anchors are loaded jointly in tension via a fixture, as in a baseplate application, then an aggregated concrete cone breakout may occur (Fig. 4.1b<sub>2</sub>). If an anchor is installed near the edge of a concrete component and loaded in tension to failure, the breakout cone may involve the edge as shown in Fig. 4.1b<sub>3</sub>. Headed studs and undercut anchors placed very close to an edge and loaded in tension may precipitate a local blow-out failure of the concrete in the vicinity of the anchor head (Fig. 4.1b<sub>4</sub>). In all of these cases the load-carrying capacity of the anchor is diminished relative to that associated with larger anchor spacing and edge distances. The load-displacement behaviour of anchors exhibiting these failure modes generally corresponds to that of curve c in Fig. 4.2, whereby the stiffness is unaffected,

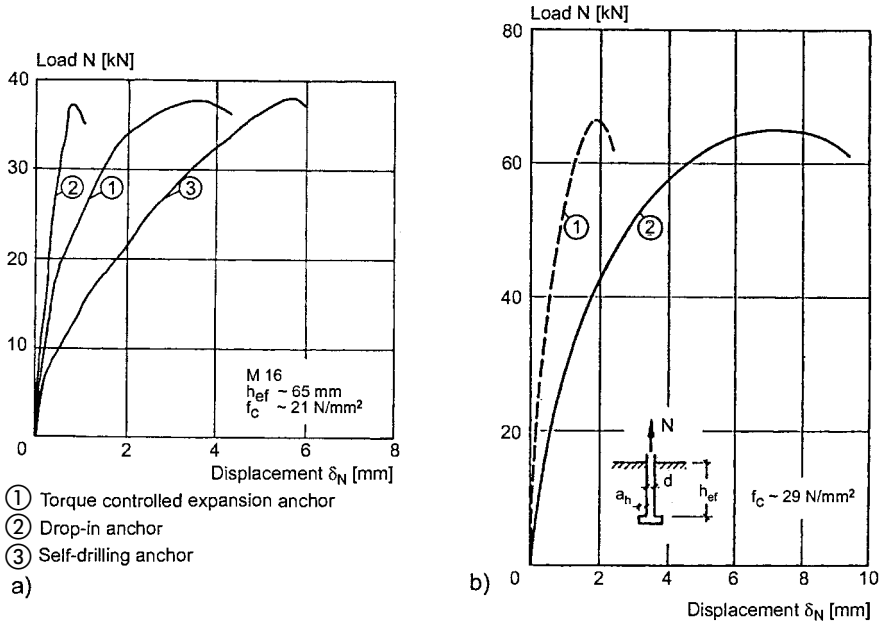


**Fig. 4.3** Load-displacement curves for various anchor types  
 a) Metal expansion anchors (Eligehausen, Pusill-Wachsmuth (1982))  
 b) Undercut anchors and headed studs (Rehm, Eligehausen, Mallée (1988))

Line	Type of anchor	d [mm]	a <sub>h</sub> [mm]	h <sub>ef</sub> [mm]
1	Headed anchor	22	6.5	80
2	Undercut anchor	18	3.0	80

but the ultimate load is determined by the anchor spacing and/or edge distance.

**c) Splitting failure**

In general, anchor failure due to splitting of the concrete occurs when the dimensions of the concrete component are limited (Fig. 4.1c<sub>1</sub>), the anchor is installed close to an edge (Fig. 4.1c<sub>2</sub>) or a line of anchors are installed in close proximity to each other (Fig. 4.1c<sub>3</sub>). The failure load associated with splitting is reduced relative to that corresponding to concrete cone failure, but the load-displacement response is similar in each case (Fig. 4.2, curve c).

**d) Steel failure**

Failure of the steel stud, bolt or sleeve (Fig. 4.1d) represents an upper limit on the achievable load-carrying capacity of an anchor. A ductile load-displacement curve results if the steel is ductile and if sufficient bolt length is provided for the steel elongation to occur. A representative load-displacement curve for a ductile anchor failure is provided as curve d in Fig. 4.2.

Note that this anchor has a larger embedment depth (in order to assure steel failure and to provide the necessary bolt length) than the anchors associated with curves a, b, and c.

As a consequence of the desire to maximise load capacity for a given depth of embedment, most anchor systems currently available exhibit concrete cone breakout when loaded in tension to failure. Steel rupture rarely occurs and then only in high-strength concrete. Pull-through failures typically occur when torque-controlled expansion anchors are equipped with smaller expansion elements and a relatively small expansion reserve (as, for example, in the case of wedge-type anchors, see Fig. 2.19a<sub>3</sub>). Splitting of the concrete during anchor installation can be avoided by observing minimum anchor spacing, edge distances and component dimensions.

Headed stud anchorages in general exhibit steel failure, concrete cone failure or concrete splitting failure depending on steel grade, concrete strength, embedment depth, thickness of com-

ponent and spacing or edge distance. Pull-out failure will occur only if the mechanical interlock (bearing surface) is too small.

Anchors should be as stiff as possible in the serviceability state in order to prevent loosening of the fixture. On the other hand, visible displacement of the anchor in the limit state is desirable so that (a) imminent failure (overload) of the anchor can be recognised and (b), in the case of anchor groups, load redistribution to less highly stressed anchors in the group can occur. For anchors that typically exhibit concrete cone

breakout, or when splitting of the concrete is the controlling failure mode, these two criteria cannot necessarily be fulfilled. Some anchors exhibit a more favourable behaviour than others in this respect (Fig. 4.3). Where steel failure controls, the ideal load-displacement behaviour can only be guaranteed when the free bolt length over which tensile strains are developed is sufficiently large and the steel used is ductile. In the pull-through failure mode, anchors may behave in a pseudo-ductile fashion provided they have an adequate expansion reserve. However, in all of these cases reduced anchor spacing and edge distances can lead to concrete cone failure with correspondingly brittle behaviour.

Owing to the unique load-displacement behaviour associated with individual anchors, only anchors of *one* type and *one* size (diameter, embedment) should be used in groups. Furthermore, excessive variations in the load-displacement behaviour associated with the anchors must be avoided if the ultimate capacity of the group is to be maximised. For this reason, specific limits regarding variations in load-displacement behaviour are included in Europe's approval procedure.

#### 4.1.1.2 Failure load associated with steel rupture

If anchor failure is characterised by rupture of the steel, then the ultimate load  $N_{u,s}^0$  can be calculated from the stressed cross-sectional area and the tensile strength of the steel as follows:

$$N_{u,s}^0 = A_s \cdot f_u \tag{4.1}$$

where:

$A_s$  = tensile cross-sectional area for threaded parts or net cross-section of the headed stud shaft

$f_u$  = measured tensile steel strength

Where headed studs are welded to an embedded plate, the welded connection should be proportioned to preclude failure of the weld prior to reaching the stud ultimate strength as governed by equation (4.1).

For anchor groups loaded with a tensile force acting concentrically on a stiff fixture (Fig. 4.4a), the failure load of the group may be calculated using equation (4.2):

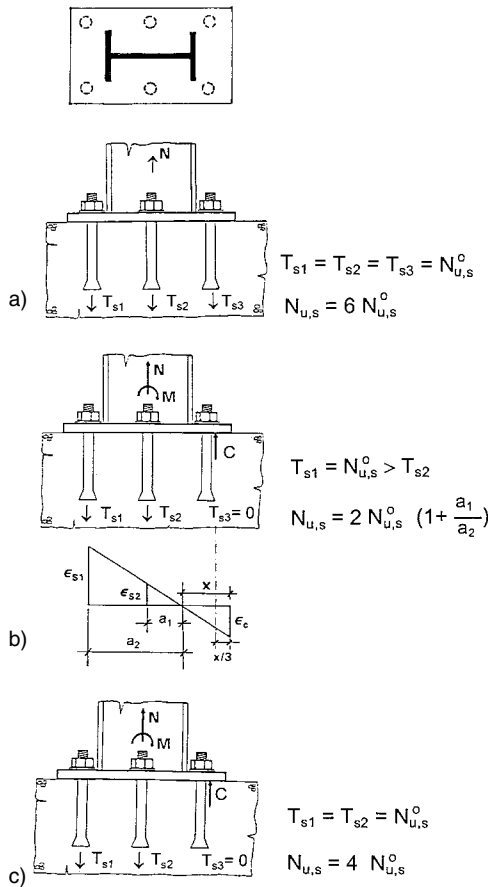


**Fig. 4.4** Steel failure load for a tension-loaded anchor group

- a) Concentric tension load
- b) Tension load and bending moment, distribution of forces calculated according to elastic theory
- c) Tension load and bending moment, distribution of forces calculated according to plastic theory



$$N_{u,s} = n \cdot N_{u,s}^0 \quad (4.2)$$

where:

$n$  = number of anchors in group

If the tensile force acts eccentrically on a stiff fixture, then the loads on the individual anchors are generally calculated assuming elastic behaviour (Fig. 4.4b), i.e. the anchor or stud carrying the highest load determines the failure load of the group. The failure load of the anchors in tension for the example shown in Fig. 4.4b is calculated using equation (4.3):

$$N_{u,s} = 2 \cdot N_{u,s}^0 \cdot \left(1 + \frac{a_1}{a_2}\right) \quad (4.3)$$

Given anchors with sufficient ductility (adequate strained length and ductile steel), plastic theory can be used for the analysis of eccentrically loaded anchor groups. This approach dictates that at ultimate all anchors in tension develop the resistance given by equation (4.1) (Cook, Klingner (1989)). For the example shown in Fig. 4.4c, the failure load of anchors in tension is calculated using equation (4.4):

$$N_{u,s} = 4 \cdot N_{u,s}^0 \quad (4.4)$$

The necessary criteria for anchors to be considered ductile is dealt with in section 14.4.13.

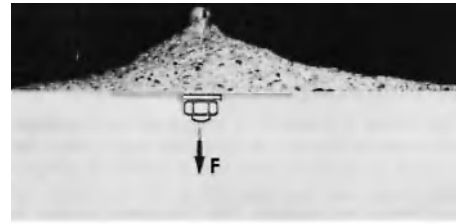
The failure load of a group for a given eccentricity  $e = M/N$  of the external action is calculated from the failure load of the anchors in tension either according to equation (4.3) or (4.4) and the connection geometry.

The failure load associated with steel rupture is not influenced by reinforcement in the concrete.

#### 4.1.1.3 Failure load associated with concrete cone breakout

##### a) General

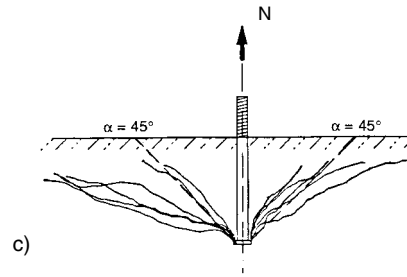
The majority of mechanical and cast-in-place anchor systems exhibit concrete cone breakout at failure. The concrete breakout surfaces produced by mechanical anchor bolts and cast-in-place headed studs are similar (Fig. 4.5a, b). The slope of the fracture surface is not constant as measured over the depth or the circumference as measured (Fig. 4.5c, d), and it varies from test to test. The slope as measured from the horizontal and averaged over the circumference lies between



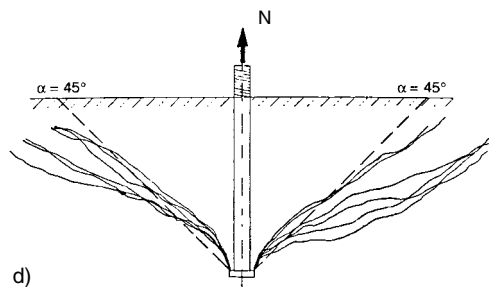
a)



b)



c)



d)

**Fig. 4.5** Concrete failure cones and sections through concrete failure cones

- a) Torque-controlled expansion anchor,  $h_{ef} = 130$  mm
  - b) Headed stud,  $h_{ef} = 520$  mm
  - c) Headed studs  $h_{ef} = 260$  mm
  - d) Headed studs  $h_{ef} = 520$  mm
- (a) after Rehm, Eligehausen, Mallée (1988),  
 (b-d) after Forschungs- und Materialprüfungsanstalt Baden-Württemberg (1985/1)

30° and 40°, and is on average about 35° (Fig. 3.28). It tends to increase with increasing embedment depth (Zhao (1993)). The slope of the failure cone also depends on the stress condition in the base material around the anchorage. Compressive or tensile stresses acting in the concrete perpendicular to the direction of the anchor load cause the slope of the failure surface to be steeper or shallower, respectively. Noting that the effective embedment depth,  $h_{ef}$ , designates the distance between the surface of the concrete and the end of the force transfer zone (Figs. 4.7 and 4.8), the depth of the concrete breakout surface varies between  $0.8 \cdot h_{ef}$  to  $1.0 \cdot h_{ef}$  for mechanical expansion anchors. For headed studs and undercut anchors the depth of the failure surface tends to be equal to  $h_{ef}$ .

The literature contains numerous analytical approaches, based on various assumptions, for calculating the failure load associated with concrete cone breakout. In the approach according to American Concrete Institute, *ACI 349* (1990) a 45° failure cone and a constant tensile stress over the projected failure surface were selected (Fig. 4.6a). The calculated failure loads correlate with the results of tests with a limited range of embedment depths (Fig. 4.41). However, this approach cannot be applied over the full range of embedment depths because the size effect is neglected (compare section 3.3.1, Fig. 3.19, and Fig. 4.42) and the assumption of a constant tensile stress over the failure surface deviates considerably from the reality (see Fig. 3.27).

In *Braestrup, Nielsen, Jensen, Bach* (1976) yield theory is employed to calculate the concrete cone breakout load of headed studs. However, concrete in tension does not exhibit the elasto-plastic behaviour assumed in this approach. Therefore, an artificially low concrete tensile strength is used to calibrate the calculated failure loads with the test results considered.

A realistic analysis of the concrete cone breakout load is only possible when the non-linear behaviour of concrete in tension is taken into account. Therefore, *Pusill-Wachsmuth* (1982) assumes that failure occurs when the tensile stress in the concrete, calculated with the help of elastic theory and averaged over the so-called characteristic unit volume, equals the uniaxial tensile strength. However, this method cannot

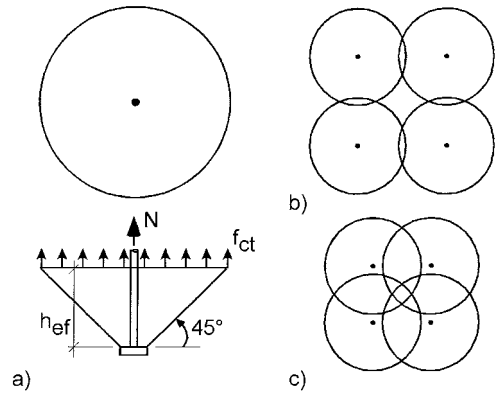


**Fig. 4.6** Shape of concrete cone according to *ACI 349* (1990)

- a) Single anchor
- b) Projected areas of a group of four anchors, large spacing
- c) Projected areas of a group of four anchors, small spacing

be applied generally because the size of the characteristic unit volume is not constant and must be calibrated with test results. The failure load associated with concrete cone breakout can be realistically assessed with the help of non-linear fracture mechanics. The corresponding work in this area is described in section 3.3.1. However, these numerical studies are relatively time-consuming and elaborate, and the required numerical analysis tools are not widely available. A more practical solution is to assess the failure loads of anchors via empirically derived equations that encompass theoretical models. This approach has led to the development of the CC (Concrete Capacity) Method (*Fuchs, Eligehausen, Breen* (1995/1) and (1995/2), *Fuchs, Eligehausen* (1995)), which is described below. In the US, this approach is termed CCD (Concrete Capacity Design) Method.

The CC-Method is based on the same mechanical model as the  $\kappa$ -Method, which is described in detail in *Rehm, Eligehausen, Mallee* (1992). The CC-Method visualises the  $\kappa$ -factors in the  $\kappa$ -Method and is very user friendly.

#### b) Single anchors with large edge distance subjected to axial tension loading

Figs 4.7 and 4.8 plot failure loads associated with concrete cone breakout as a function of anchor effective embedment depth. Repre-

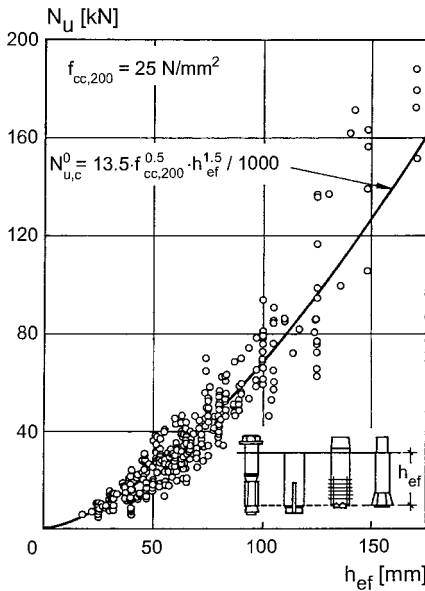


**Fig. 4.7** Concrete cone failure loads of expansion anchors and undercut anchors subjected to concentric tension as a function of embedment depth (test results after Fuchs, Eligehausen, Breen (1995))

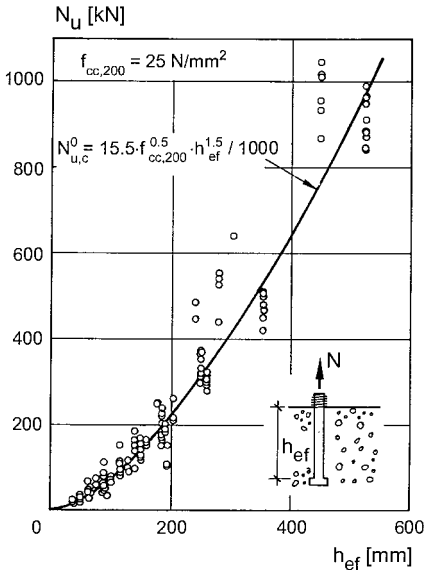


**Fig. 4.8** Concrete cone failure loads of headed studs subjected to concentric tension as a function of embedment depth (test results after Eligehausen, Fuchs, Ick, Mällée, Reuter, Schimmelpfennig, Schmal (1992) and Eligehausen, Bouska, Cervenka, Pukl (1992))

sented are results of tests with expansion anchors, undercut anchors with standard undercut dimensions, and headed studs, all conducted with large spacing and edge distance. The tests were conducted in concrete specimens of varying strength and as such, the measured failure loads have been normalised via the concrete tensile strength, assumed to be proportional to  $f_{cc,200}^{0.5}$ , to a concrete compressive strength  $f_{cc,200} = 25 \text{ N/mm}^2$ . Fig. 4.7 illustrates the results of 519 test series and Fig. 4.8 represents 318 individual tests. The mean failure load may be calculated as follows:

$$N_{u,c}^0 = k_1 \cdot f_{cc,200}^{0.5} \cdot k_2 \cdot h_{ef}^2 \cdot \frac{k_3}{h_{ef}^{0.5}} \quad (4.5a)$$

$$= k \cdot h_{ef}^{1.5} \cdot f_{cc,200}^{0.5} \quad [\text{N}] \quad (4.5b)$$

where:

$k = 13.5 \text{ [N}^{0.5}/\text{mm}^{0.5}]$  (expansion anchor)

(Eligehausen, Fuchs, Mayer (1987))

$= 15.5 \text{ [N}^{0.5}/\text{mm}^{0.5}]$  (headed stud)

(Eligehausen, Fuchs, Ick, Mällée,

Reuter, Schimmelpfennig, Schmal

(1992))

$h_{ef}$  = embedment depth [mm]

(see Figs 4.7 and 4.8)

$f_{cc,200}$  = concrete cube compressive strength [N/mm<sup>2</sup>] at the time of the test

If in equation (4.5) the cylinder strength  $f_c$  is used instead of the cube strength  $f_{cc,200}$  we get with  $f_c = 0.85 \cdot f_{cc,200}$ :

$$N_{u,c}^0 = k' \cdot h_{ef}^{1.5} \cdot f_c^{0.5} \quad [\text{N}] \quad (4.5c)$$

where:

$k' = 14.6 \text{ [N}^{0.5}/\text{mm}^{0.5}]$  (expansion anchor)

$= 16.8 \text{ [N}^{0.5}/\text{mm}^{0.5}]$  (headed stud)

In equation (4.5a) the factor  $k_1 \cdot f_{cc,200}^{0.5}$  specifies the concrete tensile capacity,  $k_2 \cdot h_{ef}^2$  the surface area of the concrete failure cone, and  $k_3 / h_{ef}^{0.5}$  the size effect, whereby the largest possible size effect predicted by linear fracture mechanics is assumed. The size effect predicts that at ultimate load the tensile stresses in the concrete averaged over the fracture surface decrease as the thickness of the component increases. It applies not only to the anchorage problem but more generally to concrete subjected to tensile strain gradients, as exemplified by flexural

stresses in non-reinforced beam sections, punching shear and shear in beams and slabs without shear reinforcement. The size effect was verified with fracture mechanics in a general sense by *Bazant* (1984), and for anchors by *Sawade, Eligehausen* (1989), *Eligehausen, Ozbolt* (1990) and *Ozbolt* (1995) (see section 3.3.1). Equation (4.5) is a simplification of equation (3.5).

The failure load as given by equation (4.5) depends solely on the concrete compressive strength (as a placeholder for the concrete tensile capacity) and the embedment depth. Test

results indicate that the diameter of the anchor has no significant influence.

Evaluation of test results indicates that headed studs produce failure loads approximately 15% higher than those developed by expansion anchors.

This is due to the favourable influence of the head, which theoretically results in a larger fracture surface for a given embedment depth, and lower stresses in the concrete in the force transfer zone. Undercut anchors that produce a sufficiently large undercut area can match the concrete cone breakout failure loads of headed studs.

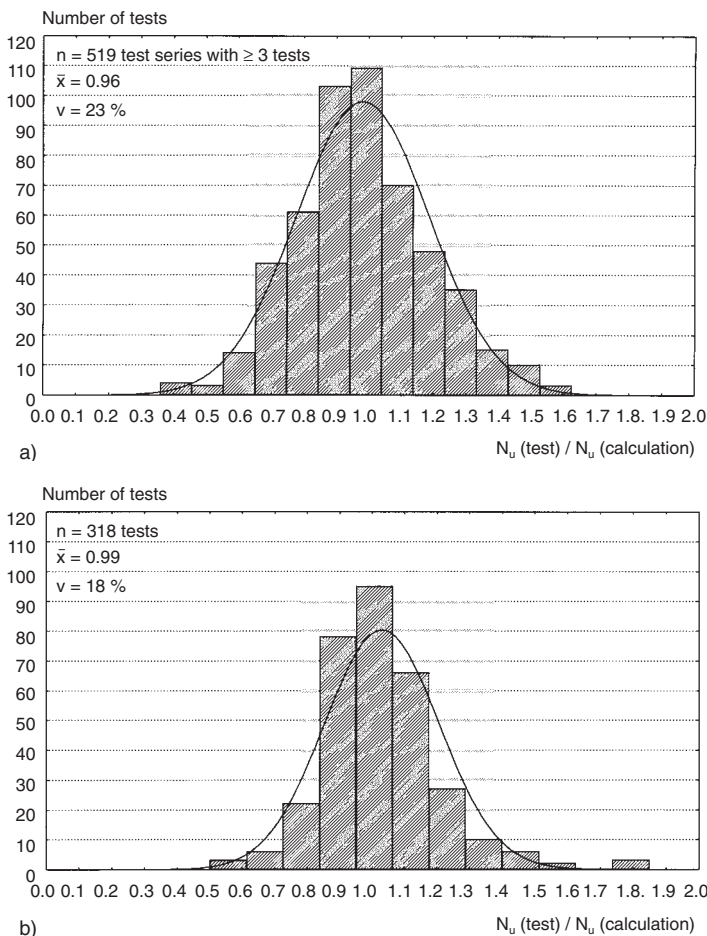


**Fig. 4.9** Histogram of measured to calculated concrete cone failure loads for anchors subjected to concentric tension

a) Expansion anchors, test data corresponding to Fig. 4.7

b) Headed studs, test data corresponding to Fig. 4.8

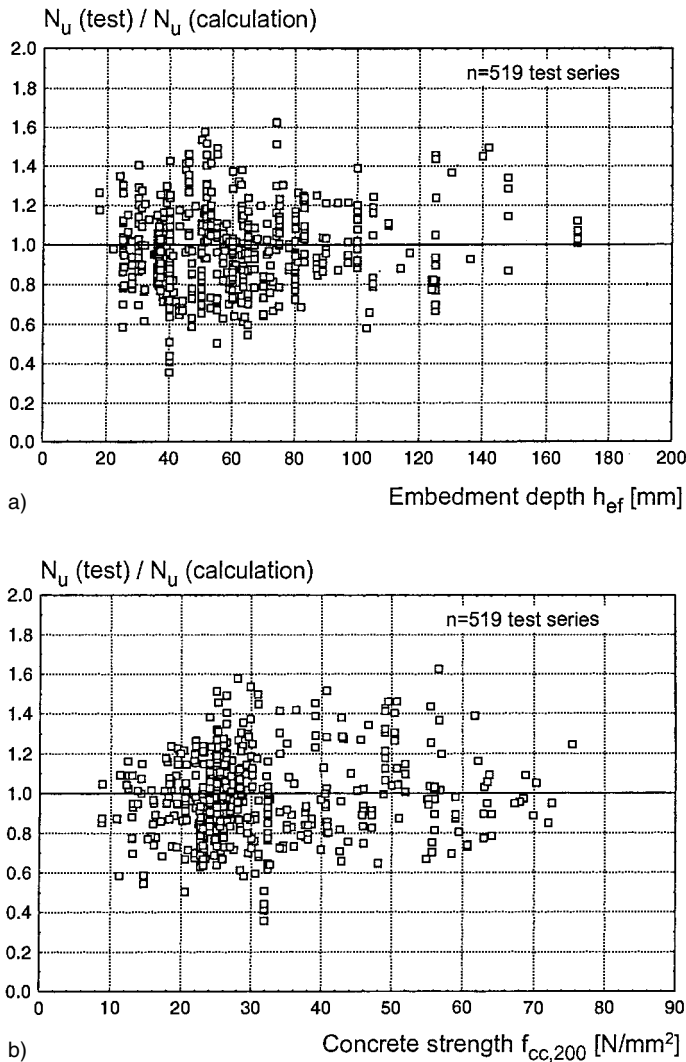


**Fig. 4.10** Ratio of measured to calculated concrete cone failure loads for anchors subjected to concentric tension (test data corresponding to Fig. 4.7)  
 a) As a function of embedment depth  
 b) As a function of concrete compressive strength

The ratio  $N_u(\text{test})/N_u(\text{calculation})$  exhibits a normal distribution (Fig. 4.9). The average value is  $\bar{x} \sim 1.0$ , with coefficients of variation  $v \sim 23\%$  (expansion anchors) and  $v \sim 18\%$  (headed studs). These values are greater than the scatter associated with measurements of concrete tensile strength. The increased scatter, especially for the expansion anchor base,

can be attributed to the fact that several different anchor systems are represented in the tests. In addition, the tests were conducted in specimens made from a range of concrete mix designs. In tests with *one* type of anchor in *one* concrete type, the scatter of the failure loads ( $v < 10\%$ ) corresponds roughly to that associated with the concrete tensile strength.

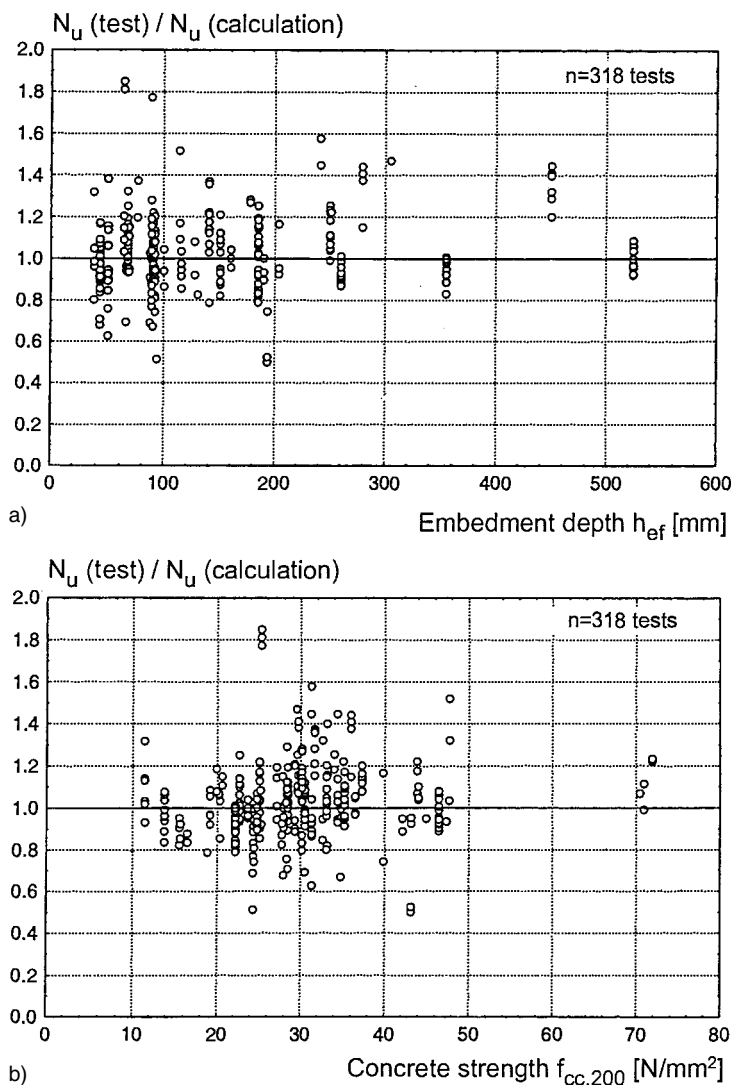


**Fig. 4.11** Ratio of measured to calculated concrete cone failure load of headed studs (test data corresponding to Fig. 4.8)

- a) As a function of embedment depth  
 b) As a function of concrete compressive strength

The ratio of measured to calculated failure loads for expansion anchors is plotted in Fig. 4.10 as a function of the embedment depth (Fig. 4.10a) and of the concrete compressive strength (Fig. 4.10b). Fig. 4.11 is valid for headed studs. Analysis of the data reveals that the failure loads are distributed roughly evenly above and

below a line corresponding to  $N_u(\text{test})/N_u(\text{calculation}) = 1$ , indicating that the influence of these parameters on the concrete cone breakout failure load is correctly assessed in equation (4.5).

To date, the validity of equation (4.5) has been experimentally verified for embedment depths  $h_{ef}$  up to 525 mm. However, as equation (4.5) is based on linear fracture mechanics and therefore takes into account the largest possible size effect, it is equally well suited to larger embedment depths (Fig. 3.19b).

Equation (4.5) has been experimentally verified for the concrete strength range  $13 \text{ N/mm}^2 \leq f_c \leq 60 \text{ N/mm}^2$ , i.e. for concrete grades C12/15 to C60/75. Tests with undercut anchors are described in *Zeitler, Wörner* (1995), with concrete strengths ranging from  $f_c \approx 30 \text{ N/mm}^2$  to  $f_c \approx 110 \text{ N/mm}^2$ . These test results indicate that the concrete cone breakout failure load rises roughly in proportion to  $f_c^{2/3}$ . In studies by *Sawade* (1994) and *Ozbolt* (1995) the concrete cone breakout failure load was found to be proportional to  $(E_c \cdot G_f)^{0.5}$  (see Fig. 3.29). According to *Remmel* (1994)  $E_c$  increases in proportion to  $f_c^{0.3}$  and  $G_f$  is approximately constant for  $f_c \geq 70 \text{ N/mm}^2$  (see Fig. 3.8b). Therefore, the concrete compressive strength can be expected to have less of an influence on the concrete cone breakout failure load in high-strength concrete than in low-strength concrete. This was confirmed in tests conducted by *Primavera, Pinelli, Kalajian* (1997). Their results indicate that the increase in concrete cone breakout failure loads of headed studs and undercut anchors is less than proportional to  $f_c^{0.5}$  as the concrete compressive strength ranges from  $f_c \approx 40 \text{ N/mm}^2$  to  $f_c \approx 70 \text{ N/mm}^2$ . The apparent differences in the results of *Zeitler, Wörner* (1995) and *Primavera, Pinelli, Kalajian* (1997) may be accounted for by differences in concrete composition. However, pending clarification of the relationship, it is recommended that the concrete cone breakout failure load be calculated using equation (4.5), but to restrict its application to concrete grades  $\leq C 70$ .

Analysis of the existing data indicates that post-installed anchors with the same embedment depth in concrete of the same compressive strength achieve similar concrete cone breakout failure loads regardless of whether the load is transferred to the base material by means of friction (torque- or displacement-controlled expansion anchors), mechanical interlock (undercut anchors with standard bearing area) or a combination of these two principles (self-drilling anchors). Note that this applies only to anchors installed in non-cracked concrete as discussed in this section.

Equation (4.5) applies to expansion anchors for which the expansion force is matched to the design embedment depth in such a way that concrete cone breakout precedes pull-out of the

anchor. For each diameter of a given anchor type there is an associated embedment depth corresponding to concrete cone breakout. Theoretically, if an expansion anchor is installed deeper than the embedment associated with fulfilment of this criterion, the failure load does not increase further. Either the anchor slips in the hole until a concrete cone failure takes place at a correspondingly reduced embedment depth, or, in the case of torque-controlled expansion anchors, the cone may be pulled through the sleeve (pull-through failure). In practice the failure loads associated with deeper set anchors are generally higher (Fig. 4.12) because the

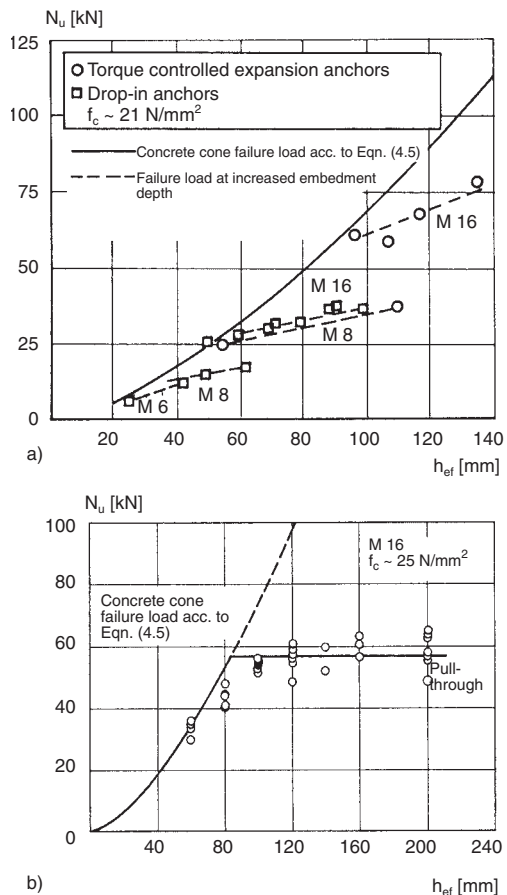


**Fig. 4.12** Failure load as a function of embedment depth for anchors installed at increasing embedments and loaded in tension (a) after *Eligehausen, Pusill-Wachsmuth* (1982), (b) after *Eligehausen, Okelo* (1996))



expansion force, which may be affected by varying concrete properties, hole tolerances and local defects in the concrete, is rarely matched precisely to the design embedment depth. For a torque-controlled expansion anchor of a given diameter, the limit on load-carrying capacity with increasing embedment is represented by pull-through (Fig. 4.12b) or steel rupture. However, additional embedment may be beneficial because the displacements associated with peak load are increased.

If the concrete bearing stress generated in the load transfer zone of undercut or headed anchors at peak load exceeds a limiting value, the failure load will be reduced as a consequence of increased displacement (and corresponding reduction in the effective embedment depth) as compared to the value predicted by equation (4.5) (see section 4.1.1.5).

Local flaws in the concrete and abandoned bore holes exert a minor influence on the concrete cone breakout load, provided they are not located in the direct vicinity of the load transfer zone. As a rule, empty holes in the concrete should be filled completely with cement grout or a synthetic resin mortar if they are nearer than twice the hole diameter to the anchor location (*Burdette, Sen, Ismen* (1982)).

#### c) Anchor groups with large edge distance subjected to axial tension loading

Consideration of the overlap of failure surfaces is a convenient way of measuring the effect of spacing on ultimate capacity. The concrete cone breakout load given by equation (4.5) assumes that a sufficient volume of concrete is available for each anchor to develop its full capacity. If, however, anchors are grouped such that the individual failure cones overlap or a common

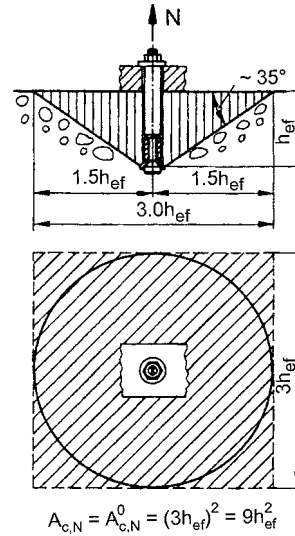


**Fig. 4.14** Concrete cone failure surface (idealised) (after *Fuchs, Eligehausen* (1995))

failure cone develops (Fig. 4.13), the failure load is reduced with respect to the sum of the individual anchor maximum capacities as determined by concrete cone breakout.

For the purpose of evaluating the effect of anchor spacing on group capacity, the slope of the concrete failure surface measured with respect to the surface of the concrete may be taken as approximately 35°, defining a projected surface whose diameter is approximately three times the embedment depth (Fig. 4.14). This implies that the distance between individual anchors or headed studs should be at least  $s = 3 \cdot h_{ef}$  to prevent overlap of the individual failure surfaces (Fig. 4.15a). If this condition is met, a group of  $n$  anchors or headed studs subjected to a concentric

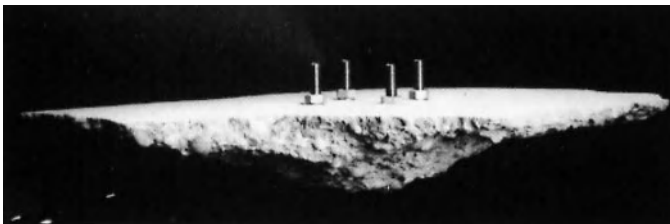


**Fig. 4.13** Concrete cone failure of a group of four undercut anchors (*Rehm, Eligehausen, Mallée* (1988))

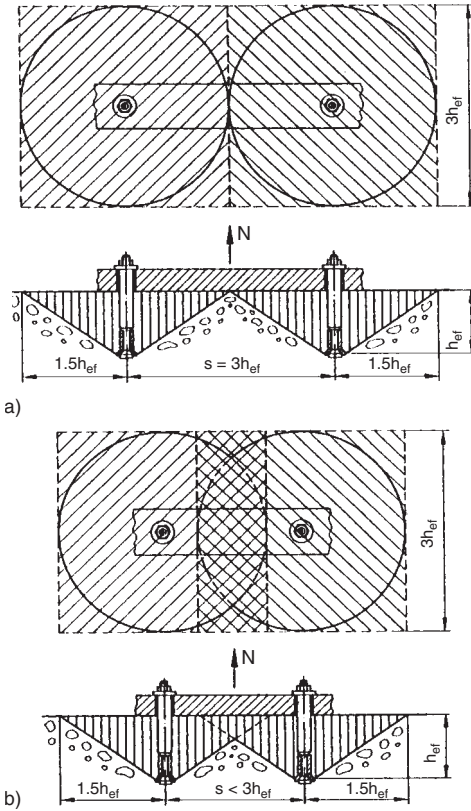


**Fig. 4.15** Influence of anchor spacing on shape of concrete cone failure surface of a group with two anchors loaded in tension (idealised) (after Fuchs, Eligehausen (1995))  
 a) Large spacing, b) Small spacing

tension load should be able to carry  $n$  times the failure load of one anchor calculated according to equation (4.5). This assumes that the tension load is distributed evenly to all anchors, e.g. via a stiff fixture. If the spacing  $s$  of the anchors within a group is  $s < 3 \cdot h_{ef}$  (Fig. 4.15b), then the concrete failure surfaces overlap and the failure load is reduced.

The concrete cone failure load of multiple anchors with a spacing  $s \leq 3 \cdot h_{ef}$  can be readily calculated using the CC-Method (Fuchs, Eligehausen (1995), Fuchs, Eligehausen, Breen (1995)) as follows:

$$N_{u,c} = \frac{A_{c,N}}{A_{c,N}^0} \cdot N_{u,c}^0 \quad [\text{N}] \quad (4.6)$$

where:

$A_{c,N}^0$  = projected area of a single anchorage with large spacing and edge distance with the concrete cone idealised as a pyramid of height  $h_{ef}$  and base length  $s_{cr,N} = 3 \cdot h_{ef}$  (Fig. 4.14)  
 $= 9h_{ef}^2$

$A_{c,N}$  = projected area of the concrete cone for the anchorage under consideration, limited by the overlap of the individual concrete cones of adjacent anchors ( $s \leq s_{cr,N}$ ) and the edges of the component ( $c \leq c_{cr,N}$ ). Fig. 4.16 provides examples for the calculation of  $A_{c,N}$

$s_{cr,N}$  = spacing required to allow the formation of an unrestricted concrete cone, i.e. development of the tension resistance of one anchor according to equation (4.5)  
 $= 3 \cdot h_{ef}$

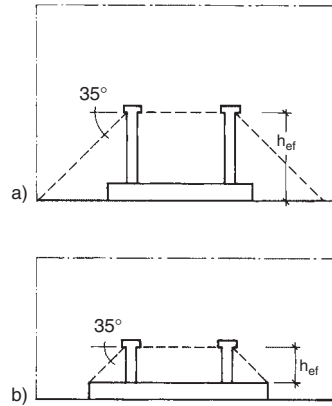
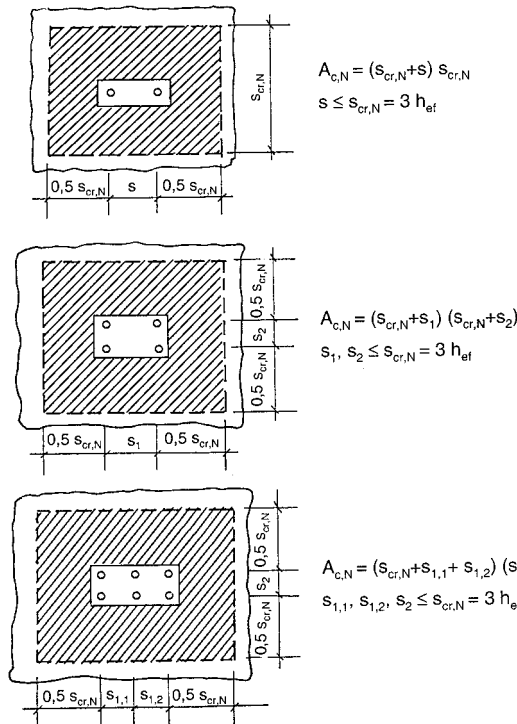
$c_{cr,N}$  = edge distance required to allow the formation of an unrestricted shear cone, i.e. development of the tension resistance of one anchor according to equation (4.5)  
 $= 1.5 \cdot h_{ef}$

$N_{u,c}^0$  as per equation (4.5b) or (4.5c)

The factor  $A_{c,N} / A_{c,N}^0$  takes into account the geometrical influence of anchor spacing on the concrete cone breakout load. It is assumed that the failure load increases in proportion to the area  $A_{c,N}$ .

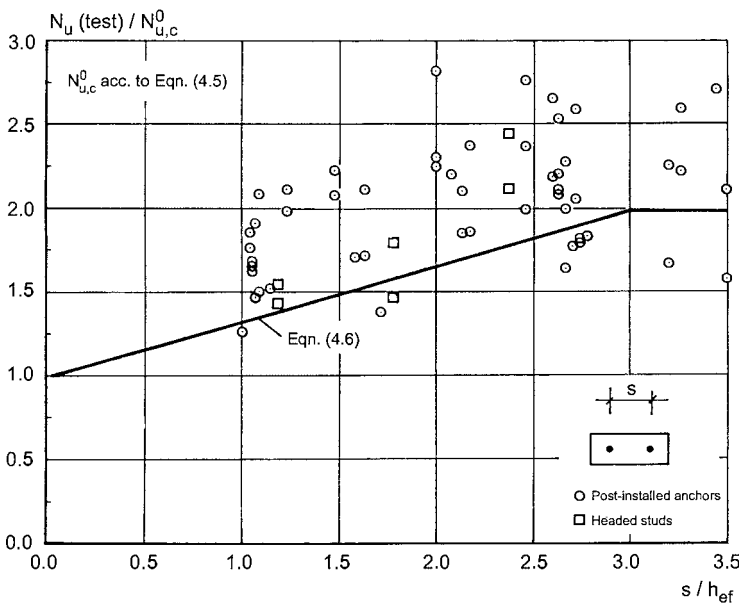
The embedment depth in equations (4.5) and (4.6) for anchorages with headed studs welded to an embedded fixture is to be taken as the distance between the surface of the concrete and the bearing surface of the head provided that the fixture lies fully within the projection of the idealised concrete cone (Fig. 4.17a). If this condition is not satisfied, then the embedment depth should be taken as the distance between the bearing surface of the head and the inside face of the fixture (Fig. 4.17b).

Fig. 4.18 compares measured concrete cone failure loads with calculated values using equation (4.6) for pairs of anchors. At a spacing  $s = 3 \cdot h_{ef}$  the failure load of the pair corresponds



**Fig. 4.17** Definition of embedment depth for anchors attached to a cast-in-place baseplate

**Fig. 4.16** Definition of projected area for groups of anchors in tension and with large edge distance



**Fig. 4.18** Influence of anchor spacing on the concrete cone failure load of groups with two anchors subjected to concentric tension (after Eligehausen, Fuchs, Mayer (1987))

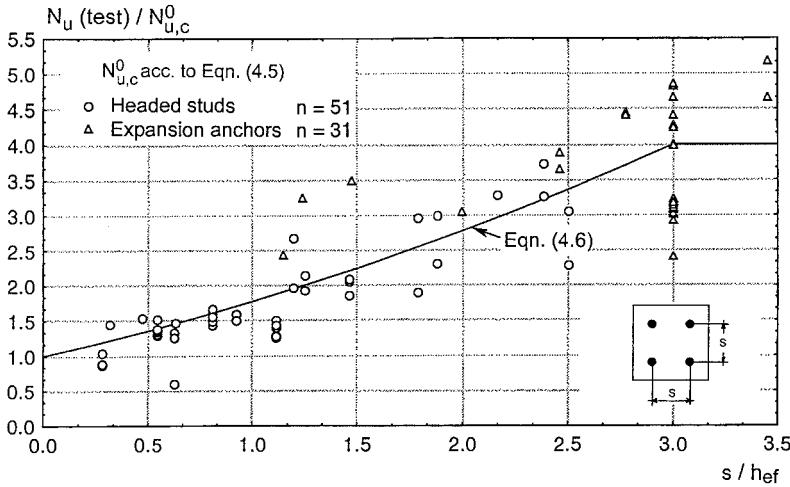


**Fig. 4.19** Influence of anchor spacing on the concrete cone failure loads of groups with four anchors subjected to concentric tension (test data from *Eligehausen, Fuchs, Mayer (1987)* (expansion anchors) and *Eligehausen, Fuchs, Ick, Mallée, Reuter, Schimmelpfennig, Schmal (1992)* (headed studs))

to two times the failure load for one anchor. At the theoretical limit state of  $s = 0$ , the concrete cone corresponding to one anchor is developed and the failure load for the group corresponds to that for one anchor. According to the CC-Method, a linear relationship is assumed between these two limits. Fig. 4.18 indicates that this approach is conservative.

Fig. 4.19 compares the concrete cone failure loads of square groups with four expansion anchors or headed studs as a function of spacing relative to the embedment depth. Fig. 4.20 gives the frequency distribution of measured to calculated concrete cone failure loads for the tests in Fig. 4.19, while Fig. 4.21 plots these ratios as a function of the embedment depth  $h_{ef}$ . Taken

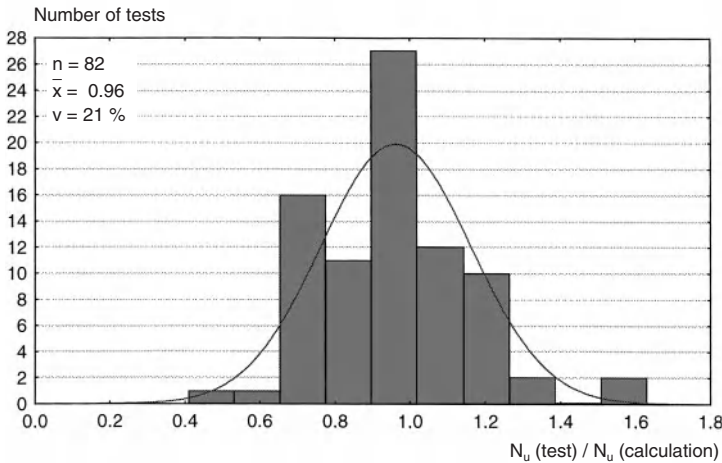


**Fig. 4.20** Histogram of measured to calculated concrete cone failure loads of groups with four expansion anchors and headed studs (test data corresponding to Fig. 4.19)

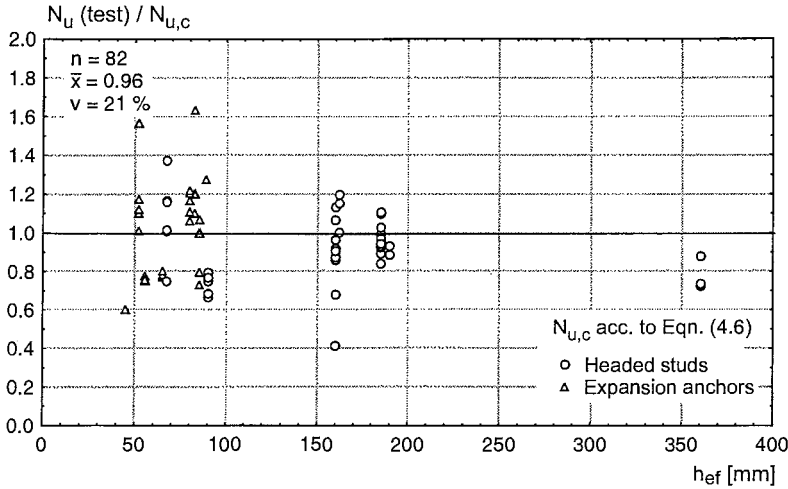


**Fig. 4.21** Measured to calculated concrete cone failure loads of groups with four anchors or headed studs in relation to embedment depth (test data corresponding to Fig. 4.19)

together, Figs. 4.19 to 4.21 indicate that equation (4.6) describes the mean failure load with sufficient accuracy for practical applications.

Fig. 4.22 illustrates the relationship between measured and calculated failure loads for groups of headed studs, arranged orthogonally, with embedment depth  $h_{ef} = 185$  mm, in relation to the spacing  $s_t$  of the outer studs. The number of studs in each group ranged from 4 up to 36 and the spacing of the individual studs was varied between 100 mm and 400 mm. Con-

centric tension was applied in a manner that assured equal distribution of load to all anchors, and all failures were characterised by concrete cone breakout. That equation (4.6) is sufficiently accurate to describe these cases is indicated by Fig. 4.22.

Equation (4.6) also applies to fastenings with any number of expansion anchors, undercut anchors or headed studs. The individual spacing within the group can be constant (Fig. 4.23a, b) or may vary (Fig. 4.23c). Conditions which

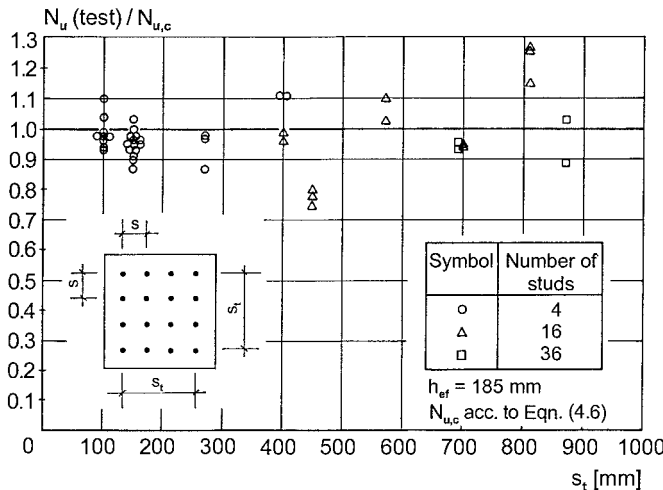


**Fig. 4.22** Measured to calculated concrete cone failure loads of groups with headed studs in orthogonal arrays as a function of the spacing of the outermost anchors (after Eligehausen, Fuchs, Ick, Mällée, Reuter, Schimmlpfennig, Schmal (1992))

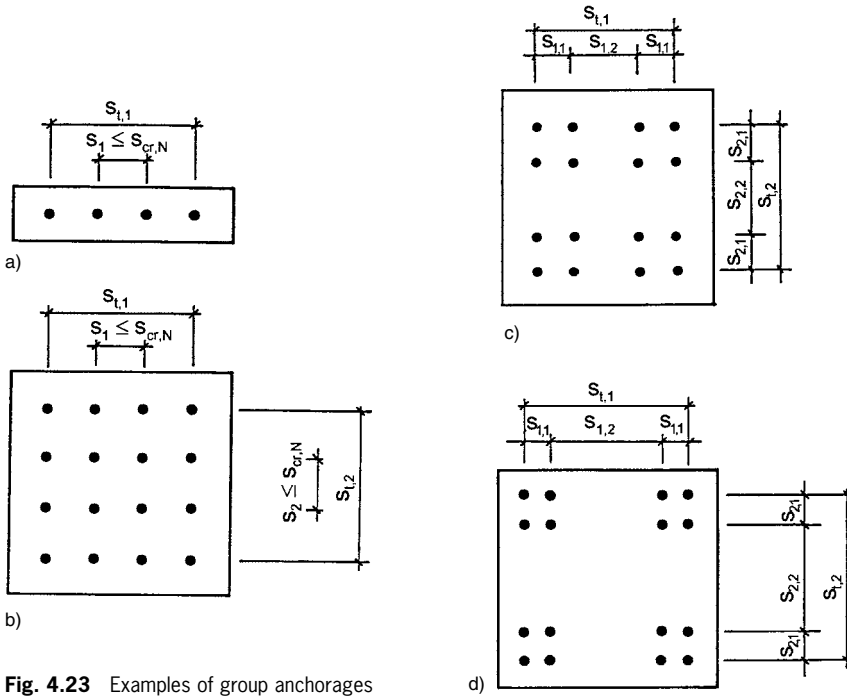


Fig. 4.23 Examples of group anchorages

must be fulfilled are as follows: (a) the fixture must be sufficiently stiff in order to assure an even distribution of applied concentric tensile force to all anchors or headed studs and (b) the spacing between all individual anchors must be less than the characteristic value  $s_{cr,N} = 3 \cdot h_{ef}$ . If the distance  $s_1$  or  $s_2$  is larger than  $s_{cr,N}$ , then a common concrete cone will not be developed. If as shown in Fig. 4.23d the distances  $s_{1,2}$  and  $s_{2,2}$  are both greater than  $s_{cr,N} = 3 \cdot h_{ef}$ , the application reduces to four independent groups with four anchors whose failure loads must be calculated separately.

**d) Anchors near an edge subjected to axial tension loading**

If anchors are positioned near a free edge, then a complete concrete cone cannot form (Fig. 4.24). This reduces the failure load.

Fastenings near the edge of a component should be positioned at a distance from the edge equal to at least half the diameter of the failure cone ( $c > 1.5h_{ef}$ ) (Fig. 4.25a) in order to develop the failure load predicted by either equation (4.5)

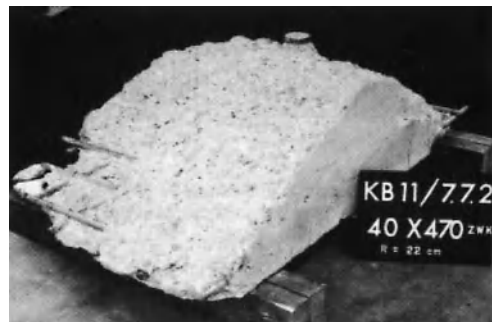


Fig. 4.24 Concrete failure cone of a large headed stud located near the edge and loaded in concentric tension (Forschungs- und Materialprüfungsanstalt Baden-Württemberg (1985/1))

for single anchors or equation (4.6) for anchor groups. In theory, a smaller edge distance will result in truncation of the concrete cone as depicted in Fig. 4.25b with a corresponding reduction in failure load. In the CC- Method the concrete cone breakout load is calculated using equation (4.7):

$$N_{u,c} = \frac{A_{c,N}}{A_{c,N}^0} \cdot \psi_{s,N} \cdot N_{u,c}^0 \quad [\text{N}] \quad (4.7)$$

where:

$$\psi_{s,N} = 0.7 + 0.3 \cdot c / c_{cr,N} \leq 1.0 \quad (4.7a)$$

$c_{cr,N}, A_{c,N}, A_{c,N}^0, N_{u,c}^0$  see equations (4.5) and (4.6)

If more than one edge is involved (e.g. a fastening in a corner or in a narrow member), the smallest edge distance  $c$  is used in equation (4.7a).

The factor  $A_{c,N}/A_{c,N}^0$  takes into account the geometric influence of anchor spacing and edge distance on the concrete cone failure load. At  $c = 1.5 \cdot h_{ef}$  the full concrete cone is developed, whereas at the limit condition of  $c = 0$  the concrete cone is theoretically reduced in volume by 50%. Examples of projected area  $A_{c,N}$  calculation for anchors proximate to an edge are shown in Fig. 4.26.

The rotationally symmetric stress condition produced in the concrete by a tension loaded anchor away from an edge is disrupted when the edge distance is reduced (Fig. 4.27). This leads to a further reduction in the failure load as represented by the factor  $\psi_{s,N}$  in equation (4.7a). In terms of the stress field generated in the con-

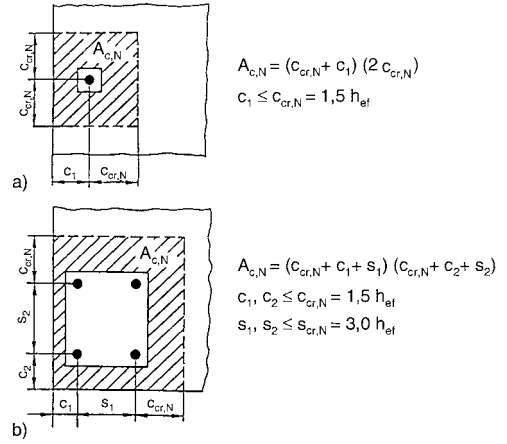


**Fig. 4.26** Projected area for near-edge anchorages loaded in tension  
a) Close to an edge, b) In a corner

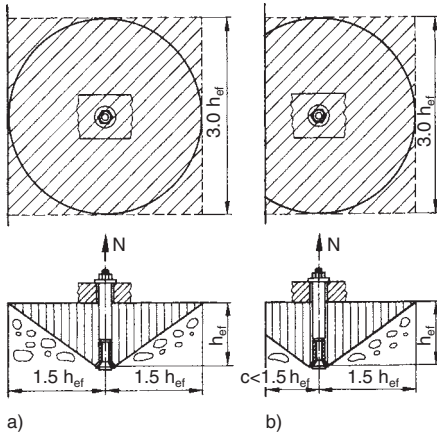


**Fig. 4.25** Influence of edge distance on the shape of the concrete cone failure surface for a single anchor loaded in tension (idealised) (after Fuchs, Elgehausen (1995))  
a) Remote from an edge, b) Close to an edge

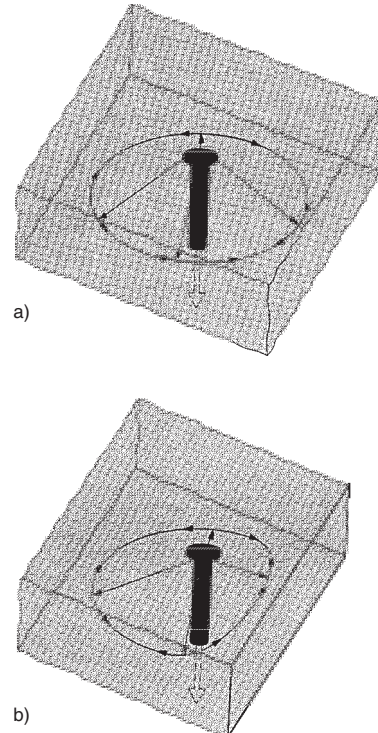


**Fig. 4.27** Distribution of forces in the concrete anchorage zone of a headed stud  
a) Remote from an edge, b) Close to an edge



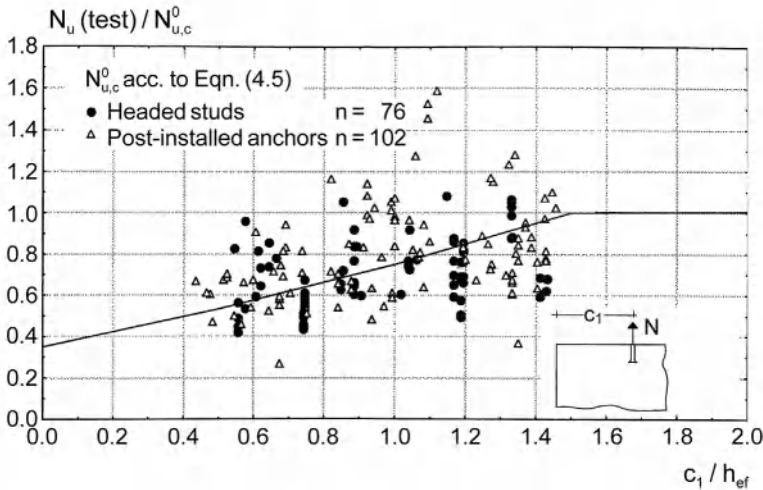


**Fig. 4.28** Influence of edge distance on the concrete cone failure load under tension (tests according to *Eligehausen, Fuchs, Mayer* (1987) (post-installed anchors) and *Eligehausen, Fuchs, Ick, Mallée, Reuter, Schimmelpfennig, Schmal* (1992) (headed studs))

crete, tension loaded anchors positioned near a free edge can be compared to anchors located in cracks (see section 4.2.1.3). Comprehensive analysis of test results by *Eligehausen, Balogh* (1995) and the numerical analyses of *Eligehausen, Ozbolt* (1992) have demonstrated that concrete cone breakout loads in cracked concrete are roughly 70% of the values developed in non-cracked concrete. Therefore,  $\psi_{s,N} = 0.7$  is assigned to the limit case of  $c = 0$  (maximum disruption of rotationally symmetric stress condition), and  $\psi_{s,N} = 1.0$  for  $c \geq 1.5 \cdot h_{ef}$  (no disruption of stress condition), with a linear relationship assumed between these two limits. For anchors positioned in a corner or in a narrow member, the determination of  $\psi_{s,N}$  is simplified by using the smallest edge distance.

Fig. 4.28 shows failure loads for single expansion anchors and single headed studs divided by the value predicted by equation (4.5), plotted as a function of edge distance over embedment depth. The frequency distribution is shown in Fig. 4.29. All tests represented in these figures resulted in concrete cone breakout. Equation (4.7) (solid line in Fig. 4.28) predicts the concrete cone breakout load of anchors positioned near an edge with sufficient accuracy. The ratio

of measured to calculated failure loads is, on average, approximately 1.04 (Fig. 4.29). The scatter of the test results is large ( $v \approx 26\%$ ). Presumably this is due to different concrete mixes used in the tests and variations in internal tensile stresses resulting from shrinkage of the concrete.

It should be noted that minimum edge distances must be maintained for cast-in-place headed studs in order to ensure good concrete placement. Minimum edge distances are required for post-installed expansion and undercut anchors to prevent splitting during anchor installation (see section 4.1.1.6).

#### e) Anchor groups subjected to eccentric tension loading or moment

The foregoing discussion has been limited to anchor groups in which all anchors share the applied load equally. In practice, however, unsymmetrical actions also may occur, e.g. bending moments or eccentric tension loads acting on a fixture. *Riemann* (1985) offers a method of estimating the failure load associated with eccentric tension loads in cases where the fixture may be assumed to be rigid. This approach is described by way of example con-

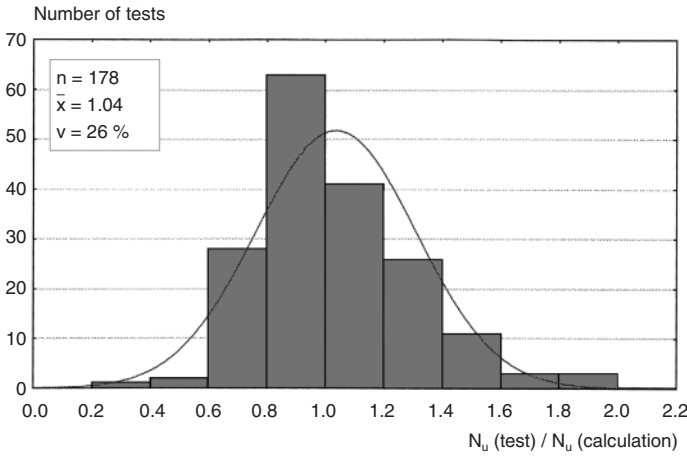


**Fig. 4.29** Histogram of measured to calculated concrete cone failure loads for tension-loaded expansion anchors and headed studs close to an edge (tests according to Fig. 4.28)

sidering a pair of anchors with edge distance  $c \geq 1.5 \cdot h_{ef}$  (Fig. 4.30). In the figure,  $R$  is the resultant of the forces in the anchors which are caused by an external load.

Equation (4.6) applies to a concentric load (Fig. 4.30a). If the resultant tensile force  $R$  is applied directly in line with the anchor (Fig. 4.30c) and the projection of the fixture is neglected, then the failure load of the group corresponds to

the value of a single anchor regardless of the spacing. If the resultant tensile force is applied at any other position within the group (Fig. 4.30b), then the failure load for the group may be assumed to follow a hyperbolic progression between the extreme cases a and c. Thus the influence of the eccentricity of the resultant tensile force on the failure load of a group can be taken into account by multiplying the concrete

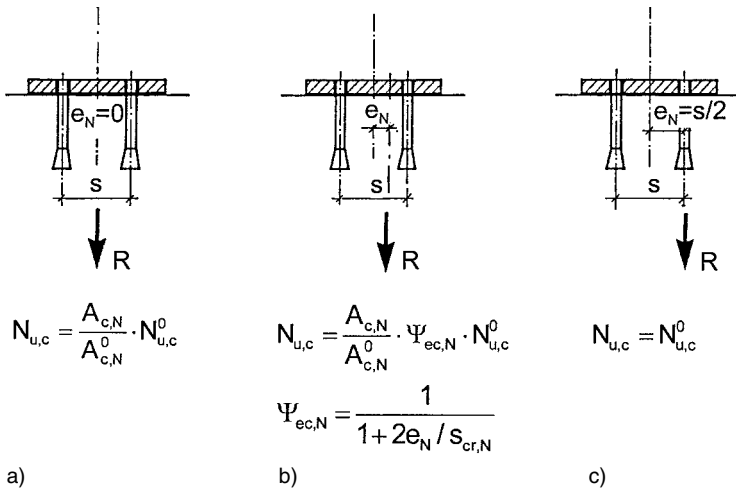


**Fig. 4.30** Accounting for the eccentricity of the external load in the CC-Method (after Riemann (1985))

cone failure load derived from equation (4.7) by an additional factor  $\psi_{ec,N}$  as follows:

$$N_{u,c} = \frac{A_{c,N}}{A_{c,N}^0} \cdot \psi_{s,N} \cdot \psi_{ec,N} \cdot N_{u,c}^0 \quad [N] \quad (4.8)$$

where:

$$\psi_{ec,N} = \frac{1}{1 + 2 \cdot e_N / s_{cr,N}} \leq 1.0 \quad (4.8a)$$

$e_N$  = distance between the resultant tensile force and the geometric centroid of the tension-loaded anchors. Where there is an eccentricity in two directions (see Fig. 4.33a), then equation (4.8a) is used to calculate  $\psi_{ec,N}$  for each axis separately and the product of both factors is used in equation (4.8)

$s_{cr,N}$ ,  $A_{c,N}$ ,  $A_{c,N}^0$ ,  $\psi_{s,N}$ ,  $N_{u,c}^0$  are according to equations (4.5) to (4.7)

In equation (4.8a) it is the internal lever arm  $e_N$  of the resultant tensile force corresponding to the tension-loaded anchors that applies. Note that in the cases where a compressive force is induced in the concrete via the fixture, the internal lever arm  $e_N$  differs from the external eccentricity  $e'_N$  of the tension load applied to the fixture. This is illustrated in Fig. 4.31 for a line anchorage.

A further case arises when some of the anchors in the group are located in the compression zone generated by the applied moment or eccentric

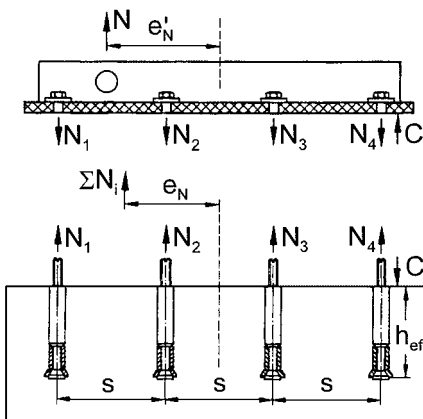


Fig. 4.31 Definition of inner and outer eccentricity for a row of anchors (Fuchs, Eligehausen (1995))

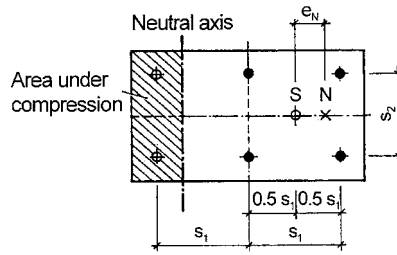


Fig. 4.32 Example for the eccentricity of tensile force resultant corresponding to an external moment (Eligehausen, Mallée, Rehm, (1997))

tension load. Then the eccentricity of the resultant anchor tensile force is derived with respect to the centre of gravity of the tension-loaded anchors only (Fig. 4.32). The same applies if the anchors are detailed such that they can resist compression loads (i.e. with levelling nuts).

If there is an eccentricity about two axes and the tensioned anchors do not form a rectangular pattern, the eccentricities of the resultant tensile force in both directions are derived with respect to the centre of gravity of the tension-loaded

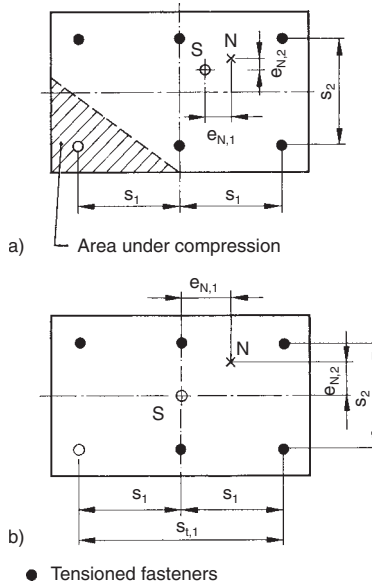
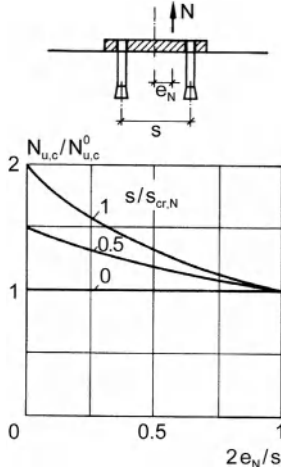


Fig. 4.33 Anchors a) subjected to an obliquely eccentric tension load, and b) imaginary rectangular array for purpose of determining tension resultant location (Eligehausen, Mallée, Rehm (1997))



**Fig. 4.34** Influence of eccentricity of tensile force on the concrete cone failure load for a pair of anchors (after Riemann (1985))

anchors (Fig. 4.33a) and the area  $A_{c,N}$  is calculated for the tensioned anchors. In this application, for reasons of simplicity, the group of tensioned anchors may be resolved into a group rectangular in shape, that means the centre of gravity of the tensioned anchors may be assumed in the centre of gravity of the resolved group (Fig. 4.33b). Furthermore the area  $A_{c,N}$  is calculated for all anchors of the resolved group. This approach should represent a conservative simplification.

Fig. 4.34 shows the concrete cone failure load of a pair of anchors in relation to the eccentricity of the tensile force as predicted by Riemann (1985). In deriving the loads carried by the individual anchors, the projection of the fixture was neglected. For large anchor spacing ( $s \geq s_{cr,N}$ ), the failure load of the group decreases with increasing eccentricity down to 50% of the value corresponding to a concentrically applied load. The effect of the eccentricity lessens considerably for decreased anchor spacing.

The expression for  $\psi_{ec,N}$  as proposed in equation (4.8a) was chosen based on the punching shear analysis of eccentrically loaded flat slabs as described in Moe (1961). Tests conducted by Zhao (1993) indicate that it is conservative. This is demonstrated by Fig. 4.35. It compares predicted versus measured effects of the eccen-

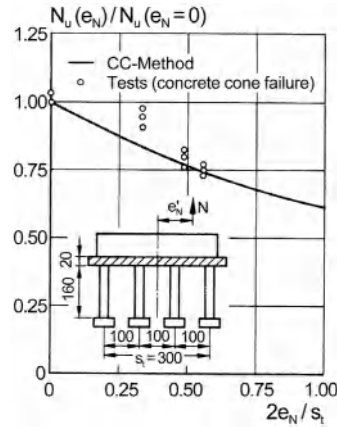


**Fig. 4.35** Ratio of failure loads for an eccentrically loaded row of four headed studs to value for concentric loading as a function of related internal eccentricity, comparison of measured and calculated values (after Zhao (1993))

tricity of the tension-loaded anchor resultant on the concrete cone failure load in the case of a line anchorage of four headed studs welded to a rigid fixture. The headed studs are located in non-cracked concrete and the eccentricity  $e'_N$  of the external tensile force is varied between  $e'_N = 0$  and  $e'_N = 0.5 \cdot s_i$ . The tensile forces in the individual anchors as required for derivation of the internal lever arm  $e_N$  are calculated assuming uniform anchor axial stiffness and elastic behaviour. Further tests on square shaped groups with four headed studs loaded eccentrically with respect to both axes (Zhao (1993)) indicate that equation (4.8) provides conservative predictions of ultimate capacity for this case as well.

Note that equation (4.8) is only valid if the flexural stiffness of the fixture with respect to the anchor axial stiffness is large, i.e. if the fixture is rigid. Furthermore, it will provide accurate predictions of ultimate capacity only if the anchor load distribution is calculated according to elastic theory.

When a fastening consisting of two anchors is subjected to a bending moment, a couple is set up consisting of a tensile force in the anchor and a compressive force beneath the fixture. This is shown in Fig. 4.36 for a fastening with headed studs welded to the fixture. If the tensile force

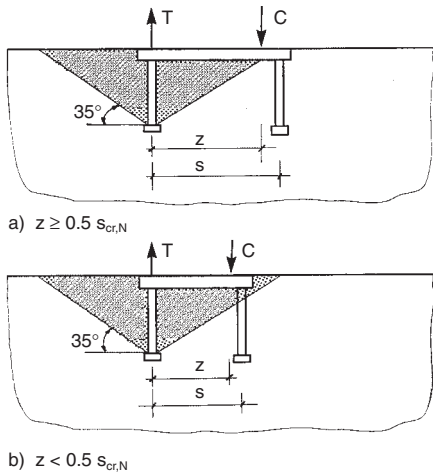


**Fig. 4.36** Influence of an externally applied moment on the concrete cone failure load of studs welded to an anchor plate (after Zhao (1993))

in the anchor exceeds the concrete cone breakout capacity, then a concrete cone failure will result. In this situation, however, the concrete cone failure load may be influenced by the adjacent compression stress block beneath the fixture. This case was investigated by Zhao (1993). If the distance between the resultant tension and compressive forces is larger than the radius of the theoretical concrete cone, i.e.  $z \geq 1.5 \cdot h_{ef}$ , then the concrete cone failure load should not be influenced by the compressive

force beneath the fixture (Fig. 4.36a). With a smaller inner lever arm, however, the development of the concrete cone is partially restrained by the compressive force (Fig. 4.36b), thus increasing the concrete cone failure load. The smaller the distance between the resultant tensile and compressive forces, the greater the increase in the load required to precipitate concrete cone failure.

Figure 4.37 shows the ratio of experimentally or numerically obtained failure loads of groups of headed anchors loaded by normal force and bending moment and the values calculated in accordance with equation (4.8) – which neglects the influence of the compression stresses beneath the fixture – as a function of the internal lever arm  $z$  related to the embedment depth. The lever arm was calculated according to the theory of elasticity assuming a stiff fixture. Zhao (1993) tested groups with four headed anchors under bending moment and shear force in one direction. Varga, Eligehausen (1995, 1996) performed tests with groups with four and nine headed anchors under tension force and bending moment in one direction as well as tests on groups of four anchors under tension force and bi-axial bending moments. Bruckner, Eligehausen, Ozbolt (2001) analysed numerically the behaviour of groups with four anchors under bending moment in one direction using the non-linear Finite Element program MASA which is well suited to predict concrete failure.

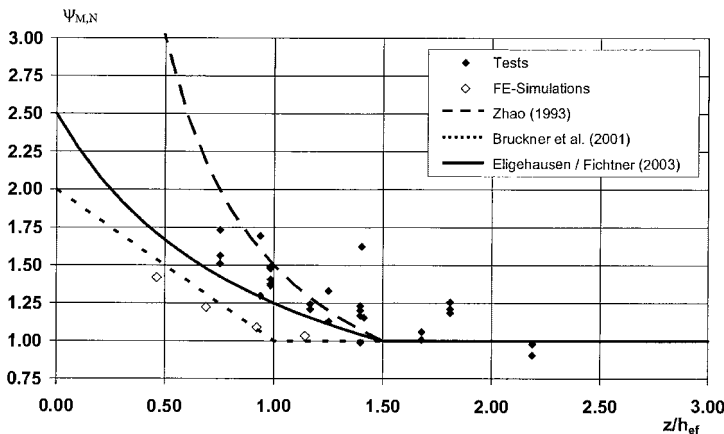


**Fig. 4.37** Influence of bending compression force under the baseplate on the concrete cone failure load as a function of ratio internal lever arm to embedment depth (Eligehausen, Fichtner (2003))

In literature three proposals are given to consider the influence of compression stresses beneath the fixture on the concrete cone failure load. The results of these proposals are also plotted in Fig. 4.37. *Zhao* (1993) assumes that for groups with  $s \geq 1.5 \cdot h_{ef}$  the influence of the compression stresses is negligible while for  $z / h_{ef} = 0$  the concrete cone failure load is infinitely large. In Fig. 4.37 it is assumed that the internal lever arm  $z$  coincides with the spacing  $s$ . The proposal by *Bruckner, Eligehausen, Ozbolt* (2001) describes the lower bound of the test results while *Eligehausen, Fichtner* (2003) predict the test results with sufficient accuracy ( $F_{u, test} / F_{u, calc} \approx 1.1$  with a coefficient of variation  $v \approx 15\%$ ). Following the proposal of *Eligehausen, Fichtner* (2003) the concrete cone failure load can be calculated in accordance with equation (4.9).

$$N_{u,c} = \frac{A_{c,N}}{A_{c,N}^0} \cdot \psi_{s,N} \cdot \psi_{ec,N} \cdot \psi_{m,N} \cdot N_{u,c}^0 \quad [\text{N}] \quad (4.9)$$

where:

$$\psi_{m,N} = 1.0 \quad \text{for } z / h_{ef} \geq 1.5$$

$$\psi_{m,N} = \frac{2.5}{1 + z / h_{ef}} \quad \text{for } z / h_{ef} < 1.5$$

$z$  = internal lever arm calculated in accordance with the theory of elasticity

The results plotted in Fig. 4.37 are valid for fastenings with large edge distances. For fastenings close to an edge two cases should be distinguished which are plotted in Fig. 4.38. If the compression force between baseplate and concrete is closer to the edge than the tensioned anchors (Fig. 4.38a), the formation of the concrete cone is restrained by the compression force and equation (4.9) is valid. However, if the tensioned anchors are located closer to the edge than the compression force (Fig. 4.38b), the failure mechanism is dominated by the

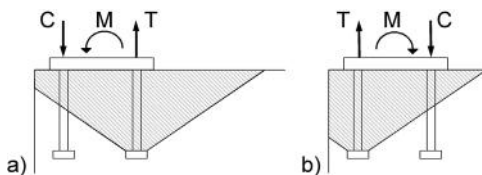


**Fig. 4.38** Anchorage with two anchors perpendicular to the edge loaded by a bending moment

crack running towards the edge. Therefore the influence of the concrete compression force on the cone failure load may be much smaller than in the applications discussed above and should be neglected.

#### f) Influence of reinforcement near the surface of the concrete

For simplicity, the presence of reinforcing steel in the concrete has been neglected in sections 4.1.1.3a to 4.1.1.3e. While structural concrete is typically reinforced, the presence of orthogonal reinforcement near the surface of slabs and walls does not typically increase the tension capacity of anchors because its orientation perpendicular to the direction of the force does not provide sufficient stiffness relative to that of the concrete in diagonal tension. It can in some circumstances give rise to ductile post-cracking behaviour if the concrete cone is sufficiently engaged by the reinforcement, however, this occurs only if the reinforcement is closely spaced and is further engaged by stirrups (*Rehm, Pusill-Wachsmuth* (1979)).

Anchoring headed studs or expansion anchors in the concrete cover zone or near the surface reinforcement can in fact have a detrimental effect on the concrete cone failure load. In such cases the bond stresses (tensile hoop stresses) associated with the reinforcing bars overlap with the tensile stresses generated by the anchorage. Furthermore, the presence of the reinforcement may act as a discontinuity and effectively reduce the volume of concrete available to transfer tensile forces precisely in a zone where the concrete strength, particularly in heavily reinforced sections, is often inferior. These influences can be taken into account by an additional factor, the so-called spall factor (equation (4.10a)), developed by *Eligehausen, Fuchs, Lotze, Reuter* (1989). Equation (4.10a) was derived for anchors in cracked concrete (see section 4.2.1.3) and is conservative for anchors in non-cracked concrete.

$$N_{u,c} = \frac{A_{c,N}}{A_{c,N}^0} \cdot \psi_{s,N} \cdot \psi_{ec,N} \cdot \psi_{m,N} \cdot \psi_{re,N} \cdot N_{u,c}^0 \quad [\text{N}] \quad (4.10)$$

where:

$$\psi_{re,N} = 0.5 + h_{ef} / 200 \leq 1.0 \quad (\text{closely spaced reinforcing bars}) \quad (4.10a)$$

$$\psi_{re,N} = 1.0 \text{ (widely spaced rein-} \\ \text{forcing bars)} \quad (4.10b)$$

$h_{ef}$  = embedment depth [mm]

$A_{c,N}$ ,  $A_{c,N}^0$ ,  $\psi_{s,N}$ ,  $\psi_{ec,N}$ ,  $\psi_m$ ,  $N_{u,c}^0$  are according to equations (4.5) to (4.9)

For the purposes of this expression, the reinforcing bars are assumed to be widely spaced when the tensile stresses in the concrete due to the bond effect of the reinforcing bars and due to the load introduced via the anchor are no longer in superimposition. As a simplification it may be assumed that this is the case for reinforcing bars at a spacing  $s \geq 100$  mm for bar diameters approximately equal to or less than 10 mm, or alternately  $s \geq 150$  mm for bar diameters greater than 10 mm.

**g) Special cases**

If the development of the concrete cone is constrained by the presence of three or more edges with  $c_{max} < 1.5 \cdot h_{ef}$  ( $c_{max}$  = largest of the edge distances), then equations (4.7) to (4.10) may be used to conservatively predict the concrete cone failure load (Eligehausen, Balogh, Fuchs, Breen (1992)). This is illustrated with the case of a single tension-loaded anchor embedded in the end of a square concrete column (Fig. 4.39a). The projected area  $A_{c,N}$  is constant for  $c \leq 1.5 \cdot h_{ef}$  and amounts to  $A_{c,N} = (2 \cdot c)^2$ . Hence, the failure load as predicted by equation (4.7) becomes:

$$N_{u,c} = \frac{4 \cdot c^2}{9 \cdot h_{ef}^2} \cdot \left( 0.7 + 0.3 \cdot \frac{c}{1.5 \cdot h_{ef}} \right) \cdot k \cdot f_{cc200}^{0.5} \cdot h_{ef}^{1.5} \approx K \cdot \frac{1}{h_{ef}^{0.5}}$$

This implies that the concrete cone failure load is inversely proportional to  $h_{ef}^{0.5}$ . However, in reality the failure load must be constant for all embedment depths  $h_{ef} \geq 1.5 \cdot c$  since the concrete fracture surface comprises the same area regardless of the embedment. More accurate results are obtained if in equation (4.5b) or (4.5c) respectively the embedment depth  $h_{ef}$  is replaced by

$$h'_{ef} = \max(c_{max}/1.5; s_{max}/3) \quad (4.11a)$$

and in equations (4.7a) and (4.8a) the values  $s_{cr,N}$  and  $c_{cr,N}$  are replaced by

$$s'_{cr,N} = 2 \cdot c'_{cr,N} = 3 \cdot h'_{ef} \quad (4.11b)$$

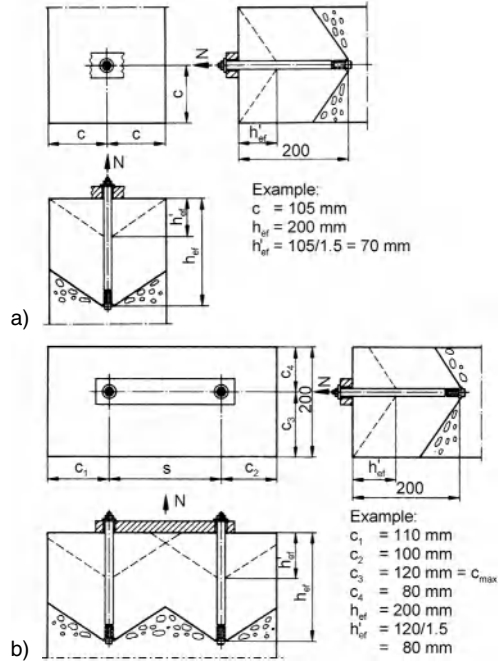


**Fig. 4.39** Determination of the effective embedment depth (taken from Fuchs, Eligehausen (1995))  
a) For a single anchor in tension with three proximate edges ( $c_{max} < 1.5 h_{ef}$ )  
b) For a pair of anchors in tension with four proximate edges ( $c_{max} < 1.5 h_{ef}$ )

Furthermore when calculating  $A_{c,N}^0$  and  $A_{c,N}$  as per Figs. 4.14, 4.16 and 4.26 the values  $h_{ef}$ ,  $s_{cr,N}$ , and  $c_{cr,N}$  should be replaced by  $h'_{ef}$ ,  $s'_{cr,N}$ , and  $c'_{cr,N}$ . Taking the example shown in Fig. 4.39a we obtain a concrete cone failure load  $N_{u,c}^0$  for  $h'_{ef} = c/1.5$  that is not dependent on the embedment depth as follows:

$$N_{u,c} = \frac{4 \cdot c^2}{9 \cdot (c/1.5)^2} \cdot \left( 0.7 + 0.3 \cdot \frac{c}{1.5 \cdot c/1.5} \right) \cdot k \cdot f_{cc200}^{0.5} \cdot (c/1.5)^{1.5} \\ = 1 \cdot 1 \cdot k \cdot f_{cc200}^{0.5} \cdot (c/1.5)^{1.5}$$



The above method may also be applied to anchor groups as shown in Fig. 4.39b.

#### h) Influence of hanger reinforcement (hairpins and stirrups)

The provision of hanger reinforcement in the form of stirrups or hairpins located directly adjacent the anchor load-transfer zone and adequately anchored in the anticipated failure cone, as well as in the surrounding concrete (Fig. 4.40), can substantially increase the tension failure load and provide increased ductility (Rehm, Schlaich, Schäfer, Eligehausen (1985)). Typically, tension hanger reinforcement is practical only for cast-in-place anchors, and it may generally be more effective to simply increase the embedment depth of the anchors by a suitable amount, thereby providing a more direct load path.

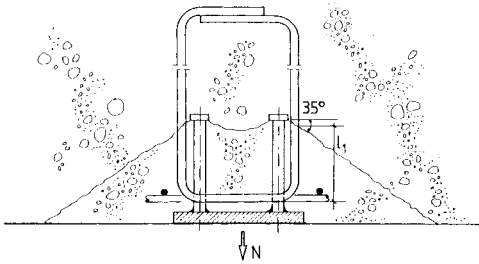


**Fig. 4.40** Group of anchors with hanger reinforcement (stirrups) (Rehm, Eligehausen, Mallée (1992))

The load-bearing capacity of an anchorage supplemented with hanger reinforcement results from the anchorage in the concrete cone achieved by means of bond and bearing of a hook or bend. The hanger reinforcement is only fully activated upon the development of the concrete cone. Therefore it should be conservatively assumed for design purposes that the applied load is carried solely by the hanger reinforcement, i.e. the share of the load carried by the concrete is ignored. The determination of anchorage capacity follows from normal considerations of reinforcement bond length. As an example, the calculation of the anchorage force for one leg of the hanger reinforcement according to the *Eurocode 2: ENV 1992-1-1:1991* (1992) is as follows:

$$N_{ub} = \pi \cdot d_s \cdot l_1 \cdot f_{bm} / \alpha_a \leq A_s \cdot f_y \quad [\text{N}] \quad (4.12)$$

where:

- $d_s$  = nominal diameter of hanger reinforcement [mm]
- $l_1$  = anchorage length measured from the intersection of the concrete cone with stirrup or hairpin (see Fig. 4.40),
- $f_{bm}$  = average bond strength [N/mm<sup>2</sup>]  
=  $2.25 \cdot f_{ctm}$
- $f_{ctm}$  = average concrete tensile strength,  
=  $0.3 \cdot f_c^{2/3}$
- $\alpha_a$  = factor to take into account influence of hook  
= 0.7
- $A_s$  = cross-sectional area of one leg of hanger reinforcement [mm<sup>2</sup>]
- $f_y$  = yield stress of hanger reinforcement  
≤ 500 N/mm<sup>2</sup>

According to *Eurocode 2: ENV 1992-1-1:1991*(1992) the average bond strength may be increased by a factor 1.5 if the edge distance of the hanger reinforcement is  $c \geq 10 \cdot d_s$  in all directions. Equation (4.12) is valid for a hanger reinforcement positioned close to the anchor. The total ultimate tension capacity of the anchorage is obtained by summing the individual capacities of the legs of the hanger reinforcement.

Tests employing headed studs with an embedment depth  $h_{ef} \geq 150$  mm, as described in Ramm, Greiner (1991) and Eligehausen, Fuchs, Ick, Mallée, Reuter, Schimmelpfennig, Schmal (1992), indicate that equation (4.12) supplies a sufficiently reliable estimate of ultimate tension capacity (compare Fig. 5.14 in which results of tests with anchor channels with an embedment depth  $h_{ef} \geq 65$  mm are also evaluated). In the tests with headed anchors the hanger reinforcement was arranged as illustrated in Fig. 4.40. If the hanger reinforcement also encloses the flexural reinforcement, then an increase in tension capacity of approximately 20% may be expected (Ramm, Greiner (1991)). Tests with anchor channels show that equation (4.12) may be used for embedment depths as small as  $h_{ef} \approx 70$  mm (compare Fig. 5.14).

#### i) Comparing the CC-method with other approaches given in the literature

Figures 4.41 and 4.42 plot the mean concrete cone failure load as predicted by equation (4.5)

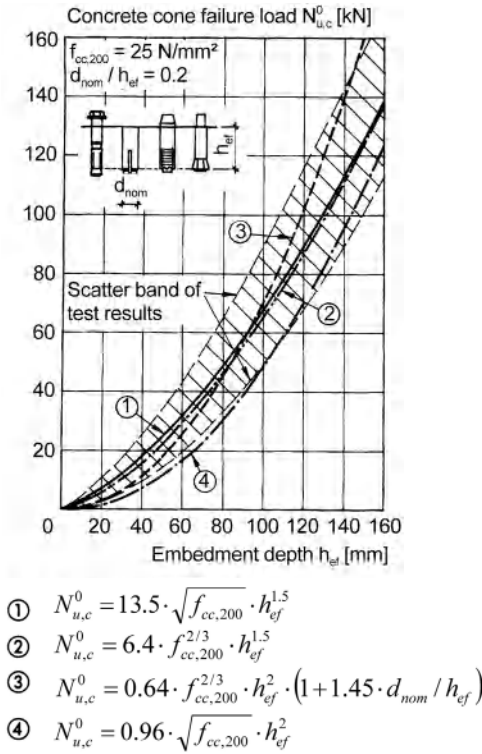


**Fig. 4.41** Concrete cone failure load of expansion and undercut anchors loaded in concentric tension as a function of embedment depth; comparison of various proposals (curve 1 as predicted by equation (4.5), curve 2 according to *Eligehausen, Pusill-Wachtsmuth* (1982), curve 3 according to *Pusill-Wachtsmuth* (1982), curve 4 according to *American Concrete Institute, ACI 349-90* (1990))

for expansion anchors and headed studs, respectively, together with various proposals described in the literature. The scatter of measured concrete cone failure loads is also provided along with the plotted expressions for  $N_{u,c}^0$ .

The approach suggested by *Eligehausen, Pusill-Wachtsmuth* (1982) for expansion anchors predicts failure loads that are nearly equivalent to those given by equation (4.5) for normal concrete strengths ( $25 \text{ N/mm}^2$ ) (compare curve 2 and curve 1 in Fig. 4.41), but predicts higher capacities at higher concrete strengths due to the use of the  $2/3$  exponent on the concrete strength term. The proposal of *Bode, Hanenkamp* (1985), which was developed for headed

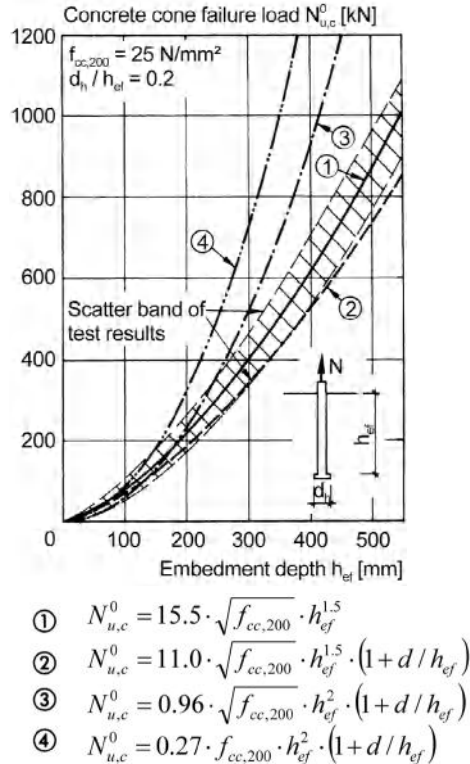


**Fig. 4.42** Concrete cone failure load of headed studs loaded in concentric tension as a function of embedment depth; comparison of various proposals (curve 1 as predicted by equation (4.5), curve 2 according to *Bode, Hanenkamp* (1985), curve 3 according to *American Concrete Institute, ACI 349-90* (1990), curve 4 according to *Braestrup, Nielsen, Jensen, Bach* (1976))

studs, predicts failure loads for all embedment depths which are about 15% lower than those given by equation (4.5) (compare curve 2 and curve 1 in Fig. 4.42). This difference may well be attributable to the different concrete mixes used in the tests. In *Braestrup, Nielsen, Jensen, Bach* (1976), *Klingner, Mendonca* (1982/2), *Pusill-Wachtsmuth* (1982) and *ACI 349-90* (1990) it is assumed that the concrete cone failure load increases with the square of the embedment depth ( $h_{ef}^2$ ). However, regression analyses indicate (and fracture mechanics considerations dictate) that the increase in concrete cone breakout capacity is more closely related to  $h_{ef}^{1.5}$ , and therefore the failure loads predicted by these approaches agree with test results over only a

relatively narrow range of embedment depths. Failure loads for smaller and larger embedment depths are under-predicted and over-predicted, respectively. The range of embedment depths where a good correlation between prediction and tests is achieved for the individual proposals is shown in Figs. 4.41 and 4.42. The approach provided by *Braestrup, Nielsen, Jensen, Bach* (1976), although it has the advantage of being units-independent, significantly overestimates the influence of the concrete compressive strength because the concrete cone failure load is assumed to be proportional to  $f_c$  (see curve 4 in Fig. 4.42).

The measured concrete cone failure loads associated with the group tests represented in Fig. 4.22 are shown in Fig. 4.43 in relation to the spacing  $s_i$  of the outermost anchors. While concrete mix design and strength ( $f_{cc,200} \sim 25 \text{ N/mm}^2$ ) as well as embedment depth ( $h_{ef} = 185 \text{ mm}$ ) were kept constant, the number of studs in the group ranged from 4 to 36, and the spacing of the outer studs was varied. The groups were loaded concentrically, whereby a very stiff fixture was utilised to ensure a roughly even distribution of forces among the individual anchors. Single studs were tested to establish baseline values. Fig. 4.43 also plots the calculated failure loads per equation (4.6) and *American Concrete Institute, ACI 349-90* (1990). In both approaches the

failure load of a group is assumed to be proportional to the area of the overlapping failure cones. While in the CC-Method the calculation of the projected failure surface is simple (see Figs. 4.16 and 4.26) it is rather complicated with the  $45^\circ$  cone method (Fig. 4.6b, c). A further significant difference between the two methods is the assumption of the characteristic spacing ( $s_{cr,N} = 3 \cdot h_{ef}$  (CC-Method) and  $s_{cr,N} = 2 \cdot h_{ef}$  ( $45^\circ$  cone method)). It is clear that equation (4.6) predicts the concrete cone failure loads as derived by tests with remarkable accuracy, while *American Concrete Institute, ACI 349-90* (1990) clearly over-predicts the capacity of the group as the spacing  $s_i$  increases. Since the failure loads for single studs with embedment depth  $h_{ef} = 185 \text{ mm}$  as predicted by equation (4.6) and *American Concrete Institute, ACI 349-90* (1990) are practically identical, the likely explanation for the error is that the failure cone assumed in *American Concrete Institute, ACI 349-90* (1990) ( $\alpha = 45^\circ$ ) is too steep.

In *Farrow, Klingner* (1995), *Farrow, Frigui, Klingner* (1996) and *Klingner, Muratli, Shirvane* (1998) the predictions by the  $45^\circ$  cone method of *American Concrete Institute, ACI 349-90* (1990) and the CC-Method for the concrete cone failure load were compared with the results of a very large data base (more than 1600 tests). The data base comprises tests on

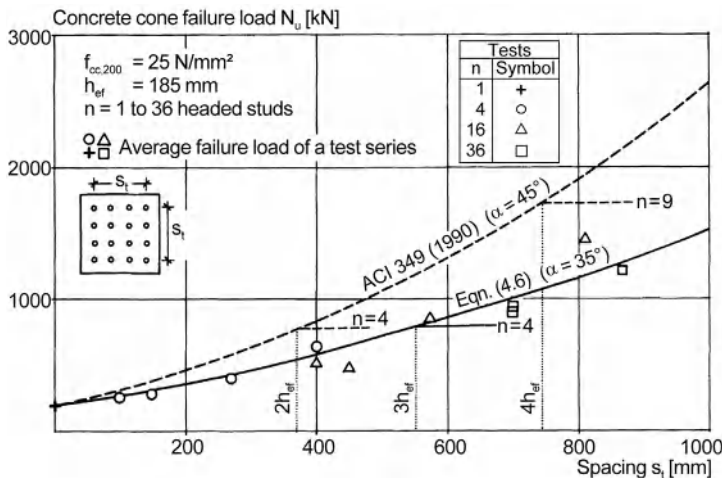


**Fig. 4.43** Concrete cone failure load of groups of headed studs as a function of the spacing of the outermost studs (tests according to *Eligehausen, Fuchs, Ick, Mallée, Reuter, Schimmelpfennig, Schmal* (1992))

headed studs and post-installed expansion and undercut anchors with concrete cone failure performed in Europe and the US. Tested were single anchors with varying embedment depth ( $h_{ef} \approx 20 \text{ mm}$  to  $h_{ef} = 525 \text{ mm}$ ) with and without edge influence and groups with two or four anchors with varying spacing without edge influence. Furthermore the probability of failure of fastenings under known loads and the probability for brittle concrete cone failure under unknown loads of fastenings designed for steel failure associated with the two methods were calculated, using the load and understrength factors of *American Concrete Institute, ACI 349-90* (1990). Based on the evaluation the authors found that the CC-Method predicts the concrete cone capacity more accurately than the  $45^\circ$  cone method and they recommend the CC-Method for use in design.

**4.1.1.4 Failure load for local concrete side blow-out failure**

Tension-loaded headed studs provided with small edge distances can generate local blow-out failures in the vicinity of the head (Fig. 4.44). Expansion anchors do not generally exhibit this type of failure since at the relevant edge distances the installation torque required to properly set the anchor will cause the concrete to split.

In a local concrete side blow-out failure, the failure load is independent of the embedment



**Fig. 4.44** Local side blow-out failure of a headed stud loaded in tension with small edge distance (Furche, Eligehausen (1991))

depth (Fig. 4.45). Side blow-out failure will govern the concrete capacity of studs having small edge distance (concrete cover) in combination with large embedment depth. Local concrete side blow-out failure is caused by the quasi-hydrostatic pressure in the region of the head of the stud which gives rise to a lateral bursting force  $F_b$  equal to  $\alpha$  times the applied tension load  $N$  (Fig. 4.46). The bursting force at failure can be approximated using equation (4.5) if the edge distance  $c_1$  is substituted for the embedment depth term,  $h_{ef}$ . The following expression is thus obtained:

$$N_{u,cb}^0 = \frac{1}{\alpha} \cdot 15.5 \cdot c_1^{1.5} \cdot f_{cc,200}^{0.5} \quad [\text{N}] \quad (4.13a)$$

The value  $\alpha$  describes the ratio lateral bursting force to tension force. It depends on the specific concrete bearing pressure  $p / f_{cc,200}$  beneath the

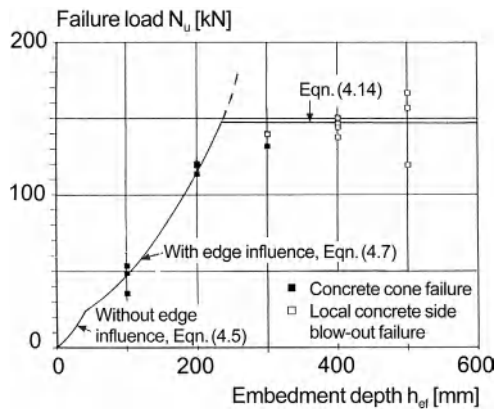


**Fig. 4.45** Failure load of single tension-loaded headed studs with constant edge distance as a function of the varied embedment depth (Furche, Eligehausen (1991))

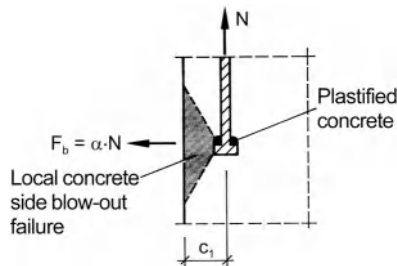


**Fig. 4.46** Local side blow-out failure of headed stud near an edge (schematic) (Rehm, Eligehausen, Mällée (1988))

head since the lateral strain in the concrete increases with the stress in the concrete beneath the head. According to *Furche, Eligehausen* (1991)  $\alpha = 0.11 \cdot (p/f_{cc,200})^{0.5}$ . This results in  $\alpha = 0.2$  for  $p/f_{cc,200} \approx 3.5$  or  $\alpha = 0.4$  for  $p/f_{cc,200} \approx 13$ .

Substituting  $\alpha = 0.11 \cdot (p/f_{cc,200})^{0.5}$ , where  $p = N_{u,cb}^0/A_h$ , in equation (4.13a), the following expression is obtained for the concrete side blow-out capacity:

$$N_{u,cb}^0 = 27 \cdot A_h^{1/3} \cdot f_{cc,200}^{2/3} \cdot c_1 \quad [N] \quad (4.13b)$$

where:

$$A_h = \text{bearing area of head} \\ = \frac{\pi}{4} \cdot (d_h^2 - d^2)$$

$d_h$  = diameter of head [mm]

$d$  = shaft diameter [mm]

While equation (4.13b) predicts that the failure load will increase in proportion to the edge distance  $c_1$ , equation (4.13a) indicates that it is proportional to  $c_1^{1.5}$ . The difference can be ascribed to the fact that equation (4.13a) contains the factor  $\alpha$ , which increases with increasing pressure beneath the head, i.e. with increasing edge distance. According to equation (4.13b) the failure load increases in proportion to  $f_{cc,200}^{2/3}$ , while normally a rise in proportion to  $f_{cc,200}^{0.5}$  is assumed. A comparison with test results shows furthermore that equation (4.13b) underestimates the influence of the bearing pressure under the head. A regression analysis of test data, assuming that the average failure load is proportional to  $f_{cc,200}^{0.5}$ , leads to equation (4.14) (*Furche, Eligehausen* (1991)):

$$N_{u,cb}^0 = 15 \cdot c_1 \cdot A_h^{0.5} \cdot f_{cc,200}^{0.5} \quad [N] \quad (4.14a)$$

Based on a multiple regression analysis of results of tests *De Vries* (1996) proposes equation (4.14b).

$$N_{u,cb}^0 = 25.2 \cdot c_1^{0.609} \cdot A_h^{0.577} \cdot f_c^{0.671} \quad [N] \quad (4.14b)$$

*Hofmann, Eligehausen* (2002) performed extensive non-linear numerical investigations with single anchors at an edge and at a corner and anchor rows at the edge. They propose as ratio lateral bursting force and tension force  $\alpha =$

$0.045 \cdot p/f_{cc,200} \leq 0.5$  with  $p = N/A_h$ . Substituting this expression in equation (4.13a) leads to:

$$N_{u,cb}^0 = 18.5 \cdot c_1^{0.75} \cdot A_h^{0.5} \cdot f_{cc,200}^{0.75} \quad [N] \quad (4.14c)$$

In Fig. 4.47a results of tests by *De Vries* (1996) are plotted as a function of the edge distance. In the tests the concrete strength was varied between  $f_{cc,200} = 24 \text{ N/mm}^2$  and  $f_{cc,200} = 29 \text{ N/mm}^2$ . The bearing area was altered between  $A_h = 2,200 \text{ mm}^2$  and  $A_h = 7,100 \text{ mm}^2$ . Therefore the measured failure loads were normalised to  $f_{cc,200} = 25 \text{ N/mm}^2$  and the bearing area to  $A_h = 5,000 \text{ mm}^2$  using equation (4.14c). The figure demonstrates that equation (4.14c) predicts the influence of the edge distance on the failure load better than equation (4.14a).

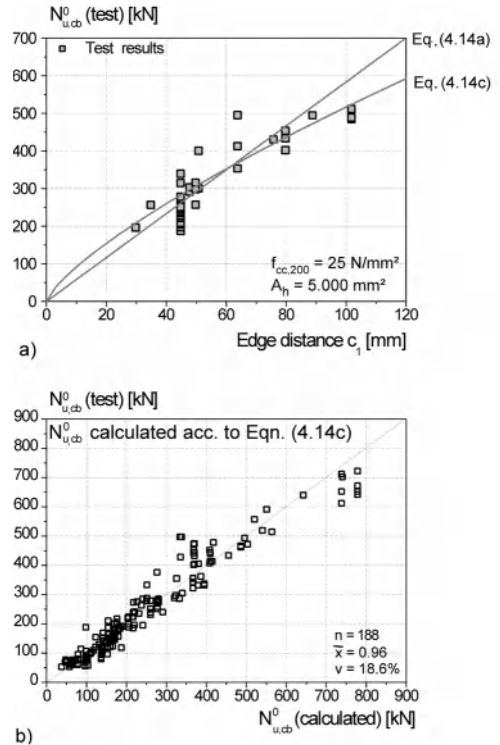


**Fig. 4.47** Comparison of measured blow-out failure loads with predictions (after *Hofmann, Eligehausen* (2003))  
 a) Failure loads as a function of the edge distance  
 b) Measured failure loads as a function of the calculated values



Fig. 4.47b plots predicted failure loads given by equation (4.14c) against test results published in *Hasselwander, Jirsa, Breen (1987)*, *Furche, Eligehausen (1991)*, *Varga, Eligehausen (1995)*, *Bashandy (1996)* and *DeVries (1996)*. The agreement is acceptable.

The edge distance at which there is a transition from a local side blow-out failure to a concrete cone breakout failure depends on the bearing area of the headed stud and the embedment depth (*Furche, Eligehausen (1991)*). For single studs at embedment depths  $h_{ef} < 300$  mm the value is  $c_1 = 0.3 \cdot h_{ef}$  to  $0.5 \cdot h_{ef}$ .

Equation (4.14c) applies to single anchors positioned near a free edge. If several closely spaced headed anchors are positioned parallel with the edge, then the side blow-out failure cones can overlap and, at the corner of a member, the failure surface may be truncated. In such situations *Furche, Eligehausen (1991)* propose that the failure load can be determined in a manner analogous to that used by the CC-Method for concrete cone breakout capacity. With this approach the failure load corresponding to a row of anchors parallel to the edge or an anchor in the corner can be calculated using equation (4.15). This is structured similarly to equation (4.8):

$$N_{u,cb} = \frac{A_{c,Nb}^0}{A_{c,Nb}^0} \cdot \psi_{s,Nb} \cdot \psi_{ec,Nb} \cdot N_{u,cb}^0 \quad [\text{N}] \quad (4.15a)$$

where:

$A_{c,Nb}^0$  = projected area of the side blow-out cone for a single stud

$A_{c,Nb}$  = projected area of cone for the group of anchors. In this calculation the effect of neighbouring anchors, proximate corners and the member thickness on the shear cone geometry are taken into account

$\psi_{s,Nb}$  = influence of corner distance  $c_2$  on the stress distribution in the concrete

$$= 0.7 + 0.3 \cdot \frac{c_2}{c_{cr,Nb}} \leq 1.0 \quad (4.15b)$$

$\psi_{ec,Nb}$  = influence of eccentricity of the applied tension load relative to the geometrical centroid of the group

$$= \frac{1}{1 + 2 \cdot e_N / s_{cr,Nb}} \leq 1.0 \quad (4.15c)$$

$e_N$  = eccentricity of resultant tensile force on the anchors relative to their geometrical centroid

$s_{cr,Nb}$  = characteristic spacing for local side blow-out failure

$c_{cr,Nb}$  = characteristic edge distance for local side blow-out failure

$N_{u,cb}^0$  according to equation (4.14c)

According to *Furche, Eligehausen (1991)* the diameters of the side blow-out cones are relatively large and measure approximately six times the edge distance  $c_1$  (Fig. 4.48). However, if this value is applied as a characteristic spacing  $s_{cr,Nb}$  for full capacity, the failure loads of single anchors at a corner and of anchor rows parallel to the edge are underestimated. Therefore *Hofmann, Eligehausen (2002)* propose  $s_{cr,Nb} = 2 \cdot c_{cr,Nb} = 4 \cdot c_1$  as characteristic distances. Examples for  $A_{c,Nb}^0$  and  $A_{c,Nb}$  based on this proposal are shown in Fig. 4.49.

According to equation (4.15) the failure load of an anchor row with  $s = 0$  is equal to the ultimate load  $N_{u,cb}^0$  of a single anchor. However, according to the results of numerical analysis by *Hofmann, Eligehausen (2002)* in the above application the failure load is  $N_{u,cb} = n^{0.5} \cdot N_{u,cb}^0$ . This can be explained as follows. The bearing area of  $n$  anchors parallel to the edge is  $n$  times the bearing area of a single anchor. If the spacing between the anchors is reduced to  $s = 0$  the bearing area of the fictitious anchor is  $n$  times the bearing area of a single anchor. The failure

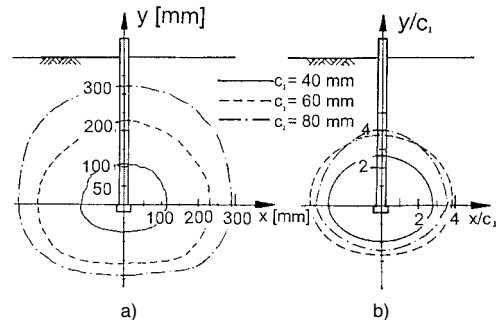


**Fig. 4.48** Dimensions at concrete surface of concrete cones associated with local side blow-out failure (after *Furche, Eligehausen (1991)*)

a) Absolute dimensions

b) Diameter as a function of edge distance

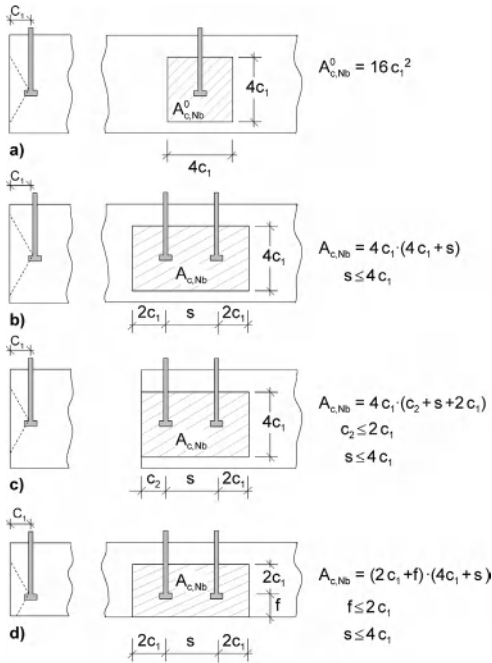


**Fig. 4.49** Idealised cones (left hand side) and projected surface areas  $A_{c,Nb}^0$  or  $A_{c,Nb}$  (right hand side) for local blow-out failure of headed studs (Hofmann, Eligehausen (2003))  
 a) Single headed stud  
 b) Two studs near an edge  
 c) Two studs in the corner  
 d) Two studs in a thin member

load is proportional to  $A_h^{0.5}$ . Therefore the ultimate capacity of  $n$  anchors with  $s = 0$  is  $n^{0.5} \cdot N_{u,cb}^0$ . If the spacing between the anchors is increased to  $s_{cr,Nb}$ , the ultimate capacity of the anchor row is  $n \cdot N_{u,cb}^0$ . Between these two extremes a linear relationship is proposed. Considering this behaviour an additional factor  $\psi_{g,Nb}$  should be introduced to equation (4.15).

$$N_{u,cb} = \frac{A_{c,Nb}}{A_{c,Nb}^0} \cdot \psi_{g,Nb} \cdot \psi_{s,Nb} \cdot \psi_{ec,Nb} \cdot N_{u,cb}^0 \quad [N] \quad (4.15d)$$

where:

$$\psi_{g,Nb} = (1 - n^{0.5}) \cdot s / s_{cr,Nb} + n^{0.5} \quad (4.15e)$$

$n$  = number of anchors of an anchor row parallel to the edge  
 according to equation (4.14c)  
 $s_{cr,Nb} = 2 \cdot c_{cr,Nb} = 4 \cdot c_1$

$A_{c,Nb}^0$ ,  $A_{c,Nb}$  according to equation (4.15a)  
 $\psi_{s,Nb}$  according to equation (4.15b)  
 $\psi_{ec,Nb}$  according to equation (4.15c)

In Fig. 4.50 the measured failure loads of tests by Eligehausen, Varga (1995) and De Vries (1996) on pairs of headed studs near the edge and on single studs in the corner of a concrete member are compared with the calculated values according to equation (4.15d). Furthermore the results of numerical analysis by Hofmann, Eligehausen (2002) are plotted. Equation (4.15d) predicts the failure loads with sufficient accuracy.

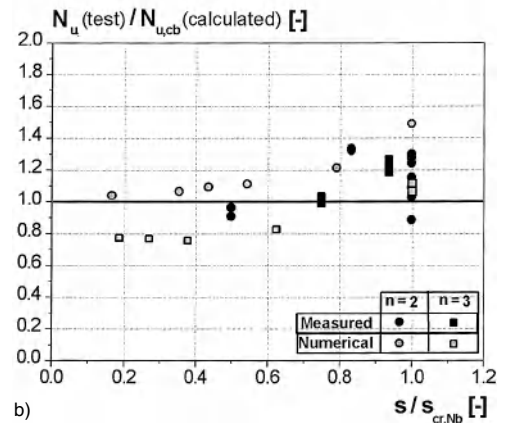
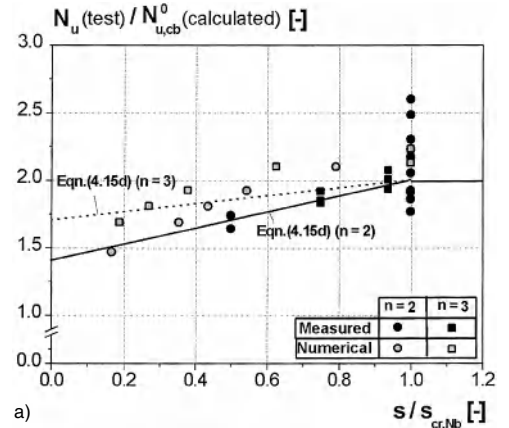


**Fig. 4.50** Comparison of measured and numerically obtained failure loads of groups of headed studs close to an edge (Hofmann, Eligehausen (2002))  
 a) With the calculated values according to equation (4.14c) as a function of related spacing  
 b) With the calculated values according to equation (4.15d) as a function of related spacing



Equation (4.15d) may also be used to predict the local blow-out failure of undercut anchors. However, the minimum edge distance to prevent splitting of concrete during installation is large enough to preclude a local side blow-out failure.

Limited studies have shown that the failure load associated with a local concrete side blow-out failure can be increased by confining the concrete with closely spaced stirrups or spiral reinforcement (Hasselwander, Jirsa, Breen (1987), Eligehausen, Varga (1995), De Vries (1996)). Again, there are insufficient test results to support the development of a reliable predictive equation for this condition.

#### 4.1.1.5 Failure loads associated with pull-out and pull-through failures

Setting and subsequent loading of an expansion anchor induces local deformations in the concrete around the drilled hole (see section 2.3.3.1), giving rise to a radial expansion pressure whose integration over the contact area is used to derive the expansion force  $F_{ex}$ . The failure load  $N_{u,p}$  of the anchor for the pull-out failure mode is proportional to the expansion force:

$$N_{u,p} = \mu \cdot F_{ex}$$

According to Wagner-Grey (1977/1) the force transfer coefficient  $\mu$  between expansion sleeve and concrete is about 0.2 to 0.3 for torque-controlled expansion anchors and about 0.35 for displacement-controlled expansion anchors. A later study by Mayer (1990) estimates the force transfer coefficient for torque-controlled expansion anchors to vary from  $\mu = 0.35$  (high-strength concrete) to  $\mu = 0.6$  (low-strength concrete).

Wagner-Grey (1977/1) proposes an approach for calculating the expansion force and associated pull-out load for an expansion anchor. Linear-elastic, ideal-plastic material behaviour is assumed for the concrete, and a failure criterion based on Mohr-Coulomb is employed. To calculate the expansion pressure or expansion force resulting from a given expansion displacement, equations are developed that may either be solved by iteration or with the help of diagrams developed for this purpose. The validity of this approach was checked in Rehm,

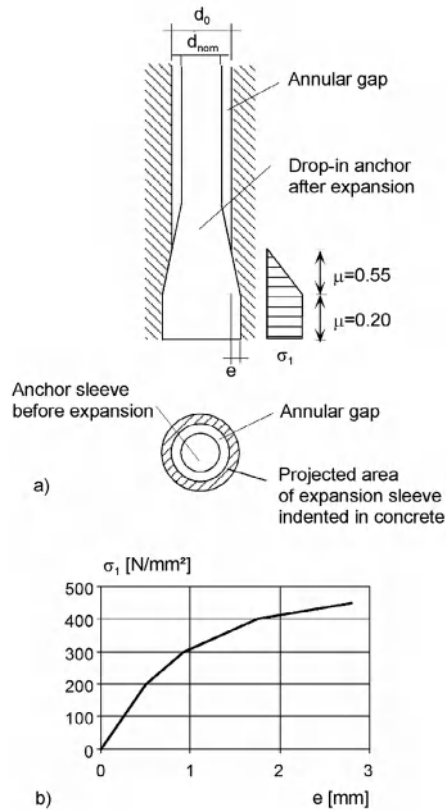


**Fig. 4.51** Assumptions when calculating the pull-out loads of drop-in anchors in non-cracked concrete (after Lehmann (1993))

- a) Indentation of anchor expansion elements in concrete and resulting concrete bearing stress  
b) Concrete bearing stress as a function of concrete indentation

Pusill-Wachtsmuth (1978) via the evaluation of approximately 900 tests using 11 different expansion anchors. This study concludes, as did the original study, that the Wagner-Grey (1977/1) approach provides at best a rough approximation of the pull-out load and that additional investigations are necessary.

The pull-out loads of metal expansion anchors were investigated in detail by Lehmann (1993). Fig. 4.51 illustrates the assumptions applied in the analysis using the example of a drop-in anchor. The indentation in the concrete caused by setting the anchor is determined from the geometry of the expanded anchor and the diameter of the drilled hole (Fig. 4.51a). The pres-

sure developed in the concrete is shown in Fig. 4.51b in relation to the degree of incursion of the expansion sleeve into the concrete; it was developed for a concrete cube compressive strength  $f_{cc,200} \approx 30 \text{ N/mm}^2$ . The curve shown in Fig. 4.51b was derived from the results of tests carried out by *Lieberum* (1987) in which concrete specimens were subjected to extreme concentrated loads. The expansion force  $F_{ex}$  is derived by integrating the pressure between anchor and concrete around the circumference and the length of the expansion zone. The load transfer coefficient in the zone of concrete deformation (idealised as a conical shape) was taken to be  $\mu = 0.55$  while the coefficient of friction in the cylindrical part of the contact zone was taken as  $\mu = 0.20$  (see Fig. 4.51a). These coefficients were determined from tests in which variously shaped steel elements were pulled through holes drilled in concrete. The same model is also applied to predict the pull-out loads associated with torque-controlled expansion anchors. It has been further extended to include anchors in cracked concrete and provides a usable correlation between analysis and test results. It is well suited to analytical studies of the influence of installation parameters (actual drill bit diameter, measured anchor expansion displacement) on the pull-out load.

Torque-controlled expansion anchors that do not exhibit concrete cone breakout at ultimate should be designed such that failure of the anchor is characterised by *pull-through* rather than *pull-out*. Extraction of the entire anchor, including the expansion elements, indicates failure of the anchor to develop follow-up expansion and therefore represents a less stable and predictable behaviour, whereas pull-through is an extension of the follow-up expan-

sion process (see section 2.3.3.1). It should be noted that expansion anchors that exhibit reliable follow-up expansion may also fail by concrete cone breakout if sufficiently high expansion forces are developed. Follow-up expansion is achieved only if the frictional resistance developed between the cone and sleeve is less than the resistance developed between the sleeve and the hole surface (*Mayer* (1990)). The pull-through load can be predicted by multiplying the expansion force  $F_{ex}$  determined according to *Lehmann* (1993) in relation to the anchor geometry (see Fig. 4.51) with the load transfer coefficient  $\mu_{ce}$  between cone and expansion sleeve. This factor should be determined as  $\mu_{ce} = \tan(\alpha + \rho)$  with  $\alpha =$  angle of cone and  $\rho =$  angle of friction between cone and expansion sleeve.

Predictions for pull-out and pull-through loads essentially depend on the assumptions made concerning the normal force generated at the load transfer zone, as well as the applicable coefficients of load transfer (friction). These material parameters exhibit relatively large scatter, and further testing is necessary to adequately assess the analytical results of *Mayer* (1990) and *Lehmann* (1993).

Increasing bearing pressure below the contact surface of a headed stud or undercut anchor leads to a significant increase in anchor displacement, which in turn can result in a reduction of the effective embedment depth and the associated concrete cone breakout load as predicted by equation (4.5) (Fig. 4.52). These displacements are attributable to the fact that the concrete is crushed locally in the bearing area. This can be seen at the head of the stud in Figs 4.5b and 4.44. *Eligehausen, Fuchs, Ick, Mallée,*

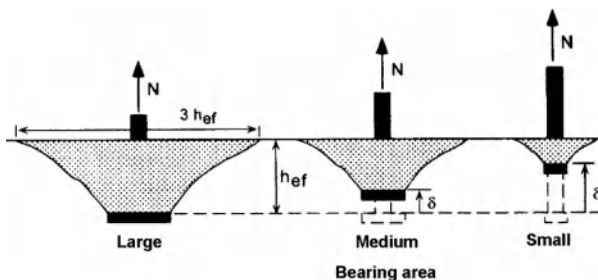


**Fig. 4.52** Concrete breakout cones of headed studs with heads of various diameters (schematic) (after *Furche* (1994))

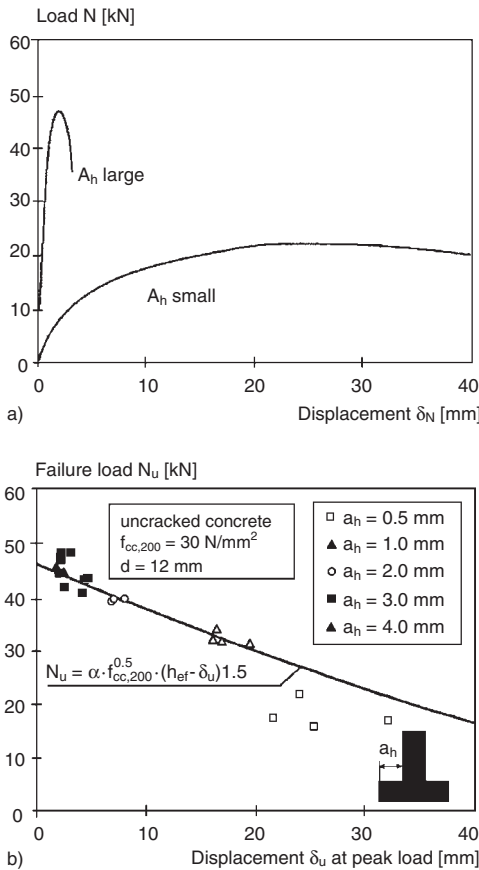


**Fig. 4.53** Influence of head size on behaviour of headed studs (after *Furche* (1994))  
 a) Load-displacement curves for two different head sizes (schematic)  
 b) Ultimate loads of headed studs as a function of displacement at failure

*Reuter, Schimmelpfennig, Schmal* (1992) estimate the magnitude of the critical maximum bearing pressure to ensure the concrete cone breakout load as predicted by equation (4.5) to be about  $15 \cdot f_{cc,200}$ . This value was derived from tests on headed studs with an embedment depth  $h_{ef} = 185 \text{ mm}$ .

The load-bearing behaviour of headed studs exhibiting concrete cone and pull-out failure modes was investigated in detail by *Furche* (1994), whereby a smooth transition from concrete cone failure to pull-out failure was assumed. The analytical correlation between

concrete pressure beneath the head and the displacement  $\delta$  of the head was determined using a physical model. This displacement reduces the effective embedment depth and the associated concrete cone breakout load for a headed anchor as a function of the bearing stress or bearing area. The derived expressions for the failure load address both the concrete cone breakout and pull-out failure modes as well as the intervening transition range. Fig. 4.53a plots typical load-displacement curves of two headed studs having large and small bearing area. In Fig. 4.53b the measured failure loads are shown as a function of the displacement  $\delta_u$  at peak load together with the relation for the failure load developed by *Furche* (1994). Fig. 4.53b reveals a usable correlation between calculated and measured ultimate loads. Expressed as a function of the concrete cube compressive strength, the critical maximum bearing pressure corresponding to concrete cone breakout as per equation (4.5) is, according to *Furche* (1994), about  $10 \cdot f_{cc,200}$  for  $h_{ef} = 40 \text{ mm}$  and  $14 \cdot f_{cc,200}$  for  $h_{ef} = 200 \text{ mm}$  (Fig. 4.54). The latter value coincides well with the limit derived by *Eligehausen, Fuchs, Ick, Mallée, Reuter, Schimmelpfennig, Schmal* (1992).

The pull-out failure load is not influenced by the presence of orthogonal surface reinforcement or by normally spaced stirrups, ties, etc. An increase in the pull-out load is theoretically possible if the concrete in the force transfer zone is confined by means of closely spaced spirals or hoops sufficient to restrict lateral

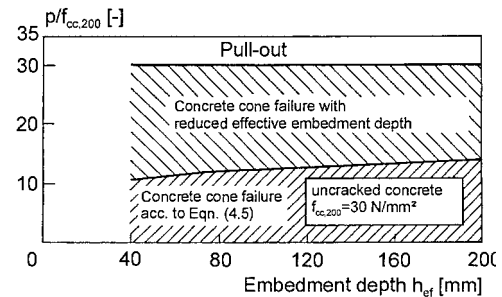


**Fig. 4.54** Maximum average bearing pressure under the head related to the concrete compressive strength required to assure the concrete cone failure load in non-cracked concrete predicted by equation (4.5), as a function of embedment depth (after *Furche* (1994))

strains. However, such closely spaced reinforcement is generally not feasible in practice.

#### 4.1.1.6 Failure load associated with splitting of the concrete

The splitting failure mode can occur during installation when applying a torque moment to fasteners or during anchor loading (see section 4.1.1.1c). These two cases are addressed separately.

##### a) Splitting during installation

Displacement-controlled and torque-controlled expansion anchors as well as undercut anchors generate a radial expansion pressure in the concrete during the installation process. This is also valid for headed studs that are prestressed. Integration of the expansion pressure over the contact area yields the expansion force  $F_{ex}$  (Fig. 4.55, left). Integrating the pressures along one axis only yields the splitting force  $F_{sp}$  (Fig. 4.55, right) across that axis. In the case of displacement-controlled expansion anchors, the magnitude of the splitting force depends on the expansion displacement and the deformation resistance of the concrete. For torque-controlled expansion anchors, the magnitude of the applied torque, the translation of the torque into axial tension (equation (3.8)) as well as the geometry and friction characteristics of the anchor in the expansion zone are all influencing factors. The splitting forces associated with undercut anchors that are installed in pre-drilled undercuts depend on the magnitude of applied prestressing and the resulting concrete pressures in the region of the undercut. Undercut anchors that form the undercut during anchor installation generate splitting forces during the undercutting process.

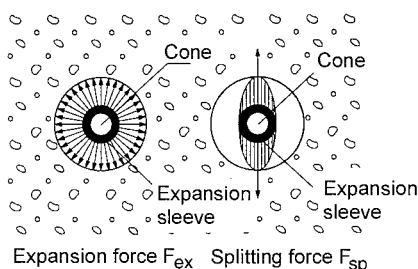


**Fig. 4.55** Definition of expansion force and splitting force (after Mayer (1990))

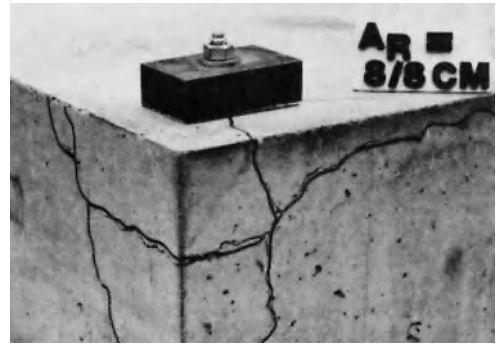


**Fig. 4.56** Splitting cracks which occurred during the installation of a torque-controlled expansion anchor in the corner of a concrete member (Rehm, Eligehausen, Mallée (1988))

The ratio of the splitting force generated in the concrete to the tensile force in the anchor bolt is approximately 1.0 to 2.0 for torque-controlled expansion anchors, 0.7 to 1.0 for undercut anchors, and 0.5 for headed studs (Asmus (1999)).

The splitting resistance depends on the concrete strength, thickness of the member, edge or corner distance and, in the case of anchor groups, the anchor spacing. If anchors are installed too close to an edge, splitting may occur during anchor installation (Fig. 4.56). The minimum spacing, edge distance and component thickness necessary to prevent splitting depend on the type of anchor and type of construction – for the reasons outlined above. They should be determined experimentally and in some countries are specified in the product approval. They may vary from product to product, even for similar anchor systems. The following values should be regarded as a guide. They are applicable for a component thickness  $h \geq 2h_{ef}$  and concrete grades  $\geq C 20/25$ .

Minimum edge distance:

$$\begin{aligned}
 c_{min} &\sim 1.0 \cdot h_{ef} \text{ undercut anchors,} \\
 &\sim 2.0 \cdot h_{ef} \text{ torque-controlled expansion} \\
 &\quad \text{anchors with one expansion} \\
 &\quad \text{cone,} \\
 &\sim 3.0 \cdot h_{ef} \text{ torque-controlled expansion} \\
 &\quad \text{anchors with two opposing} \\
 &\quad \text{expansion cones,} \\
 &\sim 3.0 \cdot h_{ef} \text{ drop-in anchors.}
 \end{aligned}$$

Minimum spacing:

- $s_{min} \sim 1.0 \cdot h_{ef}$  torque-controlled expansion anchors with one expansion cone and undercut anchors,  
 $\sim 1.5 \cdot h_{ef}$  torque-controlled expansion anchors with two opposing expansion cones,  
 $\sim 2.5 \cdot h_{ef}$  drop-in anchors.

The minimum spacing and edge distance required to prevent splitting during installation are greatest for drop-in type anchors because the expansion displacement generates very high splitting forces. Due to their follow-up expansion capability torque-controlled expansion anchors need smaller expansion forces during installation and therefore smaller minimum distances than drop-in anchors. Undercut anchors require smaller minimum distances than do torque-controlled expansion anchors because the splitting forces during installation are considerably lower due to the larger cone angle and the increased bearing area.

Headed studs welded to fixtures are not pre-stressed. Therefore, no splitting forces occur during installation. It should be noted that a minimum edge distance is required to protect against corrosion and to ensure adequate placement of the concrete. Minimum values of  $c = 2.5 \cdot d \geq 50$  mm and  $s = 5 \cdot d \geq 50$  mm are recommended.

### b) Splitting failure of loaded fasteners

Analytical studies to determine the failure load associated with the splitting failure mode for expansion anchors were conducted by *Pusill-Wachtsmuth* (1982) and *Weyerhäuser* (1984). However, the simplifying assumptions employed, especially with regard to concrete behaviour, do not permit a generalisation of the results.

The behaviour of headed studs that exhibit the splitting failure mode when loaded in tension was investigated by *Pukl, Ozbolt, Schlottke, Eligehausen* (1993) with the aid of three-dimensional computer models. The behaviour of the concrete was simulated using a model based on non-linear fracture mechanics. The results of the calculations show that there is stable growth of the radial cracks before attainment of peak load. As the edge distance is

increased, the splitting failure mode gradually changes to a concrete cone breakout. This analysis indicates that the splitting failure load depends on the ratio of splitting force to tensile force (a function of anchor geometry), on anchor spacing, edge distance and component thickness, as well as on concrete tensile strength. In components with a minimum thickness ( $h \approx h_{ef} + 30$  mm), the transition from splitting failure to concrete cone breakout occurs at an edge distance of  $c \approx 2 \cdot h_{ef}$ .

The load-bearing behaviour of expansion and undercut anchors as well as headed studs that exhibit splitting failure was investigated in detail both numerically (using non-linear FEM) and experimentally by *Asmus* (1999). It is assumed that splitting failure, analogous to other concentrated load problems, is influenced by the magnitude of the bearing stress, the anchor location relative to other loaded anchors and free edges, and the concrete strength. The stress in the concrete is assessed from the geometrical dimensions, and the ratio of splitting force to applied tension load is found to increase with increasing bearing stress (compare with section 4.1.1.4). Size effect is taken into account in determining the resistance of the concrete to splitting.

The equations derived by *Asmus* (1999) are well suited to calculating the splitting failure load for anchorages comprised of headed studs, undercut anchors and torque-controlled expansion anchors near an edge or corner of a component or in a narrow member. However, they are less suitable for design purposes. Therefore, a simplified approach is proposed below.

This simplified method for predicting the splitting failure load uses an equation similar to that developed for the CC-Method, as shown below:

$$N_{u,sp} = \frac{A_{c,sp}}{A_{c,sp}^0} \cdot \psi_{s,sp} \cdot \psi_{ec,sp} \cdot \psi_{re,sp} \cdot \psi_{h,sp} \cdot N_{u,c}^0 \quad [\text{N}] \quad (4.16)$$

where:

$$\psi_{h,sp} = \left( \frac{h}{2 \cdot h_{ef}} \right)^{2/3} \leq 1.0 \quad (4.16a)$$

$\psi_{re,N}$  according to equation (4.10a)  
or (4.10b)

$N_{u,c}^0$  according to equation (4.5)



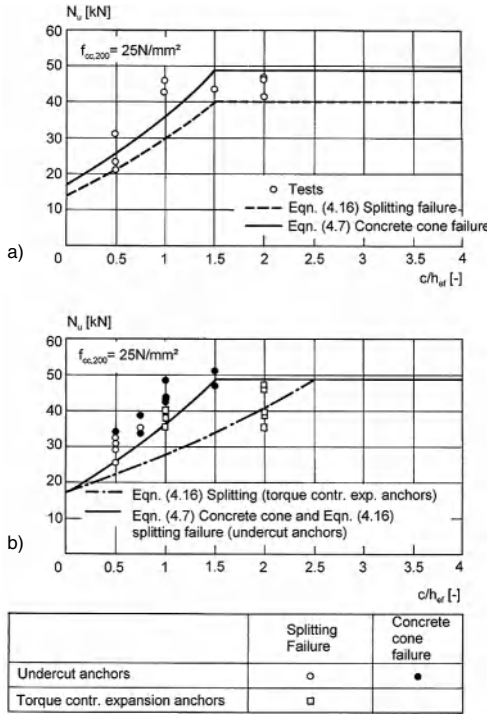


**Fig. 4.57** Comparison of measured failure loads of single anchors ( $h_{ef} = 80 \text{ mm}$ ) close to the edge of a concrete member with the calculated values for concrete cone failure and splitting (after Asmus (1999))  
 a) Undercut anchors, member thickness  $h = 1.5h_{ef}$   
 b) Undercut and torque-controlled expansion anchors, member thickness  $h = 2 h_{ef}$

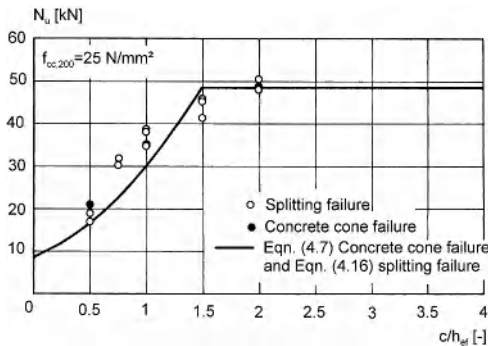


**Fig. 4.58** Measured failure loads of single undercut anchors ( $h_{ef} = 80 \text{ mm}$ ) in the corner of a concrete member ( $h = 2 h_{ef}$ ) compared to the calculated values for concrete cone failure and splitting failure (after Asmus (1999))

Projected areas  $A_{c,sp}$  and  $A_{c,sp}^0$  are calculated in accordance with the instructions given for equation (4.6) and the factors  $\psi_{s,sp}$  and  $\psi_{ec,sp}$  are obtained with equations (4.7a) and (4.8a) whereby in calculating the projected areas and associated factors  $\psi_{s,sp}$  and  $\psi_{ec,sp}$ , the values  $c_{cr,N}$  and  $s_{cr,N}$  are replaced by  $c_{cr,sp}$  and  $s_{cr,sp}$ . The characteristic edge distance and spacing  $c_{cr,sp}$  and  $s_{cr,sp}$  ensure that the splitting failure load corresponds to the concrete cone failure load. These values are explained below.

Equation (4.16) is structured similarly to equation (4.10) for calculating the concrete cone breakout load. In addition, the influence of a thin component ( $h < 2 \cdot h_{ef}$ ) on the splitting failure load is taken into account by the factor  $\phi_{h,sf}$ . As the splitting failure load cannot exceed the concrete cone failure load, for anchorages meeting the conditions  $s \geq s_{cr,sp}$ ,  $c \geq c_{cr,sp}$  and  $h \geq 2 \cdot h_{ef}$  equation (4.16) reduces to equation (4.10). The characteristic spacing and edge distance values  $s_{cr,sp} = 2 \cdot c_{cr,sp}$  as required to ensure development of the full concrete cone breakout load depend on the particular characteristics of the anchor. The characteristic edge distance for fastenings near the edge of a component in components with a thickness  $h \approx 2 \cdot h_{ef}$  is approximately:

- $c_{cr,sp} \sim 1.0 \cdot h_{ef}$  headed studs
- $\sim 1.5 \cdot h_{ef}$  undercut anchors
- $\sim 2.5 \cdot h_{ef}$  torque-controlled expansion anchors with one expansion cone
- $\sim 3.0 \cdot h_{ef}$  drop-in anchors, torque-controlled expansion anchors with two opposing expansion cones

The above values should be increased by about 20% for anchors close to an edge on two sides (narrow member or corner of a concrete element).

Equation (4.16) should be regarded as a conservative approximation to the real behaviour. The splitting failure load is in part dependent on other parameters which do not affect the concrete cone breakout load. However, it can safely predict the splitting capacity of an anchor as confirmed by Figs. 4.57 and 4.58, which apply

to single anchors near the edge and in the corner of a component, respectively.

If the characteristic edge distance associated with splitting failure for a given anchor is less than or equal to the value associated with concrete cone breakout ( $c_{cr,sp} \leq c_{cr,N}$ ) and the component thickness is  $h \geq 2 \cdot h_{ef}$ , then splitting does not occur and equation (4.16) can be neglected for all applications.

### c) The influence of reinforcement on the splitting failure mode

Reinforcement parallel to the edge can be effective for accommodating splitting forces although it will not prevent the occurrence of splitting cracks. If reinforcement is designed to carry the induced splitting forces, its role is to prevent splitting cracks from widening excessively. In the case of anchors that are designed for use in cracked concrete, the concrete cone breakout capacity or pull-out capacity associated with cracked concrete will be maintained (see section 4.2.1) if sufficient crack control reinforcing is present. Given a constant tension load  $N$  applied to an anchor, the associated splitting force  $F_{sp}$  generated in the concrete will depend on the relevant details of the anchor construction. The following values can be taken as first approximations:

$$\begin{aligned} F_{sp} &\approx 0.5 \cdot N && \text{headed studs} \\ F_{sp} &\approx 0.8 \cdot N && \text{undercut anchors} \\ F_{sp} &\approx 1.5 \cdot N && \text{torque-controlled expansion} \\ &&& \text{anchors with one expansion cone} \end{aligned}$$

## 4.1.2 Shear

### 4.1.2.1 Load-displacement behaviour and modes of failure

Fig. 4.59 depicts a typical load-displacement curve for a preloaded (torqued) anchor loaded in shear with no proximate edges. The corresponding curve associated with tension loading for the same anchor is provided for comparison. At the steep start of the shear loading curve, the shear force is transferred between the concrete and the baseplate via friction as generated by the preload in the anchor. When the externally applied shear load exceeds the available friction resistance the plate slips as required to engage the anchor in bearing. The lateral deformation of the anchor as it bears against the surface concrete generates a

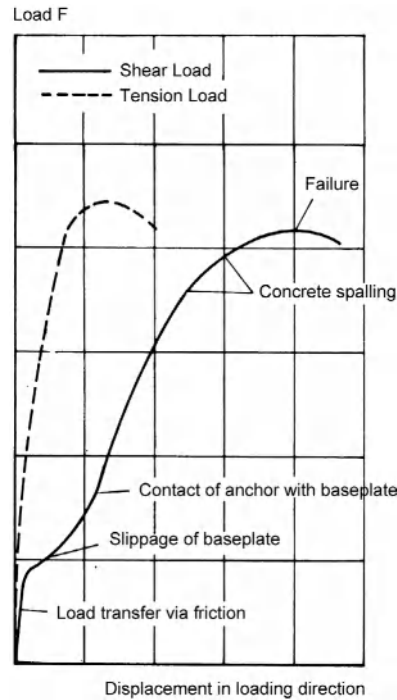


**Fig. 4.59** Idealised load-displacement curves for anchors subjected to tension and shear (Rehm, Eligehausen, Mällée (1988))

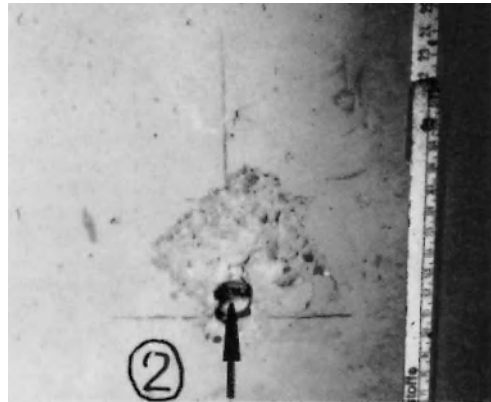


**Fig. 4.60** Fracture pattern of an anchor remote from an edge when subjected to shear (taken from Fuchs, Eligehausen (1990))

corresponding catenary tensile force in the anchor bolt. As the shear load increases the bearing stress in the surface concrete increases until of a shallow spall occurs (Fig. 4.60). The fracture



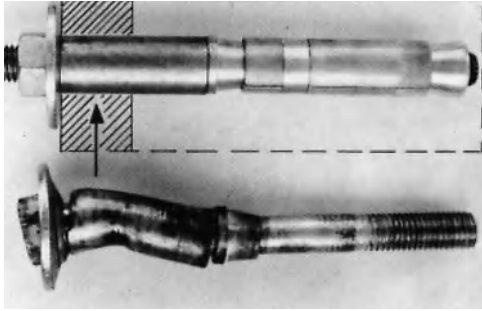


**Fig. 4.61** Expansion anchor before and after shear load test (taken from *Eligehausen, Pusill-Wachsmuth (1982)*)

of the surface concrete transfers the bearing resultant to a location further from the point of load application thus increasing the lever arm and the associated flexural stress in the anchor (Fig. 4.61). With sufficient embedment depth the anchor may be capable of resisting additional load until the failure of the anchor bolt (Fig. 4.60). Owing to the locally high bearing stresses, the spalling of the concrete and the associated bending deformation of the anchor, displacements associated with shear loading at ultimate are markedly greater than for axial loading (Fig. 4.59).

Anchor bolts with variable cross-sectional area (e.g. of the type depicted in Fig. 2.19a<sub>3</sub>) may fracture at the reduced cross-section due to the catenary tensile force induced in the anchor. Alternately, anchors with small embedment depths may break out or be pulled out of the concrete before reaching their steel capacity.

The load-displacement behaviour of a cast-in-place headed stud subjected to shear is similar to that of a post-installed anchors. Headed studs that are welded to an embedded plate (e.g. shear studs) lack the benefit of pretensioning; on the other hand, the load path is direct (no annular gap) and the embedded plate adds to the stiffness of the fastening until the concrete in front of the plate is spalled away. Shear studs also produce concrete spalls at the point of bearing because load eccentricity and the associated catenary tension in the studs causes the base-plate to lose contact with the concrete at near-ultimate load levels. Fig. 4.62 provides an example of such spalling, albeit in this case for



**Fig. 4.62** Shell-shaped concrete spalling for a headed stud remote from an edge when subjected to shear (taken from *Fuchs (1990)*)

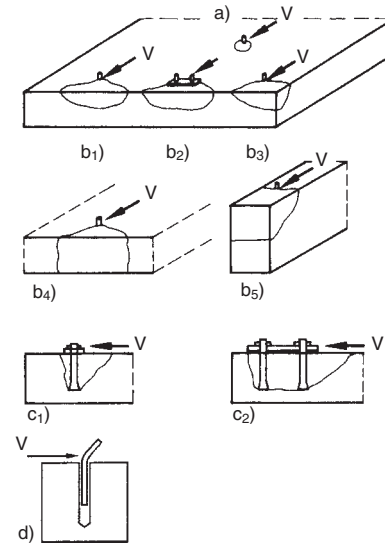


**Fig. 4.63** Failure modes for shear loading (*Eligehausen, Malleé, Rehm (1997)*)

- Steel failure
- Concrete edge failure
- Concrete pry-out failure
- Pull-out failure

a headed stud bolted to the not embedded base-plate.

Possible failure modes associated with anchors subjected to shear loading are illustrated in Fig. 4.63.

#### a) Steel failure

Anchors loaded in shear exhibit steel failure when the edge distance and the embedment depth are sufficiently large, whereby conical

spalling of the surface concrete precedes steel failure (Figs. 4.60, 4.62, and 4.63a). For a given anchor, steel failure represents a limit on the maximum shear capacity. Anchors made of ductile steels can develop relatively large displacements at failure.

#### b) Concrete edge failure

Anchors loaded in shear toward a proximate free edge may fail by development of a semi-conical fracture surface in the concrete originating at the point of bearing and radiating to the free surface (Fig. 4.63b<sub>1</sub>). A group of anchors loaded in shear and proximate to an edge may develop a common conical fracture surface (Fig. 4.63b<sub>2</sub>), and the development of the fracture surface is interrupted by the presence of a corner (Fig. 4.63b<sub>3</sub>), by the limited depth of the member (Fig. 4.63b<sub>4</sub>) or by proximate edges parallel with the load direction (Fig. 4.63b<sub>5</sub>). In these cases the failure load associated with the anchor or one anchor of the group is reduced compared to the application shown in Fig. 4.63b<sub>1</sub>.

#### c) Pry-out failure

Anchors and shear studs having limited embedment and loaded in shear can exhibit sufficient rotation to produce a pry-out fracture whereby the primary fracture surface develops 'behind' the point of load application (Fig. 4.63c<sub>1</sub>). Anchor groups may develop a common pry-out fracture surface. (Fig. 4.63c<sub>2</sub>). This failure mode does not depend on the presence of free edges.

#### d) Pull-out failure

Pull-out failure under shear loading is generally associated with expansion anchors that cannot develop sufficient frictional resistance to accommodate the catenary tension force generated in the anchor bolt as a result of lateral deformation. This failure mode is rarely observed and is not dealt with in any further detail here.

As in the case of anchors loaded in tension and failing by concrete cone breakout or by splitting, concrete edge breakout and pry-out failures under shear load represent the maximum capacity of the concrete to transmit tensile stresses. Anchor lateral displacements associated with concrete edge breakout and with pry-out failure are dependent on edge distance and anchor embedment, nevertheless, they are gen-

erally significantly smaller than those corresponding to steel failure.

### 4.1.2.2 Failure load associated with steel rupture

#### a) Shear load without lever arm

In addition to shear stresses and catenary tension stresses, anchors subjected to shear loads also experience secondary bending stresses. The influence of bending stresses on the failure load associated with anchor steel rupture is generally negligible for cast-in-place embedded plates with welded shear studs and for baseplates secured with pretensioned anchors. Thin grout layers ( $\leq 3$  mm), e.g. as required to smooth out the concrete surface, will generally not contribute significantly to these bending stresses. However, in instances where thicker grout pads are used, e.g. to permit baseplate levelling, spalling of the grout in front of the leading anchors may result in the shear load being transferred primarily via bending in the anchors as opposed to shear in the grout pad. According to *Bouwman, Gresnigt, Romeijn* (1989) grout pads with a thickness of less than 20 mm do not have a negative effect on the shear strength of column connections.

At present, there is no generally acknowledged theoretical approach to calculate the steel failure load associated with the complex interaction of shear, tension and bending stresses developed in a shear-loaded anchor. It is frequently assumed that failure occurs when the bending stresses in the anchor exceed the tensile strength of the steel. This leads to solutions based on the classical indeterminate problem of a beam on an elastic or elasto-plastic foundation (*Friberg* (1940), *Basler, Witta* (1967), *Wiedenroth* (1971), *Cziesielski, Friedmann* (1983)). *Rasmussen* (1963) and *Vintzeléou, Tassios* (1987) assume a distribution of concrete bearing stress and the onset of full plastic moment in the anchor bolt at a defined distance from the surface of the concrete to determine the associated bolt failure load.

The failure loads predicted by *Friberg* (1940) and *Wiedenroth* (1971) average roughly 50% of measured values (*Fuchs* (1990)). Although failure loads predicted by other approaches coincide, on average, reasonably well with measured loads, the coefficient of variation associ-

ated with the ratio of measured to calculated failure loads is quite high ( $v \approx 30\%$  to  $40\%$ ). Thus a simple and straightforward approach based on the relation  $V_{u,s} = \alpha \cdot A_s \cdot f_u$  appears more reasonable. Using regression analysis, *Fuchs, Eligehausen* (1986/1) have established the coefficient  $\alpha = V_{u(test)}/V_{u(calculation)}$  associated with approximately 220 test series. A variety of post-installed anchor systems are represented in this database for which all tests resulted in steel failure. Taking  $f_u$  as the nominal steel strength, a mean value  $\alpha = 0.68$  results. However, steel strengths associated with the test specimens, while generally not recorded, likely exceeded nominal values. Past experience indicates that the actual steel strength is 1.1 times to 1.2 times the nominal value, resulting in a mean value  $\alpha \approx 0.6$ .

Tests with welded shear studs produce a higher coefficient  $\alpha$ . This is attributable to the strengthening of the cross-section provided by the weld metal and the reduced bending moment associated with the fixity of the stud and resulting double curvature. When the measured steel strength is taken for  $f_u$ , a value  $\alpha \approx 0.7$  was found by *Klingner, Mendonca* (1982/3) and *Roik* (1982) and  $\alpha \approx 1.0$  by *Anderson, Meinheit* (2000).

The following equation is proposed for calculating the mean shear capacity of the steel bolt:

$$V_{u,s} = \alpha \cdot A_s \cdot f_u \quad (4.17)$$

where:

$\alpha = 0.6$  for anchors

$\alpha = 0.7$  for headed studs welded to the baseplate

$f_u$  = measured tensile steel strength

Strictly speaking, equation (4.17) is valid only for the conditions present in the tests used for the evaluation, i.e. single headed studs with shank diameter  $d \leq 22$  mm and measured steel strength  $f_u \leq 500$  N/mm<sup>2</sup> and single post-installed anchors with bolt size less than M20 and measured steel strength  $f_u \leq 1000$  N/mm<sup>2</sup>. Furthermore, the embedment depth must be sufficient to preclude pry-out failure of the anchor (section 4.1.2.3).

The *Huber-Hencky-Mises* yield condition predicts a value for  $\alpha$  associated with shear yield of  $1/\sqrt{3} = 0.57$ . *Valtinat* (1982) specifies a value of

$\alpha = 0.625$  for machine bolts as derived from tests. According to *Schmidt, Knoblauch* (1988) the coefficient  $\alpha$  is dependant on the steel strength of the bolt and can be taken as  $\alpha = 0.68$  for ISO Grade 4.6 bolts and  $\alpha = 0.60$  for ISO Grade 10.9 bolts. *Klingner, Mendonca* (1982/3) recommend a value of  $\alpha = 0.675$  for shear studs, whereas for headed studs welded to baseplates *Roik* (1982) proposes  $\alpha = 0.70$  and *Anderson, Meinheit* (2000) recommend  $\alpha = 1.0$ . For undercut anchors *Cook, Klingner* (1989) recommend that  $\alpha$  be taken as 0.60. Thus the coefficients proposed in equation (4.17) are – with the exception of the proposal of *Anderson, Meinheit* (2000) – generally in accordance with published results.

*Ollgaard, Slutter, Fisher* (1971) and *Roik* (1982) identify concrete spalling as a failure criterion in addition to pure steel failure. *Ollgaard, Slutter, Fisher* (1971) propose equation (4.18) for the average shear failure load of studs welded to baseplates when concrete spalling occurs. Nevertheless, for standard concrete and steel strengths and sufficiently large embedment depths, *Klingner, Mendonca* (1982/3), *Meinheit, Heidbrink* (1985) and *Fuchs* (1990) all report failure loads in accordance with equation (4.17) for specimens exhibiting spalling prior to steel rupture.

$$V_{u,sp} = 0.5 \cdot A_s \cdot \sqrt{E_c \cdot f_c} \quad (4.18)$$

For group anchorages where a shear force acts concentrically on the baseplate, the failure load is theoretically  $n$  times the value given by equation (4.17) for a single anchor, where  $n$  is the number of anchors. However, for anchorages comprises of anchors arranged linearly in the direction of applied shear load, uniform load distribution at ultimate load levels occurs only if there is no play between the anchors and the holes in the baseplate, or if the anchors are welded to the baseplate. If, however, the anchors have play or are not welded to the baseplate, then the random positioning of the anchors within the hole clearance will result in uneven load sharing. Similarly, the anchors will experience different displacement demands at ultimate load depending on hole clearances and the relative anchor positions. Nevertheless, the effect of the unevenly distributed load on the steel failure load for fastenings with up to three

anchors in a row collinear with the load direction may be marginal (Fuchs, Eligehausen (1990)) if the anchors have sufficient plastic deformation capacity and are installed with standard hole clearances as specified in Table 3.2, (e.g. 2 mm for M12). This has also been confirmed experimentally via tests on reinforced concrete corbels connected to columns with HSFG bolts (Eibl, Schürmann (1982)). A clear reduction in the failure load resulted only: (a) if the anchors possessed insufficient plastic deformational capacity and/or (b) they were installed with significantly greater hole tolerances than the maximum values given in Table 3.2, or (c) the anchorage consisted of more than three anchors in a row collinear with the load direction. In such cases it is recommended to reduce the coefficient  $\alpha$  in equation (4.17) by 20% (Fuchs, Eligehausen (1990)). The resulting coefficient  $\alpha \approx 0.5$  is also recommended in Cook, Klingner (1989) for group anchorages.

**b) Shear load with lever arm**

In stand-off installations (e.g. facade anchors), anchors are clearly subjected to cantilever bending. Flexural failure of the steel rod generally defines the capacity of such anchorages provided the distance to the edge of the component is sufficiently large.

The average bending moment in a bolt at failure  $M_{u,s}^0$  can be calculated using equation (4.19a) (Scheer, Peil, Nölle (1987)). It corresponds to the plastic bending moment at failure:

$$M_{u,s}^0 = 1.7 \cdot W_{el} \cdot f_y \tag{4.19a}$$

where:

- $W_{el}$  = section modulus for the threaded part calculated based on the net tensile area
- $f_y$  = measured steel yield stress

The 5% fractile of the bending moment corresponding to rupture is approximately 90% of the average value. It is calculated using equation (4.19b):

$$M_{u,s,5\%}^0 = 1.5 \cdot W_{el} \cdot f_y \tag{4.19b}$$

In deriving equation (4.19a) a 10° rotation of the threaded stud was defined as the failure criterion. The angle of rotation corresponds to the angle between the non-deformed axis of the bolt and a line joining the point of fixation with the point at which the load is applied in the deformed state.

Fig. 4.64 shows the bending moments at failure as measured in tests compared to the theoretical 5% fractile of the bending moments at failure as predicted by equation (4.19b). This diagram

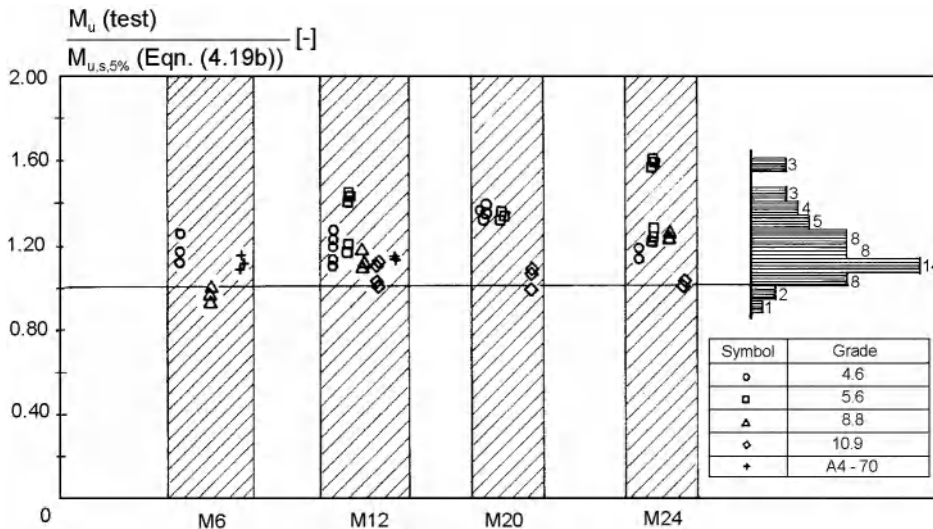


**Fig. 4.64** Ratio of measured ultimate and calculated characteristic bending moments as a function of bolt diameter (after Scheer, Peil, Nölle (1987))

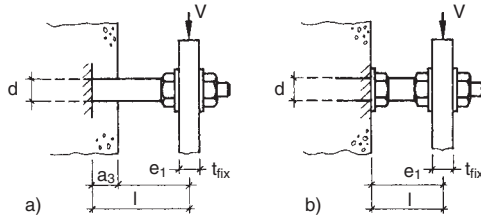


**Fig. 4.65** Definition of shear load lever arm for stand-off installation (after Comité Euro-International du Béton (1995))

applies to cases in which the point of fixity was located in the bolt shank. It shows that equation (4.19b) produces sufficiently accurate results.

Extensive tests on specimens subjected to bending reveal that equation (4.19) is also valid for post-installed anchors (Varga, Eligehausen (1994)). However, when calculating the acting bending moment an adjustment to the lever arm  $l$  according to equation (4.20) is required for the application shown in Fig. 4.65a to account for local spalling caused during the drilling process. If additional rotational restraint is provided as shown in Fig. 4.65b, the effect of spalling on the ultimate capacity may be neglected.

$$l = e_1 + a_3 \tag{4.20}$$

where:

$e_1$  = distance between shear load and surface of concrete

$a_3 = 0.5 \cdot d$  (Fig. 4.65a)

= 0 (Fig. 4.65b)

According to Scheer, Peil, Nölle (1987) the average bending moment at failure decreases if tensile forces are applied simultaneously (equation (4.21)).

$$M_{u,s} = M_{u,s}^0 (1 - N / N_u) \tag{4.21}$$

where:

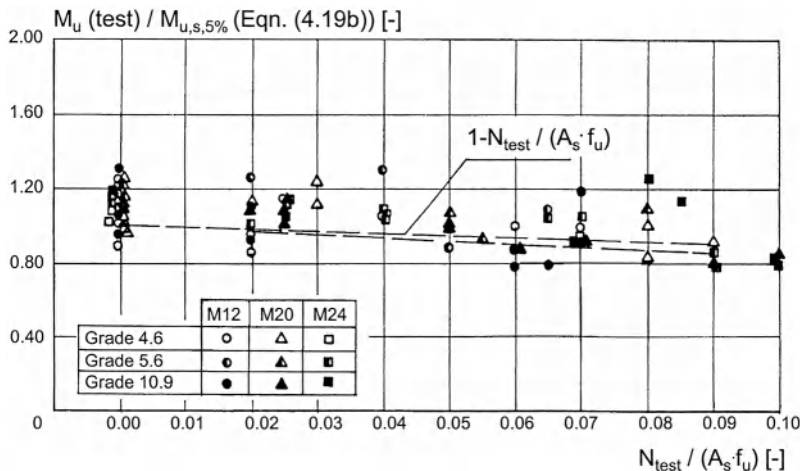
$M_{u,s}^0$  according to equation (4.19a)

$N$  = tensile force

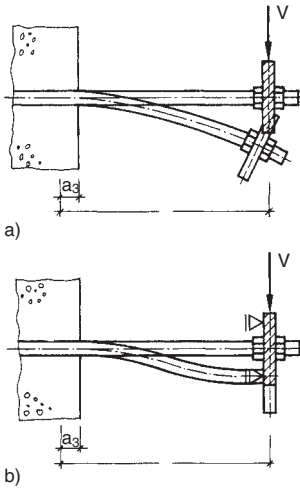
$N_u$  = failure load according to equation (4.1)

Fig. 4.66 shows the bending moments at failure measured in tests compared to the values calculated using equation (4.19b) in relation to the relative tensile load. The diagram shows that equation (4.21) describes the test results with sufficient accuracy.

According to Scheer, Peil, Nölle (1987) the influence of a shear force on the bending moment at failure does not need to be considered for related load eccentricities  $e_1/d \geq 1$ . This condition normally exists for fastenings with



**Fig. 4.66** Ratio of measured ultimate and calculated characteristic bending moments at failure as a function of the applied related tensile force (after Scheer, Peil, Nölle (1987))



**Fig. 4.67** Anchor with and without full fixity provided by the attachment (after Comité Euro-International du Béton (1995))  
 a)  $\alpha_M = 1.0$   
 b)  $\alpha_M = 2.0$

post-installed anchors, because when determining the lever arm  $l$ , the point of fixity is assumed to be a distance of  $0.5d$  behind the face of the concrete and, in addition, 0.5 times the thickness of the fixture is included (Fig. 4.65a). Therefore, the shear failure load for a stand-off installation can be calculated from the bending moment at failure according to equation (4.21), the lever arm of the shear load and the structural system (equation (4.22)):

$$V_{u,s} = \alpha_M \cdot M_{u,s} / l \tag{4.22}$$

where:

- $\alpha_M = 1.0$  when rotation of the baseplate and/or anchor is not restrained (Fig. 4.67a)
- $= 2.0$  when the anchor is restrained from rotation at the baseplate (Fig. 4.67b)

$M_{u,s}$  according to equation (4.21)

$l$  according to equation (4.20)

The coefficient  $\alpha_M$  depends on the degree of rotational fixity of the anchor where it joins the baseplate. A conservative figure should be chosen. If it is assumed that the anchor is restrained by the baseplate as shown in Fig. 4.67b, then the baseplate must have sufficient stiffness to resist the induced moment without significant deformation.

### 4.1.2.3 Failure load associated with pry-out

The load-bearing mechanism of a single headed stud anchorage subjected to a shear load is illustrated schematically in Fig. 4.68 (Zhao (1993)). The applied shear load gives rise to bearing stresses in the concrete. With increasing load the surface concrete is crushed or spalled, shifting the centroid of resistance  $V_b$  to a location deeper in the concrete. Also with increasing load and stud elongation, the baseplate rotates and loses contact with the concrete on the loaded side. These two mechanisms act to further increase the eccentricity between the applied shear load  $V$  and the stress resultant  $V_b$  in the concrete. The moment resulting from this eccentricity generates a compressive force  $C$  between baseplate and concrete and a tensile force  $N$  in the stud. If the tensile force in the stud exceeds the tensile capacity associated with the maximum fracture surface that can be activated by the stud, a fracture surface originating at the head of the stud and projecting in conical fashion behind the stud forms (Fig. 4.69). This is defined as a pry-out failure.

The tensile force in the stud or anchor depends on a number of factors, including the size of the baseplate. In the tests carried out by Zhao (1993) the clear distance of the shear studs from the edge of the baseplate corresponds more or less with the limits of constructibility. The tensile force in the studs at ultimate as measured with the aid of strain gauges is on average about 35% of the applied shear load. According to investigations by Fuchs (1990) using a non-linear finite element program, the tensile force developed in post-installed anchors at ultimate is approximately 40% of the applied shear load. The fracture surface area is approximately 60% to 70% of the area corresponding to a concentric tension load applied to an anchor with the

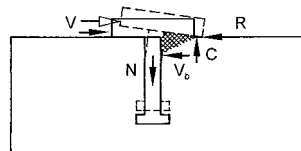


**Fig. 4.68** Load-bearing mechanism of headed stud anchorage subjected to shear loading (schematic) (after Zhao (1993))



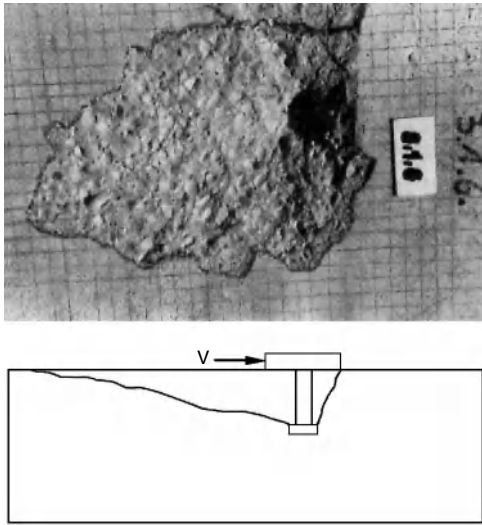


**Fig. 4.69** Typical failure body of a stud anchorage far from an edge loaded in shear (after Zhao (1993))  
 Top: Photo (taken from above)  
 Bottom: Cross-section of failure body (schematic)

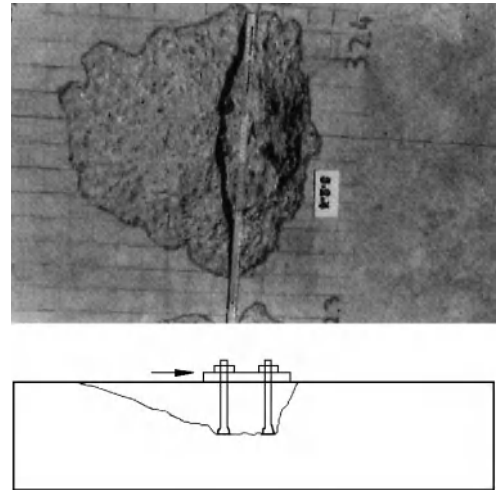


**Fig. 4.70** Typical failure body of a group of four headed studs far from an edge loaded in shear (after Eligehausen, Lehr (1993))  
 Top: Photo (taken from above)  
 Bottom: Cross-section of failure body (schematic)

same embedment. Owing to the compressive force  $C$ , the failure surface originates at the toe of the baseplate. The slope of the fracture surface is also characteristically shallower than that measured for a typical concrete cone breakout resulting from tension loading. Assuming that the distribution of the tensile stresses over the fracture surface is similar for shear and tension loads and ignoring the positive influence of the compressive force  $C$  on the concrete cone failure load, then the failure load of a single anchor corresponding to pry-out  $V_{u,cp}^0$  can be taken as:

$$V_{u,cp}^0 = \frac{R_u}{N/V} \tag{4.23a}$$

where:

$R_u$  = resistance associated with concrete cone breakout  $\approx 0.6 N_{u,c}^0$  to  $0.7 N_{u,c}^0$

$N/V$  = ratio of the tension force in the anchor to the applied shear force 0.35

Substituting:

$$V_{u,cp}^0 = \frac{0.6 \cdot N_{u,c}^0 \text{ to } 0.7 \cdot N_{u,c}^0}{0.35} = 1.7 \cdot N_{u,c}^0 \text{ to } 2.0 \cdot N_{u,c}^0 \tag{4.23b}$$

This may be simplified as follows:

$$V_{u,cp}^0 = k_1 \cdot N_{u,c}^0 \tag{4.23c}$$

where:

$$k_1 = 2.0$$

$N_{u,c}^0$  is determined in accordance with equation (4.5)

Tests by *Eligehausen, Lehr* (1993) indicate that the coefficient  $k_1$  is dependent on the embedment depth and may be less than 2.0 for  $h_{ef} < 60$  mm. These tests also show that pry-out failure occurs in anchor groups (Fig. 4.70), whereby the failure load can be approximated with the same approach used for single anchors.

The general case then becomes:

$$V_{u,cp} = k_1 \cdot N_{u,c} \tag{4.24}$$

where:

$$k_1 = 2.0 \text{ for } h_{ef} \geq 60 \text{ mm}$$

$$k_1 < 2.0 \text{ for } h_{ef} < 60 \text{ mm}$$

$N_{u,c}$  according to equation (4.10)

Here, the concrete cone failure load is calculated for the anchors that resist the shear loads. If the shear load is applied concentrically with respect to the anchorage centroid, then calcula-



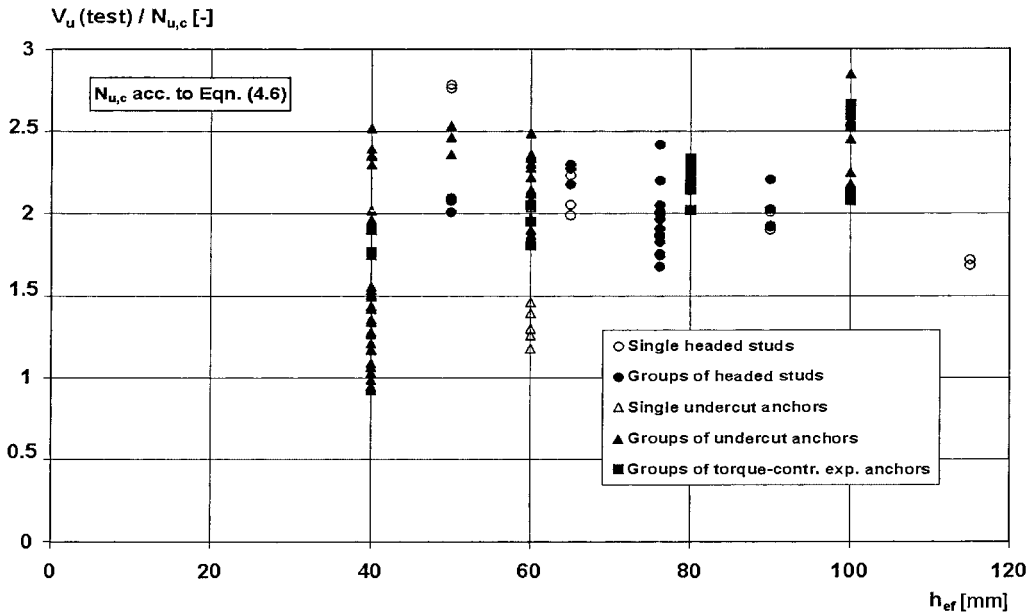


**Fig. 4.71** Ratio of measured shear failure load and calculated tension concrete cone failure load as a function of embedment depth (Elgehausen, Graf, Fuchs (1997))

tion of the projected area  $A_{c,N}$  includes all anchors in the group and the eccentricity factor  $\psi_{ec,N}$  in equation (4.8a) is taken as 1. If the shear load is applied eccentrically with respect to the anchorage centroid but still within the boundary of the anchor group, then again all anchors in the group are considered when calculating the projected area  $A_{c,N}$ , but for calculating  $\psi_{ec,N}$  the eccentricity  $e_N$  is taken relative to the centroid of the shear-resisting anchors only. Due to the complex nature of the shear load distribution to the anchors in the group, no approach is currently available for calculating the pry-out failure load associated with a shear load applied outside of the geometric boundary of the anchor group.

Fig. 4.71 shows the relationship of failure loads as measured in tests (concentric shear acting on fastenings with large edge distance) to the calculated concrete cone failure loads for tension calculated per equation (4.6) as a function of the embedment depth. All data points represent pry-out failures. It is apparent that the ratio  $V_u(test)/N_{u,c}$  is scattered about the value  $k_1 = 2.0$  for  $h_{ef} \geq 60$  mm, but that the value of  $k_1$  can

clearly be lower for  $h_{ef} = 40$  mm. For headed stud anchorages with  $h_{ef} \geq 60$  mm at an edge, loaded towards the edge, with special reinforcement to carry the shear load, a coefficient  $k_1 = 1.5$  is indicated from tests conducted by Ramm, Greiner (1991).

The embedment depth required to preclude pry-out failure, or rather to assure failure of the steel, depends on the steel strength, the diameter of the anchor, and the concrete strength. For groups, the anchor spacing is relevant as well. Therefore, the required embedment depth can vary substantially. Pry-out failure is often critical for the design of fastenings remote from an edge.

In theory, equation (4.24) applies also to fastenings located near the edge of a component that are subjected to shear loads parallel to or directed away from the edge. In calculating  $N_{u,c}$  the presence of the near-edge condition is accounted for in determining the projected area  $A_{c,N}$  and the factor  $\psi_{s,N}$  as per equation (4.7a). Further experimental studies are required to confirm this approach.

#### 4.1.2.4 Concrete edge failure for a shear load perpendicular to the edge

Anchorage close to an edge subjected to a shear load perpendicular to the edge may fail via fracture of the concrete before the load-carrying capacity of the steel is reached. Figures 3.2 and 4.72 show the resulting failure bodies of single anchors loaded perpendicular to the edge. Experimental investigations show that the fracture crack presents an angle with respect to the edge of  $35^\circ$  on average and develops to a depth at the face of the edge equal to approximately 1.3 times to 1.5 times the edge distance (*Stichting Bouwresearch* (1971), *Fuchs, Eligehausen* (1986/2)).

The load-bearing behaviour of such fasteners depends on the behaviour of the concrete in tension. Development of a satisfactory analytical procedure to predict the concrete cone breakout load of fasteners loaded in shear remains quite complex for the reasons explained in section 4.1.1.3a. It is therefore necessary to employ empirical methods to determine the load-carrying capacity of shear-loaded fasteners near an edge, whereby rational engineering models should be considered. The application of the CC-Method as described below fulfils this condition.

##### a) Concentric shear load acting on a single anchor adjacent to the edge of a member

*Fuchs* (1984) proposes an equation for predicting the average concrete failure load of a single anchor subjected to a shear load applied perpendicular to the edge of a member. This is based on the evaluation of approximately 80



**Fig. 4.72** Concrete edge failure of a shear-loaded anchor close to an edge (taken from *Fuchs, Eligehausen* (1986))

tests on post-installed anchors and headed studs with  $d \leq 25$  mm. The applicability of this equation is confirmed in *Zhao, Fuchs, Eligehausen* (1989) on the basis of a some additional 160 tests on various types of anchors whereby the influence of the anchor geometry is also established. In addition, *Eligehausen, Mallée, Rehm* (1997) performed a further analysis of a database of shear tests on anchors conducted since 1989. The combined test results are represented by equation (4.25):

$$V_{uc}^0 = 0.9 \cdot \sqrt{d_{nom}} \cdot \sqrt{f_{cc,200}} \cdot \left( \frac{l_f}{d_{nom}} \right)^{0.2} \cdot c_1^{1.5} \quad [\text{N}] \quad (4.25)$$

where:

- $d_{nom}$  = outside diameter of a post-installed anchor, or shank diameter  $d$  of a headed stud [mm]  
 $\leq 25$  mm
- $c_1$  = edge distance, measured from the longitudinal axis of the anchor (see Fig. 4.73b) [mm]
- $l_f$  = effective load transfer length [mm]  
 $= h_{ef}$  for anchors with constant flexural stiffness over the length of the anchor  
 $=$  length of the embedded distance sleeve for post-installed anchors with a non-uniform flexural stiffness (i.e. sleeve-type anchors)

$$l_f/d_{nom} \leq 8$$

Equation (4.25) indicates that the concrete failure load of a near-edge shear loaded anchor is strongly influenced by the edge distance since it is this parameter – analogous to the embedment depth for a tension loaded anchor – that determines the size of the fracture surface (Fig. 4.73). Nevertheless, the failure load is proportional to  $c_1^{1.5}$ , whereby the area of the fracture surface is proportional to  $c_1^2$ . This is likewise attributable to the size effect discussed in section 3.3.1 (*Fuchs* (1990)). The ultimate load is further influenced by the tension capacity of the concrete, assumed to be proportional to  $f_{cc,200}^{0.5}$ , and on the distribution of bearing stresses along the anchor length, which in turn depends both on the bearing stiffness of the concrete and the flexural stiffness of the anchor. The diameter and effective load transfer length terms are used to account for the bearing stress distribution.

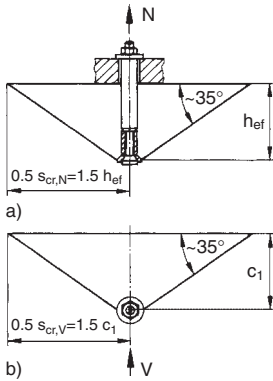


**Fig. 4.73** Comparison of concrete failure bodies (Fuchs, Eligehausen (1995))  
 a) Concentric tension load (cross-section)  
 b) Shear load towards the edge (seen from above)

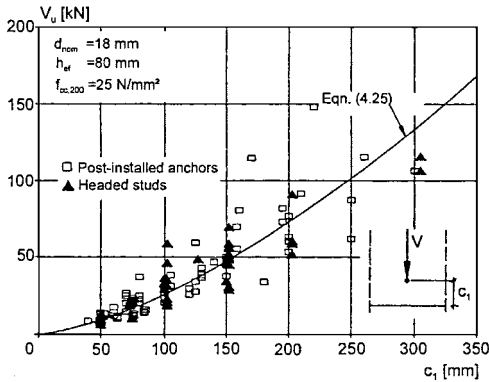


**Fig. 4.74** Influence of edge distance on the concrete cone breakout load associated with shear towards a free edge (Eligehausen, Mallée, Rehm (1997))

Failure loads for post-installed anchors and headed studs exhibiting concrete edge failures under shear loading perpendicular to the edge are plotted as a function of the edge distance in Fig. 4.74. The failure loads measured in the tests were normalised with the aid of the relationships given in equation (4.25) to an outside diameter  $d_{nom} = 18$  mm, an embedment depth  $h_{ef} = 80$  mm and a concrete strength  $f_{cc,200}^{0.5} = 25$  N/mm<sup>2</sup>. A friction-reducing surface was used in all tests in order to minimise the friction between concrete and loading plate. The results of the tests are scattered about the calculated values according to equation (4.25). The ratio of

measured to calculated failure load exhibits a normal distribution and is on average 0.95 with a coefficient of variation of 17 % (Fuchs, Eligehausen, Breen (1995/1)). This degree of scatter is somewhat larger than that generally associated with the concrete tensile strength. This can be attributed to the variety of tested systems (post-installed anchors and headed studs), and the different concrete mix designs represented in the database. Moreover, tensile stresses resulting from shrinkage of the concrete may further influence the failure load, leading to increased scatter.

Extensive experimental and numerical research on headed studs and post-installed bonded anchors described in Eligehausen, Hofmann (2003) reveals that equation (4.25) overestimates the influence of the anchor diameter, specially for anchors with a diameter  $d > 25$  mm. A more accurate approach for the average concrete edge failure load is given by equation (4.26).

$$V_{uc}^0 = 3.0 \cdot d_{nom}^\alpha \cdot l_f^\beta \cdot f_{cc,200}^{0.5} \cdot c_1^{1.5} \quad [N] \quad (4.26)$$

where:

$$\alpha = 0.1 \cdot \left( \frac{l_f}{c_1} \right)^{0.5}$$

$$\beta = 0.1 \cdot \left( \frac{d_{nom}}{c_1} \right)^{0.2}$$

$l_f, d_{nom}$  as defined in equation (4.25)

According to equation (4.26) the influence of the anchor diameter and of the value  $l_f$  on the concrete edge failure load depends on the edge distance. For anchors with a constant  $l_f$  the failure load is approximately proportional to  $d_{nom}^{0.15}$  for a small edge distance and there is almost no influence of the anchor diameter for a large edge distance. Likewise for an anchor with a constant diameter and a small edge distance the failure load is approximately proportional to  $l_f^{0.07}$ , while for large edge distances the influence of  $l_f$  is negligible.

Figs. 4.75 and 4.76 show that the influence of anchor diameter  $d_{nom}$  and the effective load transfer length  $l_f$  on the concrete edge failure load are correctly taken into account by equa-

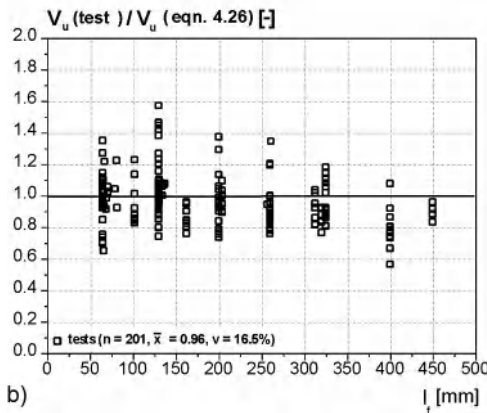
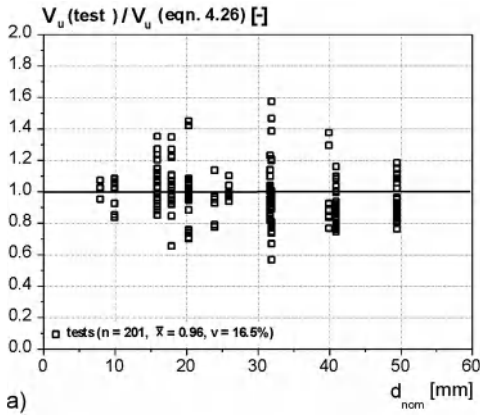


**Fig. 4.75** Ratio of measured concrete edge failure loads and values calculated according to equation (4.26) (Hofmann (2004))  
 a) As a function of anchor diameter  
 b) As a function of the effective load transfer length

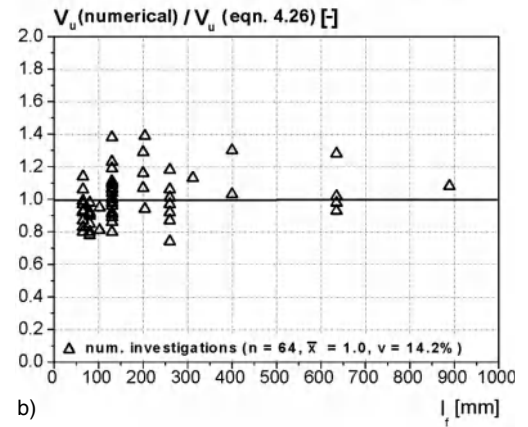
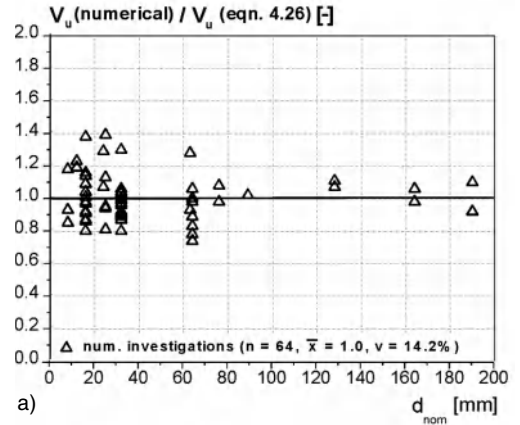


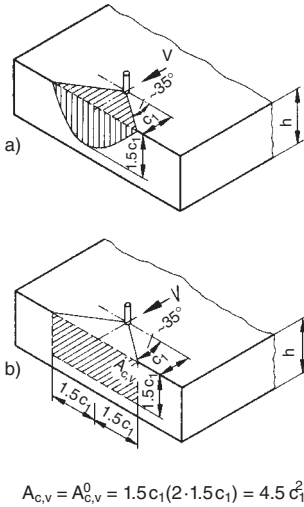
**Fig. 4.76** Ratio of concrete edge failure loads obtained numerically and values calculated according to equation (4.26) (Hofmann (2004))  
 a) As a function of anchor diameter  
 b) As a function of embedment depth

tion (4.26). In the tests  $d_{nom}$  was varied between 8 mm and 50 mm and  $l_f$  between 60 mm and 450 mm (Fig. 4.75). The numerical analysis covered diameters from 8 mm to 190 mm and effective load transfer lengths from 60 mm to 900 mm (Fig. 4.76).

For standard applications (diameter up to 20 mm and edge distance up to 200 mm) the failure loads predicted by equation (4.25) or (4.26) are almost identical. Only for larger anchor diameters and/or larger distances, equation (4.25) predicts significantly higher failure loads than equation (4.26).

**b) Concentric shear load acting on a group of anchors adjacent to an edge**

In theory, the failure load predicted by equation (4.25) or (4.26) will be reached only if the fracture surface can fully develop as shown schematically in Fig. 4.63b<sub>1</sub> or Fig. 4.77a. Assuming a failure surface angle of 35°, this condition is met only if the distance(s) to the adjacent loaded anchor(s) is  $s \geq 3 \cdot c_1$  and the member thickness is  $h \geq 1.5 \cdot c_1$ . Anchor groups with spacing  $s < 3c_1$  form a common concrete fracture surface (Figs. 4.63b<sub>2</sub> and 4.78) and hence develop a lower failure load than would



$$A_{c,v} = A_{c,v}^0 = 1.5c_1(2 \cdot 1.5c_1) = 4.5c_1^2$$

**Fig. 4.77** Anchor loaded in shear towards an edge (after Fuchs, Elgehausen (1995))  
 a) Idealised shape of typical concrete failure body  
 b) Projected area for same anchor per the CC-Method

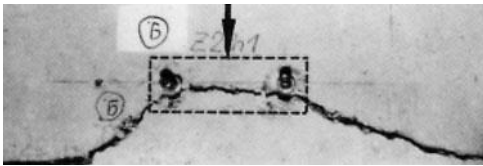


**Fig. 4.78** Concrete failure body of a pair of shear-loaded anchors close to an edge (taken from Fuchs, Elgehausen (1986/2))

be predicted based on the individual anchor capacities. The failure load can be evaluated with the CC-Method in a manner similar to that used for fastenings loaded in tension, i.e. by means of projected areas. Equation (4.27) applies generally to anchors in members having a thickness  $h \geq 1.5 \cdot c_1$ :

$$V_{u,c} = \frac{A_{c,v}}{A_{c,v}^0} \cdot V_{u,c}^0 \quad [\text{N}] \quad (4.27)$$

where:

$A_{c,v}^0$  = projected area of the fully developed failure surface for a single anchor idealised as a half-pyramid with height  $c_1$  and base lengths  $1.5 \cdot c_1$  and  $3 \cdot c_1$  (Fig. 4.77b)

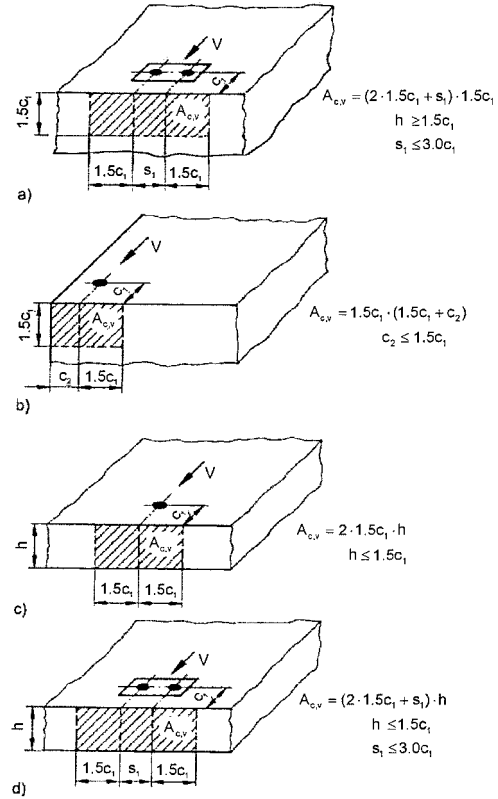


**Fig. 4.79** Projected areas for various shear-loaded anchor configurations  
 a) Pair of anchors close to an edge  
 b) Single anchor in the corner of a concrete member  
 c) Single anchor in a thin concrete member  
 d) Pair of anchors in a thin concrete member

$= 4.5 \cdot c_1^2$   
 $A_{c,v}$  = projected area of the failure surface for the anchorage as defined by the overlap of individual idealised failure surfaces of adjacent anchors ( $s < 3 \cdot c_1$ ) (see Fig. 4.79a for example of calculation of  $A_{c,v}$ )  
 $V_{u,c}^0$  according to equation (4.26)

The factor  $A_{c,v}/A_{c,v}^0$  takes into account the influence of anchor spacing on the concrete breakout shear load in a manner directly analogous to the tension loading case. In the case of two anchors with a spacing  $s \geq 3 \cdot c_1$ , the equation predicts a failure load equal to twice the failure load asso-

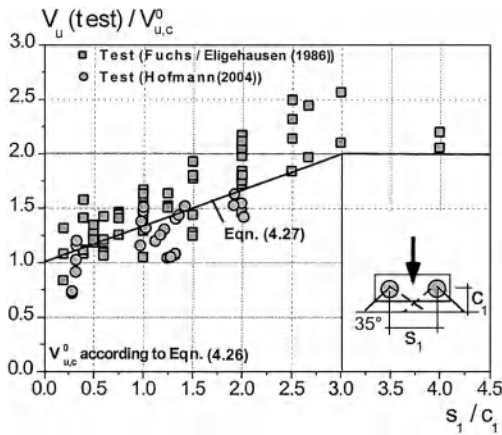


**Fig. 4.80** Influence of spacing on the concrete edge failure load of pairs of anchors subjected to shear (tests according to *Fuchs, Eligehausen (1986/2)*)

ciated with a single anchor having the same edge distance. At the limit condition  $s = 0$ , the failure load reduces to the capacity of a single anchor. A linear interpolation between these two extremes is assumed, as given by equation (4.27). Fig. 4.80 indicates that this approach is sufficiently conservative.

Anchor groups with more than two anchors in a row have not been tested extensively, however, for anchorages that do not exhibit slip between the anchor and the baseplate (e.g. welded shear studs), equation (4.27) should be applicable.

*Stichting Bouwresearch (1971)* similarly identifies  $s = 3 \cdot c_1$  as the spacing required to avoid shear cone overlap. While *American Concrete Institute, ACI 349-90 (1990)* proposes  $s = 2 \cdot c_1$  as the critical spacing, analysis by *Fuchs, Eligehausen, Breen (1995/1)* demonstrates that this can lead to unconservative predictions. A non-linear relationship between the shear capacity of groups located near the edge of a member and the anchor spacing as a function of edge distance is assumed in *Uéda, Stitmannaitum, Matupagout (1991)*. Assuming a linear correlation as given by the CC-Method leads to  $s \approx 4 \cdot c_1$ .

Equation (4.27) is applicable only if the individual anchor spacings of anchors in a group are  $s < 3 \cdot c_1$ . If this is not the case, then the shear cones of neighbouring anchors do not overlap and equation (4.25) or (4.26) applies to each anchor.

A few special aspects should be noted with respect to anchor groups loaded in shear where the anchors are arranged perpendicular to a proximate edge. A distinction should be made here between anchors installed through a baseplate and welded shear studs.

When anchors are installed through a baseplate, some degree of hole clearance is typically present around the anchor. Consider a pair of anchors located perpendicular to a free edge, as shown in Fig. 4.81 (*Fuchs, Eligehausen (1995)*). If the shear load is initially resisted by

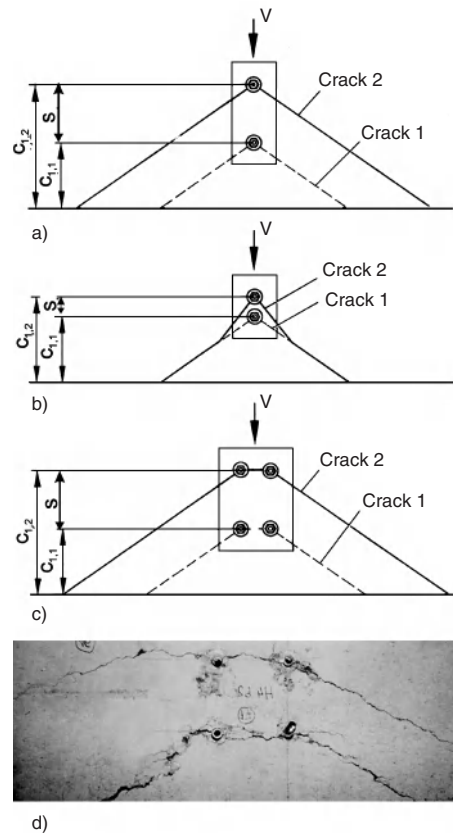


**Fig. 4.81** Fracture patterns of shear-loaded anchorages with hole clearance close to an edge (after *Fuchs, Eligehausen (1995)*)

- a) Two anchors perpendicular to the edge with large spacing
- b) Two anchors perpendicular to the edge with small spacing
- c) Four anchors with large spacing
- d) Test of four anchors with large spacing – photo of crack pattern



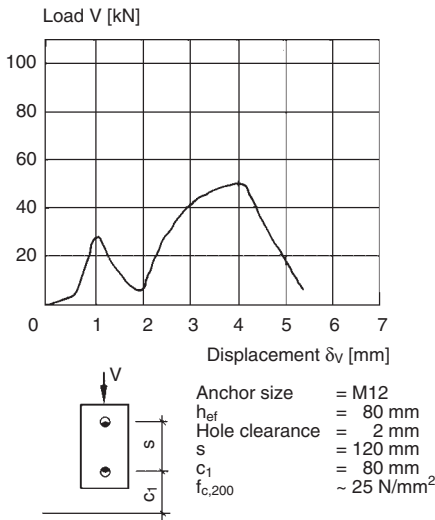


**Fig. 4.82** Load-displacement curve for a pair of shear-loaded anchors oriented perpendicular to the edge (after Fuchs, Eligehausen (1986))

the near-edge anchor alone, it will generate a concrete breakout (crack 1 in Fig. 4.81a). Following displacement sufficient to bring the rear anchor into a bearing condition, that anchor will then resist the entire shear load. Due to its larger concrete breakout capacity, the rear anchor governs the ultimate capacity of the group, all other factors being equal (see crack 2 in Fig. 4.81a). The progression of load distribution is readily seen in Fig. 4.82 (Fuchs, Eligehausen (1986/2)), which shows the load-displacement curve measured in a deformation-controlled test on a pair of anchors positioned perpendicular to the edge. A hole clearance of 2 mm was provided for the anchor furthest from the edge. Following formation of a concrete breakout fracture at the near-edge anchor, the shear resistance of the group decreases with increasing displacement up to 2 mm, at which point the anchor furthest from the edge engages the baseplate. The ultimate capacity of the group is reached upon formation of a concrete breakout fracture originating at the rear anchor. This capacity has been experimentally shown to correspond to the ultimate load of a single anchor having the same edge distance as the rear anchor, which implies that for the anchor spacing in this case ( $s = 120$  mm), the ultimate

capacity of the group is not influenced by the concrete breakout fracture generated by the near-edge anchor. The shear load fracture pattern associated with a four-anchor group with a relatively large spacing between the front and rear anchors is shown schematically in Fig. 4.81c. The experimental result is shown in Fig. 4.81d. In this case the shear capacity at failure is governed by the anchors furthest from the edge. Therefore, equation (4.28) applies:

$$V_{u,c} = V_{u,c}(c_{1,2}) \quad (4.28)$$

Theoretically, if a small relative spacing is provided between the front and rear anchors (Fig. 4.81b), crack 2 may merge with crack 1. In this case, the capacity of the group would be only slightly increased over that associated with the formation of crack 1. This failure mode has not been verified experimentally to date. The minimum spacing  $s_1$  perpendicular to the edge at which cracks 1 and 2 are more or less parallel to each other may depend on the edge distance associated with the near-edge anchor(s). Tests on groups of anchors carried out by Eligehausen, Fuchs (1988) with  $c_{1,1} = 80$  mm to 120 mm confirmed that a distance of  $s_1 = 120$  mm is sufficient to assure parallel crack formation. Tests conducted by Wong, Donahey, Lloyd (1988) on shear stud assemblies (edge distances and spacing  $c_{1,1} = s_1 \approx 60$  mm) also generated parallel cracks. Parallel cracks were also found in tests with post-installed bonded anchors with  $c_{1,1} = 140$  mm and  $s_1 = 70$  mm by Eligehausen, Hofmann (2003). It may be conservatively assumed that calculation of the concrete edge failure load using equation (4.28) is justified for a spacing  $s_1 \geq c_{1,1}$ . If the spacing  $s_1$  is less than  $c_{1,1}$ , it should be assumed that the near edge anchors govern the concrete edge failure load. That is:

$$V_{u,c} = V_{u,c}(c_{1,1}) \quad (\text{valid for } s_1 < c_{1,1}) \quad (4.29)$$

The formation of crack 1 has implications for the behaviour of the anchorage at service load levels. This should be taken into account in the design of the anchorage (section 14).

Welded shear stud connections (see Fig. 4.83) tend to distribute shear loads evenly to the individual studs, regardless of location, up to a load corresponding to  $V = 2 \cdot V_{u,c}(c_{1,1})$  where

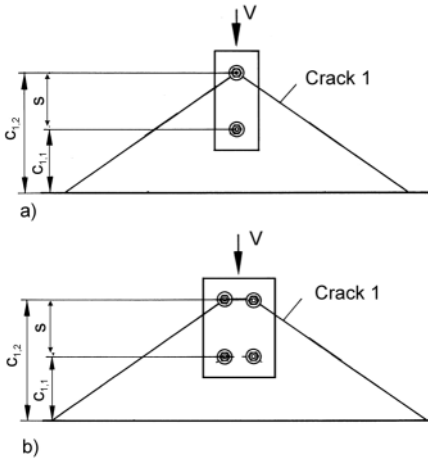


**Fig. 4.83** Fracture patterns of shear-loaded headed studs close to an edge (Hofmann (2004))  
 a) Two anchors perpendicular to the edge with large spacing  
 b) Group of four anchors with large spacing

$V_{u,c}(c_{1,1})$  is equal to the capacity of the near-edge stud(s) according to equation (4.27). With increasing load the stiffness of the near-edge stud(s) decreases and the load is re-distributed to the rear stud(s) (Anderson, Meinheit (2000/1), Eligehausen, Hofmann (2003)). According to the experimental investigations of Anderson, Meinheit (2000/1) this re-distribution of load takes place without the formation of a crack from the front studs. However, according to the numerical investigations of Eligehausen, Hofmann (2003) a crack will form at the front anchors before reaching the failure load if the spacing  $s_f$  is larger than  $\approx 1.5 \cdot c_{1,1}$ . If the spacing between front and rear stud(s) is sufficiently large, the failure crack is formed from the rear stud(s) (crack 1 in Fig.

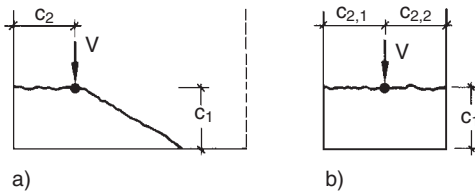


**Fig. 4.84** Fracture pattern of a single shear-loaded anchor (Rehm, Eligehausen, Mallée (1992))  
 a) In the corner of a concrete member  
 b) In a narrow concrete member (schematic)

4.83), which defines the ultimate load of the group ( $V_{u,c} = V_{u,c}(c_{1,2})$ ). The concrete breakout capacity of the group may therefore be predicted with equation (4.30) as follows:

$$V_{u,c} = \max\{2 \cdot V_{u,c}(c_{1,1}), V_{u,c}(c_{1,2})\} \quad (4.30)$$

**c) Concentric shear load acting on anchors in a corner or in a narrow member**

In the case of shear-loaded anchors positioned in the corner of a component or in a narrow component, development of the concrete fracture surface may be restricted (Fig. 4.84) if the distance to the edge parallel to the load direction is  $c_2 < 1.5 \cdot c_1$ . The critical value  $c_2 = 1.5 \cdot c_1$  corresponds to a fracture angle of  $35^\circ$ .

At the limit condition of  $c_2 = 0$  (refer to Fig. 4.84a) the volume of the theoretical shear cone associated with a shear-loaded anchor in a corner is reduced by 50%. In addition, the stress distribution – which is at edges symmetric in the direction of the load – is disrupted by the presence of the corner, leading to further capacity reduction. This may be taken into account with a reduction factor in a manner similar to that adopted for tension loads:

$$V_{u,c} = \frac{A_{c,V}}{A_{c,V}^0} \cdot \psi_{s,V} \cdot V_{u,c}^0 \quad [\text{N}] \quad (4.31)$$

where:

$$\psi_{s,V} = 0.7 + 0.3 \cdot c_2 / (1.5 \cdot c_1) \leq 1.0 \quad (4.31a)$$

$c_2$  = distance to the edge that is parallel to the direction of load

$A_{c,V}, A_{c,V}^0, V_{u,c}^0$  are evaluated as for equation (4.27) (Fig. 4.79b illustrates the calculation of  $A_{c,V}$ )

Equation (4.31) may also be applied to shear-loaded anchors located in stem walls or other narrow members (see Fig. 4.84b). Note that the smaller of the edge distances  $c_{2,1}$  and  $c_{2,2}$  should be inserted into equation (4.31a) in lieu of  $c_2$ .

The accuracy of equation (4.31) was checked with shear tests on single anchors located in the corner of a component with  $c_2 = c_1$ . These resulted in adequate correlation between predicted and tested failure loads (Fuchs (1990)). As shown in Fig. 4.85, equation (4.31) also supplies sufficiently accurate predictions for single anchors positioned symmetrically in narrow members. Tests involving unequal edge distances

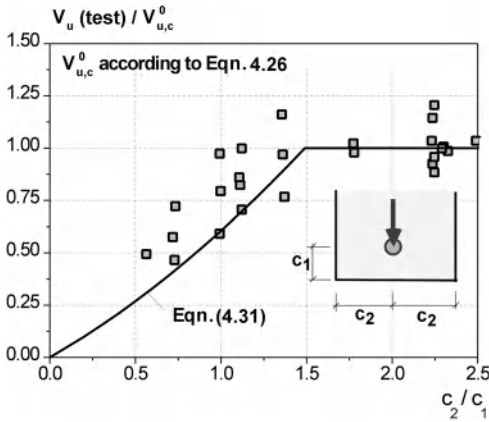


**Fig. 4.85** Ratio of ultimate loads measured in tests with cast-in-place dowel bars in thin members and values calculated according to equation (4.26) as a function of the ratio corner distance to edge distance (tests after Paschen, Schönhoff (1983))

( $c_{2,1} \neq c_{2,2}$ ) are not available, but it is expected that the CC-Method should supply conservative results if the differences are not too large.

**d) Concentric shear load acting on anchors in a member with limited thickness**

The failure load predicted by equation (4.31) is valid only if the member thickness is sufficient to permit the formation of the complete fracture surface. A shear loaded anchor located in a thin member generates a fracture surface that is truncated by the lower edge of the component (Fig. 4.63b<sub>4</sub>). In this case, the failure load associated with concrete fracture will increase roughly linearly with the edge distance (Fig. 4.86). The minimum member thickness required to permit formation of a complete fracture surface is roughly 1.3 times to 1.5 times the edge distance in the loading direction. In the CC-Method the value is taken as  $h = 1.5 \cdot c_1$ .

Equation (4.31) predicts that the failure load will be proportional to the projected area and hence directly proportional to the thickness of the component where shear-loaded anchors are located in members with  $h < 1.5 \cdot c_1$  (see calculation of  $A_{c,V}$  in Fig. 4.79c and d). However, this is not confirmed by shear tests in thin members (Zhao, Fuchs, Eligehausen (1989), whereby the failure load is shown to be less than proportional to the

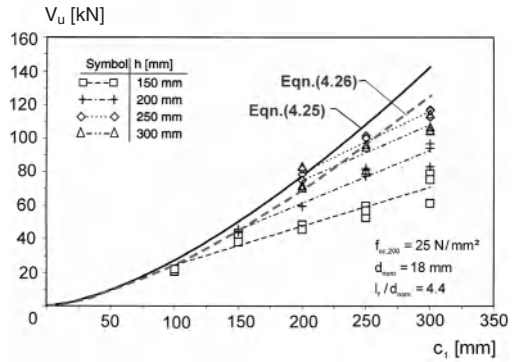


**Fig. 4.86** Measured shear failure loads (concrete edge failure) as a function of edge distance for different member thickness (tests according to Zhao, Fuchs, Eligehausen (1989))

member thickness. This is taken into account by the factor  $\psi_{h,V}$  (Zhao, Eligehausen (1992/2)):

$$V_{u,c} = \frac{A_{c,V}}{A_{c,V}^0} \cdot \psi_{s,V} \cdot \psi_{h,V} \cdot V_{u,c}^0 \tag{4.32}$$

where:

$$\psi_{h,V} = (1.5 \cdot c_1 / h)^{1/3} \geq 1.0 \tag{4.32a}$$

$A_{c,V}, A_{c,V}^0, \psi_{s,V}, V_{u,c}^0$  are evaluated as for equation (4.31)

Fig. 4.87 shows the ratio of the failure load of single anchors in tests to the value calculated

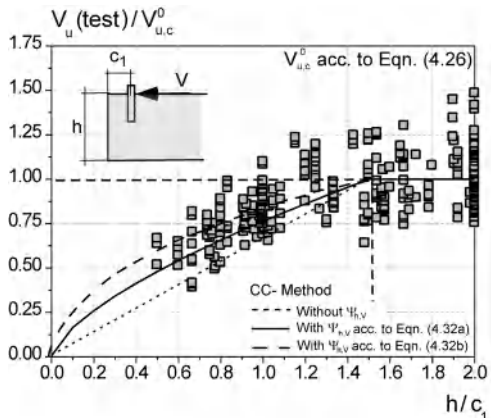


**Fig. 4.87** Influence of member thickness on the shear failure load (concrete edge failure) (after Hofmann (2004))

according to equation (4.26) as a function of the ratio member thickness to edge distance (*Hofmann* (2004)). The full line is valid for equation (4.32) with  $\psi_{h,V}$  according to equation (4.32a). It can be seen that equation (4.32a) is still conservative. Therefore in *Eligehausen, Fuchs, Hofmann* (2004) the factor  $\psi_{h,V}$  according to equation (4.32b) is proposed which predicts the average failure loads with sufficient accuracy.

$$\psi_{h,V} = (1.5 \cdot c_1/h)^{0.5} \geq 1.0 \quad (4.32b)$$

**e) Eccentric shear load acting on multiple anchors adjacent to an edge**

The effect of an eccentricity of the shear load (Fig. 4.88) on the concrete breakout load  $V_{u,c}$  of an anchor group located near an edge can be assessed in a manner similar to that proposed by *Riemann* (1985) for the tension case by formulating the reduction factor  $\psi_{ec,V}$  as follows (equation (4.33)):

$$V_{u,c} = \frac{A_{c,V}}{A_{c,V}^0} \cdot \psi_{s,V} \cdot \psi_{h,V} \cdot \psi_{ec,V} \cdot V_{u,c}^0 \quad (4.33)$$

where:

$$\psi_{ec,V} = \frac{1}{1 + 2 \cdot e_V / (3 \cdot c_1)} \leq 1 \quad (4.33a)$$

$e_V$  = eccentricity of resultant applied shear load relative to the centroid of the anchors resisting shear in the direction of the edge of the member

$A_{c,V}$ ,  $A_{c,V}^0$ ,  $\psi_{s,V}$ ,  $\psi_{h,V}$ ,  $V_{u,c}^0$  are evaluated as for equation (4.32)

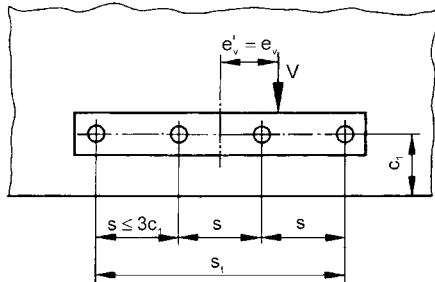


**Fig. 4.88** Shear stud anchorage at the edge of a concrete member subjected to an eccentric shear load (taken from *Eligehausen, Mällée, Rehm* (1997))

In the case of a row of welded shear studs arrayed parallel to the edge, the distribution of a shear load applied perpendicular to the edge to the individual studs of the group should be calculated according to elastic theory, whereby the same stiffness is assumed for all studs. For bolted anchor connections with the attendant hole clearance variations, this geometry becomes more problematic since the distribution of the shear load to the individual anchors is not easily definable. Equation (4.33) applies only to pairs of (non-welded) anchors parallel to an edge. For larger groups of non-welded anchors, conservative assumptions should be made regarding the distribution of loads to the individual anchors.

Equation (4.33) applies only when all of the anchors arrayed parallel to the edge are loaded in the direction of the edge (Fig. 4.89a). If however the applied torque  $M_T$  is sufficiently large, the direction of shear resistance may be reversed for one or more of the anchors in the group (Fig. 4.89b). According to the results of tests by *Mällée* (2002) with ratios  $s/c \geq 1$  failure of the group is governed by the anchor resisting a shear load in the direction of the edge and the ultimate capacity is not influenced by the reverse-loaded anchor. Non-linear numerical investigations by *Hofmann* (2004) show that this is also valid for ratios  $s/c < 1$ .

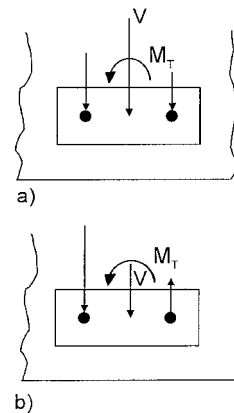


**Fig. 4.89** Anchor group close to an edge loaded by shear load and torsion moment  
 a) Both anchors loaded in shear acting towards the edge  
 b) Shear loads on anchors acting in different directions

**f) Special cases**

Equation (4.33) provides conservative predictions for anchor groups positioned in narrow members with  $\max. c_2 < 1.5c_1$  ( $\max. c_2 =$  larger of the two edge distances to the edges oriented parallel to the load direction) and with limited member thickness  $h < 1.5 \cdot c_1$  (Eligehausen, Balogh, Fuchs, Breen (1992)). This is illustrated for the case of a single shear-loaded anchor in the centre of a narrow member of limited thickness in Fig. 4.90.

For  $c_2 < 1.5 \cdot c_1$  and  $h < 1.5 \cdot c_1$ , the existing projected area  $A_{c,V}$  is constant and becomes  $A_{c,V} = 2 \cdot c_2 \cdot h$ . Hence, the failure load according to equation (4.33) is given by:

$$V_{u,c} = \frac{2 \cdot c_2 \cdot h}{4.5 \cdot c_1^2} \cdot \left(0.7 + 0.3 \cdot \frac{c_2}{1.5 \cdot c_1}\right) \cdot \left(\frac{1.5 \cdot c_1}{h}\right)^{1/3} \cdot k \cdot c_1^{1.5}$$

where:

$$k = 0.9 \cdot \sqrt{d_{nom}} \cdot (l_f / d_{nom})^{0.2} \cdot \sqrt{f_{cc200}}$$

Note that the above equation predicts that the concrete breakout failure load decreases as the edge distance  $c_1$  increases, which is not consistent with observed behaviour because the failure area is constant. This anomaly may be corrected by substituting the value  $c'_1$ , defined as the larger of  $\max. c_2/1.5$  or  $h/1.5$ , for the edge distance  $c_1$  in equations (4.25) or (4.26), (4.31a), (4.32a) and (4.33a), as well in the determination of  $A_{c,V}^0$  per Fig. 4.77. Furthermore the area  $A_{c,V}$  is taken as the cross-section of the concrete member. For the example in Fig. 4.90 with  $h = c_2$ , this approach results in a prediction for the concrete breakout failure load that is

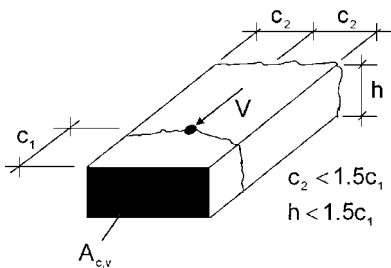
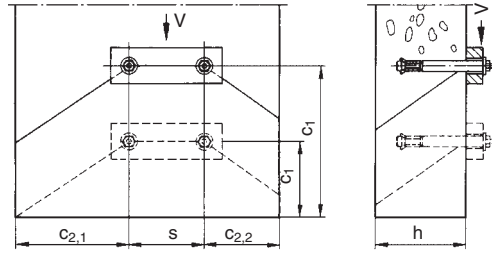


**Fig. 4.90** Single anchor in a thin, narrow concrete member



Example  
 $s = 100 \text{ mm}$ ,  $c_1 = 200 \text{ mm}$ ,  $h = 120 \text{ mm}$   
 $c_{2,1} = 150 \text{ mm}$ ,  $c_{2,2} = 100 \text{ mm}$   
 $c'_1 = \max(150/1.5; 120/1.5; 100/3) = 100 \text{ mm}$

**Fig. 4.91** Determination of effective edge distance for a pair of anchors loaded in shear towards the edge in a thin, narrow concrete member (Fuchs, Eligehausen (1995))

independent of the edge distance  $c_1$  and reduces to the value  $V_{u,c}^0$  associated with an edge distance  $c'_1 = c_2/1.5$ .

$$V_{u,c} = \frac{2 \cdot c_2 \cdot c_2}{4.5 \cdot (c_2/1.5)^2} \cdot \left(0.7 + 0.3 \cdot \frac{c_2}{1.5 \cdot (c_2/1.5)}\right) \cdot \left(\frac{1.5 \cdot (c_2/1.5)}{c_2}\right)^{1/3} \cdot k \cdot (c_2/1.5)^{1.5}$$

$$= 1 \cdot 1 \cdot 1 \cdot k \cdot (c_2/1.5)^{1.5}$$

$$= k \cdot (c_2)^{1.5}$$

This approach is also valid for anchor groups (see Fig. 4.91). It results in

$$c'_1 = \max(\max. c_2/1.5; h/1.5; \max. s/3)$$

**g) Anchors subjected to a shear load and overturning moment near an edge**

In a stand-off installation (e.g. a baseplate elevated with levelling nuts off the surface of the concrete), shear loading induces secondary overturning moments in the connection (Fig. 4.92a). The resolution of this secondary moment in the anchor results in an additional shear component towards the edge as shown in Fig. 4.92c. The net effect is to reduce the capacity of the anchorage as governed by concrete breakout. This situation was investigated by Paschen, Schönhoff (1983) in limited experiments with single shear connectors. They predict the shear force  $V_{u,c}(M)$  corresponding to

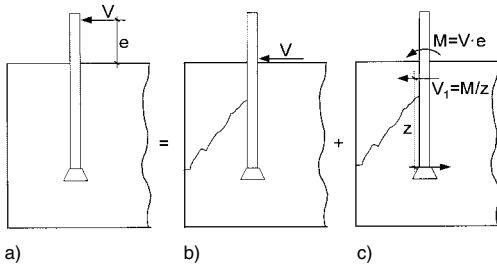


**Fig. 4.92** Anchor close to an edge subjected to a shear load with lever arm

concrete breakout in the case of single anchors near the edge subjected to shear and moment as:

$$V_{u,c}(M) = \psi_M \cdot \psi_{h,V} \cdot V_{u,c}^0 \quad (4.34)$$

where:

$$\psi_{h,V} = (110 - e)/90 \leq 1.0 \quad (4.34a)$$

$$\geq 0.3$$

$e$  = distance between shear load and concrete surface [mm]

$\psi_{h,V}$  according to equation (4.32a)

$V_{u,c}^0$  according to equation (4.25)

Equation (4.34) is a first approximation that does not account for the effect of such parameters as anchor embedment and diameter on the magnitude of the secondary forces induced in the anchor. This type of application, which occurs frequently in the anchorage of facade elements, requires further investigation.

**h) The influence of hanger reinforcement on shear capacity**

The shear capacity of anchorages located near the edge of a member can be increased through the use of hanger reinforcement. This is illustrated in Fig. 4.93, which shows load-displacement curves from deformation-controlled shear tests on headed studs (shank diameter  $d = 22$  mm) with an edge distance of approximately 75 mm. Curve 1 applies to the case where no hanger reinforcement is present. Curve 2 represents a case with one edge bar ( $d_s = 12$  mm) restrained by stirrups ( $d_s = 12$  mm) at a spacing of 150 mm. Curves 3 and 4 address the case of a hairpin ( $d_s = 12$  mm) near the surface of the concrete. In curve 3, the hairpin is placed with a clearance of 30 mm from the stud. Curve 4 shows the case where the hairpin is placed in

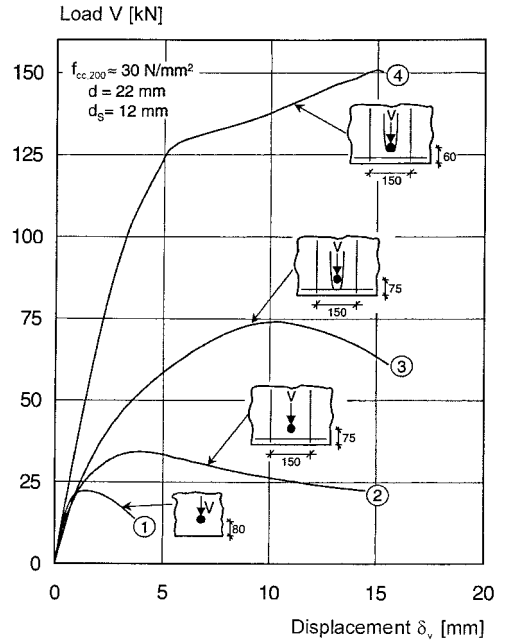


**Fig. 4.93** Effect of reinforcement on the load-displacement behaviour of single anchors close to an edge loaded in shear (curves 1 to 3 from *Forschungs- und Materialprüfungsanstalt (1985/2)*, curve 4 from *Ramm, Greiner (1991)*)

contact with the stud at the concrete surface. Clearly, the initial stiffness of the anchorage is not influenced substantially by the presence of hanger reinforcement, but ultimate capacity can be increased dramatically depending on the extent and arrangement of the reinforcement.

When the edge reinforcement is anchored by widely spaced stirrups (curve 2), the effect on anchor capacity is relatively small since the reinforcement is inadequately anchored beyond the fracture plane. The addition of a hairpin not in contact with the stud increases the capacity considerably but the ultimate load is still not maximised since the concrete between the stud and the hairpin failed in bearing at approximately 60% of the stud shear capacity, or 65% of the hairpin tension capacity. Placement of the hairpin in contact with the stud and directly below the base plate results in development of the full strength of the stud following yielding of the hairpin. Note that positioning the hairpin close to the surface, while maximising the shear



resistance of the anchor, may require special consideration of the bar exposure from a corrosion standpoint.

The effectiveness of orthogonal edge reinforcement that is designed to accommodate anchor shear loads can be improved by providing anchorage for the anchor stirrups beyond the concrete breakout fracture surface (Fig. 4.94 a–c) adequate to accommodate the node forces. The behaviour of nodes in strut-and-tie models is discussed in *Schlaich, Schäfer* (1989). The effectiveness of hanger reinforcement can be improved by reducing the stirrup spacing (Fig. 4.94b) or, for a given stirrup spacing, by increasing the anchor edge distance (Fig. 4.94c). Welded reinforcing bar assemblies also provide superior performance, as do welded wire meshes with small bar spacing ( $s \sim 50$  mm) (*Paschen, Schönhoff* (1983)).

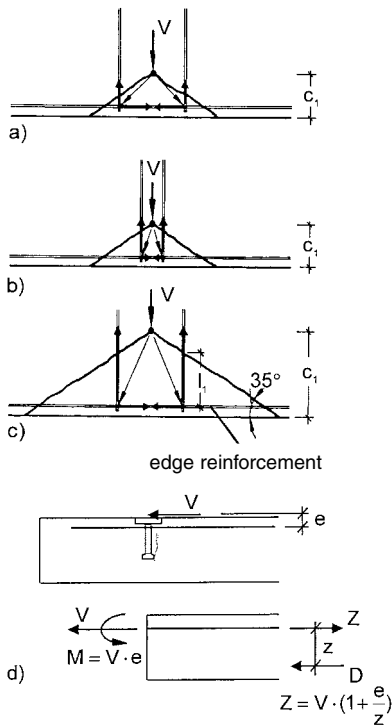


**Fig. 4.94** Models of anchorages with anchor reinforcement close to an edge  
 a) to c) Strut-and-tie models (*Rehm, Eligehausen, Mällée* (1988))  
 d) Model for calculating the tensile force in the hanger reinforcement (*Lotze* (1998))

*Lotze* (1998) provides a method for estimating the force acting on the anchor reinforcement based on consideration of a reinforced concrete section subjected to a tensile force and a bending moment (Fig. 4.94d). The tensile force corresponds to the applied shear load and the bending moment corresponds to the shear load multiplied by the distance to the level of the reinforcement. This additional bending moment increases the tensile stress in the reinforcement beyond that corresponding to the applied shear load.

The force to be carried by one leg of the hanger reinforcement (stirrups) can be estimated from the anchorage in the shear cone by way of development length and the effect of the hook or of welded transverse bars using equation (4.35) (analogous to equation (4.12)).

$$V_{ua} = \pi \cdot d_s \cdot l_1 \cdot f_{bm} / \alpha_a \leq A_s \cdot f_y \quad [\text{N}] \quad (4.35)$$

where:

- $d_s$  = diameter of stirrup
- $l_1$  = anchorage length measured from the intersection of the concrete break-out body with stirrup (see Fig. 4.94c)
- $f_{bm}$  = average bond strength [N/mm<sup>2</sup>]  
 $= 2.25 \cdot f_{ctm}$
- $f_{ctm}$  = average concrete tensile strength  
 $= 0.3 f_c^{2/3}$
- $\alpha_a$  = factor to take into account influence of hook or welded transverse bars  
 $= 0.7$
- $A_s$  = cross-sectional area of one stirrup leg [mm<sup>2</sup>]
- $f_y$  = yield strength of stirrup [N/mm<sup>2</sup>]

Equation (4.35) applies for edge distance  $c_1 \geq 50$  mm (*Sippel, Eligehausen* (2003)).

The shear capacity of the anchorage is derived by summing the capacities for all stirrup legs as predicted by equation (4.35), whereby only those stirrup legs near the surface should be included. The edge reinforcement should also be checked for the tensile force corresponding to the strut-and-tie model used to establish the forces in the stirrups (Fig. 4.94c).

Equation (4.35) also applies to welded reinforcing assemblies because the anchorage provided by the weld to the edge bar is at least equal to that provided by a hook.

Hairpins are highly effective when the anchor and the hairpin are placed in direct contact with one another at the apex of the hairpin bend (Fig. 4.93, curve 4) (Klingner, Mendonca, Malik (1982/1), Paschen, Schönhoff (1983), Ramm, Greiner (1991)). If the hairpin is positioned away from the surface of the concrete, larger deformations of the stud are required to activate the hairpin. According to the limited experimental investigations of Ramm, Greiner (1991) the failure load associated with this geometry decreases as much as 30%, depending on the edge distance, if the hairpin is positioned at a depth of 50 mm rather than with normal concrete cover. A U-shaped or V-shaped hairpin formed from deformed bar ( $d_s \leq 12$  mm, steel yield strength 420 N/mm<sup>2</sup>) can, according to Paschen, Schönhoff (1983), develop a load corresponding to bar yield if minimum cover for the hairpin is observed, if the hairpin directly engages the anchor, and if the hairpin is fully anchored on the opposing side of the shear load. The edge distance must be at least  $c_1 = 3d_b$  or 50 mm. In shear tests with welded shear stud assemblies as described by Ramm, Greiner (1991), hairpins made from deformed bars with a yield strength of 500 N/mm<sup>2</sup> having diameters up to 16 mm developed stresses in excess of yield. The hairpins were positioned below the baseplate with the minimum concrete cover and directly engaged the welded shear studs.

The force that can be carried by a hairpin in conjunction with a welded shear stud assembly can be calculated using equation (4.36):

$$V_{u,s} = 2 \cdot \eta_1 \cdot A_s \cdot f_y \quad [\text{N}] \quad (4.36)$$

where:

$\eta_1$  = effectiveness factor for hairpin

$A_s$  = cross-sectional area of one leg of hairpin [mm<sup>2</sup>],

$f_y$  = yield strength of hairpin [N/mm<sup>2</sup>]

The effectiveness factor depends on the position of the hairpin relative to the concrete surface and relative to the stud locations. If the hairpin is positioned beneath the baseplate with the minimum concrete cover and directly engages the shear studs,  $\eta_1 \approx 1.0$ . A gap between studs and hairpin of only a few centimetres, in conjunction with a hairpin location below the concrete sur-

face can result in a reduction of the effectiveness factor to a value as small as  $\eta_1 \approx 0.5$ .

Fig. 4.95 illustrates various hairpin layouts for welded shear stud assemblies. The hairpins should directly engage the studs and be positioned with the minimum concrete cover to the concrete surface. They may also be sloped to provide additional cover for the balance of the hairpin. Hairpin bend diameters should conform to the applicable requirements for reinforcing assemblies and development of the hairpins in the balance of the concrete should be adequate to fully develop the hairpin. It may be desirable to provide hairpin reinforcement for each row of studs as shown in Fig. 4.95c. Note that when calculating the force developed by angled hair-

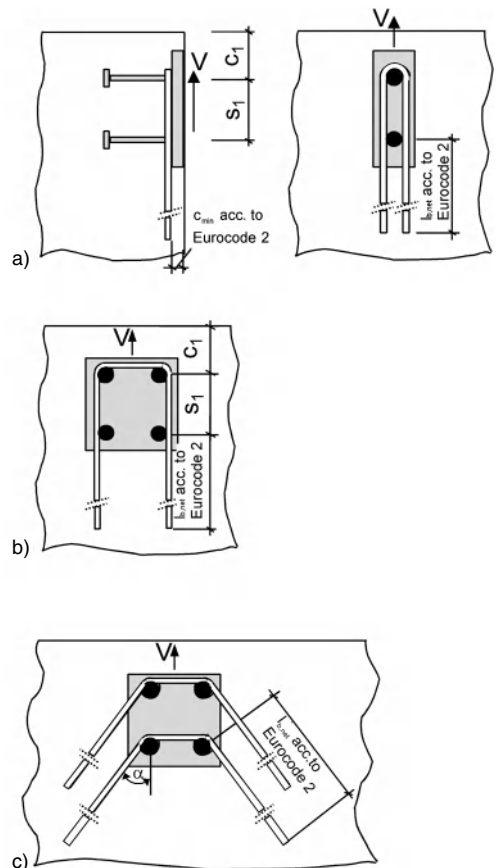


**Fig. 4.95** Suitable hanger reinforcement detailing for shear-loaded headed studs close to an edge (Ramm (1993))

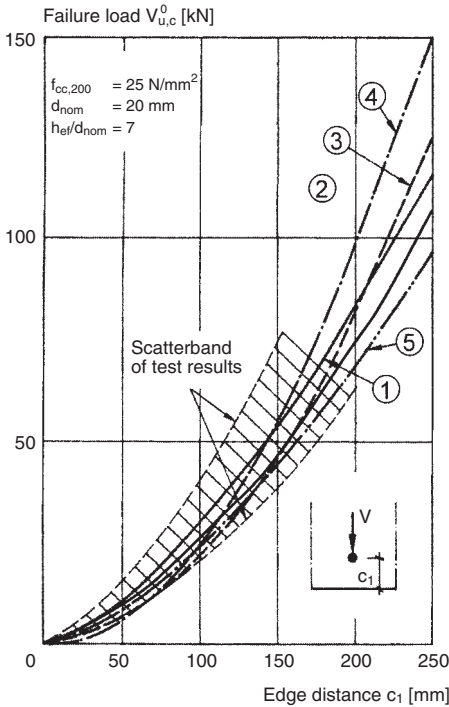
pins of this type, the value of  $V_{u,s}$  in equation (4.36) must be multiplied by  $\cos \alpha$ .

Hanger reinforcement not in contact with the anchors as represented by curves 2 and 3 in Fig. 4.93, and as shown in Fig. 4.94, becomes effective only after the formation of cracks in the concrete. As shown by *Sippel, Eligehausen* (2003) at service load level the crack width will not exceed the allowable values ( $w_k = 0.3 \text{ mm}$ )

if the resistance of the hanger reinforcement is calculated according to equation (4.35). In contrast, hairpins positioned to directly engage the shear-loaded anchors near the concrete surface are generally sufficiently stiff to develop resistance well before the formation of cracks in the concrete. Visible cracks may be expected only after service load levels have been exceeded (*Ramm, Greiner* (1991)).

**i) Comparing the CC-Method with other approaches in the literature**

Fig. 4.96 compares predictions of mean failure load for a single anchor in non-reinforced concrete as calculated using equation (4.25) (curve 1) or equation (4.26) (curve 2) as well as a number of other relations found in the literature. A representation of test results in the form of a scatter band is also depicted. The mean failure load predictions for edge distances  $c_1 < 200 \text{ mm}$ , while markedly different in some instances, all lie within the relatively wide scatter band of the test results. The failure loads predicted by equations (4.25) and (4.26) are almost equal. For larger edge distances *American Concrete Institute, ACI 349-90* (1990) (curve 4) overestimates the influence of the edge distance on the concrete breakout load because the size effect is neglected. In addition, for smaller edge distances the scatter associated with the ratio  $V_u(\text{test})/V_u(\text{calculation})$  is large (*Fuchs, Eligehausen, Breen* (1995/2)). This also applies to the proposal of *Paschen, Schönhoff* (1983) (curve 3). According to *Shaikh, Whayong* (1985) the concrete edge failure load is proportional to  $c_1^{1.5}$  (curve 5), as in the CC-Method, however, the influences of anchor diameter and embedment depth are neglected.



- ①  $V_{u,c}^0 = 0.9 \cdot \left( \frac{l_f}{d_{nom}} \right)^{0.2} \cdot \sqrt{d_{nom}} \cdot \sqrt{f_{cc,200}} \cdot c_1^{1.5}$
- ②  $V_{u,c}^0 = 3 \cdot d_{nom}^\alpha l_f^\beta \cdot f_{cc,200} \cdot c_1^{1.5}$
- ③  $V_{u,c}^0 = f_{cc,200}^{2/3} \cdot (190 + 0.23 \cdot c_1^2)$
- ④  $V_{u,c}^0 = 0.48 \cdot \sqrt{f_{cc,200}} \cdot c_1^2$
- ⑤  $V_{u,c}^0 = 4.8 \cdot \sqrt{f_{cc,200}} \cdot c_1^{1.5}$

**Fig. 4.96** Concrete edge failure loads for shear-loaded single anchors close to an edge as a function of edge distance; comparison of various proposals for a concrete member thickness (curve 1 corresponding to equation (4.25), curve 2 after *Paschen, Schönhoff* (1983), curve 3 after *American Concrete Institute, ACI 349-90* (1990), curve 4 after *Shaikh, Whayong* (1985))

**4.1.2.5 Concrete edge breakout load associated with shear loads oriented at an angle  $\alpha < 90^\circ$  to the edge**

The treatment of shear loading of near-edge anchorages has thus far been concerned only with shear loads oriented perpendicular to the edge (Fig. 4.97a). If a near-edge anchorage is subjected to a shear force acting parallel to the free edge (Fig. 4.97b), a splitting force acting perpendicular to the edge is generated. According to *Stichting Bouwresearch* (1971) and

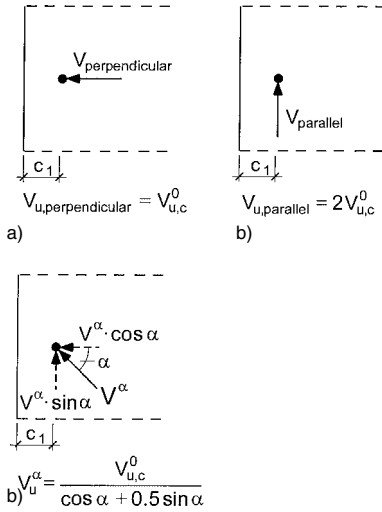


**Fig. 4.97** Shear concrete failure loads for single anchors (after Riemann (1990))  
a) Loaded perpendicular to the edge  
b) Loaded parallel to the edge  
c) Loaded in an oblique angle to the edge

Fuchs (1990) this splitting force is roughly 50% of the applied shear load. This implies that for a constant edge distance, the shear capacity associated with concrete edge breakout for shear loading parallel to the edge is about twice as large as the capacity associated with shear loading perpendicular to the edge.

Riemann (1990) proposed an equation to calculate the failure load for cases where the angle of the shear load with respect to the free edge is between  $90^\circ$  and  $0^\circ$  (Fig. 4.97c). This approach assumes a linear interaction equation (4.37a).

$$\frac{V_u^\alpha \cdot \cos \alpha}{V_{u,perpendicular}^\alpha} + \frac{V_u^\alpha \cdot \sin \alpha}{V_{u,parallel}^\alpha} = 1 \quad (4.37a)$$

where (see Fig. 4.97c):

- $V_u^\alpha$  = failure load in the case of shear applied at angle  $\alpha$  to the edge
- $\alpha$  = angle of the shear load
- $V_{u,perpendicular}^\alpha$  = failure load in the case of shear perpendicular to the edge  
= according to equation (4.25) or (4.26)
- $V_{u,parallel}^\alpha$  = failure load in the case of shear parallel to the edge  
=  $2 \cdot V_{u,c}^0$

One obtains:

$$V_{u,c} = \frac{V_{u,c}^0}{\cos \alpha + 0.5 \cdot \sin \alpha} \quad (4.37b)$$

$$= \psi_{\alpha,V} \cdot V_{u,c}^0 \quad (4.37c)$$

$$\text{with } \psi_{\alpha,V} = \frac{1}{\cos \alpha + 0.5 \cdot \sin \alpha} \geq 1 \quad (4.37d)$$

Generalising this approach for single anchors and groups of anchors near an edge or in a corner, the concrete edge breakout load is given by:

$$V_{u,c} = \frac{A_{c,V}}{A_{c,V}^0} \cdot \psi_{s,V} \cdot \psi_{h,V} \cdot \psi_{ec,V} \cdot \psi_{\alpha,V} \cdot V_{u,c}^0 \quad (4.38)$$

where (see Fig. 4.98):

$$\psi_{\alpha,V} = 1.0 \quad \text{for } 0^\circ \leq \alpha \leq 55^\circ \quad (4.38a)$$

$$= \frac{1}{\cos \alpha + 0.5 \cdot \sin \alpha} \quad \text{for } 55^\circ < \alpha \leq 90^\circ \quad (4.38b)$$

$$= 2.0 \quad \text{for } 90^\circ < \alpha \leq 180^\circ \quad (4.38c)$$

Equation (4.37d) yields a factor  $\psi_{\alpha,V} > 0.9$  for  $\alpha \leq 55^\circ$ . However, as the concrete edge breakout loads associated with shear load orientations corresponding to small angles  $\alpha$  are not measurably less than that for a load applied perpendicular to the edge, a default value of  $\psi_{\alpha,V} = 1.0$  is used for the angle range  $0^\circ$  to  $55^\circ$ . Beyond  $55^\circ$ , as the angle  $\alpha$  increases, the coefficient  $\psi_{\alpha,V}$  increases to  $\psi_{\alpha,V} = 2.0$ . For angles  $90^\circ < \alpha \leq 180^\circ$  it is conservatively assumed that the concrete edge breakout load is at least as large as that associated with a load applied parallel to the edge.

For the case shown in Fig. 4.98c (load perpendicular to edge and acting towards the interior of the member) equation (4.38) provides only a rough estimate of the capacity because the failure mechanism is similar to that of the pry-out failure mode with the resultant shear cone truncated by the edge of the component. Tests carried out by *Mesureur* (1995) indicate, however, that equation (4.38) provides conservative predictions for small edge distances. Pry-out failure can be critical for larger edge distances (section 4.1.2.3) independent of the angle of the shear load.

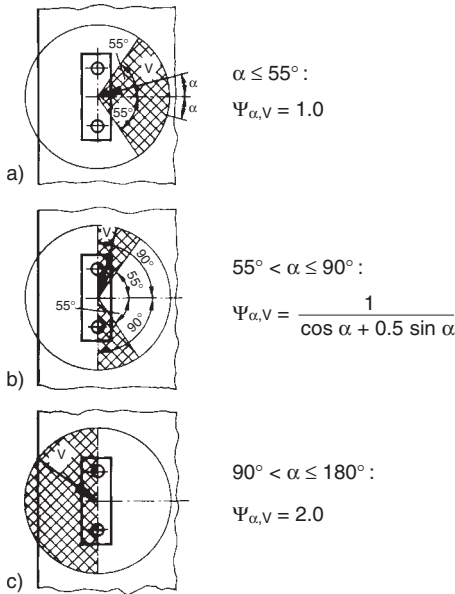


**Fig. 4.98** Factor  $\psi_{\alpha,V}$  for different angles between shear load and edge

According to research performed by *Hofmann* (2004), the ratio concrete break-out load of an anchor loaded in shear parallel to the edge to the value valid for loading perpendicular to the edge is not constant, but depends on the concrete pressure generated by the anchor. For headed anchors loaded in tension the splitting force is approximately linearly proportional to the ratio pressure under the head and concrete compressive strength. Assuming a) a linear relationship between splitting force generated by an anchor loaded in shear parallel to the edge and the anchor pressure on the concrete and b) the size of the compressed concrete area as proportional to the square of the anchor diameter, *Hofmann* (2004) deduced equation (4.39):

$$V_{u.c.,parallel}^0 = \psi_{parallel}^0 \cdot V_{u.c.,perpendicular}^0 \quad (4.39)$$

where:

$$\psi_{parallel}^0 = 4 \cdot \left[ \frac{d^2 \cdot f_{cc}}{V_{u.c.,perpendicular}^0} \right]^{0.5} \quad (4.39a)$$

$V_{u.c.,perpendicular}^0$  according to equation (4.26)

Equation (4.39) can be generalised to groups parallel to the edge (equation (4.40)).

$$V_{u.c.,parallel} = \Psi_{parallel} \cdot V_{u.c.,perpendicular} \quad (4.40)$$

where:

$$\Psi_{parallel} = 4 \cdot k_4 \cdot \left[ \frac{n \cdot d^2 \cdot f_{cc}}{V_{u.c.,perpendicular}} \right]^{0.5} \quad (4.40a)$$

$k_4 = 1.00$  for fastenings without hole clearance

$= 0.75$  for fastenings with hole clearance

$n =$  number of anchors loaded in shear,  
 $V_{u.c.,perpendicular}$  according to equation (4.33)

Equation (4.40a) takes into account that in case of a group of  $n$  anchors without hole clearance parallel to the edge and loaded parallel to the edge each anchor takes only  $1/n$ -times the applied shear load. Therefore the splitting force generated by each anchor is  $1/n$ -times of the value for a fastening with one anchor loaded by the same shear load. For fastenings with hole clearance loaded parallel to the edge it is generally assumed that all anchors share equally the applied shear load. However, in reality the distribution of the shear load to the different anchors is not uniform. This is taken into account by a reduction factor  $k_4 = 0.75$ .

According to *Hofmann* (2004) the linear interaction equation (4.37a) is conservative. A more accurate prediction of test results is given by a quadratic interaction equation.

$$\left( \frac{V_u^\alpha \cdot \cos \alpha}{V_{u,perpendicular}^\alpha} \right)^2 + \left( \frac{V_u^\alpha \cdot \sin \alpha}{V_{u,parallel}^\alpha} \right)^2 = 1 \quad (4.41)$$

The failure surface associated with group anchorages located in the corner of a member and loaded in shear at an angle to the corner is difficult to estimate. Therefore, it is advisable to check both failure modes depicted in Fig. 4.99. The notations of the edge distances and spacing are such that  $c_1$  and  $s_1$  are measured in the direction of the failing edge. The lower resistance calculated for the two failure modes controls the capacity of the connection. Fig. 4.99 is valid for fastenings with a ratio  $s_1/c_1 \geq 1$ . For fastenings with post-installed anchors with hole clearance

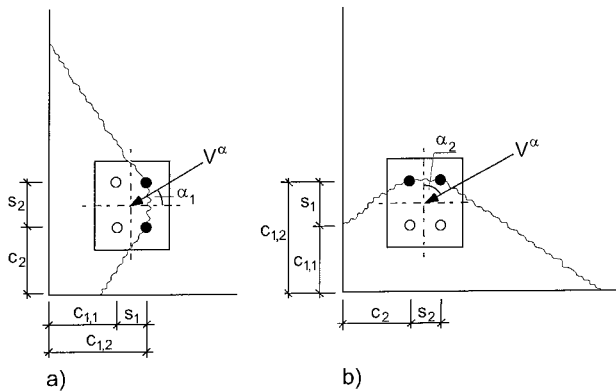


**Fig. 4.99** Example of a shear-loaded anchorage without hole clearance in the corner of a member  
 a) Assumption: Failure of left edge  
 b) Assumption: Failure of bottom edge

and a ratio  $s_1/c_1 < 1$  it should be assumed that the failure crack starts from the front anchors.

### 4.1.3 Combined tension and shear (oblique loading)

#### 4.1.3.1 Load-displacement behaviour and modes of failure

The load-bearing behaviour of anchors subjected to oblique loading lies somewhere between the response to concentric tension and the response to shear loading, and is dependent on the angle of load. All failure modes associated with tension and shear are possible. Therefore the following combined failure modes may occur:

- steel rupture under tension and shear loads,
- concrete failure due to tension and steel failure caused by shear,
- concrete failure under tension *and* shear load,
- steel rupture due to tension and concrete failure due to shear.

Concrete failure modes associated with tension loads include concrete cone or localised breakout, pull-out/pull-through, as well as splitting. Concrete failure modes associated with shear include concrete edge breakout and pry-out.

Failure combination (a) is characterised by rupture of the steel regardless of the angle at which the load is applied. This type of failure is asso-

ciated with larger embedment depths and edge distances. Failure combination (b) is associated with anchors having average embedment depth and large edge distance. As the angle of load increases, the failure mode transitions from concrete to steel failure, whereby the angle at which this transition takes place is primarily influenced by the diameter and embedment depth of the anchor, as well as the concrete and steel strength. In failure combination (c) concrete failure occurs for any angle of load application. This type of failure can be expected with anchors near an edge or those with small embedment depths remote from an edge. Failure combination (d) is theoretically associated with small diameter anchors having a large embedment depth positioned near an edge, however, this failure mode has not been observed experimentally.

*Bode, Hanenkamp* (1985) investigated the load-bearing behaviour of headed studs ( $d = 22$  mm) with a large edge distance subjected to combined tension and shear. The embedment depth was  $h_{ef} = 90$  mm. The anchors were so proportioned that shear loading alone induced steel failure and direct tension precipitated concrete cone breakout. For the combined tension and shear load test, a defined tension load was first applied and the shear load was subsequently increased until the anchor failed. The angle of load application was thus continuously varied during the test. Fig. 4.100 depicts shear load-



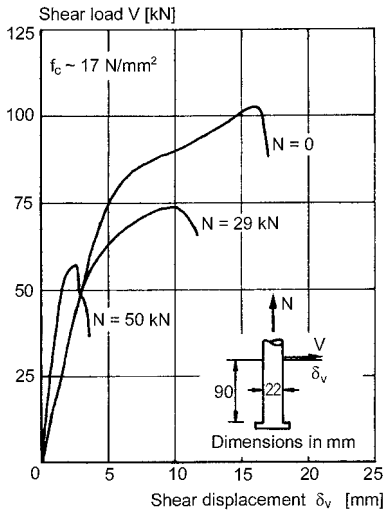


**Fig. 4.100** Shear load as a function of shear displacements for headed bolts subjected simultaneously to various levels of tension loading (after Bode, Hanenkamp (1985))

lateral displacement curves resulting from these tests. It can be seen that lateral displacement and shear load at failure decrease as the tension component of the load is increased.

The load-bearing behaviour of torque-controlled expansion anchors and undercut anchors subjected to combined tension and shear was studied in detail by Lotze, Klingner (1997). Tests included single sleeve anchors in pre-positioned and in-place configurations (see section 2.3.2) in concrete slabs of strength  $f_{cc,200} \approx 40 \text{ N/mm}^2$ . In the pre-positioned installations the shear load was carried solely by the threaded bolt, whereas in the in-place installations the shear sleeve participated in resisting the shear load. The angle of application of the load was varied from  $\alpha = 0^\circ$  (tension load) to  $\alpha = 90^\circ$  (shear load) and was kept constant during each test. Figs. 4.101 to 4.103 depict average load-displacement curves approximated by mathematical functions. The figures contain a) the tension load component as a function of the displacement in the tension direction, and b) the shear load component as a function of the lateral displacement. All curves represent undercut anchors with bolt diameter 5/8 inch ( $\approx 16$  mm).

Figs 4.101 and 4.103 are derived from anchors in pre-positioned installations and Fig. 4.102 represents anchors in in-place installations. For the tests represented in Figs. 4.101 and 4.102 the embedment depth is  $h_{ef} = 178$  mm and the edge distance is large. Consequently, these tests resulted in steel rupture regardless of load angle. In contrast, the tests represented in Fig. 4.103 reflect a reduced embedment depth of  $h_{ef} = 89$  mm and an edge distance  $c = 140$  mm, chosen so that a concrete failure occurred in all tests.

The tests reveal that the tension component of the failure load decreases as the shear load increases, or conversely, that the shear component of failure load decreases as the tension load increases. This result is obtained irrespective of the failure mode.

Steel tension failures were accompanied by large plastic deformations. Ultimate tension displacements declined noticeably as the shear component was increased (Figs. 4.101a and 4.102a). The undercut anchors installed in a pre-positioned configuration (i.e. without participation of the sleeve in resisting shear) achieved a failure load under shear which was approximately 60% of the value applicable for tension and the displacements at ultimate load were considerably smaller than those associated with un-iaxial tension (Fig. 4.101). As the tension component of the load was increased, the shear stiffness of the anchor declined, whereby significant reductions were associated with load application angles  $\alpha < 45^\circ$ . The decline in shear stiffness can be attributed to the decline in the longitudinal stiffness of the anchor rod upon approaching or exceeding tension yield. When the anchors were installed with the in-place configuration (shear sleeve engaged), the load-bearing behaviour under tension did not differ significantly from that of the pre-positioned installation (compare Figs. 4.102a and 4.101a). However, as might be expected, failure loads and displacements associated with shear loading were significantly increased (compare Figs. 4.102b and 4.101b). Again, the shear stiffness was reduced considerably as the tension component of the load was increased, and an almost plastic behaviour was observed for  $\alpha = 45^\circ$  and  $\alpha = 60^\circ$ .

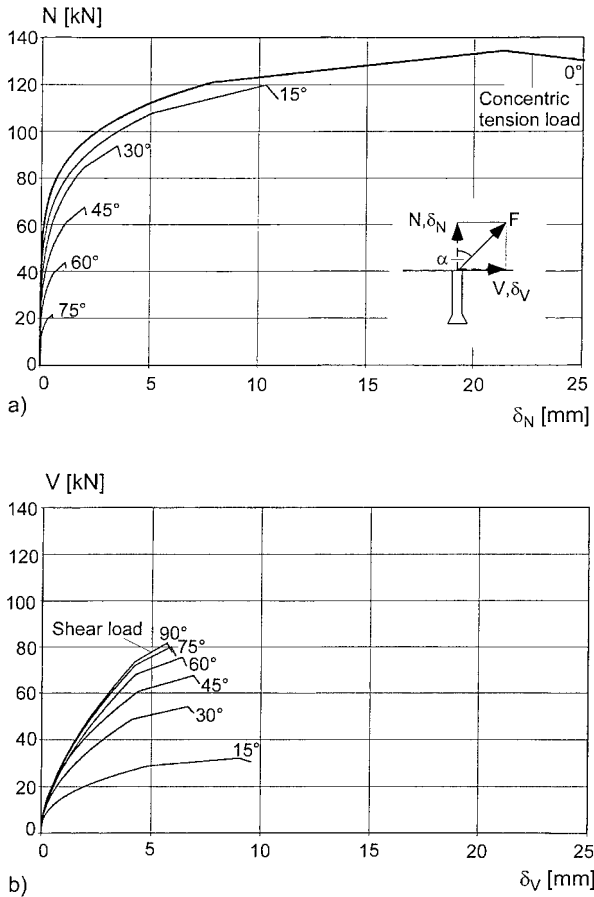


**Fig. 4.101** Load-displacement behaviour of undercut anchors subjected to combined tension and shear in the case of steel failure – pre-positioned installation of anchors (*Lotze, Klingner (1997)*)  
 a) Tension component as a function of displacement in axial direction  
 b) Shear component as a function of displacement transverse to axis

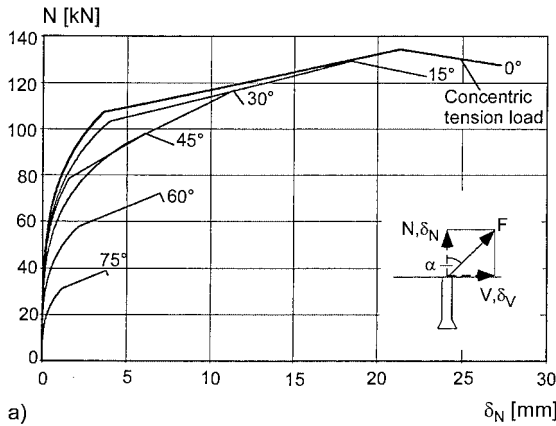
Tests with small diameter pre-positioned anchors in higher strength concrete ( $f_{cc,200}$  50 N/mm<sup>2</sup>) resulted in relatively brittle failures even in the case of steel failure.

Anchors failing by concrete cone breakout exhibited more brittle behaviour than those producing steel failure (compare Fig. 4.103 with Figs. 4.101 and 4.102). The shear stiffness of the anchors was influenced only slightly by the angle of load application because the axial stresses in the anchor rod remained well below steel yield. With anchors exhibiting concrete failure in tension and steel failure under shear a

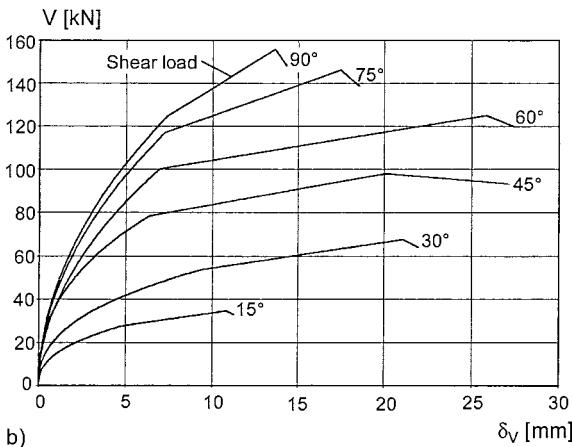
load-displacement behaviour similar to the one shown in Fig. 4.103 may be expected, whereby lateral displacements will increase.

The displacement behaviour of sleeve anchors as observed by *Lotze, Klingner (1997)* applies, in principle, to cast-in-place headed anchors as well.

The observed load-displacement behaviour associated with combined tension and shear tests affects the distribution of forces to individual anchors in group anchorages subjected to eccentric tension loads or combined bending moment and shear load.



a)



b)

**Fig. 4.102** Load-displacement behaviour of undercut anchors subjected to combined tension and shear in the case of steel failure – in-place installation of anchors (Lotze, Klingner (1997))

- a) Tension component as a function of displacement in axial direction
- b) Shear component as a function of displacement transverse to axis

In the case of steel failure, the shear stiffness depends on the magnitude of the tension load. Therefore, as the failure limit is approached, redistribution of shear load from the highly (tensile) stressed anchors to those with lower tensile stress (as in the case of eccentric tension) or those without tensile stress (as in the case of bending) will occur. In the case of welded shear studs possessing adequate ductility, the force distribution to individual studs can be determined using plastic theory, provided equilibrium conditions are maintained. With post-installed anchors, hole tolerances must be accounted for in the distribution of shear loads. With increasing shear loads, failure is characterised by shearing of the compression side anchors. If the tension side anchors are installed with typical hole tolerances, their shear dis-

placement at failure of the anchorage (as precipitated by shear failure of the compression-side anchors) may be less than the displacement of the compression side anchors by an amount equivalent to the hole tolerance. The shear capacity of the tension-side anchors is in this case not fully utilised. Therefore, in cases involving hole tolerances (i.e. non-welded anchorages), the distribution of shear forces should be calculated assuming elastic behaviour, even where steel failure is anticipated. This approach is always conservative.

In the case of an anchor or headed stud exhibiting concrete failure, the shear stiffness of the anchor is more or less independent of the load angle. Therefore, in group anchorages involving anchors failing by concrete cone breakout, there is no significant redistribution of shear loads

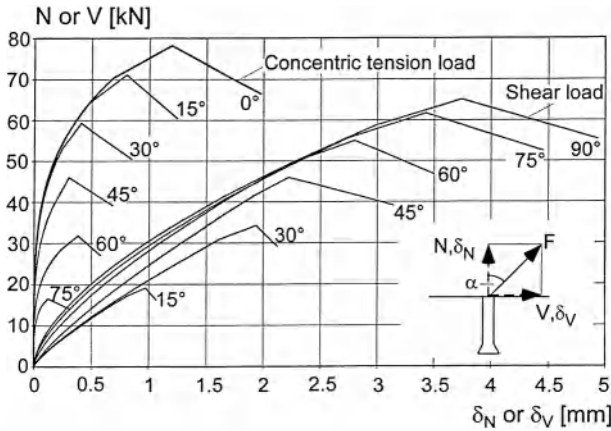


**Fig. 4.103** Load-displacement behaviour of undercut anchors subjected to combined tension and shear in the case of concrete edge failure – pre-positioned installation of anchors; tension component as a function of displacement in axial direction and shear component as a function of displacement transverse to axis (Lotze, Klingner (1997))

and the shear forces on the individual anchors should likewise be calculated assuming elastic behaviour.

#### 4.1.3.2 Failure load

To determine the failure load of anchors subjected to combined tension and shear, tests on bolts, headed studs and post-installed anchors, in which the angle of application of the load is varied systematically between  $\alpha = 0^\circ$  (concentric tension) and  $\alpha = 90^\circ$  (shear load) are relevant. Most of these types of investigations have been conducted on single anchors, but results for groups of two and four anchors are also available. Zhao, Eligehausen (1992/1) provide an evaluation of over 400 such tests.

In Figs. 4.104 to 4.106 test results are represented in the form of interaction diagrams segregated by failure mode. Fig. 4.104 represents anchor tests in which steel rupture occurred irrespective of the angle of application of the load, whereas Fig. 4.105 represents test specimens exhibiting concrete failure under concentric tension load and steel failure when loaded in shear. Figs. 4.106a and 4.106b depict tests that resulted exclusively in concrete failure. In each case, the ratio  $N/N_u$  is plotted as a function of the relationship  $V/V_u$ , where  $N$  and  $V$  are the tension and shear components of the measured failure load under inclined loading, and  $N_u$  and

$V_u$  are the average failure loads under concentric tension and straight shear, respectively, for the corresponding test series. (In some cases the normalising failure loads  $N_u$  and  $V_u$  were not determined by tests, but were instead calculated using the equations given in sections 4.1.1 and 4.1.2.)

Plotted in each figure 4.104 to 4.106 is the trilinear interaction relationship proposed by Bode, Hanenkamp (1985) as follows:

$$N/N_u = 1.0 \quad (4.42a)$$

$$V/V_u = 1.0 \quad (4.42b)$$

$$N/N_u + V/V_u = 1.2 \quad (4.42c)$$

where:

$N$  = tension component of failure load under combined tension and shear

$V$  = shear component of failure load under combined tension and shear

$N_u$  = mean tension failure load

$V_u$  = mean shear failure load

Also plotted in each figure 4.104 to 4.106 is the interaction curve given by equation (4.43) with a best-fit  $k$ -value as determined by regression analysis:

$$(N/N_u)^k + (V/V_u)^k = 1.0 \quad (4.43)$$

Equation (4.43) with  $k = 2$  corresponds to a circle in the interaction diagram, with  $k = 1$  to a straight line.

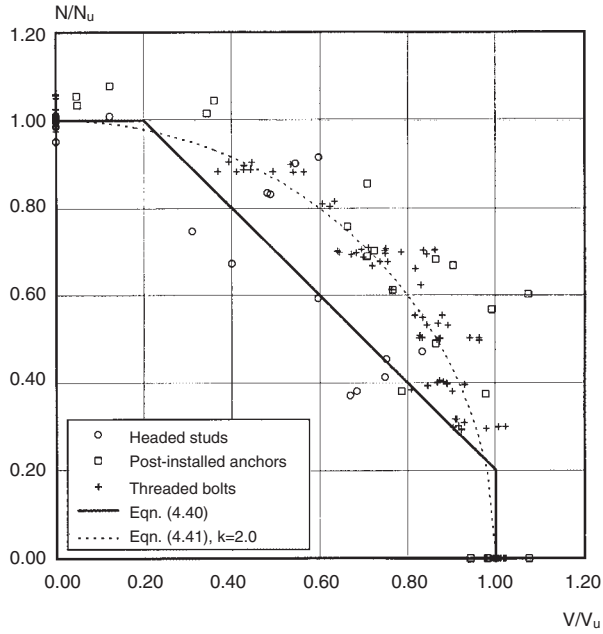


**Fig. 4.104** Interaction diagram of threaded bolts, headed studs and post-installed anchors in the case of steel failure (Zhao, Eligehausen (1992/1))

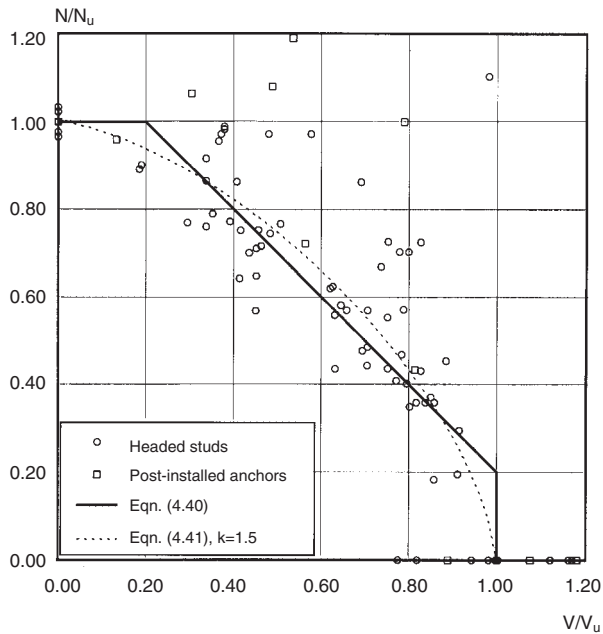
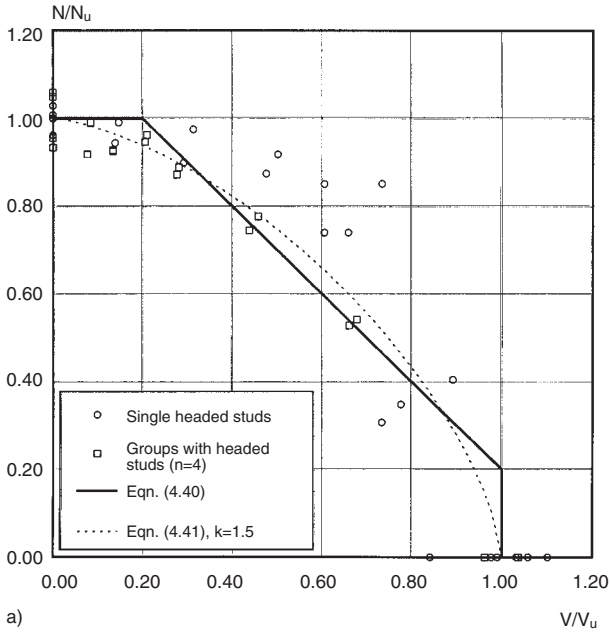
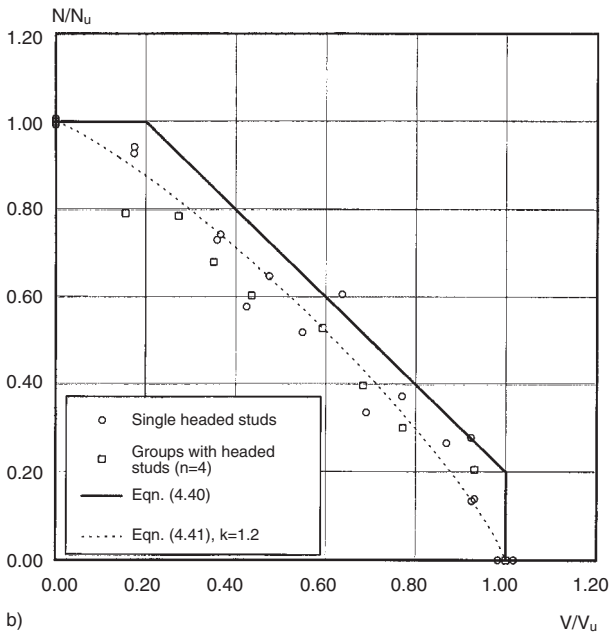


**Fig. 4.105** Interaction diagram for combined failure (concrete failure in tension and steel failure in shear) of headed studs and post-installed anchors (Zhao, Eligehausen (1992/1))



a)



b)

**Fig. 4.106** Interaction diagram of headed studs in the case of concrete breakout (Zhao, Elgehausen (1992/1))  
 a) Anchors remote from an edge, b) Anchors close to an edge



Fig. 4.104 indicates that a circular interaction relationship (equation (4.43) with  $k = 2$ ) most accurately predicts the steel failure load under combined tension and shear. Lotze, Klingner (1997) derived an exponent  $k \approx 1.75$  from tests on torque-controlled tension and undercut anchors. For the common case of anchors that exhibit concrete failure under concentric tension and steel failure under straight shear, the test results are approximated equally well by a tri-linear interaction equation (4.42) and by equation (4.43) with  $k = 1.5$  (Fig. 4.105). The same equations provide equally reasonable predictions for anchors remote from the edge that exhibit concrete failure regardless of the direction of the load (Fig. 4.106a). Equation (4.43) with  $k = 1.2$  supplies reasonable results for near-edge anchors that exhibit concrete failure (Fig. 4.106b).

Fig. 4.107 (Zhao, Eligehausen (1992/1)) offers an explanation for the unfavourable behaviour associated with near-edge anchors subjected to oblique loading where the shear component of the load is directed towards the edge. Fracture patterns associated with concentric tension and with straight shear loading are shown. For a single anchor loaded in tension (Fig. 4.107a), concrete fracture is initiated at approximately 25 to 40% of the ultimate load, depending on the embedment depth. Cracking progresses steadily up to ultimate load at which point the crack length is approximately 30 to 50% of the subsequent concrete cone side length (Ozbolt (1995)). With increasing deformation the resis-

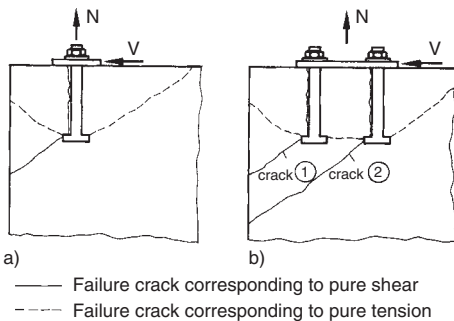


**Fig. 4.107** Crack pattern associated with anchors close to an edge subjected to oblique loading towards the edge (schematic) (Zhao, Eligehausen (1992/1))

tance decreases and the concrete cone is fully developed. The crack formation process associated with shear loading is, in principle, similar to the tension load case, whereby the extent of fracture at ultimate load is approximately 40 to 70% of the shear cone side length, depending on the edge distance (Fuchs (1990)). If an anchor having embedment depth and edge distance such that  $N_u \approx V_u$  is subjected to an oblique load ( $45^\circ$ ), cracking associated with both load directions is initiated well before attainment of the inclined tension failure load. This lowers the tension capacity of the concrete and hence the failure load associated with oblique loading. With groups of two anchors oriented perpendicular to the edge or groups of four anchors, the shear component may cause the formation of crack 1 (Fig. 4.107b) at a relatively low load level (compare section 4.1.2.4b). The crack reduces the tension capacity of the near-edge anchor(s). This explains the lower failure loads under combined tension and shear associated with anchors in groups compared to single anchors.

Grouping all failure modes together (Fig. 4.108a), the mean failure load corresponding to oblique load is reasonably predicted by the tri-linear interaction equation (4.42) or the elliptical interaction equation (4.43) with  $k = 1.5$ . Test values for which steel failure occurred regardless of the direction of load lie in the upper part of the scatter band while data points representing concrete failure of near-edge anchors lie in the lower extreme. If the test results are normalised with the 5% fractile of the tension and shear capacities rather than the mean capacities (Fig. 4.108b), then all test values lie beyond the interaction curve (Zhao, Eligehausen (1992/1)).

The form of interaction relationship given by equation (4.43) is commonly found in the literature, albeit with varying recommendations for  $k$ . In *American Concrete Institute, ACI 349-90* (1990) and *Cook, Klingner* (1989)  $k = 1.0$  is recommended, whereas in *McMackin, Slutter, Fisher* (1973), *Meinheit, Heidbrink* (1985) and *Johnson, Lew* (1990)  $k = 5/3$  is proposed, and in *Shaik, Whayong* (1985)  $k$  is given as 2.0. Using  $k = 1.0$  provides conservative results for all failure combinations. The use of  $k = 2.0$  provides unconservative predictions for all cases except

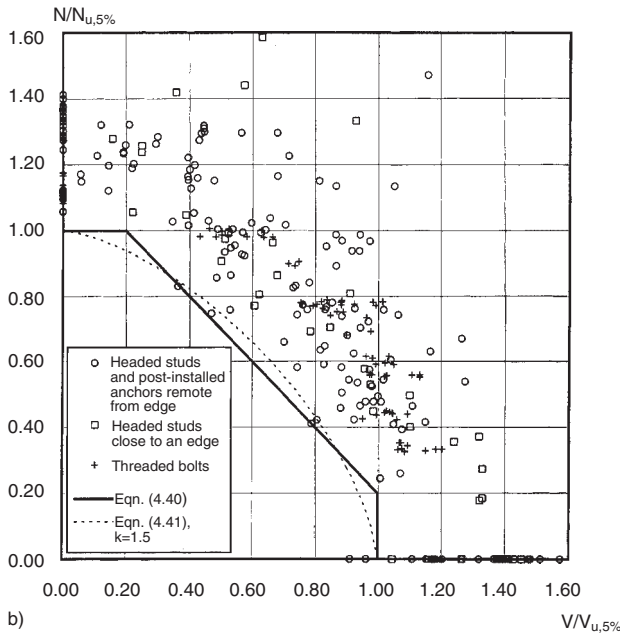
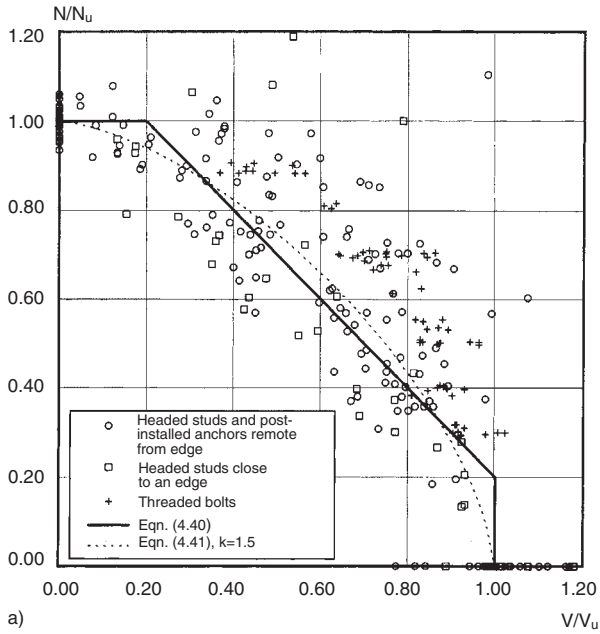


**Fig. 4.108** Interaction diagram for threaded bolts, headed studs and post-installed anchors independent of failure mode (Zhao, Elgehausen (1992/1))

a) Test results related to the mean values for  $N_u$  and  $V_u$   
 b) Test results related to the characteristic values for  $N_{u,5\%}$  and  $V_{u,5\%}$

steel failure under tension and shear. The exponent  $k = 5/3$  provides reasonable predictions for the common case where anchor capacity is governed by concrete failure and steel rupture in tension and shear, respectively.

The foregoing discussion is valid for anchors subjected to combined tension and shear loads *without* hanger reinforcement. Near-edge anchors provided with hanger reinforcement to take up the shear loading generate a complete shear cone well before attainment of the failure load. This shear cone is restrained by the hanger reinforcement (compare cracks 1 and 2 in Fig. 4.107b). If the anchorage is simultaneously subjected to a tension load component, the fractured concrete must likewise carry this load. This case has not been investigated experimentally, however, it is likely that the tension capacity associated with this geometry is relatively low. It is suggested to use conservative predictions that can be obtained from equation (4.43) with  $k$  set to  $2/3$ . The interaction curves given by equation (4.43) for  $k = 2/3$  and  $k = 1.5$  are shown in Fig. 4.109.

An anchor remote from an edge and provided with hanger reinforcement (Fig. 4.110) develops a concrete breakout fracture (crack 1) that is restrained by the hanger reinforcement well before the ultimate tension load is reached. Application of a simultaneous shear load causes the formation of crack 2, which overlaps with crack 1 on the lee side of the anchorage. There-

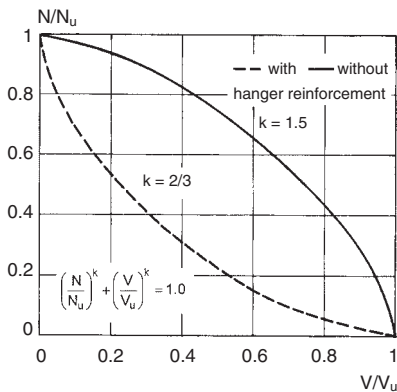


**Fig. 4.109** Proposed interaction diagram for anchors with and without hanger reinforcement for one loading direction (Eligehausen, Mallée, Rehm (1997))

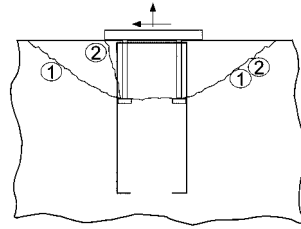


**Fig. 4.110** Crack pattern for an anchorage with hanger reinforcement with large edge distance subjected to oblique loading (schematic)

fore, the hanger reinforcement must be able to accommodate forces resulting from both the tension *and* shear loads on this side. This geometry has not been investigated experimentally. Based on the above reasoning, it is anticipated that the shear capacity associated with this case is relatively low. Conservatively the use of equation (4.43) with  $k = 2/3$  is recommended.

**4.1.4 Bending of the baseplate**

It is common in practice that a bending moment is applied to the baseplate via a rigidly attached (generally welded) structural member. For the typical connection shown in Fig. (4.111a), this

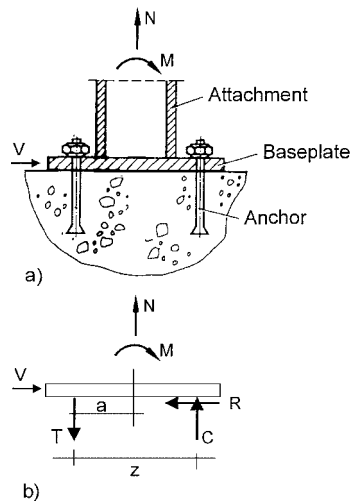


**Fig. 4.111** Anchorage subjected to bending moment and shear force  
 a) Cross-section  
 b) Forces acting on baseplate, shear force taken up by friction force

moment generates tensile forces in the anchors, as well as a compressive reaction beneath the baseplate (Fig. 4.111b). The position of the compression force depends on the stiffness of the plate. If the baseplate flexural stiffness is sufficiently large relative to the anchor axial stiffness (rigid baseplate), to be taken as rigid, elastic theory may be used to establish the location of the compression resultant. In the case of non-rigid baseplates, the compressive resultant may be assumed to lie at the edge of the welded structural member that is responsible for the imposed moment. If, as is generally the case, a shear force is applied in conjunction with a sufficiently large bending moment, the shear is resisted entirely by the friction force associated with the compression resultant, i.e. the anchors are not loaded in shear. The friction force  $R$  is given by:

$$R = \mu \cdot C \quad (4.44)$$

where (see Fig. 4.111b):

$C$  = resultant compressive force

$$= M/z - N \cdot a / z$$

$M$  = applied bending moment

$z$  = lever arm of internal forces (distance between resultant tension and compression force)

$a$  = distance between normal force  $N$  and resultant tension force

$N$  = applied axial force

$\mu$  = friction coefficient

According to *Cook, Klingner* (1989) the average value of the friction coefficient for baseplates in direct contact with the concrete may be taken as  $\mu = 0.43$ , whereby  $\mu$  is not significantly affected by either the concrete surface properties or the magnitude of the compressive stress beneath the baseplate. According to *Roik* (1982) the friction coefficient depends on the surface roughness of the steel plate but is not dependent on the concrete strength. Values for the mean coefficient of friction ranging from  $\mu = 0.46$  (painted baseplate) to  $\mu = 0.77$  (baseplate with mill finish) are given. In *Eurocode 3: EN 1993 1-1 (2002)* a value  $\mu = 0.2$  is recommended for baseplates on normal grout.

If the applied shear force exceeds the friction force as given by equation (4.44), movement of the baseplate will engage the anchors to resist

the balance of the applied shear. The distribution of the shear force to the individual anchors depends on the anchor stiffness and hole tolerances in the baseplate. If the anchors are welded to the baseplate and are dimensioned to generate concrete cone failure under tension loading, it may be reasonably assumed that a concentric applied shear load will be distributed evenly to all anchors. For anchors that exhibit ductile behaviour (ductile steel failure), *Cook, Klingner* (1989) provide the following model for distributing the applied loads.

The distribution of the tensile forces carried by the individual anchors of the group can be determined irrespective of the magnitude of the applied shear load according to plastic theory. If the friction force as predicted by equation (4.44) is exceeded, anchors located in the compression zone under the anchor plate can resist an ultimate load corresponding to equation (4.17). Only when the applied shear force is greater than the sum of the frictional resistance given by equation (4.44) plus the shear capacity of the anchors in the compression zone under the anchor plate as given by equation (4.17) are the tension-loaded anchors assumed to participate in resisting the applied shear forces. Their load-bearing capacity can be determined using equation (4.43) with  $k = 2$ . The conditions under which anchors can be regarded as sufficiently ductile are discussed in section 14.4.13.

According to *Lotze, Klingner* (1997) the above approach may not be conservative for anchorages with hole clearance in the baseplate or for fastenings where the tensioned anchors fail due to pull-out or concrete cone break-out.

#### 4.1.5 Sustained loads

Anchorage must be capable of safely resisting applied loads for many years. Therefore, their long-term behaviour is of interest.

Fig. 4.112a compares the characteristic load-displacement behaviour of a torque-controlled expansion anchor subjected to a monotonically increasing tension load to that of the same anchor subjected to a sustained load at an intermediate load level before being loaded to failure. The displacements due to creep of the concrete in the expansion zone increase under sus-

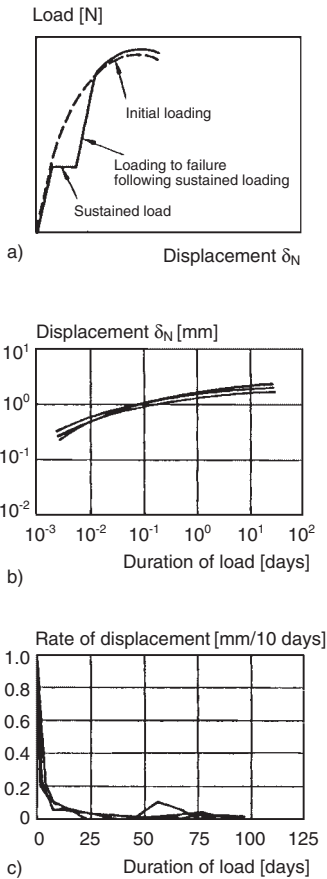


**Fig. 4.112** Effect of long-term loading on the displacement behaviour of a torque-controlled expansion anchor under concentric tension (after Seghezzi (1983))

tained loads. However, this process abates rapidly (Fig. 4.112b) and the rate of displacement declines after a relatively short time (Fig. 4.112c).

Under the usual safety requirements (see section 14), the permissible sustained load for post-installed anchors and headed studs is approximately 25 to 35% of the average short-term failure load. Sustained loads of this magnitude do not bring about anchor failure and cause only a slight increase in displacements. Likewise, as shown in Fig. 4.112a, they do not reduce the attainable failure load associated with subsequent monotonic tension loading.

#### 4.1.6 Fatigue loading

Like a static sustained load, frequently recurring loads of varying magnitude on the anchor have the effect of causing additional displacements. If the maximum load remains low (e.g.  $\leq 25\%$  of the short-term failure load) and fatigue failure of the steel components is excluded, then the behaviour is similar to that shown in Fig. 4.112a. As the maximum load and the amplitude of the variable portion of the load increases, not only fatigue failure of the steel parts, but also of the base material (concrete), must be considered.

When estimating the fatigue strength of the base material, it should be remembered that hairline cracks – initiating at the head of the stud or in the force transfer zone of the post-installed anchor – form in the concrete even at service load levels (section 3.3). However, due to the conical failure surface the area to be cracked increases with increasing crack length. Therefore, for a constant tension load, the stresses at the crack tip decrease as the crack surface extends, and consequently crack propagation remains stable (Elfgren, Broms, Cederwall, Gylltoft (1982)). It is therefore to be expected that the fatigue strength associated with concrete cone failure is at least equal to the fatigue strength of concrete subjected to uni-axial tension. This premise was confirmed in tests with single headed studs and groups with four studs (Usami, Abe, Matsuzaki (1980/1) and (1983), Lotze (1987/1)). The curve describing the relative capacity as a function of load cycles ( $S-n_{cycl}$  curve) associated with concrete cone failure is similar to those for concrete in tension, concrete in compression, and for the bond strength of ribbed reinforcing bars (Fig. 4.113). This suggests that fatigue failure of the base material (concrete cone failure) may be avoided over several million load cycles if the maximum load is maintained at less than about 50% of the average static failure load. If fatigue failure does not occur during cycling, the ultimate resistance and associated displacement of the anchorage are little influenced by the preceding load cycles.

With sufficient embedment, shear studs welded to steel plates experience fatigue fractures at the weld seam. The stress range associated with the

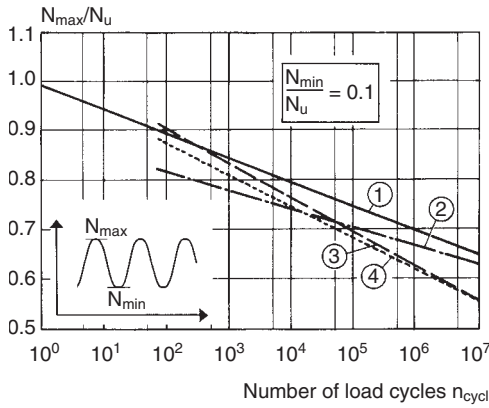


**Fig. 4.113** Comparison of  $S-n_{cycl}$  curves corresponding to concrete cone failure with  $S-n$  curves for other failure modes (after Lotze (1987/1))  
 Curve 1: concrete cone breakout (after Lotze (1987/1))  
 Curve 2: bond failure (after Rehm, Eligehausen (1977))  
 Curve 3: concrete under uni-axial tension (after Cornelissen, Reinhardt (1984))  
 Curve 4: concrete under uni-axial compression (after Klausen (1978))

cross-section of the shank for  $n_{cycl} = 2 \cdot 10^6$  load cycles is on average about  $2 \cdot \sigma_A = \sigma_{max} - \sigma_{min} \geq 100 \text{ N/mm}^2$  (Usami, Abe, Matsuzaki (1980/1) and (1983)).

The fatigue strength of headed stud anchorages subjected to shear loads is less than that for tension loads. Fig. 4.114 plots the shear stress range against the number of cycles at failure for welded shear stud specimens. The tests were

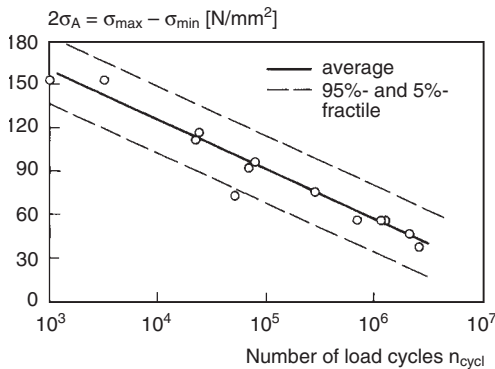


**Fig. 4.114**  $S-n_{cycl}$  curves for shear stud anchorages subjected to shear loading (after Naithani, Gupta, Gudh (1988))

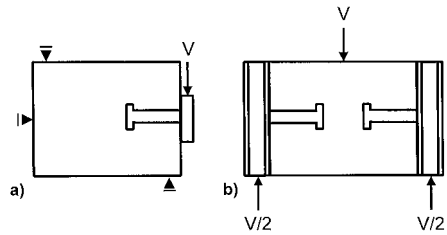


**Fig. 4.115** Set-up for testing headed studs in shear (schematic)  
 a) Single shear, b) Double shear

carried out on single headed studs in specimens representative of welded stud anchorages (single shear, see Fig. 4.115a) (Naithani, Gupta, Gudh (1988)). The fatigue strength is on average about  $2 \cdot \tau_A = \tau_{max} - \tau_{min} = 50 \text{ N/mm}^2$  for  $n_{cycl} = 2 \cdot 10^6$  load cycles. The 5% fractile is  $2 \cdot \tau_A \approx 30 \text{ N/mm}^2$ . Tests on specimens in double shear (Fig. 4.115b) result in fatigue strengths approximately 20% higher (Slutter, Fisher (1966)).

Generally, fasteners in anchorages subjected to alternating tension loads or reversing bending moments experience pulsating tension loads since the compressive forces are transferred to the base material directly via contact between the baseplate and concrete. Stand-off installations represent an exception in that the anchors must resist tension and compression loads. For the case of alternating shear loading which exceeds the friction force between the baseplate and the concrete the anchors are subjected to alternating shear loads.

Tension fatigue failures of post-installed anchors can occur in the bolt or sleeve, depending on the design of the anchor. The known values for screws (Wiegand, Illgner (1962), Illgner, Beelich (1966), Wellinger, Dietmann (1968), Wiegand (1974), Thomala (1978)) can be taken as a guide to the fatigue strength of bolts of post-installed anchors (Fuchs (1985/1), Illgner (1985)).  $S-n_{cycl}$  curves for screws (with rolled threads) in tension as proposed by various authors are shown in Fig. 4.116. This diagram is valid for pulsating loads and represents the 5%-fractiles of the test results. According to Fig. 4.116, the fatigue strength for  $n_{cycl} = 2 \cdot 10^6$  load



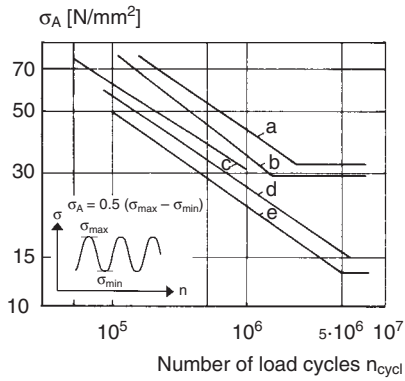


**Fig. 4.116**  $S$ - $n_{cycl}$  curves for screws subjected to axial tension – 5%-fractiles of test results (after *Lacher* (1986))  
 a) M20, grade 10.9, carbon steel (after *Lacher* (1986))  
 b) M20, grade 10.9, hot-dip galvanised carbon steel (after *Lacher* (1986))  
 c) M20, grade 10.9, carbon steel (after *Bouwman* (1979))  
 d) SIA 161 (1979), hot-dip galvanised carbon steel  
 e) Eurocode 3: EN 1993-1-1 (2002), hot-dip galvanised carbon steel

cycles is  $2 \cdot \sigma_A = \sigma_{max} - \sigma_{min} \approx 40$  to  $80$  N/mm<sup>2</sup>. It is less for larger bolt diameters and lower bolt strengths. As the European steelwork standard *Eurocode 3: EN 1993-1-1* (2002) ignores the influence of bolt diameter and grade, it specifies the lowest fatigue strength (Fig. 4.116, line e). Cut threads provide a fatigue strength that is less than that given in Fig. 4.116. Under bending loads the fatigue strength should not be less than that expected for tension loads (*Lacher* (1986)).

As in the case of pre-tensioned high strength bolts, it is the effective load beyond the level of prestress that is relevant to the fatigue resistance of the post-installed anchors. For constant load amplitude  $\Delta N_A$ , the amplitude  $\Delta F_S$  of the tension force in the anchor is critical for fatigue failure. This force increases as the prestress declines (Fig. 4.117). Of course in the absence of any prestressing force, the connection is loose.

If the shear load exceeds the friction force between baseplate and the concrete, the shear force must be resisted by the anchors. In this case shear loads generate high local stresses. Anchors that employ a threaded bolt or sleeve at the surface of the concrete are especially at risk owing to the resulting notch effect. Therefore the fatigue strength of anchors loaded in shear is much lower than that under tension. This is confirmed by tests on undercut anchors, torque-controlled expansion anchors and bonded anchors (*Henzel, Storck* (1990), *Storck* (1990), *Block* (2001), *Block, Dreier* (2002)). According to *Block* (2001) the fatigue strength of post-installed bonded anchors in the case of shear loading is about 35% of the value valid for tension (Fig. 4.118).

For fastenings with hole clearance, a movement of the baseplate corresponding to the annular gap between the anchor(s) and the baseplate will occur for shear forces larger than the friction force. In the case of alternating shear, the baseplate slides back and forth.

To avoid premature fatigue failure of the anchors and sliding of the baseplate, a perma-

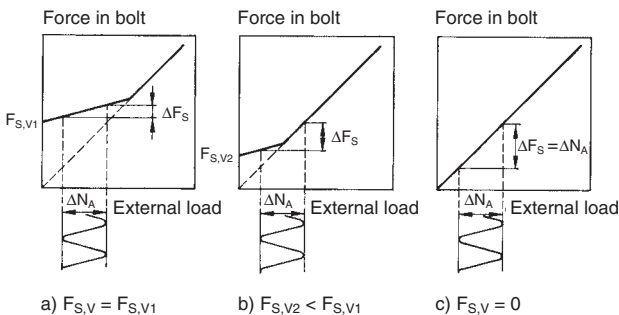


**Fig. 4.117** Influence of the degree of prestressing on the amplitude of the tensile force in the bolt for a constant amplitude of the external load (*Rehm, Eligehausen, Malleé* (1988))

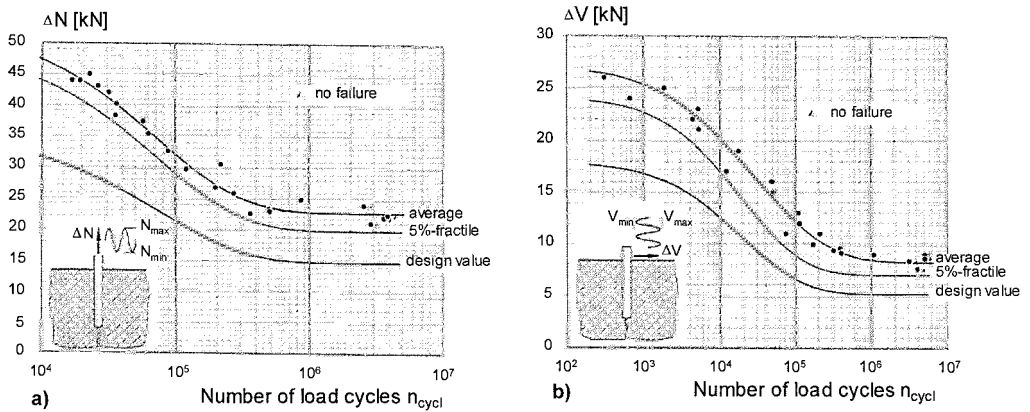


**Fig. 4.118** Load amplitude as a function of number of load cycles  $n_{cycl}$  (Block (2001)).

Tests on post-installed anchors under

a) Pulsating tension and reversed shear loading, b) Reversed shear loading

nently effective prestressing force should be present sufficient to ensure that the shear load is carried not by the anchors but rather by friction between baseplate and concrete (Lotze (1989/1 and 1993), Storck (1990)).

In general it is difficult to achieve a permanently effective level of defined prestress in anchor connections since the actual prestressing force generated upon application of the prescribed torque varies substantially, the prestress dissipates over time (see Fig. 3.38) and, finally, prestress can be lost altogether if the concrete cracks (i.e. if a crack passes through the anchor location). A nominal prestress can be assured if the connection is retightened at regular intervals. When doing so, care must be taken that the steel components are not loaded beyond their yield stress. The residual prestress at any given time can be established with a lift-off test, or with a load-indicator washer. However, some degree of uncertainty about the effective prestress will always remain.

In a group of anchors loaded by concentric tension or shear loads it is generally assumed that the loads are equally distributed to all anchors. For shear loads this assumption is only valid if a hole clearance is avoided by special measures. Even then, under tension or shear loads the amplitudes of the forces in the bolts may vary up to about 30 % from the average value owing

to differences in effective stiffness from anchor to anchor (Lotze (1993), Block (2001), Block, Dreier (2002)). This in turn leads to a reduction in the number of load cycles which can be accommodated compared to single anchors.

In Germany two torque-controlled bonded anchors and one undercut anchor are approved for use under tension and shear fatigue loading. These anchors maintain a permanent prestressing force because they are stiff and their strained length is sufficiently long. Furthermore an annular gap is avoided by special devices.

## 4.2 Cracked concrete

As discussed in section 3.4, crack formation in reinforced concrete members should be anticipated at service load levels whereby it is highly probable that anchor locations will be intersected by cracks. It is therefore necessary to assess the effect of cracking on anchor performance.

A variety of test specimens have been developed to investigate the influence of cracking on the load-bearing behaviour of anchors. These include reinforced one-way slabs loaded in flexure, reinforced tension members, and special specimens designed to generate cracks in two directions (intersecting cracks). Fig. 4.119 shows a reinforced tension member designed to

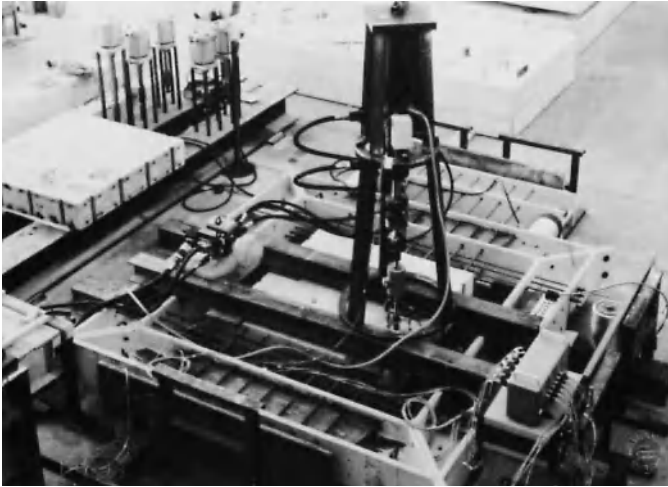


**Fig. 4.119** Test set-up for testing anchors installed in cracks in tension test members (Rehm, Eligehausen, Malleé (1988))

produce parallel cracks of roughly constant width through the depth of the member mounted in a tension testing bed. Also shown is the anchor loading hydraulic actuator elevated on a tripod frame. This testing bed is designed to also accommodate so-called intersecting crack specimens which produce an orthogonal crack pattern. Typically, post-installed anchors are positioned in pre-defined hairline cracks generated by loading and unloading of the tension specimen. The tendency of the drill holes to act as crack attractors ensures that the cracks pass through the anchor locations. In the case of cast-in-place bolts and studs, sheet metal crack inducers are incorporated to initiate cracks that are in-line with the anchor positions. In tests to assess the effect of crack width on anchor tension capacity, the cracks are opened to the prescribed width by loading the test specimen (usually via the reinforcing bars), and the anchors are then loaded monotonically to failure. During the test, the tensile load applied to the tension member is kept constant, allowing the crack width to increase slightly as the load on the anchor is increased. Variations on this test include subjecting the anchor to pulsating loads while the crack width is held constant, and cycling the crack width between two prescribed values while the anchor load is maintained at a constant level. Subjecting the anchor to a pulsating tension load simulates varying anchor loads which may occur in practice and also can

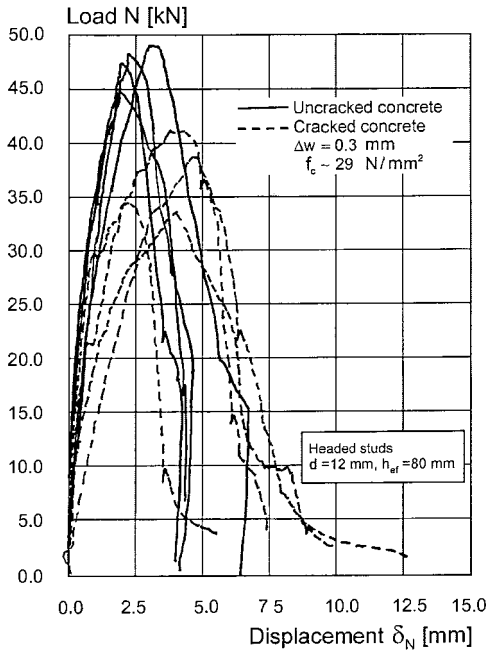
be regarded as an accelerated test to assess the effect of sustained loads. Cycling the crack width simulates the effect of varying structure loads (and hence crack widths) on anchor behaviour over time.

#### 4.2.1 Tension

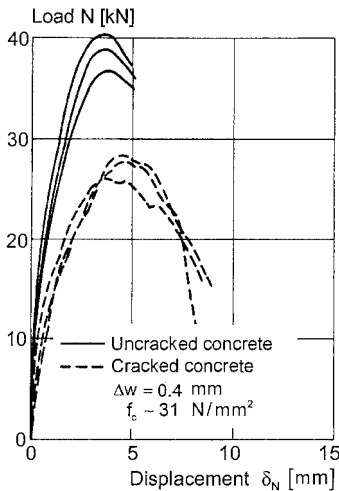
##### 4.2.1.1 Load-displacement behaviour and modes of failure

Fig. 4.120 depicts load-displacement curves from tension tests on headed studs (shank diameter  $d = 12$  mm, head diameter  $d_h = 18$  mm, embedment depth  $h_{ef} = 80$  mm) conducted in cracked and non-cracked concrete. All tests resulted in concrete cone breakout failure. The load-displacement curves associated with headed studs in cracks are flatter, peak loads are reduced and the displacements corresponding to peak load are increased when compared with tests on studs in non-cracked concrete. Undercut anchors exhibit a load-displacement behaviour that is similar to headed studs in cracked and non-cracked concrete, but the stiffness is influenced by the size of the undercut.

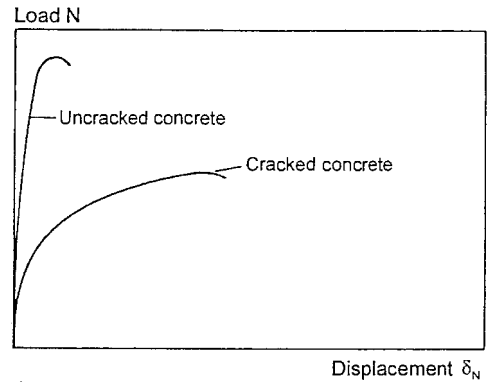
Schematic load-displacement curves for tests in non-cracked and cracked concrete conditions associated with a torque-controlled expansion anchor that is suitable for applications in cracked concrete are shown in Fig. 4.121a. Anchor failure is characterised by concrete cone



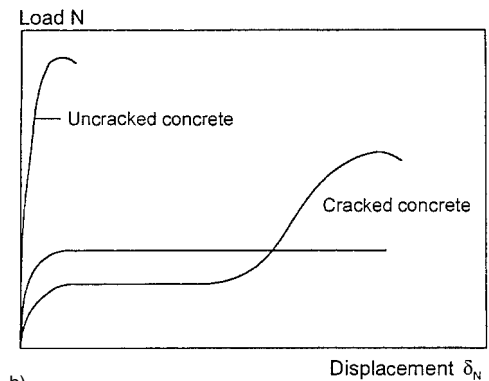
**Fig. 4.120** Load-displacement curves of headed studs tested in tension in cracked and non-cracked concrete (tests by *Furche, Dieterle* (1986))



**Fig. 4.122** Load-displacement curves of torque-controlled expansion anchors (M12,  $h_{ef} = 80$  mm) suitable for cracked concrete tested in tension in cracked and non-cracked concrete (after *Dieterle, Bozenhardt, Hirth, Opitz* (1990))



a)



b)

**Fig. 4.121** Schematic load-displacement curves of torque-controlled expansion anchors tested in tension in cracked and non-cracked concrete (after *Rehm, Lehmann* (1982))

- a) Anchors suitable for use in cracked concrete
- b) Anchors not suitable for use in cracked concrete (inadequate or non-existent follow-up expansion)

breakout in both cracked and non-cracked concrete. The effect of cracking on the load-displacement behaviour and peak load is similar to that observed for headed studs. Torque-controlled expansion anchors that are not suitable for applications in cracked concrete can exhibit so-called uncontrolled slip when loaded in tension in cracks, since such anchors may not develop follow-up expansion (necessary to re-establish anchorage in the crack) or do so only after significant displacement (Fig. 4.121b). Figs. 4.122 and 4.123 illustrate measured load-displacement curves for torque-controlled expansion anchors in cracked and non-cracked

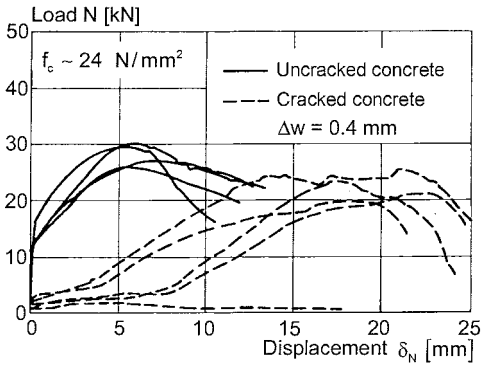


**Fig. 4.123** Load-displacement curves of torque-controlled expansion anchors (M12,  $h_{ef} = 60$  mm) developed for applications in non-cracked concrete tested in tension in cracked and non-cracked concrete (after Dieterle, Bozenhardt, Hirth, Opitz (1990))

concrete. The anchors represented in Fig. 4.122 are suitable for cracked concrete, whereby those shown in Fig. 4.123 are not. The load-displacement curves in Fig. 4.122 are characterised by uniform load development and stiffness in both

the cracked and non-cracked concrete condition. In contrast, the load-displacement curves shown in Fig. 4.123 are uniform only in the non-cracked concrete case. In cracks, these anchors exhibit large scatter in both peak load and slip, making their behaviour unpredictable.

Load-displacement curves for drop-in anchors in cracked and non-cracked concrete are shown schematically in Fig. 4.124. The load-displacement curves of fully expanded anchors are flatter in cracked concrete and exhibit greater scatter than in non-cracked concrete (Fig. 4.125). In addition, the peak load is substantially reduced. Drop-in anchors that are not fully expanded during installation (a common condition) exhibit even greater scatter in peak load, load-displacement behaviour, and stiffness in cracked concrete than fully expanded anchors (Fig. 4.126).

In general, the same modes of failure are observed with anchors in cracks as in non-cracked concrete (see Fig. 4.1). Displacement-controlled expansion anchors and torque-con-

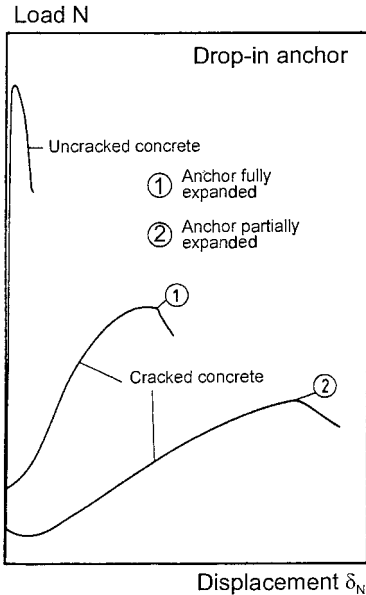


**Fig. 4.124** Schematic load-displacement curves for drop-in anchors tested in tension in cracked and non-cracked concrete (Eligehausen (1991))

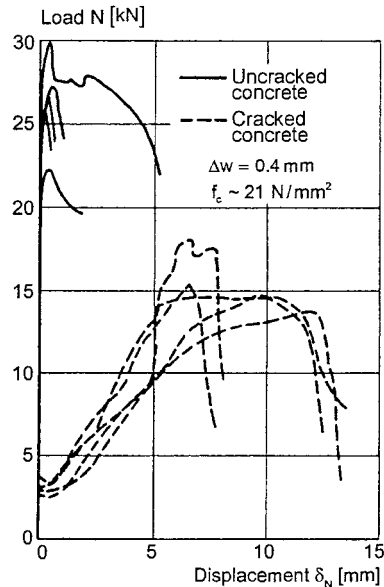


**Fig. 4.125** Load-displacement curves for fully expanded drop-in anchors (M12, 60 mm) tested in tension in cracked and non-cracked concrete (after Dieterle, Opitz (1988))

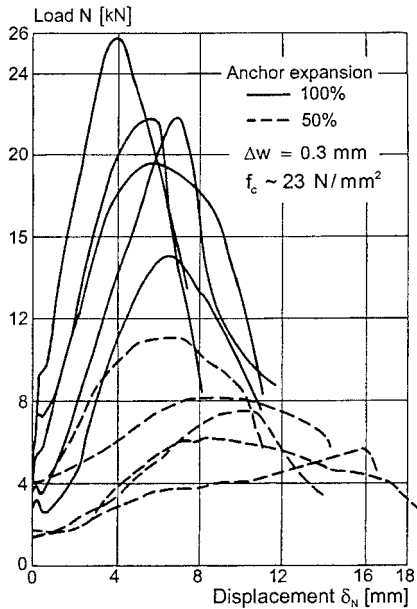


**Fig. 4.126** Load-displacement curves for fully and partially expanded drop-in anchors (M12,  $h_{ef} = 60$  mm) tested in tension in cracked concrete (after Meszaros, Eligehausen (1992))

trolled expansion anchors that cannot develop follow-up expansion or have insufficient expansion reserve (compare section 4.2.1.5) fail in cracked concrete by means of pull-out even though they may exhibit concrete cone breakout failure in non-cracked concrete.

#### 4.2.1.2 Failure load corresponding to steel failure

The failure load associated with anchors whose peak load is limited by rupture of the steel parts is not influenced by cracks in the concrete as long as the steel failure load continues to govern the capacity. Therefore, section 4.1.1.2 applies.

#### 4.2.1.3 Failure load associated with concrete cone breakout

Ultimate loads for headed studs and undercut anchors tested in cracks normalised to the predicted mean capacity in non-cracked concrete are plotted in Fig. 4.127 as a function of the crack opening  $\Delta w$  ( $\Delta w$  = difference between the crack

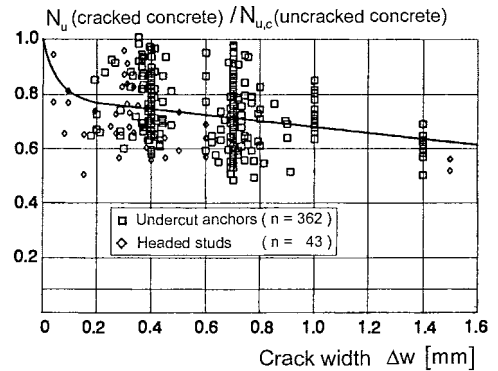


**Fig. 4.127** Effect of crack width on the concrete cone failure load of undercut anchors and headed studs subjected to concentric tension ( $N_{u,c}$  (non-cracked concrete) according to equation (4.5b)) (after Eligehausen, Balogh (1995))

width at the start of the anchor loading and before installation of the anchor). The tests in cracked concrete were carried out in reinforced tension test members and all tests resulted in concrete cone breakout failure. As the results of comparative tests in the same test specimen in the non-cracked state are not available in all cases, the concrete cone failure load in the non-cracked concrete are calculated using equation (4.5b). An assessment of only those test series in which tests were carried out in the same test specimen in the cracked *and* non-cracked states leads to roughly the same result as shown in Fig. 4.127, albeit with a smaller data population.

For crack widths  $\Delta w = 0.3$  mm to 0.4 mm, failure loads of headed studs and undercut anchors range from 0.5 to 1.0 (on average 0.75) times the value in non-cracked concrete. According to Zhang (1997), with a crack width  $\Delta w = 0.3$  mm, the average reduction in the failure loads of headed studs is only about 10 %. However, in these tests the anchors were not positioned directly in the crack in all cases. Nevertheless, the results of Zhang (1997) fall within the range of scatter of the tests assessed in Fig. 4.127. For headed studs and undercut anchors, the failure loads decrease only slightly as the crack width increases beyond the values given above. At  $\Delta w = 1.0$  mm the concrete cone breakout load is still approximately 0.70 times the value in non-cracked concrete.

*Eligehausen, Ozbolt* (1992) performed a three-dimensional non-linear FE analysis in which a pull-out test on a headed stud in cracked concrete ( $w \leq 0.3$  mm) was simulated. The “non-local microplane model” (*Bazant, Ozbolt* (1990)), which is based on non-linear fracture mechanics and is suitable for investigations of concrete behaviour, was used as the material model for the concrete. The simulation predicts that the concrete cone breakout load corresponding to a crack width  $w = 0.1$  mm is approximately 0.7 times the value in non-cracked concrete and remains constant for crack widths up to  $w = 0.3$  mm.

Headed studs and undercut anchors transfer the applied tensile force to the concrete by means of mechanical interlock (bearing). The reduced failure loads for headed studs and undercut anchors in cracked concrete must therefore be attributed to the disruption of the stress field associated with the crack (*Rehm, Eligehausen, Mallée* (1988)). In non-cracked concrete, a tension-loaded headed anchor generates a rotationally symmetric stress pattern around the anchor. Equilibrium is provided by the hoop (tangential) stresses in the concrete (Fig. 4.128a). If the anchor is located in a crack of sufficient width, these tensile stresses can no longer be transferred across the crack plane. The crack changes the way in which the forces are resolved in the concrete and effectively reduces the surface area available to transfer the tensile forces into the concrete mass (Fig. 4.128b). This model postulates the development of two independent concrete cones that are tangential to one another at the crack plane. In reality there is no significant difference in the overall shape of the fracture surface resulting from the cracked and non-cracked states, with the exception that the concrete breakout cone in cracked concrete is bisected by the crack. The model depicted in Fig. 4.128 should be regarded as a useful approximation.

The stress distribution from the non-linear FE analysis of *Eligehausen, Ozbolt* (1992) provides a better basis for explaining the reduction in the concrete cone breakout load of headed studs and undercut anchors installed in cracks. The analysis predicts that the shape of the concrete failure surface is roughly the same in cracked

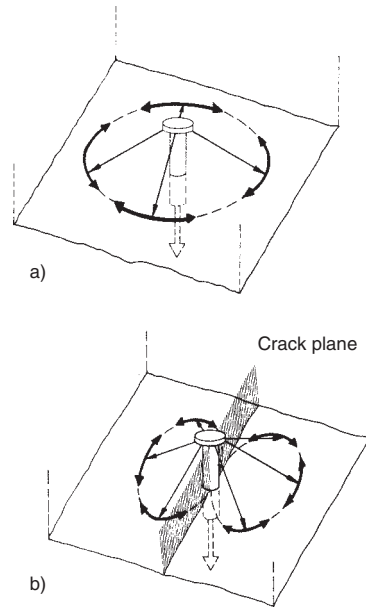


**Fig. 4.128** Distribution of forces in the concrete anchorage zone of a headed stud loaded in tension (after *Rehm, Eligehausen, Mallée* (1988))  
a) Non-cracked concrete  
b) Cracked concrete

and non-cracked concrete, which as stated above is in agreement with test results. The model predicts that only a small fraction of the load is transferred in the direction of the crack (Fig. 4.129) because the stiffness of the concrete in this direction is much lower than it is perpendicular to the crack. The distribution of the tangential stresses at the fracture surface is

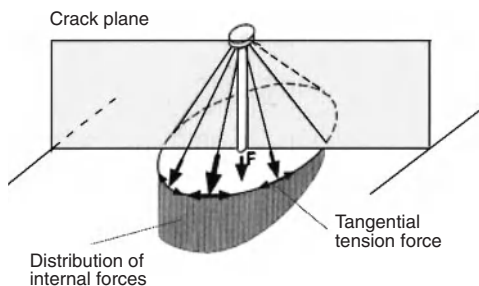


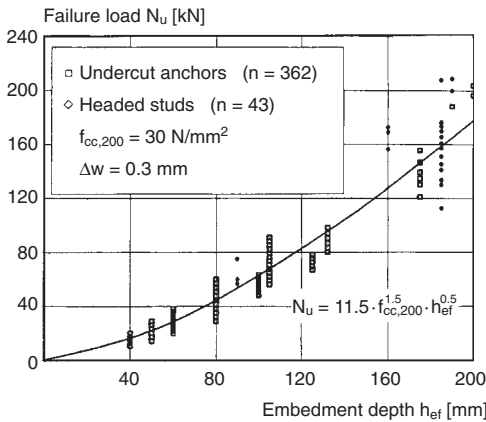
**Fig. 4.129** Load transfer mechanism of headed studs in cracked concrete (after *Eligehausen, Ozbolt* (1992))



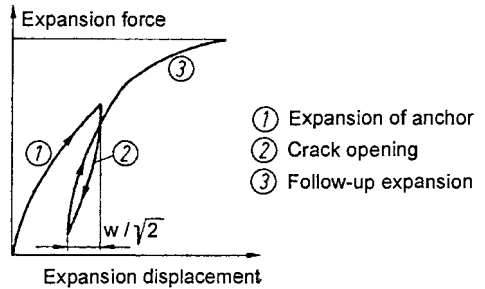
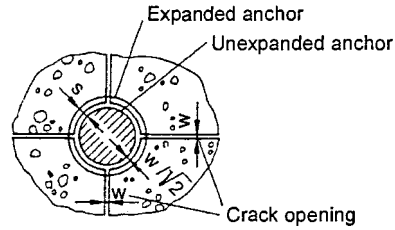
altered by shear stresses in such a way that there are no tensile stresses perpendicular to the crack.

Fig. 4.130 re-plots the failure loads represented in Fig. 4.127 as a function of embedment depth. The failure loads of the undercut anchors in the database are normalised by the factor  $15.5/13.5 = 1.15$  (see equation (4.5b)) so that they can be plotted together with the data for headed studs. As the tests were carried out in test specimens with different concrete strengths, all measured failure loads are further normalised with  $f_{cc,200}^{0.5}$  to a cube compressive strength  $f_{cc,200} = 30 \text{ N/mm}^2$ . Finally, to account for variations in the crack widths used in the tests, the measured values are normalised to a crack width  $w = 0.3 \text{ mm}$  with the aid of the regression curve shown in Fig. 4.127. Figure 4.130 indicates that the concrete cone breakout load associated with headed studs and undercut anchors in cracked concrete is proportional to  $h_{ef}^{1.5}$ . This agrees with the behaviour in non-cracked concrete (section 4.1.1.3) and can be ascribed to the size effect.

In the case of a metal expansion anchor, widening of a crack in the concrete passing through the anchor location acts to reduce the expansion force. This is depicted in Fig. 4.131, which applies to an expansion anchor located at the



**Fig. 4.130** Concrete cone failure load of undercut anchors and headed studs in cracked concrete as a function of embedment depth – test data corresponding to Fig. 4.127 (Eligehausen, Balogh (1995))



**Fig. 4.131** Effect of opening two intersecting cracks on the expansion force of a torque-controlled expansion anchor exhibiting good follow-up expansion (Eligehausen, Fuchs, Mayer (1987))

junction of two intersecting cracks. It plots the expansion force as a function of the indentation of the expansion shell in the concrete. This indentation is called expansion displacement. Line 1 represents the pre-tensioning and, if applicable, loading of the anchor in the non-cracked state. The opening of the crack to width  $w$  brings about a theoretical reduction in the existing indentation of the expansion sleeve in the concrete equal to  $w/\sqrt{2}$ . This leads to an unloading of the concrete and a reduction of the expansion force. As the unloading curve (line 2) is much steeper than the loading curve (line 1) even a small crack opening brings about an immediate loss of expansion stress. The unloading effect associated with cracking is particularly acute in high-strength concrete because of the reduced expansion displacement. Torque-controlled expansion anchors designed for applications in cracked concrete exhibit follow-up expansion in response to external tension loads which causes the expansion elements to be pressed further into the concrete, thus re-establishing the expansion force (line 3). If the

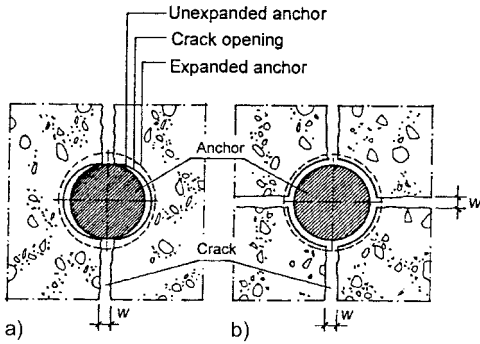


**Fig. 4.132** Effect of cracks running in one direction and orthogonal intersecting cracks on the effective indentation of the expansion elements into the concrete (schematic) (Eligehausen, Lehmann (1984))

expansion elements are sufficiently robust to prevent pull-through failure, properly designed torque-controlled expansion anchors can develop concrete cone breakout capacity in cracks.

The deformation of the concrete produced by an expansion anchor (expansion displacement) positioned in the junction of two intersecting cracks and the associated expansion force are reduced evenly over the full circumference of the anchor as the crack opens (Fig. 4.132b). In contrast, where the anchor is positioned in a crack running in one direction, crack opening produces a non-uniform decrease in the expansion displacement. It decreases perpendicular to the crack direction by the value  $w/2$  but is unchanged in the direction of the crack (Fig. 4.132a). Therefore, the influence of orthogonal intersecting cracks on the load-bearing behaviour of expansion anchors is much more severe than that associated with cracks running in one direction.

Fig. 4.133 shows the reduction in the concrete cone failure load of torque-controlled expansion anchors well-designed for use in cracked concrete as a function of the crack width opening  $\Delta w$ . The tests were carried out with reinforced tension members. The concrete cone breakout failure load in non-cracked concrete used to establish the reduction in capacity was calculated using equation (4.5b). For crack widths  $\Delta w = 0.3$  mm to 0.4 mm, the capacity is

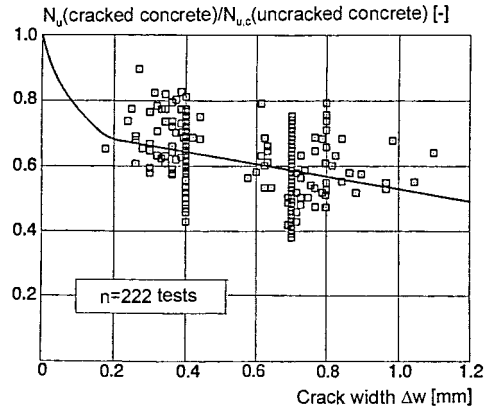


**Fig. 4.133** Effect of cracking on the concrete cone failure loads of tension-loaded torque-controlled expansion anchors exhibiting good follow-up expansion ( $N_{u,c}$  (non-cracked concrete) according to equation (4.5b)) (Eligehausen, Balogh (1995))

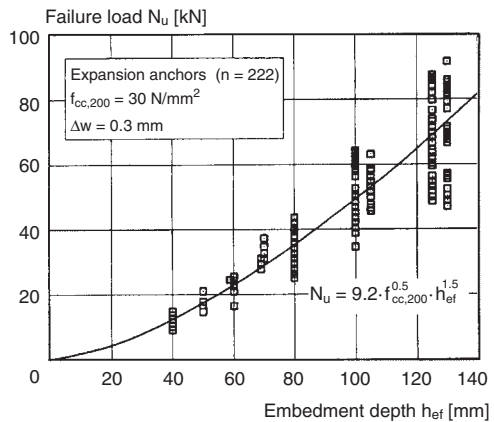


**Fig. 4.134** Concrete cone failure load of torque-controlled expansion anchors exhibiting good follow-up expansion as a function of embedment depth – test data corresponding to Fig. 4.133 (Eligehausen, Balogh (1995))

about 0.4 to 0.85, on average 0.7 of that in non-cracked concrete. Cannon (1981) and Usami, Abe, Nagano, Kowada, Kobayashi, Kodama, Koike (1988) report reductions of the same order of magnitude. Unlike bearing anchors (headed studs and undercut anchors) expansion anchors display a marked sensitivity to crack width. In part, the decrease in concrete cone breakout capacity reflects the increased degree of follow-up expansion required to compensate

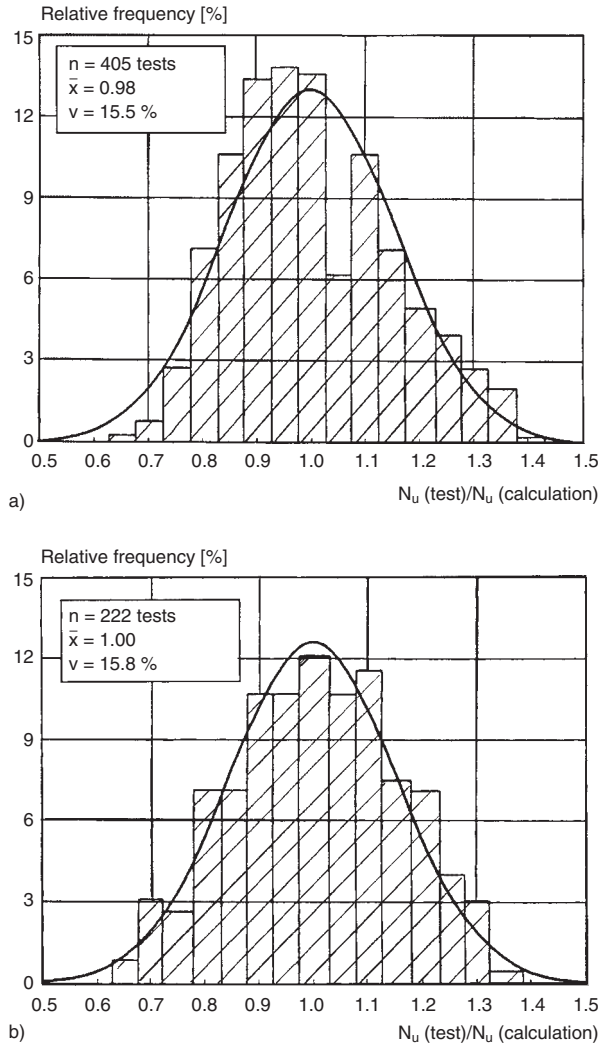


**Fig. 4.135** Histograms of measured to calculated concrete cone failure loads (Eligehausen, Balogh (1995))  
 a) Undercut anchors and headed studs  
 b) Torque-controlled expansion anchors exhibiting good follow-up expansion

for wider crack widths, which in turn acts to reduce the effective embedment depth. The extent to which torque-controlled expansion anchors are sensitive to crack opening is highly dependent on the anchor design.

Fig. 4.134 re-plots the failure loads represented in Fig. 4.133 as a function of embedment depth. The measured failure loads were normalised with  $f_{cc,200}^{0.5}$  to a concrete compressive strength  $f_{cc,200} = 30 \text{ N/mm}^2$  and via the regression curve shown in Fig. 4.133 to a constant crack width  $\Delta w = 0.3 \text{ mm}$ . Again, the increase in concrete

cone breakout capacity with increasing embedment is shown to be unchanged from the non-cracked concrete case, this is, proportional to  $h_{ef}^{1.5}$ .

The mean concrete cone breakout capacity for a single anchor positioned in a crack running in one direction and of a constant width over the member thickness  $w \approx 0.3 \text{ mm}$  is given by:

$$N_{u,c}^0(\text{cracked concrete}) = \psi_w \cdot N_{u,c}^0(\text{non-cracked concrete}) \tag{4.45}$$

where:

$\psi_w \approx 0.75$  for bearing-type anchors (headed studs and undercut anchors)

$\psi_w \approx 0.68$  for torque-controlled expansion anchors exhibiting robust follow-up expansion in cracks

$N_{u,c}^0$  according to equation (4.5b)

Histograms plotting the ratio of measured concrete cone breakout loads to the values predicted by equation (4.45) are presented in Fig. 4.135. The measured values are normalised to a crack width  $\Delta w = 0.3$  mm via the regression curves developed in Figs. 4.127 and 4.133. Fig. 4.135a represents the test data for headed studs and undercut anchors whereas Fig. 4.135b plots data from tests with torque-controlled expansion anchors showing good performance in cracked concrete. In both cases the ratio of measured to predicted values shows a normal distribution. The mean value is approximately 1.0 and the coefficient of variation is roughly 16%. This degree of scatter is not greater than that associated with tests in non-cracked concrete.

In those special cases where anchors may be positioned at the intersection of two orthogonal cracks, it is recommended to take an additional reduction in concrete cone breakout capacity of approximately 20% beyond the reduction predicted by equation (4.45) to account for the additional disruption to the stress state in the concrete.

The test record indicates that the concrete cone breakout capacity of torque-controlled expansion anchors in cracked concrete ( $w \approx 0.3$  mm) is approximately 10 % lower than that of undercut anchors, whereas no such difference has been established for the concrete cone breakout capacities in non-cracked concrete (section 4.1.1.3). Again, this additional reduction can be attributed to the fact that a torque-controlled expansion anchor in a crack experiences a greater degree of follow-up expansion than in non-cracked concrete and this movement of the anchor acts to reduce the effective embedment depth.

In reinforced concrete members subjected to flexural loading, the width of the flexural cracks decreases as the distance from the extreme tension fibre (or tension reinforcement) increases. In such cases the anchor failure load is also influ-

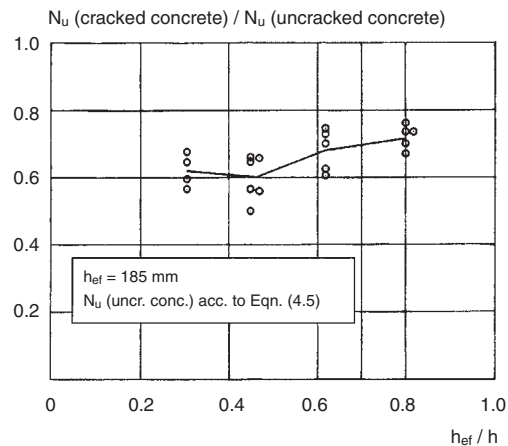


**Fig. 4.136** Ratio of concrete cone failure loads in cracked to values valid for non-cracked concrete as a function of embedment depth to component thickness (taken from *Eligehausen, Fuchs, Ick, Mallée, Reuter, Schimmelpfennig, Schmal* (1992))

enced by the ratio of the anchor embedment depth to the member depth. The influence of this parameter on the concrete cone failure load is investigated in *Eligehausen, Fuchs, Ick, Mallée, Reuter, Schimmelpfennig, Schmal* (1992). Tests were carried out on headed studs with an embedment depth  $h_{ef} = 185$  mm in beams of varying depth. The crack width at the beam soffit where the anchors were positioned was held at  $w = 0.25$  mm to 0.50 mm. The results of these tests are presented in Fig. 4.136, whereby the ratios of measured concrete cone breakout loads to the values calculated for non-cracked concrete per equation (4.5b) are plotted as a function of the embedment depth  $h_{ef}$  divided by the beam depth  $h$ . For  $h_{ef} < 0.5 \cdot h$ , the measured failure loads are on average 60% of the calculated concrete cone breakout loads in non-cracked concrete, i.e. in the lower end of the scatter band shown in Fig. 4.127. The failure loads associated with embedment depth  $h_{ef} = 0.8h$  are approximately 15% higher than for anchorages with  $h_{ef} < 0.5 \cdot h$ . Assuming that the mean crack width over the embedment depth may be taken as a predictor of the decrease in failure load, some reduction in capacity as compared to the non-cracked state should be expected even for anchorages with embedment sufficient to reach past the neutral axis into the compression zone.

All things being equal, the concrete cone breakout load associated with bearing anchors and expansion anchors that demonstrate good performance in cracked concrete is nearly independent of whether the anchors are located in or directly adjacent to the crack since in either case the distribution of stresses in the concrete is disrupted by the crack. Additionally, the failure surface may be truncated by the crack (Rehm, Lehmann (1982)).

If a group of anchors is located in the tension zone of a reinforced concrete member, it is unlikely that all of the anchors in the group will be positioned in cracks. Fig. 4.137 shows the concrete cone failure loads for groups of four anchors in relation to the number of anchors in the group that are located in cracks. The tests were carried out in reinforced tension test members (crack width  $\Delta w \approx 0.4$  mm). Expansion and undercut anchors demonstrating good performance in cracks were used for the tests. The tension loading mechanism was constructed in such a manner as to allow for free rotation of the baseplate. Failure in all cases was characterised by concrete cone breakout. Control tests were performed with groups of anchors in non-cracked concrete and these established the maximum capacity for the group. In conformance with theoretical predictions (Mayer, Eligehausen (1984)), the concrete cone failure load associated with a group of four anchors in cracked concrete was not influenced to any great extent by the orientation of the group

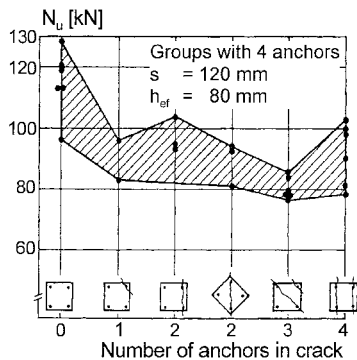


**Fig. 4.137** Effect of the number of anchors positioned in cracks on the failure load of groups with four anchors loaded in concentric tension (Mayer, Eligehausen (1984))

within the crack pattern. The lowest failure loads were recorded for cases in which three of the anchors in the group were located in cracks; these were on average approximately 30 % lower than for groups tested in non-cracked concrete. The results indicate that the concrete cone failure load of a group of anchors in cracked concrete is reduced by roughly the same percentage as is applicable to single anchors. According to Mayer, Eligehausen (1984) this assumption may also be made for rigid anchor plates unable to rotate.

Single anchors and anchor groups positioned in cracked concrete with small edge distances and/or subjected to eccentric tension have not been tested to date. It is reasonable to assume, however, that in these cases the concrete cone failure load is influenced by cracking to the same extent as for single anchors and groups subjected to concentric tension loading with a large edge distance. Accordingly, the concrete cone failure load in cracked concrete can be expressed by equation (4.46):

$$N_{u,c}(\text{cracked concrete}) = \psi_w \cdot N_{u,c}(\text{uncracked concrete}) \tag{4.46}$$

where:

$\psi_w$  according to equation (4.45)

$N_{u,c}$  according to equation (4.9)

Anchors that exhibit a continuous increase in load-displacement in both cracked and non-cracked concrete (curves a<sub>1</sub> and a<sub>2</sub> in Fig. 4.138)

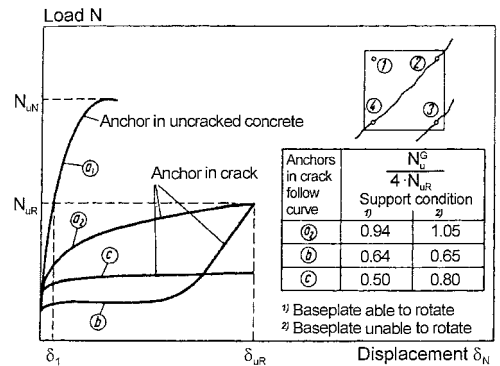


**Fig. 4.138** Effect of anchor load-displacement behaviour on the failure loads of groups with four anchors subjected to concentric tension (Mayer, Eligehausen (1984))

were used for the tests evaluated in Fig. 4.137. However, as shown in Fig. 4.123 expansion anchors located in cracks may experience significant slip prior to re-establishing resistance to the applied load via follow-up expansion or, if they fail to re-expand, they may simply be pulled out without an increase in the load. This behaviour is depicted in Fig. 4.138, curves b and c. The influence of this type of anchor behaviour on the failure load of a group of four anchors was analysed theoretically in Mayer, Eligehausen (1984). The baseplate was either assumed as hinged so that it could rotate or as rotationally stiff. The calculation of the failure load of the group is shown in Fig. 4.139b for hinged and in Fig. 4.139c for rotationally stiff baseplates. Assuming that all of the anchors located in cracks exhibit load-displacement behaviour as represented by curves  $a_1$  and  $a_2$ , and that the anchor spacing in the group is adequate to allow full development of the concrete cone breakout capacity for each anchor, the ultimate load of the group is approximately four times the capacity of a single anchor in a crack. If, however, anchor 2 and/or anchor 4 exhibit behaviour conforming to curve b, the failure load drops by approximately 1/3. The drop in the load is larger still if one of the anchors located in a crack fails to develop further capacity, i.e. exhibits the behaviour depicted by curve c in Fig. 4.138.

These studies demonstrate that anchors that are to be used in cracked concrete must satisfy very specific conditions in terms of their load-displacement behaviour. Their suitability can be assessed in special tests (see section 14.2). Current investigations indicate that only bearing-type anchors (headed studs and headed anchors, as well as undercut and bonded undercut anchors and concrete screws) and well-designed torque-controlled expansion and bonded expansion anchors can be regarded as suitable for applications in cracked concrete.

In addition to the influence of cracks, the superimposition of tensile stresses from various loading cases is also of interest for anchorages in cracked concrete. It is well known that high tensile stresses occur in the concrete surrounding overlap splices of reinforcing bars. If anchors are positioned in these zones, the tensile

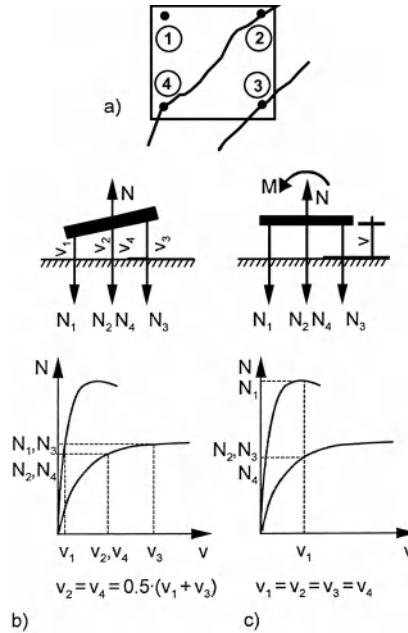


**Fig. 4.139** Calculation of the failure load of a group with four anchors from the load-displacement curves (Mayer, Eligehausen (1984))

- a) Baseplate with anchors (anchor 1 in non-cracked concrete, anchors 2 to 4 in a crack)
- b) Baseplate is able to rotate
- c) Baseplate is unable to rotate

stresses generated by the anchor are superimposed locally with those of the overlap splice. According to theoretical and experimental studies (Eligehausen (1984)) this stress superimposition can result in a reduction of up to 30 % in the concrete cone breakout load of anchors located near the splice ends of large ( $d_s = 28$  mm) reinforcing bars or welded steel fabric reinforcement as compared to the capacity of anchors in non-cracked and otherwise unloaded concrete. The reduction decreases with increasing anchor embedment depth. It is of a similar order of magnitude to the reduction in the concrete cone failure load due to cracks (Fig. 4.127). Therefore, for the capacity of anchors in the zone of reinforcing bar splices, the position of the anchors relative to cracks in the concrete is decisive.

A further unfavourable condition is created when headed studs or post-installed anchors are



terminated within the concrete cover or just at the level of a dense layer of reinforcement in a reinforced concrete member. As with an overlap splice condition, the bond stresses associated with the reinforcing bars are superimposed on the tensile stresses generated by the anchors. Additionally, the closely spaced reinforcement disrupts the transfer of the force from the anchor into the member. Aggravating this condition is the fact that the concrete strength in the concrete cover is often lower and the concrete is of poorer quality than that in the middle of the member cross-section. The cone failure load to be expected in such conditions was investigated

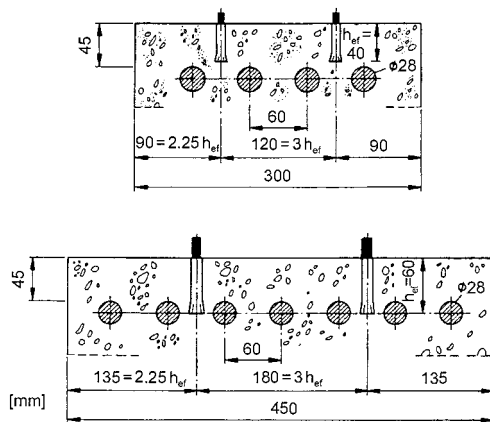


**Fig. 4.140** Anchorage in the concrete cover of heavily reinforced beams (tests by *Fuchs* (1985/2))

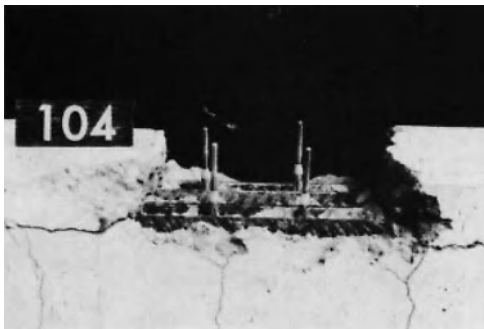


**Fig. 4.141** Failure pattern of a group with four anchors embedded in the concrete cover of a heavily reinforced beam. The anchors were put into their original place after the test (*Fuchs* (1985/2))

with single anchors and anchor groups placed in cracks (*Fuchs* (1985/2)). Undercut and sleeve-type torque-controlled expansion anchors were employed in the tests. The anchors were tested in loaded reinforced concrete beams with flexural reinforcement consisting of deformed bars ( $d_s = 28$  mm) placed with a clear spacing of about 30 mm. A concrete cover of 45 mm was chosen so that the selected anchors with embedments  $h_{ef} = 40$  mm to 60 mm were terminated in the concrete cover or just at the level of the reinforcing bars (Fig. 4.140). Failure of the anchor groups was characterised by peeling away of the concrete cover (Fig. 4.141).

The failure loads were, on average, approximately 30 % lower than could have been expected in cracked concrete with widely spaced reinforcement. A similar reduction is to be expected with headed studs.

If, on the other hand, post-installed anchors or headed studs are anchored *behind* closely spaced tension reinforcement that is enclosed by stirrups, then higher concrete cone failure loads are achieved than for widely spaced reinforcement near the surface.

The concrete cone failure load is increased by including anchor reinforcement in the form of stirrups or links directly adjacent to the fastening. This situation has not been investigated experimentally in cracked concrete. However, it can be assumed that the anchor reinforcement has a beneficial effect similar to anchors in non-cracked concrete and the capacity of the anchor can be calculated according to equation (4.12) (see section 4.1.1.3h).

#### 4.2.1.4 Failure load associated with local blow-out failure

Headed studs with large embedment depth and small edge distance may fail in non-cracked concrete via a local concrete side blow-out failure (see section 4.1.1.4). The behaviour of such anchors in cracks has not been investigated to date. Owing to the similarity between local side blow-out and cone-shaped concrete breakout failures, it is to be expected that the failure load for a local side blow-out failure would be reduced by cracking to a similar extent as for a



cone-shaped concrete failure. Consequently, the ultimate load for a local blow-out failure is:

$$N_{u,cb}(\text{cracked concrete}) = \psi_w \cdot N_{u,cb}(\text{non-cracked concrete}) \quad (4.46)$$

where:

$$\psi_w \approx 0.75$$

$N_{u,cb}$  is according to equation (4.15a)

The resistance to side blow-out type failure can be improved by confining the concrete locally with stirrups or spiral reinforcing (compare section 4.1.1.4). However, this application has not been investigated experimentally to date in cracked concrete.

#### 4.2.1.5 Failure load associated with pull-out/pull-through failure

The expansion force and hence the pull-out resistance of an expansion anchor positioned in a crack is substantially reduced as the crack widens (line 2 in Fig. 4.131). The follow-up expansion mechanism of torque-controlled expansion anchors designed for applications in non-cracked concrete may be inadequate for cracked concrete conditions. Under tension loading, the pull-out failure load of such anchors may scatter considerably and be unpredictable (Fig. 4.123). In contrast, torque-controlled expansion anchors suitable for use in cracks demonstrate reliable follow-up expansion and have sufficient expansion displacement to bridge typical crack widths. The failure mode of these anchors in a crack depends on the crack width and the geometry of the expansion elements responsible for the extent of available expansion displacement. If the crack width is not excessive and/or the expansion elements are of sufficient thickness to preclude a pull-through failure, the behaviour of the anchor will be characterised by concrete cone breakout and section 4.2.1.3 applies. If the anchor is located in a wider crack such that the effective expansion displacement is too small and hence the expansion force is not sufficient to develop a concrete cone failure, the cone may be pulled through the expansion sleeve. The corresponding failure load is reduced in comparison to the value to be expected for a concrete cone breakout. Pull-through failure can also occur in cracks of normal width if the anchor is equipped

with thinner expansion elements. Anchors failing by pull-through in cracked concrete show a normal scatter of the ultimate load which is predictable. *Lehmann* (1993) offers equations for calculating the pull-through load of torque-controlled expansion anchors in cracked concrete. However, it is recommended that these calculated values be verified with tests. In general the failure load associated with anchors that exhibit pull-through failure in both cracked and non-cracked concrete is reduced by about 30% for cracks having a width  $w \approx 0.3$  mm. With increasing crack width the reduction of the failure load is more significant than shown in Fig. 4.133.

Drop-in anchors (Fig. 2.19b<sub>1</sub>) that generate concrete cone break-out in non-cracked concrete when loaded in tension to failure usually exhibit pull-out failures when anchored in cracks because the expansion force is reduced as the crack opens (see line 2 in Fig. 4.131). Since the construction of drop-in anchors does not permit follow-up expansion, this lost expansion force cannot be restored. The capacity of such anchors is thus influenced by cracks to a much

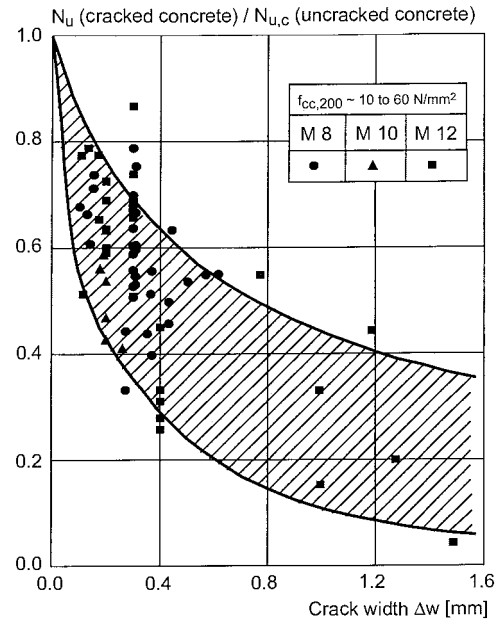


**Fig. 4.142** Effect of crack width on the failure loads of fully expanded drop-in anchors loaded in concentric tension ( $N_{u,c}$  (non-cracked concrete) according to equation (4.5b))

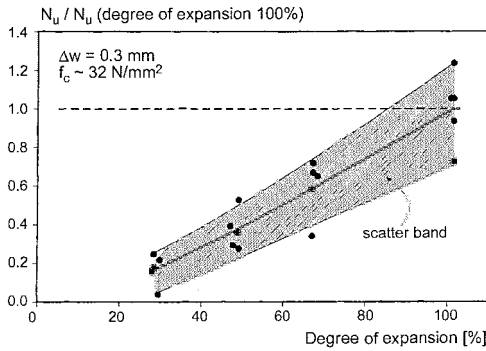


**Fig. 4.143** Failure loads of M12 drop-in anchors as a function of the degree of expansion (Meszaros, Eligehausen (1992))

greater degree than, for example, anchors that develop mechanical interlock. This is shown by a comparison of Fig. 4.142, which pertains to a fully expanded drop-in anchor, with Fig. 4.127. At a crack width  $\Delta w = 0.3$  mm, the pull-out load is reduced by approximately 50% compared to the concrete cone breakout capacity in non-cracked concrete.

In order to expand drop-in anchors fully, significant impact energy is required (see section 2.3.3.1). This fact implies that drop-in anchors are often under-expanded in practice. Accord-

ing to investigations by *Eligehausen, Meszaros* (1992) the average expansion of drop-in anchors M8 to M12 in practice was about 50%. Under-expanded drop-in anchors subjected to tension loading in cracks generate failure loads that are again significantly reduced compared to fully expanded drop-in anchors (Fig. 4.143). At 50% expansion, the pull-out load of a M12 drop-in anchor is on average only about 40% of the value applicable for full expansion in cracks and hence only about 20% of the failure load in non-cracked concrete. The influence of the degree of expansion on the pull-out load is even greater for smaller diameter anchors.

The pull-out load of drop-in anchors in cracked concrete can be assessed according to *Lehmann* (1993). The calculated pull-out loads agree reasonably well with the measured values at full expansion. However, the influence of the degree of expansion on the ultimate load is overestimated in the calculation. The probable explanation for this is that the actual shape of the drilled hole as created by a hammer drill with a carbide cutting edge deviates from the circular shape assumed in *Lehmann* (1993).

In the case of bearing-type anchors (headed studs and undercut anchors), the displacements in cracked and non-cracked concrete increase in proportion to  $p^2$ , where  $p$  is the bearing pressure

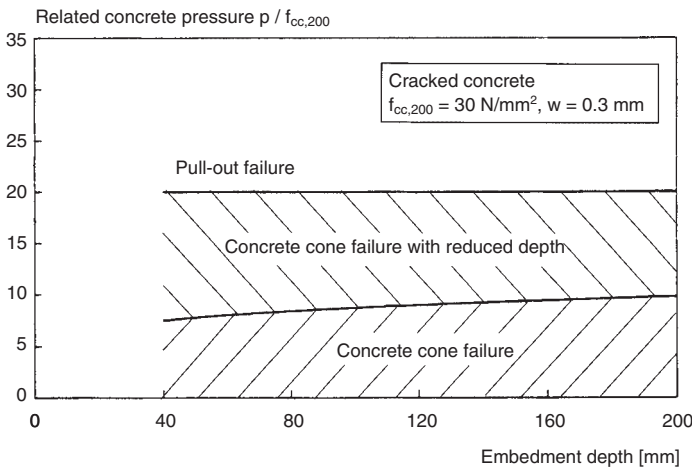


**Fig. 4.144** Maximum average bearing pressure under the head related to the concrete compressive strength required to assure the concrete cone failure load in cracked concrete predicted by equation (4.45), as a function of embedment depth (after *Furche* (1994))

at the head ( $p = N / A_n$ ) (Furche (1994)). For a pressure beyond a critical value, the effective embedment depth and hence the concrete cone failure load will be reduced. The maximum bearing pressure beneath the head of a headed stud required to assure full concrete cone breakout capacity in accordance with equation (4.45) is illustrated in Fig. 4.144 in relation to the embedment depth. Expressed in terms of the cube compressive strength, the critical pressure ranges from  $p \approx 7 f_{cc,200}$  ( $\approx 8.3 f_c$ ) for  $h_{ef} = 40$  mm to  $p \approx 10 f_{cc,200}$  ( $\approx 11.9 f_c$ ) for  $h_{ef} = 200$  mm, i.e. about 70 % of the value in non-cracked concrete (see Fig. 4.54). At higher concrete pressures, a concrete cone breakout at a reduced depth takes place. The associated ultimate load can be calculated according to Furche (1994).

#### 4.2.1.6 Failure load associated with splitting of the concrete

The splitting forces generated by expansion anchors may cause the concrete cross-section to split (see section 4.1.1.6). In reinforced concrete such forces are resisted by reinforcement near the surface (see Fig. 4.145a for the case of an anchorage in a narrow member), edge reinforcement (anchorage near the edge of a member – Fig. 4.145b) or corner reinforcement (Fig. 4.145c – anchorage in the corner of a member). The influence of a splitting crack on the ultimate load of an anchor corresponds to that of tension cracks produced by external loads or member restraint. Therefore, the reinforcement should be proportioned to resist the splitting

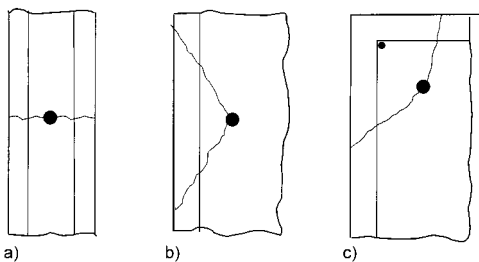


**Fig. 4.145** Restricting the width of splitting cracks by means of reinforcement

- a) Fastening in narrow concrete member
- b) Fastening at edge of concrete member
- c) Fastening in corner of concrete member

forces that are generated by the anchor (see section 4.1.1.6c) and to limit the crack width to  $w \approx 0.3$  mm. In the case of anchors suitable for cracked concrete conditions, the presence of such reinforcement will allow the anchor to develop its capacity in cracked concrete. Depending on anchor type, concrete strength, embedment depth and edge distance, either the full steel capacity or the concrete capacity as governed by concrete cone breakout or pull-through in cracked concrete is reached. In the case of anchors that exhibit poor performance in cracks, the onset of splitting cracks generally defines the ultimate load. This load corresponds to the value associated with the splitting failure mode in non-cracked concrete (see section 4.1.1.6).

#### 4.2.2 Shear

##### 4.2.2.1 Load-displacement behaviour and modes of failure

The load-displacement behaviour of anchors subjected to shear in cracked concrete depends on the direction of the load in relation to the crack trajectory. If the shear load acts perpendicular to the crack, then the load-displacement behaviour does not differ significantly from the behaviour in non-cracked concrete. If the shear load acts parallel to the crack, however, the load-displacement curves may be flattened. This is illustrated in Fig. 4.146, which represents tests resulting in steel failure.

Anchors subjected to shear fail either by rupture of the steel, pry-out failure or concrete edge breakout, depending on the edge distance and embedment depth (Fig. 4.63).

Even anchors that exhibit inferior performance when loaded in tension in cracks are usually adequate to resist shear loads in cracked concrete (Fuchs, Eligehausen (1989)).

##### 4.2.2.2 Failure load associated with steel failure

As in the case of non-cracked concrete, the ultimate shear capacity of expansion anchors or headed studs in cracks with no proximate edges and sufficient embedment depth will be governed by steel rupture. The influence of cracks

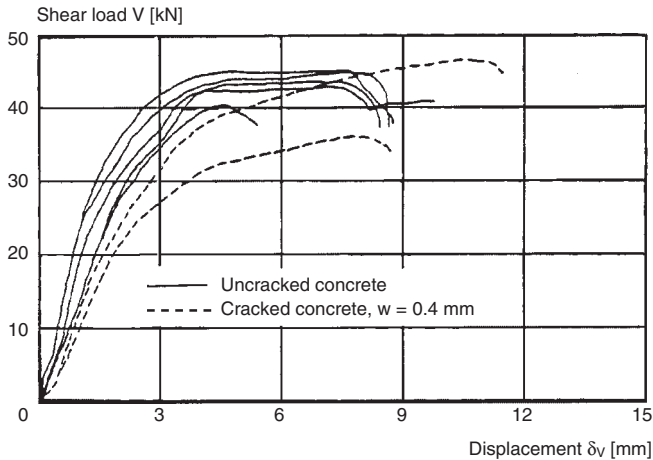


**Fig. 4.146** Load-displacement behaviour of headed studs in cracked and non-cracked concrete – shear load in direction of crack

on the failure load is relatively minor (< 10%) (*Fuchs, Eligehausen (1989)*).

#### 4.2.2.3 Failure load associated with pry-out failure

A concrete pry-out failure can occur under various conditions (compare sections 4.1.2.1c and 4.1.2.3). To date, this failure mode has not been investigated in experiments with cracked concrete. Inasmuch as the concrete breakout body on the side opposite the applied load direction resembles one half of the concrete cone generated in a tension test (compare Fig. 4.69 with Fig. 4.5), it may be conservatively assumed that the failure load associated with pry-out failure is influenced by cracks to the same degree as is the case for concrete cone breakout failure resulting from tension loads. Therefore:

$$V_{u,sp}(\text{cracked concrete}) = \psi_w \cdot V_{u,sp}(\text{uncracked concrete}) \quad (4.47)$$

where:

$\psi_w \approx 0.75$  for bearing-type anchors (e.g. headed studs and undercut anchors)

$\psi_w \approx 0.68$  for torque-controlled expansion anchors that exhibit good behaviour in cracked concrete

$V_{u,sp}(\text{uncracked concrete})$  may be evaluated as per equation (4.24)

#### 4.2.2.4 Failure load associated with concrete edge breakout

Concrete edge failure occurs with anchorages near the edge of a member and loaded with a shear component acting towards the free edge. Fig. 4.147 shows the reduction in the failure loads associated with anchors in cracks, relative to their capacity in non-cracked concrete, as a function of the crack width. The tests in cracked and non-cracked concrete were performed on test specimens produced with the same concrete mix. For comparison purposes, the mean curve valid for headed studs and undercut anchors subjected to concentric tension is also shown. The failure loads for anchors in cracks with crack widths  $\Delta w > 0.4$  mm are approx. 25% lower than the values measured in non-cracked concrete. This reduction was also established in *Vintzeleou, Eligehausen (1991)*. Consequently, the reduction in the concrete edge failure load is of the same order of magnitude as that of the concrete cone failure load associated with concentric tension in cracked concrete.

Less of a reduction is to be expected when edge reinforcement is present to restrain the concrete breakout. According to tests carried out by *Fuchs, Eligehausen (1989)*, the increase in shear capacity associated with the inclusion of straight edge reinforcement with 12 mm diameter bars, which were not enclosed by stirrups,

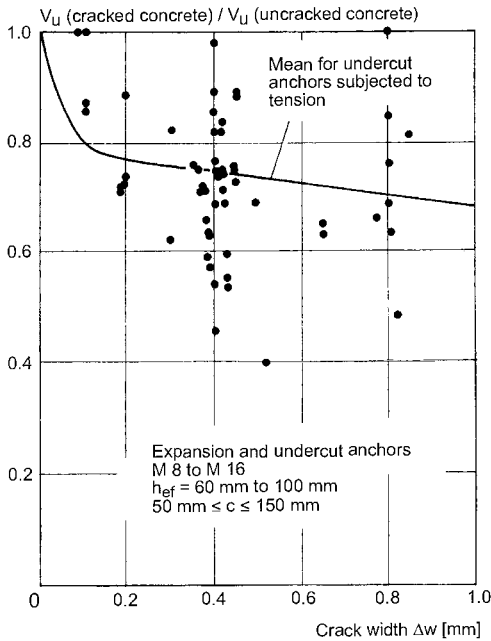


**Fig. 4.147** Influence of crack width on the concrete edge failure load of expansion and undercut anchors subjected to shear loads towards the edge (after Fuchs, Eligehausen (1989))

can be as much as 15 to 20% for small edge distances. These tests were conducted with torque-controlled expansion, undercut and bonded anchors, however, the results also apply to headed studs.

**4.2.3 Combined tension and shear**

**4.2.3.1 Load-displacement behaviour and modes of failure**

The load-bearing behaviour of torque- and displacement-controlled expansion anchors as well as undercut anchors when subjected to combined tension and shear loads in cracked concrete ( $\Delta w \approx 0.4$  mm) was investigated by Dieterle, Bozenhardt, Hirth, Opitz (1990). The angle of application of the load was varied systematically from  $\alpha = 0^\circ$  (tension load) to  $\alpha = 90^\circ$  (shear load), but was kept constant during loading.

The load-displacement behaviour observed in cracked concrete for anchors demonstrating good performance in cracks was generally comparable with that observed in non-cracked con-

crete. The same failure modes were observed in cracked concrete as in non-cracked concrete (section 4.1.3.1). The load-displacement behaviour associated with anchors that are unsuitable to transfer tension loads in cracked concrete is unpredictable in the case of oblique loading where the primary component is tension.

**4.2.3.2 Failure load**

Fig. 4.148 shows failure loads for M10 sleeve-type torque-controlled expansion anchors suitable for use in cracked concrete that were installed in cracks of width  $\Delta w \approx 0.4$  mm and subjected to oblique loading. The results for M10 undercut anchors are shown in Fig. 4.149. The interaction equations (4.42) and (4.43), with  $k = 1.5$ , are plotted in the two figures as well, using the average measured failure loads in tension and shear for  $N_u$  and  $V_u$  in equations (4.42) and (4.43). The tests were carried out in tension test members with a concrete cube compressive strength  $f_{cc,200} = 37$  N/mm<sup>2</sup>. Failure was characterised by concrete cone breakout (when the load was primarily tension) or steel rupture. The results indicate that the failure loads in cracked concrete of anchors exhibiting good

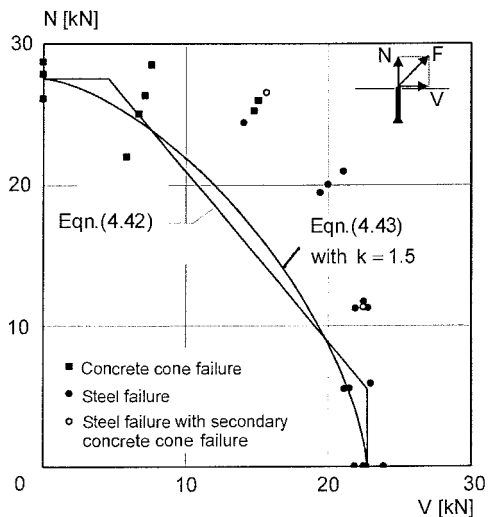


**Fig. 4.148** Interaction diagram for M10 torque-controlled expansion anchors (sleeve type) exhibiting good follow-up expansion in cracked concrete ( $\Delta w = 0.4$  mm,  $f_c \approx 31$  N/mm<sup>2</sup>) (after Dieterle, Bozenhardt, Hirth, Opitz (1990))

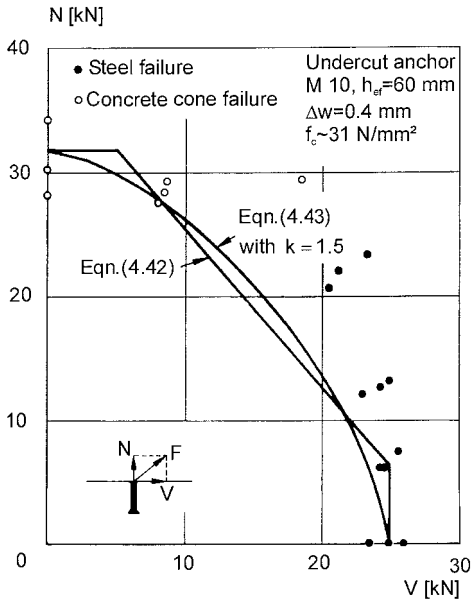


**Fig. 4.149** Interaction diagram for M10 undercut anchors in cracked concrete (after Dieterle, Bozenhardt, Hirth, Opitz (1990))

performance in cracks can be described by the same interaction equations as those used for non-cracked concrete. This would also apply to headed studs and other bearing anchors.

Expansion anchors that do not function correctly in cracked concrete when subjected to tension, e.g. experience pull-out at greatly reduced load, exhibit a different type of behaviour under oblique loading (Fig. 4.150). In this case the scatter associated with the measured failure loads for primarily tension loading is quite large. Consequently, the interaction equations (4.42) and (4.43) are inappropriate for predicting the capacity of such anchors subjected to oblique loading.

**4.2.4 Sustained loads**

In principal, post-installed anchors or headed studs positioned in cracks of a constant width respond to sustained loads in a manner comparable to their behaviour in non-cracked concrete (see section 4.1.5). In the absence of a failure during the sustained load, long-term loading does not have any significant influence on the mode of failure, the peak load and the displacement at peak load as measured in a subsequent test to failure.

In practice, however, the width of a crack is not usually constant because the loading on the member in which the anchor is located – as viewed over longer periods of time – varies. If anchors are positioned in cracks and subjected

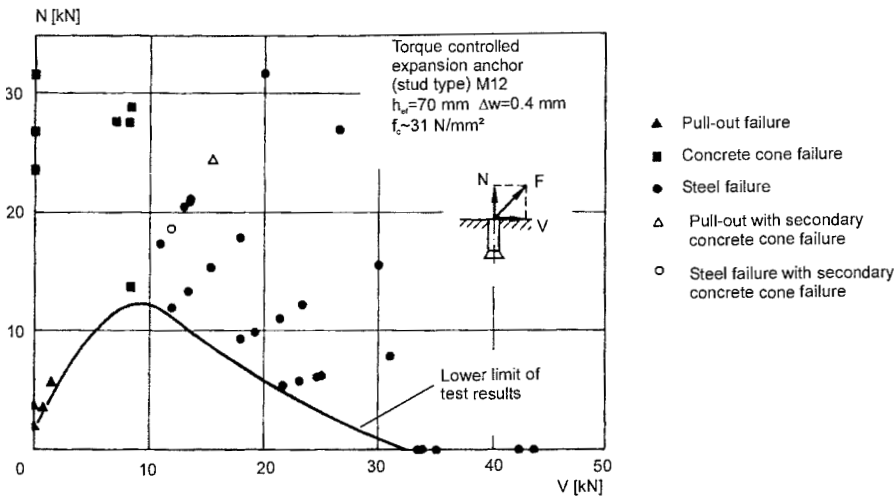


**Fig. 4.150** Interaction diagram for M12 torque-controlled expansion anchors (stud-type) exhibiting poor follow-up expansion in cracked concrete (after Dieterle, Bozenhardt, Hirth, Opitz (1990))



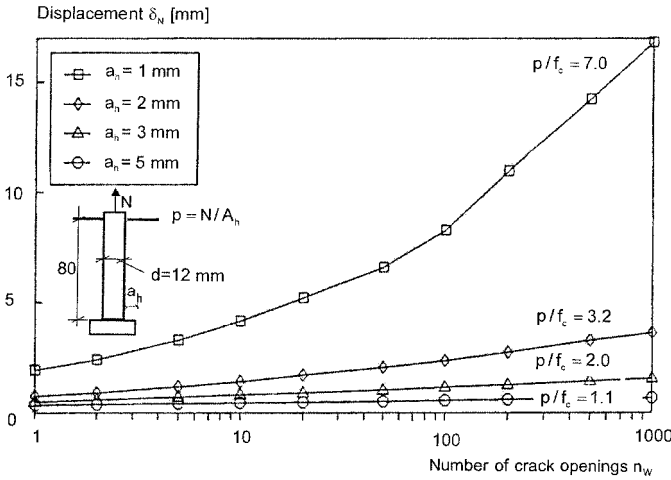


**Fig. 4.151** Displacements of headed studs subjected to a static tension load as a function of the number of crack cycles ( $N = 7.8$  kN,  $f_c \approx 27$  N/mm<sup>2</sup>, crack width cycled between  $w \approx 0.3$  mm and  $w \approx 0.1$  mm) (Furche (1994))

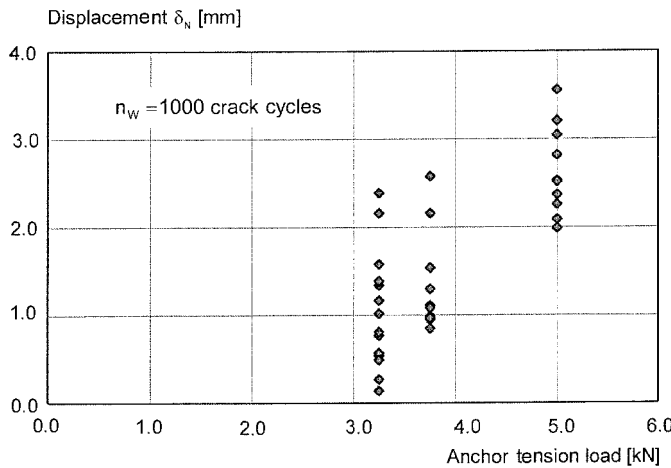


**Fig. 4.152** Displacements of M10 stud-type torque-controlled expansion anchors exhibiting good follow-up expansion after 1000 crack cycles between  $w \approx 0.3$  mm and  $w \approx 0.1$  mm as a function of the static tension load

to a constant tension load, anchor displacement increases due to the fluctuating crack width over time. The magnitude of this increase in the displacement mainly depends on the anchor system, the range of crack width fluctuation, the magnitude of the tension load and the number of crack width cycles. In the case of headed studs and undercut anchors subjected to a constant tension load, the size of the undercut or the magnitude of the concrete pressure in the load transfer zone also play a significant role (Furche (1994)) (Fig. 4.151). The increase in the displacement of torque-controlled expansion anchors that are suitable for applications in cracked concrete is also dependent on the magnitude of the tension load applied to the anchor,

i.e. on the concrete pressures in the expansion zone. This is shown in Fig. 4.152, which is representative of the behaviour of a wedge-type anchor. Anchors that exhibit poor performance in cracks can experience pull-out failure after only a few cycles (Rehm, Lehmann (1982), Eligehausen, Asmus (1991)). This particularly applies to groups loaded by a stiff baseplate (Cannon (1981)) because the anchors exhibit markedly different displacement behaviour and hence their share of the tension load applied to the group is very uneven. If displacements are small during the cycling of the crack width, then the failure behaviour and the failure load, as measured in a subsequent tension test, are not significantly influenced.

### 4.2.5 Fatigue loading

It is necessary to distinguish between the following cases in the context of fatigue loading:

- The member in which the anchor is located is loaded by fatigue loading and the anchor is statically loaded.
- The member in which the anchor is located is loaded statically and the anchor is subjected to fatigue loading.
- Both the member in which the anchor is located and the anchor are subjected to fatigue loading.

In case a), members subjected to repetitive loads may experience several millions of crack cycles (crack opening and closing). If the anchor is placed under constant tension, then the displacements increase as a result of the crack cycling (Fig. 4.151). If the structural member is subject primarily to static loading, no more than  $n_w = 1,000$  crack cycles, with a clear variation in crack width ( $\Delta w = w_{\max} - w_{\min} \approx 0.2$  mm), should be expected. For the case where the load is not primarily static, although well over 1,000 crack cycles may occur, the difference in crack widths is generally small, with  $< 0.2$  mm. Therefore, we can often assume that anchors whose suitability for cracked concrete has been verified, as described in section 14.2 will also exhibit satisfactory load-bearing behaviour in structural members subjected to repetitive loads (*Mesureur (1995/1)*).

In case b) the anchor is located in a crack of constant width and subjected to fatigue loading. In this case the load-bearing behaviour of the anchor is influenced in a manner similar to that described for non-cracked concrete (section 4.1.6). If a fatigue failure does not occur, repetitive loading of the anchor does not have any significant influence on the ultimate load behaviour and the peak load as measured in a subsequent test to failure (Fig. 4.153).

A particularly critical design condition exists when both the member in which the anchor is located, as well as the anchor itself, are repetitively loaded (case c). To date this case has not been investigated experimentally.

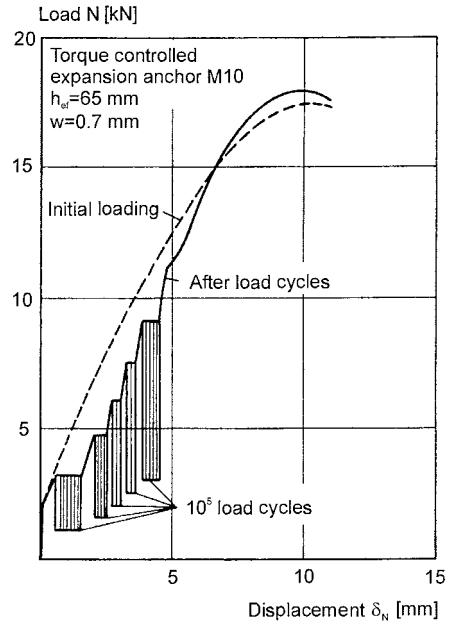


**Fig. 4.153** Influence of a cycling load on the load-displacement behaviour of a M10 torque-controlled expansion anchor subjected to concentric tension (*Rehm, Lehmann (1982)*)

When an anchorage is subjected to fatigue loading (e.g. anchors for crane rails or elevator guide rails) or is anchored in a component subjected to repetitive loads (e.g. in bridge decks or structural slabs carrying traffic), the anchor displacement will increase. If this happens, the prestressing force will be reduced. *Lotze (1993)* proposes a method for determining the residual prestressing force to be expected depending on the stiffness of the anchors. Often the prestressing force will be completely eliminated and the anchorage will be loosened. To avoid this a permanently effective prestressing force should be provided (*Storck (1990), Lotze (1993)*), e.g. by using spring elements. In Germany two torque-controlled bonded anchors and one undercut anchor are approved for use under tension and shear fatigue loading in cracked and non-cracked concrete. These anchors maintain a permanent prestressing force without spring elements because they are stiff and their strained length is sufficiently long. Furthermore an annular gap is avoided by special devices.

## 5 Behaviour of cast-in anchor channels in non-cracked and cracked concrete

This chapter addresses the behaviour of cast-in anchor channel systems. Only those anchor channel configurations shown in Fig. 2.9 are included for discussion. In this section the anchor channels are denoted by the width and height of the channel. This notation is used in Europe.

### 5.1 Non-cracked concrete

#### 5.1.1 Tension

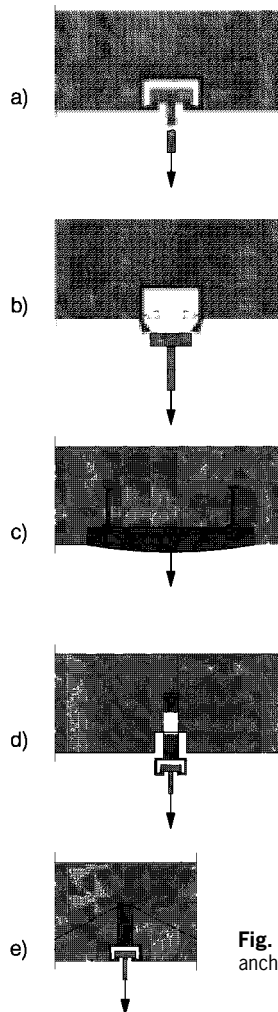
##### 5.1.1.1 Load-displacement behaviour and modes of failure

The following failure modes have been observed for anchor channels in response to tension loading:

- bolt failure (Fig. 5.1a)
- distortion of channel flanges followed by extraction of bolt (Figs. 5.1b and 5.3)
- channel bending failure (Figs. 5.1c and 5.4)
- separation of the anchor element from the back of channel (not shown)
- fracture of the anchor element (Fig. 5.1d)
- concrete breakout or splitting failure (Fig. 5.1e)

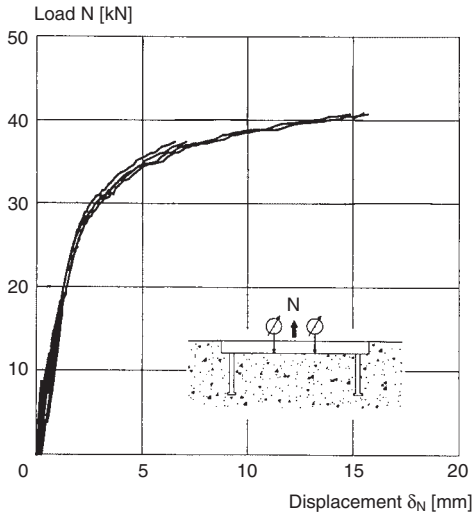
Typically, anchor channel systems currently available on the market preclude pull-out failure of the anchor element by providing a sufficiently large anchor head.

Fig. 5.2 provides load-displacement curves for short channel segments (50/30 profile[JS2]) equipped with two anchors tested in tension to failure. A concentrated load was applied midway between the anchors. Failure was characterised by flexural yielding of the channel followed by distortion of the channel flanges or rupture of the connection between anchor and channel. Fig. 5.3 illustrates one such failure whereby the channel distortion is clearly visible. Fig. 5.4 shows the large displacements associated with flexural failure of the channel.



**Fig. 5.1** Failure modes of anchor channels

A ductile behaviour is associated with such failure. In cases where failure is precipitated by concrete breakout before reaching the bending strength of the anchor channel, e.g. when the tension load is applied at or near one of the



**Fig. 5.2** Load-displacement curves of channels with two anchors; failure was caused by flexural yielding of the channel followed by distortion of the channel flanges or rupture of the connection between anchor and channel (Wohlfahrt (1996))



**Fig. 5.3** Photo of an anchor channel after test; failure by distortion of anchor flanges (Wohlfahrt (1996))

anchors, the load-displacement behaviour is very similar to that of tension-loaded headed studs (cf. Fig. 4.3b). Failure in such cases is relatively sudden (non-ductile).

#### 5.1.1.2 Failure load associated with steel failure

The ultimate load associated with tension failure of the steel bolt or anchor may be determined with equation (4.1). The failure load corresponding to rupture of the weld between the

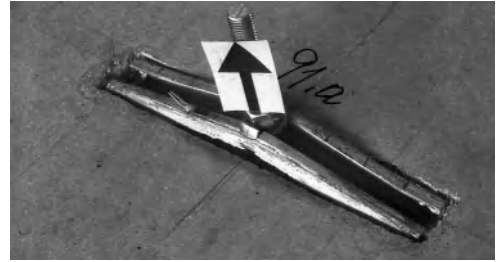


**Fig. 5.4** Photo of an anchor channel after test; failure by bending of channel and distortion of anchor flanges (Forschungs- und Materialprüfungsanstalt Baden-Württemberg (1995/1))

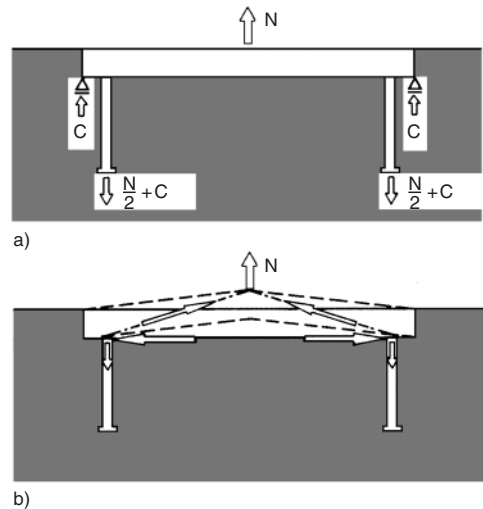


**Fig. 5.5** Behaviour of anchor channels loaded in bending (schematic) (Wohlfahrt (1996))

anchor and the channel web may be assessed using ordinary structural steel design principles. In contrast, the ultimate load associated with distortion of the channel flanges is quite difficult to establish without testing. The flanges are to some degree supported by the surrounding concrete and therefore exhibit a different load-bearing behaviour compared to a free-standing channel. Similarly, the failure load corresponding to separation of an anchor element that is swaged onto or pressed into the back of the channel can only be determined through testing.

An extensive treatment of the flexural load-bearing behaviour of anchor channels may be found in Wohlfahrt (1996). Consider a short

segment of anchor channel with two anchors loaded midway between the two anchors. The load is transferred to the anchors via channel flexure. Compression developed at the toe of the channel where it projects beyond the anchor provides some degree of fixity (Fig. 5.5a). This fixity decreases as the load increases owing to displacement of the anchor. When the yield moment of the channel is reached, a plastic hinge forms in the centre of the span. Subsequent loading is resisted via cable tension in the channel segments balanced by shear and tension forces in the anchors (Fig. 5.5b). The ultimate load associated with this condition can be approximated with equation (5.1) (Wohlfahrt (1996)):

$$N_{u,s} = k_2 \cdot M_{u,s} / l \quad (5.1)$$

where:

$M_{u,s}$  = yield moment of anchor channel

$$= W_{pl} \cdot f_{yk}$$

$W_{pl}$  = plastic section modulus of the channel

$l$  = anchor spacing

$k_2$  = 8 for profiles  $\leq 38/17$

= 6 for profiles  $\geq 40/22$

In small profiles, at ultimate most of the load is carried via this cable mechanism. This is taken into account in the analysis by assuming full fixity. Tests on larger profiles show that exces-

sive distortion of the channel flanges limits the capacity of the system, and thus the cable mechanism plays a smaller role in resisting the load. This is accounted for with an assumption of 50% restraint at the supports.

### 5.1.1.3 Failure load associated with concrete cone breakout

If the anchors are short, or if they are closely spaced or positioned near a free edge, a cone-shaped concrete breakout may limit the tension capacity of the anchor. For this type of failure the load-bearing behaviour of channels with two anchors or of channels with more than two anchors and equal load on each anchor mimics that of headed studs. According to Wohlfahrt (1996) the failure load can be determined using the CC-Method as it applies to headed studs (see section 4.1.1.3). However according to Kraus (2003) some modifications to the CC-Method are necessary.

The presence of the channel profile in the breakout cone may influence the load-carrying capacity depending on the ratio of the height of the channel to embedment depth. This can be seen from Fig. 5.6 which is based on numerical calculations. For anchor channels used in Europe this influence on the average concrete

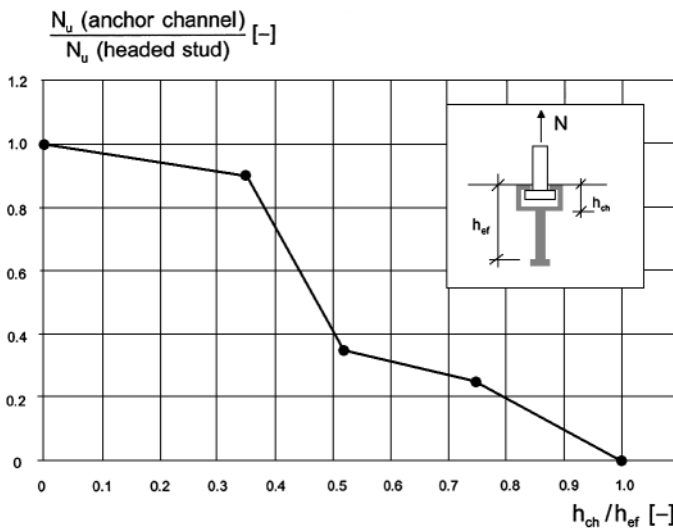


**Fig. 5.6** Concrete cone failure load of an anchor channel related to value valid for a headed stud as a function of the ratio of the height of channel to embedment depth; results of numerical analysis (Kraus (2003))

cone failure load of a single anchor may be considered in accordance with equation (5.2) (Kraus (2003)).

$$N_{u,c}^0 = 15.5 \cdot h_{ef}^{1.5} \cdot f_{cc,200}^{0.5} \cdot \alpha_{ch,N} \quad (5.2)$$

where:

$$\alpha_{ch,N} = (h_{ef} / 180)^{0.15} \leq 1 \quad (5.2a)$$

According to equation (5.2) the concrete cone failure load of a single anchor without edge and spacing effects varies between 80% (small channels with  $h_{ef} = 40$  mm) and 100% (large channels with  $h_{ef} > 180$  mm) of the capacity of one headed stud.

According to analytical and experimental studies, a channel with two anchors that receives a concentrated tension load applied just directly over one of the anchors will not exhibit any significant redistribution of load to the unloaded anchor up to ultimate (Wohlfahrt (1996)). This is shown in Fig. 5.7, in which the failure loads of channel segments equipped with two anchors and loaded directly over one anchor are plotted as a function of the anchor embedment depth. The curve represents the calculated concrete cone breakout load for a single anchor according to equation (5.2). The measured failure loads correlate rather well with the prediction.

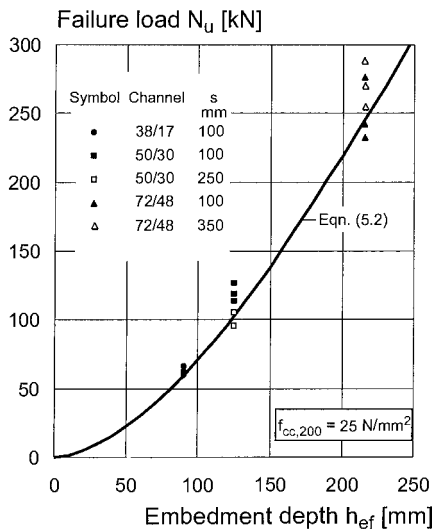


Fig. 5.7 Concrete cone failure load of channels with two anchors and loaded directly above one anchor as a function of embedment depth (Wohlfahrt (1996))

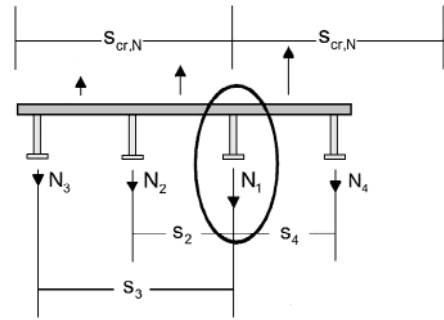


Fig. 5.8 Example of an anchor channel with different tension loads on each anchor (Kraus (2003))

Channels with more than two anchors and loaded in the span behave like continuous beams on springs, whereby the stiffness of the springs corresponds to the load-displacement curve of the anchor. The anchors carry different loads and the CC-Method does not apply.

Kraus (2003) proposes a method to calculate the forces on the anchors (see section 3.7.3) and the resistance of one anchor of such an application (Fig. 5.8). The concrete cone capacity of the anchor in question is influenced by the distance of and the load on neighbouring anchors. This is taken into account by multiplying the basic concrete cone capacity  $N_{u,c}^0$  with the factor  $\alpha_{s,N}$ .

$$N_{u,c} = \alpha_{s,N} \cdot N_{u,c}^0 \quad (5.3)$$

where:

$$\alpha_{s,N} = \frac{1}{1 + \sum_2^i (1 - s_i / s_{cr,N})^{1.5} \cdot N_i / N_1} \quad (5.3a)$$

$$s_{cr,N} = 2 \cdot c_{cr,N} = (5.6 - 2.6 \cdot h_{ef} / 180) \cdot h_{ef} \geq 3 \cdot h_{ef} \quad (5.3b)$$

- $N_i$  tension force of a neighbouring anchor
- $N_1$  tension force of the anchor which resistance is determined
- $N_{u,c}^0$  according to equation (5.2)

According to Kraus (2003) the characteristic spacing depends on the embedment depth. It varies linearly between  $s_{cr,N} = 5 \cdot h_{ef}$  ( $h_{ef} = 40$  mm) and  $s_{cr,N} = 3 \cdot h_{ef}$  ( $h_{ef} > 180$  mm).

For the example shown in Fig. 5.8 the factor  $\alpha_{s,N}$  amounts to:

$$\alpha_{s,N} = \frac{1}{1 + (1 - s_2 / s_{cr,N})^{1.5} \cdot N_2 / N_1 + (1 - s_3 / s_{cr,N})^{1.5} \cdot N_3 / N_1 + (1 - s_4 / s_{cr,N})^{1.5} \cdot N_4 / N_1}$$

The factor  $\alpha_{s,N}$  replaces the ratio  $A_{c,N} / A_{c,N}^0$  and the factor  $\psi_{ec,N}$  in equation (4.9). For channels with two anchors the factor  $\alpha_{s,N}$  and the product  $(A_{c,N} / A_{c,N}^0) \cdot \psi_{ec,N}$  give practically the same results.

Equation (5.3) is valid for anchor channels with an edge distance  $c \geq c_{cr,N}$  in all directions. For applications  $c < c_{cr,N}$ , e. g. close to an edge or in a corner, equation (5.4) is proposed based on Kraus (2003).

$$N_{u,c} = N_{u,c}^0 \cdot \alpha_{s,N} \cdot \alpha_{e,N} \cdot \alpha_{c,N} \cdot \psi_{re,N} \quad (5.4)$$

where:

$N_{u,c}$  = average failure load of one anchor of an anchor channel

$$\alpha_{e,N} = \left( \frac{c}{c_{cr,N}} \right)^{0.5} \leq 1.0 \quad (5.4a)$$

$c$  = edge distance of the channel (Fig. 5.9a)

$$\alpha_{c,N} = \left( \frac{c_2}{c_{cr,N}} \right)^{0.5} \leq 1.0 \quad (5.4b)$$

$c_2$  = corner distance of the anchor for which the resistance is calculated (Fig. 5.10a, b)

$N_{u,c}^0$ ,  $\alpha_{s,N}$  according to equation (5.3)

$\psi_{re,N}$  according to equation (4.10a, b)

With anchor channels located parallel to an edge (Fig. 5.9a) a crack below the channel in the longitudinal direction occurs during loading (Kraus (2003)). Due to this crack the activated

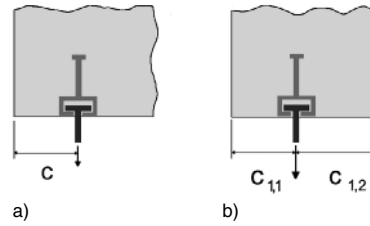


Fig. 5.9 Anchor channel bar at an edge (a) or in a narrow member (b)

concrete area on the opposing side of the edge is limited to the edge distance  $c$  (Fig. 5.11). In contrast to that for headed studs, the characteristic edge distance  $c_{cr,N}$  may be taken (Fig. 4.26). With channel bars in a narrow concrete member with different edge distances  $c_{1,1}$  and  $c_{1,2}$  (Fig. 5.9b) the lower value of  $c_{1,1}$  and  $c_{1,2}$  should be inserted in equation (5.4a).

The influence of a corner is taken into account by the factor  $\alpha_{c,N}$ . If a channel bar is influenced by two corners (Fig. 5.10c) the minimum value of  $c_{2,1}$  and  $c_{2,2}$  should be inserted in equation (5.4b).

Fig. 5.12 shows the failure loads measured in tests with anchor channels (profile 50/30,  $h_{ef} = 85$  mm,  $s = 300$  mm) at an edge as a function of the related edge distance normalised to a concrete strength  $f_c = 20$  N/mm<sup>2</sup>. For comparison the values calculated according to equation (5.4) are plotted as well. Fig. 5.13 shows the failure loads measured in tests with different

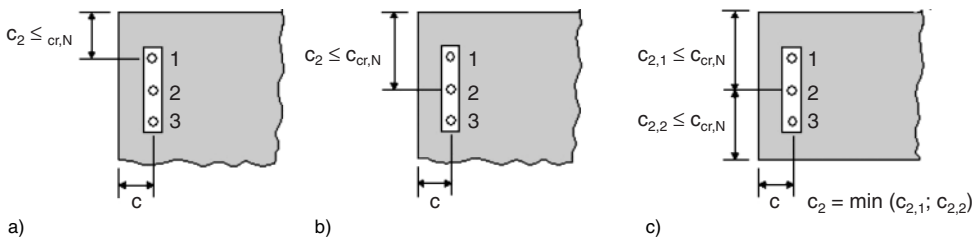
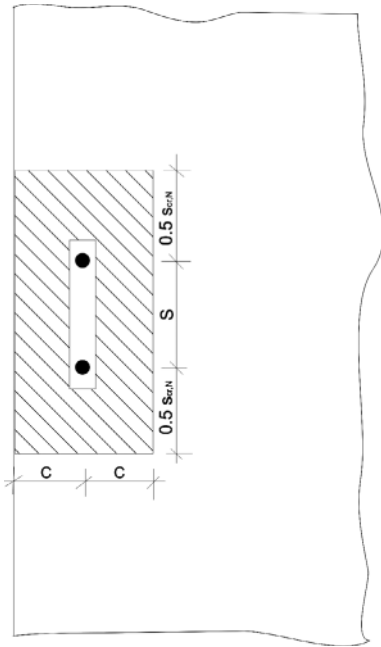


Fig. 5.10 Anchor channel in a corner (a, b) or in a narrow member (c)  
 a) Corner distance if resistance of anchor 1 is calculated  
 b) Corner distance if resistance of anchor 2 is calculated  
 c) Corner distances if resistance of anchor 2 is calculated





**Fig. 5.11** Activated concrete area of anchor channels close to an edge (Kraus (2003))

anchor channels as a function of the calculated values. Both figures show a good agreement between test results and predictions.

The tension load-bearing behaviour of anchor channels is improved by anchor reinforcement specially designed for that purpose (Eligehausen (1995/1)). The reinforcement may be designed according to the procedure developed for headed studs (section 4.1.1.3h). This can be seen from Fig. 5.14 which shows the ratio of measured and calculated failure load as a function of the embedment depth for tests with anchor channels and headed studs.

**5.1.1.4 Failure load associated with local concrete side blow-out failure**

The equations for calculating the failure load for a local concrete blow-out failure as given in section 4.1.1.4 for headed studs may also be applied to anchor channel. Minimum edge distances should be specified to prevent local concrete blow-out failures. These limits should be evaluated from the results of tests.

**5.1.1.5 Failure load associated with pull-out failure**

The discussion provided in section 4.1.1.5 regarding pull-out as it pertains to headed studs generally applies to the anchor channel situation as well. Typically, however, the bearing contact area (head diameter) of the anchors of anchor channels is sufficiently large to preclude pull-out failure.

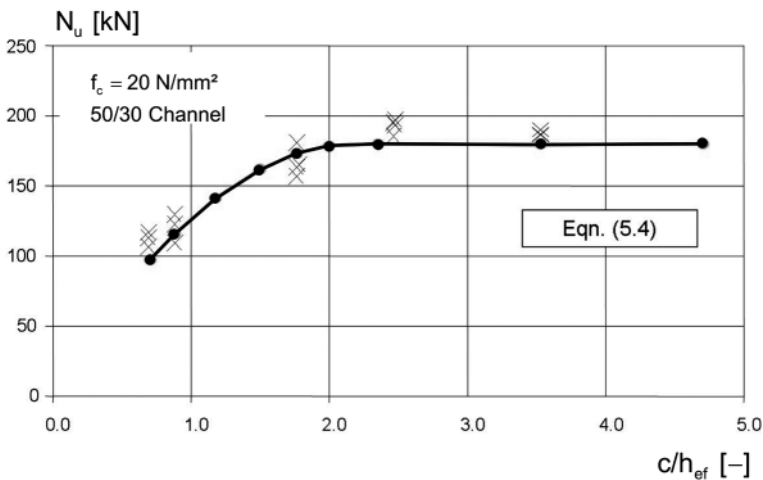


**Fig. 5.12** Failure load of anchor channels (profile 50/30,  $h_{ef} = 85$  mm,  $s = 300$  mm) normalised to  $f_c = 20$  N/mm<sup>2</sup> as a function of the related edge distance (Kraus (2003))

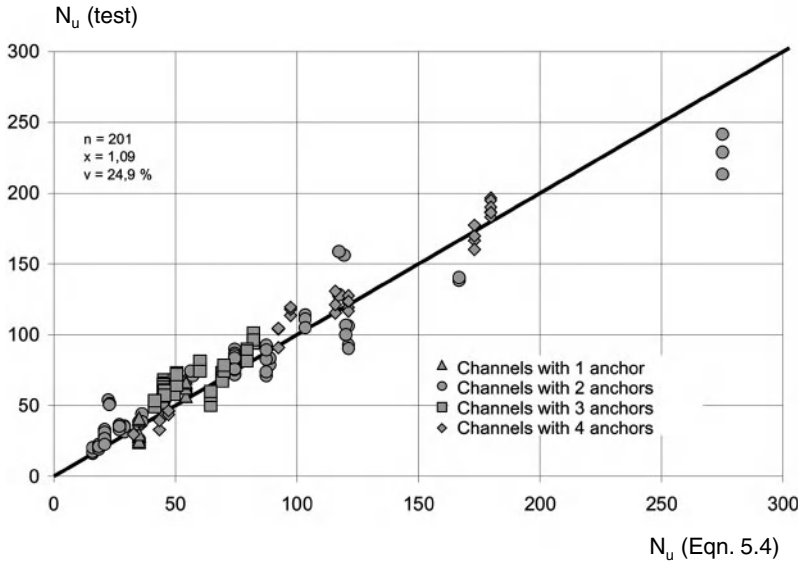


Fig. 5.13 Measured failure loads of anchor channels as a function of calculated values (Kraus (2003))

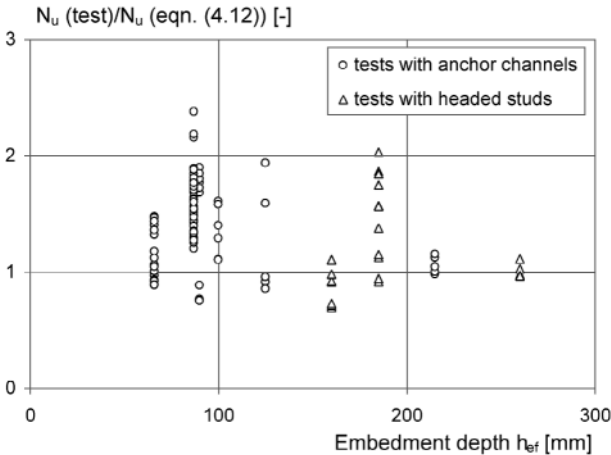


Fig. 5.14 Measured to calculated failure loads as a function of embedment depth. Tests with anchor channels and headed studs with hanger reinforcement in the form of stirrups or loops (Sippel, Eligehausen (2003))

**5.1.1.6 Failure load associated with splitting of the concrete**

The discussion provided in section 4.1.1.6 regarding splitting as it pertains to headed studs generally applies to anchor channels as well. It should be noted, however, that if the channel is cast flush with the surface of the concrete, tightening the T-head bolt will not induce compression in the concrete since the fixture is tightened

directly against the channel flanges. However, if the surface of the concrete is uneven and/or the channel is recessed due to installation inaccuracies, tightening the bolts will induce splitting forces in the concrete as the fixture is clamped against the concrete surface. As with side blow-out, minimum edge distances are required to prevent splitting of the concrete due to torquing of the bolts.

## 5.1.2 Shear

### 5.1.2.1 Load-displacement behaviour and modes of failure

As a rule, shear loads should be restricted to those occurring *perpendicular* to the anchor channel longitudinal axis. The transfer of shear loads *along* the length of the channel may be accommodated when using specially designed systems with serrated edges (Fig. 2.12) that provide for interlock of the T-headed bolt and the channel flange.

The following failure modes have been observed for anchor channels in response to shear loading:

- bolt failure
- distortion of channel flanges followed by bolt extraction
- concrete edge breakout failure
- pry-out failure

Failures resulting from bolt rupture and from channel flange distortion are typically associated with large displacements and ductile behaviour. Concrete edge breakout and pry-out are brittle failure modes, and displacements at failure depend mainly on edge distance (concrete edge breakout) or embedment depth (pry-out failure).

### 5.1.2.2 Failure load associated with steel failure

The ultimate load associated with shear failure of the steel bolt or anchor may be determined with equation (4.17). The shear failure load associated with channel flange distortion and subsequent bolt extraction must be established through testing. It is typically equal to or greater than the tension capacity associated with this failure mode.

### 5.1.2.3 Failure load associated with pry-out failure

The equations given in section 4.1.2.3 for calculating the failure load associated with pry-out failure also apply to anchor channels (*Eligehausen* (1995/1)). The modifications regarding tension loading (see section 5.1.1.3) should be taken into account.

### 5.1.2.4 Failure load associated with concrete edge failure

The behaviour of anchor channels loaded towards the free edge is discussed in detail in *Wohlfahrt* (1996) and *Eligehausen, Potthoff, Grewin, Lotze* (2004), based on numerical and experimental investigations.

According to *Wohlfahrt* (1996) the shear load is initially transferred into the concrete via the channel and the anchors. Owing to the edge distance from the front face of the channel closer to the edge, which is smaller than the edge distance of the anchor, a local concrete failure starting at the front edge of the channel frequently occurs before the ultimate load is reached. Thereafter, the entire load is transferred to the concrete via the anchors. The ultimate load for a channel with *one* anchor can then be determined using equation (4.25) (for headed studs), whereby the diameter of the anchor is used for  $d_{nom}$ . However, early separation of the back face of the channel from the concrete leads to a disruption in the concrete stress state.

As a consequence, the concrete between the anchors of a channel with multiple anchors experiences higher stresses than would be the case for headed studs installed at the same spacing. Thus the spacing  $s_{cr,V}$  required to achieve the maximum capacity of the concrete (two times the capacity of a single anchor for channels equipped with two anchors) is substantially greater than the value assumed for headed studs. *Wohlfahrt* (1996) proposes  $s_{cr,V} = 5 \cdot c_1$ . Fig. 5.15 shows the fracture pattern of an



**Fig. 5.15** Photo of an anchor channel after test; concrete edge failure. Spacing of anchors equal to 5 times the edge distance (*Forschungs- und Materialprüfungsanstalt Baden-Württemberg* (1995/2))

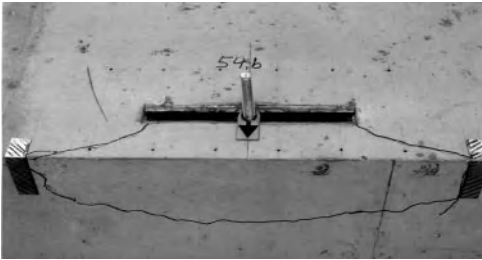


**Fig. 5.16** Photo of an anchor channel after test; concrete edge failure. Shear load applied between anchors (Forschungs- und Materialprüfungsanstalt Baden-Württemberg (1995/2))

anchor channel with an anchor spacing corresponding to five times the edge distance. The common shear cone is readily visible. Also in the case of anchor channels equipped with two anchors whereby the shear load is applied as a concentrated load in the centre between the anchors, a common breakout body occurs (Fig. 5.16). In anchor channels with two anchors where the load is applied at *one* anchor, there is no significant redistribution of the load to the other anchor. Furthermore, for the same reasons discussed above, the component thickness to guarantee the maximum concrete edge failure load must be about  $h \geq 2.5 \cdot c_1$  for anchor channels, while for headed studs  $h = 1.5 \cdot c_1$  is sufficient.

Based on these studies, Wohlfahrt (1996) proposes to determine the concrete edge failure load of a channel – analogous to equation (4.33) – as follows:

$$V_{u,c} = \frac{A_{c,V}}{A_{c,V}^0} \cdot \psi_{s,V} \cdot \psi_{h,V} \cdot \psi_{ec,V} \cdot V_{u,c}^0 \quad (5.5)$$

where:

$A_{c,V}^0$  = projected area of the concrete breakout failure surface for a single anchor, idealised as a half pyramid of height  $c_1$  and base dimensions  $h = 2.5 \cdot c_1$  and  $s_{cr,V} = 5 \cdot c_1$  (compare Fig. 4.77 which is valid for headed studs)

$$= 12.5 \cdot c_1^2$$

$A_{c,V}$  = projected area of the concrete breakout surface of the group of anchors – limited by overlap of individual breakout cones of adjacent anchors ( $s < 5 \cdot c_1$ ),

as well as by proximate edges of the concrete member *parallel* to the loading direction ( $c_2 < 2.5 \cdot c_1$ ) and the thickness of the member ( $h < 2.5 \cdot c_1$ ) (compare Fig. 4.79 which is valid for headed studs)

$$\psi_{s,V} = 0.7 + 0.3 \cdot c_2 / (2.5 \cdot c_1) \leq 1.0 \quad (5.5a)$$

$c_2$  = edge distance parallel to loading direction (the smaller value of  $c_2$  is to be used in equation (5.5a) for anchorages with two edges parallel to the loading direction (e.g. in a narrow component)

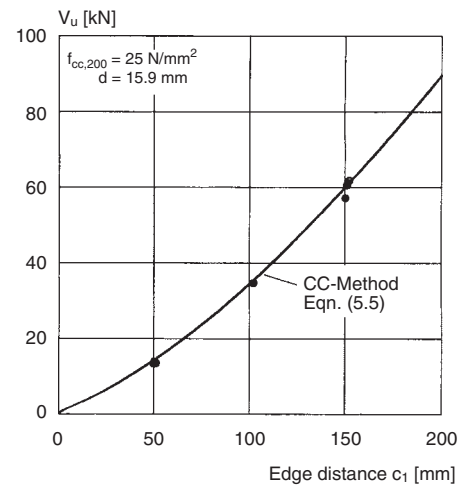
$$\psi_{h,V} = (2.5 \cdot c_1 / h)^{1/3} \geq 1.0 \quad (5.5b)$$

$$\psi_{ec,V} = \frac{1}{1 + 2 \cdot e_V / (5 \cdot c_1)} \quad (5.5c)$$

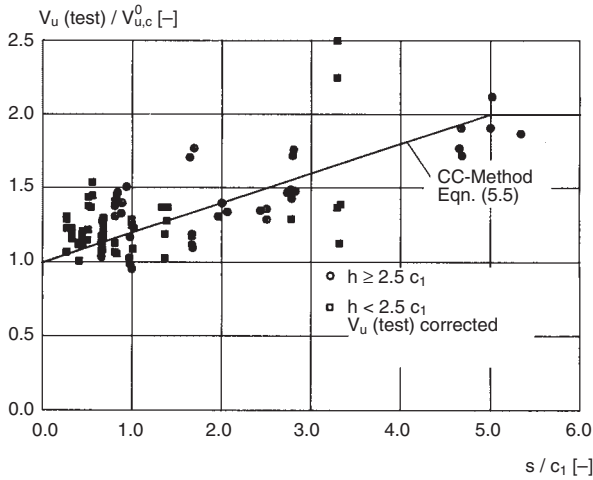
$e_V$  = eccentricity of resultant shear load of anchor related to geometrical centre of gravity of anchors loaded in shear (compare Fig. 4.88)

$V_{u,c}^0$  according to equation (4.25), with edge distance, diameter and embedment depth related to the anchor(s)

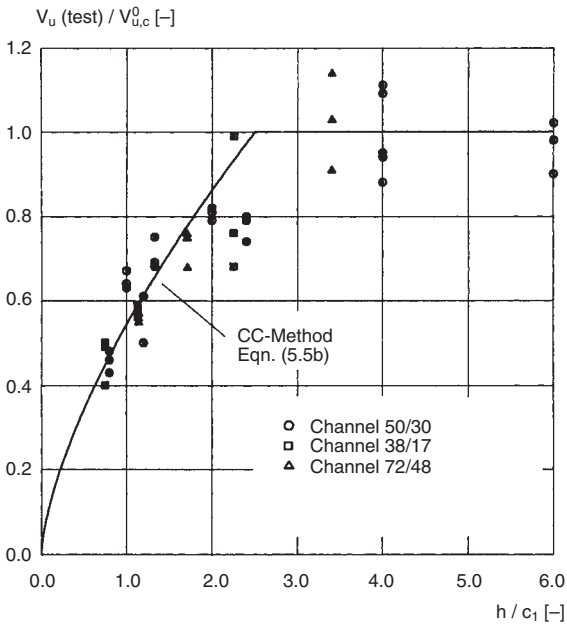
Figs. 5.17 to 5.20 illustrate comparisons between test results (Wohlfahrt (1996)) and equation (5.5). All the tests were carried out on anchor channel segments with two anchors in non-cracked concrete.



**Fig. 5.17** Concrete edge failure load of anchor channels with two anchors as a function of edge distance (Wohlfahrt (1996))



**Fig. 5.18** Influence of spacing related to edge distance on concrete edge failure load ( $V_{u,c}^0$  according to equation (4.25)) (Wohlfahrt (1996))



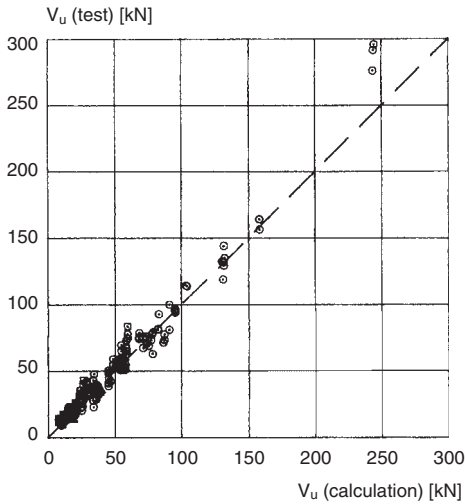
**Fig. 5.19** Influence of embedment depth related to edge distance on concrete edge failure load ( $V_{u,c}^0$  according to equation (4.25)) (Wohlfahrt (1996))

Fig. 5.17 represents failure loads of anchor channels 50/30 as a function of edge distance. The failure loads measured in tests were normalised via  $\sqrt{f_{cc,200}}$  to  $f_{cc,200} = 25 \text{ N/mm}^2$ . The diameter of the anchor is  $d = 15.9 \text{ mm}$  and the spacing  $s = 100 \text{ mm}$ .

Fig. 5.18 illustrates shear ultimate loads of channel segments related to  $V_{u,c}^0$  for a single anchor as predicted by equation (4.25) and plotted as a function of anchor spacing over anchor

edge distance. Ultimate loads from tests in which the component thickness was less than  $2.5 \cdot c_1$  have been adjusted for the influence of the component thickness with equation (5.5b).

Fig. 5.19 illustrates measured failure loads of channel segments related to  $V_{u,c}^0$  for a single anchor as predicted by equation (4.25) and plotted as a function of component thickness over edge distance.



**Fig. 5.20** Measured concrete edge failure load of anchor channels with two anchors over the values calculated in accordance with equation (5.5) (Wohlfahrt (1996))

Fig. 5.20 shows the measured failure loads as a function of the value calculated according to equation (5.5). The diagonal line represents an optimum correlation between analysis and test results. Figs 5.17 to 5.20 confirm the good correlation between predicted and measured failure loads. For  $n = 108$  tests the mean ratio of calculated to measured failure loads is 1.0 with a coefficient of variation  $v = 13\%$ . This is valid for anchor channels equipped with two anchors.

However, further research by *Eligehausen, Potthoff, Grewin, Lotze* (2004) show that equation (5.5) predicts failure loads that are rather conservative for an anchor channel equipped with more than two anchors, especially if the anchor channel is located in a deep member and provided with a large edge distance. Furthermore, the influence of arbitrary loading on channels with more than two anchors can not be taken into account by equation (5.5). Therefore *Eligehausen, Potthoff, Grewin, Lotze* (2004) propose a modified model which is analogous to the model by *Kraus* (2003) for tension loading (compare section 5.1.1.3).

In contrast to *Wohlfahrt* (1996), *Eligehausen, Potthoff, Grewin, Lotze* (2004) show that also at failure the shear load is transferred mainly by the channel and only to a smaller extend by the

anchors into the concrete. However, due to the eccentricity between the applied shear load and the resultant of the shear resistance in the concrete, the anchors are highly stressed in tension. The ultimate load of a channel segment with one anchor depends on the size of the channel and anchor and is given by:

$$V_{uc}^0 = \alpha_p \cdot c_1^{1.5} \cdot \sqrt{f_{cc}} \quad (5.6)$$

where:

$$\begin{aligned} \alpha_p &= \text{channel factor depending on dimensions} \\ &\quad \text{of profile and anchor} \\ &= 5 \text{ for channels } \leq 38/17 \\ &= 6 \text{ for channels } 50/30 \\ &= 7 \text{ for channels } 72/48 \end{aligned}$$

The above given numerical values for the factor  $\alpha_p$  are valid for anchor channels with thickness of the flanges and with anchor diameters as used in Germany.

The model by *Eligehausen, Potthoff, Grewin, Lotze* (2004) described below (equation (5.7)) for the calculation of the concrete edge capacity of anchor channels under shear loading towards the edge assumes that shear forces are transferred by bending of the channel to the anchors and from the anchors into the concrete. This approach simplifies the real behaviour. It has been chosen to allow for a simple interaction between tension and shear forces acting on the channel. Equation (5.7) gives the failure load of one anchor of an anchor channel.

$$V_{uc} = V_{uc}^0 \cdot \alpha_{s,V} \cdot \alpha_{h,V} \cdot \alpha_{c,V} \quad (5.7)$$

where:

$$\begin{aligned} V_{uc} &= \text{average failure load of one anchor of} \\ &\quad \text{an anchor channel} \\ V_{uc}^0 &= \text{according to equation (5.6)} \\ \alpha_{s,V} &= \text{factor taking into account the influence} \\ &\quad \text{of distance to and load on neighbouring} \\ &\quad \text{anchors} \end{aligned}$$

$$\alpha_{s,V} = \frac{1}{1 + \sum_{i=2}^n \left[ (1 - s_i / s_{cr,V})^{1.5} \cdot V_i / V_1 \right]} \quad (5.7a)$$

$$s_{cr,V} = 4 \cdot c_1 + 2 \cdot b_{ch} \quad (5.7b)$$

$$b_{ch} = \text{width of anchor channel}$$

$$V_i = \text{calculated shear load on neighbouring anchor } i \text{ (compare Fig. 5.21)}$$

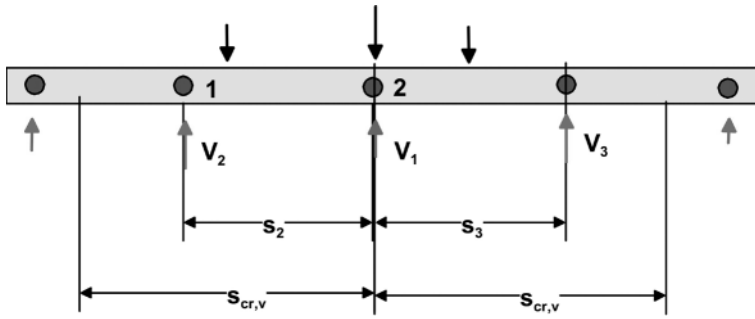


**Fig. 5.21** Example of an anchor channel with different calculated shear loads on the anchors (Eligehausen, Potthoff, Grewin, Lotze (2004))

- $V_1$  = calculated shear load on anchor 1 which resistance is determined
- $\alpha_{h,V}$  factor taking into account the influence of member thickness
- $\alpha_{h,V} = (h / h_{cr,V})^{2/3} \leq 1$  (5.7c)
- $h_{cr,V} = 2 \cdot c_1 + 2 \cdot h_{ch}$  (5.7d)
- $h_{ch}$  = height of anchor channel
- $\alpha_{c,V}$  factor taking into account the influence of a corner
- $\alpha_{c,V} = (c_2 / c_{cr,V})^{0.5} \leq 1$  (5.7e)
- $c_{cr,V} = 0.5 \cdot s_{cr,V}$  (5.7f)

The factor  $\alpha_{s,V}$  replaces the ratio  $A_{c,V} / A_{c,V}^0$  and the factor  $\psi_{ec,V}$  in equation (5.5). For channels with two anchors the factor  $\alpha_{s,V}$  and the product  $(A_{c,V} / A_{c,V}^0) \cdot \psi_{ec,V}$  give practically the same results. The factor  $\alpha_{h,V}$  gives identical results as the product  $(A_{c,V} / A_{c,V}^0) \cdot \psi_{h,V}$  in equation (5.5). The factor  $\alpha_{c,V}$  was chosen in analogy with equation (5.4).

In Figs. 5.22 to 5.27 the ratios failure loads measured in tests to values calculated according to equation (5.7) are plotted. Figs. 5.22 to 5.24

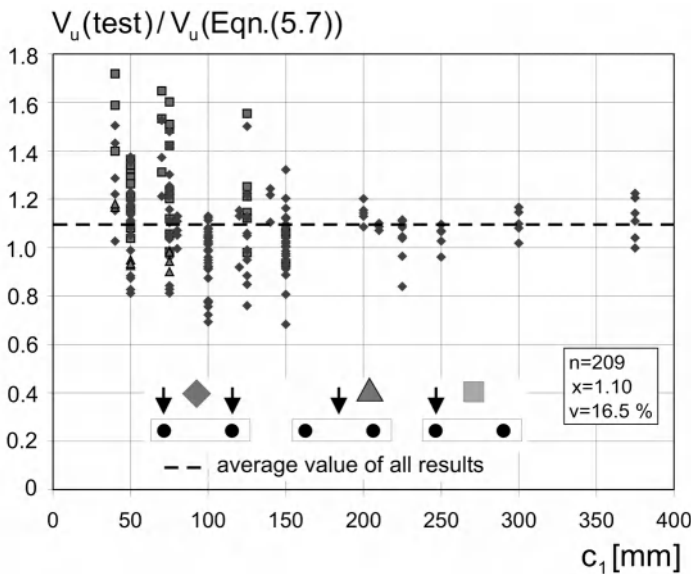


**Fig. 5.22** Ratio of the measured concrete edge failure load to the value calculated according to equation (5.7) as a function of edge distance; anchor channels with two anchors (Eligehausen, Potthoff, Grewin, Lotze (2004))



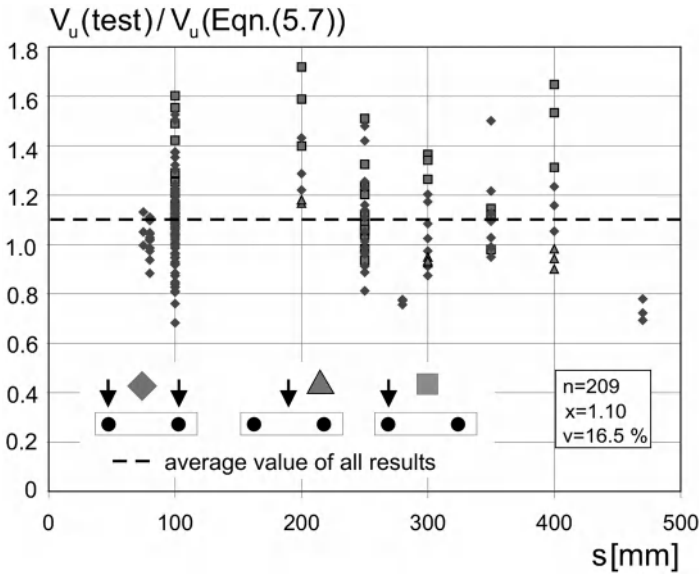


**Fig. 5.23** Ratio of the measured concrete edge failure load to the value calculated according to equation (5.7) as a function of anchor spacing; anchor channels with two anchors (Eligehausen, Potthoff, Grewin, Lotze (2004))

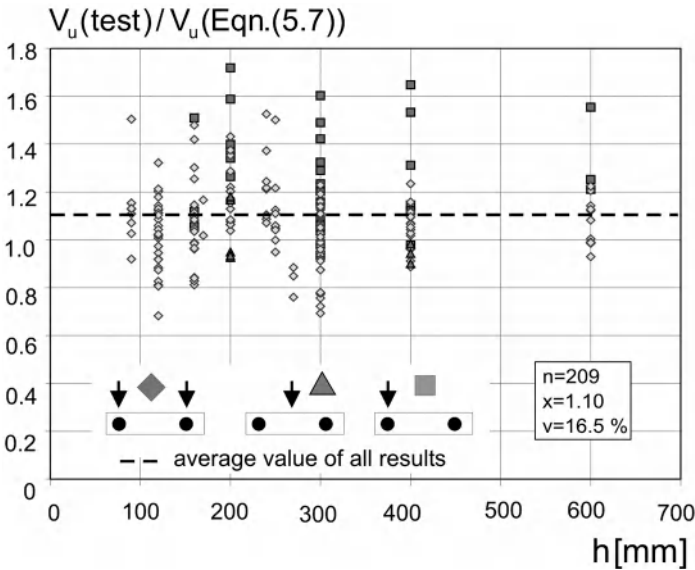


**Fig. 5.24** Ratio of the measured concrete edge failure load to the value calculated according to equation (5.7) as a function of member thickness; anchor channels with two anchors (Eligehausen, Potthoff, Grewin, Lotze (2004))

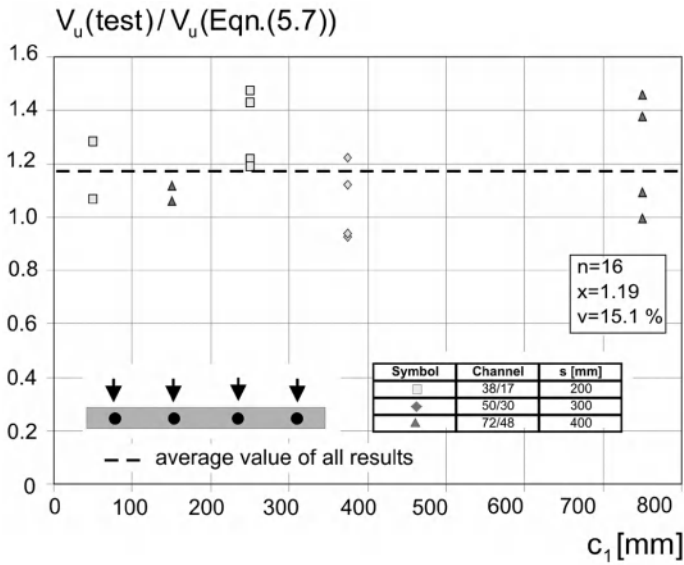


**Fig. 5.25** Ratio of the measured concrete edge failure load to the value calculated according to equation (5.7) as a function of edge distance; anchor channels with four anchors (Eligehausen, Potthoff, Grewin, Lotze (2004))

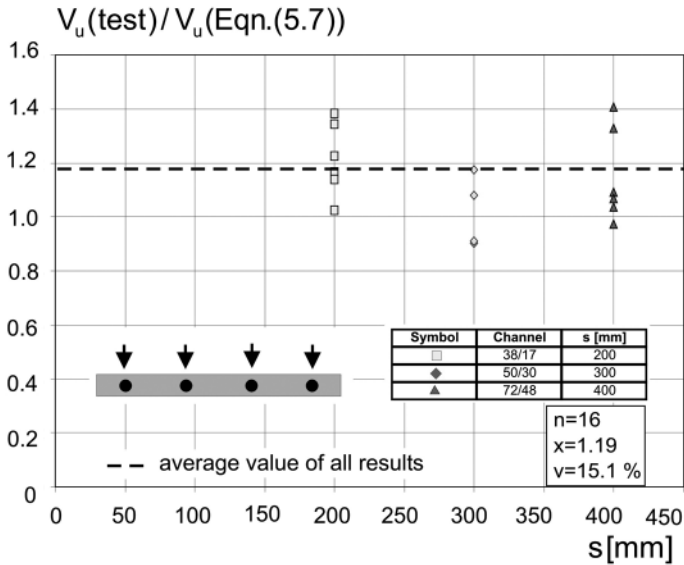


**Fig. 5.26** Ratio of the measured concrete edge failure load to the value calculated according to equation (5.7) as a function of anchor spacing; anchor channels with four anchors (Eligehausen, Potthoff, Grewin, Lotze (2004))

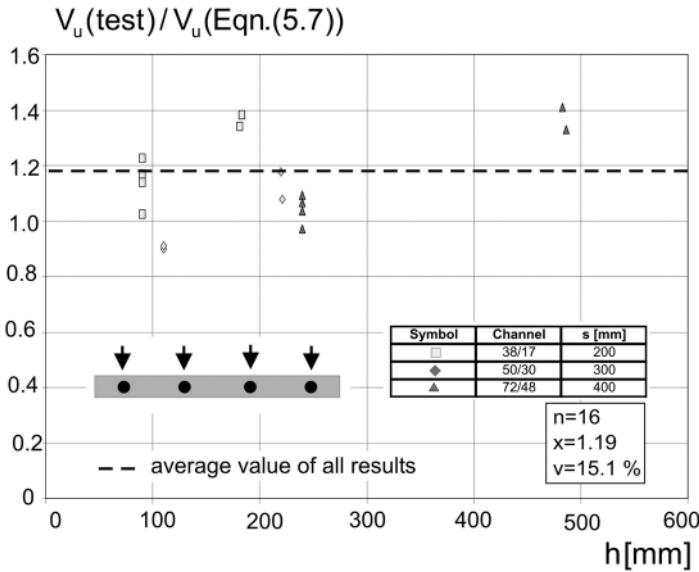


**Fig. 5.27** Ratio of the measured concrete edge failure load to the value calculated according to equation (5.7) as a function of member thickness; anchor channels with four anchors (Eligehausen, Potthoff, Grewin, Lotze (2004))

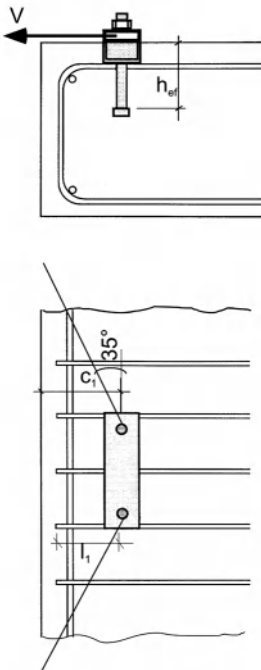


**Fig. 5.28** Anchor channel close to an edge with suitable hanger reinforcement in the form of stirrups to take up shear load

are valid for anchor channels with two anchors while Figs. 5.25 to 5.27 apply to anchor channels with four anchors. The figures show that equation (5.7) is slightly conservative but the influence of the geometric parameters edge distance, anchor spacing and component thickness is taken into account with sufficient accuracy. Further numerical studies on anchor channels with up to 25 anchors and different loads on the anchors show that equation (5.7) works sufficiently well also for these applications.

The failure load of an anchor channel located at the edge of a member and resisting a shear load towards the edge can be increased by hanger reinforcement, e. g. in the form of stirrups (Fig. 5.28). With a larger edge distance, the existing reinforcement near the surface can serve as hanger reinforcement. The shear capacity provided by the hanger reinforcement can be calculated in accordance with section 4.1.2.4h, equation (4.35) (Sippel, Eligehausen (2003)). This can be seen from Fig. 5.29 which shows the ratio of measured failure loads to calculated values as a function of the edge distance for anchor channels close to an edge with hanger reinforcement in the form of stirrups (Fig. 5.28)

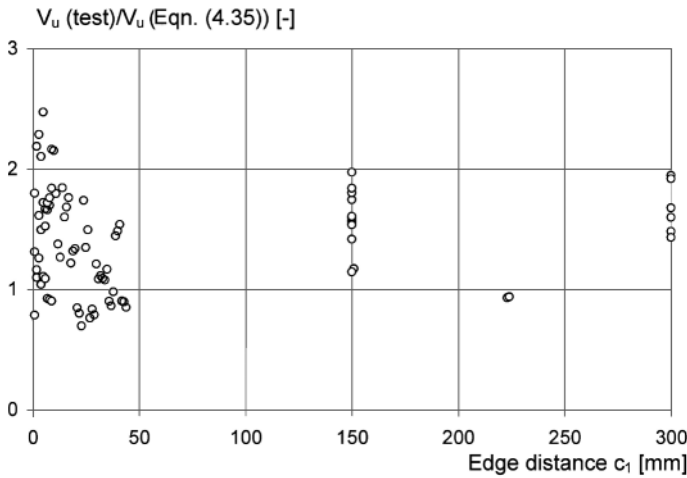


**Fig. 5.29** Measured to calculated failure loads as a function of edge distance. Tests with anchor channels with hanger reinforcement in the form of stirrups or welded wire mesh (Sippel, Elgehausen (2003))

or welded wire mesh. For small edge distances the calculated values are rather conservative. Note, however, that for close edge distances the calculated failure load is very sensitive to the position of the anchor channel with respect to the hanger reinforcement. In practice the actual

anchorage length  $l_f$  of the hanger reinforcement in the concrete breakout body may be smaller than the value assumed in the calculation due to tolerances in the position of the anchor channel or hanger reinforcement.

A hairpin that directly engages the anchors is less effective with anchor channels than when used with headed studs because the hairpin must be positioned below the channel and is therefore relatively far from the concrete surface. In addition, with the exception of T-anchors welded perpendicular to the channel axis, the connection between channel web and anchor is generally not of sufficient rigidity. Therefore equation (4.36) in section 4.1.2.4(h) may be used only with a rather low effectiveness factor ( $\eta_1 < 0.5$ ).

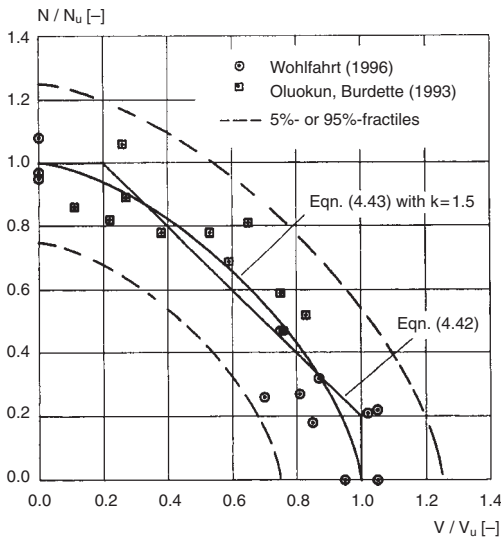


**Fig. 5.30** Interaction diagram for anchor channels without hanger reinforcement under combined tension and shear loads (Wohlfahrt 1996)

### 5.1.3 Combined tension and shear

The behaviour of anchor channels subjected to combined tension and shear loads was investigated by Oluokon, Burdette (1993) and Wohlfahrt (1996). In the tests by Oluokon, Burdette (1993), a constant shear load was imposed and an increasing tension load was applied up to failure. Wohlfahrt (1996) maintained the angle of the applied resultant force constant during the tests ( $\alpha = 30^\circ, 45^\circ, \text{ and } 60^\circ$ ). Tests with pure shear and with concentric tension were also car-

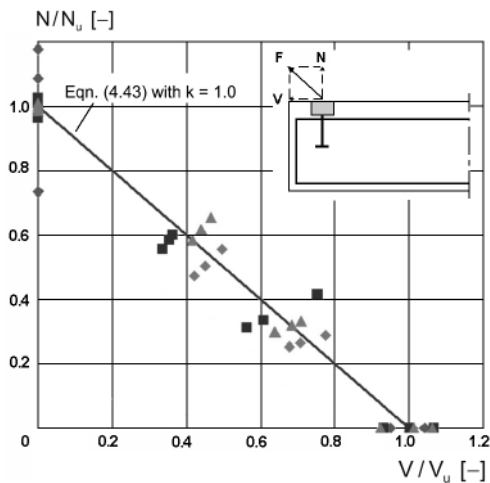


**Fig. 5.31** Interaction diagram for anchor channels close to an edge with hanger reinforcement to take up shear loads under combined tension and shear loads (Grewin, Potthoff, Eligehausen (2002))

ried out in both studies for comparison. Fig. 5.30 plots values of the tension component of the failure load related to the tension failure load as a function of the shear component of the failure load related to the shear failure load. Each symbol represents the result of one test by Wohlfahrt (1996) and the average of at least three tests by Oluokon, Burdette (1993). The figure shows that the test results can be described with sufficient accuracy by the tri-linear interaction described by equations (4.42) or by the exponential function given in equation (4.43) with  $k = 1.5$ . Tests described in Grewin, Potthoff, Eligehausen (2002) indicate that for anchor channels with a hanger reinforcement to take up the shear load and no hanger reinforcement for the tension load, a linear interaction (equation (4.43) with  $k = 1$ ) applies (Fig. 5.31).

### 5.1.4 Sustained and fatigue loading

Sustained loads lead to an increase of displacements. The discussion of this subject relating to headed studs in section 4.1.5 applies here as well.

In the case of fatigue tension loads, it is usually the connection between anchor and channel that fails first if the T-head bolt is of sufficient diameter. The fatigue strength should be established by testing for the specific geometry in question. It is dependent on the shape and method of manufacture (hot rolled, cold formed) of the channel profile, as well as the details of the connection between the anchor and the channel.

As far as the authors are aware, tests on anchor channels with fatigue shear loads have not been conducted to date. Alternating shear loads require a permanently effective prestress in order to avoid slippage of the attached fixture.

## 5.2 Cracked concrete

Cracks in the concrete have the same influence on the load-displacement behaviour of cast-in anchor channels subjected to tension and shear loading as they do on the performance of headed studs. They have only a small effect on the failure load in the case of steel failure (bolt rupture, channel failure). However, cracks affect significantly the concrete cone breakout and the pull-out capacity under tension and the concrete edge or pry-out capacity associated with shear loading. According to Wohlfahrt (1996) the cracking factor for concrete cone failure under tension as determined from a limited number of tests is  $\psi_w = 0.74$ . This corresponds to the value applicable for headed studs (see section 4.2.1.3). In the case of concrete edge breakout under shear, the cracking factor increases slightly with the edge distance. At an edge distance  $c \leq 150$  mm it is  $\psi_w \approx 0.7$ , which corresponds to the value for headed studs and expansion anchors (see section 4.2.2.4). Therefore the concrete cone capacity in tension, the pry-out failure load and the concrete edge capacity under shear towards the edge in cracked concrete should be calculated by multiplying the equations given in sections 5.1.1.3 and 5.1.2.4 by 0.7.

To the authors' knowledge, tests with combined tension and shear in cracked concrete have not been carried out to date. However, it may conservatively be assumed that the interaction equations (4.42) and (4.43) with  $k = 1.5$  also apply to anchor channels.

## 6 Behaviour of bonded anchors in non-cracked and cracked concrete

Sections 6.1 and 6.2 address the behaviour of conventional bonded anchor systems with  $d_p/d \leq 1.5$  installed in cylindrical drilled holes. The mortar consists of aggregates and binder in the form of unsaturated polyester, vinylester, vinylester with cement (hybrid systems) or epoxy. The behaviour of bonded undercut and bonded expansion anchors is discussed in section 6.3.

### 6.1 Non-cracked concrete

#### 6.1.1 Tension load

##### 6.1.1.1 Load-displacement behaviour and modes of failure

In principle, bonded anchors exhibit the same basic failure modes as expansion and undercut anchors (see Fig. 4.1). Fig. 6.1 depicts the typical failure modes associated with single anchors loaded in tension. At small embedment depths ( $h_{ef} \approx 3 \cdot d$  to  $5 \cdot d$ ) concrete failure is characterised by a cone-shaped concrete breakout originating at the base of the anchor (Fig. 6.1a). The slope of the cone envelope with respect to the surface of the concrete member is approxi-

mately  $35^\circ$ , i.e. the same as for headed studs, undercut anchors, and expansion anchors. For greater embedment depths, the concrete failure mode usually transitions to a mixed-mode (bond/concrete breakout) type of failure. A concrete cone with a depth of approximately  $2 \cdot d$  to  $3 \cdot d$  forms at the top end of the anchor and the bond fails over the balance of the embedment depth. Bond failure occurs either at the boundary between concrete and mortar (Fig. 6.1b) or at the boundary between the mortar and anchor rod (Fig. 6.1c). Often a failure between concrete and mortar occurs in the upper part of the embedment, with the failure of the bond between mortar and anchor rod confined to the deeper end (Fig. 6.1d). Fig. 6.2 provides a photo of a bonded anchor that has failed in this way. For large embedment depths the bond resistance developed over the length of the anchor can exceed the rupture strength of the steel rod, leading to steel failure (Fig. 6.1e). The minimum embedment depth of a single anchor without edge or spacing effects required to ensure failure of the steel rod depends on the grade of steel, the concrete mechanical properties and the properties of the mortar. In cases of anchor

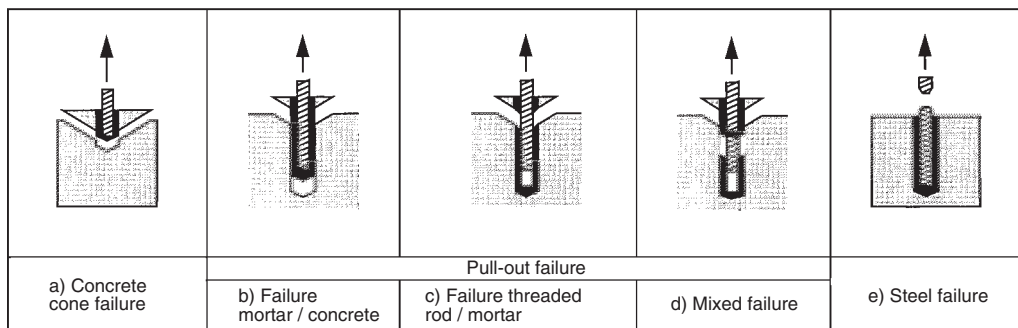
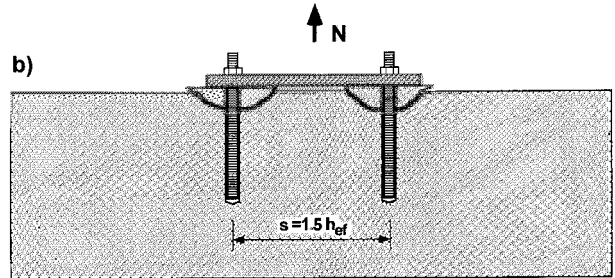
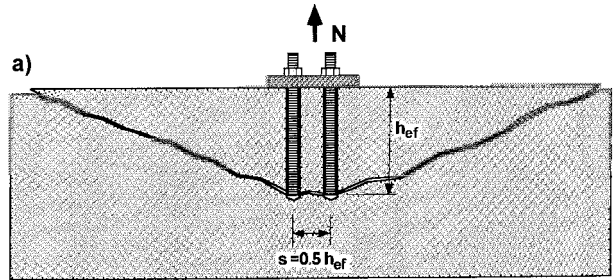


Fig. 6.1 Failure modes of bonded anchors under tension load (Cook, Kunz, Fuchs, Konz (1998))



**Fig. 6.2** Photo of a bonded anchor after tension test (Eligehausen, Mallée, Rehm (1984))



**Fig. 6.3** Failure modes of groups with bonded anchors M12 with constant embedment depth,  $h_{ef} = 12d$ , for different spacings (Lehr, Eligehausen (1998))

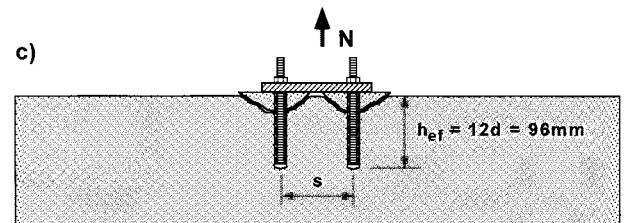
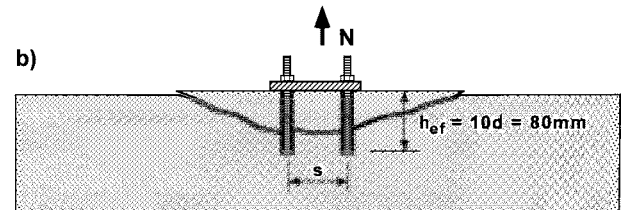
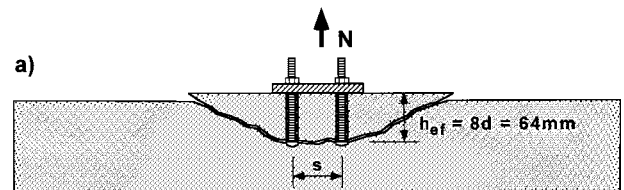


**Fig. 6.4** Failure modes of groups with bonded anchors M8 with constant ratio of spacing to embedment depth for different embedment depths (Lehr, Eligehausen (1998))



groups or anchorages close to an edge, the geometry of the anchorage is also important. Anchorages close to an edge or in a corner can precipitate splitting of the concrete (see Fig. 4.1c).

Failure modes of anchor groups observed in tests are shown in Figs. 6.3 and 6.4. Anchor groups with a small anchor spacing generate a common concrete cone breakout in response to tension loading (Figs. 6.3a and 6.4a), whereas anchor groups with large anchor spacing generally exhibit mixed mode failure of the individual anchors (Fig. 6.3b). In numerical analysis at intermediate spacing, cracks were observed that initiate at the end of the anchors and propagate towards each other and connect at peak load (*Li, Eligehausen, Ozbolt, Lehr* (2002)). Final failure was caused by mixed mode failure of the individual anchors. A similar transition between failure modes is seen when, for a constant spacing-to-embedment depth ratio, the embedment depth is increased (Fig. 6.4). Group anchorages near an edge can split the concrete.

Schematic load-displacement curves for non-prestressed, single bonded anchors loaded in tension and exhibiting pull-out failure are plotted in Fig. 6.5. The load-displacement behaviour essentially depends on the stiffness and adhesion of the mortar. Given a stiff mortar having good adhesion, bonded anchors can exhibit an approximately elastic behaviour nearly up to failure (Fig. 6.5a). Post-peak behaviour is dependent on which interface has experienced bond failure. If bond is lost between the concrete and mortar (Fig. 6.1b), the anchor rod with mortar is pulled through the non-uniform surface of the drilled hole and frictional resistance is generated. If this frictional resistance is lower than the adhesion strength, then the load that can be resisted shows steady decline as the displacement increases (Fig. 6.5a). If the adhesion strength is less than the frictional resistance generated between mortar and hole, the ultimate load is attained at relatively large displacements. However, the ultimate load associated with frictional resistance typically exhibits a relatively large degree of scatter. The ratio of adhesion resistance to ultimate load can be relatively high (Fig. 6.5b) or, as in the case of less robust systems, quite low (Fig. 6.5c).

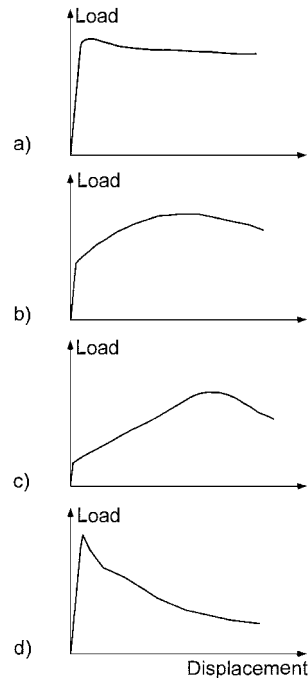


**Fig. 6.5** Load-displacement curves of single bonded anchors (schematic) (*Meszaros* (1999))

- a) Failure between mortar and wall of drilled hole (bond force between mortar and concrete higher than friction force)
- b) Failure between mortar and wall of drilled hole (bond force between mortar and concrete lower than friction force)
- c) Failure between mortar and wall of drilled hole (bond force between mortar and concrete significantly lower than friction force)
- d) Failure between mortar and rod

If, on the other hand, bond failure takes place between mortar and anchor rod (Fig. 6.1c), resistance will drop rapidly with increasing displacement (Fig. 6.5d) since the mortar projections into the anchor rod deformations (generally, threads) are sheared off at small displacements followed by extraction of the anchor rod. After shearing off the mortar between the threads, the surface of the mortar is relatively smooth and therefore frictional resistance tends to be small. The load-displacement behaviour represented by Fig. 6.5a is clearly more favourable than that of Fig. 6.5d, most importantly because it allows for redistribution of loads in group anchorages.

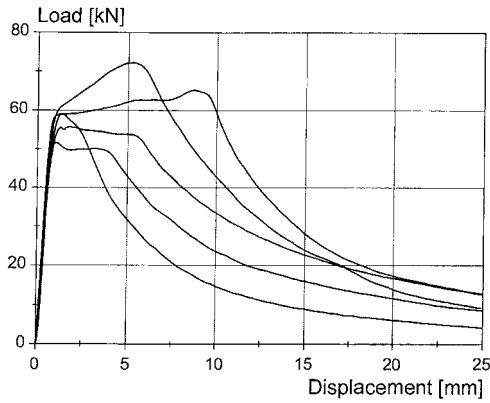


**Fig. 6.6** Load-displacement curves of capsule type bonded anchors M12,  $h_{ef} = 110$  mm,  $f_c \approx 25$  N/mm<sup>2</sup>, well-cleaned drill hole, dry concrete (Meszaros, Eligehausen (1996/1))

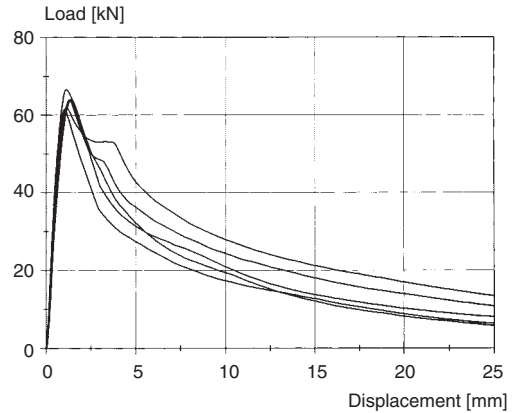


**Fig. 6.8** Load-displacement curves of injection type bonded anchors M12,  $h_{ef} = 110$  mm,  $f_c \approx 25$  N/mm<sup>2</sup>, well-cleaned drill hole, dry concrete (Meszaros, Eligehausen (1996/1))

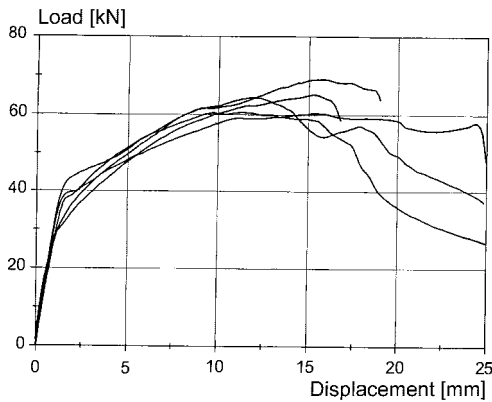


**Fig. 6.7** Load-displacement curves of injection type bonded anchors M12,  $h_{ef} = 110$  mm,  $f_c \approx 25$  N/mm<sup>2</sup>, well-cleaned drill hole, dry concrete (Meszaros, Eligehausen (1998))

Figs. 6.6 to 6.8 provide load-displacement curves derived from tests with various bonded anchor systems (diameter 12 mm, embedment depth  $h_{ef} = 110$  mm). All holes were drilled with a hammer drill. This drilling technique results in a relatively rough hole surface, which in addition presents a uneven geometry in the longitudinal direction and so deviates from the straight cylindrical form. These curves are valid for anchors installed in thoroughly cleaned holes in dry concrete. Typically, a bonded

anchor system will consistently exhibit *one* of the methods of behaviour described above (Figs. 6.7 and 6.8). However, it is also possible for varying load-displacement relationships to occur in a single test series (Fig. 6.6).

#### 6.1.1.2 Failure load associated with steel failure

Section 4.1.1.2 applies.

#### 6.1.1.3 Failure load associated with concrete breakout/pull-out failure

The distribution of the bond stresses over the embedment depth depends on the magnitude of the load, the stiffness of the mortar, and the embedment depth. At peak load the bond stresses are distributed unevenly over the embedment depth, however, for simplicity, a uniform distribution is typically assumed. According to *Cook, Kunz, Fuchs, Konz* (1998), a constant bond stress over the embedment depth and a bond strength not dependent on the embedment depth may be assumed for embedment depths  $4.5 \leq h_{ef}/d \leq 25$ . This is shown in Fig. 6.9, in which the quotients from measured failure loads and those calculated using equation (6.4) are plotted against the ratio of embedment depth to anchor rod diameter for eight different products and a total of 888 individual results. In equation (6.4) product-specific bond

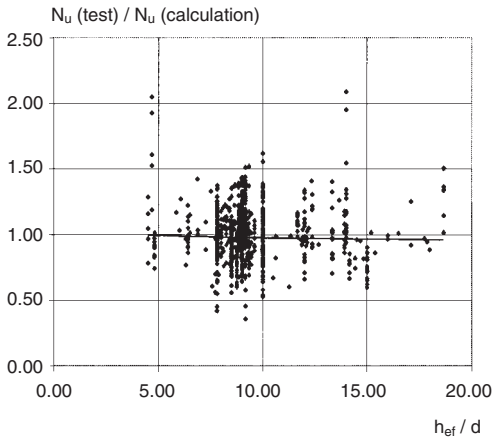


**Fig. 6.9** Ratio between measured failure loads and values calculated according to equation (6.4) as a function of the ratio between embedment depth and anchor diameter (Cook, Kunz, Fuchs, Konz (1998))

strengths are assumed that are constant for all embedment depths. In the tests, edge distance ( $c \geq h_{ef}$ ) and the support spacing were chosen to allow the formation of a complete concrete cone breakout. Cartridge and injection systems were investigated in conjunction with various types of mortar. The holes were drilled in dry concrete and carefully cleaned with brushes and compressed air. Pull-out failure was observed in all tests. An earlier less comprehensive test program described in Lang (1979) revealed that

bond strength decreases at embedment depths  $h_{ef} > 9d$ .

Strictly speaking, any measure of bond strength should be related to the fracture surface area generated during the test. However, it is often not possible to predict the failure surface associated with the anchor ultimate capacity, particularly in the case of mixed-mode failures. Additionally, the failure mode can vary within a test series or with variations in concrete mix design. Alternatively, it is always reasonable to relate the bond strength to the anchor rod diameter. According to the studies by Cook, Kunz, Fuchs, Konz (1998) this approach is valid for bonded anchors with a small annular clearance. The ratio  $d_0/d$  for the investigated systems typically fell in the range of 1.1 to 1.3 with individual cases as high as 1.8. The following discussion applies to bonded anchors with  $d_0/d \leq 1.5$ , whereby the specified bond strengths have been determined using the anchor rod diameter.

Bond strength is primarily a function of mortar type. Cook, Bishop, Hagedoorn, Sikes, Richardson, Adams, De Zee (1994) conducted in excess of 1,000 tension tests on 20 different products. Close support spacing was employed in the tests (so-called confined tests) to force bond failure. Fig. 6.10 shows the mean bond strengths recorded for the various types of mortar investigated. The threaded anchor rods used in the

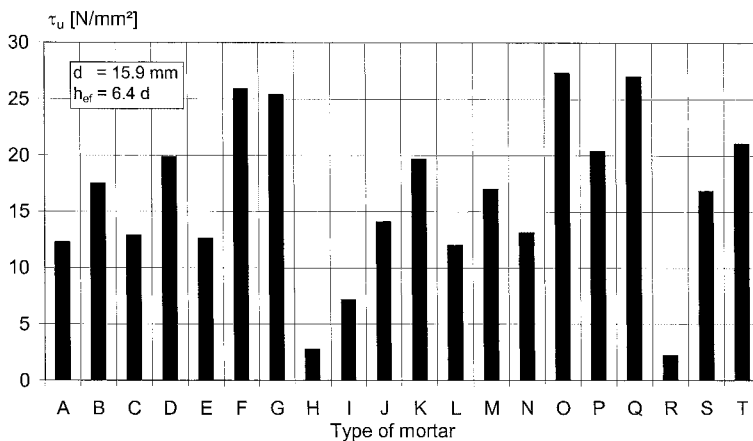


**Fig. 6.10** Average bond strength in concrete with  $f_c \approx 45 \text{ N/mm}^2$  for different mortar types (Cook, Bishop, Hagedoorn, Sikes, Richardson, Adams, De Zee (1994))

tests had a diameter of  $5/8$  in. ( $\approx 16$  mm) and were embedded with  $h_{ef} = 6.4 \cdot d$  in dry and carefully cleaned-out holes (i.e. under ideal conditions). Although three products exhibited very low bond strengths, in 11 cases the mean bond strength fell in the range of  $10$  N/mm<sup>2</sup> to  $20$  N/mm<sup>2</sup>. Six products had a bond strength exceeding  $20$  N/mm<sup>2</sup>. Clearly, bond strength is highly dependent on product type and bond values derived for one product cannot be assumed to apply to others.

According to *Cook, Kunz, Fuchs, Konz* (1998) bond strengths for the majority of mortar products currently on the market do not vary significantly with anchor rod diameter. However, some mortars do exhibit diameter sensitivity in the form of clearly lower bond strengths at specific diameters (Fig. 6.11).

Higher concrete compressive strengths can lead to improved bond strength only if bond failure occurs at the boundary between mortar and the sides of the hole. However, for most products

this influence is minimal because the sides of the hole become smoother as the concrete strength increases. Furthermore, at higher concrete strengths often the bond between mortar and anchor rod fails. The effect of the concrete compressive strength on the bond strength also varies by product. Bond strength can be either independent of concrete compressive strength or increase in proportion to  $f_c^\alpha$ , where  $\alpha \leq 0.5$  (*Cook, Kunz, Fuchs, Konz* (1998)). As a rule, bond strengths established in testing with concrete compressive strength  $f_c \approx 20$  N/mm<sup>2</sup> should be valid for concretes up to strength class C50/60 according to *Eurocode 2: EN 1992-1-1* (2003). In very high strength concretes, the bond strength can drop as a consequence of increased hole smoothness.

The bond strengths given in Fig. 6.10 are applicable to anchors installed under the following conditions: (1) dry, sound concrete, (2) holes produced with hammer drills and subsequently brush cleaned and blown out with compressed air, (3) room temperature of approximately  $20$  °C at the time of installation, and (4) installation otherwise in accordance with manufacturer instructions. Incorrect installation can measurably affect these values. For example, capsule anchor systems designed to be installed with hammering and rotation action of the drill exhibit very low ultimate tension capacity when installed with hammering action alone because the mortar is not mixed thoroughly. A low anchor capacity will also occur with injection systems if the correct mix of the mortar is not ensured (bulk systems) or if the hole is not filled completely with mortar.

Failure to remove drilling dust and concrete fragments that collect in the bottom of holes drilled vertically downward may hinder installation of the anchor rod to the specified embedment. Over-driving a capsule anchor in an attempt to force the rod through such material will typically cause expulsion of mortar from the hole, leading to gaps in the mortar coverage over the length of the anchor rod. It may also interfere with the initial gel of the resin and has been shown to cause a drop in the tension capacity of the anchor of up to  $80\%$  (*Rehm* (1985/2)).

Regardless of the direction in which the anchor is installed (vertically upwards/downwards,

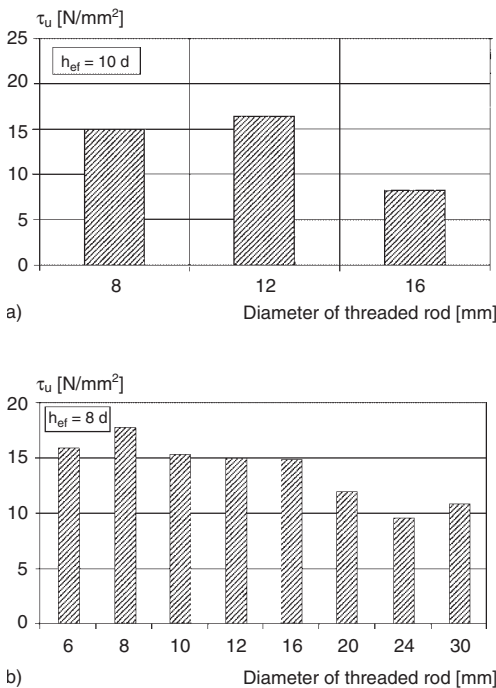


**Fig. 6.11** Average bond strength in concrete with  $f_c \approx 25$  N/mm<sup>2</sup> for different anchor diameters

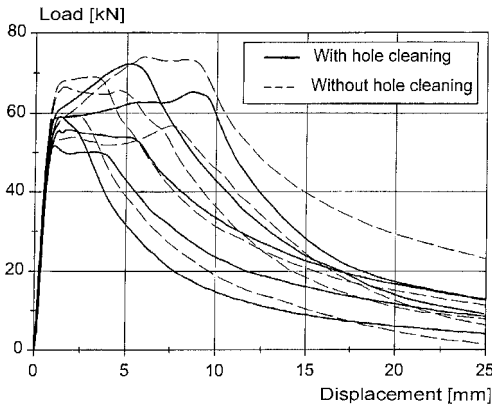


**Fig. 6.12** Load-displacement curves of bonded anchors M12,  $h_{ef} = 110$  mm,  $f_c \approx 25$  N/mm<sup>2</sup>, anchored in well-cleaned and uncleaned drill holes (anchor type not sensitive to hole cleaning) (Meszaros, Eligehausen (1996/1))

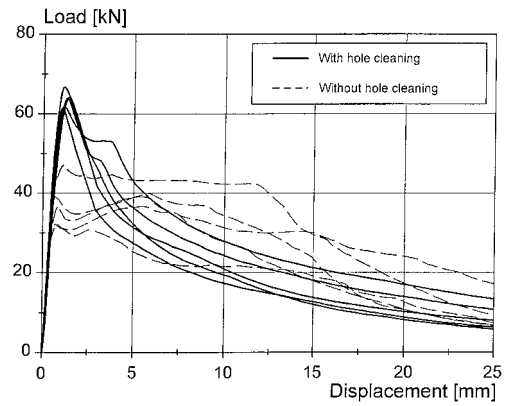
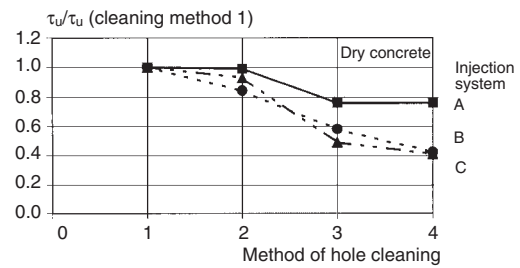


**Fig. 6.13** Load-displacement curves of bonded anchors M12,  $h_{ef} = 110$  mm,  $f_c \approx 25$  N/mm<sup>2</sup>, anchored in well-cleaned and uncleaned drill holes (anchor type sensitive to hole cleaning) (Meszaros, Eligehausen (1996/1))

horizontally), inadequate cleaning of the drilled hole allows for the retention of dust on the sides of the hole. Figs. 6.12 and 6.13 show the influence of cleaning (i.e., dust removal) on the load-displacement behaviour of anchors installed in dry concrete. Both figures compare load-displacement curves for thorough cleaning of the drilled hole by use of a stiff brush and blowing with a hand pump to those derived from anchors installed without cleaning the hole. In the latter case the holes drilled vertically downwards were drilled deeper than required in order to create a space in which the dust from drilling could collect. In imitation of typical practice, the hammer drill was retracted three times at roughly equal intervals during the drilling process to facilitate transport of the drilling dust out of the hole (and to prevent jamming of the drill bit). Depending on the mortar system, hole cleaning can have merely a minor effect (Fig. 6.12) or a more pronounced effect (Fig. 6.13) on the load-displacement behaviour and the ultimate load. Capsule anchor systems that are installed by chucking the anchor rod into the hammer drill and driving the rod through the capsule with both hammering and drilling action are generally among the least sensitive types of bonded anchor systems in this regard. This may be attributed to the drilling action which, in combination with the quartz

aggregate contained in the resin capsule, serves to scour the dust from the hole wall. The reduction in tension capacity for such systems installed in un-cleaned holes is usually less than 20%. With injection systems, whereby the mortar is pre-mixed in the injection nozzle, the reduction in tension capacity associated with inadequate hole cleaning depends on the adhesion of the resin type used, and can range from less than 20% to as much as 50% (Eligehausen,



Method of hole cleaning	
1	2 x blowing, 2 x brushing, 2 x blowing
2	1 x blowing, 1 x brushing, 1 x blowing
3	2 x blowing
4	No cleaning (drilling machine retracted 3 times)

**Fig. 6.14** Influence of intensity of hole cleaning on the bond strength of injection anchors M12 in dry concrete (Meszaros, Eligehausen (1998))

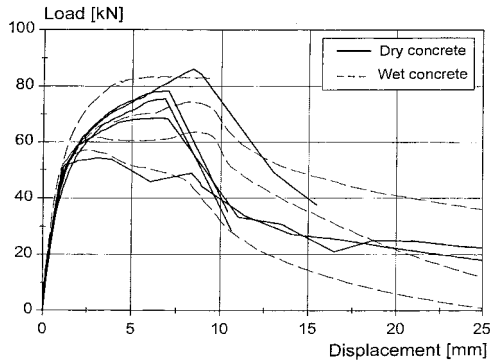


**Fig. 6.15** Load-displacement curves of bonded anchors M12,  $h_{ef} = 110$  mm, anchored in dry and wet concrete with  $f_c \approx 25$  N/mm<sup>2</sup>, drill holes cleaned thoroughly (anchor type not sensitive to moisture in concrete) (Meszaros, Eligehausen (1996/2))

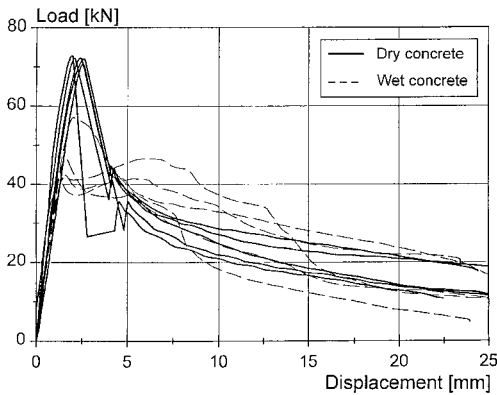


**Fig. 6.16** Load-displacement curves of bonded anchors M12,  $h_{ef} = 110$  mm, anchored in dry and wet concrete with  $f_c \approx 25$  N/mm<sup>2</sup>, drill holes cleaned thoroughly (anchor type sensitive to moisture in concrete) (Meszaros, Eligehausen (1996/2))

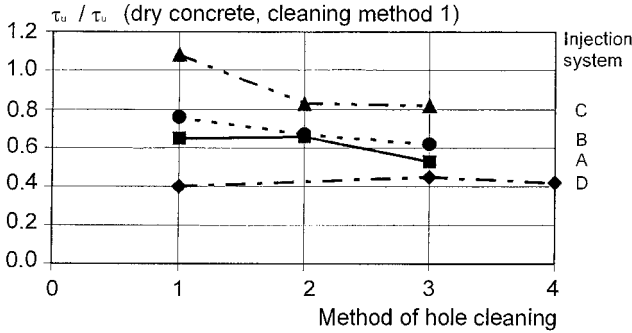
Meszaros (1996)). It is important with injection systems that the hole is mechanically cleaned with a suitably stiff brush and subsequently blown clean. Compressed air alone is generally not adequate to remove the dust from the sides of the hole. Fig. 6.14 shows the influence of the degree of hole cleaning on the bond strength attainable for three different injection system types. Capsule anchor systems in which the anchor rod is hammered but not spun into the hole should exhibit a sensitivity to hole cleaning that is on a par with injection systems using a similar resin.

The installation of bonded anchors in wet concrete can lead to reduced tension capacity. In this respect, wet concrete refers to fully hardened concrete that is water saturated. In tests this condition may be achieved by submerging the concrete specimen in water for a sufficiently long time and removing it from the water immediately prior to installing the anchors. Effective cleaning of the hole is particularly difficult in wet concrete because the drilling dust tends to adhere to the sides of the hole. In addition, depending on the type of mortar, the water film on the sides of the hole can have an unfavourable effect on bond development during curing of the resin. Figs. 6.15 and 6.16 allow for the comparison of load-displacement curves corresponding to anchors installed in dry and wet concrete. In all tests, the holes were carefully brushed and blown out after drilling. The load-bearing behaviour in wet concrete depends on the resin system used. Tested systems employing unsaturated polyester resin and vinyl ester resin containing styrene exhibited a relatively small drop (< 20%) in tension capacity (Fig. 6.15), whereas other systems (e.g. styrene-free vinyl ester, epoxy) experienced a greater reduction (Fig. 6.16). If, in addition, the drilled hole is not thoroughly cleaned, the bond strength can fall even further depending on the type of resin and intensity of hole cleaning. This can be seen from Fig. 6.17 which is valid for injection systems.

The bond strength may also be reduced if there is standing water in the hole during installation, regardless of the degree of cleaning effort. Even if the concrete is otherwise dry, the resulting bond strengths may be approximately equal to those of an anchor installed in wet (saturated) concrete.

The bond strengths associated with bonded anchors installed in wet concrete or in water-filled holes are highly product-dependent and should therefore be determined for each anchor system via testing.

The foregoing discussion applies to bonded anchors installed in holes drilled with carbide-tipped hammer drills. In practice, however, both wet- and dry-process diamond core drills are increasingly employed on jobsites for anchor installation. In particular, water-assisted core



Method of hole cleaning	
1	2 x blowing, 2 x brushing, 2 x blowing
2	1 x blowing, 1 x brushing, 1 x blowing
3	2 x blowing
4	No cleaning (drilling machine retracted 3 times)

**Fig. 6.17** Influence of intensity of hole cleaning on the bond strength of injection anchors M12 in wet concrete (Meszaros, Eligehausen (1998))

drilling produces a clean, smooth, geometrically regular cylindrical hole. Even after excess water has been evacuated from the hole, the sides of the hole are coated with drilling slurry and tend to remain wet for some time. The bond strength which can be developed under these conditions is highly dependent on the resin type. If a sufficient time interval is allowed following drilling to allow the hole to dry out completely and if the hole is then thoroughly cleaned, high-adhesion resin types can be

expected to achieve about the same bond strengths as measured in hammer-drilled holes. However, probably owing to the smoothness of the hole surface, significantly reduced bond strengths are typically recorded for low-adhesion resin systems as seen in a limited number of tests conducted at the University of Stuttgart (Fig. 6.18). The effect of diamond core drilling on the load-bearing behaviour of bonded anchor systems is again highly product-dependent and must be checked on a product by product basis.

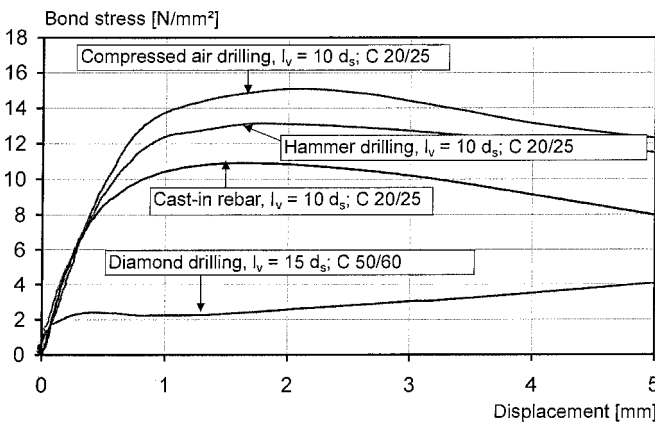


**Fig. 6.18** Bond stress-displacement curves of injection type bonded anchors with a diameter  $d_s = 20$  mm anchored in holes made by hammer and diamond drilling (Spieth, Eligehausen (2002))



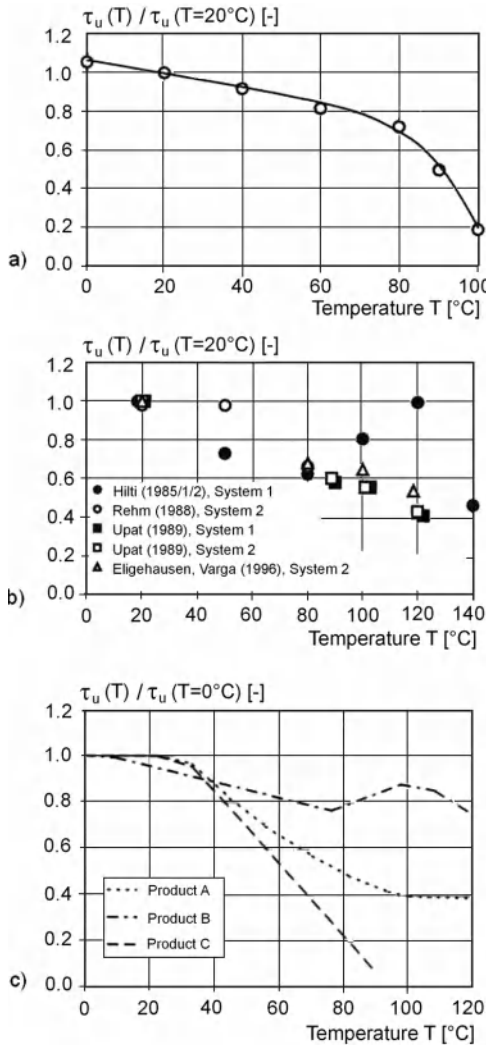


**Fig. 6.19** Influence of temperature in the concrete on bond strength  
a) Unsaturated polyester (Sell 1973/1)  
b) Vinyl ester (after different references)  
c) Different mortar types (Cook, Kunz, Fuchs, Konz (1998))

In the following discussion, bond strength at increased temperature refers to the bond strength of an anchor installed at room temperature and fully cured prior to increasing the concrete temperature. The bond strength of polymer-based bonded anchor systems decreases as the concrete temperature increases (Sell (1973/1), Rehm (1988), Eligehausen, Varga

(1996), Cook, Kunz, Fuchs, Konz (1998)). The relationship between concrete temperature and bond strength is highly product dependent (Fig. 6.19). As the glass transition temperature is reached, the bond strength drops precipitously. The bond strength of a bonded anchor utilising unsaturated polyester resin in concrete having a temperature of 80 °C is only about 70% of the value recorded in tests at 20 °C (Sell (1973/1)). The same reduction has been found for vinyl ester mortar at the same temperature, however, at higher temperatures strength loss is not as severe as with polyester resins (Rehm (1988), Eligehausen, Varga (1996)). The bond strength loss associated with temperature increase is usually much greater for bonded anchors based on epoxy resins. However, the formulation of the resin has a notable influence on this behaviour, and as such a general statement in this respect is not possible.

Numerous equations have been proposed in the literature for calculating the concrete-related failure loads of bonded anchors having large spacing and edge distance. A comprehensive treatment of this subject may be found in Kunz, Cook, Fuchs, Spieth (1998) whereby various approaches are described and evaluated, only a few of the proposed methods are discussed here.

Eligehausen, Mällée, Rehm (1984) evaluated the results of numerous tests on M8 to M30 capsule systems with a mortar based on an unsaturated polyester resin (Fig. 6.20). The embedment depth was approximately nine times the anchor rod diameter. As the concrete compressive strength of the test specimens varied from  $f_{cc,200} \sim 15 \text{ N/mm}^2$  to  $f_{cc,200} \sim 40 \text{ N/mm}^2$ , the measured failure loads were normalised to  $f_{cc,200} = 25 \text{ N/mm}^2$  using the square root of the compressive strength. Equation (6.1) predicts the measured failure loads with reasonable accuracy. It is valid only for the range of applications covered by the tests:

$$N_u^0 = 0.85 \cdot h_{ef}^2 \cdot \sqrt{f_{cc,200}} \quad (6.1)$$

The mean ratio of prediction to test is 1.0, with a coefficient of variation  $v = 14 \%$ . Within the tested ranges, neither anchor diameter nor concrete compressive strength appears to have had any significant influence on the ultimate capacity.

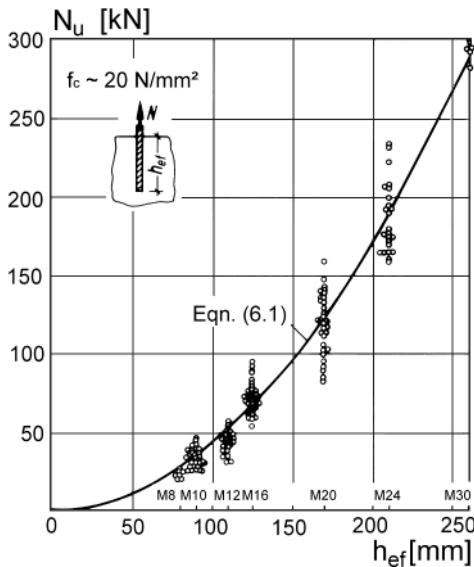


**Fig. 6.20** Failure loads of bonded anchors (capsule system on the basis of unsaturated polyester resin) under tension loading as a function of embedment depth (Eligehausen, Mallée, Rehm (1984))

Eligehausen, Mallée, Rehm (1984) characterised the anchor failure as concrete cone breakout. According to Cook (1993) bonded anchors fail primarily by pull-out at the embedment depths ( $h_{ef} \approx 9d$ ) investigated by Eligehausen, Mallée, Rehm (1984). Assuming a uniform distribution of bond stress over the embedment length, the bond strength at a concrete strength of  $f_{cc,200} = 25 \text{ N/mm}^2 = \tau_u \approx 12 \text{ N/mm}^2$ . As noted by Eligehausen, Mallée, Rehm (1984), testing by Kobarg (1982) indicates that at embedment depths  $h_{ef} > 9 \cdot d$  the failure load does not increase as rapidly as predicted by equation (6.1) but rather proportional to  $h_{ef}$ . This implies that the bond strength  $\tau_u$  remains roughly constant for  $h_{ef} > 9 \cdot d$ .

Cook, Doerr, Klingner (1993) calculated the failure loads of bonded anchors assuming elastic bond behaviour. After the formation of a concrete cone near the surface, the bond stresses are redistributed over the remaining embedment length. It is assumed that pull-out takes place when the maximum bond stress, which occurs at the loaded end of the bonded length, equals the bond strength.

Cook (1993) proposes an approach for calculating the failure loads of bonded anchors that combines the concrete cone and bond capacity. If the embedment depth  $h_{ef}$  is smaller than the depth  $h_c$  of the concrete cone near the surface as given by equation (6.2), then the failure load is calculated using equation (6.1), at larger embedment depths, equation (6.3) is used. This equation consists of two parts: the first part specifies the capacity of the shallow concrete cone, the second that of the bond:

$$h_c = \frac{\tau_u \cdot \pi \cdot d}{1.8 \cdot \sqrt{f_c}} \quad (6.2)$$

$$N_u^0 = 0.85 \cdot h_c^2 \cdot \sqrt{f_{cc,200}} + \pi \cdot d \cdot (h_{ef} - h_c) \cdot \tau_u \quad (6.3)$$

Cook, Kunz, Fuchs, Konz (1998) propose to assume a constant bond strength along the embedment depth. The failure load is thus given by equation (6.4):

$$N_u^0 = \pi \cdot d \cdot h_{ef} \cdot \tau_u \quad (6.4)$$

Equation (6.4) is sufficiently accurate for embedment depths  $4.5 \leq h_{ef}/d \leq 20$  (Fig. 6.9), diameters  $d \leq 50 \text{ mm}$  and bond areas  $\pi \cdot d \cdot h_{ef} \leq 55,000 \text{ mm}^2$ , independent of type of failure (pull-out, mixed concrete and pull-out, concrete cone).

The bond strength  $\tau_u$  is product-specific. It is influenced by the state of the concrete (dry, water saturated), the manner in which the hole is drilled (hammer drill, diamond core drill), the degree to which the hole is cleaned out, and the temperature of the base material. Therefore, the ultimate bond strength must be determined with product- and application-specific testing.

Fig. 6.21 shows failure loads measured in tests on bonded anchors as a function of their embedment depth. While in Fig. 6.20 the various embedment depths were associated with multiple anchor rod diameters, in Fig. 6.21 the rod diameter ( $d = 3/8 \text{ inch} \approx 9.5 \text{ mm}$ ) was held constant for all embedment depths. Failure loads corresponding to equations (6.1), (6.3) and (6.4) are plotted as well as those predicted by the elastic bond model of Cook, Doerr, Klingner (1993). It can be seen that equation (6.1) coincides well with the test results for  $h_{ef} = 9d$ , but underestimates the capacity for smaller embed-

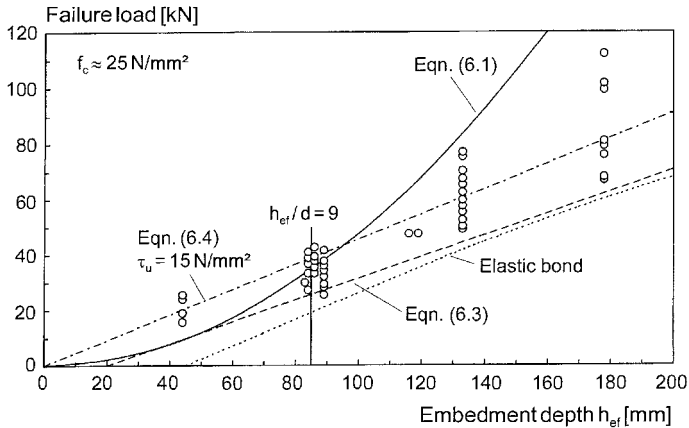


**Fig. 6.21** Comparison of different proposals for calculating the failure load of single bonded anchors ( $d = 9.5$  mm) with test results (Kunz, Cook, Fuchs, Spieth (1998))

ments and overestimates the capacity at embedments greater than  $9d$ . This is not surprising given that equation (6.1) was developed solely on the basis of tests with bonded anchors having an  $h_{ef} \approx 9 \cdot d$ . Both the elastic bond model of Cook, Doerr, Klingner (1993) and equation (6.3) underestimate the failure loads at all tested embedments. In contrast, the constant bond stress equation (6.4) predicts failure loads that agree reasonably well with the test results.

Bonded anchor groups may fail by pull-out of the individual anchors (Figs. 6.3b and 6.4c). Despite the lack of visible overlapping failure surfaces, testing indicates that for an anchor spacing less than a critical value the failure load of a group of four anchors is less than four times the pull-out load of a single anchor. Numerical analyses using the MASA non-linear FEM program (Ozbolt (1998)) were carried out to shed light on this behaviour (Li, Eligehausen, Ozbolt, Lehr (2002)). This analysis indicates that the reduced pull-out load of multiple anchors compared to the value applicable for a single anchor with large spacing can be attributed to changes in the bond stress distribution around the anchor. Single anchors exhibit a uniform bond stress distribution in the circumferential direction. Closely spaced anchors, on the other hand, develop a bond stress distribution that is circumferentially skewed, with higher bond stresses on the outward facing surfaces and lower bond stresses on the inward facing sides.

According to Pukl, Ozbolt, Eligehausen (1998) and Schou, Christiansen, Andersen (1998) this is attributable to tensile stresses in the concrete between the anchors of the group which serve to effectively reduce the bond stresses that can be accommodated. In addition, Li, Eligehausen, Ozbolt, Lehr (2002) report that a horizontal crack, which develops at the base of the anchor group, is responsible for the uneven distribution of the bond stresses around the anchors at ultimate load.

As the anchor spacing is reduced the failure mode transitions to concrete cone breakout (Figs. 6.3a and 6.4a,b) and the failure load is further reduced.

Bonded anchors positioned at the edge of a member can also fail via pull-out or concrete cone breakout, whereby failure loads associated with edge distances less than a characteristic value are reduced when compared with anchors placed well away from the edge.

Irrespective of the failure mode, tension failure loads associated with bonded anchor groups or single anchors positioned near an edge can be approximated similar to the CC-Method (see section 4.1.1.3) (Lehr, Eligehausen (1998)), however, with some modifications.

$$N_u = \frac{A_{c,N}}{A_{c,N}^0} \cdot \psi_{s,N} \cdot \psi_{ec,N} \cdot N_u^0 \quad [\text{N}] \quad (6.5)$$

where:

$N_u^0$  is calculated according to equation (6.4)

$A_{c,N}$  = existing area of fastening projected onto surface of concrete limited by the overlap of individual projected areas of neighbouring anchors ( $s < s_{cr,N}$ ) as well as by edges ( $c < c_{cr,N}$ )

$$A_{c,N}^0 = s_{cr,N}^2$$

$$\psi_{s,N} = 0.7 + 0.3 \cdot \frac{c}{c_{cr,N}} \leq 1.0 \quad (6.5a)$$

$$\psi_{ec,N} = \frac{1}{1 + 2 \cdot e_N / s_{cr,N}} \leq 1.0 \quad (6.5b)$$

$e_N$  = eccentricity of tensile force resultant associated with tension-loaded anchors from their geometrical centroid

$s_{cr,N}$  = characteristic spacing

$c_{cr,N}$  = characteristic edge distance

The ultimate load of a single anchor  $N_u^0$  not influenced by adjacent anchors or edges is calculated according to the uniform bond model (equation (6.4)). Note that with this equation the failure load for different types of failures (pull-out, mixed concrete and pull-out, concrete cone) is approximated.

The projected area calculation for bonded anchors may be made in the same manner as for

the concrete cone breakout of headed anchors (see Figs 4.16 and 4.26) but with the characteristic spacing and edge distance  $s_{cr,N} = 2 \cdot c_{cr,N} = 3 \cdot h_{ef}$  replaced by different values.

*Lehr, Eligehausen* (1998) assume  $s_{cr,N} = 2c_{cr,N} = 2h_{ef}$  and *Kunz, Cook, Fuchs, Spieth* (1998) recommend  $s_{cr,N} = 2 \cdot c_{cr,N} = 1.75 \cdot h_{ef}$ . *Cook, Konz* (1998) also propose  $s_{cr,N} = 1.75 \cdot h_{ef}$ , but for the influence of the edge they assume that the failure load decreases linearly from for  $c = 10 \cdot d$  to  $N_u^0$  for  $c = 0$ .

According to the above proposals the characteristic spacing of bonded anchors depends – as for headed studs – on the embedment depth. Based on the results of numerical and experimental investigations, *Lehr* (2003) assumes that the characteristic spacing depends on the anchor diameter. He proposes  $s_{cr,N} = 2 \cdot c_{cr,N} = 16 \cdot d$ . According to the results of numerical investigations of *Li, Eligehausen* (2001) the characteristic spacing is additionally influenced by the bond strength. Based on results with 415 tests with anchor groups *Eligehausen, Appl, Lehr, Meszaros, Fuchs* (2005) propose  $s_{cr,N} = 2 \cdot c_{cr,N} = 20 \cdot d \cdot (\tau_u / 10)^{2/3}$ .

According to equation (6.5) the failure load of a fastening with  $n = 2$  or  $n = 4$  anchors with a spacing  $s = d$  corresponds approximately to the value

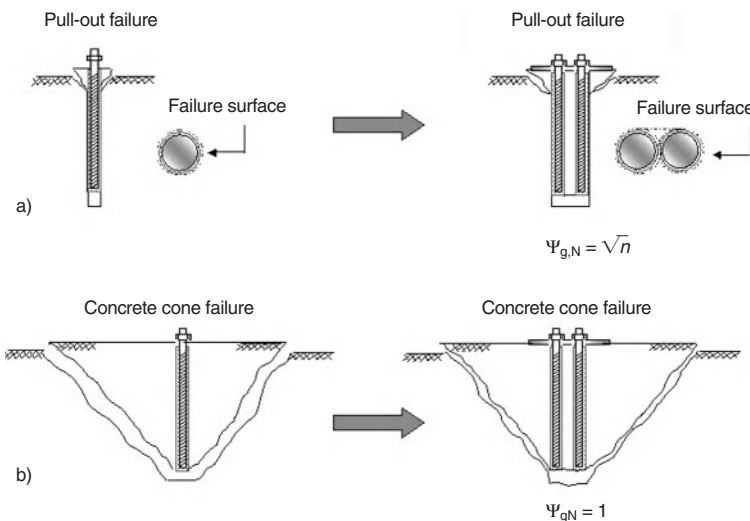


**Fig. 6.22** Failure of a pair of bonded anchors ( $s = d$ ) (*Eligehausen, Appl, Lehr, Meszaros, Fuchs* (2005))  
 a) Pull-out failure, b) Concrete cone failure

valid for one anchor. However, the load that can be introduced into the concrete by bond is by the factor  $\sqrt{n}$  larger than that of a single anchor because of the increased bond area (Fig. 6.22a) but may be limited by concrete cone failure (Fig. 6.22b). To consider this *Eligehausen, Appl, Lehr, Meszaros, Fuchs (2005)* propose equation (6.6) in which an additional factor  $\psi_{g,N}$  is added to equation (6.5). Furthermore, based on the results of tests with single anchors at the edge the factor  $\psi_{s,N}$  is omitted.

$$N_u = \frac{A_{c,N}}{A_{c,N}^0} \cdot \psi_{g,N} \cdot \psi_{ec,N} \cdot N_u^0 \quad [\text{N}] \quad (6.6)$$

where:

$$\psi_{g,N} = \psi_{g,N}^0 + \frac{s}{s_{cr,N}} \cdot (1 - \psi_{g,N}^0) \geq 1 \quad (6.6a)$$

$$\psi_{g,N}^0 = n^\alpha$$

$$\alpha = 0.7 \cdot (1 - \tau_u / \tau_{u,max}) \leq 0.5 \quad (6.6b)$$

$$\tau_{u,max} = 4.3 \cdot (h_{ef} \cdot f_{cc,200}) / d \quad (6.6c)$$

$$s_{cr,N} = 2 \cdot c_{cr,N} = 20 \cdot d \cdot (\tau_u / 10)^{2/3} \quad (6.6d)$$

$n$  = number of anchors in a group

$A_{c,N}, A_{c,N}^0, \psi_{ec,N}, N_u^0$  as defined in equation (6.5)

The rationale for the group factor  $\psi_{g,N}$  is shown in Fig. 6.23. Plotted is the factor  $\psi_{g,N}^0$  as a function of the anchor bond strength related to a

maximum value. The maximum bond strength  $\tau_{u,max}$  to ensure concrete cone failure of a single anchor is given by equation (6.6c). It is obtained by equating equation (4.5b) using  $k = 13.5$  for concrete cone failure with equation (6.4) for bond failure. For a bond strength of a single anchor equal to  $\tau_{u,max}$  groups will fail by concrete cone failure. In this case the group factor is  $\psi_{g,N}^0 = 1$ . For a bond strength smaller than or equal to about  $0.5 \cdot \tau_{u,max} / \sqrt{n}$  pull-out failure is assumed and the group factor is  $\psi_{g,N}^0 = \sqrt{n}$ . For intermediate bond strengths a hyperbolic interpolation between the limiting  $\psi_{g,N}^0$ -values is assumed. With increasing spacing the group factor  $\psi_{g,N}$  decreases linearly from  $\psi_{g,N} = \psi_{g,N}^0$  for  $s = 0$  to  $\psi_{g,N} = 1$  for  $s = s_{cr,N}$ . For instance, for a group of four anchors with a low bond strength so that pull-out failure occurs, the factor  $\psi_{g,N}$  varies linearly between 2 for  $s = 0$  and 1 for  $s \geq s_{cr,N}$ .

According to equation (6.6) the failure load of fastenings with bonded anchors increases with increasing embedment depth, diameter and/or bond strength. In contrast to this the concrete cone failure load of headed studs, expansion and undercut anchors is assumed to be independent of the diameter (compare equation (4.9)). Therefore for large anchor diameters or high bond strength, failure loads calculated with

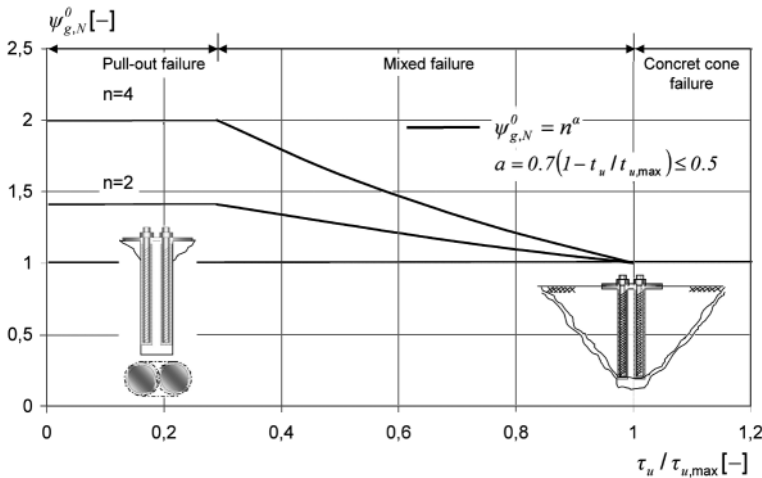


**Fig. 6.23** Factor  $\psi_{g,N}^0$  according to equation (6.6b) as a function of bond strength to maximum value (*Eligehausen, Appl, Lehr, Meszaros, Fuchs (2005)*)

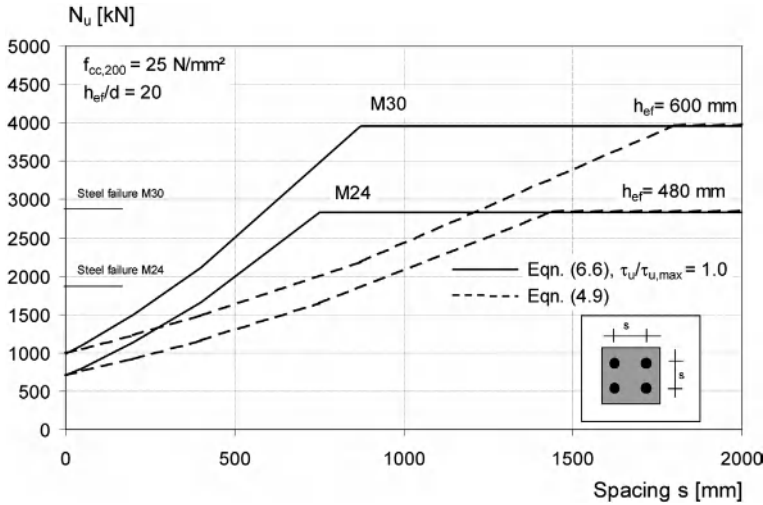


**Fig. 6.24** Calculated failure loads of groups of bonded and headed anchors as a function of spacing (Eligehausen, Appl, Lehr, Meszaros, Fuchs (2005))

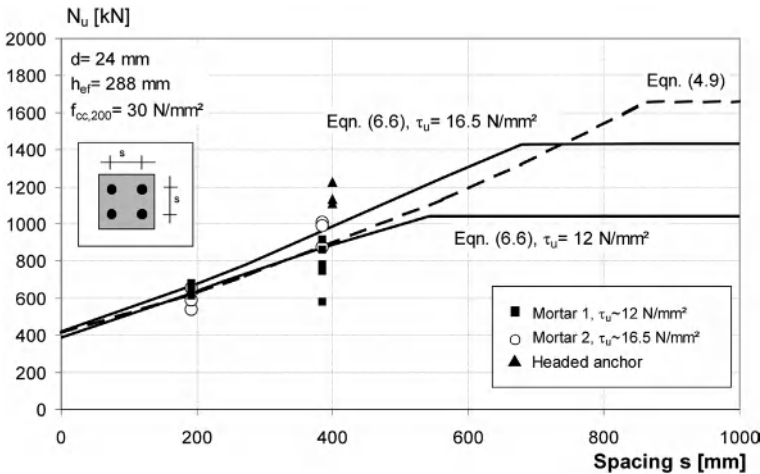


**Fig. 6.25** Comparison of measured failure loads of groups of bonded and headed anchors with calculated values as a function of spacing (tests by Lehr (2003))

equation (6.6) might be significantly larger than the concrete cone failure load of mechanical anchors. This is shown in Fig. 6.24, which is valid for a fastening with four anchors. To investigate whether the failure load of fastenings with bonded anchors may be higher than that of fastenings with mechanical anchors, tests on groups with four anchors (diameter  $d =$

24 mm,  $h_{ef} = 288$  mm) were performed by Lehr (2003). Tested were cast-in-place headed anchors and post-installed bonded anchors with two different bond strengths. The spacing between the anchors was varied. In all tests concrete cone failure occurred. The test results are plotted in Fig. 6.25. The failure loads predicted by equations (4.9) and (6.6) are also plotted in

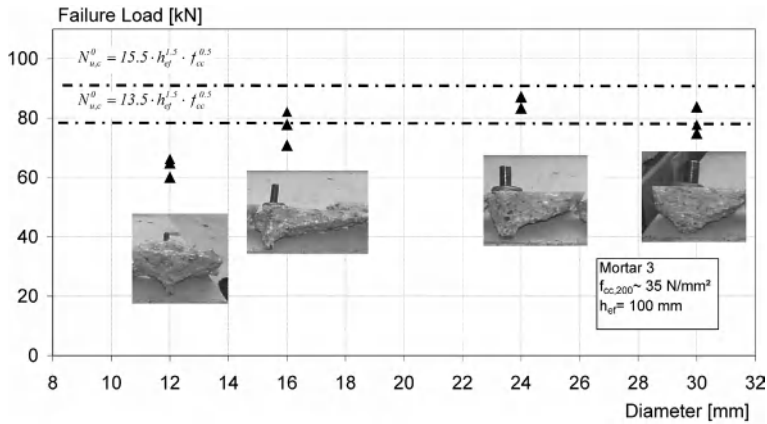


**Fig. 6.26** Failure loads of bonded anchors as a function of the anchor diameter (*Eligehausen, Appl, Lehr, Meszaros, Fuchs (2004/1)*)

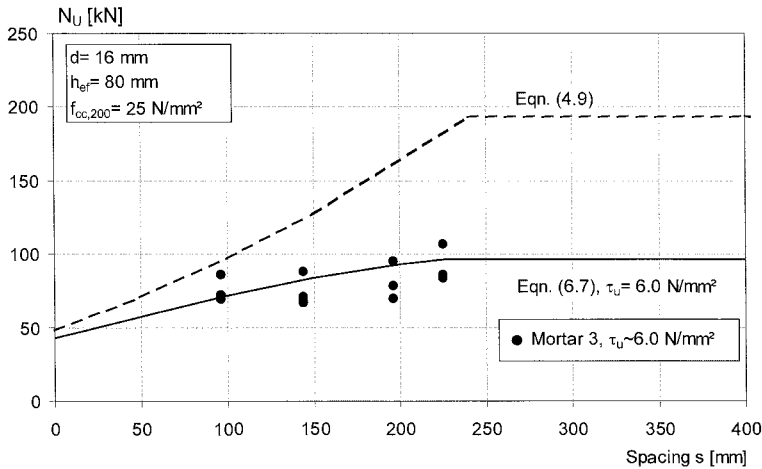


**Fig. 6.27** Comparison of measured failure loads of groups with bonded anchors M12 with calculated values as a function of spacing (tests by *Lehr (2003)*)

the figure. The measured failure loads of the headed anchors are higher than predicted. The measured capacities of the bonded anchors are less or equal to that of headed anchors.

In Fig. 6.26 the failure loads of single bonded anchors with a high strength mortar and embedment depth of 100 mm are plotted as a function of the anchor diameter. For comparison the concrete cone failure load of headed or expansion anchors according to equation (4.9) is plotted as well. With diameters of 24 mm and 30 mm the

failure cones start from the end of the anchor. The failure loads scatter around the calculated value for expansion anchors. Numerical calculations at the University of Stuttgart indicate that bonded anchors with a rather stiff mortar may reach the concrete cone failure load of headed anchors.

Based on the above considerations *Lehr (2003)* and *Eligehausen, Appl, Lehr, Meszaros, Fuchs (2005)* propose to limit the failure load according to equation (6.6) by the concrete cone failure load of expansion anchors (equation (4.9)).



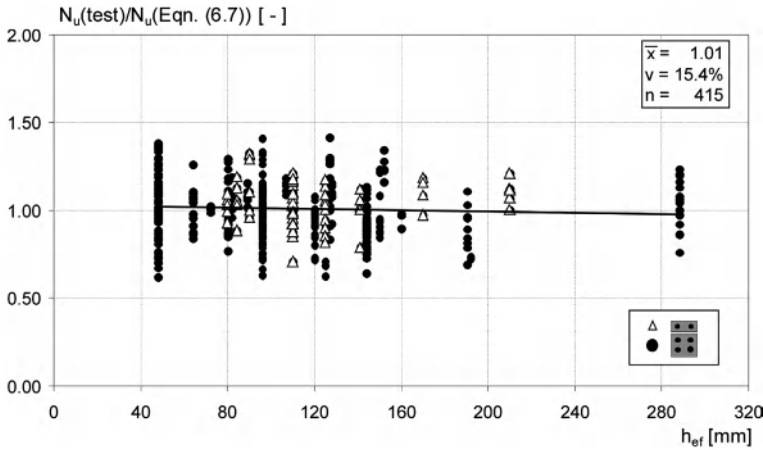


**Fig. 6.28** Ratios of measured failure loads of groups with bonded anchors to values calculated according to equation (6.7) as a function of embedment depth (Eligehausen, Appl, Lehr, Meszaros, Fuchs (2005))

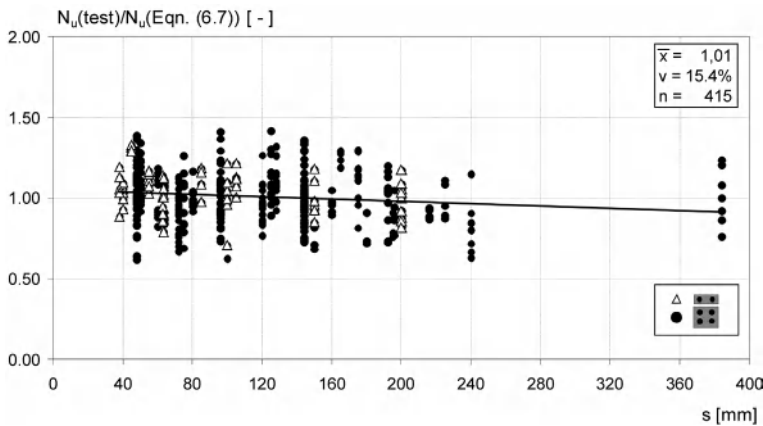


**Fig. 6.29** Ratios of measured failure loads of groups with bonded anchors to values calculated according to equation (6.7) as a function of spacing (Eligehausen, Appl, Lehr, Meszaros, Fuchs (2005))

However, if it can be shown by appropriate tests with single anchors that the concrete cone failure load of headed anchors is reached with a specific bonded anchor system, then the capacity of fastenings with bonded anchors should be limited by the concrete cone capacity of headed anchors.

$$N_u = \min[N_u(Eqn.(6.6)); N_{u,c}(Eqn.(4.9))] \quad (6.7)$$

Fig. 6.27 compares the results of tests with groups of four bonded anchors M12 with the

prediction according to equation (6.6). The calculated failure loads agree well with the test results. All failure loads are much lower than the corresponding concrete cone failure loads of headed anchors.

In Figs. 6.28 to 6.31 the ratios of measured failure loads of groups with two and four bonded anchors and the values calculated according to equation (6.7) are shown as a function of embedment depth, spacing, diameter, and ultimate bond strength. These figures show that the

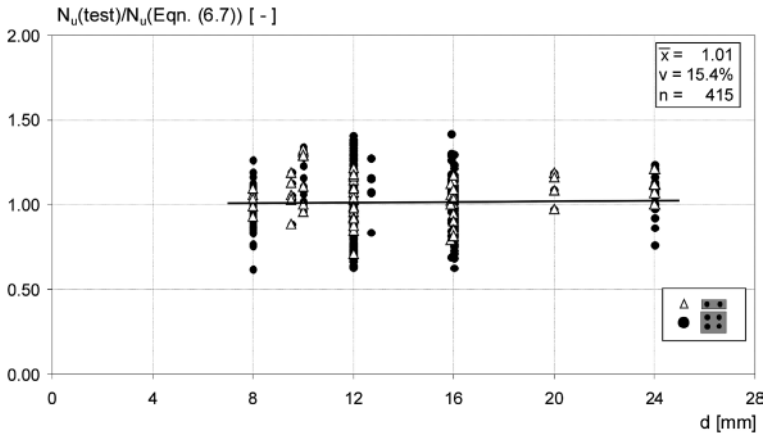


**Fig. 6.30** Ratios of measured failure loads of groups with bonded anchors to values calculated according to equation (6.7) as a function of diameter (*Eligehausen, Appl, Lehr, Meszaros, Fuchs (2005)*)

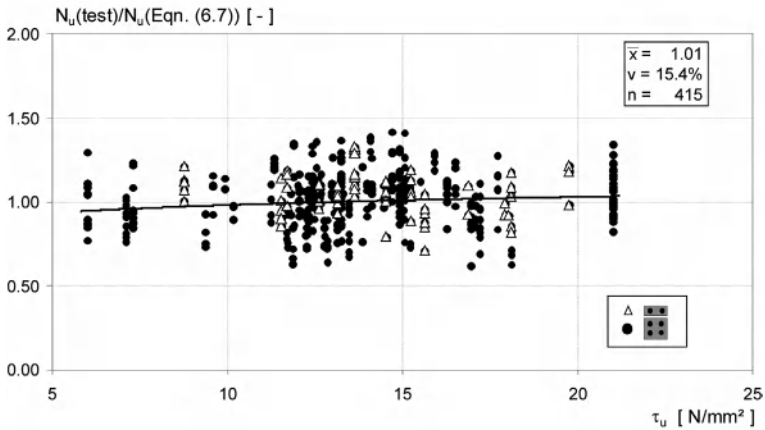


**Fig. 6.31** Ratios of measured failure loads of groups with bonded anchors to values calculated according to equation (6.7) as a function of bond strength (*Eligehausen, Appl, Lehr, Meszaros, Fuchs (2005)*)

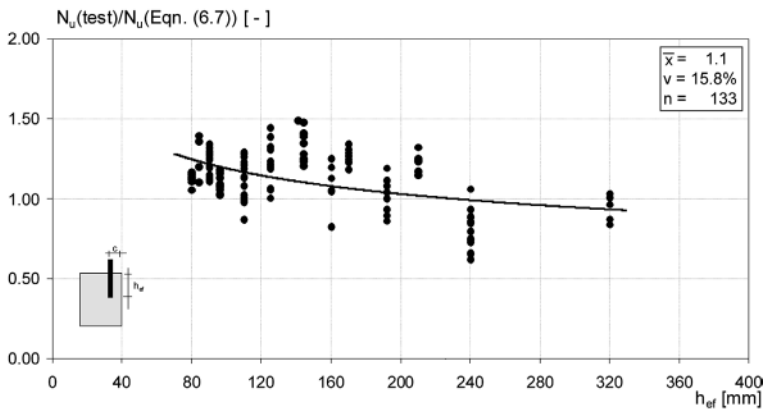


**Fig. 6.32** Ratios of measured failure loads of single bonded anchors at an edge to values calculated according to equation (6.7) as a function of embedment depth (*Eligehausen, Appl, Lehr, Meszaros, Fuchs (2005)*)

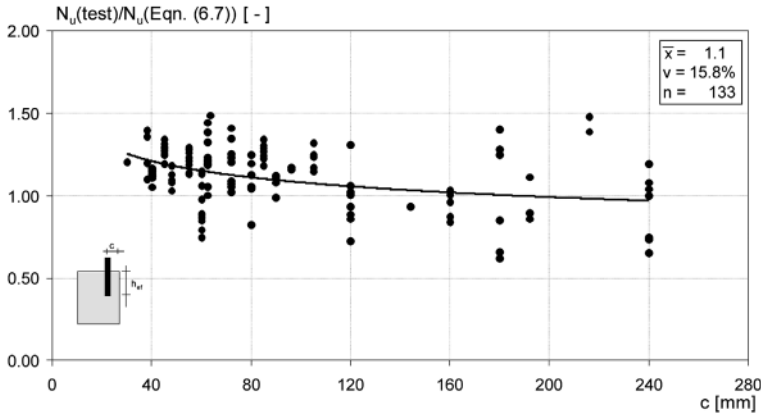


**Fig. 6.33** Ratios of measured failure loads of single bonded anchors at an edge to values calculated according to equation (6.7) as a function of edge distance (Eligehausen, Appl, Lehr, Meszaros, Fuchs (2005))

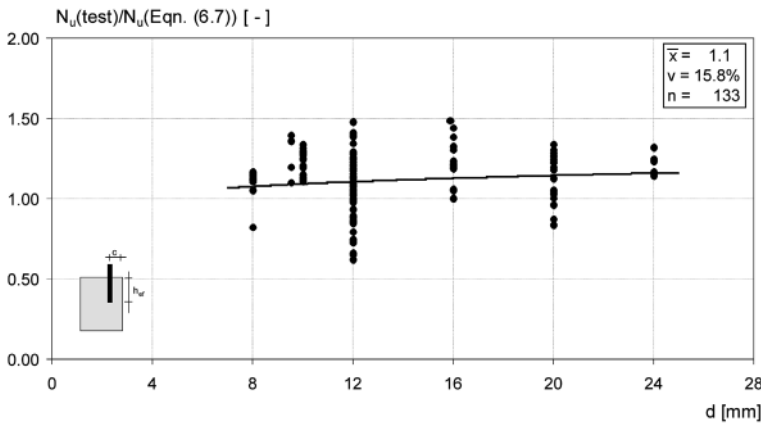


**Fig. 6.34** Ratios of measured failure loads of single bonded anchors at an edge to values calculated according to equation (6.7) as a function of diameter (Eligehausen, Appl, Lehr, Meszaros, Fuchs (2005))

failure load of groups are predicted by equation (6.7) with sufficient accuracy and the influences of the relevant parameters are taken correctly into account. The ratio of measured failure loads of single bonded anchors at an edge and the values calculated according to equation (6.7) are shown in Figs. 6.32 to 6.34 as a function of embedment depth, edge distance, and diameter. The prediction of equation (6.7) is conservative for small edge distances and embedment depths.

Equation (6.7) has the disadvantage that the failure loads of fastenings with bonded anchors must be calculated twice: According to equation (6.6) (bond model) and to equation (4.9) (concrete cone failure of headed anchors). To overcome this disadvantage Eligehausen and Appl currently work on a combined model which describes a continuous transition from the bond model (equation (6.6)) to the concrete cone model (equation (4.9)).

#### 6.1.1.4 Failure load associated with splitting

Bonded anchors loaded in tension generate splitting forces similar to those associated with deformed reinforcing bars. *Comité Euro-International du Béton* (1995) estimates the magnitude of the splitting force as  $F_{sp} \approx 0.5 \cdot N$  (where  $N$  = applied tensile force). No model is yet available for calculating the splitting failure load of bonded anchors. Therefore, the anchor spacings and edge distances, required to prevent splitting during installation (including torquing) and loading of bonded anchors must be determined experimentally.

The following values, which are valid for embedment depths  $h_{ef} \approx 9 \cdot d$  and member thickness  $h = h_{ef} + 50$  mm, should be observed in order to avoid splitting cracks during installation (torquing): min.  $c \approx 0.5 \cdot h_{ef}$  and min.  $s \approx 1.0 \cdot h_{ef}$ .

The spacings and edge distances required to avoid splitting at maximum load are still under investigation. Splitting does not generally control for member thicknesses equal to or greater than  $2 \cdot h_{ef}$  and the failure load may be calculated according to section 6.1.1.3.

### 6.1.2 Shear load

#### 6.1.2.1 Load-displacement behaviour and modes of failure

The load-displacement behaviour of shear loaded bonded anchors generally corresponds to that of headed studs and post-installed metal anchors (expansion and undercut anchors). However, the annular gap between the anchor and the sides of the drilled hole present with post-installed metal anchors does not exist with bonded anchors, provided they are grouted to the concrete surface.

Bonded anchors loaded in shear exhibit the same failure modes associated with headed studs, as well as metal expansion and undercut anchors (Fig. 4.63).

#### 6.1.2.2 Failure load associated with steel failure

The discussion in section 4.1.2.2 generally applies to bonded anchors as well.

#### 6.1.2.3 Failure load associated with pry-out failure

The authors are not aware of investigations regarding the behaviour of bonded anchors exhibiting pry-out failure. It may be assumed, however, that the failure load associated with this failure mode may conservatively be predicted using equation (6.8), which is analogous to equation (4.24).

$$V_{u,exp} = k_1 \cdot N_u \quad (6.8)$$

where:

$$k_1 < 2.0 \text{ for } h_{ef} < 60 \text{ mm}$$

$$k_1 = 2.0 \text{ for } h_{ef} \geq 60 \text{ mm}$$

$$N_u \text{ according to equation (6.7)}$$

It should be noted, however, that pry-out failures are unlikely to occur with groups of four bonded anchors with  $h_{ef} \geq 9 \cdot d$  and threaded rod steel grade 5.8 or A4-70 since this combination of  $h_{ef}/d$  and steel strength will almost always ensure steel failure.

#### 6.1.2.4 Failure load associated with concrete edge breakout

Testing by *Fuchs, Eligehausen* (1989), *Kummerow* (1996) and *Hofmann* (2004) indicates that the CC-Method presented in section 4.1.2.4 for headed studs and post-installed anchors can also be used to predict concrete edge breakout of bonded anchors. According to *Fuchs, Eligehausen* (1989) and *Kummerow* (1996) the diameter  $d_o$  of the drilled hole can be taken for  $d_{nom}$  since the mortar acts to improve load distribution. *Hofmann* (2004) proposes to use the diameter of the rod.

### 6.1.3 Combined tension and shear load

The interaction equations (4.42) and (4.43) presented in section 4.1.3.2 may be used to predict failure loads for bonded anchor under combined tension and shear loading.

### 6.1.4 Sustained and fatigue loading

Owing to variations in their visco-elastic properties, synthetic resins exhibit strength differences under short- and long-term loading. Furthermore, their tensile strength can be affected by environmental factors.

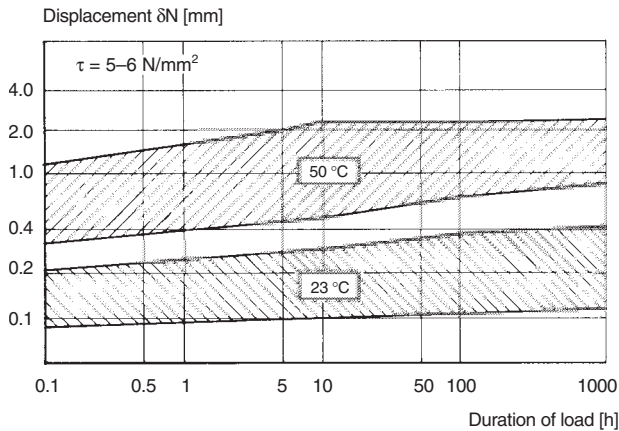


**Fig. 6.35** Displacement behaviour of bonded anchors under constant tension loading at different temperatures in the concrete (Lang (1979))

The long-term behaviour of polyester resin-based bonded anchors was investigated for specific levels of sustained load (*Forschungs- und Materialprüfungsanstalt Baden-Württemberg* (1976, 1980), *Rehm* (1978), *Lang* (1979)). Bonded anchor systems based on vinyl ester resins, both with and without styrene, were investigated at the University of Stuttgart. An increase in displacements occurs under sustained loading for all mortar types (Fig. 6.35). Both initial and final displacements depend on the resin type, the magnitude of the load, and the concrete temperature. Displacement curves tend to flatten out (i.e. become stable) as the test duration increases. Fig. 6.35 applies to bonded anchors exhibiting load-displacement behaviour corresponding to Fig. 6.5a,d. In limited tests performed at the University of Stuttgart on bonded anchors that exhibit load-displacement behaviour corresponding to Fig. 6.5b or 6.5c, it was found that much larger increases in the displacement occur when the sustained load exceeds the adhesion resistance.

Anchors exhibiting load-displacement behaviour as shown in Fig. 6.5a or 6.5d did not fail when subjected to sustained loads equal to 0.5 times the short-term failure load for up to roughly 1,000 hours at room temperature (*Lang* (1979)). Tests at the University of Stuttgart resulted in no pull-out failures for load durations up to 5,000 hours at load levels corresponding to 40% of the average short-term failure load. An assessment of results of sustained

load tests on polymer resin concrete compression specimens, reactive resin concrete joints and reinforcing dowel bars in polymer concrete as described by *Rehm, Franke* (1978), *Jagfeld* (1980), *Rehm, Franke, Zeus* (1980) and *Rehm, Franke* (1982) indicates that the long-term bond strength of unsaturated polyesters, vinyl esters and epoxy resins can be taken as roughly 60% on average of the short-term bond strength (*Rehm* (1978)). In the absence of failure under long-term loading, the residual bond strength as assessed in subsequent loading to failure is not noticeably reduced by the preceding sustained loads (*Rehm* (1978), *Lang* (1979)).

The bond strength decreases as the temperature increases (Fig. 6.19). It may be assumed that the ratio of long-term to short-term strength at temperatures up to approximately 80 °C is more or less unaffected by the ambient temperature.

Section 4.1.6 describes the fatigue behaviour of threaded rods. The fatigue behaviour of the bond between anchor rod and grout or grout and concrete has been investigated with limited testing (*Kobarg* (1982), *Spieth, Eligehausen* (2000), *Kunz* (2003)). The tests were arranged in such a way that failure occurred by pull-out. The results indicate that, in principle, the behaviour found with cast-in-place reinforcing bars also applies to threaded rods anchored with synthetic resins. This is shown in Fig. 6.36, which shows the ratio  $N_{max} / N_u$  as a function of the logarithm of the number of load cycles at fail-

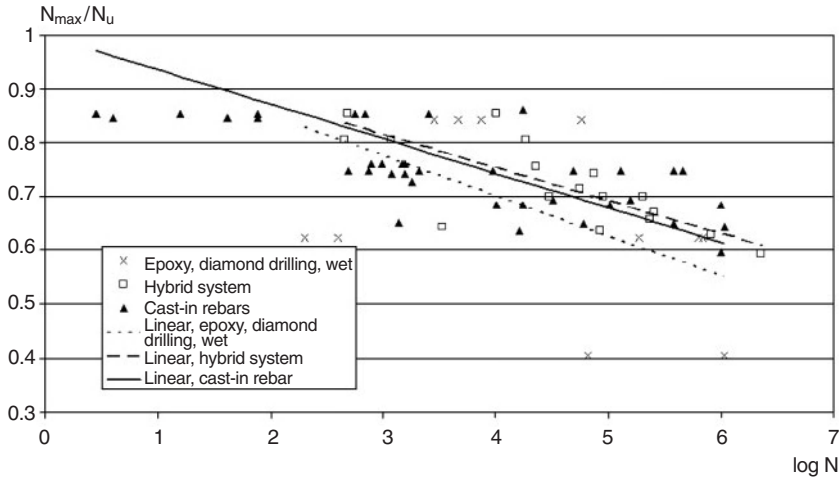


**Fig. 6.36** Ratio  $N_{max}/N_u$  as a function of number of load cycles at failure (Kunz (2003))

ure for a specific epoxy and hybrid system. For comparison the results of tests with cast-in bars (Rehm, Eligehausen (1979)) are shown as well. The ratio  $N_{min}/N_u$  was smaller than 0.1. The behaviour can be summarised as follows. The bond fatigue strength for  $2 \cdot 10^6$  load cycles is approximately 60 % of the short-term bond strength. For the epoxy resin anchored in wet diamond cored holes the fatigue strength was slightly lower. If fatigue failure does not occur, the residual bond stress measured in a subsequent short-term test to failure is not reduced compared to the value without prior fatigue loading.

### 6.1.5 Environmental factors

The discussion of section 6.1.4 regarding sustained loads applies to bonded anchors in dry interiors at a constant temperature. Anchors in exterior applications can be exposed to variations in the moisture content of the concrete, as well as temperature fluctuations and freeze-thaw cycles. Furthermore, they may be subjected to aggressive (reactive) substances.

Long-term tests on bonded anchors using unsaturated polyester resin installed in the open air and subjected to freeze-thaw cycles and moisture under a load corresponding to an average bond stress of  $\tau = 3.5 \text{ N/mm}^2 \approx 0.3\tau_u$  have

shown no indication of failure over a loading period of up to seven years (Rehm (1985/1)). However, the measured residual short-term bond strengths were reduced. This is shown in Fig. 6.37, in which the ratio of pull-out load after a loading time  $t$  to the initial value ( $t = 0$ ) is plotted over time. The anchors were installed at various geographic locations. A constant tension load corresponding to  $\tau = 3.5 \text{ N/mm}^2 \approx 0.3 \tau_u$  was applied at test locations 1 to 3. At the other locations the anchors were subjected to a service load the magnitude of which is not known. Each location represented a different climatic exposure. The anchors at test locations 1 to 3 and 8 were installed in unprotected external locations, at locations 4 and 5 they were permanently submerged in water, at location 6 the anchors were within the tidal range of a breakwater and at test location 7 in a tunnel. The reduction in the pull-out loads may be due to alkalis attacking the polyester resin. According to the findings the bond strength decreases after a long period to, on average, approximately 60%, and in isolated cases approximately 30%, of the initial value.

According to Rehm (1985/2 and 1988) vinyl ester resins are far less sensitive to climatic conditions than unsaturated polyester resins. Environmental factors (e.g. moisture) can lead to a maximum  $\approx 10\%$  decline in bond strength.

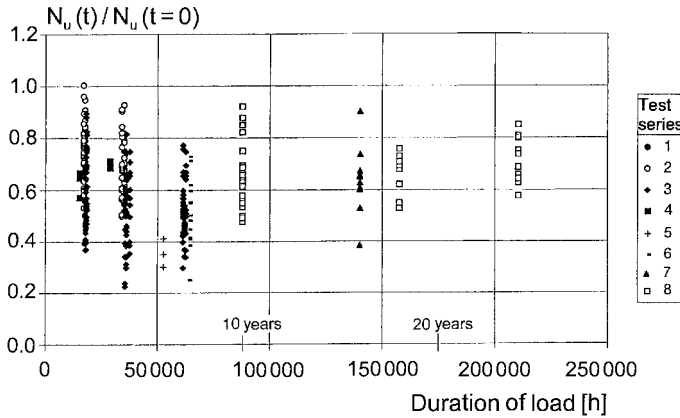


**Fig. 6.37** Ratio of pull-out load after loading over a time  $t$  to the initial value ( $t = 0$ ) as a function of time (anchors were installed at various geographic locations) (results of tests with bonded anchors based on unsaturated polyester resin, after *Rehm (1985/1), Rehm (1986)*)

The foregoing discussion concerning long-term behaviour of bonded anchors is confirmed by results of freeze-thaw tests. M12 bonded anchors were subjected to sustained loading equal to 1.35 times the permissible load and the surface of the concrete was covered with water. While the displacements of anchors using unsaturated polyester resin gradually increased with the number of freeze-thaw cycles, the increase in displacements for anchors based on vinylester resin stabilised after approximately 40 freeze-thaw cycles (*Fig. 6.38*).

The environmental influence on the behaviour of bonded anchors based on epoxy resin depends on the formulation of the resin. Therefore it should be checked by tests.

Sulphur and nitrogen in concentrations as encountered in the atmosphere do not appear to have a significant influence on the bond strengths of bonded anchors approved for use in Europe.

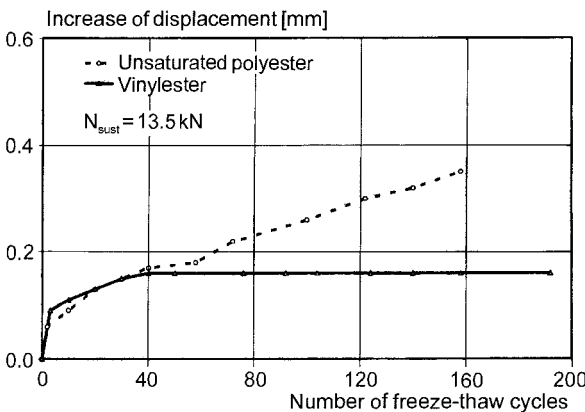


**Fig. 6.38** Increase of displacements of bonded anchors M12 loaded with a constant tension load as a function of number of freeze-thaw cycles (*Rehm (1985/1), Rehm (1985/2)*)



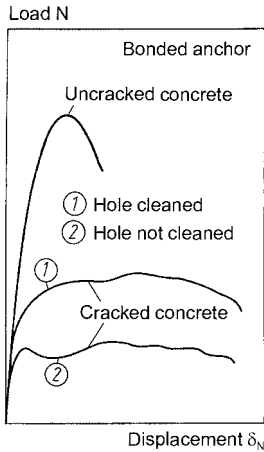


**Fig. 6.39** Load-displacement curves of bonded anchors in non-cracked and cracked concrete (schematic) (Eligehausen, Mällée, Rehm (1997))

## 6.2 Cracked concrete

### 6.2.1 Tension load

#### 6.2.1.1 Load-displacement behaviour and modes of failure

Depending on embedment depth, concrete strength, and grade of steel, bonded anchors in cracked concrete loaded in tension to failure exhibit steel rupture, pull-out or mixed failure (compare Fig. 6.1). Pull-out failure is usually a consequence of loss of bond between mortar and drilled hole, although with some systems the bond between mortar and anchor rod may fail. Anchors located close to an edge may generate splitting failures. Concrete cone failures in cracked concrete testing are rarely observed.

Fig. 6.39 shows schematic load-displacement curves for bonded anchors in cracked and non-cracked concrete. As with other anchor types, the anchor stiffness in cracked concrete is lower than it is in non-cracked concrete. After the bond between mortar and concrete is lost, the anchor rod and adhering mortar are extracted from the hole, whereby a further increase in load may occur at large slip (Fig. 6.39, curve 1). This is attributable to the friction between the mortar mass and the uneven hole surface. As the frictional resistance is strongly influenced by hole surface geometry, it is associated with a

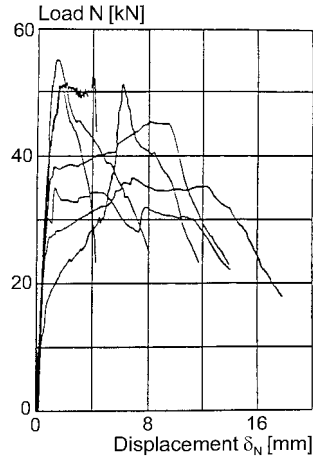


**Fig. 6.40** Load-displacement curves of capsule type bonded anchors M12,  $h_{ef} = 110$  mm in cracked concrete ( $f_c \approx 25$  N/mm<sup>2</sup>,  $\Delta w \approx 0.4$  mm) (Dieterle, Opitz (1988))

high degree of variability and leads to highly unpredictable load-displacement behaviour following initial bond loss (Fig. 6.40).

Inadequate hole cleaning may lead to further reductions in ultimate tension capacity (curve 2 in Fig. 6.39). The degree of influence that hole cleaning has on the pull-out load is product-dependent (see section 6.1.1.3) and tends to be more severe in cracked concrete than in non-cracked concrete (Eligehausen, Meszaros (1996)). Not cleaning the drilled hole can lead to tension failure load reductions of up to 60% for injection-type anchors (Fig. 6.41). It may be

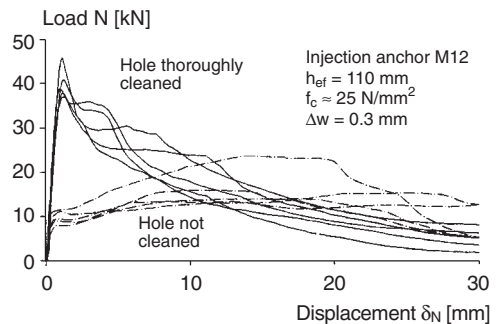


**Fig. 6.41** Load-displacement curves of injection type bonded anchors M12,  $h_{ef} = 110$  mm, anchored in cracked concrete, drill holes well-cleaned and uncleaned (Meszaros, Eligehausen (1996/1))

assumed that capsule anchors that are set with only hammering action are similarly affected. When installed with careful attention to hole cleaning (e.g. brushing followed by blowing) the system illustrated in Fig. 6.41 exhibits bond failure at the interface between anchor rod and mortar, which explains both the uniform load-displacement performance, as well as the precipitous drop in load following bond failure. Conversely, when the hole is not adequately cleaned the bond failure occurs at the mortar/concrete interface, leading to greater scatter in the post-elastic response. Depending on resin type, injection anchors and hammer-in type capsule anchors can exhibit marked capacity reductions when installed in holes that have been only blown out with compressed air but not brush cleaned (see Fig. 6.14). Capsule anchors that are installed with both rotary and hammer action display far less sensitivity to this condition for the reasons already discussed in section 6.1.1.3.

### 6.2.1.2 Failure load corresponding to steel failure

The discussion provided in section 4.1.1.2 is generally applicable to bonded anchors as well.

### 6.2.1.3 Failure load corresponding to pull-out failure

Fig. 6.42 presents the ratio of tension failure loads for bonded anchors tested in cracks to their mean capacity in non-cracked concrete, plotted as a function of crack width. The tests were conducted using both capsule-type anchors and injection anchors. The mortar was based on unsaturated polyester resin, vinylester resin, or vinylester resin with cement (hybrid systems). The cracked concrete testing was conducted mainly in tension test specimens, but some tests were performed in flexural members. The anchors were installed in hairline cracks that were subsequently opened to the desired width. The anchors were then loaded to failure with the cracks open. The scatter of the results of tests in cracked concrete is rather large. This is mainly caused by the irregular position of the crack with respect to the anchor, i.e. the crack may deviate from the plane of the anchor axis.

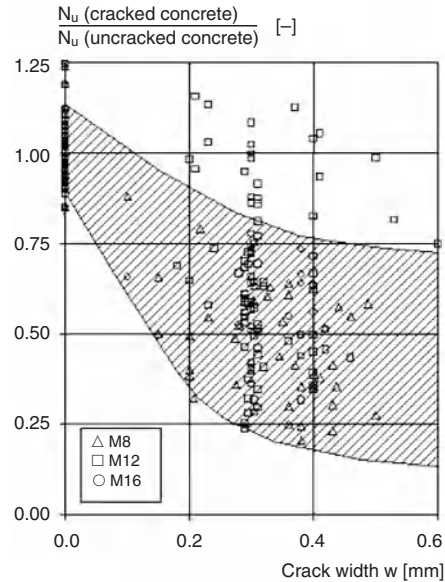


**Fig. 6.42** Influence of crack width on the failure load of bonded anchors (Meszaros (1999))

If the results of tests with a ratio  $N_u(\text{cracked concrete}) / N_u(\text{non-cracked concrete}) > 0.8$  are neglected (because in these tests it may be assumed that only the upper part of the anchor was located in the crack) then the anchor capacities in cracked concrete with a crack width  $\Delta w \approx 0.3$  mm to 0.4 mm is about 25% to 80% of the value valid for non-cracked concrete. On average the ratio is about 50%.

This large reduction of the tension capacity by cracks can be explained as follows. Owing to the high tensile strength of the polymer mortars used in the bonded anchor systems tested, crack opening after anchor installation results in the redirection of the crack around the anchor along the interface between mortar and concrete, effectively causing bond loss on *one* side of the anchor (Fig. 6.43). Assuming that the crack trajectory as shown in Fig. 6.43 occurs over the full embedment depth, the bond capacity is theoretically 50% of the capacity in non-cracked concrete. An additional effect of the bond loss associated with the crack opening is the eccentricity between the tensile load and the resultant of the bond resistance. This secondary moment

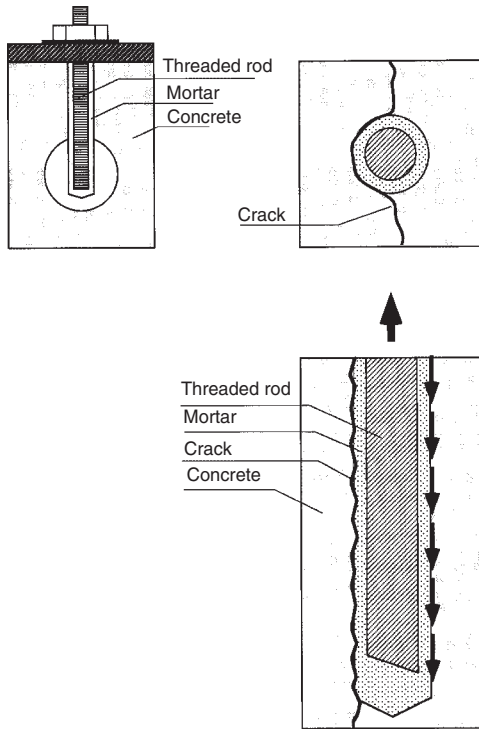


**Fig. 6.43** Disturbance of bond between mortar and concrete by a crack

generates tensile stresses perpendicular to the bond interface, which should act to further reduce the bond capacity. In theory, therefore, the pull-out load in cracked concrete should be somewhat less than 50 % of the value in non-cracked concrete. Extensive testing of bonded anchors in cracks yields, however, a pull-out capacity that is, on average, 50 % of the mean capacity in non-cracked concrete. This may be due to the additional capacity afforded by the frictional resistance between the mortar mass and the concrete following loss of adhesion resistance.

Bonded anchors tested in cracks exhibit considerably greater variation in load-displacement behaviour compared to anchors in non-cracked concrete. This can be attributed to the fact that the trajectory of the crack around the circumference of the hole and along the embedment depth varies considerably from test to test. In addition, the frictional resistance after loss of adhesion

resistance is sensitive to the unique geometry of the hole.

According to the knowledge of the authors, tests with bonded anchors where failure in cracked and non-cracked concrete is characterised by loss of bond between the anchor rod and mortar have not yet been performed. In this case cracking will also result in a reduction in failure load since the resistance to lateral strain of the mortar is diminished due to the presence of the crack. However, a smaller reduction than given above may be expected. In the best case the behaviour may be similar to cast-in-place rebars, which show a reduction by approximately 20 % to 30 % in cracks with  $w \approx 0.3$  mm (Eibl, Idda, Lucero-Cimas (1997)).

Variations in crack width over time, whether as a result of fluctuating structure loads or alternating (seismic) shear, will cause further reductions in anchor capacity. Testing by Cannon (1981), in which beam members containing anchors were loaded cyclically in flexure, indicated that bonded anchor pull-out can result in cracked concrete when the anchor is loaded with the allowable load for non-cracked concrete.

#### 6.2.1.4 Failure loads corresponding to concrete cone failure and splitting of the concrete

Concrete cone failures of single bonded anchors in cracks have generally not been observed. However, concrete cone failure may occur with groups with small spacing or with fastenings close to an edge. To the authors' knowledge, no research has been performed on these applications. The authors assume that equation (6.7) can be applied provided the bond strength valid for cracked concrete is used.

Bonded anchors installed in members with limited thickness and/or provided with small edge distance will split the concrete as a result of the circumferential tensile stresses associated with bond. If the concrete is reinforced adequately to resist the splitting forces and to control the crack widths, then the discussion provided in section 6.2.1.3 regarding pull-out behaviour generally applies. If the concrete is either unreinforced or provided with minimum

reinforcement, the onset of splitting defines the ultimate capacity and section 6.1.1.4 is applicable.

**6.2.2 Shear load**

Shear testing of anchors in cracks by *Fuchs, Eligehausen (1989)* and *Vintzeleou, Eligehausen (1991)* indicates that cracks have only a minor influence on the stiffness of bonded anchors. Provided the edge distance and embedment depth are sufficient, failure is characterised by steel failure, and the failure load is not significantly influenced by cracking (<10%). As with headed studs and expansion anchors, bonded anchors located near an edge and loaded in shear towards the edge generate concrete edge breakout failures. Limited testing by *Fuchs, Eligehausen (1989)* indicates that the reduction in the concrete edge failure load caused by cracks tends to be somewhat larger than it is for headed studs or expansion and undercut anchors (compare Figs. 6.44 and 4.147).

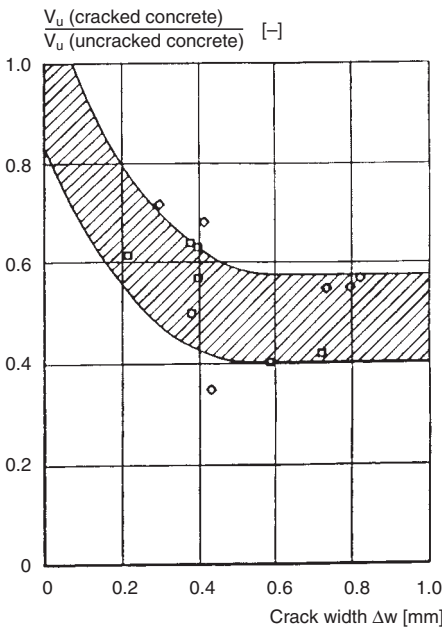
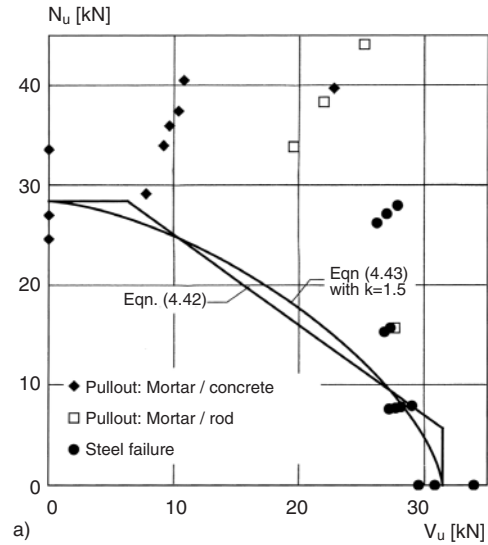
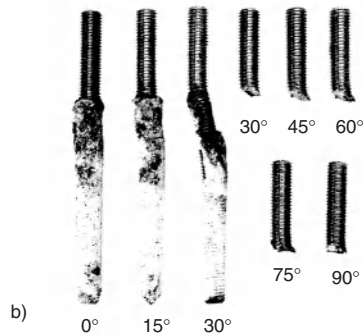


**Fig. 6.44** Influence of crack width on the concrete edge failure load of bonded anchors loaded in shear towards the edge (*Fuchs, Eligehausen (1989)*)



a)



b)

**Fig. 6.45** Bonded anchors M12,  $h_{ef} = 110$  mm under combined tension and shear loads in cracked concrete ( $f_c \approx 23$  N/mm<sup>2</sup>,  $\Delta w = 0.4$  mm) (*Dieterle, Bozenhardt, Hirth, Opitz (1990)*)

- a) Interaction diagram
- b) Photos of anchors after tests (0° = tension, 90° = shear)

**6.2.3 Combined tension and shear load**

*Dieterle, Bozenhardt, Hirth, Opitz (1990)* investigated the behaviour of M12 bonded anchors (capsule anchors utilising vinylester resin) subjected to combined tension and shear loads in cracked concrete. The tests were carried out in tension test members. After installing the anchors in thoroughly cleaned holes, the cracks were opened by  $\Delta w = 0.4$  mm. Under predominantly tensile loading, bond failure

occurred between mortar and concrete (Fig. 6.45b). With the load applied at an angle of  $30^\circ$ , bond failure between anchor rod and mortar or between mortar and concrete was observed. At angles  $\geq 45^\circ$  failure was exclusively due to rupture of the steel. Up to an angle of  $30^\circ$  the tension component of the failure load exceeded the pull-out load corresponding to concentric tension (Fig. 6.45a), a consequence of the friction forces resulting from the shear component of the load. Failure loads can be conservatively predicted with either equation (4.42) or equation (4.43) with  $k = 1.5$  (Fig. 6.45a).

The behaviour of bonded anchors installed in inadequately cleaned holes and subjected to combined tension and shear loading has not been investigated. However, if the tension pull-out load is influenced significantly by the type and degree of hole cleaning, then a behaviour similar to that shown in Fig. 4.150 should be anticipated when the anchor is subjected to combined tension and shear.

### 6.2.4 Sustained and fatigue loads

To the knowledge of the authors test results are not available for bonded anchors subjected to sustained and fatigue loads in cracked concrete. If the magnitude of the sustained load (in the case of fatigue loading, the peak load) remains below  $\sim 60\%$  of the load needed to overcome the bond between mortar and concrete, the behaviour should not differ significantly from that observed in non-cracked concrete (see section 6.1.4). Under higher levels of sustained or fatigue loading, large increases in displacement, possibly leading to pull-out failure, may be expected.

When bonded anchors are positioned in cracks and subjected to a constant tension load, the displacements increase as the crack in the base material is opened and closed several times. If the tension load is well below that required to overcome the adhesion resistance between mortar and concrete, then only a small increase in displacements should be expected (*Opitz, Eligehausen* (1989)). With increasing load, pull-out failure may occur after only a few crack cycles.

## 6.2.5 Environmental factors

In general, the discussion provided in section 6.1.5 is applicable to the case of bonded anchors in cracks. However, it is highly probable that the bond strength in cracked concrete will be more severely affected by environmental factors than in non-cracked concrete due to the greater access of aggressive media afforded by the presence of the crack.

## 6.3 Bonded undercut anchors and bonded expansion anchors

### 6.3.1 Non-cracked concrete

In non-cracked concrete, the behaviour of bonded undercut and expansion anchors subjected to tension loading does not differ significantly from that of common types of bonded anchors. With respect to hole cleaning, however, the undercut or expansion action associated with these systems has a beneficial effect. Assuming sufficient debris has been removed from the hole to permit installation of the anchor to the desired embedment, hole cleaning has only a minor influence on the load-bearing behaviour of these anchors since they function as undercut or expansion anchors once the bond between mortar and concrete is lost. The effects of temperature, sustained loading and environmental aggressors on the load-bearing behaviour of bonded undercut and expansion anchors are similar to those addressed for conventional bonded anchor systems (see sections 6.1.3, 6.1.4, and 6.1.5).

Bonded undercut and expansion anchors subjected to shear loads behave in a manner similar to conventional bonded anchor types.

### 6.3.2 Cracked concrete

#### 6.3.2.1 Tension load

Fig. 6.46 compares load-displacement curves for bonded expansion anchors without prestressing subjected to tension loading in cracked and non-cracked concrete. As with expansion anchors, both stiffness and ultimate load are decreased in cracked concrete. Bonded undercut anchors exhibit similar behaviour.

In principle, the failure modes depicted in Fig. 4.1 are applicable to bonded undercut and

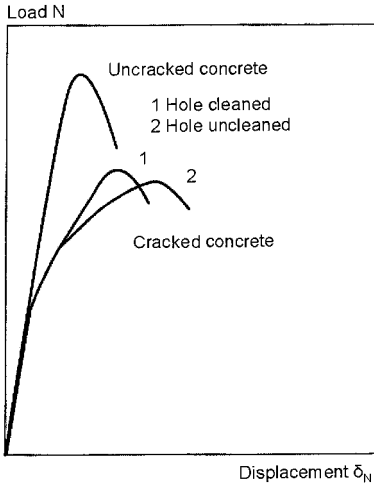


**Fig. 6.46** Load-displacement curves of bonded expansion anchors in non-cracked and cracked concrete (schematic)

expansion anchors. Bonded expansion anchors may fail by pull-through if the mortar between the conical projections is sheared off and the anchor element is pulled through the mortar.

As with a conventional bonded anchor, a crack passing through the mortar-concrete interface of a bonded undercut or expansion anchor can lead to bond loss. A bonded undercut anchor that suffers bond degradation under tension loading will subsequently transfer the load to the concrete via the undercut (Fig. 6.47). In the case of bonded expansion anchors, however, loss of bond leads to the formation of radial cracks in the mortar annulus as the anchor element is pulled into the mortar mass and expands the mortar segments against the wall of the hole (Fig. 6.48). This mechanism may be compared to the follow-up expansion normally associated with metal torque-controlled expansion anchors, and is effective in bridging normal crack widths. The onset of anchor expansion can be identified by the kink in each load-displacement curve shown in Fig. 6.46. Expansion force and associated friction resistance is developed between the mortar segments and the concrete and these friction forces are sufficient to transfer the applied tension without participation of bond. If the force required to break the bond between the anchor element and the mor-

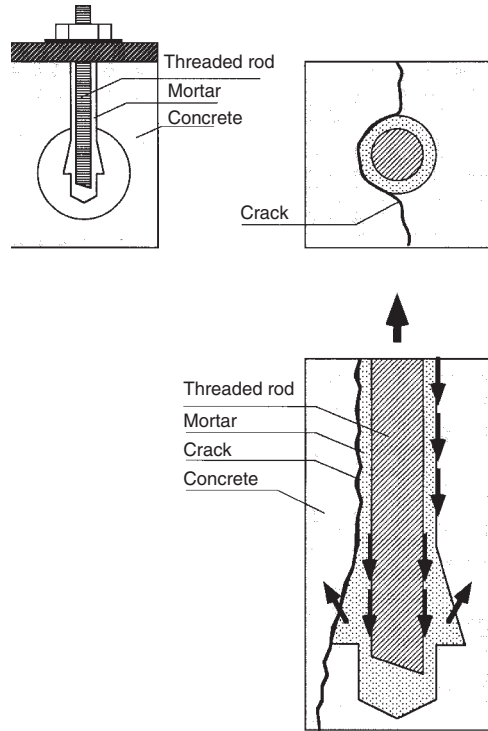


**Fig. 6.47** Disturbance of bond between mortar and concrete by a crack and transfer of a tension load with bonded undercut anchors

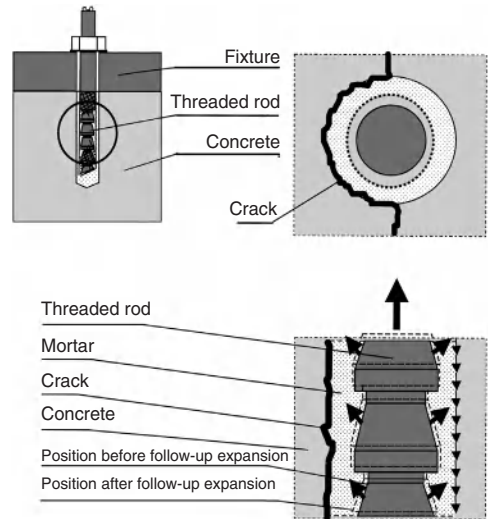


**Fig. 6.48** Disturbance of bond between mortar and concrete by a crack and transfer of a tension load with bonded expansion anchors

tar is sufficiently low, a bonded expansion anchor exhibits follow-up expansion even in an inadequately cleaned hole and reaches the same ultimate capacity as in thoroughly cleaned holes (Fig. 6.46).

Bonded undercut and expansion anchors that function according to these principles are generally suitable for applications in cracked concrete.

In absence of steel rupture, bonded undercut anchors generally exhibit concrete cone breakout when loaded in tension to failure. In cracked concrete the failure loads may be expected to reflect a reduction similar to that found for headed studs and conventional undercut anchors (see Fig. 4.127). For a crack width  $w =$

0.3 mm, the reduction in tension capacity may be taken as 25 %. Bonded expansion anchors in cracked concrete fail via pull-through of the anchor element through the mortar segments. Failure loads for bonded expansion anchors are reduced approximately 30 % in concrete with cracks of a width  $w \approx 0.3$  mm.

### **6.3.2.2 Shear and combined tension and shear load**

When subjected to shear or combined tension and shear loading, bonded undercut and expansion anchors behave in a manner essentially similar to conventional expansion and undercut anchors. Sections 4.2.2 and 4.2.3 address these loading cases.



## 7 Behaviour of plastic anchors in non-cracked and cracked concrete

A plastic anchor consists of a plastic anchor sleeve and a steel expansion element (tapered screw or profiled nail). Insertion of the screw into the sleeve cuts a thread into the plastic and forces the sleeve against the wall of the drilled hole. Hammering in a nail into the sleeve displaces the material in a similar fashion. An expansion force is created by expanding the sleeve which presses the sleeve against the wall of the hole. The distribution and magnitude of this contact pressure are dependent on the design of the anchor.

The load-bearing behaviour of plastic anchors is mainly dependent on the particular polymer material used for the anchor sleeve. The studies discussed in this chapter were conducted with anchors fabricated from modified polyamides 6 and 66 (Ultramid® B3L and B3S, Durethan® BC30, Grilon® A28DZ, Maranyl® XA328) and designed for use with screws.

### 7.1 Non-cracked concrete

#### 7.1.1 Tension load

External loads are transferred from the screw to the anchor sleeve by virtue of the thread cut into the plastic material, and from the sleeve to the base material primarily via friction. A limited form of mechanical interlock may occur between the sleeve and the base material if the plastic adapts to the unevenness of the sides of the drilled hole over the course of time (Ehrenstein (1976/2)).

The distribution of expansion forces generated by plastic anchors along the anchor axis and their magnitude depend on the design of the anchor and is therefore product-dependent. The expansion forces are generally not sufficient to initiate concrete cone failure of single anchors. The predominant tension failure mode of the plastic anchors is pull-out of the expansion ele-

ment from the base material. Concrete cone failure may occur with anchor groups with small spacing.

Fig. 7.1 illustrates typical load-displacement curves of a qualified plastic anchor with diameter  $d_{nom} = 10$  mm and embedment depth  $h_{ef} = 70$  mm. The initial part of the load-displacement curve is nearly linear. If the tension load exceeds the static friction between the anchor sleeve and the hole wall, the resistance drops rapidly to a level corresponding to the dynamic friction with correspondingly large displacements.

Pull-out loads achievable with plastic anchors are dependent on the level of expansion force  $F_{ex}$  generated during insertion of the screw into the anchor sleeve and the coefficient of friction  $\mu$  between sleeve and concrete:

$$N_u = \mu \cdot F_{ex} \quad (7.1)$$

The magnitude of the expansion force is influenced by the design of the anchor including the relative diameter of screw (minor diameter) and inside diameter of the plastic sleeve. Also the

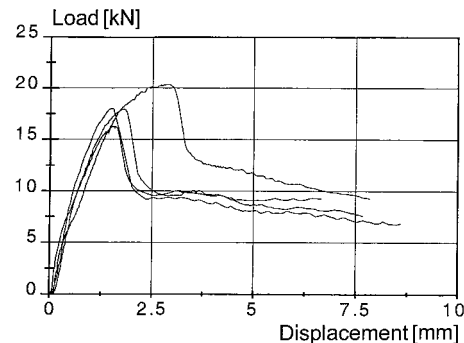


Fig. 7.1 Load-displacement curves of plastic anchors with  $d_{nom} = 10$  mm and  $h_{ef} = 70$  mm

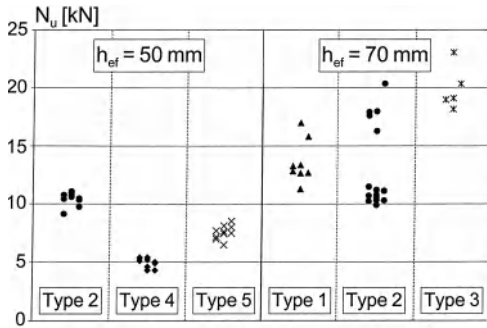


Fig. 7.2 Pull-out loads of different types of plastic anchors with  $d_{nom} = 10$  mm

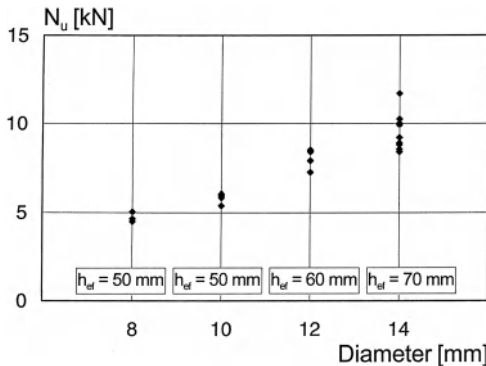


Fig. 7.3 Pull-out loads of a particular type of plastic anchor as a function of the anchor diameter

coefficient of friction is influenced by the design of the anchor. There are very many designs of plastic anchors available and pull-out loads of plastic anchors having the same diameter vary widely between manufacturers. This is shown in Fig. 7.2, in which the pull-out loads of plastic anchors of diameter  $d_{nom} = 10$  mm are plotted for various anchor manufacturers.

Pull-out resistance for plastic anchors generally increases with increasing anchor diameter (Fig. 7.3). Note that in Fig. 7.3 for anchors with  $d_{nom} \geq 12$  mm the failure loads are also influenced by the larger embedment depth.

Manufacturing tolerances of plastic anchors are typically small and do not have an influence on the anchor capacity. In contrast, screw tolerances can have a very marked effect on capacity. Standards governing common wood screws

such as slotted countersunk screws and hexagon-head wood screws do not control the dimensional tolerances (minor diameter, thread form, tip geometry) relevant to the load-bearing behaviour of plastic anchors. Manufacturing tolerances for these products are large and pull-out loads show a correspondingly wide scatter (Plank (1977)). To rule out or minimise the effects of screw tolerances, matched screws are required for approved plastic anchors in Europe.

The degree to which the screw is inserted into the plastic sleeve is an important factor for tension capacity. This is demonstrated in Fig. 7.4, which presents the results of tension tests wherein the degree of screw insertion has been systematically varied for a plastic anchor with  $d_{nom} = 10$  mm. As the degree of screw insertion is reduced the generated expansion force generally falls disproportionately. For the anchors tested, screw insertion 10 mm less than the specified depth leads to a mean capacity drop of approximately 30%. The influence of the depth of the screw insertion is considerably greater with smaller diameter anchors (Güth (1982)).

A plastic anchor is susceptible to inadequate screw insertion if (a) the screw is too short or (b) if the anchor sleeve is pushed too far into the hole during installation of the screw (Fig. 7.5). The first problem may be avoided by using screws that are dimensionally matched to the sleeve. The second problem is overcome by using anchor

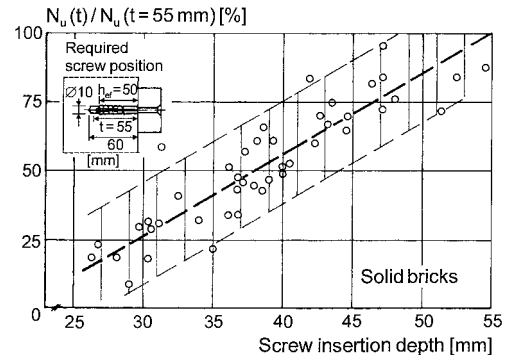
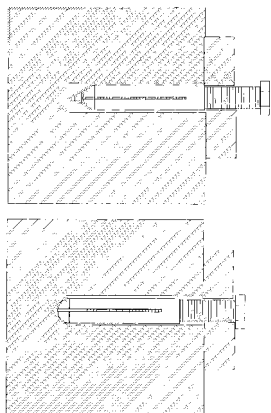


Fig. 7.4 Influence of screw insertion depth on the pull-out failure load of plastic anchors with  $d_{nom} = 10$  mm (Plank (1977))



**Fig. 7.5** Reduction of screw insertion depth by pushing the sleeve too far into the hole  
 a) Correct anchor installation  
 b) Installation with sleeve pushed too far into the hole

systems equipped with a collar at the top of the sleeve that prevents it from being driven too deep into the base material (see Fig. 2.49).

As discussed before, the capacity of plastic anchors with the same diameter and embedment depth from different manufacturers varies widely. In Europe this problem is addressed through the approval process, whereby only approved anchors whose suitability and load capacity have been verified are permitted for general building construction. Owing to choice of materials, optimisation of expansion forces through coordinated sleeves and screws, and installation instructions, these anchors are highly reliable when used for their intended applications.

The load-carrying capacity of approved systems depends on installation tolerances – particularly hole diameter and embedment depth – as well as on the moisture content and temperature of the plastic sleeve.

Fig. 7.6 shows the influence of the drill bit diameter (diameter of cutting tip  $d_{cut}$ ) on the tension capacity of plastic anchors with a sleeve diameter of 10 mm. The capacity drops as the bit diameter increases because the expansion force is diminished. For example, if for the installation of an approved plastic anchor an 11 mm drill bit is used instead of the specified 10 mm bit, the failure load may drop to 30 % of the normal value. The influence of the drill bit

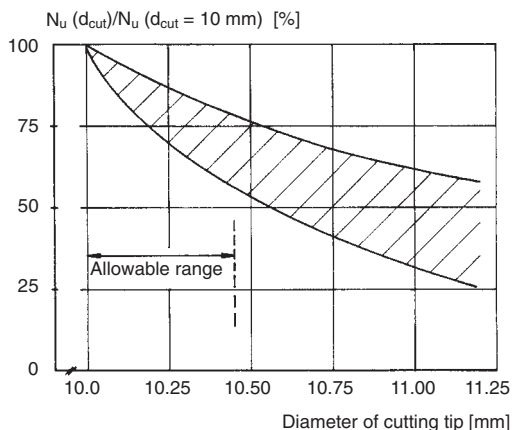


**Fig. 7.6** Influence of the diameter of the drill bit cutting tip on the pull-out failure load of plastic anchors with  $d_{nom} = 10$  mm (after Ehrenstein (1976/2), Plank (1977), Rehm Eligehausen, Mällée (1988))

is even greater for smaller diameter anchors (Güth (1982)). Therefore, holes for plastic anchors should only be drilled with matched tolerance drill bits.

The second major factor in determining plastic anchor tension capacity is the embedment depth. Even with correct screw insertion, reduced embedment has a marked influence on the failure load (Fig. 7.7) since the available friction surface decreases. Testing with a partic-

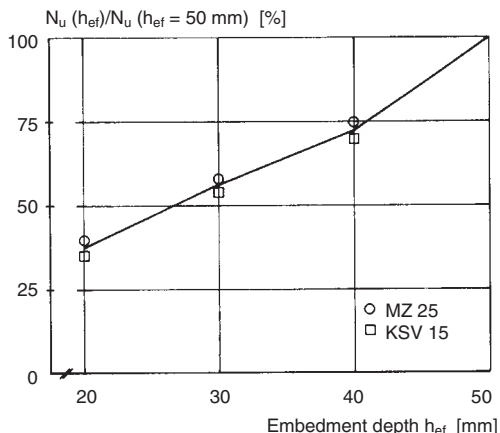


**Fig. 7.7** Influence of embedment depth on the pull-out failure load of plastic anchors with  $d_{nom} = 10$  mm (Plank (1977))

ular 10 mm plastic anchor revealed a roughly 25 % reduction in the load-carrying capacity for an embedment reduction of 20 % (from 50 mm to 40 mm). The results shown in Fig. 7.7 were obtained from tests in solid masonry units, but they may also be assumed to apply to applications in concrete.

Reduced embedment depth may result from a variety of circumstances, such as incorrect assessment of the thickness of a non-load-bearing layer through which the anchor must penetrate (e.g. plaster, insulation) (compare Fig. 2.18), incorrect determination of the fastened component thickness, or a drilled hole depth that is insufficient for the length of the anchor.

As shown in Fig. 7.8 the pull-out load decreases as the moisture content of the anchor sleeve increases. A moisture content of 0 % is possible after a sufficiently long period of storage in dry conditions whereas a moisture content of about 8 % to 9 % may be expected after the sleeve has been immersed in water for a long time. However, these moisture contents should be regarded as extreme values. The influence of the moisture content on the pull-out load of the anchor is negligible under the conditions to be expected in practice (moisture content  $f \approx 2\%$  to 3 %).

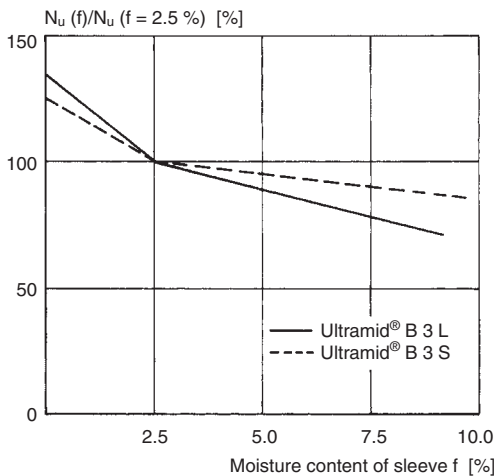


**Fig. 7.8** Influence of moisture content of plastic sleeve on the pull-out failure load of plastic anchors (Ehrenstein (1976/1) and (1976/2))

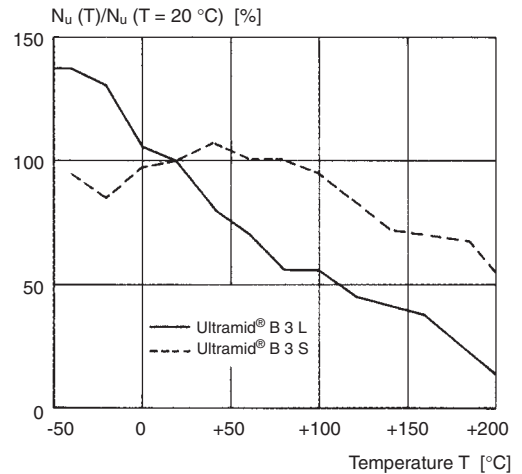


**Fig. 7.9** Influence of concrete temperature on the pull-out failure load of plastic anchors (Ehrenstein (1976/1) and (1976/2))

Fig. 7.9 shows how temperature variations affect the pull-out loads of plastic anchors differently depending on the material used in their manufacture. Anchors made from Ultramid® B3L show a continuous decrease in tension capacity as the temperature is increased from – 50 °C to + 200 °C because the stiffness of the material and hence the contact pressure between anchor and sides of hole decreases as the temperature increases. In contrast, the pull-out loads derived for anchors made from Ultramid® B3S are more or less constant between about – 40 °C and + 100 °C, and only show steady decrease at temperatures above + 100 °C.

Single anchors close to an edge or groups of plastic anchors with small spacing may fail due to concrete cone failure. The failure load can be calculated in accordance with the CC-method (section 4.1.1.3) if a reduced embedment depth is used in equation (4.10) (Pregartner (2003)). This reduced embedment depth is calculated under the assumption that the measured pull-out failure load of single anchors is equal to the concrete cone failure load according to equation (4.5b). This leads to equation (7.2).

$$h'_{ef} = (N_u / (13.5 \cdot f_{cc,200}^{0.5}))^{2/3} \tag{7.2}$$

where:

$N_u$  = measured pull-out failure load

The ratio  $h'_{ef}/h_{ef}$  depends on the anchor design and anchor diameter and varies between approximately 0.3 and 0.7.

Anchors close to an edge or positioned in narrow and thin components may fail due to splitting of the component. This failure load was observed in tests with groups of four anchors close to an edge or in the corner of a thin concrete member (Pregartner (2003)). To the authors' knowledge no proposal is available for the calculation of the failure load due to splitting.

### 7.1.2 Shear and combined tension and shear load

Plastic anchors with a large edge distance loaded in shear with the load applied at the surface of the base material generally fail due to screw rupture. The mean shear capacity in this case may be estimated from the net cross-section of the screw and the steel strength using equation (4.17) (Pregartner (2003)). If the shear load is applied eccentrically (i.e. at some distance from the surface of the base material), the screw fails in flexure. The failure load can likewise be predicted with equation (4.22). Pry-out failure typically will not occur even with groups with small anchor spacing (Pregartner (2003)).

Plastic anchors loaded in shear towards the edge may fail in consequence of concrete edge failure. The failure load can be calculated according to section 4.1.2.4 (Pregartner (2003)).

The authors do not know of any tests involving combined tension and shear loads. The failure load corresponding to oblique loading can probably be reasonably predicted with interaction equation (4.42) or (4.43) with  $k = 1.5$ .

### 7.1.3 Long-term behaviour

With time, the expansion force that creates a contact pressure between the anchor sleeve and the wall of the hole decreases owing to relaxation of the polyamide. This is shown for a particular anchor in Fig. 7.10, in which the splitting force (which is equal to the integration of contact pressure in one direction, compare Fig. 4.55) is plotted over time. The splitting force falls considerably in the first minutes after

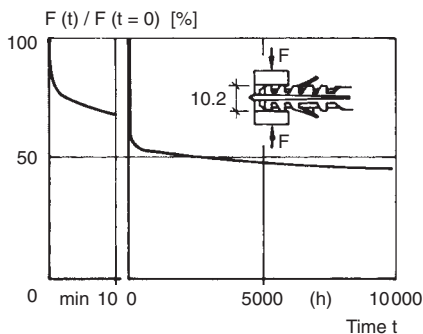
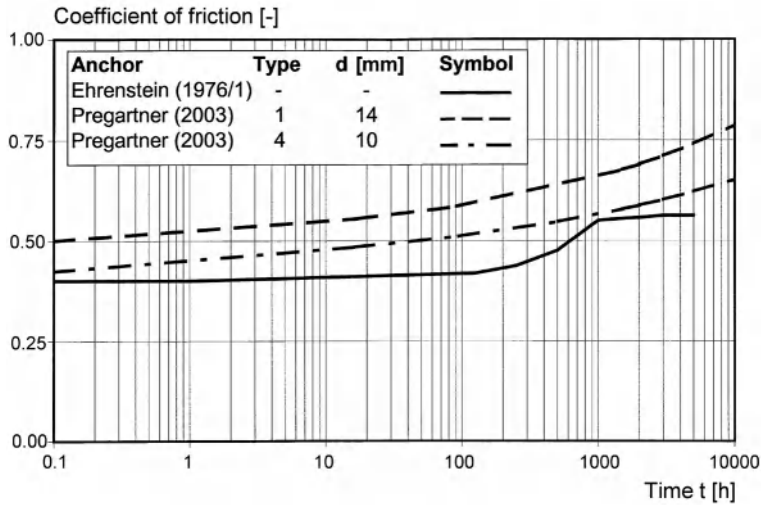


Fig. 7.10 Splitting force of a plastic anchor with  $d_{nom} = 10$  mm as a function of time (Ehrenstein (1976/1))

installation, then stabilizes after a few hours, and at this point is very close to its final value (Ehrenstein (1976/1), Wagner-Grey (1977/1), Roeder (1984), Pregartner (2003)). The final splitting force depends on the design of the anchor. The pull-out load is proportional to the expansion force. Therefore a decrease of the failure load with time should be expected. However, the static friction increases over time (Fig. 7.11). The reason for this is that the plastic sleeve, subjected to high levels of expansion stress, plastically deforms into the irregularities in the wall of the drilled hole and thus increases the micro interlock (Ehrenstein (1976/1)). This is shown schematically in Fig. 7.12a, b. As a result, pull-out resistance drops slightly after installation but rises again after a longer period and reaches at least the initial value. This can be seen from Fig. 7.13, which shows the ultimate loads of different plastic anchors in relation to the elapsed time between installation and testing. The dotted lines denote the average values of the different test series while the full lines give the scatter band of the test average results. If, directly after installation, the anchor is loaded with a tension load equal to the allowable value, the failure load is not reduced by the sustained load even after a long period of time. This has been found in tests by Ehrenstein (1976/1 and 2) and Pregartner (2003).

Similar positive results were obtained in pulsating tension load tests in which the maximum load was set well-above the working load. The load-carrying capacity was at least equal to the



**Fig. 7.11** Coefficient of friction between plastic sleeve and wall of the drilled hole as a function of time (Pregartner (2003))

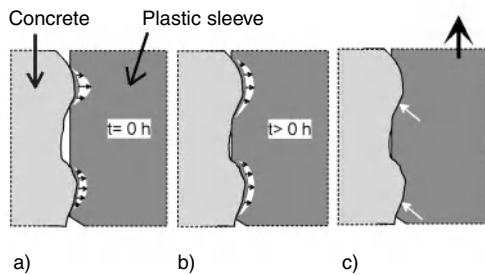


**Fig. 7.12** Detail of a longitudinal section through a plastic anchor (schematic) (Pregartner (2003))  
 a), b) Increase of micro interlock with time  
 c) Increase of expansion force due to tension loading

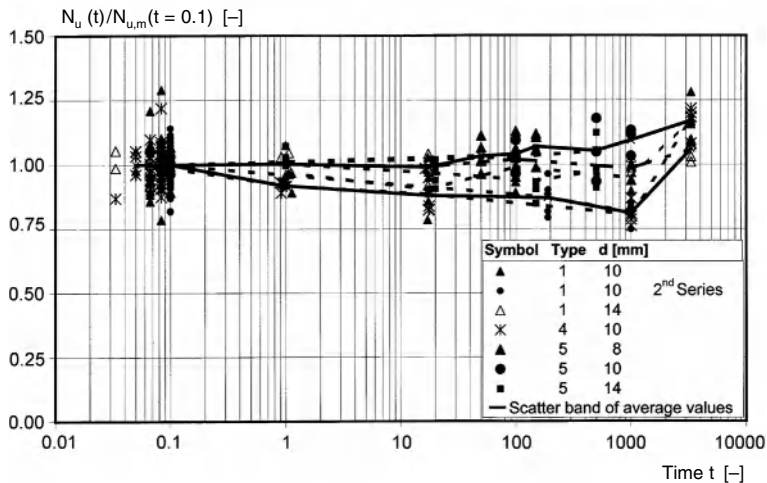


**Fig. 7.13** Influence of time between pull-out test and anchor installation on the relative pull-out failure load (Pregartner (2003))

short-term value after  $N = 10^5$  loading cycles (Ehrenstein (1976/1 and 2)). This behaviour was confirmed in numerous tests conducted within the scope of product approval investigations.

Plastic anchor displacements increase over time in the case of sustained loads or loading cycles. Fig. 7.14 shows the displacements measured over a loading period of up to 9,500 hours plotted in a non-logarithmic scale. The permanent load was set at about 1.9 times the allowable tension load. It can be seen that the increase in displacements per unit of time becomes smaller, i.e. the displacements approach a final value. According to Stampfer, Ehrenstein (1995) displacements measured under sustained load can be approximated by the approach of Findley (1960):

$$s(t) = s_0 + a \cdot t^b \quad (7.3)$$

where:

$t$  = time [h]

$s_0, a, b$  = constants

The constant  $s_0$  can normally be taken as the displacement at time  $t = 0$ .

The displacements measured in one of the tests corresponding to Fig. 7.14 are plotted in Fig.

7.15. The conformity with equation (7.3) is also shown whereby the constants were calibrated with measurements between 300 hours and 2,000 hours. It is clear that the displacements measured up to 9,500 hours are adequately predicted by equation (7.3). Fig. 7.16 shows the displacements of the anchor corresponding to the measurements in Fig. 7.15 extrapolated to a period of 50 years. It can be seen that the displacements after a service life of 100,000 hours (about 11 years) increase only marginally.

According to Ehrenstein (1999), if the displacements in the first 100 hours are neglected and the constants in equation (7.3) are calibrated using the displacements measured during a sustained load test up to only 1,000 hours the displacements for a long time calculated with equation (7.3) overestimate the measured values. The longer the calibration or measurement period is extended the smaller the overestimation error will be. This statement was confirmed by the results of long-term tests carried out over a period of more than 20 years.

The assertions in Ehrenstein (1999) were also confirmed by evaluating the displacements of plastic anchors subjected to sustained loading equivalent to two times the permissible load over a period of about 10 years. Fig. 7.17a

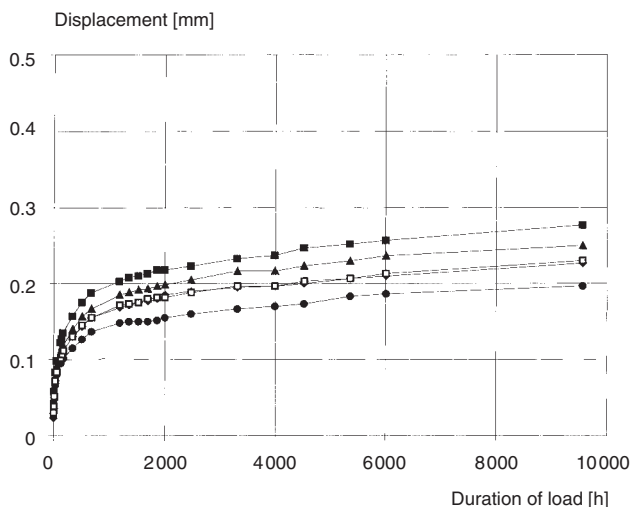


**Fig. 7.14** Displacement of plastic anchors with  $d_{nom} = 10$  mm and  $h_{ef} = 70$  mm as a function of duration of sustained test; sustained load = 3 kN  $\approx 1.9 N_{adm}$ ,  $T \approx 20$  °C



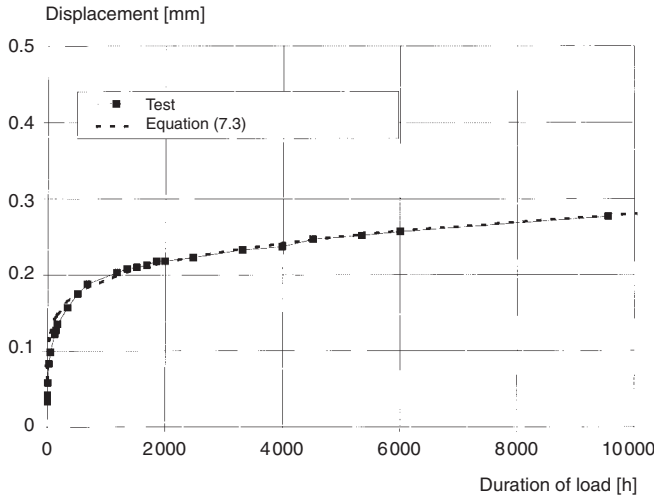


**Fig. 7.15** Displacement of one plastic anchor from Fig. 7.14 as a function of duration of sustained test, fitting of test results by equation (7.3)

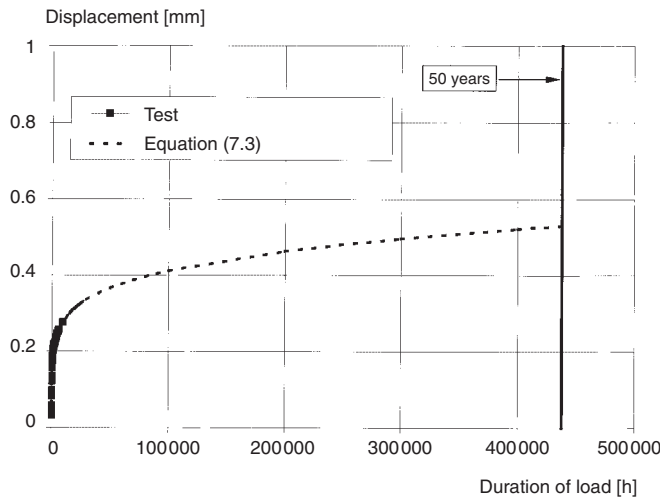
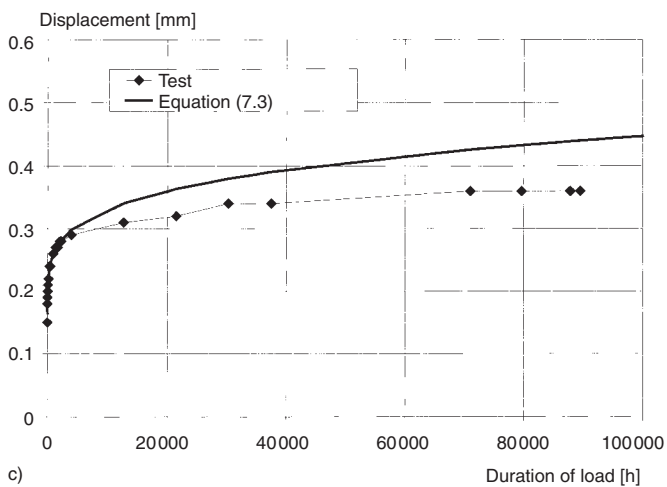
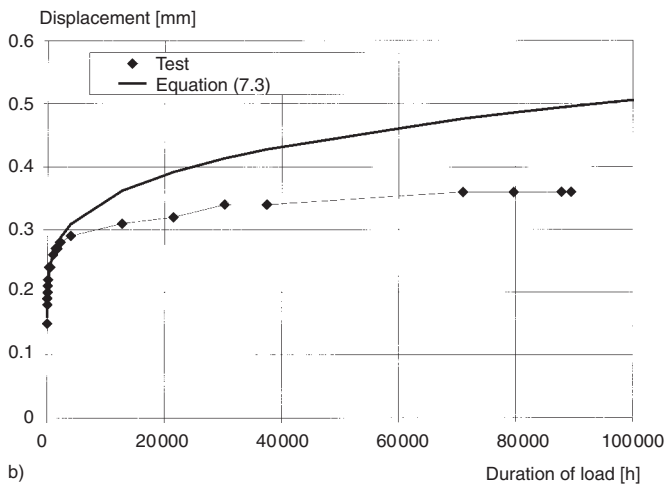
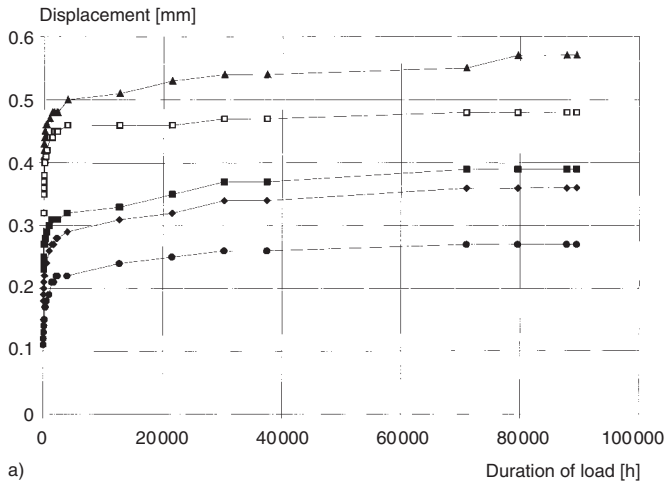


**Fig. 7.16** Displacement of one plastic anchor from Fig. 7.14 as a function of duration of sustained test, extrapolation to 50 years according to equation (7.3)

**Fig. 7.17** Displacements of plastic anchors with  $d_{nom} = 10$  mm and  $h_{ef} = 50$  mm as a function of duration of sustained load; sustained load =  $1.6$  kN  $\approx 2 N_{adm}$ ,  $T = 23$  °C (tests by fischerwerke (1999))

- a) Test results
- b) Test results of one anchor and values calculated according to equation (7.3); calibration with values measured between 100 hours and 1000 hours
- c) Test results of one anchor and values calculated according to equation (7.3); calibration with values measured between 100 hours and 2500 hours



shows the measured displacements and Fig. 7.17b, c the results of individual tests, in each case plotted together with the calibrated Findley equation (7.3). In Fig. 7.17b calibration was conducted with measurements between 100 hours and 1,000 hours, in Fig. 7.17c with measurements between 100 hours and 2,500 hours.

The results illustrated in Figs. 7.14 to 7.17 are valid for room temperature. Larger creep displacements can be expected at higher temperatures.

During sustained load, failure by pull-out will occur if the total displacement (initial value and creep displacement) reaches a critical value. A proposal to evaluate this critical value from the load-displacement curves of short term pull-out tests is given by *Pregartner* (2003). If no failure occurs during the sustained load test the pull-out load measured in a subsequent short time test is not negatively influenced by the sustained load.

Laboratory tests and tests on anchors in use for more than 10 years indicate that the Ultramid® used in these tests is resistant to the chemicals found in concrete under normal environmental conditions (*Ehrenstein* (1976/1)). This statement is also valid for the other plastic materials mentioned in the second paragraph of section 7.

The above described investigations show that approved plastic anchors can safely resist tension loads over the anticipated service life of 50 years.

## 7.2 Cracked concrete

### 7.2.1 Tension load

As with other types of expansion anchors, cracks in concrete cause a reduction in the expansion force generated by plastic anchors. The extent of this reduction depends on the anchor design and on the expansion direction with respect to the crack direction. The greatest reduction occurs when the expansion direction is the same as the direction in which the crack opens. Fig. 7.18 shows the splitting force as a function of time. The maximum force is reached directly after installation and decreases with time (compare Fig. 7.10). In the test, after 10 minutes the crack is opened by 0.2 mm and the splitting force is measured for a further 10 minutes after which the anchor is loaded to failure. Due to the crack opening the splitting force in the direction of the crack opening is reduced significantly. It increases again with increasing time due to the visco-elastic behaviour of the plastic material. This is known as memory effect and can be explained by a rheological 4-parameter-model (*Pregartner* (2003)). When loading the anchor, the splitting (expansion)

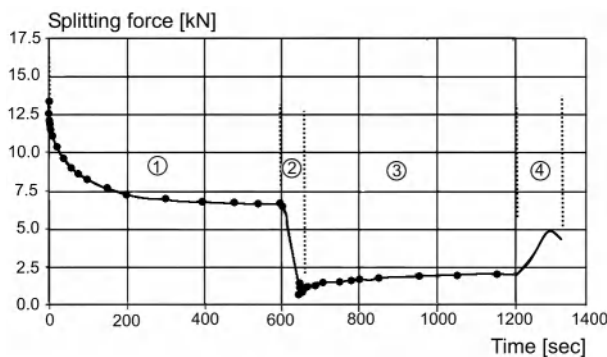


**Fig. 7.18** Splitting force of a plastic anchor with  $d_{nom} = 10$  mm and  $h_{ef} = 70$  mm as a function of time;  $f \approx 2.5$  %,  $T \approx 20$  °C (*Pregartner* (2003))

- 1 Relaxation in non-cracked concrete
- 2 Crack opening  $w = 0.2$  mm
- 3 Memory effect in cracked concrete
- 4 Loading to failure

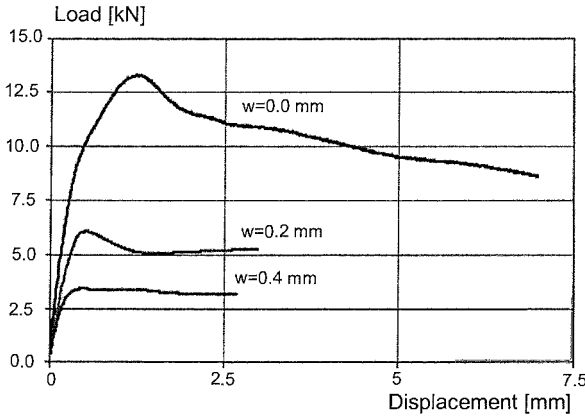


**Fig. 7.19** Influence of crack width on average load-displacement curves of a plastic anchor with  $d_{nom} = 10$  mm and  $h_{ef} = 70$  mm (Pregartner (2003))

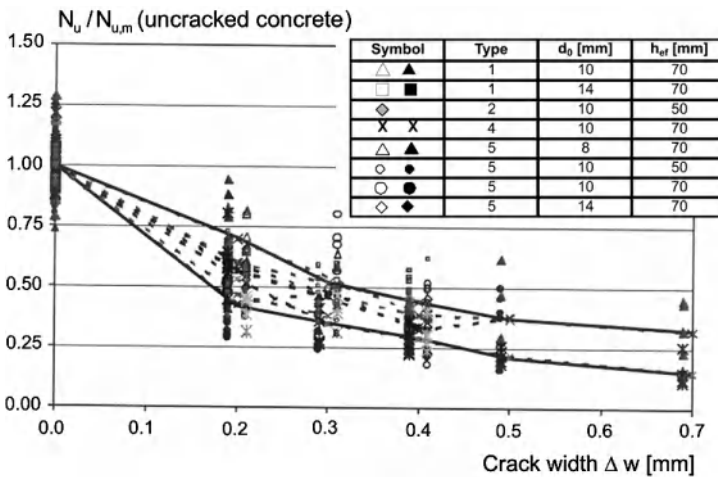


**Fig. 7.20** Influence of crack width on the related pull-out failure load (Pregartner (2003))

force increases because the sleeve may be pulled through the irregularities of the wall of the drilled hole (compare Fig. 7.12c) or the screw may be pulled through the sleeve.

Fig. 7.19 shows average measured load-displacement curves for a plastic anchor ( $d_{nom} = 10$  mm,  $h_{ef} = 70$  mm) tested in non-cracked and cracked concrete ( $w = 0.2$  mm and  $w = 0.4$  mm). The crack reduces the stiffness and the pull-out load of the anchor.

The ratio of the pull-out load in cracked concrete to the value in non-cracked concrete is plotted in Fig. 7.20 as a function of the crack width  $\Delta w$  for different types of anchors. If there

are two symbols for one anchor type the open and full symbol denote values where the main expansion direction was parallel or perpendicular to the crack respectively. While the dotted lines denote the average test results of the different test series, the full lines give the scatter band of the average test results. The pull-out loads decrease as the crack widens. For a crack width  $\Delta w = 0.3$  mm the average pull-out load is approximately 0.3 times to 0.5 times the mean value measured in non-cracked concrete depending on anchor type and diameter. The pull-out tests used in Fig. 7.20 were carried out less than 10 minutes after crack opening. If the time between crack opening and pull-out test is

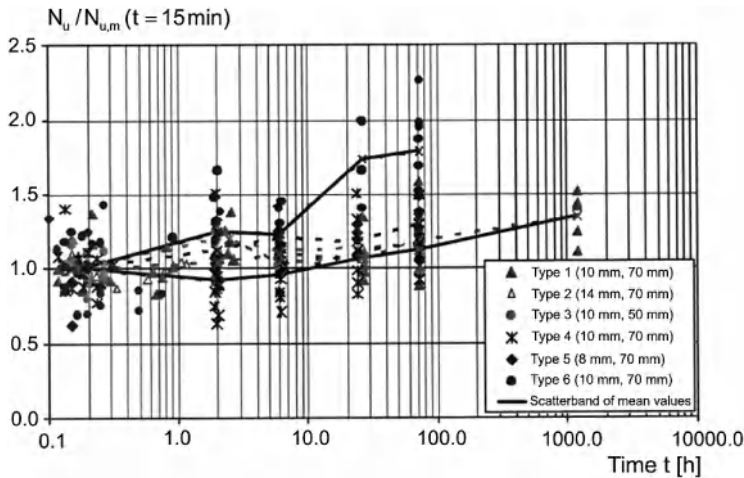


**Fig. 7.21** Influence of time between pull-out test and crack opening on the related pull-out failure load (Pregartner (2003))

increased the failure loads increase (Fig. 7.21) due to the memory effect and an increase of the friction coefficient (Pregartner (2003)).

While the influence of the temperature on the pull-out load in cracks is much the same as in non-cracked concrete the influence of the moisture content of the sleeve is much less pronounced than for non-cracked concrete (Pregartner (2003)).

### 7.2.2 Shear and combined tension and shear load

The behaviour of plastic anchors subjected to shear loads or combined tension and shear loads in cracked concrete has not been investigated up

to now. However, it may be assumed that the ultimate loads corresponding to oblique loading are at least equal to the uniaxial tension capacity.

### 7.2.3 Long-term behaviour

Plastic anchors in cracked concrete subjected to sustained or pulsating loads have not been investigated to date. If anchors are loaded with a tension load equal to the allowable value and the crack is opened and closed the anchor displacements may increase significantly depending on anchor type, diameter and difference in crack width (Pregartner (2003)). Special tests are required for the assessment of this behaviour.

## 8 Behaviour of power actuated fasteners in non-cracked and cracked concrete

### 8.1 Non-cracked concrete

#### 8.1.1 Tension load

Driving a power actuated fastener into concrete is achieved by displacing the base material. The concrete in the immediate vicinity of the pin is compacted and high compressive stresses are generated. The high velocity with which the fastener is driven into the concrete generates locally high temperatures, leading to a partial fusion of concrete and steel. In addition, the driving process scarifies the surface of the pin. These two effects lead to improved bond between fastener and concrete, and power actuated fasteners can exhibit sufficiently robust interlock with the base material such that failure under tension loading occurs not at the interface but rather in the adjacent concrete (Fig. 8.1). The load-displacement behaviour of power actuated fasteners under applied load is almost linear up to failure. Displacements at ultimate load are typically very small ( $< 0.3$  mm) and tension failure is very brittle.

The load-carrying capacity essentially depends on the penetration depth of the pin (Fig. 8.2)



**Fig. 8.1** Pulled out power actuated fastener (Patzak (1979))

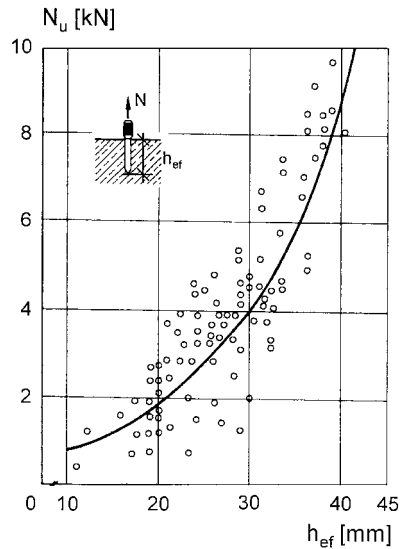


**Fig. 8.2** Pull-out failure load of power actuated fasteners as a function of embedment depth (taken from Patzak (1979))

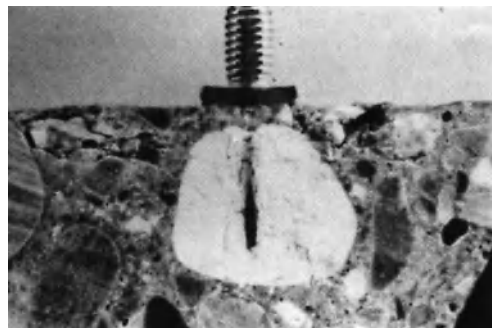


**Fig. 8.3** Penetration of soft aggregate by a power actuated fastener (Seghezzi (1984))

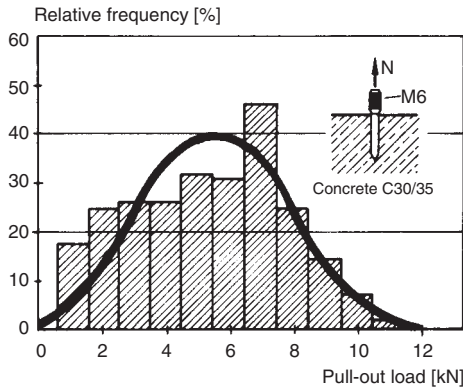


**Fig. 8.4** Relative frequency of the pull-out failure loads of power actuated fasteners (Seghezzi (1984))

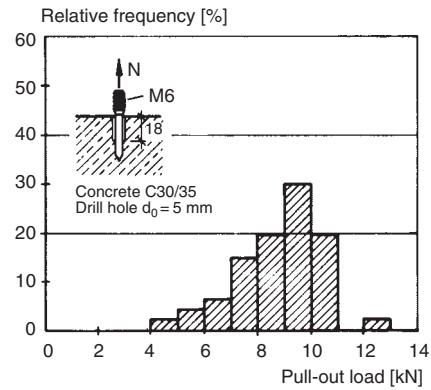


**Fig. 8.5** Relative frequency of the pull-out failure loads of power actuated fasteners installed in pre-drilled pilot holes (Bereiter (1986))

and, to a lesser extent, pin diameter, concrete strength and drive velocity (Patzak (1979)). The pin can penetrate softer aggregates (Fig. 8.3), but harder aggregates and those struck at an oblique angle may deflect the pin (see Fig. 2.58a). This can result in a failed installation. The proportion of failed installations to successful ones climbs as the concrete compressive strength and maximum aggregate size increase; this percentage is typically about 10 % to 20 %. As a result, tension failure loads exhibit severe scatter (Fig. 8.4) with a coefficient of variation  $v = 30\%$  to  $45\%$  (Patzak (1979), Seghezzi (1984)).

Gerber (1987) presents a theory for calculating the pull-out loads of power actuated fasteners in concrete. However, this approach is not generally applicable owing to the assumptions made concerning the concrete behaviour.

Installation failures do not occur when the pins are driven into pre-drilled pilot holes having a depth of approximately 20 mm (see Fig. 2.58b). The concrete breakout load increases due to the larger embedment depth and failure loads are more consistent (Fig. 8.5).

Minimum spacing and edge distances are necessary in order to achieve the failure loads represented in Fig. 8.5. The minimum edge distance to avoid spalling of the free edge during installation is 70 mm to 100 mm (Seghezzi (1984)). The failure load per fastener is reduced

in groups with a fastener spacing less than about 100 mm (Seghezzi (1984)). These figures apply to concrete grades up to about C30/35. Higher strengths require larger spacings and edge distances.

### 8.1.2 Shear and combined tension and shear load

Displacements associated with shear loading to failure are in general relatively large. The shear capacity of commonly available power actuated fasteners is greater than that associated with tension loading (Seghezzi (1984)). The shear failure load can be calculated using equation (4.17) with  $\alpha \approx 0.4$  (Rehm, Eligehausen, Mallée (1992)). As limited by bending of the pin, the shear failure loads associated with power actuated fasteners installed in pilot holes are of roughly the same order of magnitude as those associated with pins loaded in tension. When subjected to combined tension and shear, the ultimate loads can be calculated using the interaction equations (4.42) and (4.43) with  $k = 1.5$ .

### 8.1.3 Sustained and repetitive loading

Relaxation of the concrete causes concrete compressive stresses developed in the immediate vicinity of the pin during installation to diminish over time, theoretically resulting in a decrease in pull-out loads. Investigations by



Hilti (1988) demonstrate that this effect stabilizes after approximately 24 hours and subsequent pull-out loads remain constant. Pull-out tests on power actuated fasteners installed eight months prior to testing resulted in failure loads roughly 10 % lower than those measured in tests performed directly after installation. Therefore concrete relaxation has only a small influence on the pull-out load.

Long-term tests on 4.5 mm studs subjected to a 3 kN constant tension load ( $\approx N_u$ ) showed no failures after two years, and displacement increase of less than 0.2 mm.

Rankweil (1989) reports on studies into the load-carrying capacity of power actuated fasteners installed in pre-drilled pilot holes and subjected to pulsating tension loads. The power actuated fasteners were installed in a concrete slab ( $f_c \approx 25 \text{ N/mm}^2$ ) and subjected to up to  $2 \cdot 10^6$  loading cycles. The minimum load was roughly zero and the maximum load varied. Failure of the steel occurred in every case. These tests indicate that the fatigue strength corresponding to pull-out is typically greater than that of the pin, which in this case was approximately 2.5 kN.

## 8.2 Cracked concrete

### 8.2.1 Tension load

Radial compressive stresses in the concrete result from driving the pin into the concrete. The stresses perpendicular to the crack direction are diminished by cracks that form in the concrete after installation and are reduced to negligible levels at crack widths greater than 0.2 mm. Partial fusion of the pin with the concrete and scarring of the pin surface during installation both contribute to the development of bond (adhesion) that typically exceeds the concrete tensile strength. As a result, cracks that transect the pin location do not destroy the interface between pin and concrete but instead tend to remain in the adjoining concrete. Crack widening leads to a condition whereby the load-bearing behaviour of the pin is essentially governed by the interlocking effect of the rough sides of the crack (micro- and macro-interlocking). Failure is always characterised by pin pull-out with the sintered concrete adhering to the



**Fig. 8.6** Photo of a power actuated fastener after a tension test in cracked concrete (taken from Eligehausen (1988/2))

pin (Fig. 8.6). The depth of adhered concrete can be up to 0.8 mm independent of pin diameter (Eligehausen (1988/2)).

As in non-cracked concrete the load-displacement behaviour is almost linear up to peak load with small displacements and failure is rather brittle.

The pull-out load of power actuated fasteners decreases markedly with increasing crack width (Figs 8.7 and 8.8).

Fig. 8.7, which applies to power actuated fasteners installed *without* a pilot hole, shows mean values derived from  $n \geq 12$  tests per crack width in each case. At a crack width of  $\Delta w = 0.4 \text{ mm}$  the pull-out load is, on average, about 30 % of the value in non-cracked concrete. Fig. 8.8 shows the results of about 320 tests (260 tests in cracks) on power actuated fasteners

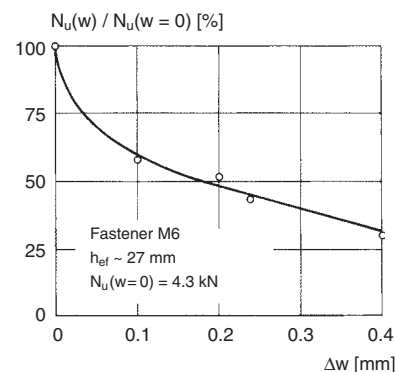


**Fig. 8.7** Influence of crack width on the relative tension failure load of power actuated fasteners (Patzak (1979))

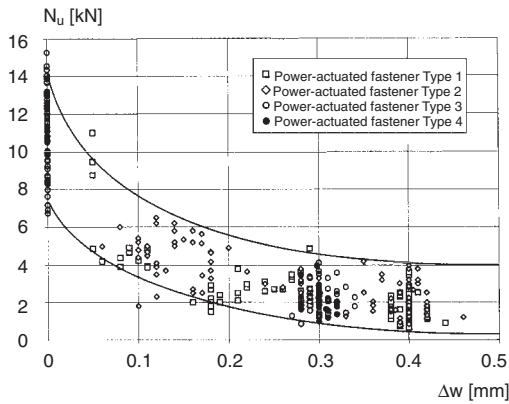


**Fig. 8.8** Influence of crack width on the relative tension failure load of power actuated fasteners installed in pre-drilled pilot holes (Eligehausen (1995/2))

installed in a pre-drilled pilot hole. The mean failure load in non-cracked concrete is approximately 11 kN. The pull-out load at a crack width of  $\Delta w = 0.3$  mm is, on average, about 25 % and the lowest measured individual value approximately 10 % of the mean failure load in non-cracked concrete. Similar results were observed in the tests described by Bergmeister (1988).

Tests in opening and closing flexural cracks were carried out by Patzak (1979) to establish the influence of varying loads (applied to the component serving as the base material) on the tension load-bearing behaviour of power actuated fasteners installed without a pilot hole. However, the maximum crack width and crack width difference ( $w \approx 0.1$  mm and  $\Delta w \approx 0.02$

mm, respectively) were quite small. Pull-out loads measured in the open crack after  $10^4$  crack width cycles were on the same order of magnitude as the tests evaluated in Fig. 8.7. Power actuated fasteners with pilot holes have also been tested in opening and closing flexural cracks (Eligehausen (1988/2)), whereby the constant tension load was approximately 1.5 times the allowable load, the crack width at maximum load was  $w \approx 0.2$  mm and the crack width difference between minimum and maximum was  $\Delta w \approx 0.15$  mm. None of the pins were pulled out during the tests and the increase in displacement was less than 0.1 mm after  $10^4$  crack openings. The failure loads measured after  $10^4$  crack cycles were within the same range of scatter as those of control tests without crack cycling.

### 8.2.2 Shear and combined tension and shear load

The authors are not aware of shear tests on power actuated fasteners in cracked concrete. It may be assumed that failure loads are significantly higher than those associated with tension loading. Eligehausen (1995/2) evaluates tests with power actuated fasteners in pilot holes subjected to combined tension and shear loads. The angle of application of the load was varied between  $\alpha = 0^\circ$  (tension) and  $\alpha = 30^\circ$ . Up to this angle of application the tension component of the failure load was at least equal to that associated with concentric tension. This can be attributed to the fact that the shear component of load acts to wedge the pin against the wall of the pilot hole and thus increases the frictional resistance to pull-out.

## 9 Behaviour of screw anchors in non-cracked and cracked concrete

### 9.1 Installation

During installation, screw anchors cut a thread into the wall of the drilled hole (Fig. 9.1). Therefore, tensile loads are transferred into the base material by diagonal compression struts, i.e. mechanical interlock (Fig. 9.2a). The load transfer mechanism is similar to that of deformed reinforcing bars cast into concrete (Fig. 9.2b), whereby the flanks of the screw thread function in a similar manner as the ribs of reinforcing bars. However, some differences from deformed reinforcing bars should be considered. Damage to the threads cut into the wall of the drilled hole (compare Fig. 9.1) may reduce the area of the mechanical interlock. Additionally, the core diameter of the concrete screw is smaller than the drill hole diameter to allow for easier installation. Consequently, the lateral restraint of the concrete is lost in the



**Fig. 9.1** Screw anchor and a thread cut into the wall of the drilled hole (Küenzlen, Sippel (2001))

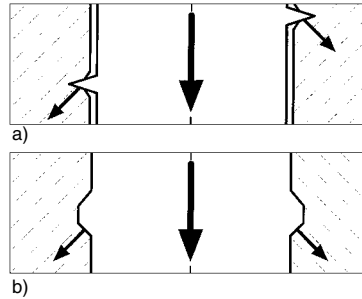


**Fig. 9.2** Transmission of tension load into concrete (Eligehausen, Küenzlen (2002))

a) Screw anchor

b) Cast-in deformed reinforcing bar

region of the highly loaded concrete consoles below the thread. To achieve sufficient load transfer into the concrete, the depth of the threads cut into the wall of the drilled hole is usually larger than the height of the ribs of commercially available deformed reinforcing bars.

Screw anchors are normally screwed into the concrete using an electric screw-gun. They can also be screwed in with a torque wrench. The necessary torque for cutting the threads into the concrete should be small in order to achieve an easy installation. Moreover, the resistance against shearing-off of the threads should be as high as possible, so that the threads cut into the concrete are not destroyed while tightening the screw anchors.

Fig. 9.3 shows the measured torque while screwing in a screw anchor with a drill bit diameter  $d_0 = 8$  mm as a function of the angle of rotation (swing angle). The embedment depth was chosen such that failure was caused by shearing of the concrete threads. The concrete, which was of the strength class C20/25, was produced from fine-grained aggregate (maximum aggregate size 8 mm). Before the screw head touched

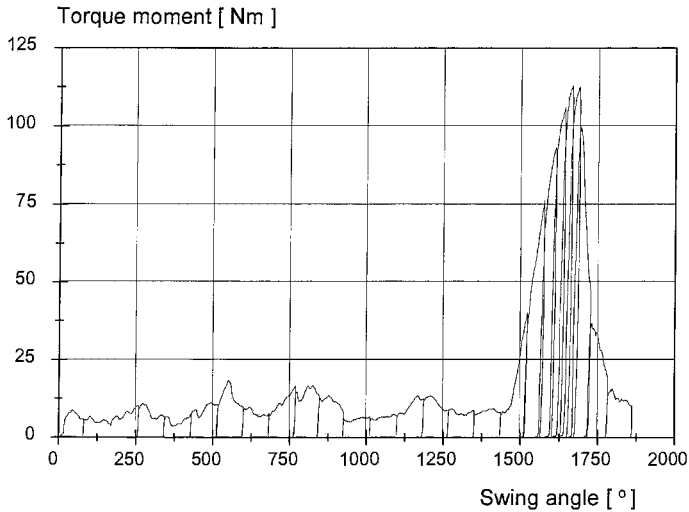


**Fig. 9.3** Typical relationship between torque moment and swing angle (Küenzlen (2004))

the fixture, the installation torque  $T_{inst}$  varied only slightly. If the concrete contains coarser aggregates, the variation in installation torque will be larger. After the screw head reaches the fixture, the torque increases steeply up to the peak value  $T_u$ . With a further increasing of the angle of rotation, the concrete threads are sheared off and the torque decreases rapidly to

zero. Fig. 9.4a shows the threads just after the screw head reaches the fixture. The damaged concrete threads after over-tightening the screw anchor are shown in Figs 9.4b.

The installation torque necessary to screw the anchor into the concrete depends significantly on the type of the screw anchor, the cutting diameter of the drill bit, and the hardness and size  $d_{max}$  of the large aggregates (Fig. 9.5). A further influencing factor is the anchor diameter. By increasing the embedment depth the installation torque increases only slightly because the threads are mainly cut into the concrete by the flanks of the screw thread at the tip of the screw. The concrete strength influences the installation torque only to a minor extent.

The failure torque  $T_u$  when the concrete threads are sheared off is influenced by the same parameters as the installation torque. However, it increases with increasing embedment depth (Fig. 9.6) because more threads have to be sheared off. When the embedment depth is increased beyond a critical value failure is caused by steel rupture (shearing of the shaft of the screw anchor) and not by shearing of the threads cut into the concrete.

While the installation of a screw anchor with a torque wrench requires more than 30 seconds,

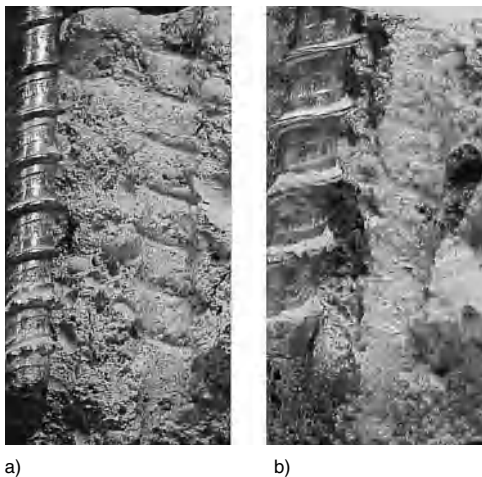


**Fig. 9.4** Threads cut into the wall of the drilled hole (Küenzlen (2004))

- a)  $T = T_{inst}$   
 b)  $T = 0.19 \cdot T_u$  (after passing maximum torque)

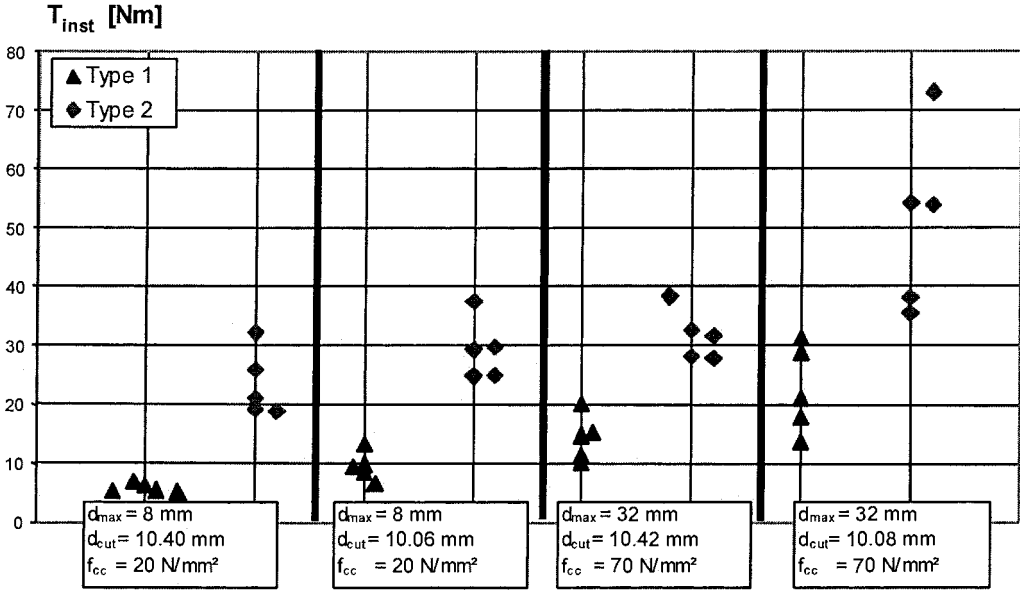


**Fig. 9.5** Required installation torque moment  $T_{inst}$  for two types of screw anchors ( $d_0 = 10\text{ mm}$ ,  $h_{ef} = 50\text{ mm}$ ) under different test conditions (Küenzlen, Sippel (2001))

installation with a high-performance electric screw-gun requires only a few seconds. For this reason, in practice concrete screws are usually screwed-in with an electric screw-gun. In the setting tests described in Küenzlen (2004), electric screw-guns with a maximum torque higher than the steel failure torque of the screw anchors were

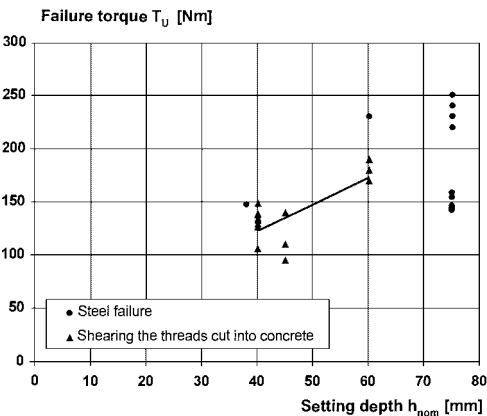


**Fig. 9.6** Influence of the embedment depth on the failure torque moment (Küenzlen (2004))

used. Nevertheless, the screw anchors failed by shearing of the threads cut into the concrete after the screw head reached the fixture. The difference  $t_u$  between the time when the anchor head reaches the fixture and the shearing-off of the threads increases with increasing embedment depth (Fig. 9.7). It is influenced by the same parameters that affect the failure torque  $T_U$ . A further significant influencing factor is the power output of the electric screw-gun.

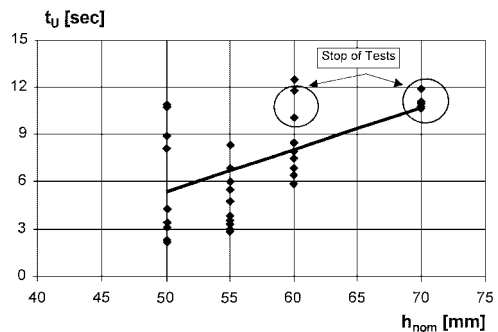


**Fig. 9.7** Influence of the embedment depth on the time until shearing the threads cut into the wall of the drilled hole (Eligehausen, Küenzlen (2002))

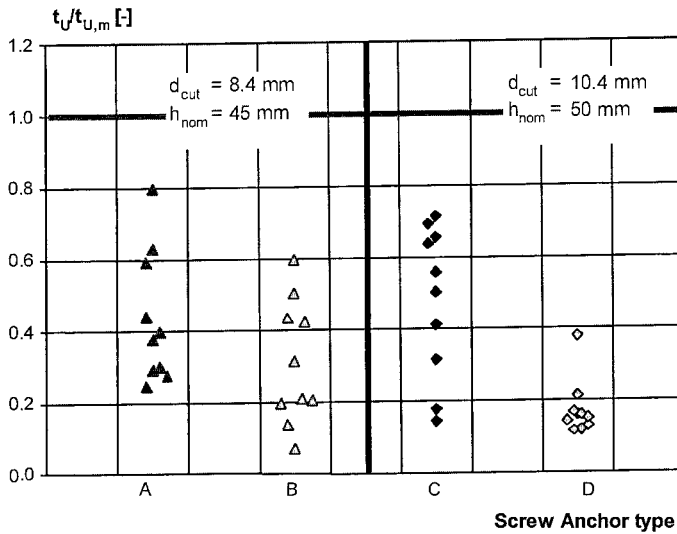


**Fig. 9.8** Time  $t_u$  until shearing the threads cut into the wall of the drilled hole of screw anchors after un-screwing related to the average time  $t_{u,m}$  of screw anchors without un-screwing (Küenzlen (2004))

In practice it may occur that screw anchors are unscrewed after the screw head reaches the fixture (e.g. for easier installation of an anchor group). Upon reinstallation of the screw anchor, this unscrewing reduces the time  $t_u$  until failure by 60 to 80% compared to screw anchors that were not unscrewed. This is shown in Fig. 9.8, in which the times  $t_u$  after un-screwing related to

the average time  $t_{u,m}$  of screw anchors without unscrewing are plotted for different anchor types.

If the thread cut into the concrete is not damaged during installation, neither the load-displacement behaviour nor the pull-out failure load are significantly influenced by the magnitude of the applied torque. However, if the screw anchors are overtorqued, the failure load is significantly reduced (Fig. 9.9) because the thread cut into the wall of the drilled hole is damaged (compare Fig. 9.4).

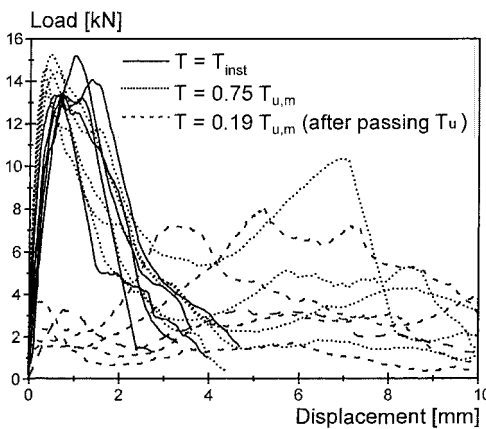


**Fig. 9.9** Load-displacement behaviour of screw anchors installed with different torque moments (Küenzlen (2004))

In practice it cannot be excluded that screw anchors are further tightened after the screw head reaches the fixture, e. g. if the electric screw-gun is not stopped immediately or if the fixture is tightened against the surface of the concrete with a standard wrench. Un-screwing of the screw anchors and screwing them in again can also occur. Damage of the threads cut into the wall of the drilled hole should be avoided by using a sufficiently large embedment depth. Corresponding tests are required in the approval process in Europe (*Deutsches Institut für Bautechnik* (2003/1)).

## 9.2 Non-cracked concrete

### 9.2.1 Tension load

#### 9.2.1.1 Load-displacement behaviour and failure modes

Figure 9.9 shows typical load-displacement curves of screw anchors measured in pull-out tests under tension load in non-cracked concrete. If the screw anchors are not over-torqued during installation the load-displacement curves increase steeply with a small scatter. The failure was caused by concrete cone breakout.

In general, with screw anchors the same failure modes are observed as with expansion and undercut anchors (see Fig. 4.1). Screw anchors with a thread over the entire embedment depth fail due to a concrete cone that starts at the first bearing thread at the tip of the concrete screw when the embedment depth is small (Fig. 9.10a). As the embedment depth increases, only the concrete at the surface breaks out and the remaining portion of the screw is pulled out (Fig. 9.10b). By further increasing the embedment depth, steel failure will occur. Anchor groups fail due to a common concrete cone breakout and with anchors very close to an edge in a thin concrete member splitting might be expected.

The failure mode shown in Fig. 9.10b is similar to that of bonded anchors. However the failure

load of bonded anchors increases nearly linearly with increasing embedment depth (*Cook, Kunz, Fuchs, Konz (1998)*), while the failure load of screw anchors with standard embedment depth increases with  $h_{ef}^{1.5}$  (Fig. 9.11).

#### 9.2.1.2 Failure loads associated with steel failure

Section 4.1.1.2 applies.

#### 9.2.1.3 Failure loads associated with pull-out failure

Pull-out failure occurs only with screw anchors with a standard anchorage length and a thread over less than about 80% of the embedment depth (*Küenzlen (2004)*). The failure load depends on the length of the thread, the diameter and the type of the screw anchor, and the concrete strength. The pull-out resistance should be determined from test results.

#### 9.2.1.4 Failure loads associated with concrete cone failure

In Fig. 9.11 the failure loads of screw anchors with a thread over the entire embedment depth from different manufacturers and with different diameters are plotted as a function of the effective embedment depth. The tests were performed in concrete with different strengths. Therefore the failure loads were normalized to

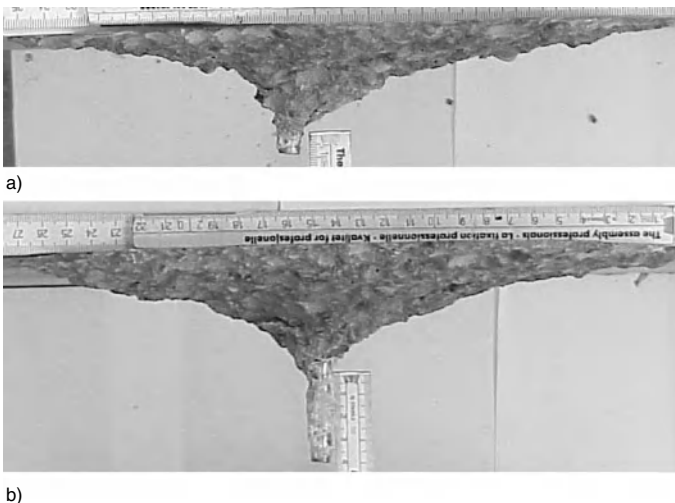


**Fig. 9.10** Typical concrete failure cones (*Küenzlen, Sippel (2001)*)  
 a)  $h_{nom} = 50$  mm  
 b)  $h_{nom} = 90$  mm



$f_{cc,200} = 30 \text{ N/mm}^2$  by assuming a square root function. The effective embedment depth was determined according to equation (9.1).

$$h_{ef} = h_{nom} - 0.5 \cdot h - h_s \tag{9.1}$$

where:

- $h_{nom}$  = length between end of the screw anchor and the concrete surface
- $h$  = distance between the threads
- $h_s$  = distance between the tip of the screw anchor and first thread

Equation (9.1) considers that load transfer starts at a distance from the tip of the screw anchor that is dependent on the type of screw anchor. It enables a better comparison of the test results of screw anchors from different manufacturers.

Fig. 9.11 shows that the failure load increases with  $h_{ef}^{1.5}$ . The influence of the type and diameter of the screw anchor is small. The average failure load is given by equation (9.2).

$$N_{u,c}^0 = 10.5 \cdot f_{cc,200}^{0.5} \cdot h_{ef}^{1.5} \tag{9.2}$$

The failure loads are about 20 % smaller than found for expansion anchors with the same embedment depth (Fig. 9.11). This can be attributed to the different form of the failure cone.

When using a reduced embedment depth

$$h_{ef,1} = 0.85 \cdot h_{ef} \tag{9.3}$$

where  $h_{ef}$  is calculated in accordance with equation (9.1), the average concrete cone failure load can be calculated with equation (9.4).

$$N_{u,c}^0 = 13.5 \cdot f_{cc,200}^{0.5} \cdot h_{ef,1}^{1.5} \tag{9.4}$$

Equation (9.4) is valid for screw anchors with a thread length larger than about 0.8 times  $h_{ef}$ , and an embedment depth  $h_{ef} \leq 10 \cdot d_0$  and not larger than  $h_{ef} \approx 150 \text{ mm}$ . According to numerical investigations by K uenzlen (2004), for larger embedment depths the failure load increases – similar to bonded anchors – in proportion to  $h_{ef}$ .

Equation (9.4) is identical with equation (4.5b) with  $k = 13.5$ , which is valid for expansion anchors.

In Fig. 9.12 the failure loads of groups with four screw anchors related to the failure load of a single anchor according to equation (9.4) are plotted as a function of the ratio of spacing  $s$  to the reduced embedment depth  $h_{ef,1}$ . The measured failure loads can be predicted by the CC-Method (see section 4.1.1.3) when the characteristic spacing is taken as  $s_{cr,N} = 3 \cdot h_{ef,1}$ . Similarly the failure loads of screw anchors close to

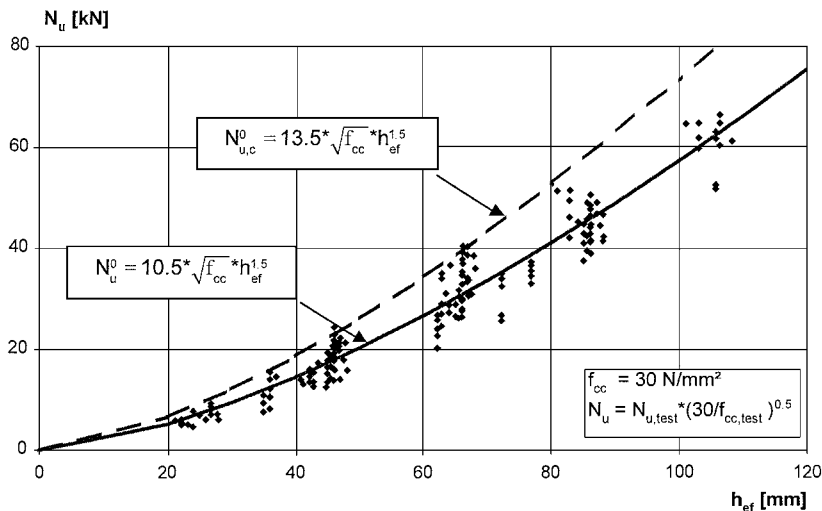


**Fig. 9.11** Failure load of screw anchors in non-cracked concrete as a function of the embedment depth (Elgehausen, K uenzlen (2002))

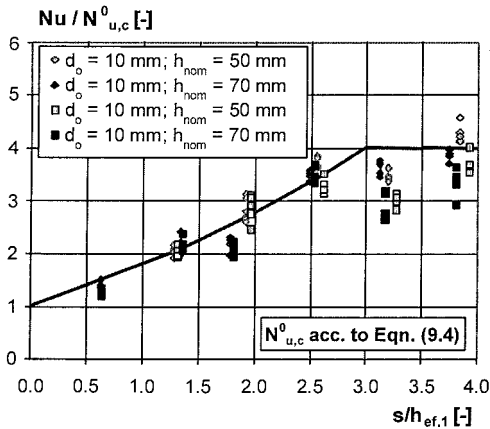


**Fig. 9.12** Measured failure loads  $N_u$  of groups with screw anchors related to the values  $N_{u,c}^0$  of single anchors according to equation (9.4) as a function of the ratio anchor spacing  $s$  to reduced embedment depth  $h_{ef,1}$  (Küenzlen (2004))

an edge can be predicted with sufficient accuracy using the CC-Method when the reduced embedment depth  $h_{ef,1}$  is used (Fig. 9.13).

**9.2.2 Shear load**

**9.2.2.1 Load-displacement behaviour and modes of failure**

The load-displacement behaviour of shear loaded screw anchors generally corresponds to

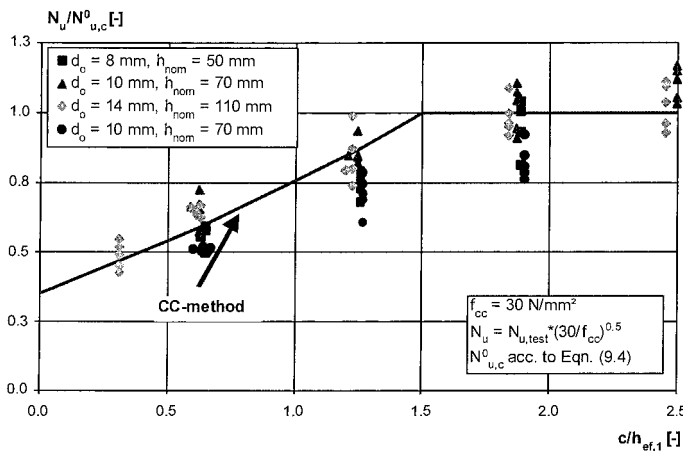


**Fig. 9.13** Measured failure loads  $N_u$  of single screw anchors related to the values according to equation (9.4) as a function of the ratio of anchor edge distance  $c$  to reduced embedment depth  $h_{ef,1}$  (Küenzlen (2004))

that of post-installed metal anchors (expansion and undercut anchors). Screw anchors exhibit the same failure modes associated with metal expansion and undercut anchors (see Fig. 4.63).

**9.2.2.2 Failure load associated with steel failure**

The discussion in section 4.1.2.2 generally applies to screw anchors as well, however, due to the high steel strength and hardness, the factor  $\alpha$  in equation (4.17) might be smaller than 0.6.

**9.2.2.3 Failure load associated with pry-out failure**

The authors are not aware of investigations regarding the behaviour of screw anchors exhibiting pry-out failure. It may be assumed, however, that the failure load associated with this failure mode may conservatively be predicted using equation (4.24), however, the ultimate load  $N_u$  is calculated using the reduced embedment depth  $h_{ef,1}$  according to equation (9.3).

**9.2.2.4 Failure load associated with concrete edge breakout**

Limited testing at the University of Stuttgart indicates that the CC-Method presented in section 4.1.2.4 for headed studs and post-installed anchors can also be used to predict concrete edge breakout of screw anchors.

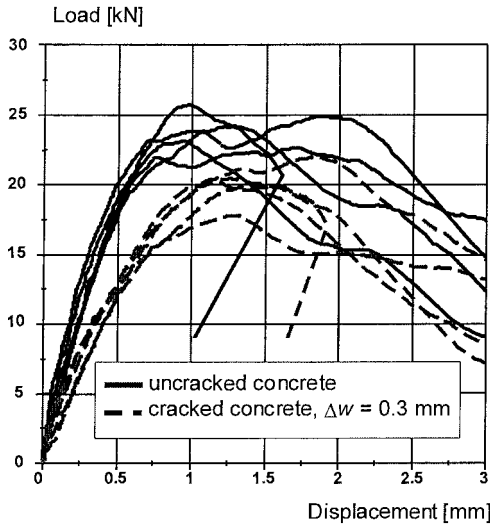


**Fig. 9.14** Typical load-displacement curves of screw anchors ( $h_{nom} = 65$  mm) in non-cracked and cracked concrete ( $f_{cc,200} = 30$  N/mm<sup>2</sup>) (Küenzlen (2004))

**9.2.3 Combined tension and shear load**

The interaction equations (4.42) and (4.43) presented in section 4.1.3.2 may be used to predict failure loads for screw anchors under combined tension and shear loading.

**9.2.4 Sustained and fatigue loads**

To the knowledge of the authors, tests under sustained load have not been performed yet. However, due to the load transfer, which is similar to that of deformed reinforcing bars, it may be assumed that a sustained load in the magnitude of the allowable load will slightly increase the displacements but will not have an influence on the failure load.

Under fatigue loading steel failure must be expected. Due to the high steel strength and hardness the fatigue strength of screw anchors is rather low. It depends significantly on the screw anchor type and should be evaluated by tests. Furthermore, special measures are required to avoid loosening of the screw anchor.

**9.3 Cracked concrete**

**9.3.1 Tension load**

If a screw anchor is positioned in a crack, the bearing area of the thread flanks is reduced in comparison to non-cracked concrete. Furthermore, the axially symmetric state of stress around the screw is disturbed by the crack. These effects reduce the stiffness and failure load of screw anchors in comparison to non-cracked concrete (Fig. 9.14). The decrease of

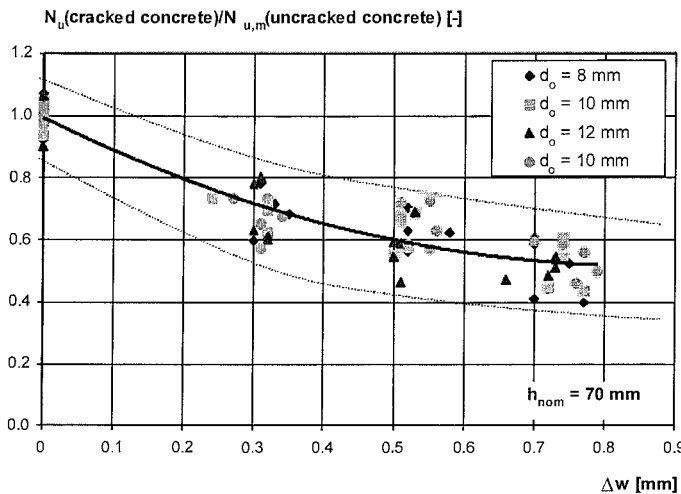


**Fig. 9.15** Effect of crack width on the concrete cone failure load of screw anchors under tension loading (according to equation (9.4)) (Küenzlen (2004))

the failure load averages about 30 % at a crack width of 0.3 mm (Fig. 9.15). This reduction is on the same order of magnitude as that for expansion or undercut anchors.

### **9.3.2 Shear load and combined tension and shear load**

The authors are not aware of results of tests with screw anchors under shear load or combined tension and shear load in cracked concrete. However, it may be assumed that the findings in sections 4.2.2 and 4.2.3 for anchors that

are suitable for use in cracked concrete are valid for screw anchors.

### **9.3.3 Sustained and fatigue loads**

According to the authors' knowledge, tests with screw anchors under sustained or fatigue loads in cracked concrete have not been carried out. In principle, the findings in section 9.2.4 apply. The behaviour of screw anchors positioned in a crack and loaded by a constant tension load while the cracks are opened and closed 1000 times is similar to that of undercut anchors.

## 10 Behaviour of anchors under seismic loading

Owing to the tremendous hazard posed by earthquakes, the design of structures to resist seismic actions (so-called strong ground motion) has been the subject of intensive research and field investigations over the past half-century. While much attention has been focused on the global response of structures and their analysis for earthquake loading, it is also recognised that good seismic performance is equally dependent on robust connection design. The design of anchorages used to transfer earthquake loads between steel and concrete elements represents an essential part of ensuring a continuous load path for inertial forces generated in a structure.

### 10.1 Anchor applications

Examples of typical anchor applications found in both seismic and non-seismic regions, as well as some anchor applications related specifically to seismic strengthening and rehabilitation of structures, are listed in Fig. 10.1.

When discussing anchorages for seismic applications, it is often useful to distinguish between structural and non-structural applications (Fig. 10.2). This distinction is important for the design of anchorages, since different loadings exist for the two cases and different factors of safety may need to be considered.

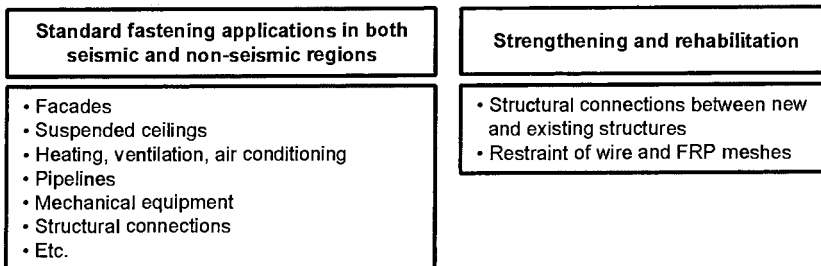
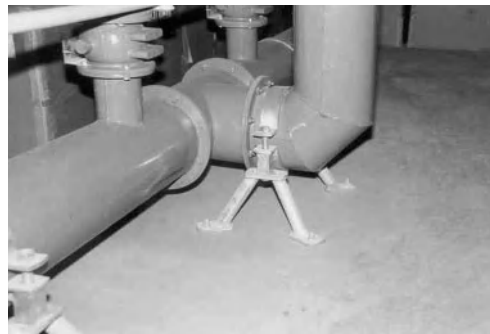


Fig. 10.1 Applications for anchor systems (Eligehausen, Hoehler (2003))



a)



b)

Fig. 10.2 Examples of applications for anchors  
a) Steel brace (structural) (Courtesy of S. Otani), b) Pipe support (non-structural)

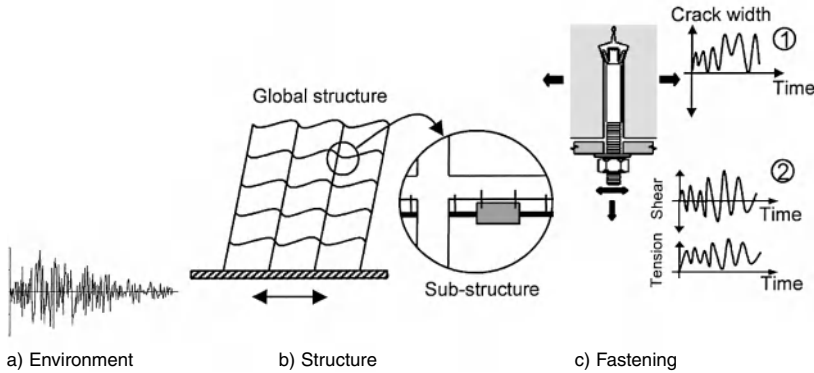


**Fig. 10.3** Actions acting on a non-structural anchorage under earthquake loading (Eligehausen, Hoehler (2003))

In the current practice, it is regrettably the case that many connections intended to transfer earthquake loads are designed using methods intended for non-seismic design situations without consideration of the special conditions that exist for seismic loading. This is particularly true for connections for non-structural elements.

## 10.2 Seismic actions

Earthquakes generate actions (forces and displacements) on a structure in a variety of ways. These include acceleration of the ground (strong ground motion), differential settlement of the foundations resulting from liquefaction or other ground phenomena, and lateral and vertical displacement across a fault trace (for those structures unlucky enough to be located directly on a fault rupture). From a design perspective, induced structure acceleration represents the most obvious and prevalent loading case to be considered. However, imposed deformations, not inertial forces, are frequently the cause of connection failures in earthquakes, particularly when those connections have not been designed to accommodate large deformations.

Typically, ground accelerations are translated through a structure via the foundations, which interact with the surrounding and supporting soil and rock via a complex interplay of frictional and bearing forces. The input motions from the ground will generate varying responses in the structure, depending on the

magnitude, frequency content and duration of the ground motion, the efficiency of the soil-structure interface, and the dynamic characteristics of the structure. As the structure responds to the ground motion, degradation of the global structure, which serves as the anchorage material, can occur. In reinforced concrete structures this degradation is in large part expressed through cracking in the structural elements. Additionally, the motion of the global structure will generate actions on sub-structures. If the sub-structure is connected to the global structure by anchors, the motion of the global structure generates tension and shear forces on the anchors (Fig. 10.3c).

Earthquake induced forces vary with time and are designated as dynamic forces. Although many forces encountered in civil engineering practice vary with time, slowly varying forces can be treated as quasi-static (Fig. 10.4a), since the inertial and damping components of the forces are negligible. The presence of inertial and damping forces, which arise in structures as a result of strong ground motion, is the critical distinction between dynamic and static loading.

If the forces on the anchor (Fig. 10.3c<sub>2</sub>) lead to load cycles only in the tension or compression range, they are referred to as 'pulsating' forces (Fig. 10.4b). If changes from the tensile to the compressive range and vice versa occur, the forces are referred to as 'alternating' forces (Fig. 10.4c). Axial forces on pre-positioned and in-place mounted anchorages are typically pul-

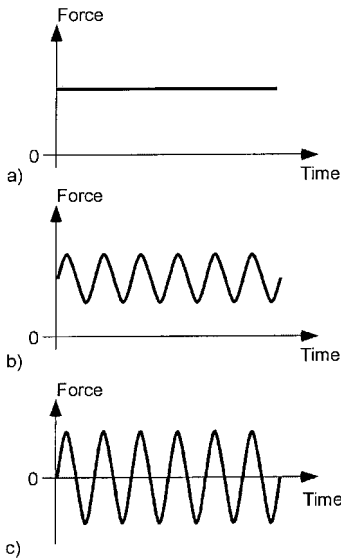


**Fig. 10.4** Types of force (Ammann (1980))  
 a) Static, b) Pulsating, c) Alternating

sating tensile forces because compression forces are transferred to the anchorage material via the fixture (Fig. 10.5a, b). Axial loads on stand-off mounted anchorages can be either pulsating or alternating (Fig. 10.5c). Shear loads on anchorages during earthquakes can be pulsating or alternating, however, are in general alternating.

Important features of the force-time function are:

- the number of load cycles  $n_{cycle}$ ,
- the strain rate or rate of loading on anchor and base material,
- the peak values of the dynamic force and their sequence in time, and

- the probability of occurrence of the earthquake induced force during the life of the anchor.

Strong ground motion associated with earthquakes typically induces actions in a structure with fewer than 30 cycles with large amplitudes and generates strain rates on the order of  $10^{-5}$  to  $10^{-2}$  (1/sec) (Ammann (1980)). The random nature of earthquakes makes the sequence of the loading difficult to generalise.

**10.3 Assumptions regarding the condition of the concrete**

Earthquakes place severe demands on structures, typically in excess of nominal design assumptions. In general, it may be expected that the deformations of a reinforced concrete structure caused by ground shaking will lead to cracking in both primary and secondary structural concrete elements. Consequently, all anchorages intended to transfer earthquake loads should be suitable for use in cracked concrete and their design should be predicated on the assumption that cracks in the concrete will cycle open and closed for the duration of strong ground motion.

During large earthquakes, parts of a structure may be subject to extreme inelastic deformation (Fig. 10.6). In reinforced concrete structures, yielding of reinforcement and cycling of cracks may result in crack widths of several millimetres, particularly in regions of plastic hinging. Qualification procedures for anchors do not currently anticipate such large crack widths. For this reason, anchorages in regions where plastic hinging is expected to occur, such as the base of shear walls, joint regions of frames, and spandrel beams, should be avoided unless suitable

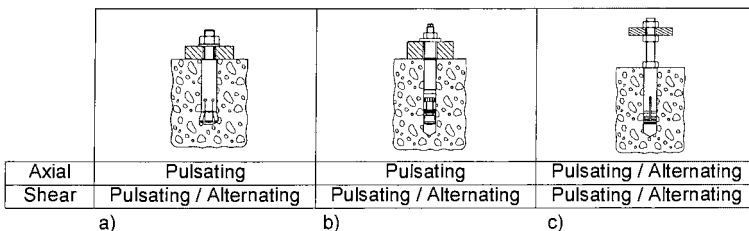


**Fig. 10.5** Typical axial and shear loading on anchors for various mountings  
 a) Pre-positioned installation, b) In-place installation, c) Stand-off installation



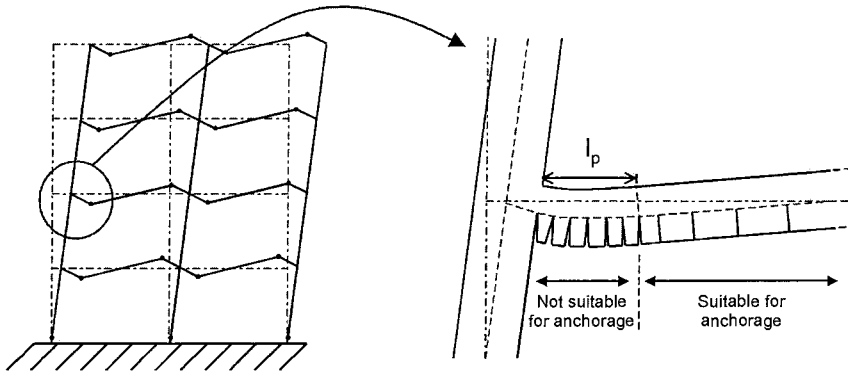


**Fig. 10.6** Mechanism for accommodating transverse motion of a building through member cracking assuming a strong-column, weak-girder design ( $l_p$  = plastic hinge length) (Eligehausen, Hoehler (2003))

design measures are taken. Outside of the regions of inelastic deformation, crack widths may be assumed not to exceed those that are reached in a member in which the longitudinal reinforcement steel is at the onset of yield strain. Such crack widths are typically less than 1 mm (Eligehausen, Hoehler (2003)). The crack widths vary as a function of time and can be idealised as a pulsating function (Fig. 10.3c<sub>1</sub>) with a minimum crack width that is almost zero.

#### 10.4 Behaviour of anchors under seismic conditions

As shown in Fig. 10.3c, during a seismic event an anchor may be subjected to a combination of cyclic tension and shear forces. Furthermore, the anchor may be located in a crack that either forms during the earthquake or has traversed the anchor location at some prior time. The crack width will typically vary with time, e.g. the crack will open and close several times. Therefore, the seismic behaviour of anchorages depends on numerous parameters, including:

- the amplitude, rate, sequence, and number of cycles of the imposed actions,
- the direction of application of the actions (axial, shear, combined),
- the state of the surrounding concrete (non-cracked or cracked, crack orientation relative to the anchor axis, crack behaviour during the strong ground motion),

- quantity and orientation of reinforcement in the vicinity of the anchorage, and
- the characteristics of the anchor, including load transfer mechanism, material properties, diameter and embedment.

Seismic loading exhibits several characteristics that may affect the failure mode of the anchor. These include high rates of load increase and repeated excursions into the post-elastic range. Limited testing indicates that high strain rates do not have an adverse effect on anchor tension performance. However, repeated loading beyond the elastic capacity of the concrete and the anchor components (steel rod, sleeve, etc.) may have several consequences for the anchor. Crushing of the concrete in the load bearing regions of the anchor may lead to increased displacements and re-distribution of load between anchors in a group. Surface spalling and crushing of surface concrete around anchors loaded in shear will lead to increased bending in the anchor body and increase the likelihood of low-cycle fatigue failure of the steel components brought on by repeated yielding cycles.

Due to the scarcity of experimental results, the design of anchorages for seismic actions should be based on systematic experimental investigations of the main parameters that influence the behaviour of the anchorages.

The available experimental results illustrating some of the main influencing parameters are presented in the following sections.

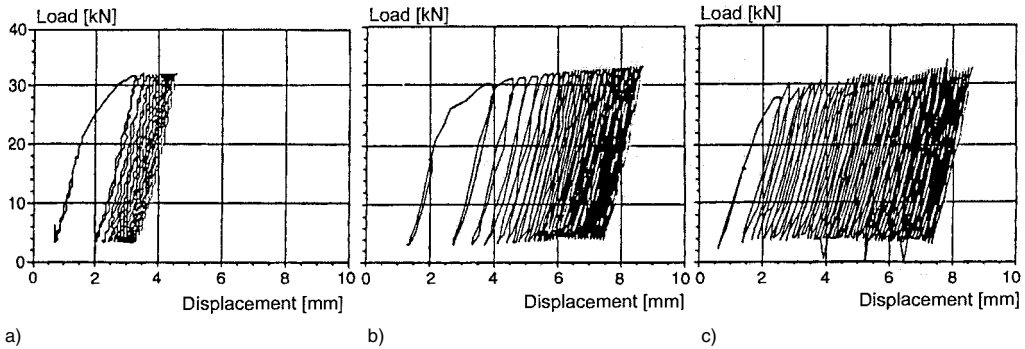


**Fig. 10.7** Load-displacement curves of undercut anchors M12 ( $h_{ef} = 80$  mm) in cracked concrete ( $w = 0.7$  mm) under cyclic loading (Eibl, Keintzel (1989))  
 a) Frequency 1 Hz, b) Frequency 5 Hz, c) Frequency 10 Hz

#### 10.4.1 Tension cycling

Fig. 10.7 shows the results of cyclic tension tests with undercut anchors situated in cracks having a width of  $w = 0.7$  mm. The load was cycled between 2 kN and 0.8 times the average failure load as determined from monotonic tests. The anchors were cycled for 10 seconds, so that with increasing frequency the number of the load cycles increased from  $n_{cyc} = 10$  ( $f = 1$  Hz) to  $n_{cyc} = 100$  ( $f = 10$  Hz). The results indicate that anchors suitable for use in cracked concrete exhibit increasing displacements with successive load cycles but that these displacements tend to stabilise in fewer than 50 cycles.

Cycling performed at load levels below the peak monotonic capacity do not typically result in anchor failure. Furthermore, the anchor post-cycling capacity and displacement at peak load as measured under monotonic loading do not generally differ significantly from normal monotonic behaviour (Fig. 10.8).

Mechanical anchors and cast-in-place headed bolts are not typically subjected to direct axial compression. In most cases, compression loads are transferred to the concrete via the fastened component. Where anchors are used in a stand-off or cantilever configurations, they are typically equipped with a bearing washer and nut.

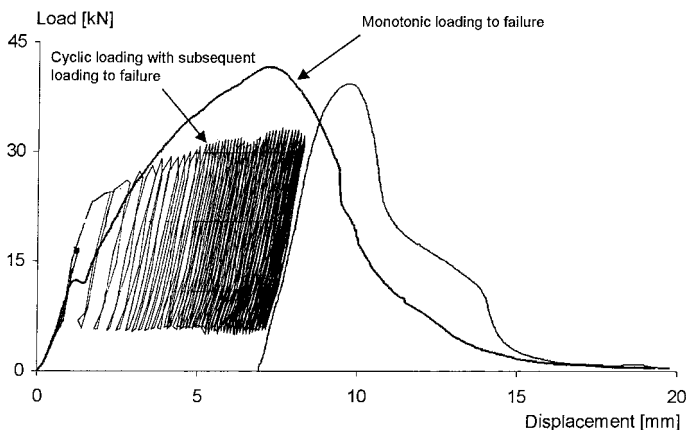


**Fig. 10.8** Influence of cycling on the tension load-displacement behaviour of undercut anchors M12 ( $h_{ef} = 80$  mm) in cracked concrete ( $w = 0.7$  mm) failing due to concrete cone break-out (after Eibl, Keintzel (1989))

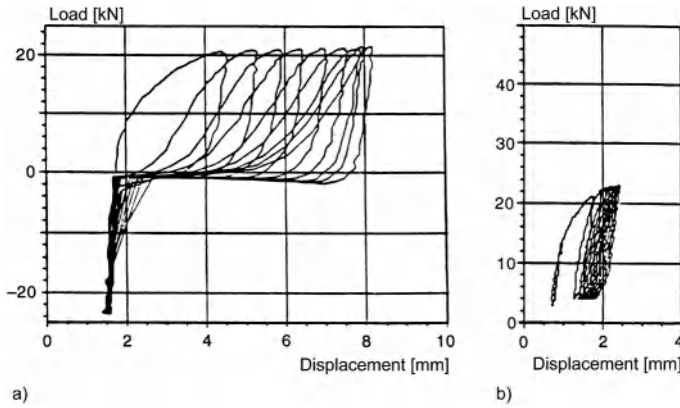


**Fig. 10.9** Behaviour of undercut anchors M12 ( $h_{ef} = 80$  mm) in cracked concrete ( $w = 0.7$  mm) (Eibl, Keintzel (1989))  
 a) Alternating tension-compression loading, b) Pulsating tension loading

This is necessary for several reasons. First, direct transference of compression loads to the embedded end of the anchor could result in a concrete breakout failure of the backside of the member in which the anchor is embedded. Second, and most important, the load-transfer mechanisms of most post-installed mechanical anchors are not suitable for transferring compression loads. Consequently, fasteners subjected to cyclic tension/compression loads may be expected to exhibit less favourable results (compare Fig. 10.9 a with Fig. 10.9 b).

The effect of crack width on the concrete cone capacity during tension cycling is the same as for the case of monotonic loading (refer to Figs. 4.127, 4.133, and 4.142).

Although sufficient experimental data is not available to establish the effect of tension cycling on failure modes other than concrete cone breakout, e.g. steel failure or pull-out failure, preliminary tests indicate that tension cycling well below the peak monotonic capacity does not significantly influence the load bearing capacity and displacement at peak load upon subsequent monotonic loading.

#### 10.4.2 Shear cycling

Reverse cyclic shear loading on anchorages during earthquakes is of critical importance due to the likelihood of low-cycle fatigue failure of

the anchor steel components. The low-cycle fatigue strength of anchors depends on the number and type of load cycles (pulsating or alternating) and the degree of inelastic deformation of the anchor during cycling. Reverse cyclic shear loading, which is the most common type of shear loading during an earthquake, is more critical for low-cycle fatigue than pulsating shear loading. Usami, Abe, Matsuzaki (1980/2) found that the low-cycle fatigue capacity of anchors subjected to reverse cycling is typically on the order of 70% to 80% of the value corresponding to pulsating shear loading (Fig. 10.10). The low-cycle fatigue strength of an anchor may be assumed to be less than 40% of the monotonic shear strength.

Fig. 10.11 illustrates typical hysteretic loops for an anchor located far from any edges and subjected to cyclic shear loading. The anchor was subjected to symmetric alternating displacements followed by monotonic loading to failure. Cycling did not reduce the ultimate load indicating that low-cycle fatigue had not taken place. The loops show a high degree of pinching, i.e. the energy dissipated by the anchor (damping) during cycling is low. In addition, the peak load associated with each successive cycle is reduced. This progressive reduction of peak load for anchors subjected to constant displacements is illustrated for several anchor types in Fig. 10.12. The load reduction tends to stabilise during

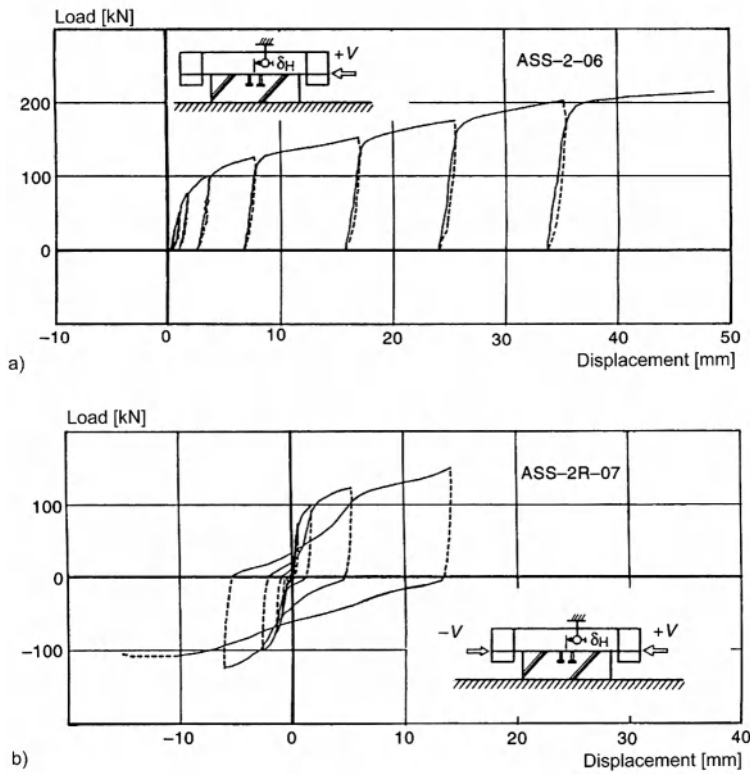


**Fig. 10.10** Load-displacement curves for a group of two headed anchors ( $d = 19$  mm) in non-cracked concrete (Usami, Abe, Matsuzaki (1980/2))  
 a) Pulsating shear loading, b) Alternating shear loading

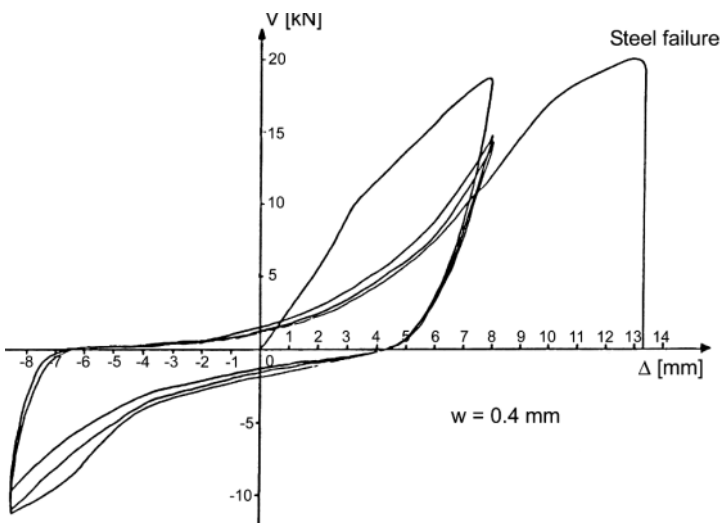


**Fig. 10.11** Typical load-displacement curve for a post-installed metal anchor in cracked concrete ( $w = 0.4$  mm) located far from edges loaded under alternating shear displacements (Vintzeleou, Eligehausen (1991))

cycling. After 5 cycles the load resisted by the anchorage is between 60 % to 80 % of the load developed upon initial loading (Fig. 10.12). Conversely, when the anchor is subjected to force-controlled reverse cyclic loading, displacements during cycling tend to increase with increasing numbers of cycles.

Shear loading of anchors located close to an edge may result in concrete edge failure with an attendant sudden loss of capacity. The provision

of tieback reinforcement placed directly against the anchor and close to the surface of the concrete can result in a more ductile behaviour (Fig. 10.13).

In most cases where anchorages are installed in existing structures, such appropriately detailed tieback reinforcement is lacking. Thus the case of anchorages installed close to edges of unreinforced concrete sections should be carefully considered in the design process.

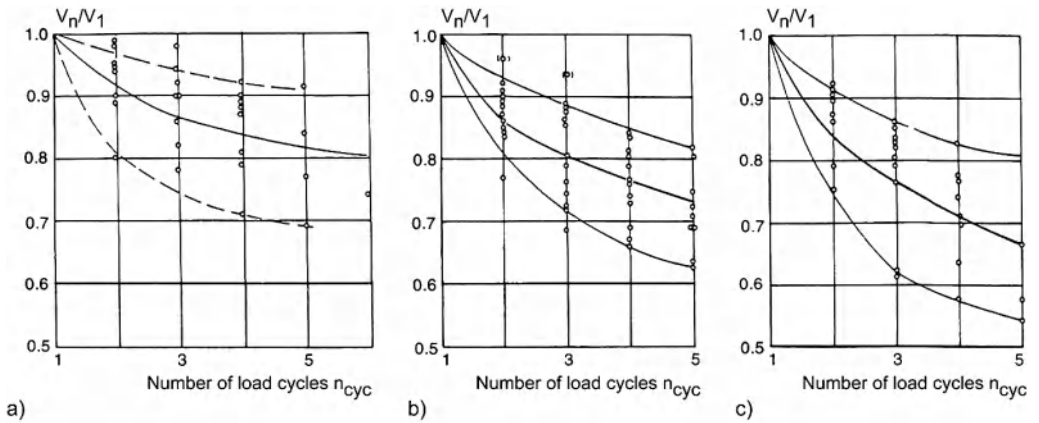


**Fig. 10.12** Force response degradation due to alternating shear cycling (Vintzeleou, Eligehausen (1991))  
 a) Undercut anchors ( $M12, h_{ef} = 80 \text{ mm}$ )  
 b) Torque-controlled expansion anchors ( $M12, h_{ef} = 80 \text{ mm}$ )  
 c) Bonded anchors ( $M12, h_{ef} = 100 \text{ mm}$ )

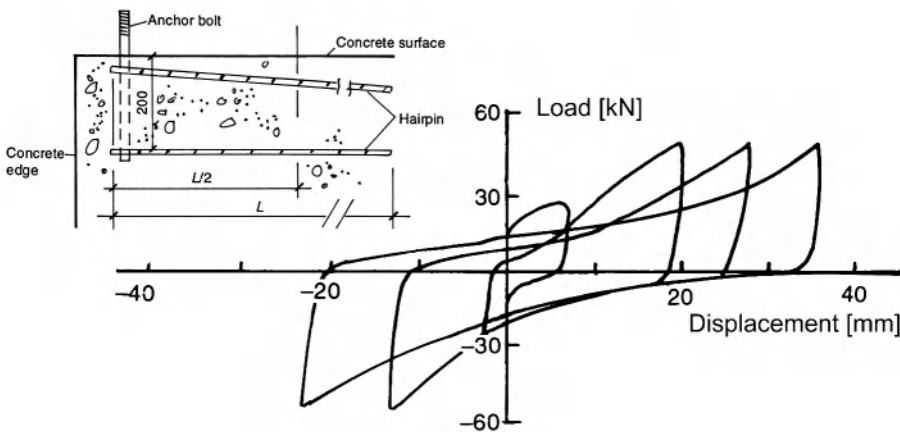


**Fig. 10.13** Load-displacement curve of an anchor at a small edge distance in suitably reinforced concrete (Klingner, Mendonca, Malik (1982/1))

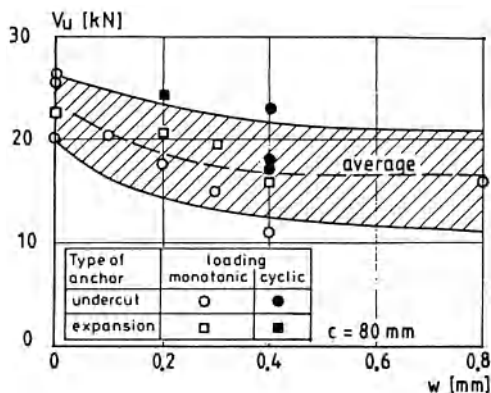


**Fig. 10.14** Influence of crack width on concrete edge failure load (Vintzeleou, Elgehausen (1991))

The effect of cracking on fasteners loaded under reverse cyclic shear, regardless of the direction of loading relative to the crack orientation (parallel, perpendicular), is comparable to monotonic shear loading (Fig. 10.14).

Testing to date indicates that if low-cycle fatigue failure of the anchor material can be prevented, the peak capacity of an anchor loaded monotonically in shear subsequent to shear cycling will be similar to that achieved without cycling. In reverse cyclic shear tests with 30 or

fewer alternating shear cycles, low-cycle fatigue failure is avoided if the peak load during the cycles is kept to less than about 40 to 50% of the monotonic shear strength of the anchor. It should be noted that these tests are designed to avoid secondary moments such as might result from fixture rocking, standoff, etc., and that such secondary moments can have a significant influence on the low-cycle fatigue performance of the anchor.

### 10.4.3 Combined tension and shear cycling

In practice, anchorages under seismic loading will typically be subjected to simultaneous tension and shear cycling. At the present, little experimental data is available on this topic. Recent design specifications (*American Concrete Institute* (2005)), however, have adopted an interaction relationship that is the same for static and dynamic (seismic, wind) loading (refer to section 14.5.5.4).

### 10.4.4 Loading rate

Fig. 10.15 shows results from anchors loaded in tension with a ramp loading function corresponding to loading rates typical for strong ground motion. The capacity of all fasteners tested in non-cracked concrete conditions under dynamic loading was greater than that observed

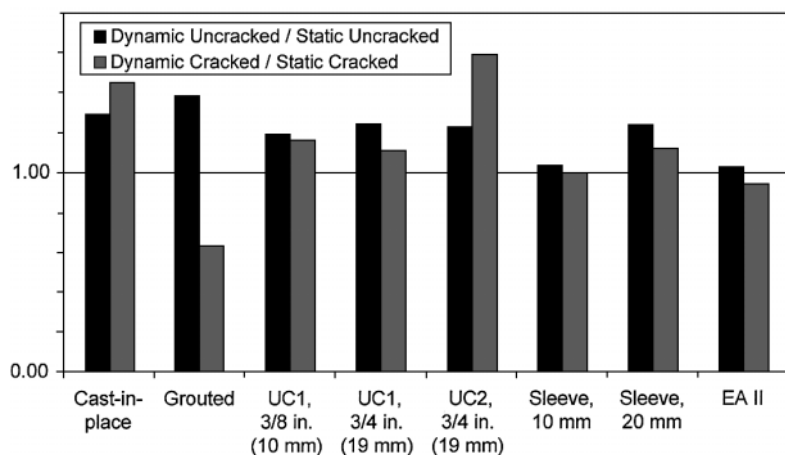


**Fig. 10.15** Ratio of tensile dynamic to static bearing capacity of several anchor types in non-cracked and cracked ( $w = 0.3 \text{ mm}$ ) concrete (Cast-in-place = cast-in-place headed anchor, Grouted = grouted anchor, UC = undercut anchor, Sleeve = sleeve type torque-controlled expansion anchor, EA = wedge-type torque-controlled expansion anchor) (after Klingner, Hallowell, Lotze, Park, Rodriguez, Zhang (1998))

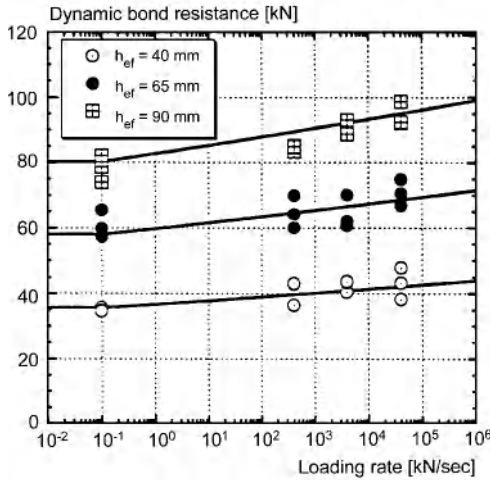


**Fig. 10.16** Dynamic bond resistance in non-cracked concrete as a function of loading rate (Fujikake, Nakayama, Sato, Mindess, Ishibashi (2003))

under static loading. In tests with a variety of anchor types positioned in cracks ( $w = 0.3$  mm) reduced capacity under dynamic loading was observed for the tested cementitious grouted anchor system and, to a lesser degree, for the tested wedge-type anchor. This reduction of capacity was associated with a change in the failure mode from concrete failure under static load to pull-out under dynamic load.

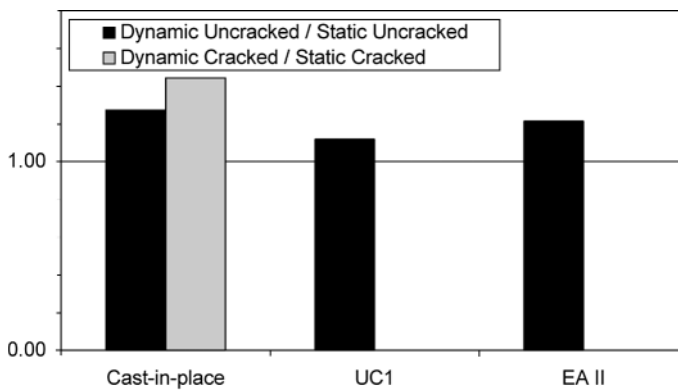


**Fig. 10.17** Ratio of shear dynamic to static bearing capacity of several anchor types in cracked ( $w = 0.3$  mm) and non-cracked concrete (Cast-in-place = cast-in-place headed anchor, UC = undercut anchor, EA = wedge-type torque-controlled expansion anchor) (values for UC1 and EA II in cracked concrete not available) (after Klingner, Hallowell, Lotze, Park, Rodriguez, Zhang (1998))

Similar results have been obtained for bonded (adhesive) anchors loaded in tension in non-cracked concrete. Fig. 10.16 demonstrates the increase in bond resistance with increasing loading rate. Under cracked concrete conditions, behaviour similar to that of grouted anchors may be expected (compare Fig. 10.15).

Tests of anchors loaded in shear at dynamic loading rates show similar results as for tension loading (Fig. 10.17).

Summarising, dynamic loading rates typical for sub-structure response in buildings subjected to earthquake excitations have little or no effect on the load-bearing capacity of anchors, provided that concrete failure governs the behaviour. Dynamic loading rates can, however, lead to a change in the tension failure mode for certain anchor types; that is, the failure mode that the anchor exhibits under rapid loading is different from that associated with static load.

### 10.4.5 Load cycle sequence

Where concrete failure governs the anchor behaviour, the capacity is primarily determined by the maximum load or displacement applied during a cyclic input motion (Weigler, Lieberum (1984)). The sequence of the load steps (increasing, cascading, random) does not appear to be significant (Fig. 10.18). Fig. 10.18b illustrates how anchor displacements



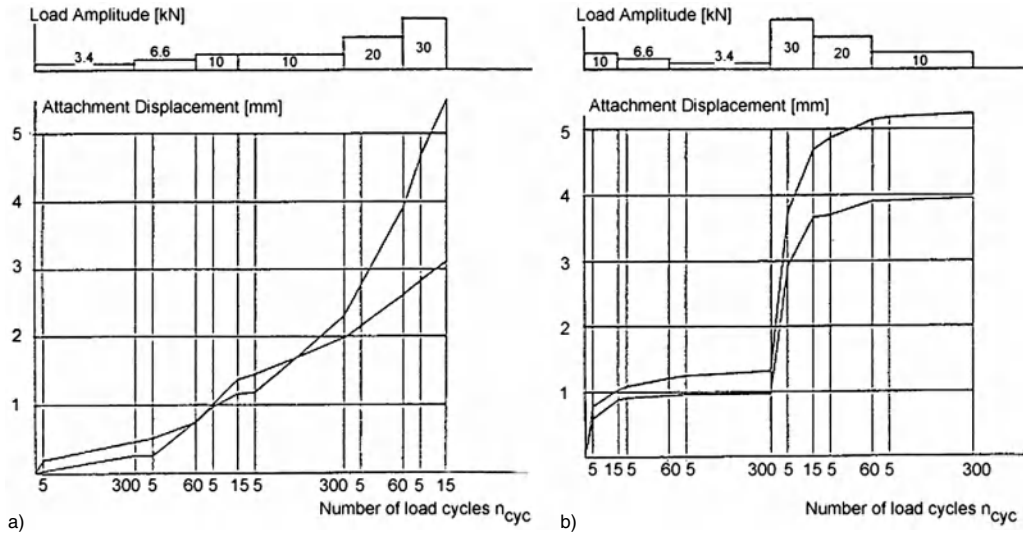


**Fig. 10.18** Influence of the order of load cycles on the tension load-displacement behaviour of anchors suitable for use in cracked concrete (Weigler, Lieberum, (1984))  
 a) Increasing load levels, b) Cascading load levels

tend to stabilise during cycling at loads levels below the previous maximum. In cases where the low-cycle fatigue behaviour of the anchor material is relevant, the sequence, number and intervals of the cycling sequence will be of greater importance.

**10.4.6 Crack cycling**

The tension performance of anchors located in cracks can be significantly affected by the number of cycles of crack width variation,  $n_w$ , and the ratio of minimum to maximum crack width during cycling. Fig. 10.19 shows that the difference between the maximum and minimum crack width can be decisive for the failure of certain anchor types, even for the relatively low number of cycles ( $n_w \sim 30$  cycles) expected in a reinforced concrete structural component during an earthquake.

Investigations described by Sippel, Asmus, Eligehausen (2001) for different types of undercut anchors tested in cycled cracks are shown in Fig. 10.20. In the figure the average displacement of 5 tests with anchors located in cracks of a tension member is plotted as a function of the number of crack cycles. The anchors

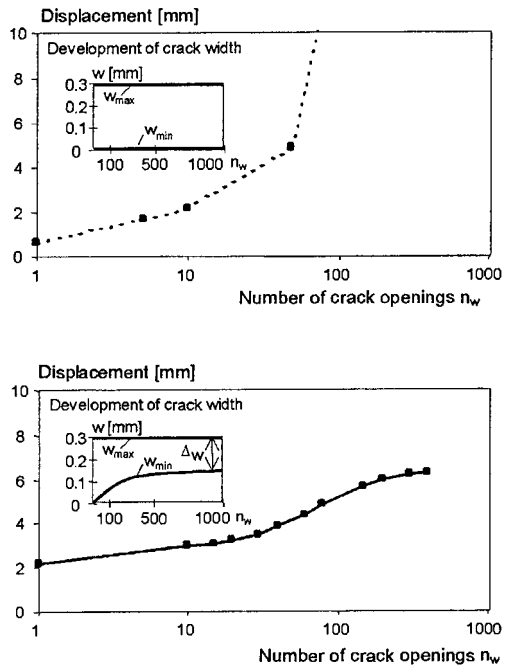


**Fig. 10.19** Effect of the difference between the maximum and minimum crack width during crack opening and closing on anchor displacement (Seghezzi (1985))

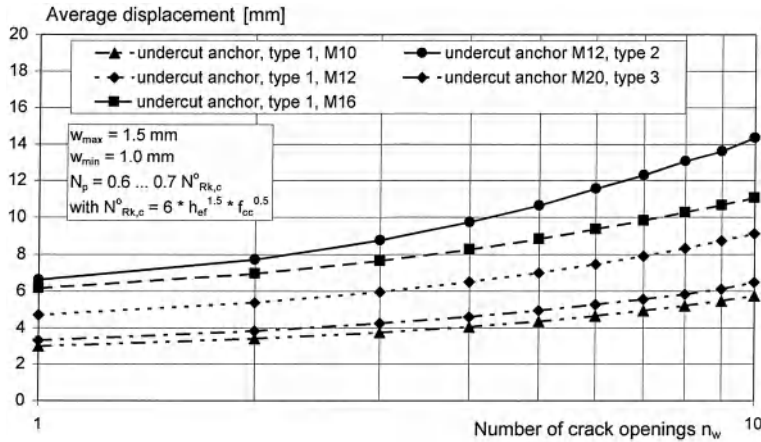


**Fig. 10.20** Average displacements of different undercut anchors in tests with opening and closing cracks as a function of the number of crack openings (Sippel, Asmus, Elgehausen (2001))

were loaded with a constant tension load  $N_p = 0.6 \cdot N_{Rk,c}^0$  to  $0.7 \cdot N_{Rk,c}^0$ , where  $N_{Rk,c}^0 = 6 \cdot \sqrt{f_{cc}} \cdot h_{ef}^{1.5}$  is the 5%-fractile of the concrete cone failure loads in cracked concrete with a large crack width. In the tests, the maximum crack width was  $w_{max} = 1.5$  mm and the minimum crack width was  $w_{min} = 1.0$  mm. The figure shows that displacements increase with the number of crack opening cycles. This increase depends mainly on the load bearing area of the undercut system, the magnitude of the constant tension load on the anchor and the number of crack cycles. During crack cycling none of the tested anchors failed. Experience has shown, however, that anchors possessing an insufficient bearing area may be pulled out after a small number of cycles. Furthermore, in general the increase in anchor displacement caused by

crack cycling is typically larger than the displacement that occurs due to load cycling in a constant crack width.

Clearly, cracking behaviour in structures subjected to strong ground motion may be quite different from that represented by typical crack cycling tests performed in the current approval procedures (compare section 14.2). Shear reversal in walls and diaphragms may result in crack widths significantly greater than those currently employed in anchor testing. Furthermore, while flexural members undergoing moment reversal will tend to exhibit cracking behaviour more closely mimicked by crack cycling testing, it remains unclear how strongly anchor performance is affected by an additional pre-compression stress induced in the concrete upon moment reversal.

## 11 Behaviour of anchors in fire

The fire resistance of anchorages is strongly dependent on the construction of the entire fastening assembly. In general, fire resistance can only be determined through testing unless protective measures are provided (e.g. casing, cladding, protective coating or concrete encasement of steel parts) that permit a classification according to a relevant standard, such as *DIN 4102 part 4* (1994).

Fire tests can be performed using various time-temperature curves. The considerations in this chapter are valid for test room temperatures following the standard time-temperature curve according to *ISO 834-1* (1999), which is plotted in Fig. 11.1.

At high temperatures the strength of steel decreases markedly (*Kordina, Meyer-Ottens* (1981)). According to studies by *Latenser* (1993) and *Reick* (2001), the anchor steel stress at failure during a fire is a function of the duration of the fire, the type of steel (galvanised or

stainless) and the diameter of the anchor. In Fig. 11.2 the results of more than 300 fire tests on different anchor types and sizes are evaluated. The tests were performed at different testing institutes using several different fixtures. The anchors were installed in both non-cracked and cracked concrete and loaded with a sustained tension load. Failure was caused by rupture of the anchor bolt or stripping of the threads. In Fig. 11.2 each data point represents the steel stress calculated from the applied load at the time of failure. The curves shown in the figure represent the trend line for the average behaviour. The figure demonstrates that the rupture steel stress decreases significantly with increasing fire duration and is much higher for stainless steel than for galvanised steel. The scatter of the test results is very large. This is mainly due to the different anchor sizes used in the tests. Therefore, in Fig. 11.3 the test results shown in Fig. 11.2 for anchors made from galvanised steel are plotted again, according to anchor size. The rupture steel stress increases with increasing anchor diameter. The influence of the diameter is very pronounced for a fire duration up to about 60 minutes and is smaller for longer duration. This can be explained by the increasing temperature in the bolt with decreasing diameter (Fig. 11.4).

Even for a constant anchor diameter, the scatter of the test results is quite large. This is particularly true for a short fire duration. One explanation for this is given in Fig. 11.5. The figure shows the temperature in the fixture as a function of the fire duration. The temperature was measured at the back of the fixture at a distance of about 10 mm from the anchor. Because of the high thermal conductivity of steel, the temperatures of the fixture and the anchor are almost identical. The different curves in Fig. 11.5 apply to various form factors  $A/V$ , where  $A$  is the area

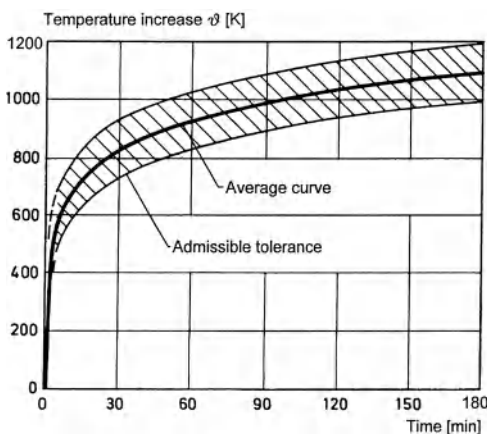


**Fig. 11.1** Standard time-temperature curve according to *ISO 834-1* (1999)

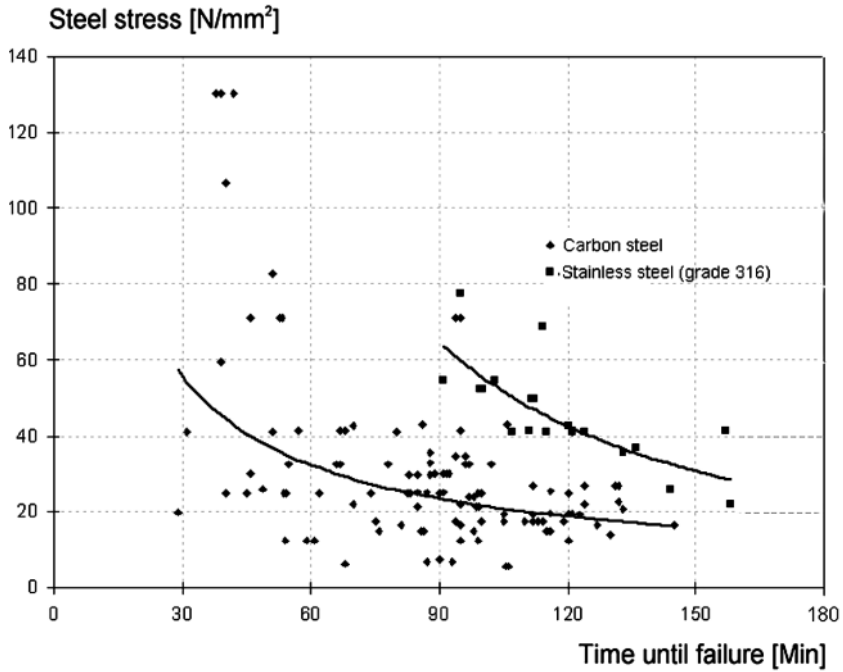


Fig. 11.2 Steel stress at failure as a function of the time until failure (Reick (2001))

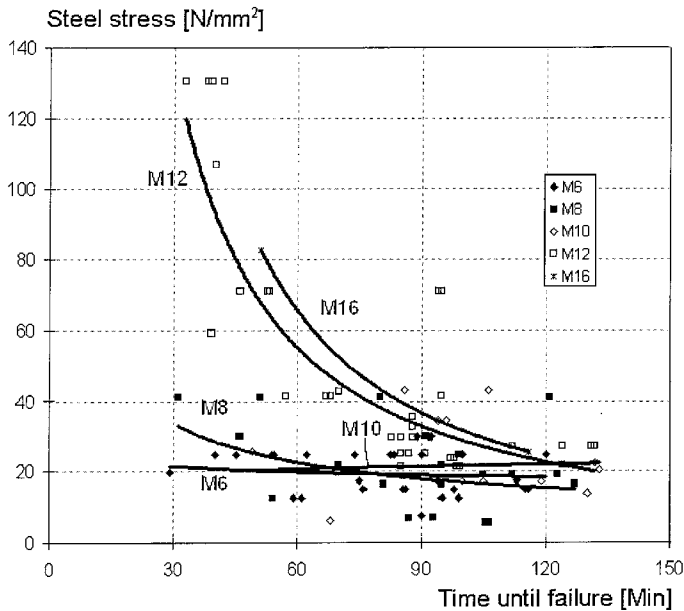
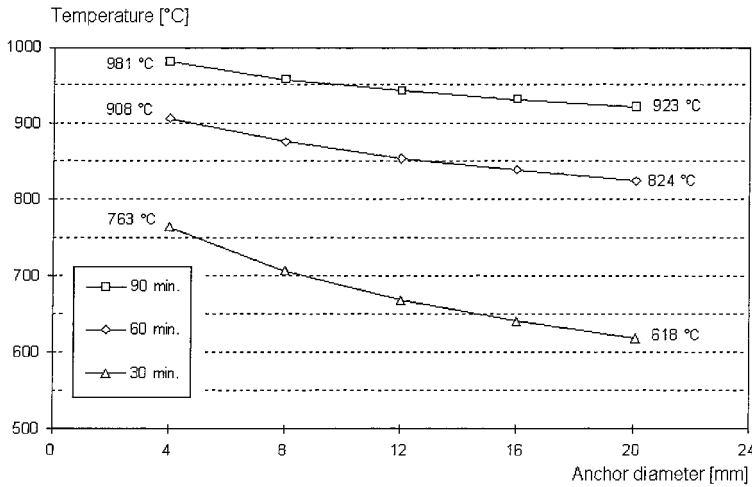
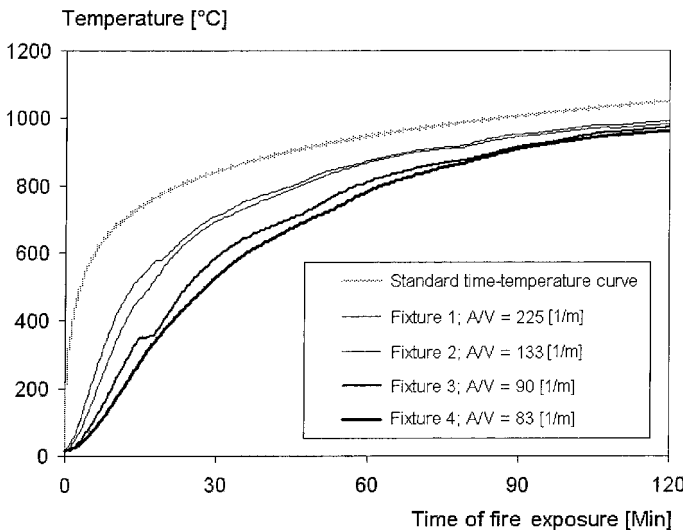


Fig. 11.3 Steel stress at failure as a function of the time until failure for anchors M6 to M16 made from galvanised carbon steel (Reick (2001))



**Fig. 11.4** Calculated temperature of anchors as a function of the anchor diameter for various duration of fire exposure (Reick (2001))



**Fig. 11.5** Measured temperature of fixtures as a function of the duration of fire exposure; fasteners located in non-cracked concrete (Reick (2001))

of the fixture and  $V$  is its volume. It can be seen that for a short fire duration the fixture temperature is lower for massive fixtures (fixture 4) compared to less massive fixtures (fixture 1). A further reason for the scatter of the test results is that some of the anchors were located in cracks and some in non-cracked concrete. During the first approximately 30 minutes of a fire test, water evaporates from the concrete. Evaporation is especially large at cracks. The evaporat-

ing water temporarily cools the fixture. This effect can be seen in Fig. 11.6 in which the measured fixture temperatures are plotted. In these tests the anchors were located in cracks. With less massive fixtures (fixtures 1 and 2), extensive water evaporation was observed during the test, which caused a decrease in the steel temperature to about 100 °C. The influence of water evaporation diminishes after approximately 60 minutes fire duration.

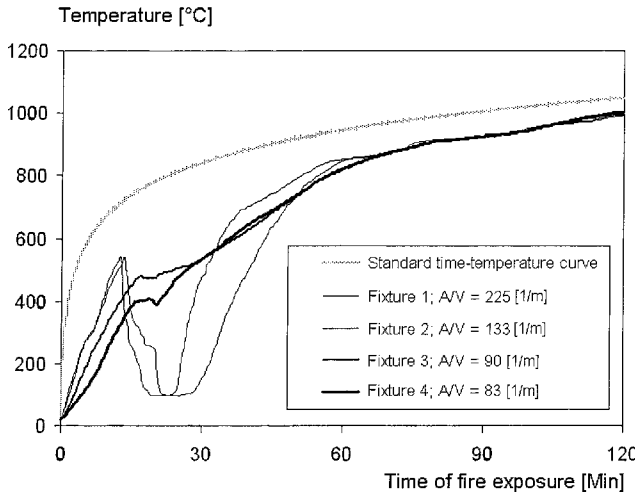


**Fig. 11.6** Measured temperature of fixtures as a function of the duration of fire exposure; fasteners located in cracked concrete (Reick (2001))

**Table 11.1** Characteristic tension strength of a fastener made of galvanised carbon steel under fire exposure (Deutsches Institut für Bautechnik (2003))

Diameter of anchor bolt or thread [mm]	Anchorage depth [mm]	Characteristic tension strength $\sigma_{Rk,s,fire}$ [N/mm <sup>2</sup> ] of an unprotected fastener made of galvanised carbon steel in the case of fire exposure up to a time (fire resistance class R) of			
		30 min (R 15 to R30)	60 min (R45 and R60)	90 min (R90)	120 min ( $\leq$ R120)
6	$\geq 30$	10	9	7	5
8	$\geq 30$	10	9	7	5
10	$\geq 40$	15	13	10	8
$\geq 12$	$\geq 50$	20	15	13	10

**Table 11.2** Characteristic tension strength of a fastener made of stainless steel A4 (grade 316) under fire exposure (Deutsches Institut für Bautechnik (2003))

Diameter of anchor bolt or thread [mm]	Anchorage depth [mm]	Characteristic tension strength $\sigma_{Rk,s,fire}$ [N/mm <sup>2</sup> ] of an unprotected fastener made of stainless steel in the case of fire exposure up to a time (fire resistance class R) of			
		30 min	60 min (R 15 to R30)	90 min (R45 and R60)	120 min (R90) ( $\leq$ R120)
6	$\geq 30$		10	9	7
8	$\geq 30$		20	16	12
10	$\geq 40$		25	20	16
$\geq 12$	$\geq 50$		30	25	20

To minimise the scatter of results found at different testing laboratories, the conditions for performing fire tests on anchors must be standardised. A proposal is given in *Deutsches Institut für Bautechnik* (2003).

Based on the results plotted in Fig. 11.2, the characteristic steel strengths of fasteners under fire exposure have been evaluated and are summarised in *Deutsches Institut für Bautechnik* (2003) (compare Tables 11.1 and 11.2).

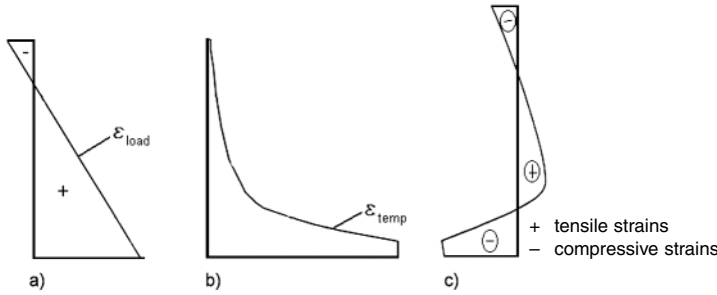


**Fig. 11.7** Strains and stresses in a reinforced concrete slab under three-point bending exposed to fire (Reick (2001))  
 a) Strains due to external load  
 b) Unrestrained thermal strains due to temperature increase in the concrete  
 c) Resultant strains in the concrete

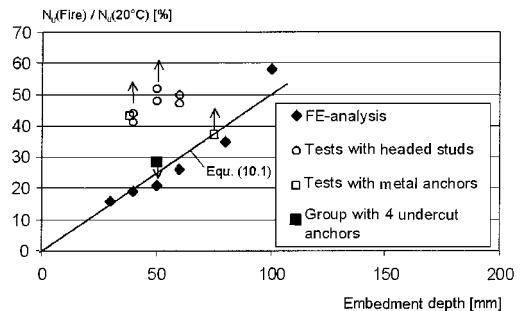
Limited test results have indicated that under fire exposure the shear and tension strength of an anchor are similar. Therefore in *Deutsches Institut für Bautechnik* (2003) it is recommended that the values given in Tables 11.1 and 11.2 also be used for the characteristic shear strength of fasteners under fire exposure.

Fig. 11.7a shows the distribution of strains  $\epsilon_{load}$  in a cross-section of a slab under three-point bending and Fig. 11.7b the strains  $\epsilon_{temp}$  due to unrestrained thermal expansion caused by fire exposure on the bottom of a slab. Due to the high concrete temperature under fire exposure, large temperature induced strains are generated. Superposition of the strains  $\epsilon_{temp}$  with the strained and displaced, but still plain, concrete cross-section due to external load results in compressive strains on the top and bottom surfaces of the slab (Fig. 11.7c). In the interior of the cross-section, large tensile strains occur that may lead to cracks with large widths. Furthermore, the stiffness of the concrete is reduced. These conditions can lead to anchor pull-out for expansion anchors with an embedment depth  $h_{ef} > 40$  mm (Reick (2001)). According to Reick, Elgehausen (2003) torque-controlled expansion anchors that are suitable for use in cracked concrete and undercut anchors loaded with a tensile load less than 25 % of the characteristic resistance for pull-out will show only small displacements during a fire up to 90 minutes. For displacement-controlled anchors a slip of up to 15 mm was observed. Generally, the pull-out

capacity of anchors exposed to fire should be determined by testing.

The large expansive forces developed inside of the concrete member during a fire are balanced by compressive stresses at the surface of the member (Fig. 11.7c). As consequence, existing cracks at the concrete surface tend to close. Anchors for suspended ceilings generally have a small embedment depth and are anchored in the surface concrete. Nevertheless, if such anchors are not protected against fire they typically exhibit steel failure.

The temperature beyond which concrete begins to experience strength decrease is approximately 100 °C (Weigler, Fischer, Dettling (1964), Kordina, Meyer-Ottens (1981)). Consequently, the concrete cone failure load of an anchor may be reduced in a fire. This has been



**Fig. 11.8** Relative concrete cone capacity after a fire exposure of 90 min as a function of embedment depth



confirmed in limited tests by *Paterson* (1978), as well as in tests on undercut anchors and headed studs performed by *Eligehausen, Reick* (1996), *Reick* (2001), and via numerical analyses as described by *Eligehausen, Pukl, Reick* (1995) and *Reick* (2001). Fig. 11.8 shows the results of tests performed by *Eligehausen, Reick* (1996) and *Reick* (2001), as well as the results of numerical analysis by *Reick* (2001). The ratios of the concrete cone capacities at a fire duration of 90 minutes to the average values at normal temperature are plotted as a function of the embedment depth. In some tests with single anchors, failure occurred after 90 minutes and the group with four undercut anchors failed after 75 minutes. These cases are indicated by arrows in the figure. In the numerical analysis the compressive stresses at the bottom of the concrete member due to temperature strains were not taken into account. Therefore the calculated concrete cone failure loads were smaller than the values observed in the experiments. According to the results of tests with single headed or undercut anchors exposed to fire, the diameter of the concrete cone is larger than under standard temperature (20 °C). This explains the relatively low capacity of the group with four undercut anchors. The concrete temperature increase and associated drop in strength associated with fire exposure attenuate rapidly with increasing depth in the concrete. Correspondingly, the relative concrete capacity increases with increasing embedment depth. The lower bound of the test results can be described by equation (11.1).

$$N_{u,fire,90} = \frac{h_{ef}}{200} \cdot N_{Rk,c} \leq N_{Rk,c} \quad (11.1)$$

where:

- $N_{u,fire,90}$  = concrete cone capacity for a fire exposure of 90 minutes according to the ISO standard time-temperature-curve
- $N_{u,c}$  = concrete cone capacity according to equation (4.10)
- $h_{ef}$  = embedment depth [mm]

Because of the larger cone diameter of anchors exposed to fire, the characteristic spacing and edge distance should be increased to  $s_{crN} = 2 \cdot c_{crN} = 4 \cdot h_{ef}$ .

For design for fire resistance, in general a global safety factor of  $\gamma = 1$  is required. This means that a structure may fail immediately after the required fire resistance duration. Taking into account the different safety concepts under normal temperature and fire exposure, it can be deduced from Fig. 11.8 that anchors having an embedment  $h_{ef} \geq 80$  mm and a load corresponding to the admissible working load at normal temperature will attain a fire resistance at least equal to a fire resistance class R 90 (90 minutes, standard ISO time-temperature curve).

The strength of synthetic resin grouts decreases considerably at temperatures over 80°C. Therefore, fire reduces the load-carrying capacity of bonded anchors. The rapid temperature decrease with increasing depth in the concrete implies that bonded anchors with a large embedment depth exhibit better performance than those with shallow embedment. The behaviour of synthetic resin grouts at high temperatures is product dependent. Therefore, the permissible load for each system in a fire must be determined experimentally.

Explosive spalling of the concrete cover may occur during fire exposure. Spalling is more prevalent with small member dimensions, high concrete moisture content and the presence of concrete compressive stresses (*Kordina, Meyer-Ottens* (1981), (1999)). Spalling is especially pronounced for high-strength concrete. To reduce the influence fire induced spalling on the capacity of fastenings, the concrete should be made using quartzite aggregates, direct contact of the concrete with moisture content should be avoided and the concrete humidity should be equal to the equilibrium humidity valid for dry interior rooms. If these conditions are not fulfilled, the outer concrete layer with a thickness of approximately 30 mm to 40 mm should be not considered when calculating the concrete cone and pull-out capacity of the anchors.

## 12 Corrosion of anchors

Steel anchor bolts are generally provided with some form of corrosion protection. Typically, they are electrogalvanised (electrochemically zinc plated) to provide a zinc thickness of 5 to 10  $\mu\text{m}$ . For exterior applications or aggressive environments, they may be hot-dip galvanised to produce a coating thickness ranging between 40 to 100  $\mu\text{m}$ . For mechanical anchors, hot-dip galvanising may not provide sufficient control of coating thickness for friction-sensitive parts. For such cases, the steel parts may be sheradised, a process by which zinc is deposited via temperature diffusion bonding. While achievable coating thicknesses are similar to hot-dip galvanising, thickness control is superior. For increased corrosion resistance, anchors may also be manufactured from austenitic stainless steels.

Because it is far less noble than steel, zinc provides sacrificial or cathodic protection from corrosion for the underlying steel. In addition, the primary product of zinc oxidation is zinc carbonate, which forms a protective layer and slows the progress of zinc corrosion. The rate of zinc dissolution determines the duration of protection for the steel. Since the rate of weathering is relatively constant and uniform, the life of the coating is directly proportional to its thickness. The rate depends mainly on the presence of sulphur dioxide. Under atmospheric conditions as noted, the rates of loss given in Table

**Table 12.1** Average rates of zinc plating loss under atmospheric conditions (after *Beratung Feuerverzinken* (1983))

Atmosphärentyp	Loss [ $\mu\text{m}/\text{Jahr}$ ]
Rural	1.3 – 2.5
Urban	1.9 – 5.2
Industrial	6.4 – 13.8
Marine	2.2 – 7.2

12.1 can be used as a guideline for calculating the service life of a zinc coating.

These rates of loss can also be used as a guide for anchors in facades when the facade is correctly ventilated, i.e. when there is no interstitial condensation nor condensation in the ventilation space. In these cases, brief periods of condensation followed by periods of drying out with good ventilation can be assumed for the anchors. Inadequately ventilated facades result in higher rates of loss than those given in Table 12.1.

Permanently damp, poorly ventilated narrow spaces are problematic for the use of zinc coating because these conditions lead to the formation of porous, loose corrosion products (white rust) which do not offer any protection. Such conditions can occur in the annular gap between the anchor and the sides of the drilled hole where the anchor is directly exposed to the weather or where it is installed in a wall subject to condensation, or where the anchor must penetrate through layers of thermal insulation or adhesive.

Contact between galvanised parts and concrete is not generally a problem provided the cement does not have a high alkali content (*Menzel* (1985), *Menzel* (1992)). Annual rates of zinc loss of 1  $\mu\text{m}$  to 1.4  $\mu\text{m}$  have been measured in concrete at 80 % relative humidity. This rate is generally valid for carbonated concrete as well. Periodic wetting or permanent exposure to moisture can increase the rate of loss to 7 to 15  $\mu\text{m}$  per year. The zone of transition from the concrete to the atmosphere represents the greatest risk for accelerated zinc loss.

After the zinc coating has been lost, the alkalinity of the concrete does not usually provide any additional protection for the anchor since the

concrete close to the surface of the drill hole carbonates within a few years (*Menzel (1992)*).

At present, most anchors approved for building work are electrogalvanised (coating thickness 5  $\mu\text{m}$  to 10  $\mu\text{m}$ ). The protection afforded by this galvanising is only adequate for *dry* interiors, e.g. in houses, shops, schools, or hospitals. It should only be regarded as temporary corrosion protection for anchors installed externally, in damp interior conditions, or behind curtain walls. This can be seen from the rates of loss given in Table 12.1 and has been confirmed by investigations of fastenings in structures. For these conditions, in just 5 years to 10 years after installation, electrogalvanised anchors exhibited an unacceptable degree of corrosion (Fig. 12.1). In contrast, *Theiler (1993)* first observed substantial levels of corrosion in galvanised

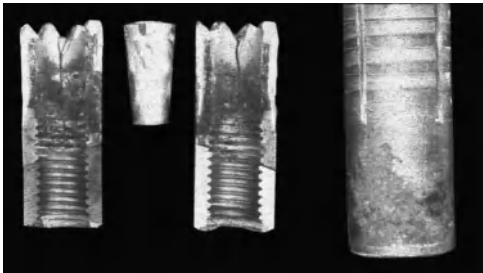


**Fig. 12.1** Photo of a galvanised expansion anchor after 3 years of use behind a facade (*Rehm, Lehmann, Nürnberger (1980)*)

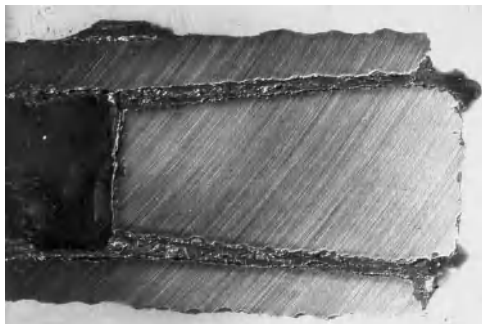


**Fig. 12.2** Photo of the expansion zone of a torque-controlled expansion anchor after 5 years of use; fastening of a road crash barrier, exterior environmental conditions (*Nürnberger, private correspondence*)

steel facade anchorages after 15 years service. It is also important to note that corrosion products (Fig. 12.2) can impair the function (follow-up expansion) of torque-controlled expansion anchors, and this can significantly reduce the failure load. Zinc-coated screw anchors may be sensitive to stress corrosion cracking and hydrogen embrittlement when used under outdoor or damp interior conditions and may fail after a rather short time.

The electroplated screws typically employed with plastic anchors in normal-weight concrete are sufficiently resistant to corrosion when used externally (also in industrial and coastal regions) if the head of the screw is protected in such a way that moisture cannot penetrate to the shaft of the screw. This protection can take the form of, for example, a fitted plastic cap, but suitable paints, injected sealant or plastic coatings provided by injection moulding are generally superior.

Non-galvanised headed studs are generally suitable for connections in dry interior locations only. Anchor plates should be painted.

As a rule, cast-in anchor channels are hot-dip galvanised (coating thickness  $\geq 50 \mu\text{m}$ ). When electrogalvanised bolts are employed, cast-in anchor channels should be used in *dry* interiors only; when hot-dip galvanised bolts are employed (coating thickness  $\geq 40 \mu\text{m}$ ), they may be used in damp interior conditions as well.

The corrosion behaviour of stainless steels as used for anchors has been studied in detail by several researchers including *Bäumel, Kügler (1975)*, *Ergang, Rockel (1975)*, *Bock, Kügler, Lennartz, Michel (1984)*, *Stichel (1986)*, *Böhni, Haselmair, Übeleis (1992)*, *Nürnberger (1995)*, *Arnold, Gümpel, Heitz, Pscheidl (1997)* and *Arnold, Gümpel, Heitz (1998, 1999)*. These studies led to the publication of Table 12.2 by the *Deutsches Institut für Bautechnik (1998)*, which covers stainless steels for use in building construction in Germany. In the table the equivalent AISI designations are also provided. This table also provides information on corrosion protection classes and typical applications. Class II and III steels are normally designated as A2 (304) and A4 (316), respectively.

**Table 12.2** Stainless steels approved for use in building construction in Germany and their permissible applications (after *Deutsches Institut für Bautechnik* (1998))

No.	Material No.	AISI designation	Corrosion protection class	Typical applications
1 2	1.4003 1.4016		I / Low	Interiors
3 4 5 6	1.4301 1.4541 1.4318 1.4567	304 321	II / Moderate	Accessible constructions without significant chloride or sulphur dioxide loads
7 8 9 10	1.4401 1.4404 1.4571 1.4439	316 316L 316Ti 317LN	III / Medium	Inaccessible constructions <sup>1)</sup> with moderate chloride or sulphur dioxide loads
11 12 13 14 15	1.4539 1.4462 1.4565 1.4529 1.4547	904L 318LN	IV / Severe	Installations with high corrosion potential due to exposure to chlorides or sulphur dioxide (or due to chemical concentrations, e.g. as found in seawater and road tunnel atmosphere); for indoor pools see footnotes <sup>2),3)</sup>

- 1) Inaccessible means constructions whose condition cannot be inspected or can only be inspected with difficulty and can only be repaired, if necessary, at very great expense.
- 2) Steel with material No. 1.4539 for components in indoor pool atmospheres without regular cleaning of the steel and water complying with Germany's Drinking Water Statute.
- 3) Steels with material Nos 1.4565, 1.4529 and 1.4547 for components in indoor pool atmospheres without regular cleaning of the steel and water rich in chloride salt (e.g. brine water).

Typical stainless steel grades used for anchors in the U.S. are *AISI 304* (1995) and *AISI 316* (1995). *AISI 303* (1995) (1.4305) stainless steel is also used, but less commonly. Class I stainless steels are not used for anchors in Germany. Class II steels are used only for headed studs which are welded to anchor plates made from class III steel. Class III steels are used for the manufacture of headed studs, anchor plates, cast-in channel anchors and their associated fittings, as well as anchors. A number of companies also supply torque-controlled expansion, undercut, bonded and bonded expansion anchors in highly corrosion-resistant class IV steels.

Stainless steels resist corrosion by forming a protective passivation layer that prevents further corrosion attack. If this layer is breached and cannot repair itself in response to an external aggressor, corrosion will occur. In contrast to the uniform surface corrosion associated with plain-carbon and low-alloy steels, however, corrosion of stainless steel is always local (pitting, crevice corrosion) but the rate of deterioration can be very fast. The corrosion products may not be readily visible. This may render

austenitic stainless steels of class II and class III unsuitable for certain applications.

It is primarily chlorides (sea or de-icing salt), and to a lesser extent sulphur dioxide, which trigger corrosion of stainless steels. Deposits of dust have an unfavourable effect. Narrow spaces, such as the interstitial gaps between plates, washer, nuts, etc., are particularly at risk for crevice corrosion.

Owing to the proportion of molybdenum in class III stainless steel (A4 steel), it is sufficiently resistant in exterior environmental conditions including industrial conditions and coastal regions (however, not directly in contact with seawater), and in damp interiors provided no further aggressive conditions occur. Class II stainless steel (A2 steel) is only adequate for less aggressive conditions (*Menzel* (1985)).

The high concentration of pollutants and the possibility of dust deposits in road tunnels (particularly at entrances and exits) render A4 steel (corrosion resistance class III) inadequate for tunnel applications (*Böhni, Haselmair, Übeleis* (1992)).

Stainless steels of classes II and III are particularly at risk of stress corrosion cracking in structures covering indoor chlorinated pools (*Stichel* (1986)). This also applies to their use in seawater (*Bock, Kügler, Lennartz, Michel* (1984)). Therefore, in some countries these steels are prohibited for load-bearing elements in such applications. Stress corrosion cracking in indoor swimming pools is triggered by acidic, oxidising condensation containing chloride due to the chlorination of the water (*Stichel* (1986)).

Contact with less noble metals (e.g. zinc) can result in galvanic corrosion of the less noble metal. This can be prevented by including non-conductive, isolating, intermediate layers (plastic washers etc.) or by coating the *noble* metal.

Although class II steels are suitable for less aggressive environmental conditions (e.g. rural atmosphere), it cannot be generally assured that atmospheric conditions will remain constant for the lifetime of the anchor. Furthermore the use of these anchors in more aggressive conditions or higher temperatures (e.g. behind dark facade panels) cannot be ruled out (*Eggert, Kulessa, Strassburg* (1975)). For this reason, some countries prohibit the use of class II stainless steels for anchors, e.g. Germany (*Deutsches Institut für Bautechnik* (1998)). One exception is headed studs made from class II steel and welded to class III anchor plates because here the concrete provides additional protection for the headed studs.

According to the current regulations in Europe (*European Organisation for Technical Approvals* (EOTA) (1997)) anchors made from class

III stainless steel (A4 steel) which are to be used in the open air (also in industrial conditions and in coastal regions), in damp interiors or for anchoring curtain walls are considered as corrosion resistant. Alternatively, permanent protection against corrosion may be provided by a special coating.

As described above the degree of protection offered by stainless steels of class III (A4 steels) is not adequate in certain special applications, e.g. in seawater, in atmospheres containing chlorides (e.g. indoor chlorinated pools), in road tunnels (particularly at entrances and exits) and in environmental technology applications (landfill sites, flue gas de-sulphurising plants). Therefore in Europe anchors made from A4 steel shall not be used for such applications (*European Organisation for Technical Approvals* (EOTA) (1997)). Class IV stainless steels are available for such situations. *Nürnberg* (1995) recommends the approved steel 1.4565, which exhibits good corrosion resistance and adequately high yield stresses, and *Böhni, Haselmair, Übeleis* (1992) recommend the approved steel 1.4529. Some anchor types have been successfully produced with this material and they fulfil the strict requirements for tunnel construction in Switzerland. Another alternative is to provide non-alloyed steel with double corrosion protection (e.g. hot-dip galvanising with a coating thickness of 70 µm to 100 µm plus a plastic coating). The advantage of this alternative is that any corrosion that does occur affects the entire surface of the bolt (uniform surface corrosion) and pitting corrosion or stress corrosion cracking is avoided.

### 13 Influence of fastenings on the capacity of components in which they are installed

Fastenings make use of the local tensile strength of the concrete. In a number of cases the concrete component also relies directly on that concrete tensile capacity. Examples include the region surrounding reinforcing bar anchorages and splices, the shear zone of slabs without shear reinforcement, and the interface of precast elements with cast-in-place composite toppings when shear dowels are not used. The introduction of loads by fastenings into these zones of tensile stress results in superposition of the tensile stresses caused by the overall structure response to external loading with those gener-

ated in response to the localized anchor loads. This can have the net effect of reducing both the capacity of the fastening and of the component (Rehm, Eligehausen (1984)). In addition, fasteners generate splitting forces (in the form of hoop stresses) as a result of both anchor preloading and external loading; these must be resisted by the orthogonal member reinforcement upon the initiation of splitting cracks.

The potential interactions of the fastening and the concrete component in which the anchor is installed are outlined schematically in Fig. 13.1.

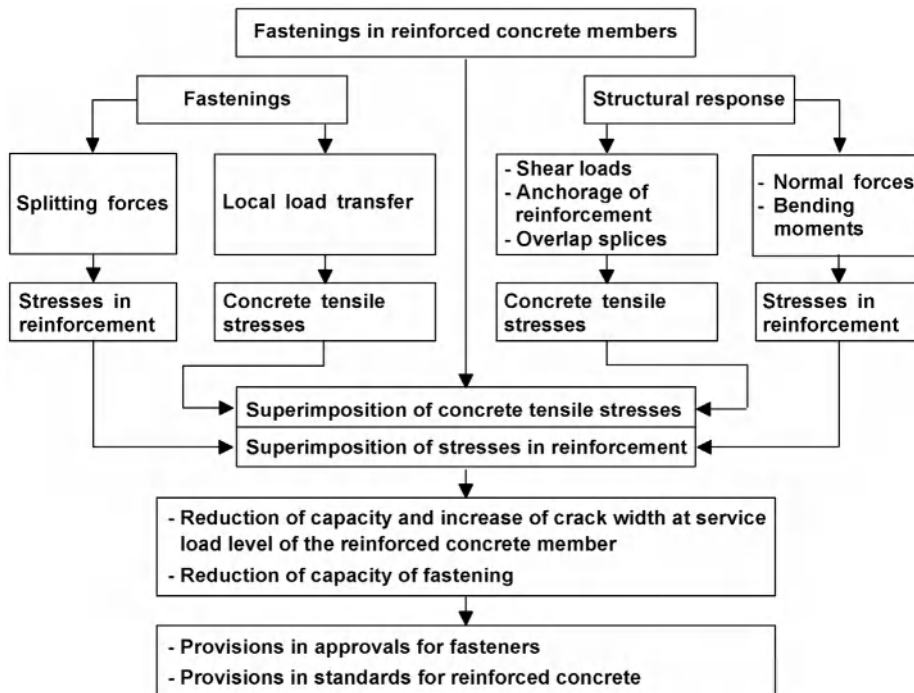
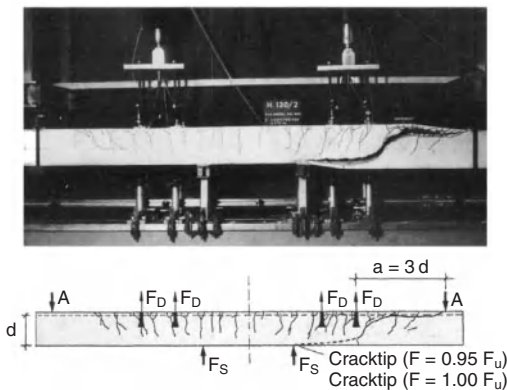


Fig. 13.1 Superimposition of concrete- and reinforcement tensile stresses due to local load transfer by anchors with stresses due to structural response (Reuter, Eligehausen (1992))

The manner in which the superposition of tensile stresses in the concrete and the onset of concrete cracking can affect the capacity of the fastener is addressed in section 4.2.1.3. In the following, the potential influence of anchor-induced local loads on the structural performance of a reinforced concrete member is reviewed.

The possible reduction of the capacity of a flexural reinforced concrete component as a result of the introduction of anchor-induced loads in the member tension zone is not explicitly considered in U.S. or European codes. The German code *DIN 1045-1* (2001) requires appropriate hanger or tieback reinforcement anchored in the compression zone where loads are introduced in the flexural tension side of the member; however, transmission of the anchor load back into the compression side of the member by means of tieback reinforcing is generally not practical where post-installed anchors are employed. Provision of such reinforcing in the case of cast-in anchor channels and embed plates with welded studs requires additional effort and attention to detail.

If special tieback reinforcement is not included, then loads transferred into the tension zone via fasteners can have a measurable reduction of the shear capacity of slabs containing no shear reinforcement (*Lieberum* (1986), *Lieberum, Reinhardt, Walraven* (1987), *Reuter, Eligehausen* (1992)). This can be explained in that the portion



**Fig. 13.2** Crack pattern at failure of a slab without shear reinforcement; a part of the load was transferred via anchors into the slab tensile zone (*Reuter, Eligehausen* (1992))

of the anchor load that cannot be accommodated by aggregate interlock across the shear crack or by dowel action of the flexural tension reinforcement must be transferred to the supports via the non-cracked concrete beyond the tip of the longest shear crack (Fig. 13.2). This results in higher tensile stresses in the vicinity of the crack tip which in turn initiate shear crack growth at a lower load than if the loads had been transferred into the compression zone (e.g., from the top side of the member).

If the entire member external load is introduced via fasteners into the tension zone, then the reduction in shear capacity for a shear span ratio of  $a/d \geq 3$  is about 14 % on average, in individual cases up to about 20 % compared to the value for a load in the compression zone (*Reuter, Eligehausen* (1992)). The ratio of embedment depth to component thickness does not seem to have any affect for  $h_{ef}/h < 0.7$ .

Non-linear FEM analyses by *Cervenka, Pukl, Eligehausen* (1990) confirm the experimental results. The analyses were based on the smeared crack approach and the crack band method of *Bazant, Oh* (1983), using a realistic description of the material behaviour of concrete. They indicate that a load introduced into the tensile zone leads to a deepening and widening of the characteristic dip in member flexural capacity

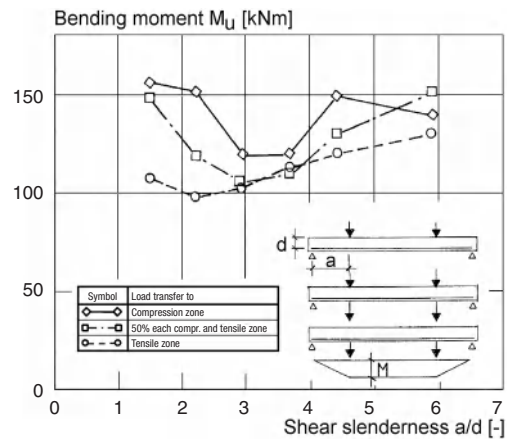


**Fig. 13.3** Bending moment  $M_u$  at failure of slabs without shear reinforcement as a function of the shear slenderness; results of numerical analysis (*Cervenka, Pukl, Eligehausen* (1990))



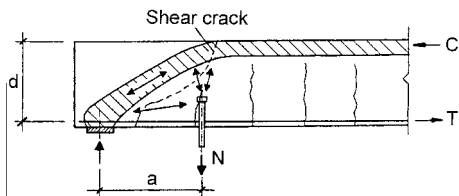


**Fig. 13.4** Load transfer mechanism in a slab without shear reinforcement; anchor loads are transferred into the tensile zone at a distance  $a < 2 \cdot d$  from the support (Lieberum, Reinhardt, Walraven (1987))

associated with shear span ratios between 2 and 4 first identified by Kani (1966) (see Fig. 13.3).

If fastenings are positioned near a support, part of the load is carried directly into the support while the other part is resisted by strut action, resulting in additional transverse tensile stresses in the compression strut (Fig. 13.4). The shear capacity is correspondingly reduced. Lieberum, Reinhardt, Walraven (1987) propose a simple model for calculating the shear failure load depending on the embedment depth of the anchor. It applies to shear span ratios  $1.5 \leq a/h \leq 2.5$ . Tests on flexural members with shear span ratio  $a/h = 1.5$  and the proportion of anchor loads exceeding 40 % of the total member load indicate a small decrease in the shear capacity of thick slabs ( $h = 470$  mm) and an approximately 50 % decrease in the case of thin slabs ( $h = 160$  mm) (Lieberum, Reinhardt, Walraven (1987)).

Transferring a load into the tension zone of a beam with shear reinforcement has less effect on the shear capacity – for an identical suspended

load – than in a slab without shear reinforcement. Tests described in Eligehausen, Mesureur, Okelo (1996) showed no significant reduction of the shear capacity when the anchor-induced load remained at or below 30 % of the permissible shear capacity of the member.

Another critical application common in building construction is anchorage into floor or roof structures consisting of precast components acting compositely with a site-cast topping slab. If the precast and site-cast components are not connected by adequately sized reinforcement (e.g. in form of stirrups), failure can occur if the adhesion strength at the interface is exceeded (Fig. 13.5). Fig. 13.6 plots the shear stress at the interface at failure as a function of the shear span ratio. The evaluated tests are described in Dardare (1973), Rehm, Eligehausen, Paul (1980) and Daschner (1986). For the common case where the slab is loaded from above and assuming that the interface has been roughened, the load-carrying capacity of the joint is typically sufficient to preclude the need for bond reinforcement between precast and on-site concrete. Corresponding design proposals are provided in Seiler, Kupfer, Manleitner (1989) and have been incorporated in building authority approvals for prestressed floor construction in Germany. If, on the other hand, the load is introduced into the precast concrete from below, then the load-carrying capacity of the joint is relatively low owing to the additional tension across the interface (Fig. 13.6). Therefore, in composite slab systems of this type constructed without bond reinforcement, the fasteners

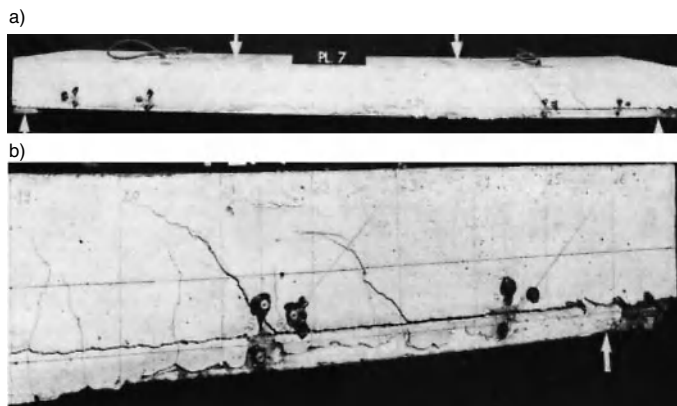


**Fig. 13.5** Failure of a reinforced concrete slab consisting of a precast concrete girder and cast in-situ concrete without connecting reinforcement (Rehm, Eligehausen, Paul (1980))  
a) Total view, b) Detail

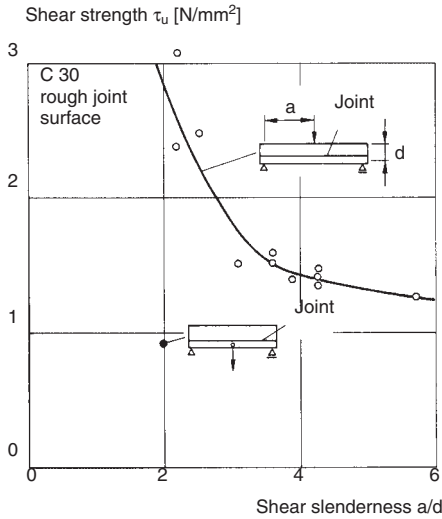


**Fig. 13.6** Shear stress at failure of the joint between pre-cast and cast in-situ concrete as a function of the shear slenderness (Rehm, Eligehausen (1984))

should extend into the topping concrete (Seiler, Kupfer, Manleitner (1989)). A limit on suspended loads of 0.5 kN/m<sup>2</sup>, corresponding to lightweight suspended ceilings or similar construction, is recommended by Seiler, Kupfer, Manleitner (1989) for cases where the anchorage terminates in the precast elements. If sufficient bond reinforcement is provided and well anchored in the compression zone, the composite member behaves like a beam or slab with shear reinforcement. In this case the influence of loads introduced by fastenings on the shear capacity is the same as described above for members with shear reinforcement.

Tests were conducted on reinforced concrete slabs in which all the reinforcing bars were spliced in the region of constant moment in order to determine the influence of fasteners on the capacity of overlap splices (Reuter, Eligehausen (1992)). The splices were designed to produce relatively large tensile stresses in the concrete (splices of welded wire meshes with stacked longitudinal bars and splices of 14 mm reinforcing bars with transverse bars not encompassing the splice). To force splice failure, the splice length was limited to about 60 % of code values. Tension loads of approximately

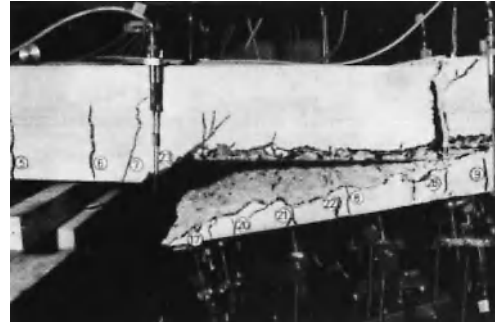


**Fig. 13.7** Failure of an overlap splice of reinforcing bars; anchor loads transferred into tensile zone (Reuter, Eligehausen (1992))

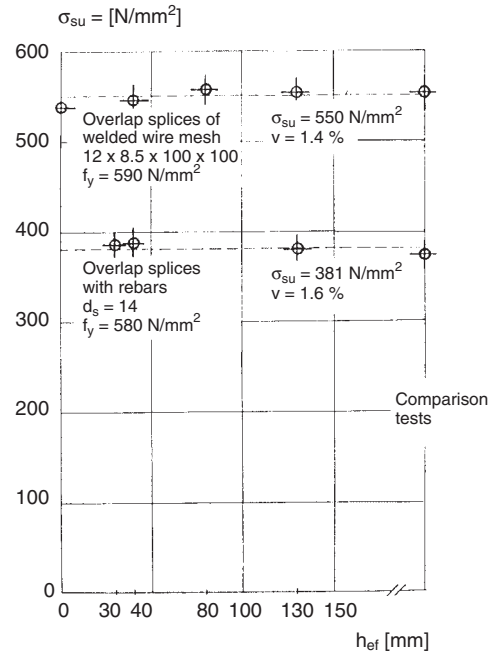


**Fig. 13.8** Steel stresses in reinforcement at failure of the overlap splices as a function of the embedment depth of the anchors in the region of the splice; the comparison tests were performed with loads applied via the compression zone (Reuter, Eligehausen (1992))

30 kN per loading point were introduced in the region of the splice via expansion and undercut anchors as well as bonded steel plates. Anchor embedment depth was varied between 30 mm and 130 mm. For comparison, tests were also

conducted in which the load was introduced only via the compression zone. As intended, a splice failure occurred in every case (Fig. 13.7). Nevertheless, no reduction in the capacity of the splice was noted in tests with the load introduced via the tension side anchors as measured against the control tests (Fig. 13.8), despite the fact that embedments having  $h_{ef} \leq 40$  mm were transferring tensile loads across the crack plane and the average tensile stress introduced by the anchors was approximately 10 % of the concrete tensile capacity. This result, while unexpected, may in fact be attributable to redistribution of localized concrete tensile stress peaks via micro-cracking (Reuter, Eligehausen (1992)).

Lieberum (1986) and Lotze (1989/2) investigated how splitting forces or loads introduced via anchorages affect the serviceability and

flexural capacity of a reinforced concrete member. They found that serviceability and flexural capacity are not affected by anchorages in the flexural tension zone provided: (a) the reinforcement is adequate to resist the attendant splitting forces, (b) the tension load per anchorage point does not exceed 30 kN and c) the reinforcement is proportioned in accordance with the code and is concentrated in both directions in the anchorage region.

The area of the transverse distribution bars should be at least 60% of the area of the main (longitudinal) bars required to carry the anchor loads. Tension loads exceeding 30 kN generally require additional reinforcement to accommodate the increased splitting forces. The magnitude of the splitting forces is given in section 4.1.1.6c.

## 14 Design of fastenings

### 14.1 General

The design of fastenings is becoming increasingly important for both design professionals and the construction community. Post-installed mechanical anchors on the market today offer the potential to routinely transfer loads of relatively large magnitude into concrete (e.g. an M20 single point fastening can develop upwards of 100 kN safe working load in tension). With the potential for deeper embedments, bonded anchors can develop even greater capacities. For loads of this scale it is clear that more rigorous analysis is required. Additionally, recent emphasis on the performance of building components under adverse loading conditions (seismic, wind) has focused increased attention on the anchorage problem. Conversely, the structural engineer has a duty to the building owner to design economically in the sense of using design methods which permit the best possible utilisation of the anchors.

Optimum utilisation of anchors is only possible if the design explicitly considers not only the direction of load (tension, shear, combined tension and shear) but the modes of failure as well. In 1995 the Comité Euro-International du Béton (CEB) published a new analysis method for anchors which fulfils these requirements (*Comité Euro-International du Béton* (1995)). The design concept, designated as the CC-Method, or Concrete Capacity-Method (in the U.S. it is known as the Concrete Capacity Design or CCD-Method) is based on the research findings described in chapter 4. It applies to cast-in-place headed anchors without or with supplementary reinforcement and to post-installed expansion and undercut anchors. That part of the method dealing with post-installed expansion and undercut anchors was finalised by the CEB Working Group in 1992,

and was endorsed by the German Building Technology Institute in 1993 (*Deutsches Institut für Bautechnik* (1993)). In 1997 the CC-Method was adopted in toto by the European Organisation for Technical Approvals (EOTA) (*European Organisation for Technical Approvals* (1997)). Subsequently the American Concrete Institute published a method for the design of fastenings with headed and post-installed anchors to concrete in Appendix D of *ACI 318-05* (*American Concrete Institute* (2005)) which is based on the Concrete Capacity-Method. A similar set of design provisions adapted for the use in the design of nuclear power plants was also published as Appendix B of *ACI 349-01* (*American Concrete Institute* (2001/1)). Currently a Working Group of the European Committee for Standardisation (CEN) is finishing a Technical Specification (pre-standard) for the design of fastenings for use in concrete (*European Committee for Standardisation* (2004)). The Technical Specification covers fastenings with headed fasteners, anchor channels and post-installed fasteners (expansion, undercut and bonded anchors).

A safe anchorage requires not only detailed planning and design but also anchor systems that function reliably under job-site conditions. In Europe this is verified by the building authority approval procedure. In other countries, job-site inspection and proof-loading supplement the approval process. In order to ensure consistent product quality, robust quality control measures are necessary. For products approved by the building authority, this typically includes manufacturer quality audits as well as third-party inspections. Finally, it is essential that the installation of anchors on-site proceeds according to the manufacturer's instructions. This cooperation between manufacturer, user, planner and installer, is illustrated in Fig. 14.1.

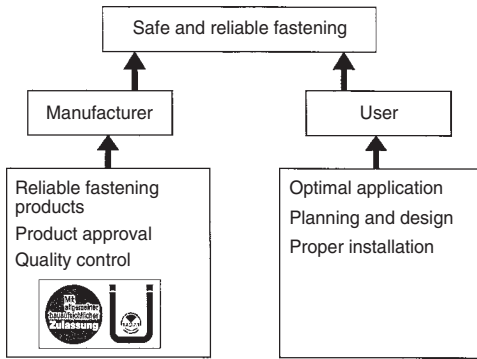


**Fig. 14.1** Co-operation between manufacturer, user and installer to ensure safe fastenings

The provisions described in sections 14.3 to 14.5 are intended for fastenings for use in structural and non-structural applications in which failure will result in collapse or partial collapse of the structure or cause risk to human life or lead to significant economic loss. If seismic resistance is a factor in the design, sections 14.4.11 and 14.5 apply. The fire resistance is dealt with in section 14.4.13.

## 14.2 Verifying the suitability of an anchor system

Fundamentally, anchors should be designed in such a way that they are resistant and durable under service loads and provide an adequate margin of safety against failure. The occurrence of gross installation errors should be mitigated by making the anchors as simple as possible to install and by training of the installer. Reductions in the load-carrying capacity of the anchorage due to unavoidable installation inaccuracies should be kept within permissible bounds. The anchor system should not be overly sensitive to site conditions since even comprehensive inspection measures cannot compensate for inadequate system reliability (Bauer (1980)). Appropriate installation controls are generally indispensable – depending on the system – as a means of offsetting the potential for human error on the job site. Proper instruction and training of installers and users is likewise essential.

Given the large variety of anchor systems available on the market today, design professionals may find it difficult to independently assess and select the appropriate anchor for a specific application. In the European Union, United States and other countries, approval processes exist to provide an independent assessment. Approvals are based on tests intended to verify the suitability of a system and to determine the admissible conditions of use.

Suitability tests are designed to verify the proper functioning of the anchor under unfavourable application conditions. These tests are generally conducted in concrete with a strength at the lower and upper end of the usual field of application, and may include tests in cracked concrete as well as in non-cracked concrete specimens depending on the intended use of the anchor. The effects of installation variances are checked in detail, insofar as they are relevant. Factors investigated may include drill bit tolerance extremes, varying techniques and effort applied to cleaning the drilled hole, variations in the degree of anchor expansion, proximity of the anchor to reinforcing bars, and variations in the moisture content and temperature of the concrete. The tests may account for the influence of sustained and repetitive loads acting on the anchorage itself as well as on the component in which the anchor is placed. Limited reductions in the failure load or an increase in the relative anchor displacement associated with suitability tests are acceptable given the relative infrequency of the conditions investigated, i.e., the overall probability of failure remains approximately the same under all conditions. In any case, the functional characteristics of the anchor must be unimpaired (e.g. torque-controlled expansion anchors must be able to develop proper follow-up expansion) in the suitability tests.

Suitability tests take into account circumstances which may occur while installing the anchor and during its service life. Gross installation errors are not covered by these tests. Gross installation errors may include:

- Using a drill bit of incorrect diameter (e.g. +1 mm) or a non-approved drill bit.
- Using a non-approved drilling system, e.g. for undercut anchors.

- Using the wrong setting tools.
- Omitting the specified hole cleaning.
- Installing a pre-positioned anchor such that the sleeve projects above the concrete surface and prevents clamping of the component against the surface of the concrete.
- Using the hammer-only setting on a hammer drill to install an anchor that requires both rotation and hammering action, such as a capsule type bonded anchors or self-undercutting undercut anchors.
- Installing the anchor with less than specified embedment depth.

Gross installation errors can be mitigated through proper training of installers and diligent job-site inspection.

Design parameters which are product-specific and therefore cannot be established theoretically are determined via admissible service condition tests. These parameters include characteristic pull-out resistance, minimum spacing and edge distances as well as characteristic spacing and edge distances as required to preclude splitting of the concrete.

In Germany, a variety of provisions for the testing and assessment of anchors have been developed. Many of these provisions have been incorporated into the European approval guidelines of the EOTA (*European Organisation for Technical Approvals* (1997, 1998, 2002, 2003)) and Common Understanding Assessment Procedures (CUAP) (*Deutsches Institut für Bautechnik* (2003/1, 2003/2)), which are the basis for issuing European Technical Approvals (ETA) for expansion anchors, undercut anchors, bonded anchors, torque-controlled bonded anchors and concrete screws as well as cast-in-place headed anchors.

In applications where statically indeterminate structures like lightweight suspended ceilings, pipes, railings and lightweight facades are fastened to concrete, the failure of one anchor will not lead to the collapse of the fastened structure but rather to a new state of equilibrium due to redistribution of the load among neighbouring anchor points, provided that the fastened structure is sufficiently strong. For these applications EOTA has drawn up an approval guideline for metal anchors for multiple use for non-struc-

tural applications (*European Organisation for Technical Approvals* (2002)). In addition, European approval guidelines for plastic anchors in concrete are also in preparation.

Recently, the American Concrete Institute has published guidelines for testing and assessing metal expansion and undercut anchors for applications in cracked and non-cracked concrete (*American Concrete Institute* (2001)). These guidelines are based in large part on the EOTA provisions (*European Organisation for Technical Approvals* (1997 and 1998)).

### 14.3 Design of fastenings with post-installed metal expansion, undercut and bonded expansion anchors according to the EOTA Guideline

#### 14.3.1 General

The *European Organisation for Technical Approvals* (1997) describes in Appendix C a design approach for anchors using the CC-Method which is based on the concept of partial safety factors. The method applies to fastenings in concrete using anchors approved by a European Technical Approval (ETA) in accordance with *European Organisation for Technical Approvals*. The characteristic anchor parameters required for calculating the resistance must be obtained from the respective approval document.

Three different methods of design are described in Appendix C. In method *A* the characteristic resistances depend on the direction of loading and take into account all conceivable failure modes. In method *B* one characteristic resistance is taken which is independent of the loading direction and the influence of reduced spacings and edge distances is allowed for by way of reduction factors. In method *C* one characteristic resistance is specified. This applies to all loading directions and predefined minimum spacings and edge distances which *must* be adhered to. The respective approval document specifies which design method may be used. In the following only the design method *A* is explained.

Anchors made from galvanised steel (coating thickness  $\geq 5 \mu\text{m}$ ) may only be used for components in *dry* interior conditions, e.g. in housing, offices, schools, hospitals, shops. Anchors made

from stainless steel of corrosion protection class III (A4 steel, *AISI 316* (1995) grade 316) may also be used in damp interior conditions and in the open air, also in industrial conditions and in coastal regions (but not directly in contact with seawater). However, these anchors may not be used in atmospheres containing chlorine, e.g. in conjunction with chlorinated water in indoor pools, road tunnels or in environmental technology applications (e.g. landfill sites, flue gas desulphurising plants – see section 12). For these applications European Technical Approvals for torque-controlled expansion, undercut and torque-controlled bonded anchors suitable for cracked and non-cracked concrete and made from steel of corrosion protection class IV have been issued.

**14.3.2 Scope**

Fig. 14.2 depicts the anchorage types included in the design guideline of the EOTA. Fastenings remote from an edge may employ a single anchor or groups of up to six anchors, whereby an anchorage is assumed to be remote from edges when the edge distance is  $c \geq 10h_{ef}$  in all directions. This edge distance is assumed to preclude concrete edge failure under shear loading. Near an edge ( $c < 10h_{ef}$ ), only single anchors or groups of two or four anchors may be considered. This restriction is deemed necessary because at smaller edge distances failure of

the edge is usually critical under shear loads and deformations at ultimate load are small. Furthermore, given the likelihood of unequal tolerances between the anchors and the baseplate in a group anchorage, the distribution of a shear load to the individual anchors in configurations consisting of three or six anchors is more difficult to predict.

The concrete member shall be of normal-weight concrete of strength classes C 20/25 to C 50/60 according to *EN 206-1:2001-07* (2001) and shall be subjected to predominantly static loads. The design methods apply to anchors subjected to static or quasi static loading and not to anchors subjected to fatigue, impact or seismic loading or loaded in compression.

The concrete in the region of the anchorage may be cracked or non-cracked. In each case the condition of the concrete shall be decided by the designer on the basis of national regulations. In the absence of national regulations the following approach may be taken. Non-cracked concrete may be considered if it is verified that under service conditions the anchor with its entire embedment depth is located in non-cracked concrete. This can be assumed if equation (14.1) is satisfied.

$$\sigma_L + \sigma_R \leq 0 \tag{14.1}$$

where:

$\sigma_L$  = stress in concrete caused by external loads, including anchor-induced loads

$\sigma_R$  = stress in concrete caused by restraint of internal deformations (e.g. shrinkage of the concrete) or of external deformations (e.g. displacement at the supports, temperature fluctuations). If no detailed analysis is conducted, then  $\sigma_R = 3 \text{ N/mm}^2$  should be assumed

Stresses  $\sigma_L$  and  $\sigma_R$  should be calculated assuming that the concrete is non-cracked. In the case of planar components which carry loads in two directions (e.g. slabs, walls), equation (14.1) should be checked for both directions.

The use of  $\sigma_R$  in equation (14.1) is intended to guarantee that the probability of cracks forming in the concrete is very low even when deformations are unintentionally restrained. The value of  $\sigma_R = 3 \text{ N/mm}^2$  is used in *Eurocode 2: ENV*

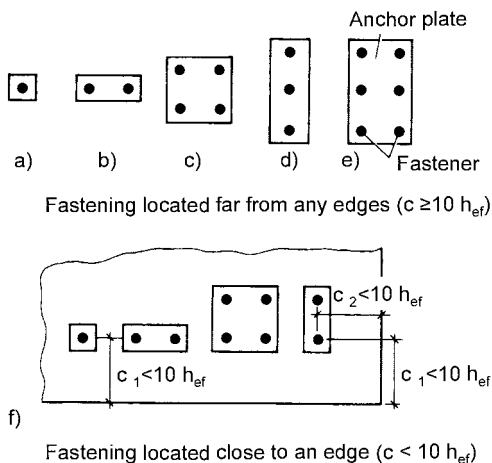


**Fig. 14.2** Fastenings covered by the EOTA Guideline



1992-1-1:1991 (1991) when calculating the minimum reinforcement required to limit crack widths at the serviceability limit state in reinforced concrete components. This value may only be reduced if the tensile restraint stresses can be shown to be less than 3 N/mm<sup>2</sup>.

The above definition of non-cracked concrete agrees with that given in *DIN 1045* (1988) and *Eurocode 2: ENV 1992-1-1:1991* (1991).

### 14.3.3 Design concept

As in modern codes (e.g. *Eurocode 2: EN 1992-1-1* (2003), *Eurocode 3: EN 1993-1-1* (2002)) the safety concept of partial safety factors is used for better handling uncertainties associated with both actions and resistance. According to this concept it shall be shown that the value of the design actions  $S_d$  does not exceed the value of the design resistance  $R_d$  (equation (14.2)).

$$S_d \leq R_d \quad (14.2)$$

In the absence of national regulations the design actions in the ultimate limit state or serviceability limit state should be calculated according to *Eurocode 1: EN 1990:2002* (2002).

The design resistance is calculated as follows:

$$R_d = R_k / \gamma_M \quad (14.3)$$

where:

$R_k$  = characteristic value (5%-fractile) of resistance

$\gamma_M$  = partial safety factor for material strength

Partial safety factors for the ultimate and serviceability limit states are established independently.

#### 14.3.3.1 Analysis for the ultimate limit state

The actions on the fastenings are determined according to the same rules and using the same partial safety factors employed in reinforced concrete design (see *Eurocode 1: EN 1990:2002* (2002)). For the simplest case (dead and one live load acting in the *same* direction), the design values for load-effects (actions) are to be calculated using equation (14.4):

$$S_d = \gamma_G \cdot G_k + \gamma_Q \cdot Q_k \quad (14.4)$$

where:

$G_k$  = characteristic dead load at serviceability limit state

$Q_k$  = characteristic live (variable) load at serviceability limit state

$\gamma_G$  = partial safety factor for dead loads  
= 1.35

$\gamma_Q$  = partial safety factor for live (variable) loads  
= 1.5

If the dead load and the live load act in *different* directions, then the following analyses is required:

$$S_d = 1.35 \cdot G_k + 1.50 \cdot Q_k \quad (14.5a)$$

$$S_d = 1.00 \cdot G_k + 1.50 \cdot Q_k \quad (14.5b)$$

$$S_d = 1.35 \cdot G_k \quad (14.5c)$$

If several live loads act together, then the design values of the actions are to be determined according to *Eurocode 1: EN 1990:2002* (2002).

If the anchorage provides deformation restraint for the fastened member or component (e.g. as in the case of temperature loads), then the resulting load effects  $Q_{ind}$  acting on the anchorage, multiplied by the safety factor  $\gamma_{ind}$ , are to be added into equations (14.4) and (14.5). However, *Eurocode 2: EN 1992-1-1* (2003) does not specify a figure for  $\gamma_{ind}$ . *Comité Euro-International du Béton* (1995) proposes the value  $\gamma_{ind} = 1.3$  for the design of anchorages when failure of the concrete is critical for the characteristic resistance. If failure of the steel is critical, then  $\gamma_{ind}$  may be taken as zero because internal restraint forces are assumed to be alleviated through ductile steel deformations.

Partial safety factors for material strength depend on the mode of failure.

The partial safety factors for concrete cone failure ( $\gamma_{Mc}$ ), splitting failure ( $\gamma_{Msp}$ ) and pull-out failure ( $\gamma_{Mp}$ ) are given in the relevant ETA. They are valid only if after installation the actual dimensions of the effective anchorage depth, spacing and edge distance are not less than the design values (only positive tolerances allowed).

The partial safety factor  $\gamma_{Mc}$  is determined from:

$$\gamma_{Mc} = \gamma_c \cdot \gamma_1 \cdot \gamma_2 \quad (14.6)$$

where:

$\gamma_c$  = partial safety factor for concrete under compression = 1.5

$\gamma_1$  = partial safety factor for taking account of the scatter of the tensile strength of site concrete  
= 1.2 for concrete produced and cured with normal care

$\gamma_2$  = partial safety factor taking account of the installation safety of an anchor system

For tension loading the partial safety factor  $\gamma_2$  is evaluated from the results of the installation safety tests which are carried out during the approval process. It amounts to:

$\gamma_2$  = 1.0 for systems with high installation safety

= 1.2 for systems with normal installation safety

= 1.4 for systems with low but still acceptable installation safety

For shear loading the installation partial safety factor is taken as  $\gamma_2 = 1.0$ , because it depends mainly on the accuracy of the anchor placement and only *positive* tolerances are allowed for spacing and edge distances.

For the partial safety factors  $\gamma_{Msp}$  and  $\gamma_{Mp}$  the value for  $\gamma_{Mc}$  may be taken.

The above figures for  $\gamma_c \cdot \gamma_1$  were derived from *Gollwitzer, Abdo, Rackwitz* (1989) and *Bergmeister* (1989). In deriving the safety factor  $\gamma_{Mc}$  a reliability index  $\beta = 4.7$  was assumed.

In the *European Organisation for Technical Approvals (EOTA)* (2004) it is recommended to set the factor that takes into account of the scatter of the tensile strength of site concrete  $\gamma_1$  equal 1.0 since in *Eurocode 2: EN 1992-1-1* (2003) the same partial safety factor is used for concrete loaded in compression or in tension.

The partial safety factors  $\gamma_{Ms}$  for steel failure are given in the relevant ETA. They are determined as follows:

Tension loading:

$$\gamma_{Ms} = \frac{1.2}{f_{yk}/f_{uk}} \geq 1.4 \quad (14.7a)$$

Shear loading of the anchor with and without lever arm:

$$\gamma_{Ms} = \frac{1.0}{f_{yk}/f_{uk}} \geq 1.25 \quad \text{for}$$

$$f_{uk} \leq 800 \text{ N/mm}^2 \text{ and } f_{yk}/f_{uk} \leq 0.8 \quad (14.7b)$$

$$\gamma_{Ms} = 1.5 \quad \text{for}$$

$$f_{uk} > 800 \text{ N/mm}^2 \text{ or } f_{yk}/f_{uk} > 0.8 \quad (14.7c)$$

The above safety factors for tension and shear on the thread apply to rolled threads. It is recommended to increase these by the factor  $1/0.85 = 1.18$  for cut threads.

The above partial safety factors  $\gamma_{Ms}$  were derived from *Eurocode 3: EN 1993-1-1* (2002). In the design method for anchors the characteristic resistance for steel failure under tension and shear with or without lever arm is calculated using the tensile strength of the steel. Therefore, introducing the quotient  $f_{yk}/f_{uk}$  into equations (14.7a) to (14.7c) assures that the yield stress of the material is not exceeded under the design action  $S_d$ .

In Europe safety issues are under the responsibility of the building authorities of the member states. Therefore they may adjust the partial safety factors given above to their specific conditions. However, the value of  $\gamma_2$  given in the European Technical Approval may not be changed because it describes a characteristic of the anchor. To the knowledge of the authors no such adjustments have been done up to now.

#### 14.3.3.2 Analysis for the serviceability limit state

In the serviceability limit state it shall be shown that the displacement occurring under the characteristic actions is not larger than the admissible displacement. The characteristic displacements are given in the European Technical Approval as a function of the magnitude and direction of the applied load. The admissible displacement depends on the application in question and should be specified by the design professional. In doing so, the function(s) of the fixed component and any redistribution of internal forces in the anchored component should be taken into account.

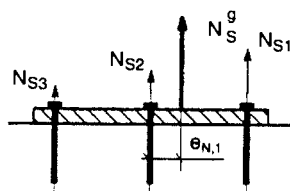
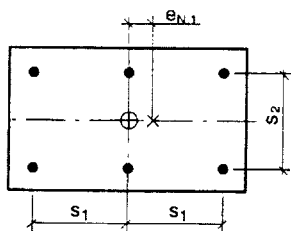
In this check the partial safety factors on actions and on resistance may be assumed to be equal to 1.0.

**14.3.4 Forces on anchors**

The European Technical Approvals require that anchorages be planned and designed according to engineering principles and that verifiable calculations and construction documents be produced. Additional stresses which could occur in

the anchorage, in the adjoining component or in the base material as a result of restraint of deformations (e.g. due to changes of temperature) must be taken into account when determining the load effects acting on the anchorage. This is particularly important when designing anchorages for facades.

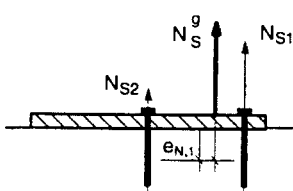
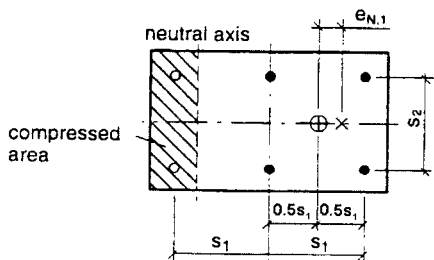
Through the design the local transfer of force into the base material is verified. Crack widths according to *Eurocode 2: EN 1992-1-1* (2003)



$$N_s^o = \sum N_{S_i}$$

$$N_{S_1} = N_s^h$$

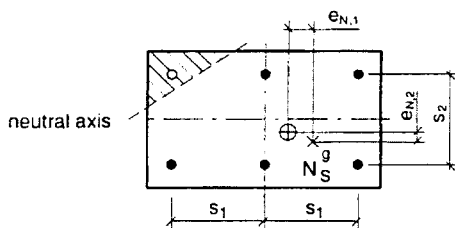
a) eccentricity in one direction, all anchors are loaded by a tension force



$$N_s^o = \sum N_{S_i}$$

$$N_{S_1} = N_s^h$$

b) eccentricity in one direction, only a part of the anchors of the group are loaded by a tension force



c) eccentricity in two directions, only a part of the anchors of the group are loaded by a tension force

- tensioned anchors
- ⊕ centre of gravity of tensioned anchors
- × location of resulting tension force

**Fig. 14.3** Examples for fastenings subjected to an eccentric tensile force  $N_{sd}$

are presumed in the case of anchorages in cracked concrete. The transmission of the forces on the anchorage within the structure (e.g. to supports, columns or foundations) must be verified in each individual case using the standard analyses. In the case of small loads on the anchorage this is usually achieved by adding a surcharge to a uniformly distributed load. Larger loads are to be treated as point loads.

The forces in the anchor at the surface of the concrete are to be calculated from the forces and moments (bending and torsion) acting on the fixture assuming a linear material behaviour for the concrete and the anchor (elastic theory) (see section 3.7.1, Fig. 3.40). In doing so, when determining the distribution of tension loads over the anchors of a group, the following assumptions are made:

- The fixture remains plane under the action of the load-effects. To guarantee this, the fixture must be sufficiently stiff and – except in the case of stand-off installations – must be in contact with the concrete or grout leveling bed over its full surface. Assuming a fixture which remains plane corresponds to the Bernoulli hypothesis in reinforced concrete, which states that the cross-section remains plane.
- All the anchors of a group have the same stiffness. This is given by the steel cross-section of the anchor and the modulus of elasticity of the steel. As a simplification, the steel cross-section can be taken as the stressed cross-section of the connecting thread and the modulus of elasticity as  $E_s = 210\,000\text{ N/mm}^2$ . The modulus of elasticity of the concrete may be taken from *Eurocode 2: EN 1992-1-1* (2003). As a simplification it may be assumed as  $E_c = 30\,000\text{ N/mm}^2$ .
- The anchors do not act in tension or compression in the compressed zone below the fixture.

If in special cases the fixture is not sufficiently stiff, then the flexibility of the fixture should be taken into account when calculating forces on anchors.

In the case of anchor groups with different levels of tension forces  $N_{Si}$  on the individual anchors of the group the eccentricity  $e_N$  of the

resulting tension force may be calculated to enable a more accurate assessment of the anchor group resistance. Examples for calculating the eccentricity are shown in Fig. 14.3. If the tensioned anchors do not form a rectangular pattern (Fig. 14.3c), for reasons of simplicity, the group of tensioned anchors may be resolved into a group rectangular in shape. In this case the centre of gravity of the tensioned anchors may be assumed in the centre of the axis.

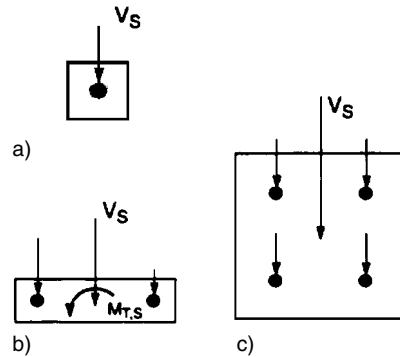


**Fig. 14.4** Examples of load distribution when all fasteners take up shear loads

When calculating the distribution of shear loads or torsion moments over the anchors of a group, it is generally assumed that all anchors contribute to carrying the shear (Fig. 14.4). In Fig. 14.4  $V_s$  and  $M_{T,s}$  are the shear loads and torsion moments respectively which act in the serviceability limit state. However, only the most critical anchors are assumed to take shear loads if the hole clearance is larger than the values given in Table 3.2. Examples are shown in Fig. 14.6. Furthermore in the case of anchorages near an edge (edge distance in at least one direction  $c < 10h_{ef}$ ) it is assumed that only the anchors nearest to the edge carry the shear. Examples are given in Fig. 14.5. It can be useful to provide slotted holes for anchors near the edge of a component so that only the anchors remote from the edge carry the shear (Fig. 14.7).

According to the above provision in case of fastenings close to an edge ( $c < 10h_{ef}$ ) only the anchors nearest the edge may be taken into account when verifying the resistance against concrete edge, pry-out and steel failure. As

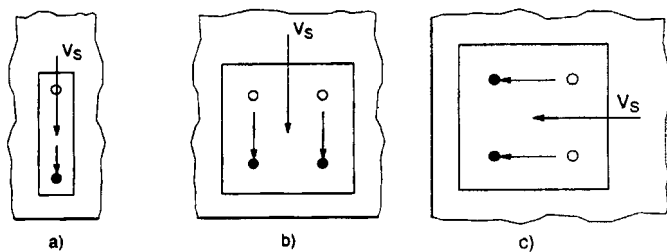


**Fig. 14.5** Examples of load distribution for fasteners close to an edge

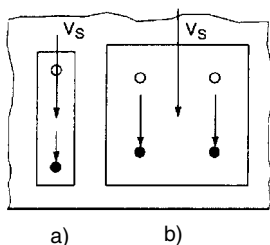


**Fig. 14.6** Examples of load distribution if the hole clearance is larger than the value according to Table 3.2

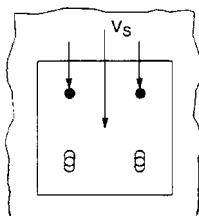


**Fig. 14.7** Examples of load distribution for a fastening with slotted holes

explained in section 4.1.2.4 this rule is a simplification of the real behaviour when checking for concrete edge failure. However, according to the opinion of the authors this rule is too conservative in case of pry-out and steel failure, because for these failure modes the displacements at failure are much larger than the play in the hole and therefore all anchors contribute to carrying the shear.

If the diameter of the holes in the fixture is greater than the values in Table 3.2, then – as shown in Fig. 14.6 – only half of the anchors are

assumed to carry the load. This is correct when the gap between the anchor and the hole is greater than the displacement at failure of the anchors carrying the load. With a smaller gap, however, this approach is unduly conservative. Furthermore with a group of six anchors it is not self-evident which anchors will be critical from a loading standpoint. In the opinion of the authors, where oversized clearance holes in the fixture are used, it should be assumed that *all* anchors in the group share the load, but that the shear load gives rise to bending in the anchors and thus a reduction in their design resistance. Such an assumption is relatively easy to implement and sufficiently conservative for most cases.

In the case of anchor groups with different levels of shear forces  $V_{si}$  acting on the individual anchors of the group the eccentricity  $e_V$  of the force of the group may be calculated to enable a more accurate assessment of the anchor group resistance. An example is shown in Fig. 14.8.

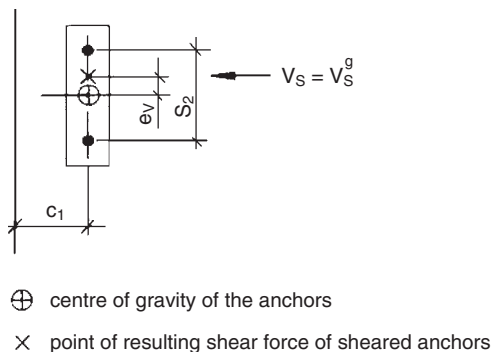
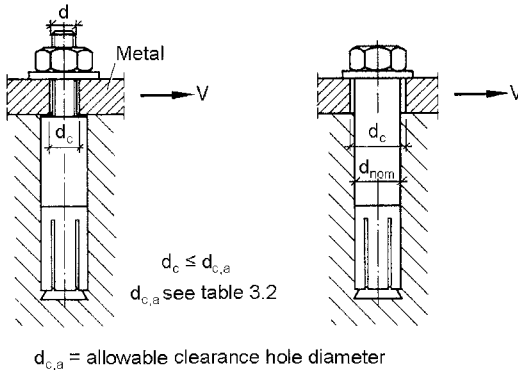


**Fig. 14.8** Example of a fastening subjected to an eccentric shear load



Pre-positioned installation

In-place installation

**Fig. 14.9** Examples of fasteners with hole clearance

Shear loads acting on the anchors may be assumed to act without lever arm if both of the following conditions are satisfied:

- The fixture is made of metal and is tightened against the concrete without any intermediate layer or with a grout levelling layer ≤ 3 mm thick in the vicinity of the anchor.
- The fixture shall be in contact with the anchor over its entire thickness (see Fig. 14.9).

If one of the above conditions is not satisfied, then the design is based on a shear load *with* lever arm. Here, the lever arm *l* between shear load and theoretical point of fixation is given by equation (14.8) (see Fig. 4.65):

$$l = a_3 + e_1 \tag{14.8}$$

where:

$e_1$  = distance between shear load and surface of concrete

$a = 0.5d$  (Fig. 4.65a)

= 0 when a washer and nut are clamped directly against the surface of the concrete (Fig. 4.65b)

$d$  = nominal diameter of anchor stud or diameter of thread

The design moment acting on the anchor is calculated using equation (14.9):

$$M_{Sd} = V_{Sd} \cdot \frac{l}{\alpha_M} \tag{14.9}$$

The value  $\alpha_M$  depends on the degree of restraint of the anchor on the fixture side (Fig. 4.67) and should be assessed according to engineering principles. An anchor not restrained by the fixture ( $\alpha_M = 1.0$ ) is to be assumed when the fixture is free to rotate (Fig. 4.67a). Full restraint ( $\alpha_M = 2.0$ ) may only be assumed when the fixture cannot rotate (Fig. 4.67b) and the clearance hole in the fixture complies with Table 3.2 or the anchor is clamped firmly against the fixture with nuts and washers on both sides (Fig. 4.65b). If we assume that the anchor is restrained in the fixture, then the fixture must be in a position to accommodate the fixing moment.

### 14.3.5 Characteristic resistances

In design method A, equation (14.2) has to be satisfied for all types of loading (tension, shear on anchors with or without lever arm, combined tension and shear) and all failure modes (steel, pull-out/pull-through, concrete cone, splitting, pry-out and concrete edge failure). Combined tension and shear requires an interaction equation to be satisfied. The mode of failure with the lowest ratio of design actions  $S_d$  and design resistance  $R_d$  governs the design. This design method fully exploits the abilities of an anchorage but the analyses required are rather time-consuming. Therefore, some manufacturers offer computer programs for the design of anchorages.

The design method only applies when the distance between individual anchors and the outer-

most anchors of groups of anchors or the clear distance between groups of anchors is  $a > s_{cr,N}$  (tension) or  $a > 3c_1$  (shear acting on anchors near an edge).

The minimum spacing and edge distances as well as minimum component thickness given in the corresponding European Technical Approval must be maintained.

The equations for calculating the characteristic resistances (5%-fractiles) for the individual loading directions and failure modes are outlined below.

The characteristic resistances specified in the following are valid for anchorages in cracked concrete. They may be used in any part of a structure without further verification. In contrast, the higher characteristic resistances for anchorages in non-cracked concrete may only be exploited when in each individual case it is verified with equation (14.1) that the anchorage lies in non-cracked concrete.

If the characteristic resistance for concrete cone failure is smaller than the value for steel failure, then the anchorage fails by way of a brittle concrete failure. This type of failure is acceptable in many cases. However, if ductile behaviour of the anchorage is called for, then anchors with adequate ductility should be used and equations (14.76), (14.77), (14.79) and (14.80) should be satisfied. This equation guarantees that rupture of the steel governs the failure of the anchorage.

**14.3.5.1 Tension resistances**

The checks required for single anchors and anchor groups are shown in Table 14.1. Here,  $N_{Sd}^h$  is the tension design value acting on the most highly loaded anchor in a group, and  $N_{Sd}^g$  is the resultant tension design value acting on the anchors in a group which are in tension.

**a) Steel failure**

The characteristic resistance  $N_{Rk,s}$  of an anchor in the case of steel failure is given in the relevant European Technical Approval. It is obtained from equation (14.10).

$$N_{Rk,s} = A_s \cdot f_{uk} \tag{14.10}$$

The most highly loaded anchor in a group subjected to an eccentric tension load is to be checked using equation (14.2) (see Table 14.1).

**b) Pull-out/pull-through failure**

The characteristic resistance  $N_{Rk,p}$  of an anchor for a pull-out/pull-through failure depends on the design of the anchor and is derived from the results of approval tests. It is specified in the respective European Technical Approval.

The most highly loaded anchor in a group subjected to an eccentric tension load is to be checked using equation (14.2) (see Table 14.1).

**c) Concrete cone failure**

The CC-Method (see section 4.1.1.3) is used to calculate the characteristic resistance  $N_{Rk,c}$  of a single tensioned anchor or a group of tensioned anchors for concrete cone failure. It is:

$$N_{Rk,c} = N_{Rk,c}^0 \cdot \frac{A_{c,N}}{A_{c,N}^0} \cdot \psi_{s,N} \cdot \psi_{re,N} \cdot \psi_{ec,N} \cdot \psi_{ucr,N} \tag{14.11}$$

The various factors in equation (14.11) are explained below.

The initial value of the characteristic resistance of an anchor with large spacing and edge distance in cracked concrete is given by equation (14.11a):

$$N_{Rk,c}^0 = 7.2 \cdot \sqrt{f_{ck,cube}} \cdot h_{ef}^{1.5} \quad [N] \tag{14.11a}$$

where:

- $f_{ck,cube}$  = nominal concrete compression strength measured on cubes with a side length of 150 mm [N/mm<sup>2</sup>]
- $h_{ef}$  = effective embedment depth [mm]

**Table 14.1** Design checks required for tension loads

	Single anchor	Anchor group
Steel failure	$N_{Sd} \leq N_{Rd,s} = N_{Rk,s} / \gamma_{Ms}$	$N_{Sd}^h \leq N_{Rd,s} = N_{Rk,s} / \gamma_{Ms}$
Pull-out/Pull-through failure	$N_{Sd} \leq N_{Rd,p} = N_{Rk,p} / \gamma_{Mp}$	$N_{Sd}^h \leq N_{Rd,p} = N_{Rk,p} / \gamma_{Mp}$
Concrete cone failure	$N_{Sd} \leq N_{Rd,c} = N_{Rk,c} / \gamma_{Mc}$	$N_{Sd}^g \leq N_{Rd,c} = N_{Rk,c} / \gamma_{Mc}$
Splitting failure	$N_{Sd} \leq N_{Rd,sp} = N_{Rk,sp} / \gamma_{Msp}$	$N_{Sd}^g \leq N_{Rd,sp} = N_{Rk,sp} / \gamma_{Msp}$



Equation (14.11a) specifies the 5% fractile of the test results in cracked concrete. It is derived from equation (4.5b) with  $k = 13.5 \text{ [N}^{0.5}/\text{mm}^{0.5}]$  taking into account the following aspects. Equation (4.5b) gives the average failure load in non-cracked concrete. The 5%-fractile is taken as 0.75 times the average value and the failure load in cracked concrete as 0.7 times the value in non-cracked concrete (see section 4.2.1.3). Furthermore the influence of the different definitions of the concrete compression strength in equations (4.5b) and (14.11a) (cubes with a side length of 200 mm or 150 mm respectively) and the curing conditions according to *EN 206-1:2001-07* (2001) are considered. In equation (14.11a) the characteristic compression strength is used instead of the mean strength because the concrete may exhibit a lower strength *locally* in the region of the anchorage (*Lewandowski* (1969)).

The geometrical influence of spacings and edge distances on the characteristic resistance is taken into account by the ratio  $A_{c,N}/A_{c,N}^0$ . Here,  $A_{c,N}^0$  is the idealised area of the concrete cone of a single anchor with large spacing and edge distance at the surface of the concrete. It is idealised as a pyramid of height  $h_{ef}$  and base length  $s_{cr,N} = 3h_{ef}$  (Fig. 4.14).  $A_{c,N}$  is the idealised area of the concrete cone of the anchorage at the concrete surface. It is curtailed through the overlaps with the individual concrete cones of neighbouring anchorages ( $s < s_{cr,N} = 3h_{ef}$ ) as well as the edges of the component ( $c < c_{cr,N} = 1.5h_{ef}$ ). Figs 4.16 and 4.26 illustrate examples of the calculation of  $A_{c,N}$ .

The factor  $\psi_{s,N}$  takes into account the fact that the edges of the component disrupt the rotationally symmetric stress condition in the concrete valid for large edge distances. If more than one edge is involved (e.g. anchorage in a corner or in a narrow component), then the smallest edge distance  $c$  is to be used in equation (14.11b):

$$\psi_{s,N} = 0.7 + 0.3 \cdot \frac{c}{c_{cr,N}} \leq 1 \quad (14.11b)$$

where:

$$c_{cr,N} = 1.5h_{ef}$$

The surface spalling factor  $\psi_{re,N}$  takes account of the negative influence of reinforcement in the area of the concrete cone (see sections 4.1.1.3f and 4.2.1.3).

$$\psi_{re,N} = 0.5 + \frac{h_{ef}}{200} \leq 1 \quad (14.11c)$$

where:

$$h_{ef} = \text{embedment depth [mm]}$$

If in the area of the anchorage there is a reinforcement with a spacing  $\geq 150$  mm (any diameter of rebar) or with a rebar diameter  $\leq 10$  mm and a spacing  $\geq 100$  mm then a surface spalling factor  $\psi_{re,N} = 1.0$  may be applied regardless of the embedment depth. This is because the tensile stresses in the concrete caused by the reinforcement are negligible compared to those due to the anchorage.

The factor  $\psi_{ec,N}$  takes account of a group effect when different tension forces are acting on the individual anchors of the group.

$$\psi_{ec,N} = \frac{1}{1 + 2 \cdot e_N / s_{cr,N}} \leq 1 \quad (14.11d)$$

where:

$e_N$  = eccentricity of the resultant tensile force acting on the tensioned anchors related to their geometrical centre of gravity  $S$  (see Fig. 14.3)

$$s_{cr,N} = 3 \cdot h_{ef}$$

Where there is an eccentricity in two directions (see Fig. 14.3c),  $\psi_{ec,N}$  is to be determined separately for each direction and the product of both factors used in equation (14.11).

Factor  $\psi_{ucr,N}$  takes into account the influence of the position of an anchorage in cracked or non-cracked concrete:

$$\psi_{ucr,N} = 1.0 \text{ for anchorages in cracked concrete} \quad (14.11e_1)$$

$$\psi_{ucr,N} = 1.4 \text{ for anchorages in non-cracked concrete} \quad (14.11e_2)$$

The coefficient  $\psi_{ucr,N} = 1.4$  for non-cracked concrete is calculated from  $\psi_{ucr,N} = 1/\psi_w = 1/0.7$ .

In the case of anchorages near three or more edges, where the edge distance  $c_{max} < 1.5 \cdot h_{ef}$  ( $c_{max}$  = largest edge distance), the calculation with equation (14.11) leads to results which are conservative (see section 4.1.1.3g). More accurate results are achieved when

$$h'_{ef} = c_{max}/1.5 \quad (14.11f)$$

is used for  $h_{ef}$  in equation (14.11a) and

$$s'_{cr,N} = 2 \cdot c_{\max} \quad (14.11g)$$

$$s'_{cr,N} = c_{\max} \quad (14.11h)$$

are substituted for  $s_{cr,N}$  and  $c_{cr,N}$  respectively when determining  $A_{c,N}^0$  and  $A_{c,N}$  according to Figs. 4.14, 4.16 and 4.26 as well as in equations (14.11b) and (14.11d). Fig. 4.39 shows one example of the application of such modified values. Note that equation (14.11f) does not consider the influence of the spacing of the anchors on  $h'_{ef}$ . This influence is taken into account by the approach given in section 14.4.6.2.1c, equation (14.31).

#### d) Splitting failure

Splitting of the concrete during installation of the anchor is prevented by adhering to the minimum spacing and minimum edge distance as well as minimum component thickness prescribed in the corresponding European Technical Approval.

Verification of the failure mode splitting of the concrete due to loading the anchor may be neglected when one of following two conditions is complied with:

- The edge distance in all directions is  $c \geq 1.5 \cdot c_{cr,sp}$  and the component thickness is  $h \geq 2 \cdot h_{ef}$ . The characteristic edge distance for splitting  $c_{cr,sp}$  is evaluated from the results of approval tests and is given in the corresponding European Technical Approval.
- The characteristic resistances for concrete cone and pull-out failure are calculated for cracked concrete and reinforcement is present which can accommodate the characteristic splitting forces and can limit crack widths to  $w_k \approx 0.3$  mm. The following values can be used as a guide for the characteristic splitting forces:

$$F_{Sp,k} = 1.0 \cdot N_{Sk} \text{ for undercut anchors}$$

$F_{Sp,k} = 1.5 \cdot N_{Sk}$  for torque-controlled expansion and torque-controlled bonded anchors

$F_{Sp,k} = 2.0 \cdot N_{Rd}$  for displacement-controlled expansion anchors

If none of the above conditions is fulfilled, then the characteristic resistance of a single anchor or a group of anchors is to be calculated using equation (14.12):

$$N_{Rk,sp} = N_{Rk,c}^0 \cdot \frac{A_{c,N}}{A_{c,N}^0} \cdot \psi_{s,N} \cdot \psi_{re,N} \cdot \psi_{ec,N} \cdot \psi_{ucr,N} \cdot \psi_{h,sp} \quad [\text{N}] \quad (14.12)$$

Here,  $N_{Rk,c}^0$  is to be determined using equation (14.11a), the factors  $\psi_{s,N}$ ,  $\psi_{re,N}$ ,  $\psi_{ec,N}$  and  $\psi_{ucr,N}$  using equations (14.11b) to (14.11e) and the values  $A_{c,N}$ ,  $A_{c,N}^0$  are to be calculated according to section 14.3.5.1c; but in doing so,  $c_{cr,N}$  and  $s_{cr,N}$  are to be replaced by  $c_{cr,sp}$  and  $s_{cr,sp} = 2 \cdot c_{cr,sp}$  respectively. The factor  $\psi_{h,sp}$ , which allows for the influence of the actual member thickness  $h$  on the splitting failure load, is found using equation (14.12a):

$$\psi_{h,sp} = \left( \frac{h}{2 \cdot h_{ef}} \right)^{2/3} \leq 1.5 \quad (14.12a)$$

According to section 4.1.1.6b the splitting failure load hardly increases for a component thickness  $h > 2h_{ef}$ . Therefore, in the opinion of the authors, the factor  $\psi_{h,sp}$  in equation (14.12a) should be taken as  $\psi_{h,sp} = 1.0$ .

If the edge distance of an anchor is  $c < c_{cr,sp}$ , then longitudinal reinforcement should be provided along the edge of the member.

#### 14.3.5.2 Shear resistances

The checks required for single anchors and anchor groups are shown in Table 14.2. Here,  $V_{Sd}^h$  is the shear design value acting on the most highly loaded anchor in a group, and  $V_{Sd}^h$  is the

**Table 14.2** Checks required for shear loads

	Single anchor	Anchor group
Steel failure, shear load without or with lever arm	$V_{Sd} \leq V_{Rd,s} = V_{Rk,s} / \gamma_{Ms}$	$V_{Sd}^h \leq V_{Rd,s} = V_{Rk,s} / \gamma_{Ms}$
Pry-out failure	$V_{Sd} \leq V_{Rd,cp} = V_{Rk,cp} / \gamma_{Mc}$	$V_{Sd}^g \leq V_{Rd,cp} = V_{Rk,cp} / \gamma_{Mc}$
Concrete edge failure	$V_{Sd} \leq V_{Rd,c} = V_{Rk,c} / \gamma_{Mc}$	$V_{Sd}^g \leq V_{Rd,c} = V_{Rk,c} / \gamma_{Mc}$

resultant shear design value acting on the anchors in a group which are loaded in shear.

#### a) Steel failure for shear loads without lever arm

The characteristic resistance  $V_{Rk,s}$  of an anchor in the case of steel failure is given in the relevant European Technical Approval. It is normally obtained from equation (14.13). However, it may be smaller for anchors with a significantly reduced section along the embedment depth, e.g. stud-type torque-controlled expansion anchors according to Fig. 2.19a<sub>3</sub>. In these cases  $V_{Rk,s}$  is determined from the results of approval tests.

$$V_{Rk,s} = 0.5 \cdot A_s \cdot f_{uk} \quad (14.13)$$

The most highly loaded anchor in a group subjected to an eccentric shear load is to be checked using equation (14.2) (see Table 14.2).

The characteristic resistance according to equation (14.13) is to be reduced by the factor 0.8 in the case of anchor groups if the anchor is made of steel with a rather low ductility (rupture elongation measured over a length of  $5d$   $A_5 \leq 8\%$ ). This takes into account the fact that the hole tolerances influence the distribution of the shear load to the individual anchors of a group and hence the load-carrying capacity of a group (see section 4.1.2.2a).

#### b) Steel failure for shear loads with lever arm

In the case of a shear load *with* lever arm, equation (14.14) is used to calculate the characteristic resistance  $V_{Rk,s}$  of an anchor:

$$V_{Rk,s} = \frac{\alpha_M \cdot M_{Rk,s}}{l} \quad [\text{N}] \quad (14.14)$$

where:

$\alpha_M$  according to section 14.3.4

$l$  = lever arm according to equation (14.8) [m]

$$M_{Rk,s} = M_{Rk,s}^0 \cdot (1 - N_{Sd} / N_{Rd,s}) \quad [\text{Nm}] \quad (14.14a)$$

$M_{Rk,s}^0$  = characteristic resistance of one anchor in bending

$$= 1.2 \cdot W_{el} \cdot f_{uk} \quad [\text{Nm}] \quad (14.14b)$$

$$N_{Rd,s} = N_{Rk,s} / \gamma_{Ms} \quad [\text{N}] \quad (14.14c)$$

Equation (14.14b) is valid only, if the anchor has not a significantly reduced section along the length of the bolt. The values  $N_{Rk,s}$ ,  $M_{Rk,s}^0$  and  $\gamma_{Ms}$

are given in the respective European Technical Approval.

#### c) Pry-out failure

Closely spaced groups are especially prone to this type of failure (see section 4.1.2.3). The associated characteristic resistance  $V_{Rk,cp}$  is calculated using equation (14.15).

$$V_{Rk,cp} = k_1 \cdot N_{Rk,c} \quad (14.15)$$

where:

$k_1$  = a coefficient given in the respective European Technical Approval, normally  $k_1 = 1.0$  for anchors with  $h_{ef} < 60$  mm, and  $k_1 = 2.0$  for anchors with  $h_{ef} \geq 60$  mm

$N_{Rk,c}$  = characteristic resistance for concrete cone failure according to equation (14.11)

The value  $N_{Rk,c}$  in equation (14.15) is to be determined for the anchors loaded in shear. For example, in Fig. 14.3b the presence of the bending moment means that only the four anchors on the right are in tension. As, however, the shear force is resisted by *all* the anchors, when calculating  $N_{Rk,c}$  in equation (14.11) all *six* anchors are included. If the shear load is applied to the fixture eccentrically, then the eccentricity of the shear load related to the centre of gravity of the anchors subjected to shear is to be used for  $e_N$  when calculating  $\psi_{ec,N}$  according to equation (14.11d).

#### d) Concrete edge failure

For anchorages shown in Fig. 14.2a–e with an edge distance in all directions  $c > 10 \cdot h_{ef}$ , a verification of the failure mode concrete edge failure may be omitted. If the verification is necessary (see applications in Fig. 14.2f) then the characteristic resistance of an anchor or group of anchors near the edge is calculated according to the CC-Method (see sections 4.1.2.4, 4.1.2.5 and 4.2.2.4). It is:

$$V_{Rk,c} = V_{Rk,c}^0 \cdot \frac{A_{c,V}}{A_{c,V}^0} \cdot \psi_{s,V} \cdot \psi_{h,V} \cdot \psi_{\alpha,V} \cdot \psi_{ec,V} \cdot \psi_{ucr,V} \quad [\text{N}] \quad (14.16)$$

The various factors in equation (14.16) are explained below.

The characteristic resistance of *one* anchor in a thick component in cracked concrete, loaded

perpendicular to the edge of the member, is calculated with equation (14.16a).

$$V_{Rk,c}^0 = 0.45 \cdot \sqrt{d_{nom}} \cdot (l_f/d_{nom})^{0.2} \cdot \sqrt{f_{ck,cube}} \cdot c_1^{1.5} \quad [\text{N}] \quad (14.16a)$$

with  $d_{nom}$ ,  $l_f$ ,  $c_1$  [mm] and  $f_{ck,cube}$  [N/mm<sup>2</sup>] measured on cubes with a side length of 150 mm.

Equation (14.16a) specifies the 5%-fractile of the test results in cracked concrete. It is derived from equation (4.25) taking into account the following aspects. Equation (4.25) gives the mean failure load in non-cracked concrete. The 5%-fractile is taken as 0.7 times the mean value and the failure load in cracked concrete as 0.7 times the value in non-cracked concrete (see section 4.2.2.4). Furthermore the influence of the different definitions of the concrete compression strength in equations (4.25) and (14.16a) (cubes with a side length of 200 mm or 150 mm respectively) and the curing conditions according to *EN 206-1:2001-07* (2001) are considered.

The geometrical influence of spacings, further edge distances parallel to the loading direction and component thickness on the characteristic resistance is taken into account by the quotient  $A_{c,V}/A_{c,V}^0$ . Here,  $A_{c,V}^0$  is the idealised area of the breakout body of a single anchor on the side face of a thick concrete component not influenced by edges parallel to the assumed loading direction or neighbouring anchors. The breakout body is assumed to be a half pyramid with

height  $c_1$  and base lengths  $1.5 \cdot c_1$  and  $3 \cdot c_1$  (see Fig. 4.77b).  $A_{c,V}$  is the actual idealised area of the breakout body of the anchorage on the side face of the concrete member. It is curtailed through the overlaps with the individual breakout bodies of neighbouring anchorages ( $s < 3 \cdot c_1$ ), through edges parallel to the assumed direction of loading ( $c_2 < 1.5 \cdot c_1$ ) and the thickness of the component ( $h < 1.5c_1$ ). Fig. 4.79 shows examples of the calculation of  $A_{c,V}$ .

In calculating  $V_{Rk,c}^0$ ,  $A_{c,V}^0$  and  $A_{c,V}$  it is assumed that the shear load acts perpendicular to the edge of the component.

Normally, there is an annular gap between the anchor and the fixture. Therefore, only the most critical anchor or the most critical anchors near the edge (Fig. 14.5) may be included when calculating  $A_{c,V}$  for groups of anchors near an edge. Anchorages in a corner of a component (Fig. 14.10) require equation (14.2) to be satisfied for both edges.

Factor  $\psi_{s,V}$  takes into account the fact that further component edges disrupt the stress condition in the concrete. Anchorages with two edge distances parallel to the loading direction (e.g. in a narrow component – see Fig. 4.84b) require the shorter edge distance of  $c_{2,1}$  and  $c_{2,2}$  to be used in equation (14.16b):

$$\psi_{s,V} = 0.7 + 0.3 \cdot \frac{c_2}{1.5 \cdot c_1} \leq 1.0 \quad (14.16b)$$

Factor  $\psi_{h,V}$  takes account of the fact that the characteristic resistance for a concrete edge failure does not decrease in proportion to the mem-

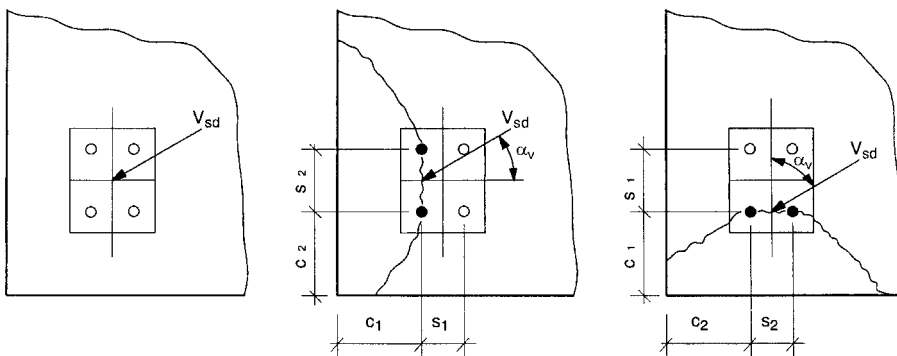


Fig. 14.10 Example of a fastener group at a corner, where resistance shall be calculated for both edges

ber thickness as assumed by the ratio  $A_{c,V} / A_{c,V}^0$  (see Fig. 4.87):

$$\psi_{h,V} = (1.5 \cdot c_1 / h)^{1/3} \geq 1.0 \quad (14.16c)$$

The factor  $\psi_{\alpha,V}$  takes into account the angle  $\alpha_V$  between the applied load  $V$  and a line perpendicular to the free edge of the concrete member (see Fig. 4.98):

$$\psi_{\alpha,V} = 1.0 \quad \text{for } 0^\circ \leq \alpha_V \leq 55^\circ \quad (14.16d)$$

$$\psi_{\alpha,V} = \frac{1}{\cos \alpha_V + 0.5 \cdot \sin \alpha_V} \quad \text{for } 55^\circ < \alpha_V \leq 90^\circ \quad (14.16e)$$

$$\psi_{\alpha,V} = 2.0 \quad \text{for } 90^\circ < \alpha_V \leq 180^\circ \quad (14.16f)$$

The factor  $\psi_{ec,V}$  allows for an eccentric shear load on a group of anchors (Fig. 14.8):

$$\psi_{ec,V} = \frac{1}{1 + 2 \cdot e_V / (3 \cdot c_1)} \leq 1.0 \quad (14.16g)$$

Here,  $e_V$  is the eccentricity of the resultant shear load on the anchors (Fig. 14.8). The eccentricity is determined from the shear forces calculated in the anchors. It is to be related to the geometrical centre of gravity of the anchors in shear. Equation (14.16g) only applies for an eccentricity  $e_V \leq s_j/2$ . At larger eccentricities the anchor near the load is loaded *towards* the edge and the anchor remote from the load *away* from the edge. This case is not covered in ETAG 001, Annex C.

The factor  $\psi_{ucr,V}$  takes into account the influence of the position of the anchorage in cracked or non-cracked concrete or the type of edge reinforcement present:

$\psi_{ucr,V} = 1.0$  anchorage in cracked concrete without edge or supplemental hanger reinforcement

$\psi_{ucr,V} = 1.2$  anchorage in cracked concrete with straight edge reinforcement ( $d_s \geq 12$  mm)

$\psi_{ucr,V} = 1.4$  anchorage in cracked concrete with edge and closely spaced supplemental hanger (bar spacing  $\leq 100$  mm), and anchorages in non-cracked concrete

For anchorages in a narrow, thin component with  $c_{2,max} < 1.5 \cdot c_1$  ( $c_{2,max}$  = larger of the two edge distances parallel to the loading direction) and  $h < 1.5 \cdot c_1$  (Fig. 4.90 shows one example), equation (14.16) leads to results which are conservative. More accurate results are obtained when the edge distance  $c_1$  is replaced by  $c'_1$  in equations (14.16a) to (14.16c) and (14.16g) as well as in the determination of areas  $A_{c,V}^0$  and  $A_{c,V}$  according to Figs. 4.77b and 4.79. Here,  $c'_1$  is the larger of the two values  $c_{max}/1.5$  and  $h/1.5$  respectively (cf. section 4.1.2.4f and Fig. 4.90). Note that the above approach does not take in to account the influence of anchor spacing on the value  $c'_1$ . This is considered in section 14.4.6.2.2c.

### 14.3.5.3 Combined tension and shear

The following checks are required in the case of combined tension and shear loads (Fig. 14.11):

$$N_{Sd} / N_{Rd} \leq 1.0 \quad (14.17a)$$

$$V_{Sd} / V_{Rd} \leq 1.0 \quad (14.17b)$$

$$N_{Sd} / N_{Rd} + V_{Sd} / V_{Rd} \leq 1.2 \quad (14.17c)$$

For single anchors, the largest value according to tables 14.1 and 14.2 is to be used for the different failure modes for the quotients  $N_{Sd} / N_{Rd}$  and  $V_{Sd} / V_{Rd}$  respectively. In the case of anchor groups, the largest of  $N_{Sd}^h / N_{Rd,s}$ ,  $N_{Sd}^h / N_{Rd,p}$ ,  $N_{Sd}^g / N_{Rd,c}$  and  $N_{Sd}^g / N_{Rd,sp}$  is to be used for the quotient  $N_{Sd} / N_{Rd}$ , and the largest of  $V_{Sd}^h / V_{Rd,s}$ ,  $V_{Sd}^h / V_{Rd,cp}$  and  $V_{Sd}^g / V_{Rd,c}$  for  $V_{Sd} / V_{Rd}$ .

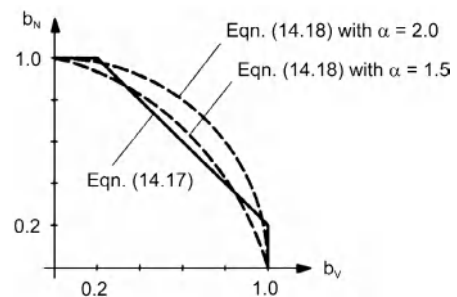


Fig. 14.11 Interaction for combined tension and shear loads

In general, equation (14.17a) to (14.17c) yield conservative results. More accurate results are obtained by equation (14.18).

$$(N_{Sd}/N_{Rd})^\alpha + (V_{Sd}/V_{Rd})^\alpha \leq 1 \quad (14.18)$$

where:

$(N_{Sd}/N_{Rd})$  and  $(V_{Sd}/V_{Rd})$  are the smallest values for the different failure modes (see above)

$\alpha = 2.0$  if  $N_{Rd}$  and  $V_{Rd}$  are governed by steel failure

$\alpha = 1.5$  for all other failure modes

### 14.3.6 Serviceability limit state

#### 14.3.6.1 Anchor displacements

At the serviceability limit state, the displacements due to the characteristic actions are to be compared with the permissible displacements. The permissible displacements depend on the construction to be anchored and are to be specified by the engineer.

The characteristic displacements of the anchor under defined tension and shear loads are given in the respective approval document. It may be assumed that the displacements are a linear function of the applied load. In the case of combined tension and shear load, the displacements for the tension and shear component of the resultant load should be geometrically added.

In the case of shear loads the influence of the hole clearance in the fixture on the expected displacement of the anchorage should be taken into account.

#### 14.3.6.2 Shear load with changing sign

If the applied shear load is reversed several times, then there is a risk of a premature failure of the anchor steel. The acceptable amplitude of the shear load depends on the design of the anchor and the number of load cycles. To avoid a fatigue failure, the shear load should be transferred by friction between the fixture and the concrete. This can be assured by a sufficiently high permanent prestressing force.

Shear loads with changing sign can occur due to temperature variations in the fastened member (e.g. facade elements). Therefore either these members are anchored such that no significant shear loads due to the restraint of deformations

imposed to the fastened element will occur in the anchor or in shear loading with lever arm (stand-off installation) the bending stresses in the most stressed anchor  $\Delta\sigma_s = \sigma_{s,max} - \sigma_{s,min}$  in the serviceability limit state caused by temperature variations should be limited to 100 N/mm<sup>2</sup>.

### 14.3.7 Additional analyses for ensuring the characteristic resistance of concrete member

#### 14.3.7.1 General

The design method described in sections 14.3.3 to 14.3.5 provides proof of the local transfer of anchor loads into the base material. Verification that the anchor loads are transferred to the supports of the concrete member is required for the ultimate and serviceability limit states. This requires the standard analyses taking into account the loads introduced by the anchors. For these verifications, the additional provisions outlined in sections 14.3.7.2 and 14.3.7.3 need to be taken into account.

If the edge distance of an anchor is less than the characteristic edge distance  $c_{cr,N} = 1.5 \cdot h_{ef}$ , then edge reinforcement with diameter  $d_s \geq 6$  mm should be provided in the edge of the component.

#### 14.3.7.2 Shear resistance of the concrete member

In *Eurocode 2: EN 1992-1-1* (2003) it is assumed that reinforced concrete flexural members are loaded from the top side. If loads are applied at the bottom side they are to be transferred to and anchored in the side of the component opposite the load, i.e. the compression zone, by way of hanger reinforcement. However, anchorages normally introduce loads into the bottom of a component, i.e. into the tension zone, and hanger reinforcement is very often not provided. In order to avoid an unfavourable effect on the shear resistance of the component serving as base material, the following additional checks are required. These provisions were discussed in detail in section 13.

In the case of precast floors and beams with a structural topping of in-situ concrete, anchor loads may only be transferred into the precast units when precast and in-situ concrete are ade-



quately connected with tie bars. In the absence of such tie bars the anchors must be anchored in the in-situ concrete with the necessary embedment depth  $h_{ef}$ . An exception is the load from lightweight suspended ceilings or similar constructions not exceeding  $1.0 \text{ kN/m}^2$ , which may be transferred into the precast units.

Generally, the shear forces  $V_{Sd,a}$  caused by the anchor loads should satisfy equation (14.19) in components made from in-situ or precast concrete as well as precast units with in-situ concrete and adequate tie bars in the joint between precast and in-situ concrete.

$$V_{Sd,a} \geq 0.4 \cdot V_{Rd1} \tag{14.19}$$

where:

$V_{Rd1}$  according to *Eurocode 2: EN 1992-1-1* (2003)

When calculating  $V_{Sd,a}$  the anchor loads shall be assumed as point loads with a width of load application  $t_1 = s_{t,1} + 2 \cdot h_{ef}$  and  $t_2 = s_{t,2} + 2 \cdot h_{ef}$ , where  $s_{t,1}$  and  $s_{t,2}$  are the spacings between the outermost anchors of the group in directions 1 and 2 respectively. For single anchors  $s_{t,1} = s_{t,2}$  is taken as 0.

Equation (14.19) needs not be checked when one of the following conditions is fulfilled:

- The shear force  $V_{Sd}$  at the support caused by the design actions including the anchor loads is:

$$V_{Sd} \leq 0.8 \cdot V_{Rd1} \tag{14.20}$$

- Under the characteristic actions, the resultant tension force,  $N_{Sk}$ , of the tensioned fasteners

is  $N_{Sk} \leq 30 \text{ kN}$  and the spacing,  $a$ , between the outermost anchors of adjacent groups or between the outer anchors of a group and individual anchors satisfies equation (14.21).

$$a \geq 200 \cdot \sqrt{N_{Sk}} ; \quad a \text{ [mm], } N_{Sk} \text{ [kN]} \tag{14.21}$$

- The anchor loads are taken up by a hanger reinforcement, which encloses the tension reinforcement and is anchored at the opposite side of the concrete member. Its distance from an single anchor or the outermost anchors of a group should be smaller than  $h_{ef}$ .

If under the characteristic actions, the resultant tension force,  $N_{Sk}$ , of the tensioned fasteners is  $N_{Sk} > 60 \text{ kN}$ , then either the embedment depth of the anchors should be  $h_{ef} \geq 0.8 \cdot h$  or a hanger reinforcement according to the requirements given above should be provided.

The necessary checks for ensuring the required shear resistance of the concrete member are summarised in Table 14.3.

The above provisions to ensure sufficient safety against shear failure of the concrete member are derived from tests on slabs *without* shear reinforcement. This approach is conservative for components *with* shear reinforcement. Preliminary test results indicate no significant reduction of the shear capacity in components *with* shear reinforcement when the load introduced via anchorages into the tension zone is less than about 30 kN.

**Table 14.3** Necessary checks for ensuring the required shear resistance of a concrete member

Calculated value of shear force of the concrete member under due consideration of the anchor loads	Spacing between single anchors and groups of anchors	$N_{Sk}$ [kN]	Proof of calculated shear force resulting from anchor loads
$V_{Sd} \leq 0.8 \cdot V_{Rd1}$	$a \geq s_{cr,N}$	$\leq 60$	not required
$V_{Sd} > 0.8 \cdot V_{Rd1}$	$a \geq s_{cr,N}$ and $a \geq 200 \cdot \sqrt{N_{Sk}}$	$\leq 30$	not required
	$a \geq s_{cr,N}$	$\leq 60$	required: $V_{Sd} \leq 0.4 \cdot V_{Rd1}$ or hanger reinforcement or $h_{ef} \geq 0.8 \cdot h$
		$> 60$	not required, but hanger reinforcement or $h_{ef} \geq 0.8 \cdot h$



### 14.3.7.3 Resistance to splitting forces

In general, the splitting forces caused by anchors should be taken into account in the design of the concrete member. This may be neglected if one of the following conditions is met:

- The load transfer area is in the compression zone of the concrete member.
- The tension component  $N_{Sk}$  of the characteristic loads acting on the anchorage (single anchor or group of anchors) is smaller than 10 kN.
- The tension component  $N_{Sk}$  is not greater than 30 kN. In addition, for fastenings in slabs and walls a concentrated reinforcement in both directions is present in the region of the anchorage. The area of the transverse reinforcement should be at least 60 % of the longitudinal reinforcement required for the actions due to the anchor loads.

If the characteristic tension load acting on the anchorage is  $N_{Sk} \geq 30$  kN and the anchors are located in the tension zone of the concrete member the splitting forces should be taken up by reinforcement. As a first indication for anchors according to current experience the values for the splitting force,  $F_{sp,k}$  given in section 14.3.5.1d may be taken.

## 14.4 Design of fastenings according to the CEN Technical Specification

### 14.4.1 General

A working group of the European Committee for Standardisation (CEN) is currently drafting a CEN Technical Specification “Design of fastenings for use in concrete” (*European Committee for Standardisation (CEN) (2004)*). In the following this specification is called CEN TS. In sections 14.4.2 to 14.4.13.3.4 the design approaches are described for different types of fasteners based on the Final Draft of July 2004. The Technical Specification applies to cast-in fasteners such as headed fasteners, anchor channels with rigid connection between fastener and channel and to post-installed anchors such as expansion anchors, undercut anchors, concrete screws, bonded anchors, bonded expansion anchors and bonded undercut anchors. The Technical Specification consists of the following parts:

Part 1: General

Part 2: Headed fasteners

Part 3: Anchor channels

Part 4: Post-installed fasteners – mechanical systems

Part 5: Post-installed fasteners – chemical systems

Numerical values for partial safety factors and other reliability parameters are recommended as basic values that provide an acceptable level of reliability. They have been selected assuming that an appropriate level of workmanship and of quality management applies. They may be applied in absence of a National Annex to the Technical Specification defining national values.

According to *Eurocode 2: EN 1992-1-1 (2003)* the local and structural effects of fasteners should be considered in the design of concrete members. The local effects are considered by fulfilling the requirements for the design of fastenings given in the Technical Specification “Design of fastenings for use in concrete”. To consider the structural effects of fastenings, in the design of the structure the anchor loads and additional design requirements given in Annex A of that Technical Specification should be taken into account.

### 14.4.2 Scope

The Technical Specification applies to fasteners covered by a European Technical Approval (ETA) and relies on characteristic resistances and distances which are stated in the ETA. It may also be used for fasteners covered by a CEN-Product Standard if the data required by the Technical Specification are provided and reference to the Technical Specification is given in the CEN-Product Standard. Up to now no CEN Product Standards for fasteners exist.

The CEN TS is intended for the design of fastening for use in structural and non-structural applications in which the failure of fastenings will:

- result in collapse or partial collapse of the structure or
- cause risk to human life or
- lead to significant economic loss.

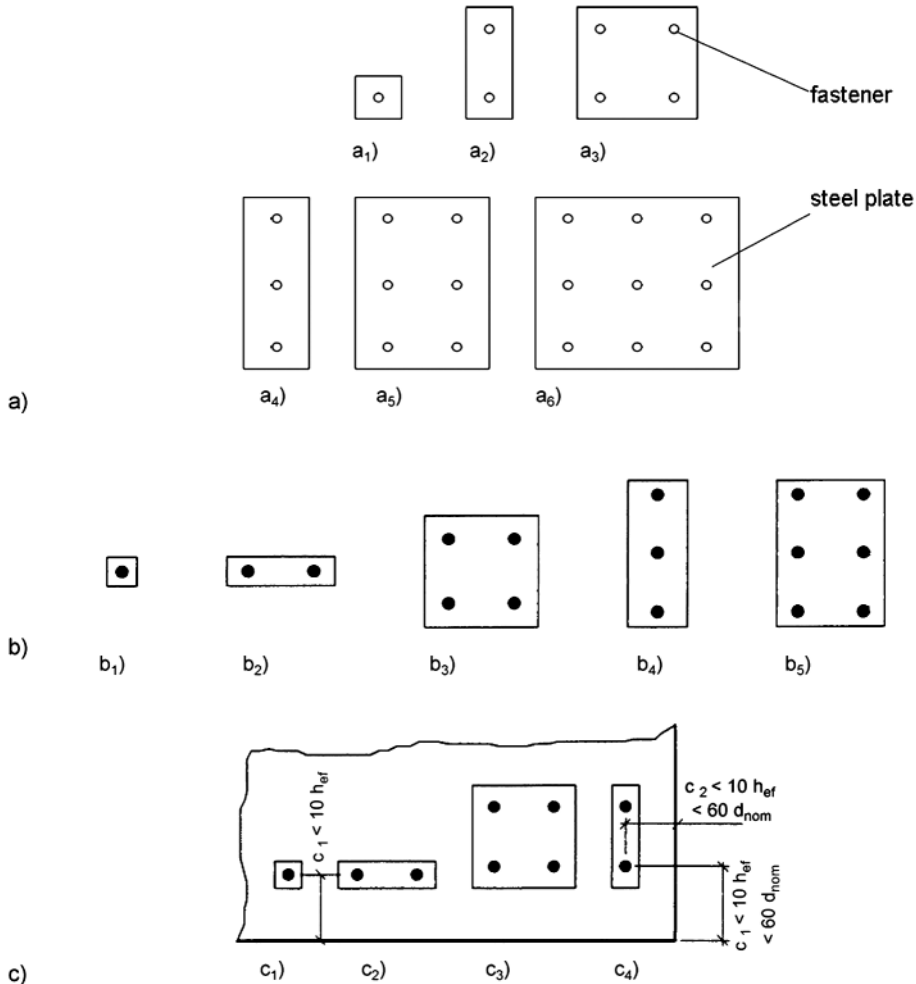


**Fig. 14.12** Configurations of fastenings:

- a) without hole clearance, all edge distances  $c \geq 10 \cdot h_{ef}$  and  $c \geq 60 \cdot d_{nom}$   
 b) with hole clearance, all edge distances  $c \geq 10 \cdot h_{ef}$  and  $c \geq 60 \cdot d_{nom}$   
 c) with hole clearance near to an edge ( $c < 10 \cdot h_{ef}$  and  $c < 60 \cdot d_{nom}$ )

It is valid for fastenings in new construction and existing structures and it may also be used for temporary fastenings e. g. for the handling of precast elements or site equipment such as scaffolding and barriers. The support of the fixture may be either statically determinate (one or two supports) or statically indeterminate. A support may consist of one fastener or a group of fasteners. In a fastening group the loads are applied to the individual fasteners of the group

by means of a common fixture. It is assumed, that in a group only fasteners of the same type and size are used.

The configurations of fasteners (cast-in place headed fasteners or post-installed fasteners) covered by the Technical Specification are shown in Fig. 14.12. A distinction is made between fastenings with or without hole clearance. The following applications may be considered to have no hole clearance:

- Bolts that are welded to or screwed into the fixture.
- Any gap between the fastener and the fixture is filled with mortar of sufficient compression strength or other means.

The configuration of fasteners for fastenings with hole clearance allowed by the CEN Technical Specification agrees with the provisions in the ETAG 001 (compare Fig. 14.12b with Fig. 14.2). For anchor channels the number of fasteners is not limited.

The Technical Specification applies to fasteners with a minimum thread size of 6 mm (M6) and a maximum thread size of 60 mm (M60) or corresponding cross-section. In general, the minimum embedment depth should be  $h_{ef} \geq 40$  mm. The Specification is valid for fasteners with a nominal steel tensile strength  $f_{tk} \leq 1000$  N/mm<sup>2</sup>.

The fastenings may be subjected to static, fatigue and seismic loading. Whether a certain type of fastener is suitable for the use under fatigue or seismic loading is stated in the relevant ETA or CEN-Product Standard. The design methods are valid for any actions on the fixture (tension, shear without or with lever arm, bending or torsion moments or any combination thereof). However, compression forces on the fixture should be transmitted to the concrete either without acting on the fastener or via fasteners suitable for resisting compression.

The Technical Specification applies to members made of concrete with normal weight aggregates according to *EN 206-1:2001-07 (2001)* and to concrete strength classes C12/15 to C90/105. The range of concrete strength classes in which a particular fastener may be used is given in the relevant ETA or CEN-Product Standard and may be more restrictive than *EN 206-1:2001-07 (2001)*. The concrete member may be subjected to static, fatigue or seismic loading. However, the use of certain types of fasteners may not be permitted for fatigue or seismic loading of the concrete member. This is again stated in the corresponding ETA or CEN-Product Standard.

In the region of the fastening, the concrete may be cracked or non-cracked. The condition of the concrete should be decided by the designer on the basis of national regulations. Non-cracked

concrete may be assumed if in each case it is verified that under service conditions the fastener with its entire embedment depth is located in non-cracked concrete. In the absence of national regulations this verification can be taken as fulfilled if equation (14.22) is observed:

$$\sigma_L + \sigma_R \leq \sigma_{adm} \quad (14.22)$$

where:

$\sigma_L$  = stresses in the concrete induced by external loads including fastener loads

$\sigma_R$  = stresses in the concrete due to restraint of intrinsic deformations (e. g. shrinkage of concrete) or extrinsic imposed deformations (e. g. due to displacement of support or temperature variations). If no detailed analysis is conducted, then  $\sigma_R = 3$  N/mm<sup>2</sup> should be assumed

$\sigma_{adm}$  = admissible stress for the definition of non-cracked concrete; in absence of national regulations  $\sigma_{adm} = 0$  is recommended

For concrete members which transmit loads in two directions (e. g. slabs, walls and shells) equation (14.22) should be fulfilled for both directions.

In general, the verification of non-cracked concrete corresponds to the requirements of *European Organisation for Technical Approvals (EOTA) (1997)* (compare equation (14.1)). The basis of the verification is described in detail in section 14.3.2.

For seismic design situations the concrete should be assumed to be cracked in the region of the fastening.

### 14.4.3 Basis of design

For fasteners the following limit states should be verified:

- ultimate limit state, including the effects of fatigue and seismic loading where appropriate,
- serviceability limit state.

Furthermore the durability (corrosion resistance) of the fastening for the intended use should be demonstrated. Where applicable, the

fastening should have an adequate fire resistance.

At ultimate limit state equation (14.23) should be fulfilled.

$$E_d \leq R_d \quad (14.23)$$

where:

$$\begin{aligned} E_d &= \text{design value of effect of actions} \\ R_d &= \text{design value of resistance} \\ &= R_k / \gamma_M \quad (14.23a) \\ R_k &= \text{characteristic resistance of} \\ &\quad \text{single fastener or group of fasteners} \\ \gamma_M &= \text{partial factor for resistance} \end{aligned}$$

At serviceability limit state it should be shown that

$$E_d \leq C_d \quad (14.24)$$

where:

$$\begin{aligned} E_d &= \text{design value of fastener displacement,} \\ &\quad \text{evaluated from information given in the} \\ &\quad \text{relevant ETA or CEN-Product Standard} \\ C_d &= \text{design value, e. g. limiting displacement.} \\ &\quad \text{It should be decided on by the designer} \\ &\quad \text{for the application in question} \end{aligned}$$

The forces in the fasteners should be derived using appropriate combinations of actions on the fixture as recommended in *EN 1990:2002* (2002), section 6. When indirect action  $Q_{ind}$  arises from the restraint of deformations (intrinsic (e. g. shrinkage) or extrinsic (temperature variations)) imposed to the fastened member (fixture, attachment), the design action shall be taken as  $\gamma_{ind} \cdot Q_{ind}$ . In general actions on the fixture may be calculated ignoring the displacement of the fasteners. However, the effect of the displacement of the fasteners may be significant when a statically indeterminate stiff element is fastened and should be considered in these cases.

The above approach agrees with the procedure described in section 14.3.3, but the term  $S_d$  in equation (14.2) has been replaced by  $E_d$ .

#### 14.4.4 Partial safety factors

In the CEN TS partial safety factors are recommended, however, the specific values to be used in a country may be found in its National Annex. Up to now no National Annex exists. In the following the recommended values are given.

##### 14.4.4.1 Static actions, indirect actions and fatigue actions

Partial safety factors for the actions to be used in the design are stated in *EN 1990 : 2002* (2002), Annex A. For the verification of indirect (ultimate limit state) and fatigue actions the following values for  $\gamma_{ind}$  and  $\gamma_{F,fat}$  respectively are recommended:

$$\gamma_{ind} = 1.2 \text{ for concrete failure} \quad (14.25a)$$

$$\gamma_{ind} = 1.0 \text{ for other modes of failure} \quad (14.25b)$$

$$\gamma_{F,fat} = 1.0 \quad (14.26)$$

##### 14.4.4.2 Resistances

###### 14.4.4.2.1 Ultimate limit state (static loading) and seismic loading

###### a) Steel failure

Tension loading on fasteners, anchors and special screws of anchor channels:

$$\gamma_{Ms} = \frac{1.2}{f_{yk}/f_{uk}} \geq 1.4 \quad (14.27a)$$

Shear loading on fasteners and special screws of anchor channels with and without lever arm:

$$\gamma_{Ms} = \frac{1.0}{f_{yk}/f_{uk}} \geq 1.25 \quad (14.27b)$$

$$f_{uk} \leq 800 \text{ N/mm}^2 \text{ and } f_{yk}/f_{uk} \leq 0.8$$

$$\gamma_{Ms} = 1.5 \quad (14.27c)$$

$$f_{uk} > 800 \text{ N/mm}^2 \text{ or } f_{yk}/f_{uk} > 0.8$$

Connection between anchor and channel of anchor channels:

$$\gamma_{Ms,c} = 1.8 \quad (14.27d)$$

Local failure of the anchor channel by bending of the lips in tension and shear:

$$\gamma_{Ms,l} = 1.8 \quad (14.27e)$$

Bending of the channel of anchor channels:

$$\gamma_{Ms,flex} = 1.15 \quad (14.27f)$$

Steel failure of supplementary reinforcement:

$$\gamma_{Ms,re} = 1.15 \quad (14.27g)$$

###### b) Concrete failure

The partial safety factor  $\gamma_{Mc}$  covers concrete break-out failure modes (cone failure, blow-out

failure, pry-out failure and concrete edge failure). It is determined from equation (14.28):

$$\gamma_{Mc} = \gamma_c \cdot \gamma_{inst} \quad (14.28)$$

where:

$\gamma_c$  = partial safety factor for concrete  
= 1.5

$\gamma_{inst}$  = partial safety factor taking into account the installation safety of a fastening system. This factor is given in the relevant ETA or CEN Product Standard. It must not be changed because it describes a characteristic of the fastener

For post-installed fasteners the partial safety factor  $\gamma_{inst}$  is equal to the value  $\gamma_2$  according to section 14.3.3.1. For cast-in place headed fasteners and for anchor channels a high installation safety ( $\gamma_{inst} = 1.0$ ) may be assumed, provided that special conditions regarding the installation are fulfilled (see sections 14.4.6 and 14.4.7).

For seismic strengthening and repair of existing structures the partial factor  $\gamma_{Mc}$  may be reduced according to the relevant sections of *Eurocode 8: EN 1998-1* (2003).

The partial factor  $\gamma_{Msp} = \gamma_{Mc}$  is valid for splitting failure.

### c) Pull-out/pull-through failure

For the partial factor  $\gamma_{Mp}$  for pull-out/pull-through failure  $\gamma_{Mp} = \gamma_{Mc}$  is recommended.

#### 14.4.4.2.2 Limit state of fatigue

Partial factors for fatigue loading  $\gamma_{Ms,fat}$ ,  $\gamma_{Mc,fat}$ ,  $\gamma_{Msp,fat}$  and  $\gamma_{Mp,fat}$  shall be considered. It is recommended to take  $\gamma_{Ms,fat} = 1.35$  (steel failure) and  $\gamma_{Mc,fat}$ ,  $\gamma_{Msp,fat}$  and  $\gamma_{Mp,fat}$  (concrete cone failure, splitting failure and pull-out/pull-through failure) according to equation (14.28).

#### 14.4.4.2.3 Serviceability limit state

A partial factor  $\gamma_M = 1.0$  is recommended.

#### 14.4.5 Forces acting on fasteners

The actions on a fixture shall be transferred to the fasteners as statically equivalent tension and shear forces. When a bending moment and/or compression force act on the fixture, which is in contact with the concrete or mortar, a friction force will develop. This friction force reduces the shear forces acting on the anchors, however, it will not alter the forces in the concrete. As it is difficult to quantify with confidence the effect of friction, the friction forces are neglected. This simplified assumption is conservative.

In this section and in the sections 14.4.6 to 14.4.12 it is assumed that the forces acting on fasteners are calculated according to the theory of elasticity. Section 14.4.13 deals with fastenings with headed and post-installed anchors designed according to a plastic design approach.

#### 14.4.5.1 Tension loads

The following assumptions apply to headed fasteners and mechanical or chemical post-installed fasteners.

The forces in headed fasteners, mechanical or chemical post-installed fasteners due to normal forces and bending moments acting on the fixture are calculated as described in section 14.3.4. Forces in anchor channels should be derived according to section 14.4.7.

#### 14.4.5.2 Shear loads

##### 14.4.5.2.1 Distribution of loads

The following assumptions apply to headed fasteners and mechanical or chemical post-

**Table 14.4** Hole clearance according to *European Committee for Standardisation (CEN)* (2004)

1	External diameter <sup>1)</sup> or $d_{nom}$ <sup>2)</sup> [mm]	6	8	10	12	14	16	18	20	22	24	27	30
2	Diameter $d_{t,1}$ of clearance hole in fixture [mm]	7	9	12	14	16	18	20	22	24	26	30	33
3	Maximum allowable diameter $d_{t,2}$ of clearance hole in fixture [mm]	8	10	14	16	18	20	22	24	26	28	33	36

<sup>1)</sup> If bolt bears against the fixture (Fig.14.9a)

<sup>2)</sup> If sleeve bears against the fixture (Fig.14.9b)

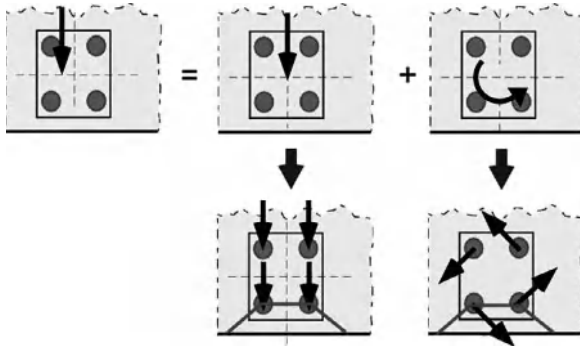


**Fig. 14.13** Examples for load distribution of an eccentrically loaded quadruple fastening without hole clearance

installed fasteners. Forces in anchor channels should be derived according to section 14.4.7.

#### a) Steel or pry-out failure

The shear forces on each anchor due to shear loads and/or torsion moments to verify steel or pry-out failure should be calculated independent of the edge distance using the theory of elasticity and statics. An example is shown in Fig. 14.13. The effectiveness of fasteners to resist shear loads depends on the hole clearance:

- If there is no hole clearance in the fixture or if the diameter of the hole in the fixture is  $d_f \leq d_{f,2}$  (Table 14.4, line 3) all fasteners are considered as effective.
- If the diameter is  $d_f > d_{f,2}$  or the hole is slotted in the direction of the shear force the fastener is considered ineffective

For external diameters larger than 30 mm which are also covered by the CEN TS the authors recommend to use  $d_{f,1} \leq 1.1 \cdot d$  and  $d_{f,2} \leq 1.2 \cdot d$  (bolt bears against the fixture, Fig. 14.9a) or  $d_{f,1} \leq 1.1 \cdot d_{nom}$  and  $d_{f,2} \leq 1.2 \cdot d_{nom}$  (sleeve bears against the fixture, Fig. 14.9b).

#### b) Concrete edge failure

No calculation of distribution of the shear forces is required to verify concrete edge failure because the resistance models of the Technical Report account for the distribution. The resistance of a group of fasteners is compared directly with the shear loads and torsion moments acting on the fixture.

The following distribution of loads is assumed in the calculation of the design resistance for concrete edge failure:

- For groups of fasteners with a hole clearance  $d_f \leq d_{f,2}$  ( $d_{f,2}$  see Table 14.4) loaded perpendicular to the edge only the front fasteners are assumed to carry shear loads.
- For all other cases it is assumed that all fasteners carry shear loads with a distribution as described in 14.4.5.2.1a.

#### 14.4.5.2.2 Shear loads without lever arm

Shear loads acting on fastenings may be assumed to act without a lever arm if all of the following conditions are fulfilled:

- The fixture must be made of metal and in the area of the fastening be fixed directly to the concrete without an intermediate layer or with a levelling layer of mortar with a compressive strength  $\geq 30 \text{ N/mm}^2$  and a thickness  $t_{Grout} \leq d/2$  (Fig. 14.14).
- The fixture is in contact with the fastener over a length of at least  $0.5 \cdot t_{fix}$  (Fig. 14.15).
- The diameter  $d_f$  of the hole in the fixture is not greater than the value  $d_{f,1}$  given in Table 14.4, line 2.

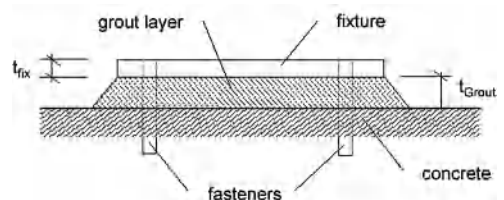


**Fig. 14.14** Fixture with grout layer

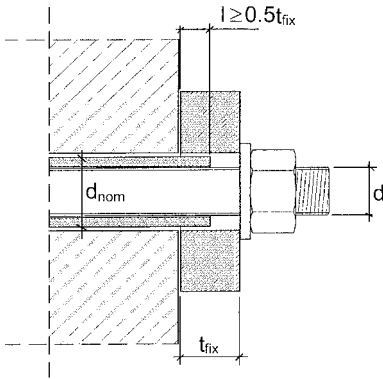


Fig. 14.15 Bearing area of a fastener

**14.4.5.2.3 Shear loads with lever arm**

If one of the conditions according to section 14.4.5.2.2 is not fulfilled, it should be assumed that the shear load acts with a lever arm according to equation (14.8).

**14.4.6 Design of headed fasteners**

**14.4.6.1 Determination of action effects**

The tension and shear loads on the fasteners due to normal forces, bending moments and shear forces should be calculated according to sections 14.4.5.1 and 14.4.5.2.

Where supplementary reinforcement is provided, the design tension forces  $N_{Ed, re}$  in the supplementary reinforcement should be established using an appropriate strut-and-tie model. The supplementary reinforcement should be designed to resist the total external force on the fastening.

The design tension forces  $N_{Ed, re}$  in a supplementary (hanger) reinforcement to take up anchor

tension forces should be calculated with an appropriate strut-and-tie model using the design load on the fastener (compare Fig. 14.17).

The design force  $N_{Ed, re}$  in the supplementary reinforcement caused by the design shear force  $V_{Ed}$  acting on the fixture is given by equation (14.29):

$$N_{Ed, re} = V_{Ed} \cdot \left( \frac{e_s}{z} + 1 \right) \tag{14.29}$$

where (compare Fig. 14.16):

- $e_s$  = distance between reinforcement and shear force acting on a fixture
- $z$  = internal lever arm of the concrete member  
 $\approx 0.85 \cdot d$
- $d$  = depth of concrete member  
 $\leq \min \{ 2 \cdot h_{ef}; 2 \cdot c_1 \}$

If the supplementary reinforcement is not arranged in the direction of the shear force then this must be taken into account in the calculation of the tension force in the reinforcement. In the case of different shear forces on the fasteners of a fixture, equation (14.29) should be solved for the shear load  $V_{Ed}$  of the most loaded fastener resulting in  $N_{Ed, re}^h$ .

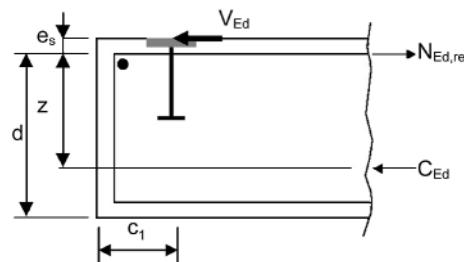


Fig. 14.16 Detailing of reinforcement to take up shear forces

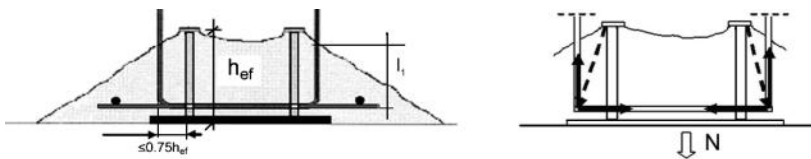


Fig. 14.17 Example for a multiple fastening with supplementary reinforcement to take up tension loads and corresponding strut and tie model



### 14.4.6.2 Verification of ultimate limit state by elastic analysis

#### 14.4.6.2.1 Tension loads

The required verifications for tension loads are shown in Table 14.5. For fasteners without supplementary reinforcement lines 1 to 5 apply. For fasteners with reinforcement lines 1,2 and 4 to 7 apply.

When the design relies on supplementary reinforcement concrete cone failure needs not to be verified but the supplementary reinforcement should be designed to resist the total load. The supplementary reinforcement should comply with the following requirements (see also Fig. 14.17):

- The same diameter of reinforcement should be provided for all fasteners of a group. The reinforcement should consist of ribbed reinforcing bars ( $f_{yk} \leq 500 \text{ N/mm}^2$ ) with a diameter not larger than 16 mm and should be detailed in form of stirrups or loops with a bending diameter according to *Eurocode 2* (2003).

- The supplementary reinforcement should be placed as close to the fasteners as practicable. Preferably, the supplementary reinforcement should enclose the surface reinforcement. Only reinforcement bars with a distance  $\leq 0.75 \cdot h_{ef}$  from a fastener should be assumed as effective.
- The minimum anchorage length of the supplementary reinforcement in the concrete failure cone is  $\min l_1 = 4 \cdot d_s$ .
- The supplementary reinforcement should be anchored outside the assumed failure cone with an anchorage length  $l_{bd}$  according to *Eurocode 2* (2003).
- A surface reinforcement should be provided designed for the forces according to the assumed strut-and-tie model and taking into account the splitting forces.

#### a) Steel failure of fastener

The characteristic resistance of a headed fastener in case of steel failure,  $N_{Rk,s}$ , is given in the relevant ETA or CEN-Product Standard. It is calculated according to equation (14.10). In

**Table 14.5** Required verifications for headed fasteners loaded in tension

		Single fastener	Fastener group	
			most loaded fastener	fastener group
1	Steel failure of fastener	$N_{Ed} \leq N_{Rd,s} = \frac{N_{Rk,s}}{\gamma_{Ms}}$	$N_{Ed}^h \leq N_{Rd,s} = \frac{N_{Rk,s}}{\gamma_{Ms}}$	
2	Pull-out failure of fastener	$N_{Ed} \leq N_{Rd,p} = \frac{N_{Rk,p}}{\gamma_{Mp}}$	$N_{Ed}^h \leq N_{Rd,p} = \frac{N_{Rk,p}}{\gamma_{Mp}}$	
3	Concrete cone failure	$N_{Ed} \leq N_{Rd,c} = \frac{N_{Rk,c}}{\gamma_{Mc}}$		$N_{Ed}^g \leq N_{Rd,c} = \frac{N_{Rk,c}}{\gamma_{Mc}}$
4	Splitting failure	$N_{Ed} \leq N_{Rd,sp} = \frac{N_{Rk,sp}}{\gamma_{Msp}}$		$N_{Ed}^g \leq N_{Rd,sp} = \frac{N_{Rk,sp}}{\gamma_{Msp}}$
5	Blow-out failure <sup>1)</sup>	$N_{Ed} \leq N_{Rd,cb} = \frac{N_{Rk,cb}}{\gamma_{Mc}}$		$N_{Ed}^g \leq N_{Rd,cb} = \frac{N_{Rk,cb}}{\gamma_{Mc}}$
6	Steel failure of reinforcement	$N_{Ed,re} \leq N_{Rd,re} = \frac{N_{Rk,re}}{\gamma_{Ms,re}}$	$N_{Ed,re}^h \leq N_{Rd,re} = \frac{N_{Rk,re}}{\gamma_{Ms,re}}$	
7	Anchorage failure of reinforcement	$N_{Ed,re} \leq N_{Rd,a}$	$N_{Ed,re}^h \leq N_{Rd,a}$	

1) Not required for fasteners with  $c > 0.5 \cdot h_{ef}$ .

case of different forces on the anchors the most loaded anchor should be verified.

### b) Pull-out failure

The characteristic resistance of a headed fastener in case of pull-out failure,  $N_{Rk,p}$ , is given in the relevant ETA or CEN-Product Standard. The resistance is limited by the concrete pressure under the head of the fastener according to equation (14.30):

$$N_{Rk,p} = 6 \cdot A_h \cdot f_{ck,cube} \cdot \psi_{ucr,N} \quad (14.30)$$

where:

$A_h$  = load bearing area of the head of the fastener

$$= \frac{\pi}{4} \cdot (d_h^2 - d_1^2) \quad (14.30a)$$

$f_{ck,cube}$  = characteristic concrete cube compressive strength measured on cubes with a side length of 150 mm, the minimum or maximum value to be inserted is given in the relevant ETA or CEN-Product Standard

$\psi_{ucr,N}$  = 1.4 for fasteners in non-cracked concrete

= 1.0 for fasteners in cracked concrete

### c) Concrete cone failure

The characteristic resistance of a tensioned headed fastener or a group of tensioned fasteners in case of concrete cone failure,  $N_{Rk,c}$ , should be calculated in accordance with section 14.3.5.1c. The factor 7.2 in equation (14.11a) is substituted by a factor  $k_1$ . The factor  $k_1$  and the characteristic spacing  $s_{cr,N}$  and  $c_{cr,N}$  are given in

the relevant ETA or CEN-Product Standard. For headed anchors according to current experience  $k_1 = 8.5$  and  $s_{cr,N} = 2 \cdot c_{cr,N} = 3 \cdot h_{ef}$  are assumed. The value  $k_1 = 8.5$  considers the higher failure load of headed studs compared to most post-installed anchors (see equation (4.5)).

The definition of the embedment depth  $h_{ef}$  is shown in Fig. 14.18.

For cases, where a fastener is located to three or more edges with distances less than  $c_{max} = 1.5 \cdot h_{ef}$  the calculation according to section 14.3.5.1c leads to conservative results. More precise results are obtained with the approach described in section 14.3.5.1c (equation (14.11f) to (14.11h)). However, for groups the value  $h_{ef}$  should be taken as the larger value of

$$h'_{ef} = \frac{c_{max}}{c_{cr,N}} \cdot h_{ef} \quad \text{and} \quad h'_{ef} = \frac{s_{max}}{s_{cr,N}} \cdot h_{ef} \quad (14.31)$$

where:

$c_{max}$  = maximum distance from centre of a fastener to the edge of a concrete member

<  $c_{cr,N}$

$s_{max}$  = maximum centre to centre spacing of anchors

<  $s_{cr,N}$

The reasoning for these provisions is given in section 4.1.1.3g.

### d) Splitting failure due to installation

Splitting failure during installation (e. g. applying a torque to the anchors according to Fig. 14.18a) is avoided by complying with minimum values for edge distance  $c_{min}$ , spacing  $s_{min}$  and

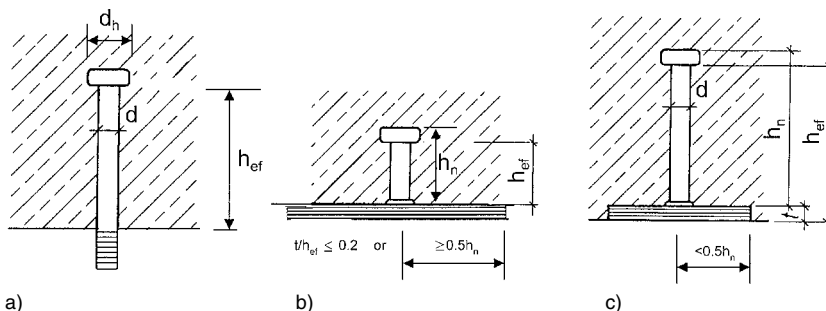


**Fig. 14.18** Definition of effective embedment depth  $h_{ef}$  for headed fasteners  
a) without anchor plate, b) with a large anchor plate, c) with a small anchor plate

member thickness  $h_{min}$  and requirements for reinforcement as given in the relevant ETA or CEN-Product Standard.

Minimum values for edge distance, spacing and member thickness should also be observed for headed anchors not torqued to allow adequate placing and compaction of the concrete

### e) Splitting failure due to loading

No verification of splitting failure due to load is required if one of the following conditions is fulfilled:

- The edge distance in all directions is  $c \geq 1.0 c_{cr,sp}$  for single fasteners or  $c \geq 1.2 c_{cr,sp}$  for groups of fasteners. The characteristic value  $c_{cr,sp}$  is given in the relevant ETA or CEN-Product Standard.
- The characteristic resistance for concrete cone failure and pull-out failure is calculated for cracked concrete and reinforcement is present that takes up the splitting forces and limits the crack width to  $w_k \leq 0.3$  mm.

The required cross-section  $A_s$  of the splitting reinforcement may be determined as follows:

$$A_s = 0.5 \cdot \frac{\sum N_{Ed}}{f_{yk} / \gamma_{Ms,rc}} \quad [\text{mm}^2] \quad (14.32)$$

where:

$N_{Ed}$  = sum of the design tensile forces of the fasteners in tension under the design value of the actions

$f_{yk}$  = characteristic yield strength of the reinforcement ( $f_{yk} \leq 500$  N/mm<sup>2</sup>)

If the two conditions given above are not fulfilled, then the characteristic resistance in case of splitting failure due to load,  $N_{Rk,sp}$ , should be calculated in accordance with section 14.3.5.1d, however, the factor  $\psi_{h,sp}$  which allows for the influence of the actual member thickness  $h$  on the splitting failure load should be calculated according to equation (14.33):

$$\psi_{h,sp} = \left( \frac{h}{h_{min}} \right)^{2/3} \leq \left( \frac{2 \cdot h_{ef}}{h_{min}} \right)^{2/3} \quad (14.33)$$

The characteristic spacing  $s_{cr,sp}$  and  $c_{cr,sp}$  should be taken from the relevant ETA or CEN Product Standard.

If the edge distance is smaller than the value  $c_{cr,sp}$  then a longitudinal reinforcement should be provided along the edge of the member.

### e) Blow-out failure

Verification of blow-out failure is not required if the edge distance in all directions exceeds  $c = 0.5 \cdot h_{ef}$ . The characteristic resistance is:

$$N_{Rk,cb} = N_{Rk,cb}^0 \cdot \frac{A_{c,Nb}}{A_{c,Nb}^0} \cdot \psi_{s,Nb} \cdot \psi_{g,Nb} \cdot \psi_{ec,Nb} \cdot \psi_{ucr,N} \quad (14.34)$$

For groups of fasteners perpendicular to the edge, which are loaded uniformly, verification of blow-out is only required for the fastener closest to the edge.

The different factors of equation (14.34) are given below:

The characteristic resistance of a single anchor,  $N_{Rk,cb}^0$ , not influenced by adjacent fasteners or free component edges placed in cracked concrete is obtained by:

$$N_{Rk,cb}^0 = 8 \cdot c_1 \cdot \sqrt{A_h} \cdot \sqrt{f_{ck,cube}} \quad [\text{N}] \quad (14.34a)$$

where:

$$\begin{aligned} f_{ck,cube} & \text{ in } [\text{N/mm}^2] \\ A_h & \text{ [mm}^2\text{] compare equation (14.30a)} \\ c_1 & \text{ [mm]} \end{aligned}$$

Equation (14.34a) is based on equation (4.14a) assuming a ratio  $N_{u,5\%} / N_{u,m} = 0.75$  and  $N_u(\text{cracked}) / N_u(\text{non-cracked}) = 0.7$ .

The geometric effect of axial spacing and edge distances on the characteristic resistance is taken into account by the value  $A_{c,Nb} / A_{c,Nb}^0$ , where:

$$A_{c,Nb}^0 = \text{reference projected area, see Fig. 4.49a} \\ = (4 \cdot c_1)^2$$

$A_{c,Nb}$  = actual area, limited by overlapping concrete break-out bodies of adjacent fasteners ( $s \leq 4 \cdot c_1$ ) as well as by edges of the concrete member ( $c \leq 2 \cdot c_1$ ) or the member depth  $h$ . Examples are shown in Fig. 4.49

The factor  $\psi_{s,Nb}$  takes account of the disturbance of the distribution of stresses in the concrete due to a corner of the concrete member. For fastenings with more than one edge distance (e. g. fastening in a corner or a narrow compo-

ment), the smallest distance  $c_2$  shall be inserted in equation (14.34b).

$$\psi_{s,Nb} = 0.7 + 0.3 \cdot \frac{c_2}{2 \cdot c_1} \leq 1 \quad (14.34b)$$

The factor  $\psi_{g,Nb}$  takes account of the bearing areas of the individual fasteners of a group.

$$\psi_{g,Nb} = \sqrt{n} + (1 - \sqrt{n}) \cdot \frac{s_1}{4 \cdot c_1} \geq 1 \quad \text{with } s_1 \leq 4 \cdot c_1 \quad (14.34c)$$

where:

$n$  = number of tensioned fasteners in a row parallel to the edge

The factor  $\psi_{ec,Nb}$  takes account of group effect, when different loads are acting on the individual fastener of the group.

$$\psi_{ec,Nb} = \frac{1}{1 + 2 \cdot e_N / (4 \cdot c_1)} \leq 1 \quad (14.34d)$$

$e_N$  = eccentricity of the resulting tensile load acting on the tensioned fasteners in respect to the centre of gravity of the tensioned fasteners

The factor  $\psi_{ucr,N}$  takes account of the position of the fastening in cracked or non-cracked concrete.

$$\psi_{ucr,N} = 1.0 \text{ for fasteners in cracked concrete} \quad (14.34e)$$

$$\psi_{ucr,N} = 1.4 \text{ for fasteners in non-cracked concrete} \quad (14.34f)$$

### f) Steel failure of the supplementary reinforcement

The characteristic resistance of the supplementary reinforcement,  $N_{Rk,re}$ , of one fastener is:

$$N_{Rk,re} = n \cdot A_s \cdot f_{yk} \quad (14.35)$$

where:

$n$  = number of legs of the supplementary reinforcement effective for one fastener

$A_s$  = cross-section of one leg of the supplementary reinforcement

$f_{yk}$  = nominal yield strength of the supplementary reinforcement  
 $\leq 500 \text{ N/mm}^2$

### g) Anchorage failure of the supplementary reinforcement in the concrete cone

The design resistance,  $N_{Rd,a}$ , of the supplementary reinforcement of one fastener should be calculated according to equation (14.36):

$$N_{Rd,a} = \sum_n \frac{l_1 \cdot \pi \cdot d_s \cdot f_{bd}}{\alpha} \quad (14.36)$$

where:

$n$  = number of legs of the supplementary reinforcement effective for one fastener (distance to fastener  $\leq 0.75 \cdot h_{ef}$ )

$l_1$  = anchorage length of the supplementary reinforcement in the assumed failure cone (see Fig. 14.17)  $\geq l_{b,min}$

$l_{b,min}$  = minimum anchorage length  
 $= 4 \cdot d_s$  (anchorage with hooked bars, loops or stirrups)

$d_s$  = diameter of supplementary reinforcement

$f_{bd}$  = design bond strength according to *Eurocode 2* (2003) taking into account the concrete cover of the supplementary reinforcement

$\alpha$  = influencing factor according to *Eurocode 2* (2003)  
 $= 0.7$  for hooked bars, loops or stirrups

#### 14.4.6.2.2 Shear loads

The required verifications for shear loads are shown in Table 14.6. For fasteners without supplementary reinforcement lines 1 to 4 apply. For fasteners with reinforcement lines 1,2 and 4 to 6 apply.

Where the design load in the fasteners exceeds the design resistance for concrete edge failure supplementary reinforcement should be provided to resist the total design load. The supplementary reinforcement may be in the form of a surface reinforcement (Fig. 14.19) or in the shape of stirrups or loops (Fig. 4.95).

The supplementary reinforcement shall be anchored outside the assumed failure cone with an anchorage length  $l_{b,net}$  according to *Eurocode 2* (2003).

The same diameter of reinforcement should be provided for all fasteners of the group. It should consist of ribbed bars with  $f_{yk} \leq 500 \text{ N/mm}^2$  and a diameter not larger than 16 mm. The bending diameter should comply with *Eurocode 2* (2003).

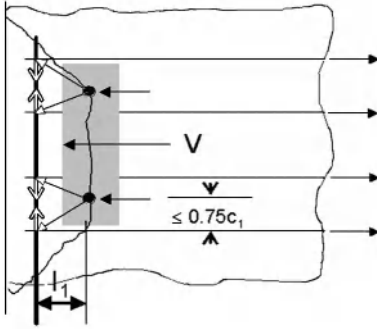


**Fig. 14.19** Surface reinforcement to take up shear forces with simplified strut and tie model to design edge reinforcement

If the shear force is taken up by a surface reinforcement according to Fig. 14.19, the following additional requirements should be met:

- Only bars with a distance  $\leq 0.75 \cdot c_1$  from the fastener should be assumed as effective.
- The minimum anchorage length in the concrete break-out body is  
 $\min l_1 = 10 \cdot d_s$  for straight bars with or without welded transverse bars,  
 $= 4 \cdot d_s$  for bars with a hook or bend.

- A reinforcement along the edge of the concrete member should be provided and be designed for the forces according to an appropriate strut-and-tie model (see Fig. 14.19).

If the shear forces are taken up by a supplementary reinforcement according to Fig. 4.95 it should enclose and contact the shaft of the fastener and should be positioned as closely as possible to the fixture.

**a) Steel failure of fastener**

**a<sub>1</sub>) Shear load without lever arm**

For headed fasteners welded or not welded to a fixture the characteristic resistance of a fastener in case of steel failure,  $V_{Rk,s}$ , is given in the relevant ETA or CEN Product Standard. For fasteners not welded to the fixture the characteristic resistance is calculated according to equation (14.13). For fasteners welded to the fixture the factor 0.5 in equation (14.13) is increased to 0.6. In case of groups with a hole clearance  $d_f < d_{f1}$  according to Table 14.4 and made of non-ductile steel, this characteristic shear resistance should be multiplied with the factor  $k_2$  which is given in the relevant ETA or CEN Product Standard. According to current experience the factor  $k_2$  for non-ductile steel is  $k_2 = 0.8$ .

**Table 14.6** Required verifications for headed fasteners loaded in shear

		Single fastener	Fastener group	
			Most loaded fastener	Fastener group
1	Steel failure of fastener without lever arm	$V_{Ed} \leq V_{Rd,s} = \frac{V_{Rk,s}}{\gamma_{Ms}}$	$V_{Ed}^h \leq V_{Rd,s} = \frac{V_{Rk,s}}{\gamma_{Ms}}$	
2	Steel failure of fastener with lever arm	$V_{Ed} \leq V_{Rd,s} = \frac{V_{Rk,s}}{\gamma_{Ms}}$	$V_{Ed}^h \leq V_{Rd,s} = \frac{V_{Rk,s}}{\gamma_{Ms}}$	
3	Concrete edge failure	$V_{Ed} \leq V_{Rd,c} = \frac{V_{Rk,c}}{\gamma_{Mc}}$		$V_{Ed}^g \leq V_{Rd,c} = \frac{V_{Rk,c}}{\gamma_{Mc}}$
4	Concrete pry-out failure	$V_{Ed} \leq V_{Rd,cp} = \frac{V_{Rk,cp}}{\gamma_{Mc}}$		$V_{Ed}^g \leq V_{Rd,cp} = \frac{V_{Rk,cp}}{\gamma_{Mc}}$
5	Steel failure of supplementary reinforcement	$N_{Ed,re} \leq N_{Rd,re} = \frac{N_{Rk,re}}{\gamma_{Ms,re}}$	$N_{Ed,re}^h \leq N_{Rd,re} = \frac{N_{Rk,re}}{\gamma_{Ms,re}}$	
6	Anchorage failure of supplementary reinforcement	$N_{Ed,re} \leq N_{Rd,a}$	$N_{Ed,re}^h \leq N_{Rd,a}$	

**a<sub>2</sub>) Shear load with lever arm**

For the characteristic resistance in the case of shear load with lever arm section 14.3.5.2b applies.

**b) Concrete pry-out failure**

Fastenings may fail due to a concrete pry-out failure at the side opposite to load direction. The corresponding characteristic resistance,  $V_{Rk,cp}$ , may be calculated from equation (14.37):

$$V_{Rk,cp} = k_3 \cdot N_{Rk,c} \tag{14.37}$$

where:

$k_3$ : factor to be taken from the relevant ETA or CEN Product Standard, valid for

applications without supplementary reinforcement. Generally  $k_3 = 1.0$  for fasteners with  $h_{ef} < 60$  mm and  $k_3 = 2.0$  for fasteners with  $h_{ef} \geq 60$  mm. In case of supplementary reinforcement the factor  $k_3$  should be multiplied by 0.75,

$N_{Rk,c}$ : according to section 14.4.6.2.1c determined for the fasteners loaded in shear.

Equation (14.37) agrees with equation (14.15) for post-installed fasteners.

**c) Concrete edge failure**

This section covers different configurations of shear forces and torsion moments acting on fastenings. They are shown in Fig. 14.20.

Applied load	Figure
Shear perpendicular to the edge	
Shear parallel to the edge	
Inclined shear	
Torsion	
Combined torsion and shear	

**Fig. 14.20** Examples for configurations of fastenings in shear and torsion

**c<sub>1</sub>) Shear without torsion**

The characteristic resistance of a fastener or a fastener group loaded in shear *perpendicular* to the edge corresponds to:

$$V_{Rk,c\perp} = V_{Rk,c\perp}^0 \cdot \frac{A_{c,V}}{A_{c,V}^0} \cdot \psi_{s,V} \cdot \psi_{h,V} \cdot \psi_{f,V} \cdot \psi_{ucr,V} \tag{14.38}$$

Unlike *European Organisation for Technical Approvals (EOTA) (1997)*, Annex C (see equation (14.16)), equation (14.38) is only valid for shear without torsion. The influence of an eccentricity of the shear force on the concrete edge resistance is separately accounted for in section c<sub>4</sub> (shear with torsion).

The different factors in equation (14.38) are explained below:

The initial value of the characteristic resistance of a fastener loaded perpendicular to the edge in cracked concrete corresponds to:

$$V_{Rk,c\perp}^0 = 1.6 \cdot d_{nom}^\alpha \cdot l_f^\beta \cdot \sqrt{f_{ck,cube}} \cdot c_1^{1.5} \tag{14.38a}$$

where:

$$\alpha = 0.1 \cdot \left( \frac{l_f}{c_1} \right)^{0.5} \tag{14.38b}$$

$$\beta = 0.1 \cdot \left( \frac{d_{nom}}{c_1} \right)^{0.2} \tag{14.38c}$$

c<sub>1</sub> = edge distance in the direction of the shear load

d<sub>nom</sub>, l<sub>f</sub>, c<sub>1</sub> in [mm]; d<sub>nom</sub> ≤ 60 mm; l<sub>f</sub> ≤ 16 · d<sub>nom</sub>; f<sub>ck,cube</sub> in [N/mm<sup>2</sup>]

Equation (14.38a) is based on equation (4.26) assuming V<sub>u,5%</sub> / V<sub>u,m</sub> = 0.75 and V<sub>u</sub>(cracked) / V<sub>u</sub>(non-cracked) = 0.7

The values d<sub>nom</sub> and l<sub>f</sub> are given in the relevant ETA or CEN Product Standard. In case of a constant diameter over the length of the shank of the headed fastener d<sub>nom</sub> = d and l<sub>f</sub> = h<sub>ef</sub> are taken.

The geometrical effect of spacing and further edge distances and the effect of thickness of the concrete member on the characteristic resistance is taken into account by the ratio A<sub>c,V</sub> / A<sub>c,V</sub><sup>0</sup> which should be calculated in accordance with section 14.3.5.2d.

The factor ψ<sub>s,V</sub> takes into account the disturbance of the distribution of stresses in the concrete due to further edges. It should be calculated in accordance with section 14.3.5.2d, equation (14.16b).

The factor ψ<sub>h,V</sub> takes account of the fact that the shear resistance does not decrease proportionally to the member thickness. It should be calculated according to equation (14.38d).

$$\psi_{h,V} = \left( \frac{1.5 \cdot c_1}{h} \right)^{0.5} \geq 1 \tag{14.38d}$$

According to *Eligehausen, Fuchs, Hofmann (2004)* the approach given in Annex C of ETAG 001 to take account of the influence of the member thickness on the concrete edge failure mode (compare equation (14.16c)) is conservative. Therefore in equation (14.38d) the power on the ratio (1.5 · c<sub>1</sub> / h) has been increased to 0.5.

The load distribution factor ψ<sub>f,V</sub> takes into account the influence of spacing s<sub>1</sub> and hole clearance in the fixture on the characteristic resistance of groups.

ψ<sub>f,V</sub> = 1.0 for fastenings with a hole clearance in the fixture

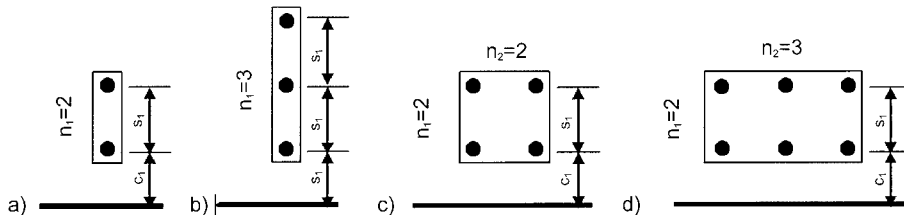


**Fig. 14.21** Definition of the number of anchors   
 a) Group of two fasteners perpendicular to the edge, b) Group of three fasteners perpendicular to the edge,   
 c) Group of four fasteners, d) Group of six fasteners parallel to the edge



$$\psi_{f,V} = 1 + (n_1 - 1) \cdot s_1 / (0.75 \cdot c_1) \leq n_1$$

(without hole clearance) (14.38e)

$n_1$  = number of anchors in a row orthogonal to the edge (Fig. 14.21)

Where there are a number  $n_1$  of fasteners in a row perpendicular to the edge (see Fig. 14.21), the resistance of a group is assumed to be a multiple ( $\psi_{f,V}$ ) of the resistance of the front fasteners. The following assumptions on the distribution of the shear loads have been made:

- For a group of fasteners with hole clearance loaded perpendicular to the edge only the front fasteners are assumed to carry shear loads.
- For a group of fasteners without hole clearance loaded perpendicular to the edge all fasteners are assumed to share the shear loads equally. Therefore the resistance of the group is  $n_1$ -times the calculated concrete edge resistance of the front row ( $\psi_{f,V} = n_1$ ). However, for a spacing  $s_1 < 0.75 \cdot c_1$  the front and back fasteners influence each other unfavourably. This is taken into account by a factor  $\psi_{f,V} \leq n_1$ .

The factor  $\psi_{ucr,V}$  takes into account the influence of the position of the fastening in cracked or non-cracked concrete or the type of reinforcement present on the edge:

$\psi_{ucr,V} = 1.0$  fastening in cracked concrete without edge reinforcement or stirrups

$\psi_{ucr,V} = 1.2$  fastening in cracked concrete with straight edge reinforcement ( $d_s \geq 12$  mm)

$\psi_{ucr,V} = 1.4$  fastening in cracked concrete with edge reinforcement and closely spaced stirrups (bar spacing  $a \leq 100$  mm and  $a \leq 2 \cdot c_1$  and fastening in non-cracked concrete

For fastenings in a narrow, thin member with  $c_{2,max} < 1.5c_1$  ( $c_{2,max}$  = larger of the two edge distances parallel to the loading direction) and  $h < 1.5c_1$  (example see Fig. 4.91) equation (14.38) leads to results which are conservative. More precise results are achieved in accordance with section 14.3.5.2d. However, for groups the value should be taken as the larger value of

$$c'_1 = \frac{c_{2,max}}{1.5}, \quad c'_1 = \frac{h}{1.5} \quad \text{and} \quad c'_1 = \frac{s_{max}}{3} \quad (14.39)$$

where:

$c_{2,max}$  = largest of the two edge distances parallel to the direction of loading

$$< 1.5 \cdot c_1$$

$h$  = member thickness

$s_{max}$  = maximum centre to centre spacing a anchors

$$< 3 \cdot c_1$$

The reasoning for these provisions is given in section 4.1.2.4f.

The characteristic resistance for a fastener or a group of fasteners loaded *parallel* to the edge is:

$$V_{Rk,c||} = V_{Rk,c\perp} \cdot \psi_{90^\circ} \cdot \psi_{I,V} \quad (14.40)$$

where:

$V_{Rk,c\perp}$  according to equation (14.38)

$$\psi_{90^\circ} = 4 \cdot k_4 \cdot \left[ \frac{n \cdot d_{nom}^2 \cdot f_{ck,cube}}{V_{Rk,c\perp}} \right]^{0.5} \leq 5.0 \quad (14.40a)$$

$k_4 = 1.0$  fastenings without hole clearance

= 0.75 fastenings with hole clearance

$n$  = number of fasteners in a group

=  $n_1 \cdot n_2$  (compare Fig. 14.21)

$\psi_{I,V} = 1.0$  fastenings without hole clearance

=  $1 + (n_1 - 1) \cdot s_1 / (0.75 \cdot c_1) \leq n_1$   
fastening with hole clearance (14.40b)

Where fasteners are loaded in shear parallel to the edge the concrete edge failure is initiated by splitting forces perpendicular to the edge (compare section 4.1.2.5). They are a fraction of the applied shear load. This fraction is equal to the factor  $1 / \psi_{90^\circ}$ . Therefore the characteristic resistance of a fastener loaded in shear parallel to the edge is taken as  $\psi_{90^\circ}$ -times the resistance  $V_{Rk,c\perp}$ .

With a row of anchors arranged and loaded parallel to the edge it is assumed that the shear load is distributed uniformly to all fasteners of the group. However, in the case of fasteners with hole clearance in the fixture arranged parallel to the edge this assumption is non-conservative. This is accounted for by the factor  $k_4 = 0.75$  in equation (14.40a).

Where there are a number  $n_1$  of anchors in a row perpendicular to the edge (see Fig. 14.21) loaded parallel to the edge it is also assumed that the shear load is distributed uniformly to all fasteners of the group and that failure is initiated by the front anchors. With fasteners without hole clearance the influence of the back anchors on the resistance is already taken into account in the calculation of  $V_{Rk,c\perp}$  by using the factor  $\psi_{f,V} > 1$ . Therefore the factor  $\psi_{i,V}$  in equation (14.40) is taken as 1. However, in case of fastenings with hole clearance when calculating the resistance  $V_{Rk,c\perp}$  it is assumed that only the fasteners closest to the edge carry shear loads ( $\psi_{f,V} = 1$ ). Consequently the resistance  $V_{Rk,c\perp}$  according to equation (14.38) is increased by the factor  $\psi_{i,V} > 1$  to meet the resistance of a group loaded parallel to the edge.

**c<sub>2</sub>) Torsion without shear**

The characteristic torsion resistance of a row of fasteners located perpendicular to the edge (see Fig. 14.22) is:

$$T_{Rk,c} = (n_1 - 1) \cdot s_1 \cdot V_{Rk,c\parallel}^0 / n_1 \tag{14.41}$$

where:

- $V_{Rk,c\parallel}^0 = V_{Rk,c\perp}^0 \cdot \Psi_{90^\circ}$
- $V_{Rk,c\perp}^0$  according to equation (14.38a)
- $\Psi_{90^\circ}$  according to equation (14.40a)
- $s_1$  spacing orthogonal to the edge
- $n_1$  number of anchors (see Fig. 14.22)

A torsion moment causes shear forces parallel to the edge as shown in Fig. 14.22. Failure is due to the shear force on the anchor closest to the edge. The failure load is not influenced by the shear load on the back anchor. Therefore the characteristic torsion moment is equal to the characteristic concrete resistance of the front anchor multiplied by the distance to the back anchor. However, the resistance  $V_{Rk,c\parallel}$  is calculated for the group under the assumption that all anchors are loaded to the same extent and in the same direction. Therefore the shear load on the front anchor at failure is equal to  $V_{Rk,c\parallel} / n_1$ .

The characteristic resistance of a row of fasteners located parallel to the edge (Fig. 14.23) is:

$$T_{Rk,c} = (n_2 - 1) \cdot s_2 \cdot V_{Rk,c\perp}^0 \tag{14.42}$$

where:

- $V_{Rk,c\perp}^0$  according to equation (14.38a)
- $s_2$  spacing parallel to the edge
- $n_2$  see Fig. 14.23

With a row parallel to the edge the failure is caused by the anchor loaded in shear towards the edge and the failure load is not influenced by the anchor loaded away from the edge (Mallée (2002), Hofmann (2004)). Therefore the characteristic torsion moment is equal to the characteristic concrete resistance  $V_{Rk,c\perp}^0$  multiplied by the distance between the outer anchors.

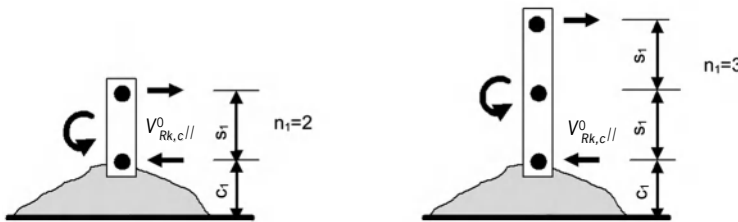


**Fig. 14.22** Examples for fastenings located perpendicular to the edge under torsion moment

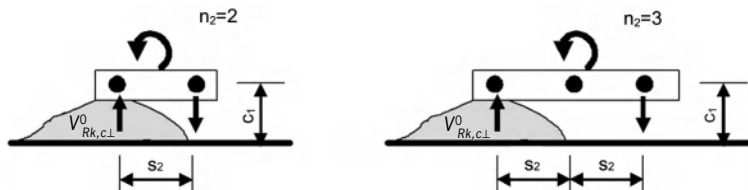


**Fig. 14.23** Examples for fastenings located parallel to the edge under torsion moment

For fastenings with four fasteners located perpendicular *and* parallel to the edge ( $n_1 = n_2 = 2$ ), the characteristic torsion resistance is:

$$T_{Rk,c} = \frac{(s_1 + s_2)^2 \cdot V_{Rk,c\perp}^0 \cdot (V_{Rk,c\parallel} / n_1)}{\sqrt{s_2^2 \cdot (V_{Rk,c\parallel} / n_1)^2 + s_1^2 \cdot (V_{Rk,c\perp}^0)^2}} \quad (14.43)$$

where:

- $V_{Rk,c\perp}^0$  according to equation (14.38a)
- $V_{Rk,c\parallel}$  according to equation (14.40)
- $s_1$  spacing orthogonal to the edge
- $s_2$  spacing parallel to the edge
- $n_1$  number of fasteners according to Fig. 14.21

For fastenings with more than one edge, the resistance for all edges shall be calculated and the smallest value is decisive for the resistance  $T_{Rk,c}$ .

### c<sub>3</sub>) Shear acting under an arbitrary angle in respect to the edge without torsion

For fastening without torsion moment the characteristic resistance is determined by solving equation (14.44).

$$\left( \frac{V_{Rk,c} \cdot \cos \alpha}{V_{Rk,1}} \right)^2 + \left( \frac{V_{Rk,c} \cdot \sin \alpha}{V_{Rk,2}} \right)^2 = 1 \quad (14.44)$$

The determination of the parameters  $V_{Rk,1}$  and  $V_{Rk,2}$  and the definition of the angle  $\alpha$  are shown in Table 14.7 for fastenings located close to an edge and in Table 14.8 for fastenings in a corner.

In equation (14.44) it is assumed that the shear force  $V_s$  acting on the fixture is equal to the characteristic resistance  $V_{Rk,c}$ . Furthermore it assumes a quadratic interaction between the portion of the shear forces acting perpendicular and parallel to the edge. In contrast to that in equations (14.16d) and (14.16e) a conservative linear interaction is assumed. Independent of the direction of the shear force the concrete capacity is limited by the concrete pry-out resistance. This is taken into account in Tables 14.7 and 14.8. In contrast to that ETAG 001, Annex C assumes that the concrete resistance for a shear load acting away from the edge is equal to the minimum of twice the resistance when the shear load acts perpendicular to the edge (equa-

tion (14.16f)) and the pry-out resistance. The approach in ETAG 001, Annex C is conservative.

### c<sub>4</sub>) Shear acting under an arbitrary angle in respect to the edge with torsion

For fastening with torsion moment the characteristic resistance is determined by solving equation (14.45).

$$\left( \frac{V_{Rk,c} \cdot \cos \alpha}{V_{Rk,1}} \right)^2 + \left( \frac{V_{Rk,c} \cdot \sin \alpha}{V_{Rk,2}} \right)^2 = \left( 1 - \frac{V_{Rk,c} \cdot e_V}{T_{Rk,c}} \right) \quad (14.45)$$

where:

- $V_{Rk,1}, V_{Rk,2}$  according to Table 14.7 or 14.8
- $T_{Rk,c}$  according to equations (14.41) to (14.43)
- $e_V$  eccentricity of the applied load  $V_{sd}$  (Fig. 14.24)

Equation (14.45) assumes a quadratic interaction between the shear forces perpendicular and parallel to the edge and a linear interaction between the resistances valid for a concentric shear force and a torsion moment.

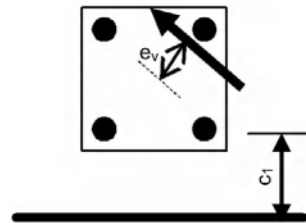


Fig. 14.24 Example for a fastening close to an edge under shear and torsion

### d) Steel failure of supplementary reinforcement

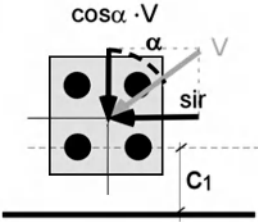
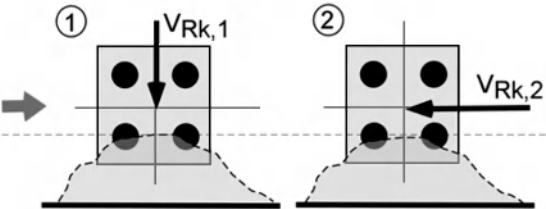
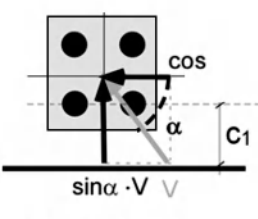
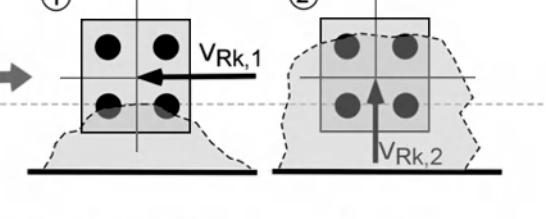
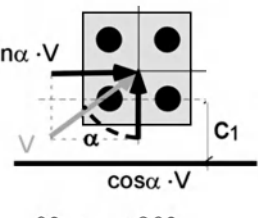
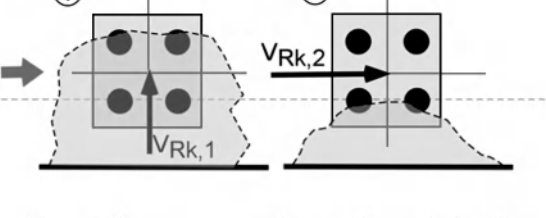
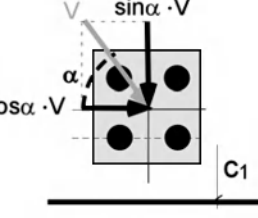
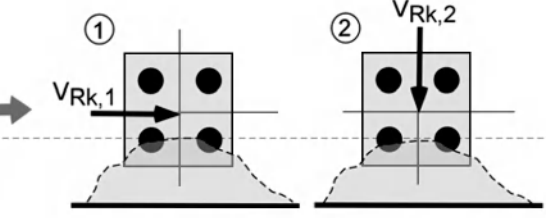
The characteristic resistance of one fastener in case of steel failure of the supplementary reinforcement may be calculated according to equation (14.46):

$$N_{Rk,re} = k_6 \cdot n \cdot A_s \cdot f_{yk} \quad (14.46)$$

where:

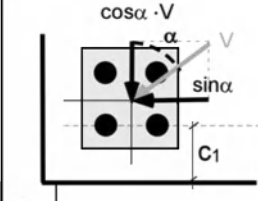
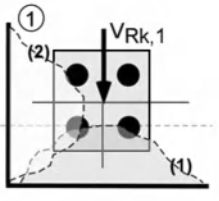
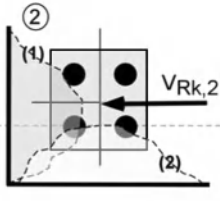
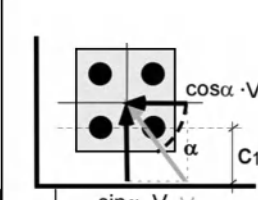
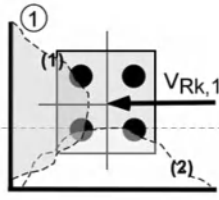
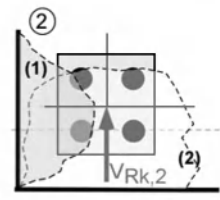
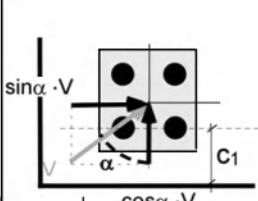
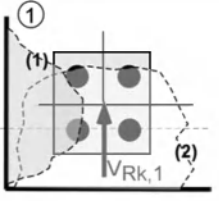
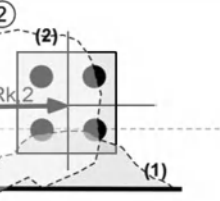
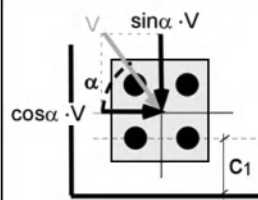
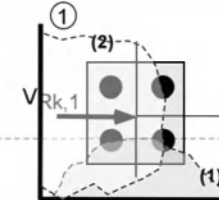
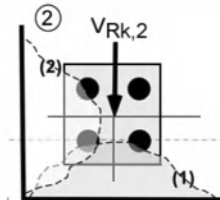
- $k_6$  = efficiency factor
- = 0.5 supplementary reinforcement in form of loops (see Fig. 4.95)

**Table 14.7** Determination of  $V_{Rk,1}$  and  $V_{Rk,2}$  for fastenings located close to an edge

Applied load	Definition of $V_{Rk,1}$ and $V_{Rk,2}$
 <p><math>\cos\alpha \cdot V</math> <math>\alpha</math> sir <math>C_1</math></p> <p><math>0^\circ \leq \alpha \leq 90^\circ</math></p>	 <p>① <math>V_{Rk,1}</math>      ② <math>V_{Rk,2}</math></p> <p><math>V_{Rk,1} = V_{Rk,c\perp}(c_1) \leq V_{Rk,cp}</math>    <math>V_{Rk,2} = V_{Rk,c\parallel}(c_1) \leq V_{Rk,cp}</math></p>
 <p><math>\cos</math> <math>\alpha</math> <math>C_1</math> <math>\sin\alpha \cdot V</math></p> <p><math>0^\circ \leq \alpha \leq 90^\circ</math></p>	 <p>① <math>V_{Rk,1}</math>      ② <math>V_{Rk,2}</math></p> <p><math>V_{Rk,1} = V_{Rk,c\parallel}(c_1) \leq V_{Rk,cp}</math>    <math>V_{Rk,2} = V_{Rk,cp}</math></p>
 <p><math>\sin\alpha \cdot V</math> <math>\alpha</math> <math>C_1</math> <math>\cos\alpha \cdot V</math></p> <p><math>0^\circ \leq \alpha \leq 90^\circ</math></p>	 <p>① <math>V_{Rk,1}</math>      ② <math>V_{Rk,2}</math></p> <p><math>V_{Rk,1} = V_{Rk,cp}</math>    <math>V_{Rk,2} = V_{Rk,c\parallel}(c_1) \leq V_{Rk,cp}</math></p>
 <p><math>\sin\alpha \cdot V</math> <math>\alpha</math> <math>C_1</math> <math>\cos\alpha \cdot V</math></p> <p><math>0^\circ \leq \alpha \leq 90^\circ</math></p>	 <p>① <math>V_{Rk,1}</math>      ② <math>V_{Rk,2}</math></p> <p><math>V_{Rk,1} = V_{Rk,c\parallel}(c_1) \leq V_{Rk,cp}</math>    <math>V_{Rk,2} = V_{Rk,c\perp}(c_1) \leq V_{Rk,cp}</math></p>

$V_{Rk,cp}$  according to equation (14.37);  $V_{Rk,c\perp}$  according to equation (14.38);  $V_{Rk,c\parallel}$  according to equation (14.40)

**Table 14.8** Determination of  $V_{Rk,1}$  and  $V_{Rk,2}$  for fastenings located in a corner

Applied load	Definition of $V_{Rk,1}$ and $V_{Rk,2}$	
	 $V_{Rk,1} = \min \begin{cases} V_{Rk,c\perp}(c_1) \\ V_{Rk,c\parallel}(c_2) \end{cases} \leq V_{Rk,cp}$	 $V_{Rk,2} = \min \begin{cases} V_{Rk,c\perp}(c_2) \\ V_{Rk,c\parallel}(c_1) \end{cases} \leq V_{Rk,cp}$
	 $V_{Rk,1} = \min \begin{cases} V_{Rk,c\perp}(c_2) \\ V_{Rk,c\parallel}(c_1) \end{cases} \leq V_{Rk,cp}$	 $V_{Rk,2} = V_{Rk,c\parallel}(c_2) \leq V_{Rk,cp}$
	 $V_{Rk,1} = V_{Rk,c\parallel}(c_2) \leq V_{Rk,cp}$	 $V_{Rk,2} = V_{Rk,c\parallel}(c_1) \leq V_{Rk,cp}$
	 $V_{Rk,1} = V_{Rk,c\parallel}(c_1) \leq V_{Rk,cp}$	 $V_{Rk,2} = \min \begin{cases} V_{Rk,c\perp}(c_1) \\ V_{Rk,c\parallel}(c_2) \end{cases} \leq V_{Rk,cp}$

$V_{Rk,cp}$  according to equation (14.37);  $V_{Rk,c\perp}$  according to equation (14.38);  $V_{Rk,c\parallel}$  according to equation (14.40)

- = 1.0 surface reinforcement according to Fig. 14.19
- $n$  = number of bars of the supplementary reinforcement of one anchor
- $A_s$  = cross-section of one bar of the supplementary reinforcement
- $f_{yk}$  = nominal yield strength of the supplementary reinforcement  
 $\leq 500 \text{ N/mm}^2$

The factor  $k_6 = 0.5$  for a supplementary reinforcement in form of loops (see Fig. 4.95) takes account of unavoidable tolerances in workmanship for the placing of the loops in respect to the anchor.

**e) Anchorage failure of supplementary reinforcement in the concrete breakout body**

For applications according to Fig. 4.95 no verification of the anchorage capacity is necessary because the efficiency of the loop is taken into account by the factor  $k_6 = 0.5$ . For applications according to Fig. 14.19 the design resistance  $N_{Rd,a}$  of the reinforcement of one fastener in case of anchorage failure is given by equation (14.47).

$$N_{Rd,a} = \sum_n \frac{l_1 \cdot \pi \cdot d_s \cdot f_{bd}}{\alpha} \quad (14.47)$$

where:

- $l_1$  = anchorage length of the supplementary reinforcement in the assumed failure cone (see Fig. 14.19)
- $\geq l_{b,min.}$
- $l_{b,min}$  =  $10 \cdot d_s$  straight bars with or without welded transverse bars
- =  $4 \cdot d_s$  bars with hook or bend
- $d_s$  = diameter of the reinforcement bar
- $f_{bd}$  = design bond strength according to Eurocode 2 (2003), taking into account the concrete cover of the supplementary reinforcement
- $\alpha$  = influencing factor according to Eurocode 2 (2003)
- = 0.7 for hooked bars
- $n$  = number of legs of the supplementary reinforcement effective for one fastener

**14.4.6.2.3 Combined tension and shear loads**

**a) Fastenings without supplementary reinforcement**

If steel failure is decisive for tension *and* shear load the following equation should be satisfied:

$$\beta_N^2 + \beta_V^2 \leq 1 \quad (14.48)$$

where  $\beta_N = N_{Ed} / N_{Rd}$  and  $\beta_V = V_{Ed} / V_{Rd}$

For other modes of failure either of the following equations shall be satisfied:

$$\beta_N + \beta_V \leq 1.2 \quad (14.49a)$$

$$\beta_N^{1.5} + \beta_V^{1.5} \leq 1 \quad (14.49b)$$

In equations (14.48) and (14.49) the largest value of  $\beta_N$  and  $\beta_V$  for the different failure modes should be taken.

The different interaction equations are plotted in Fig. 14.11.

**b) Fastenings with supplementary reinforcement**

For fastenings with a supplementary reinforcement for tension *and* shear loads section 14.4.6.2.3a applies. For fastenings with a supplementary reinforcement to take up tension or shear loads *only*, equation (14.50) shall be used for the largest value of  $\beta_N$  and  $\beta_V$  for the different failure modes.

$$\beta_N^{k_7} + \beta_V^{k_7} \leq 1 \quad (14.50)$$

The value  $k_7$  is given in the ETA or CEN-Product standard. According to current experience the factor is  $k_7 = 2/3$ .

**14.4.7 Design of anchor channels**

Fig. 14.25 shows a typical cross-section of an anchor channel.

The design method given in this section is valid for tension loads and shear loads acting on the channel. However, the direction of the shear loads must be perpendicular to the longitudinal channel axis. Shear loads acting parallel to the longitudinal channel axis are not covered.

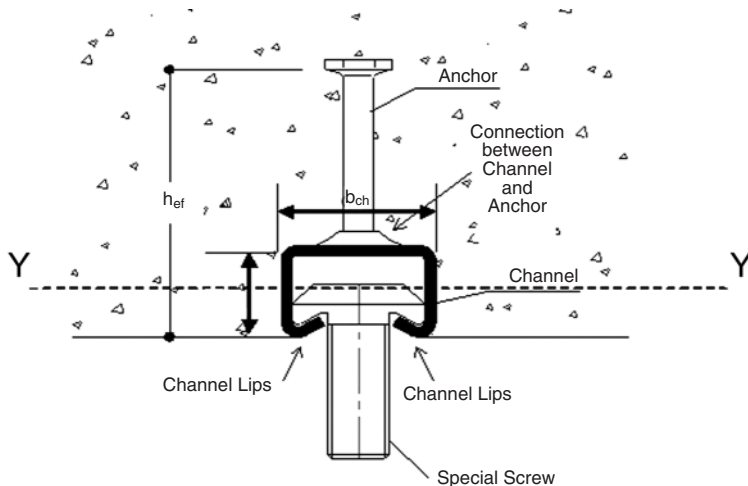


Fig. 14.25 Definitions for anchor channels

**14.4.7.1 Derivation of forces acting on the anchors of the anchor channel**

The distribution of tension loads acting on the channel to the anchors may be calculated using as static system a beam on elastic support (anchors) with a partial restraint of the channel ends. The resulting anchor forces depend significantly on the assumed anchor stiffness and degree of restraint. For shear loads the distribution is also influenced by the pressure distribution in the contact zone between channel and concrete. Therefore a simplified method (termed triangular method) is introduced in the CEN TS for calculating the anchor forces. This method is described in the following. It gives sufficiently accurate results (*Kraus (2003)*).

**14.4.7.1.1 Tension loads**

The tension forces on each anchor due to a tension load on the channel are calculated according to equation (14.51), which assumes a linear distribution over the influence length  $l_i$  and takes into account the condition of equilibrium. The influence length  $l_i$  shall be calculated according to equation (14.51b). An example for the calculation is given in Fig. 14.26.

$$N_{Sd,i}^a = k \cdot A_i' \cdot N_{Sd} \tag{14.51}$$

where:

$A_i'$  = ordinate at the position of the anchor  $i$  of a triangle with the unit height at the position of the load  $N$  and the base length  $2 \cdot l_i$

$$k = \frac{1}{\sum A_i'} \tag{14.51a}$$

$$13 \cdot I_y^{0.05} \cdot s^{0.5} \geq l_i \quad [\text{mm}] \tag{14.51b}$$

$I_y$  = moment of inertia of the channel over the axis y-y [mm<sup>4</sup>] (see Fig. 14.25)

$s$  = anchor spacing [mm]

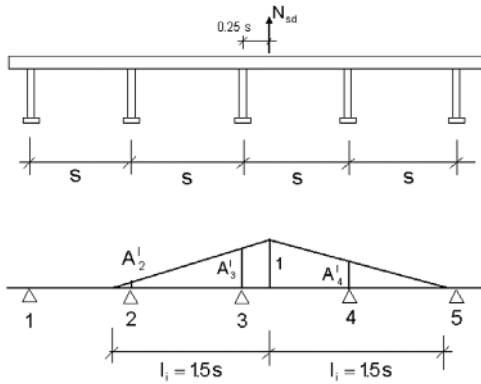
The moment of inertia  $I_y$  of the channel is given in the relevant ETA.

If several tension loads are acting on the channel a linear superimposition of the anchor forces for all loads may be assumed.

If the exact position of the tension load is not known, the most unfavourable loading position should be assumed for each failure mode (e. g. load over an anchor for the case of failure of an anchor by steel rupture or pull-out and load acting between anchors in the case of bending failure of the channel).

The bending moment on the channel due to tension loads may be calculated assuming a simply





$$\begin{aligned}
 A_2^I &= \frac{l - 1.25s}{l} = \frac{1}{6} & N_{sd,1}^a &= N_{sd,5}^a = 0 \\
 A_3^I &= \frac{l - 0.25s}{l} = \frac{5}{6} & N_{sd,2}^a &= \frac{1}{6} \cdot \frac{2}{3} \cdot N = \frac{1}{9} N_{sd} \\
 A_4^I &= \frac{l - 0.75s}{l} = \frac{1}{2} & N_{sd,3}^a &= \frac{5}{6} \cdot \frac{2}{3} \cdot N = \frac{5}{9} N_{sd} \\
 k &= \frac{1}{A_2^I + A_3^I + A_4^I} = \frac{2}{3} & N_{sd,4}^a &= \frac{1}{2} \cdot \frac{2}{3} \cdot N = \frac{1}{3} N_{sd}
 \end{aligned}$$

**Fig. 14.26** Example for the calculation of anchor forces according to triangular load distribution method for an anchor channel with 5 anchors; the influence length is assumed as  $l_i = 1.5 \cdot s$

supported beam with a span length equal to the anchor spacing.

**14.4.7.1.2 Shear loads**

The shear forces on each anchor due to a shear load acting on the channel perpendicular to its longitudinal axis may be calculated according to section 14.4.7.1.1.

A significant part of the shear load applied perpendicular to the longitudinal axis of the channel is transferred into the concrete by compression stresses in the interface between channel and concrete. In addition for reasons of equilibrium the anchors are stressed by tension forces. In the chosen approach it is assumed that shear forces are transferred by bending of the channel to the anchors and by the anchors into the concrete. This simplified approach allows an easy application of the interaction equations to account for the influence of tension and shear loads on the channel resistance.

**14.4.7.2 Tension forces in the supplementary reinforcement**

**14.4.7.2.1 Tension loads**

The design tension force  $N_{Ed,re}$  in the supplementary (hanger) reinforcement should be calculated with an appropriate strut-and-tie model using the design load on the fastener (compare Fig. 14.17).

**14.4.7.2.2 Shear loads**

The design tension force  $N_{Ed,re}$  in the supplementary reinforcement caused by the design shear force  $V_{Ed}$  acting on a fixture is given by equation (14.52).

$$N_{Ed,re} = V_{Ed} \cdot (e_s / z + 1) \tag{14.52}$$

where (see Fig. 14.27):

- $e_s$  = distance between reinforcement and shear force acting on the anchor channel
- $z$  = internal lever arm of the concrete member
- $\approx 0.85 \cdot (d - h_{ch} - 0.5 \cdot d_s)$  (14.52a)
- $d$  = member depth
- $\leq \min(2 \cdot h_{ef}; 2 \cdot c_1)$

If the supplementary reinforcement is not arranged in the direction of the shear force then this must be taken into account in the calculation of the design tension force of the reinforcement.

In the case of different shear forces on the anchors of the channel equation (14.52) should be solved for the shear load of the most loaded fastener resulting in  $N_{Ed}^h$ .

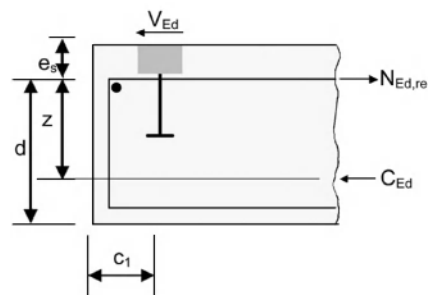


**Fig. 14.27** Surface reinforcement to take up shear forces; detailing of reinforcement

### 14.4.7.3 Verification of ultimate limit state by elastic analysis

#### 14.4.7.3.1 Tension loads

The required verifications for tension loads are shown in Table 14.9. For fasteners without supplementary reinforcement lines 1 to 9 apply. For fasteners with supplementary reinforcement lines 1 to 6 and 8 to 11 apply.

When the design relies on supplementary reinforcement, concrete cone failure according to equation 14.53 needs not to be verified but the supplementary reinforcement should be designed to resist the total load. The reinforcement should be anchored adequately on both sides of the potential failure planes.

The supplementary reinforcement to take up tension loads should comply with the following requirements (see also Fig. 14.28):

- The same diameter of reinforcement should be provided for all anchors of a channel. It should consist of ribbed bars ( $f_{yk} \leq 500 \text{ N/mm}^2$ ) with a diameter not larger than 16 mm and should be detailed in form of stirrups or loops with a bending diameter according to *Eurocode 2* (2003).
- The supplementary reinforcement should be placed as close to the anchors as practicable. Preferably, the supplementary reinforcement

should enclose the surface reinforcement. Only these reinforcement bars with a distance  $\leq 0.75 \cdot h_{ef}$  from the anchor should be assumed active.

- The minimum anchorage length of the supplementary reinforcement in the concrete failure cone is  $\min l_1 = 4 \cdot d_s$  (anchorage with bends, hooks or loops).
- The supplementary reinforcement shall be anchored outside the assumed failure cone with an anchorage length  $l_{bd}$  according to *Eurocode 2* (2003).
- A surface reinforcement should be provided as shown in Fig. 14.28 designed to resist the forces arising from the assumed strut-and-tie model, taking into account the splitting forces.

For channel bars parallel to the edge of a concrete member or in a narrow concrete component the plane of the supplementary reinforcement should be placed perpendicular to the longitudinal axis of the channel (see Fig. 14.28)).

#### a) Steel failure

The characteristic resistance  $N_{Rk,s,a}$  (failure of anchor),  $N_{Rk,s,c}$  (failure of connection between anchor and channel),  $N_{Rk,s,l}$  (local failure of channel lips),  $N_{Rk,s}$  (failure of the screw) and  $M_{Rk,s,flex}$  (bending failure of channel) are given in the relevant ETA.

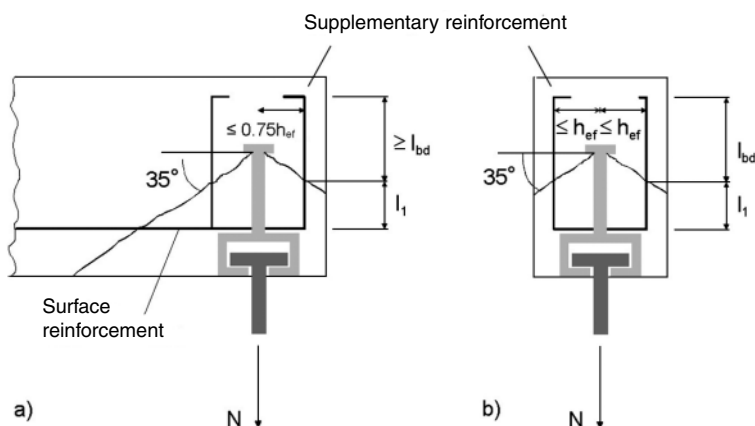


**Fig. 14.28** Arrangement of supplementary reinforcement  
a) Anchor channel located parallel to the edge of a concrete member  
b) Anchor channel in a narrow concrete member

**Table 14.9** Required verifications for channel bars loaded in tension

		Channel	Most unfavourable anchor <sup>2)</sup>
1	Steel failure	Rupture of an anchor	$N_{Ed}^a \leq N_{Rd,s,a} = \frac{N_{Rk,s,a}}{\gamma_{Ms}}$
2		Failure of the connection between anchor and channel	$N_{Ed}^a \leq N_{Rd,s,c} = \frac{N_{Rk,s,c}}{\gamma_{Ms,c}}$
3		Local flexure of channel lip	$N_{Ed} \leq N_{Rd,s,l} = \frac{N_{Rk,s,l}}{\gamma_{Ms,l}}$
4		Special screw	$N_{Ed} \leq N_{Rd,s} = \frac{N_{Rk,s}}{\gamma_{Ms}}$
5		Flexure of channel	$M_{Ed} \leq M_{Rd,s,flex} = \frac{M_{Rk,s,flex}}{\gamma_{Ms,flex}}$
6	Pull-out failure		$N_{Ed}^a \leq N_{Rd,p} = \frac{N_{Rk,p}}{\gamma_{Mp}}$
7	Concrete cone failure		$N_{Ed}^a \leq N_{Rd,c} = \frac{N_{Rk,c}}{\gamma_{Mc}}$
8	Splitting failure		$N_{Ed}^a \leq N_{Rd,sp} = \frac{N_{Rk,sp}}{\gamma_{Msp}}$
9	Blow-out failure <sup>1)</sup>		$N_{Ed}^a \leq N_{Rd,cb} = \frac{N_{Rk,cb}}{\gamma_{Mc}}$
10	Steel failure of supplementary reinforcement		$N_{Ed}^a \leq N_{Rd,re} = \frac{N_{Rk,re}}{\gamma_{Ms,re}}$
11	Anchorage failure of supplementary reinforcement		$N_{Ed}^a \leq N_{Rd,a} = \frac{N_{Rk,a}}{\gamma_{Mc}}$

<sup>1)</sup> Not required for anchors with  $c > 0.5 \cdot h_{ef}$ .

<sup>2)</sup> The load on the anchor in conjunction with the edge distance and spacing should be considered in determining the most unfavourable anchor

### b) Pull-out failure

The characteristic resistance for pull-out failure,  $N_{Rk,p}$ , is given in the relevant ETA. It is limited by the concrete pressure under the head of the fastener according to equation (14.30).

### c) Concrete cone failure

The characteristic resistance of one anchor of a channel in case of concrete cone failure may be calculated according to equation (14.53). This equation is based on the influence method

developed by Kraus (2003) which is described in detail in section 5.1.1.3.

$$N_{Rk,c} = N_{Rk,c}^0 \cdot \alpha_{s,N} \cdot \alpha_{e,N} \cdot \alpha_{c,N} \cdot \psi_{re,N} \cdot \psi_{ucr,N} \quad (14.53)$$

The different factors in equation (14.53) are explained below.

The basic characteristic resistance of one anchor not influenced by adjacent anchors, edges or corners located in cracked concrete is obtained by:

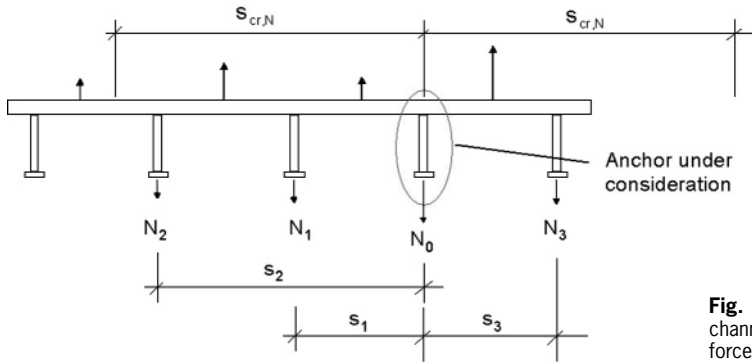


**Fig. 14.29** Example for an anchor channel with different anchor tension forces

$$N_{Rk,c}^0 = 8.5 \cdot \alpha_{ch} \cdot \sqrt{f_{ck,cube}} \cdot h_{ef}^{1.5} \quad [N] \quad (14.53a)$$

where:

$\alpha_{ch}$  = factor taking into account the influence of the channel on the concrete cone failure load. It is given in the relevant European Technical Approval  $\leq 1$

$f_{ck,cube}$  = characteristic concrete strength in [N/mm<sup>2</sup>], the minimum and maximum values to be inserted into equation (14.53a) are given in the relevant European Technical Approval

$h_{ef}$  = embedment depth of the anchor [mm] (see Fig. 14.25)

The factor  $\alpha_{ch}$  takes the unfavourable influence of the channel on the concrete cone capacity into account (see section 5.1.1.3). It may be calculated according to equation (5.2a).

The influence of neighbouring anchors on the concrete cone resistance is taken into account by the factor  $\alpha_{s,N}$ . All anchors with a distance  $\leq s_{cr,N}$  from the anchor under consideration should be included.

$$\alpha_{s,N} = \frac{1}{1 + \sum_{i=1}^n \left[ \left( 1 - \frac{s_i}{s_{cr,N}} \right)^{1.5} \cdot \frac{N_i}{N_0} \right]} \quad (14.53b)$$

where (see Fig. 14.29):

$s_i$  = distance between the anchor, for which the resistance is calculated and the neighbouring anchor  $\leq s_{cr,N}$

$$s_{cr,N} = 2 \cdot (2.8 - 1.3 \cdot h_{ef}/180) \cdot h_{ef} \geq 3 \cdot h_{ef} \quad (14.53c)$$

$N_i$  = tension force of an influencing anchor

$N_0$  = tension force of the anchor under consideration

$n$  = number of influencing anchors

The influence of an edge of a concrete member on the characteristic resistance is taken into account by the factor  $\alpha_{e,N}$  according to equation (14.53d).

$$\alpha_{e,N} = \left( \frac{c_1}{c_{cr,N}} \right)^{0.5} \leq 1 \quad (14.53d)$$

where:

$c_1$  = actual edge distance of the anchor channel (see Fig. 14.30)

$c_{cr,N}$  = characteristic edge distance  $= (2.8 - 1.3 \cdot h_{ef}/180) \cdot h_{ef} \geq 1.5 \cdot h_{ef}$  (14.53e)

With channel bars in a narrow concrete member with different edge distances  $c_{1,1}$  and  $c_{1,2}$  (see Fig. 14.30b) the minimum value of  $c_{1,1}$  and  $c_{1,2}$  shall be inserted in equation (14.53d).

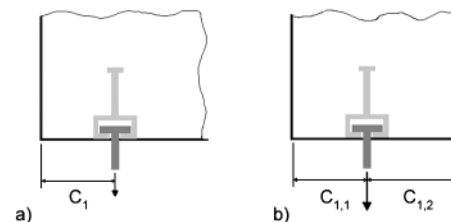


**Fig. 14.30** Anchor channel  
a) at an edge of a concrete member  
b) in a narrow concrete member

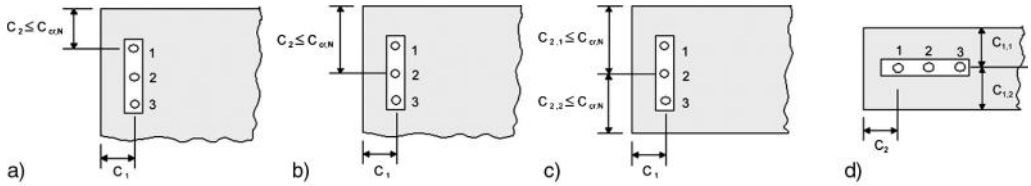


**Fig. 14.31** Definition of the corner distance of an anchor channel in the corner of a concrete member  
 a) Resistance of anchor 1 is calculated, b) Resistance of anchor 2 is calculated, c) Resistance of anchor 2 is calculated, d) Resistance of anchor 1 is calculated

The influence of a corner of the concrete member is taken into account by the factor  $\alpha_{c,N}$  according to equation (14.53f).

$$\alpha_{c,N} = \left( \frac{c_2}{c_{cr,N}} \right)^{0.5} \leq 1 \quad (14.53f)$$

where:

$c_2$  = corner distance of the anchor for which the resistance is calculated (Fig. 14.31)

If an anchor is influenced by two corners, then  $\alpha_{c,N}$  has to be calculated for the values  $c_{2,1}$  and  $c_{2,2}$  and the product of both factors  $\alpha_{c,N}$  should be inserted in equation (14.53).

The shell spalling factor  $\psi_{re,N}$  takes account of a dense reinforcement. It should be calculated according to section 14.3.5.1, equation (14.11c).

The factor  $\psi_{ucr,N}$  takes account of the position of the anchor channel in cracked or non-cracked concrete. Section 14.3.5.1, equations (14.11e<sub>1</sub>) and (14.11e<sub>2</sub>) apply.

In the special case of an anchor channel with an embedment depth  $h_{ef} > 180$  mm in an application with an edge distance  $c_{max} < c_{cr,N}$  and two corner distances with  $c_{2,max} < c_{cr,N}$  (example see Fig. 14.31c) the calculation according to equation (14.53) leads to conservative results. More precise results are obtained if the value  $h_{ef}$  is limited to the maximum of:

$$h'_{ef} = \max \left\{ \frac{c_{max}}{c_{cr,N}} \cdot h_{ef}; \frac{s_{max}}{s_{cr,N}} \cdot h_{ef} \right\} \geq 180 \quad [\text{mm}] \quad (14.53g)$$

where:

$c_{max}$  = maximum distance from centre of the anchor under consideration to any edge of the concrete member

$s_{max}$  = maximum centre to centre spacing of influencing anchors

$\leq c_{cr,N}$   
 $\leq s_{cr,N}$

This value of  $h'_{ef}$  is inserted in equation (14.53a) as well as in equations (14.53c) and (14.53e).

#### d) Splitting failure due to installation of the special screw

Splitting failure is avoided during installation of the special screw by complying with minimum values for edge distance  $c_{min}$ , spacing  $s_{min}$ , member thickness  $h_{min}$  and requirements on reinforcement as given in the relevant ETA.

#### e) Splitting failure due to loading

No verification of splitting failure due to load is required if at least one of the following conditions is fulfilled:

- The edge distance in all directions is  $c \geq 1.0 c_{cr,sp}$  for single anchors or  $c \geq 1.2 c_{cr,sp}$  for anchor channels with more than one anchor. The characteristic values of edge distance and spacing in the case of splitting due to load,  $c_{cr,sp}$  and  $s_{cr,sp}$ , are given in the relevant ETA.
- The characteristic resistance of concrete cone failure and pull-out failure is calculated for cracked concrete and reinforcement limits the crack width to  $w_k \leq 0.3$  mm.

If neither of the two conditions is fulfilled, the characteristic resistance of one anchor of a channel should be calculated according to equation (14.54).

$$N_{Rk,sp} = N_{Rk,c}^0 \cdot \alpha_{s,N} \cdot \alpha_{e,N} \cdot \alpha_{c,N} \cdot \psi_{re,N} \cdot \psi_{ucr,N} \cdot \psi_{h,sp} \quad (14.54)$$

with  $N_{Rk,c}^0$ ,  $\alpha_{s,N}$ ,  $\alpha_{e,N}$ ,  $\alpha_{c,N}$ ,  $\psi_{re,N}$ ,  $\psi_{ucr,N}$  and  $\psi_{h,sp}$  according to section 14.4.7.3.1c.

However, the values  $c_{cr,N}$  and  $s_{cr,N}$  should be replaced by  $c_{cr,sp}$  and  $s_{cr,sp}$ . The values  $c_{cr,sp}$  and  $s_{cr,sp}$  are based on the member thickness  $h_{min}$  on the splitting resistance. It may be calculated according to equation (14.33).

If the edge distance is smaller than the value  $c_{cr,sp}$  a longitudinal reinforcement should be provided along the edge of a member.

#### f) Blow-out failure

Blow-out failure may occur with anchors when the distance between the anchor and the side surface of the concrete member is  $c \leq 0.5 \cdot h_{ef}$ . The characteristic resistance is given by equation (14.55). The basis of this equation agrees with the approach for headed studs. However, equation (14.34) which gives the characteristic resistance of a group of headed studs has been re-written to yield the characteristic resistance of one anchor.

$$N_{Rk,cb} = N_{Rk,cb}^0 \cdot \alpha_{s,Nb} \cdot \psi_{g,Nb} \cdot \alpha_{c,Nb} \cdot \alpha_{h,Nb} \cdot \psi_{ucr,N} \quad (14.55)$$

The different factors of equation (14.55) are explained in the following.

The basic resistance of a single anchor,  $N_{Rk,cb}^0$ , should be calculated according to section 14.4.6.2.1e, equation (14.34a).

The factor  $\alpha_{s,Nb}$  takes into account the influence of neighbouring anchors and should be calculated analogous to equation (14.53b), however, the characteristic spacing  $s_{cr,N}$  should be replaced by  $s_{cr,Nb} = 4 \cdot c_1$ .

The factor  $\alpha_{c,Nb}$  takes into account the influence of a corner of the concrete member. It should be calculated according to equation (14.53f), however, the characteristic corner distance  $c_{cr,N}$  should be replaced by  $c_{cr,Nb} = 2 \cdot c_1$ .

If an anchor is influenced by two corners ( $c_{2,i} < 2 \cdot c_1$ ) (example see Fig. 14.31c) then the factor  $\alpha_{c,Nb}$  should be calculated for the values  $c_{2,1}$  and  $c_{2,2}$  and the product of both factors  $\alpha_{c,Nb}$  shall be inserted in equation (14.55).

The influence of the bearing area is taken into account by the factor  $\psi_{g,Nb}$  according to section 14.4.6.2.1e, equation (14.34c).

The influence of a distance  $f \leq 2 \cdot c_1$  between the anchor head and the upper or lower surface of the concrete member is taken into account by the factor  $\alpha_{h,Nb}$  according to equation (14.55a).

$$\alpha_{h,Nb} = \frac{h_{ef} + f}{4 \cdot c_1} \leq \frac{2 \cdot c_1 + f}{4 \cdot c_1} \leq 1 \quad (14.55a)$$

where:

$f$  = distance between the anchor head and the lower surface of the concrete member (see Fig. 14.32)

The influence of the position of the anchor channel is taken into account by the factor  $\psi_{ucr,N}$  according to section 14.3.5.1, equations (14.11e<sub>1</sub>) and (14.11e<sub>2</sub>).

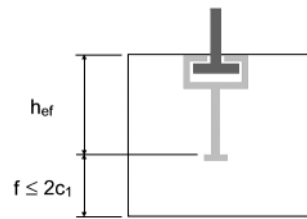


Fig. 14.32 Anchor channel at the edge of a thin concrete member

#### g) Steel failure of the supplementary reinforcement

The characteristic resistance of the supplementary reinforcement,  $N_{Rk,re}$  may be calculated in accordance with section 14.4.6.2.1f, equation (14.35).

#### h) Anchorage failure of the supplementary reinforcement in the concrete cone

The characteristic resistance of the supplementary reinforcement,  $N_{Rd,a}$  may be calculated in accordance with section 14.4.6.2.1g, equation (14.36).

#### 14.4.7.3.2 Shear loads

The required verifications for shear loads are shown in Table 14.10. For fasteners without supplementary reinforcement lines 1 to 5 apply.

**Table 14.10** Required verifications for anchor channels loaded in shear

				Channel	Most unfavourable anchor <sup>2)</sup>
1	Steel failure	Shear force without lever arm	Special screw		$V_{Ed} \leq V_{Rd,s} = \frac{V_{Rk,s}}{\gamma_{Ms}}$
2			Local bending of channel lip	$V_{Ed} \leq V_{Rd,s,l} = \frac{V_{Rk,s,l}}{\gamma_{Ms,l}}$	
3		Shear force with lever arm	Special screw		$V_{Ed} \leq V_{Rd,s} = \frac{V_{Rk,s}}{\gamma_{Ms}}$
4	Pry-out failure				$V_{Ed}^a \leq V_{Rd,cp} = \frac{V_{Rk,cp}}{\gamma_{Mc}}$
5	Concrete edge failure				$V_{Ed}^a \leq V_{Rd,c} = \frac{V_{Rk,c}}{\gamma_{Mc}}$
6	Steel failure of supplementary reinforcement				$N_{Ed,re}^h \leq N_{Rd,re} = \frac{N_{Rk,re}}{\gamma_{Ms,re}}$
7	Anchorage failure of supplementary reinforcement				$N_{Ed,re}^h \leq N_{Rd,a}$

For anchors with supplementary reinforcement lines 1 to 4 and 6, 7 apply.

Test experience shows that failure of the anchors, of the connections between anchors and channel or bending failure of the channel do not occur due to the load transfer described in section 5.1.2.4. Therefore these failure modes need not to be verified.

When the design relies on supplementary reinforcement, concrete edge failure according to equation (14.57) needs not to be verified but the supplementary reinforcement should be designed to resist the total shear load. The supplementary reinforcement may be in the form of a surface reinforcement (Fig. 14.19). It should comply with the requirements given in section 14.4.6.2.2 for headed anchors.

### a) Steel failure of fastener

#### a<sub>1</sub>) Shear force without lever arm

The characteristic resistance  $V_{Rk,s}$  (special screw) and  $V_{Rk,s,l}$  (local bending of the channel lips) are given in the relevant ETA. In general the characteristic resistance  $V_{Rk,s}$  is calculated according to equation (4.17).  $V_{Rk,s,l}$  is evaluated from test results.

#### a<sub>2</sub>) Shear force with lever arm

The characteristic resistance of a special screw in case of steel failure,  $V_{Rk,s}$ , may be obtained according section 14.3.5.2b, equation (14.14). The characteristic bending resistance  $M_{Rk,s}^0$ , calculated according to equation (14.14b) is given in the relevant ETA.

#### b) Concrete pry-out failure

The characteristic resistance for concrete pry-out failure should be calculated according to equation (14.56).

$$V_{Rk,cp} = k_5 \cdot N_{Rk,c} \quad (14.56)$$

where:

$k_5$  = factor to be taken from the relevant ETA valid for applications without supplementary reinforcement; in case of supplementary reinforcement the factor  $k_5$  should be multiplied with 0.75. In general,  $k_5 = 1.0$  ( $h_{ef} < 60$  mm) and  $k_5 = 2.0$  ( $h_{ef} \geq 60$  mm)

$N_{Rk,c}$  according to equation (14.53), determined for the most unfavourable anchor loaded in shear



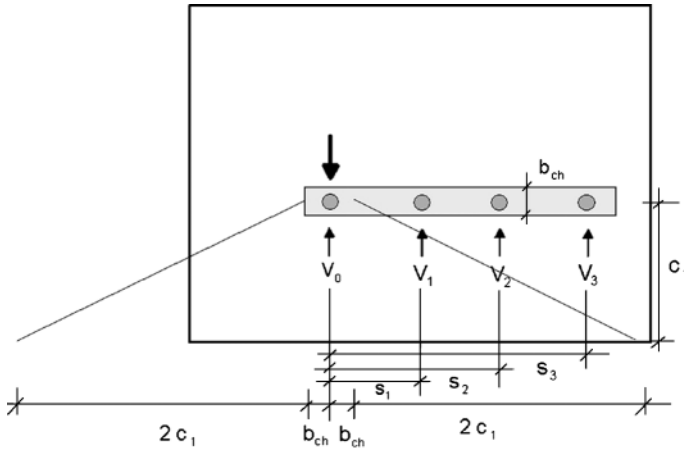


**Fig. 14.33** Example for an anchor channel with different anchor shear forces

**c) Concrete edge failure**

For anchors of a channel with an edge distance in all directions  $c \geq 10 \cdot h_{ef}$  and  $c \geq 60 \cdot d$ , a check of the concrete edge failure resistance may be omitted.

The characteristic resistance of a channel with one anchor in cracked concrete loaded perpendicular to the edge is given by equation (14.57). This equation is based on the approach described in section 5.1.2.4, equation (5.7).

$$V_{Rk,c} = V_{Rk,c}^0 \cdot \alpha_{s,V} \cdot \alpha_{c,V} \cdot \psi_{h,V} \cdot \psi_{ucr,V} \quad (14.57)$$

The different factors of equation (14.57) are given below.

The basic characteristic resistance of a channel with one anchor loaded perpendicular to the edge not influenced by neighbouring anchors, member thickness or corner should be calculated according to equation (14.57a).

$$V_{Rk,cp}^0 = \alpha_p \cdot \sqrt{f_{ck,cube}} \cdot c_1^{1.5} \quad [\text{N}] \quad (14.57a)$$

where:

$\alpha_p$  = product factor given in the relevant ETA

The product factor depends on the design and size of the anchor channel. It is evaluated from test results. As default value  $\alpha_p = 2.5$  may be taken.

The influence of neighbouring anchors is taken into account by the factor  $\alpha_{s,V}$  according to equation (14.57b).

$$\alpha_{s,V} = \frac{1}{1 + \sum_{i=1}^n \left[ \left( 1 - \frac{s_i}{s_{cr,V}} \right)^{1.5} \cdot \frac{V_i}{V_0} \right]} \quad (14.57b)$$

where (see Fig. 14.33):

$s_i$  = distance between the anchor for which the resistance is calculated and a neighbouring anchor

$$s_{cr,V} = 4 \cdot c_1 + 2 \cdot b_{ch} \quad (14.57c)$$

$b_{ch}$  = width of anchor channel (see Fig. 14.25)

$V_i$  = shear force of an influencing neighbouring anchor

$V_0$  = shear force of the anchor under consideration

$n$  = number of influencing anchors (all anchors with  $s < s_{cr,V}$  from the anchor under consideration)

The influence of a corner is taken into account by the factor  $\alpha_{c,V}$  according to equation (14.57d).

$$\alpha_{c,V} = \left( \frac{c_2}{c_{cr,V}} \right)^{0.5} \leq 1 \quad (14.57d)$$

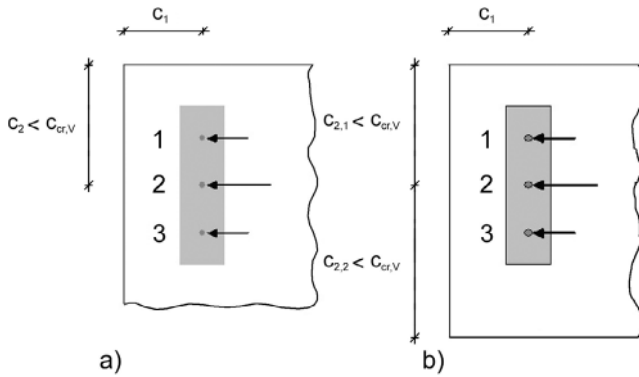


**Fig. 14.34** Example for an anchor channel with anchors where anchor No 2 is under consideration, influenced by a) one corner, b) two corners

where:

$$c_2 = \text{distance of the anchor under consideration to the corner}$$

$$c_{cr,V} = 2 \cdot c_1 + b_{ch} \quad (14.57e)$$

If an anchor is influenced by two corners (example see Fig. 14.34b) then the factor  $\alpha_{c,V}$  according to equation (14.57d) shall be calculated for each corner and the product shall be inserted in equation (14.57).

The influence of the member thickness  $h < h_{cr,V}$  is taken into account by the factor  $\alpha_{h,V}$ .

$$\alpha_{h,V} = \left( \frac{h}{h_{cr,V}} \right)^{0.5} \leq 1 \quad (14.57f)$$

where:

$$h_{cr,V} = 2 \cdot c_1 + 2 \cdot h_{ch} \quad (14.57g)$$

$$h_{ch} = \text{height of channel bar (see Fig. 14.25)}$$

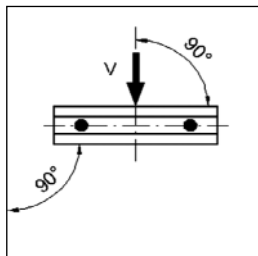


**Fig. 14.35** Anchor channel loaded parallel to the edge

For shear loads acting parallel to the edge (see Fig. 14.35),  $V_{Rk,c}$  shall be permitted to be twice the value for shear resistance determined from equation (14.57).

The factor  $\psi_{ucr,V}$  takes into account the effect of the position of the anchor channel in cracked or non-cracked concrete. The factor may be taken in accordance with section 14.3.5.2d. A factor  $\psi_{ucr,V} > 1$  shall only be used, if the height of the channel is  $h_{ch} \leq 40$  mm.

For an anchor in a narrow, thin member (see Fig. 14.36) with  $c_{2,max} \leq c_{cr,V}$  ( $c_{2,max}$  = maximum of  $c_{2,1}$  and  $c_{2,2}$ ,  $c_{cr,V}$  according to equation (14.57e)) and  $h < h_{cr,V}$  ( $h_{cr,V}$  according to equation (14.57g)), the calculation according to equation (14.57) leads to conservative results. More precise results are achieved if in equations (14.57a), (14.57c), (14.57e) and (14.57g) the edge distance  $c_1$  is replaced by the value according to equation (14.57h).

$$c'_1 = \max \{ (c_{2,max} - b_{ch})/2; (h - 2 \cdot h_{ch})/2 \} \quad [\text{mm}] \quad (14.57h)$$

**d) Steel failure of supplementary reinforcement**

The characteristic resistance of one anchor in case of steel failure of the reinforcement may be calculated according to section 14.4.6.2.2d, equation (14.46).

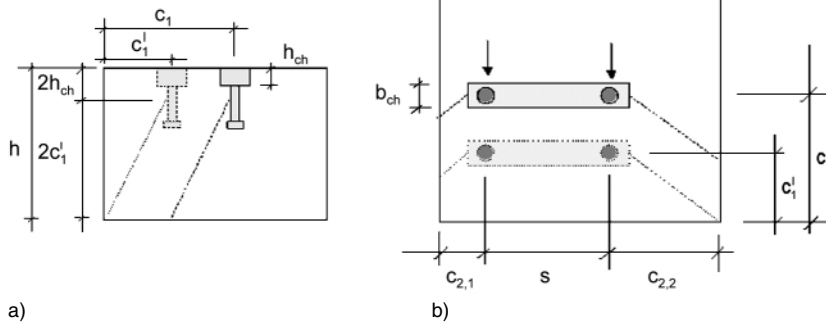


**Fig. 14.36** Anchor channel in a thin member, influenced by two corners  
a) section, b) top view

#### e) Anchorage failure of supplementary reinforcement in the concrete cone

For applications according Fig. 14.19 the design resistance of the reinforcement of one fastener in case of anchorage failure may be calculated according to section 14.4.6.2.2.e, equation (14.47).

#### 14.4.7.3.3 Combined tension and shear loads

##### 14.4.7.3.3.1 Anchor channels without supplementary reinforcement

For combined tension and shear loads section 14.4.6.2.3a applies.

##### 14.4.7.3.3.2 Anchor channels with supplementary reinforcement

For fastenings with supplementary reinforcement to take up tension and shear loads section 14.4.6.2.3.a applies. For fastenings at the edge with  $c_1 \leq c_{cr,N}$  with supplementary reinforcement to take up shear loads, equation (14.58) shall be satisfied:

$$\beta_N + \beta_V \leq 1 \quad (14.58)$$

with  $\beta_N = N_{Ed} / N_{Rd}$  and  $\beta_V = V_{Ed} / V_{Rd}$ . The largest value of  $\beta_N$  and  $\beta_V$  for the different failure modes should be used in equation (14.58).

#### 14.4.8 Design of post-installed fasteners – mechanical systems

##### 14.4.8.1 Scope

This part of the CEN Technical Specification (*European Committee for Standardisation (CEN)* (2004)) covers mechanical post-installed anchors such as expansion anchors, undercut anchors, concrete screws as well as bonded expansion anchors and bonded undercut anchors.

##### 14.4.8.2 Determination of action effects

For the determination and analysis of the condition of concrete (cracked or non-cracked concrete) serving as base material for the fastener section 14.4.2 applies. For determination of the forces acting on fasteners compare section 14.4.5.

##### 14.4.8.3 Verification of ultimate limit state by elastic analysis

###### 14.4.8.3.1 General

For the design in the ultimate limit state, there are three different methods available. They agree with the methods described in section 14.3.1. In the following only design method A is covered. This method requires proofs for all loading directions and all failure modes.

The spacing between outer fasteners of adjoining groups or the distance to single fasteners shall be  $a > s_{cr,N}$ .

**Table 14.11** Required verifications for tension loads

		Single fastener	Fastener group	
			Most loaded fastener	Fastener group
1	Steel failure	$N_{Ed} \leq N_{Rd,s} = \frac{N_{Rk,s}}{\gamma_{Ms}}$	$N_{Ed}^h \leq N_{Rd,s} = \frac{N_{Rk,s}}{\gamma_{Ms}}$	
2	Pull-out failure	$N_{Ed} \leq N_{Rd,p} = \frac{N_{Rk,p}}{\gamma_{Mp}}$	$N_{Ed}^h \leq N_{Rd,p} = \frac{N_{Rk,p}}{\gamma_{Mp}}$	
3	Concrete cone failure	$N_{Ed} \leq N_{Rd,c} = \frac{N_{Rk,c}}{\gamma_{Mc}}$		$N_{Ed}^g \leq N_{Rd,c} = \frac{N_{Rk,c}}{\gamma_{Mc}}$
4	Splitting failure	$N_{Ed} \leq N_{Rd,sp} = \frac{N_{Rk,sp}}{\gamma_{Msp}}$		$N_{Ed}^g \leq N_{Rd,sp} = \frac{N_{Rk,sp}}{\gamma_{Msp}}$

Aborted drill holes filled with high strength non-shrinkage mortar do not have to be considered in the design of fastenings.

#### 14.4.8.3.2 Tension loads

The required verifications are given in Table 14.11.

##### a) Steel failure

The characteristic resistance,  $N_{Rk,s}$ , in the case of steel failure is given in the relevant ETA.

##### b) Pull-out or pull-through failure

The characteristic resistance,  $N_{Rk,p}$ , in the case of pull-out or pull-through failure is given in the relevant ETA. In the ETAs pull-out failure is taken synonymously for pull-out and pull-through failure.

##### c) Concrete cone failure

For the characteristic resistance in the case of concrete failure section 14.4.6.2.1c applies. No influence of a supplementary reinforcement on the concrete cone failure load is considered because in general the position of the anchors in respect to the reinforcement bars is unknown.

##### d) Splitting failure due to fastener installation

Splitting failure is avoided during fastener installation by complying with minimum values for edge distance  $c_{min}$ , spacing  $s_{min}$ , member

thickness  $h_{min}$  and requirements on reinforcement as given in the relevant ETA.

##### e) Splitting failure due to loading

No verification of splitting failure due to load is required if at least one of the following conditions is fulfilled:

- The edge distance in all directions is  $c \geq 1.0 \cdot c_{cr,sp}$  for single fasteners or  $c \geq 1.2 \cdot c_{cr,sp}$  for groups of fasteners and the member thickness is  $h \geq h_{min}$ . The characteristic value  $c_{cr,sp}$  is given in the relevant ETA.
- The characteristic resistance of concrete cone failure and pull-out failure is calculated for cracked concrete and reinforcement is present to take up the splitting forces and to limit the crack width to  $w_k \leq 0.3$  mm.

If neither of the two conditions is fulfilled, then the characteristic resistance of a post-installed fastener or a group of fasteners should be calculated according to section 14.3.5.1d.

#### 14.4.8.3.3 Shear loads

The required verifications are given in Table 14.12.

##### a1) Steel failure without lever arm

For the characteristic resistance in case of steel failure without lever arm section 14.4.6.2.2a<sub>1</sub> applies.

**Table 14.12** Required verifications for shear loads

		Single fastener	Fastener group	
			Most loaded anchor	Fastener group
1	Steel failure without lever arm	$V_{Ed} \leq V_{Rd,s} = \frac{V_{Rk,s}}{\gamma_{Ms}}$	$V_{Ed}^h \leq V_{Rd,s} = \frac{V_{Rk,s}}{\gamma_{Ms}}$	
2	Steel failure with lever arm	$V_{Ed} \leq V_{Rd,s} = \frac{V_{Rk,s}}{\gamma_{Ms}}$	$V_{Ed}^h \leq V_{Rd,s} = \frac{V_{Rk,s}}{\gamma_{Ms}}$	
3	Concrete edge failure	$V_{Ed} \leq V_{Rd,c} = \frac{V_{Rk,c}}{\gamma_{Mc}}$		$V_{Ed}^g \leq V_{Rd,c} = \frac{V_{Rk,c}}{\gamma_{Mc}}$
4	Concrete pry-out failure	$V_{Ed} \leq V_{Rd,cp} = \frac{V_{Rk,cp}}{\gamma_{Mc}}$		$V_{Ed}^g \leq V_{Rd,cp} = \frac{V_{Rk,cp}}{\gamma_{Mc}}$

**a2) Steel failure with lever arm**

For the characteristic resistance in case of steel failure with lever arm section 14.3.5.2b applies.

**b) Concrete failure**

For the verification of concrete failure (concrete pry-out failure, concrete edge failure) sections 14.4.6.2.2b and c applies. The influence length  $l_f$  is given in the relevant ETA. In general it should be assumed that there is a hole clearance between anchor and fixture. Only if any gap between the fastener and the fixture is filled with mortar of sufficient compression strength or other means described in the ETA fastenings without hole clearance may be assumed.

No influence of a supplementary reinforcement on the concrete edge failure load is considered because in general the position of the anchors in respect to the reinforcement bars is unknown.

**14.4.8.3.4 Combined tension and shear loads**

For the characteristic resistance for combined tension and shear loads section 14.4.6.2.3a applies.

**14.4.9 Design of post-installed fasteners – chemical systems**

In general the verification of post-installed fasteners with chemical systems follows the rules for mechanical systems (compare section

14.4.8). However, a few modifications apply that are described in the following.

**14.4.9.1 Tension resistances**

Due to the different load transfer mechanism of bonded anchors in comparison with mechanical systems the characteristic resistance for pull-out failure is not given by a single value but should be calculated according to equation (14.59). This equation is valid for fasteners in non-cracked concrete and covers the transition from a pull-out failure to a concrete cone failure with different depths of the cone related to the embedment depth.

$$N_{Rk,p} = N_{Rk,p}^0 \cdot \psi_{c,Np} \cdot \frac{A_{p,N}}{A_{p,N}^0} \cdot \psi_{g,Np} \cdot \psi_{re} \cdot \psi_{ec,Np} \quad (14.59)$$

The various factors in equation (14.59) are explained below.

The initial value  $N_{Rk,p}^0$  of the characteristic resistance of one anchor with large spacing and edge distances in non-cracked concrete is given in the corresponding ETA. It is calculated according to equation (14.59a).

$$N_{Rk,p}^0 = \pi \cdot d \cdot h_{ef} \cdot \tau_{Rk,ncr} \quad (14.59a)$$

where:

$\tau_{Rk,ncr}$  = characteristic bond resistance in non-cracked concrete evaluated according to *European Organisation for Technical Approvals (EOTA) (2002)*

The influence of the concrete strength is taken into account by the factor  $\Psi_{c,Np}$ . The value is given in the ETA.

The geometrical influence of spacing and edge distance on the characteristic resistance is taken into account by the ratio  $A_{p,N} / A_{p,N}^0$ . The projected areas  $A_{p,N}$  and  $A_{p,N}^0$  are calculated according to Figs. 4.14, 4.16 and 4.27 using  $s_{cr,Np} = 2 \cdot c_{cr,Np}$  according to equation (14.59b) instead of  $s_{cr,N} = 2 \cdot c_{cr,N} = 3 \cdot h_{ef}$ .

The characteristic spacing and edge distance are:

$$s_{cr,Np} = 5 \cdot d \cdot \tau_{Rk}^{2/3} \quad (14.59b)$$

$$c_{cr,Np} = 0.5 \cdot s_{cr,Np} \quad (14.59c)$$

The modification factor for the influence of the failure surface of a group of bonded anchors is:

$$\psi_{g,Np} = \psi_{g,Np}^0 + \frac{s}{s_{cr,Np}} \cdot (1 - \psi_{g,Np}^0) \geq 1 \quad (14.59d)$$

where:

$$\psi_{g,Np}^0 = n^{\alpha_p} \quad (14.59e)$$

$$\alpha_p = 0.7 \cdot (1 - \tau_{Rk} / \tau_{Rk,max}) \leq 0.5 \quad (14.59f)$$

$$\tau_{Rk,max} = \text{kg} \cdot \frac{(h_{ef} \cdot f_{ck,cube})^{0.5}}{\pi d} \quad (14.59g)$$

$n$  = number of tensioned anchors in a group

kg given in the relevant ETA

$\Psi_{re}$  according to equation (14.11c)

The factor  $\psi_{ec,Np}$  takes account of a group effect when different tension forces are acting on the individual anchors of a group.

$$\psi_{ec,Np} = \frac{1}{1 + 2 \cdot e_N / s_{cr,Np}} \leq 1 \quad (14.59h)$$

where:

$e_N$  = eccentricity of the resultant tensile force related to the geometric centre of gravity of the tensioned anchors (see section 14.3.4)

$s_{cr,Np}$  according to equation (14.59b)

Equation (14.59h) agrees with equation (14.11d), however,  $s_{cr,N}$  is replaced by  $s_{cr,Np}$ .

When a bonded anchor or a group of bonded anchors is located in a region of a concrete member where analysis indicates concrete

cracking at service load levels (compare equation (14.1)) the characteristic resistance  $N_{Rk,p}$  is calculated according to equation (14.59), however with  $\tau_{Rk,cr}$  substituted for  $\tau_{Rk,ncr}$  in the calculation of the initial value of  $N_{Rk,p}^0$ .  $\tau_{Rk,cr}$  is the characteristic bond resistance in cracked concrete evaluated according to *European Organisation for Technical Approvals (EOTA)* (2002).

The resistance according to equation (14.59) is limited by the concrete cone resistance  $N_{Rk,c}$  of mechanical expansion anchors calculated according to section 14.3.5.1c. However, if it has been shown by appropriate approval tests with single anchors that the concrete cone failure load of headed anchors is reached with a specific bonded anchor system, then the capacity of fastenings with bonded anchors calculated according to equation (14.59) should be limited by the concrete cone capacity of headed anchors calculated according to section 14.4.6.2.1c. This is stated in the corresponding ETA.

#### 14.4.9.2 Shear loads

For the verification of fastenings with bonded anchors under shear loads section 14.4.8.3.3 applies. However, the characteristic resistance for concrete edge failure is calculated according to section 14.4.6.2.2c with  $l_f$  taken as embedment depth  $h_{ef}$  and  $d_{nom}$  as drill hole diameter  $d_0$ .

#### 14.4.9.3 Combined tension and shear loads

For the verification of combined tension and shear loads section 14.4.6.2.3a applies.

#### 14.4.10 Fatigue loads

The CEN Technical Specification (*European Committee for Standardisation (CEN)* (2004)) covers applications under pulsating tension or shear load (Fig. 14.37) and alternating shear load (Fig. 14.38). Fatigue verification should be carried out when fasteners are subjected to regular load cycles (e.g. fastenings of cranes, reciprocating machines, guide rails of elevators). Fatigue load cycling may also arise at restraints of members subjected to temperature (e.g. facades).

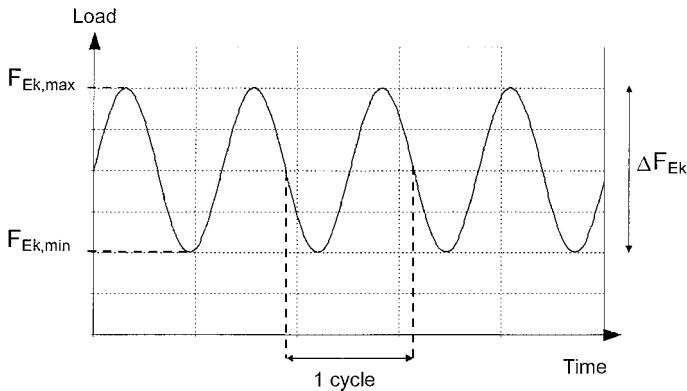


**Fig. 14.37** Definition of pulsating actions

In general, fatigue verification is not required in the following cases:

- Less than 1000 load cycles for pulsating tension, shear or combined tension and shear loads with a load range  $\Delta F_{Ek} = F_{Ek,max} - F_{Ek,min}$  equal to the allowable load for static loading, which is  $F_{Rd} / \gamma_Q$  (with  $F_{Rd}$  = design resistance for steel failure,  $\gamma_Q = 1.5$ ).
- Less than 15 load cycles of alternating shear loads with a load range twice the allowable value for static loading. For smaller load ranges the number of load cycles, where no verification is required, may be increased.
- With load cycles imposed by temperature variations (e.g. fastening of facade elements), if the stress range caused by the restraint forces in the most stressed fastener  $\Delta\sigma_{max} = \sigma_{max} - \sigma_{min}$  is limited to 100 N/mm<sup>2</sup> (bending stresses in the fastener e.g. in a stand-off installation) or in case of shear loads, if the maximum stress range in the cross-section of the most stressed fastener is limited to  $\Delta\tau = \tau_{max} - \tau_{min} \leq 60$  N/mm<sup>2</sup> ( $\tau$  = shear stress in the fastener).

Fasteners used to resist fatigue loading should be pre-qualified for this application either by a European Technical Approval or by a CEN Product Standard.

Annular gaps are not allowed and loosening of the nut or screw shall be avoided. Therefore a

permanent prestressing force on the fastener shall be present during lifetime. This requirements can be fulfilled e.g. by special installation sets.

The verification of the resistance under fatigue loading consists of both, the verification under static and fatigue loading. Under static loading the fasteners should be designed based on the design methods given in section 14.4. The verifications under fatigue loading are given in the following.

The required verifications are summarised in Table 14.13 (tension loading) and Table 14.14 (shear loading). In general, the values for resistances are considered valid up to  $2 \cdot 10^6$  cycles. The maximum number of cycles is stated in the relevant European Technical Approval or in the CEN Product Standard.

To take account for the unequal resistance of fasteners within a group arising from possible differences in stiffness the fatigue resistance of the most loaded fastener is multiplied with a reduction factor  $\psi_{FN}$  for tensile loading or of  $\psi_{FV}$  for shear loading. These factors may be taken from the corresponding European Technical Approval or from the CEN Product Standard. For groups with two fasteners under shear load perpendicular to the axis of the fasteners when the fixture is able to rotate the factor  $\psi_{FV}$  may be taken to  $\psi_{FV} = 1.0$ .



**Table 14.13** Required verifications for fatigue under tension loading

	Single fastener	Fastener group	
		Most loaded fastener	Fastener group
Steel failure	$\gamma_{F,fat} \cdot \Delta N_{Ek} \leq \frac{\Delta N_{Rk,s}}{\gamma_{Ms,N,fat}}$	$\gamma_{F,fat} \cdot \Delta N_{Ek}^h \leq \frac{\psi_{FN} \cdot \Delta N_{Rk,s}}{\gamma_{Ms,N,fat}}$	
Pull-out failure	$\gamma_{F,fat} \cdot \Delta N_{Ek} \leq \frac{\Delta N_{Rk,p}}{\gamma_{Mp,fat}}$	$\gamma_{F,fat} \cdot \Delta N_{Ek}^h \leq \frac{\psi_{FN} \cdot \Delta N_{Rk,p}}{\gamma_{Mp,fat}}$	
Concrete cone failure	$\gamma_{F,fat} \cdot \Delta N_{Ek} \leq \frac{\Delta N_{Rk,c}}{\gamma_{Mc,fat}}$		$\gamma_{F,fat} \cdot \Delta N_{Ek}^s \leq \frac{\Delta N_{Rk,c}}{\gamma_{Mc,fat}}$
Concrete splitting failure	$\gamma_{F,fat} \cdot \Delta N_{Ek} \leq \frac{\Delta N_{Rk,sp}}{\gamma_{Mc,fat}}$		$\gamma_{F,fat} \cdot \Delta N_{Ek}^s \leq \frac{\Delta N_{Rk,sp}}{\gamma_{Mc,fat}}$
Concrete blow-out failure	$\gamma_{F,fat} \cdot \Delta N_{Ek} \leq \frac{\Delta N_{Rk,cb}}{\gamma_{Mc,fat}}$		$\gamma_{F,fat} \cdot \Delta N_{Ek}^s \leq \frac{\Delta N_{Rk,cb}}{\gamma_{Mc,fat}}$

where:

- $\gamma_{F,fat} = 1.0$
- $\gamma_{Mc,fat}, \gamma_{Mp,fat}$  according to section 14.4.4.2.2
- $\gamma_{Ms,N,fat} = 1.35$
- $\Delta N_{Ek} = N_{Ek,max} - N_{Ek,min}$
- $=$  twice the amplitude of the fatigue tensile action (see Fig. 14.37)
- $\Delta N_{Rk,s}$  fatigue resistance for steel under tension loading (according to the corresponding European Technical Approval or to the CEN Product Standard)
- $\Delta N_{Rk,c}$  fatigue resistance for concrete failure under tension loading
- $= 0.6 \cdot N_{Rk,c}$
- $N_{Rk,c}$  resistance for concrete failure under predominantly static tension loading (according to the corresponding European Technical Approval or to the CEN Product Standard)

$\Delta N_{Rk,p}$

fatigue resistance for pull-out under tension loading (according to the corresponding European Technical Approval or to the CEN Product Standard)

$\Delta N_{Rk,sp}$

fatigue resistance for splitting under tension loading

$= 0.6 \cdot N_{Rk,sp}$

$N_{Rk,sp}$

resistance for splitting under predominantly static tension loading (according to the corresponding European Technical Approval or to the CEN Product Standard)

$\Delta N_{Rk,cb}$

fatigue resistance for concrete blow-out under tension loading

$= 0.6 \cdot N_{Rk,cb}$

$N_{Rk,cb}$

resistance for concrete blow-out under predominantly static tension loading (according to the corresponding European Technical Approval or to the CEN Product Standard)

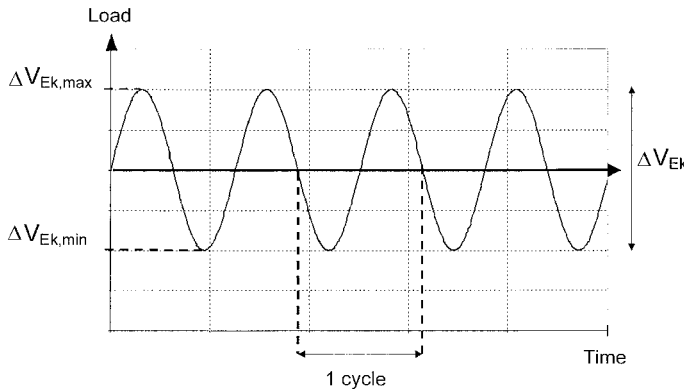


**Fig. 14.38** Definition of alternating shear actions

**Table 14.14** Required verifications for fatigue under shear loading

	Single fastener	Fastener group	
		Most loaded fastener	Fastener group
Steel failure without lever arm	$\gamma_{F,fat} \cdot \Delta V_{Ek} \leq \frac{\Delta V_{Rk,s}}{\gamma_{Ms,V,fat}}$	$\gamma_{F,fat} \cdot \Delta V_{Ek}^h \leq \frac{\psi_{FV} \cdot \Delta V_{Rk,s}}{\gamma_{Ms,V,fat}}$	
Steel failure with lever arm	$\gamma_{F,fat} \cdot \Delta V_{Ek} \leq \frac{\Delta V_{Rk,s}}{\gamma_{Ms,V,fat}}$	$\gamma_{F,fat} \cdot \Delta V_{Ek}^h \leq \frac{\psi_{FV} \cdot \Delta V_{Rk,s}}{\gamma_{Ms,V,fat}}$	
Concrete pry-out failure	$\gamma_{F,fat} \cdot \Delta V_{Ek} \leq \frac{\Delta V_{Rk,cp}}{\gamma_{Mc,fat}}$		$\gamma_{F,fat} \cdot \Delta V_{Ek}^g \leq \frac{\Delta V_{Rk,cp}}{\gamma_{Mc,fat}}$
Concrete edge failure	$\gamma_{F,fat} \cdot \Delta V_{Ek} \leq \frac{\Delta V_{Rk,c}}{\gamma_{Mc,fat}}$		$\gamma_{F,fat} \cdot \Delta V_{Ek}^g \leq \frac{\Delta V_{Rk,c}}{\gamma_{Mc,fat}}$

where:

$$\gamma_{F,fat} = 1.0$$

$\gamma_{Mc,fat}$  according to section 14.4.4.2.2

$$\gamma_{Ms,V,fat} = 1.35$$

$\Delta V_{Ek} = V_{Ek,max} - V_{Ek,min}$   
= twice the amplitude of the fatigue shear action (see Fig. 14.38)

$\Delta V_{Rk,s}$  fatigue resistance for steel under shear loading (according to the corresponding European Technical Approval or to the CEN Product Standard)

$\Delta V_{Rk,cp}$  fatigue resistance for pry-out under shear loading  
=  $0.6 \cdot V_{Rk,cp}$

$V_{Rk,cp}$

resistance for pry-out under predominantly static shear loading (according to the corresponding European Technical Approval or to the CEN Product Standard)

$\Delta V_{Rk,c}$

= fatigue resistance for concrete edge failure under shear loading

$$= 0.6 \cdot V_{Rk,c}$$

$V_{Rk,c}$

resistance for concrete edge failure under predominantly static shear loading (according to the corresponding European Technical Approval or to the CEN Product Standard)

For combined tension and shear loading equation (14.60) shall be satisfied.

$$\beta_{N,fat} = \frac{\gamma_{F,fat} \cdot \Delta N_{Sk}}{\psi_{FN} \cdot \Delta N_{Rk} / \gamma_M} \leq 1 \quad (14.60a)$$

$$\beta_{V,fat} = \frac{\gamma_{F,fat} \cdot \Delta V_{Sk}}{\psi_{FV} \cdot \Delta V_{Rk} / \gamma_M} \leq 1 \quad (14.60b)$$

$$(\beta_{N,fat})^\alpha + (\beta_{V,fat})^\alpha \leq 1 \quad (14.60c)$$

where:

$\psi_{FN}$ ,  $\psi_{FV}$ ,  $\alpha$  taken from the corresponding European Technical Approval or from the CEN Product standard  
 $\Delta N_{Rk}$ ,  $\Delta V_{Rk}$  minimum value of resistance of the governing failure mode

In equation (14.60c) the largest value of  $\beta_{N,fat}$  and  $\beta_{V,fat}$  for the different failure modes shall be taken.

## 14.4.11 Seismic loads

### 14.4.11.1 General

This section provides additional requirements for fastenings used to transmit seismic actions by means of tension, shear, or a combination of tension and shear

- between connected structural elements,
- between non-structural attachments and structural elements.

Applications for which actions are predominantly high-cycle fatigue or impact are not covered by the provisions in this section.

Fasteners used to resist seismic actions shall meet all applicable requirements for non-seismic applications. The fasteners shall be pre-qualified for seismic situations either by a European Technical Approval or by a CEN Product Standard.

In the region of the fastening, the concrete shall be assumed to be cracked. This section does not apply to the design of fastenings in plastic hinge zones (critical regions) of concrete structures. The critical length  $l_{cr}$  is defined in *Eurocode 8: prEN 1998-1* (2003).

Displacement of the fastening should be accounted for by engineering judgement e.g. when anchoring structural elements to non-structural elements of great importance or of a particularly dangerous nature.

Determination of distribution of forces to the individual fasteners of a group shall take into account the stiffness of the fixture and its ability to redistribute loads to other anchors in the group beyond yield of the fixture.

In general annular gaps between a fastener and its fixture should be avoided for seismic design situations. Where in minor non-critical applications the requirement is not fulfilled, the effect of the annular gap on the distribution of shear loads in case of groups and on the resistance should be taken into account. Loosening of the nut or screw shall be prevented by appropriate measures.

#### 14.4.11.2 Actions

The design value of the effect of seismic actions  $E_d$  acting on the fixture shall be determined according to *Eurocode 8: prEN 1998-1* (2003). While *Eurocode 8* provides requirements for the design of non-structural elements in its section 4.3.5, it ignores the vertical accelerations in the calculation of actions. Therefore additional requirements in are provided in *European Committee for Standardisation* (2004), Annex E.

In the design of fastenings for non-structural elements subjected to seismic actions, any beneficial effects of friction due to the gravity loads should be ignored.

The horizontal effects of the seismic action may be determined by applying to the non-structural element a horizontal force  $F_a$  according to equation (14.61).

$$F_a = (S_a \cdot W_a \cdot \gamma_a) / q_a \quad (14.61)$$

where:

$F_a$  = horizontal seismic force, acting at the centre of mass of the non-structural element in the most unfavourable direction

$W_a$  = weight of the element

$S_a$  = horizontal seismic coefficient applicable to non-structural elements (see equation (14.62))

$\gamma_a$  = importance factor of the element

$\geq 1.5$  for non-structural elements deemed to be of great importance

$q_a$  = behaviour factor of the element (see Table 14.15)

The horizontal seismic coefficient  $S_a$  may be calculated using equation (14.62).

$$S_a = \alpha \cdot S \cdot \left[ \left( 1 + \frac{z}{h} \right) \cdot A_a - 0.5 \right] \geq \alpha \cdot S \quad (14.62)$$

where:

$A_a$  = response amplification factor

$$= \frac{3}{1 + \left( 1 - \frac{T_a}{T_1} \right)^2} \quad (14.62a)$$

$T_a$  = fundamental vibration period of the non-structural element

$T_1$  = fundamental vibration period of the building in the relevant direction

$\alpha$  = ratio of the design ground acceleration on type A ground,  $a_g$ , to the acceleration of gravity  $g$

$S$  = soil factor

$z$  = height of the non-structural element above the level of application of the seismic action

$h$  = height of the building, measured from the foundation or from top of a rigid basement

If the values  $T_a$  and/or  $T_1$  in equation (14.62a) are not known, the values given in Table 14.15 may be used.

The vertical effects of the seismic action may be determined by applying to the non-structural element a vertical force  $F_{va}$  according to equation (14.63).

$$F_{va} = (S_{va} \cdot W_a \cdot \gamma_a) / q_a \tag{14.63}$$

where:

$F_{va}$  = vertical seismic force, acting at the centre of mass of the non-structural element

$S_{va}$  = vertical seismic coefficient applicable to non-structural elements (see equation (14.64))

$W_a, \gamma_a, q_a$  as given in equation (14.61)

$$S_{va} = \alpha_v \cdot A_a \tag{14.64}$$

where:

$\alpha_v$  = ratio of the vertical design ground acceleration on type A ground,  $a_{vg}$ , to the acceleration of gravity  $g$

$A_a$  = response amplification factor (see Table 14.15)

The vertical effects of the seismic action  $F_{va}$  for non-structural elements may be neglected when the ratio of the vertical component of the design ground acceleration  $a_{vg}$  to the acceleration of the gravity  $g$  is less than 1.0 and the gravity loads are transferred through direct bearing of the fixture on the structure (see Fig. 14.39).

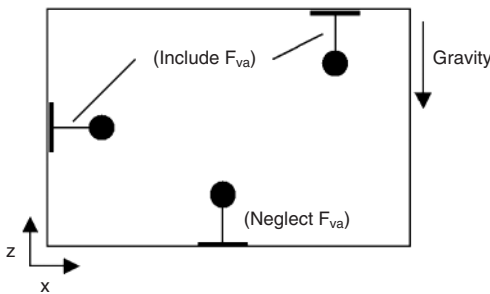


**Fig. 14.39** Vertical effects of a seismic action

Values of the response amplification factor  $A_a$  and behaviour factor  $q_a$  for non-structural elements may be selected from Table 14.15. For buildings with fewer than 10 stories, a factor  $A_a = 1.5$  may be slightly unconservative compared to the value yielded by equation (14.62a). A factor  $A_a = 3.0$  is always conservative compared to using equation (14.62a).

**Table 14.15** Non-structural elements response amplification and behaviour factors

	$A_a$	$q_a$
<b>Architectural</b>		
Exterior wall elements	1.5	2.0
Partitions	1.5	2.0
Interior veneers	1.5	2.0
Ceilings	1.5	2.0
Parapets and appendages	3.0	1.0
Canopies and marquees	3.0	1.0
Chimneys and masts <sup>1)</sup>	3.0	1.0
Stairs	1.5	2.0
<b>Mechanical equipment</b>		
Mechanical equipment	1.5	2.0
Storage vessels and water heaters <sup>1)</sup>	3.0	1.0
High-pressure piping	3.0	2.0
Fire suppression piping	3.0	2.0
Fluid piping (not fire suppression) for hazardous materials	3.0	1.0
Fluid piping (not fire suppression) for non-hazardous materials	3.0	2.0
Ductwork	1.5	2.0
<b>Electrical and communications equipment</b>		
Electrical and communications equipment	1.5	2.0
Electrical and communications distribution equipment	3.0	2.0
Light fixtures	1.5	2.0
<b>Furnishing and interior equipment</b>		
Storage racks	3.0	2.0
Bookcases	1.5	2.0
Computer access floors	1.5	2.0
Hazardous materials storage	3.0	1.0
Computer communications racks	3.0	2.0
Elevators	1.5	2.0
Conveyors	3.0	2.0
<b>Other unspecified equipment</b>		
Other rigid components (fundamental period $\leq 0.06$ sec)		
High deformability elements and attachments	1.5	2.0
Low deformability elements and attachments	1.5	1.0
Other flexible components (fundamental period $> 0.06$ sec)		
High deformability elements and attachments	3.0	2.0
Low deformability elements and attachments	3.0	1.0

<sup>1)</sup> For chimneys, masts and tanks on legs acting as unbraced cantilevers along less than one half of their total height, or braced or guyed structure at or above their centre of mass,  $A_a$  may be taken as 1.5 and  $q_a$  may be taken as 2.0

### 14.4.11.3 Resistances

For the partial safety factors  $\gamma_M$  section 14.4.4.2 applies.

The seismic design resistance  $R_{d,seis}$  of a fastening shall be taken as 75 % of the minimum design resistance as determined for the persistent and transient elastic design situation using the values for the characteristic seismic resistance  $R_{k,seis}$  provided by an European Technical Approval or a CEN Product Standard.

$$R_{d,seis} = 0.75 \cdot \frac{R_{k,seis}}{\gamma_M} \quad (14.65)$$

When the fastening design includes seismic actions one of the following conditions shall be satisfied:

- The fixture, or the element attached to the fixture, shall be designed to undergo ductile yielding at a load level not greater than 80 % of the seismic design resistance of the fastening as defined by equation (14.65).
- The fasteners shall be designed for ductile steel failure. To ensure ductile steel failure, the seismic design resistance of the fasteners, as defined by equation (14.65), failing by concrete cone, splitting or pull-out under tension loading or pry-out or concrete edge failure under shear loading shall exceed 1.25-times the characteristic seismic resistance for steel failure provided by the relevant European Technical Approval or CEN Product Standard. The nominal steel strength of the fasteners should not exceed  $f_{uk} = 800 \text{ N/mm}^2$ , the ratio nominal steel yield strength to nominal ultimate strength shall not exceed  $f_{yk}/f_{uk} = 0.8$ , and the rupture elongation (measured over a length equal to  $5 \cdot d$ ) should be at least 12 %. Fasteners with a reduced section should satisfy the following conditions:
  - For fasteners loaded in tension, the strength  $N_{uk}$  of the reduced section should either be greater than 1.1-times of the yield strength  $N_{yk}$  of the unreduced section or the stressed length of the reduced section should be  $\geq 5 \cdot d$  ( $d$  = fastening diameter outside reduced section).

- For fasteners loaded in shear or which shall redistribute shear forces, the begin of the reduced section should either be  $\geq 5 \cdot d$  below the concrete surface or in the case of a threaded fastener the threaded part should extend  $\geq 2 \cdot d$  into the concrete.
- For fasteners loaded in combined tension and shear, the two conditions given above should be met.

The steel fixture should be embedded in the concrete or fastened to the concrete surface without an intermediate layer or with a levelling layer of mortar with a compressive strength  $\geq 30 \text{ N/mm}^2$  and a thickness  $\leq d/2$ . Ductile failure modes other than ductile steel failure may be allowed. However, ductility equivalent to that which occurs during ductile steel failure shall be shown in the relevant European Technical Approval or in the CEN Product Standard.

- For non-structural elements, brittle failure of the fastening shall be allowed only if the seismic design resistance as defined by equation (14.65) is taken as at least 2.5-times the effect of the applied seismic action  $E_d$  of the attached non-structural element (see Equation 14.66). For structural elements, brittle failure of the fastening is not permitted. Non-structural elements:

$$2.5 \cdot E_d \leq 0.75 \cdot \frac{R_{k,seis}}{\gamma_M} \quad (14.66)$$

Minimum edge distance and minimum spacing between fasteners shall be determined as for persistent and transient design situations unless different values for seismic design situations are provided in the relevant European Technical Approval or in the CEN Product Standard.

### 14.4.12 Verification of serviceability limit state

For the required verification see section 14.4.3. The admissible displacement  $C_d$  should be evaluated by the designer taking into account the type of application in question (e.g. the structural element to be fastened). It may be assumed that the displacements are a linear function of the applied load. In the case of combined ten-

sion and shear loading components of the resultant load should be added vectorially. The characteristic displacements of the fastener under given tension and shear loads shall be taken from the relevant European Technical Approval or in the CEN Product Standard.

### 14.4.13 Fire

#### 14.4.13.1 General

In absence of specifications concerning the characteristic values for fire resistance in corresponding European Technical Approvals or CEN Product Standards the following modified design method may be used. It is valid for cast-in-place headed anchors, expansion and undercut anchors and concrete screws only. For bonded anchors the fire resistances in the cases of bond and concrete failure are product dependent. Anchor channels are not covered. Therefore no values can be given here and the manufacturer should be consulted.

The fire resistance is classified according to *EN 13501-2* using the Standard ISO time-temperature curve (STC).

The design method covers fasteners with a fire exposure from one side only. For fire exposure from more than one side, the design method may be used only, if the edge distance of the fastener is  $c \geq 300$  mm and  $c \geq 2 \cdot h_{ef}$ .

The design under fire exposure is carried out according to the normal design method for ambient temperature given in the CEN Technical Specification (*European Committee for Standardisation* (2004)) with the modifications described in the following.

#### 14.4.13.2 Partial safety factors

Partial safety factors for actions  $\gamma_{F,fi}$  and for materials  $\gamma_{M,fi}$  may be defined in a National Annex to the CEN Technical Specification (*European Committee for Standardisation* (2004)). The recommended values are  $\gamma_{F,fi} = 1.0$  and  $\gamma_{M,fi} = 1.0$ .

#### 14.4.13.3 Resistance

In absence of test data for a specific anchor the following characteristic resistances in the ultimate limit state under fire exposure may be

taken instead of the values given in the product specific parts of the CEN Technical Specification (*European Committee for Standardisation* (2004)), which are valid for ambient temperatures. These values are conservative.

#### 14.4.13.3.1 Tension loading

##### a) Steel failure

The characteristic resistance of a fastener in case of steel failure under fire exposure (characteristic tension strength  $\sigma_{Rk,s,fi}$ ) given in Tables 14.16 and 14.17 may be used. These values are also valid for the unprotected steel part of the fastener outside the concrete.

##### b) Pull-out/pull-through failure

The characteristic resistance of fasteners installed in concrete of strength classes C20/25 to C50/60 may be obtained from equation (14.67).

- Fire exposure up to 90 minutes:

$$N_{Rk,p,fi(90)} = 0.25 \cdot N_{Rk,p} \quad (14.67a)$$

- Fire exposure between 90 and 120 minutes:

$$N_{Rk,p,fi(120)} = 0.20 \cdot N_{Rk,p} \quad (14.67b)$$

where:

$N_{Rk,p}$  = characteristic resistance in cracked concrete C20/25 under ambient temperature given in the European Technical Approval or in the CEN Product Standard

##### c) Concrete cone failure

The characteristic resistance of a single anchor  $N_{Rk,c,fi}^0$  not influenced by adjacent fasteners or edges of the concrete member and installed in concrete with the strength classes C20/25 to C50/60 may be obtained from equation (14.68). The influence of the different effects of geometry, shell spalling, eccentricity, position and further influencing parameters may be taken from the relevant product specific part of the CEN Technical Specification (*European Committee for Standardisation* (2004)). However, the characteristic spacing and edge distance for fasteners under fire near the edge shall be taken as  $s_{cr,N} = 2 \cdot c_{cr,N} = 4 \cdot h_{ef}$ .

**Table 14.16** Characteristic tension strength of a fastener made of carbon steel under fire exposure

Anchor bolt or thread diameter [mm]	Anchorage depth $h_{ef}$ [mm]	Characteristic tension strength $\sigma_{Rk,s,fi}$ [N/mm <sup>2</sup> ] of an unprotected fastener made of carbon steel according to EN 10025 in case of fire exposure in the time up to			
		30 min (R15 to R30)	60 min (R45 to R60)	90 min (R90)	120 min ( $\leq$ R120)
6	$\geq 30$	10	9	7	5
8	$\geq 30$	10	9	7	5
10	$\geq 40$	15	13	10	8
$\geq 12$	$\geq 50$	20	15	13	10

**Table 14.17** Characteristic tension strength of a fastener made of stainless steel under fire exposure

Anchor bolt or thread diameter [mm]	Anchorage depth $h_{ef}$ [mm]	Characteristic tension strength $\sigma_{Rk,s,fi}$ [N/mm <sup>2</sup> ] of an unprotected fastener made of carbon steel according to ISO 3506 in case of fire exposure in the time up to			
		30 min (R15 to R30)	60 min (R45 to R60)	90 min (R90)	120 min ( $\leq$ R120)
6	$\geq 30$	10	9	7	5
8	$\geq 30$	20	16	12	10
10	$\geq 40$	25	20	16	14
$\geq 12$	$\geq 50$	30	25	20	16

- Fire exposure up to 90 minutes:

$$N_{Rk,c,fi(90)}^0 = \frac{h_{ef}}{200} \cdot N_{Rk,c}^0 \leq N_{Rk,c}^0 \quad (14.68a)$$

- Fire exposure between 90 and 120 minutes:

$$N_{Rk,c,fi(120)}^0 = 0.8 \cdot \frac{h_{ef}}{200} \cdot N_{Rk,c}^0 \leq N_{Rk,c}^0 \quad (14.68b)$$

where:

$h_{ef}$  = effective embedment depth [mm]

$N_{Rk,c}^0$  = characteristic resistance of a single fastener in cracked concrete C20/25 under ambient temperature given in the European Technical Approval or in the CEN Product Standard

#### d) Splitting failure

The assessment of splitting failure due to loading under fire exposure is not required because the splitting forces are assumed to be taken up by reinforcement.

### 14.4.13.3.2 Shear loading

#### a) Steel failure

##### a1) Shear load without lever arm

For the characteristic shear resistance  $\tau_{Rk,s,fi}$  of a fastener in case of steel failure under fire exposure (characteristic strength) the values given in

Tables 14.16 and 14.17 apply. They are also valid for the unprotected steel part of the fastener outside the concrete. Limited tests have indicated, that the ratio of shear strength to tensile strength increases under fire conditions above that for ambient temperature design.

##### a2) Shear load with lever arm

The characteristic resistance of a fastener may be calculated according to the relevant product specific part of the CEN Technical Specification (*European Committee for Standardisation* (2004)). However, the characteristic bending resistance of a single fastener under fire exposure is limited to the characteristic tension strength according to section 14.4.13.3.1a. The characteristic bending resistance may be taken from equation 14.69.

$$M_{Rk,s,fi}^0 = 1.2 \cdot W_{el} \cdot \sigma_{Rk,s,fi} \quad (14.69)$$

where:

$\sigma_{Rk,s,fi}$  given in Tables 14.16 and 14.17

##### b) Concrete pry-out failure

The characteristic resistance in case of fasteners installed in concrete with strength classes C20/25 to C50/60 may be taken from equation (14.70).



- Fire exposure up to 90 minutes:

$$V_{Rk,cp,fi(90)} = k \cdot N_{Rk,c,fi(90)} \quad (14.70a)$$

- Fire exposure between 90 and 120 minutes:

$$V_{Rk,cp,fi(120)} = k \cdot N_{Rk,c,fi(120)} \quad (14.70b)$$

where:

$k$  taken from the relevant European Technical Approval or CEN Product Standard (ambient temperature)

$N_{Rk,c,fi(90)}, N_{Rk,c,fi(120)}$  calculated according to 14.4.13.3.1c

**c) Concrete edge failure**

The characteristic resistance of a single fastener installed in concrete with strength classes C20/25 to C50/60 may be taken from equation (14.71). The influence of the different effects of geometry, thickness, load direction, eccentricity, may be taken from the relevant product specific part of the CEN Technical Specification (*European Committee for Standardisation (2004)*).

- Fire exposure up to 90 minutes:

$$V_{Rk,c,fi(90)}^0 = 0.25 \cdot V_{Rk,c}^0 \quad (14.71a)$$

- Fire exposure between 90 and 120 minutes:

$$V_{Rk,c,fi(120)}^0 = 0.20 \cdot V_{Rk,c}^0 \quad (14.71b)$$

where:

$V_{Rk,c}^0$  initial value of the characteristic resistance of a single fastener in cracked concrete C20/25 under ambient temperature according to the relevant product specific part of the CEN Technical Specification (*European Committee for Standardisation (2004)*)

**14.4.13.3.3 Combined tension and shear loading**

The interaction conditions according to the relevant product specific part of the CEN Technical Specification (*European Committee for Standardisation (2004)*) may be taken with the characteristic resistances under fire exposure for the different loading directions.

**14.4.14 Plastic design of fastenings with headed fasteners and post-installed fasteners**

**14.4.14.1 Field of application**

In a plastic analysis it is assumed that significant redistribution of tension and shear forces will occur in a group. Therefore, this analysis is acceptable only when the failure is governed by ductile steel failure of the fastenings under tension, shear or combined tension and shear loading.

To ensure ductile steel failure, the following conditions shall be met:

- Fastening arrangements as shown in Fig. 14.40 are covered. Other forms of the attachment than shown in Fig. 14.40 are possible. The number of fastenings parallel to the axis of bending might be larger than 2. The fixture may be loaded by normal and shear forces and by a bending moment. Flexible fixtures may be used if the resultant non-linear load distribution and associated prying forces are taken into account (Fig. 14.41).
- The design resistance of a fastener as governed by concrete failure should exceed the design resistance as governed by steel failure. Resistance models as given in section 14.4.14.3 will satisfy this requirement.

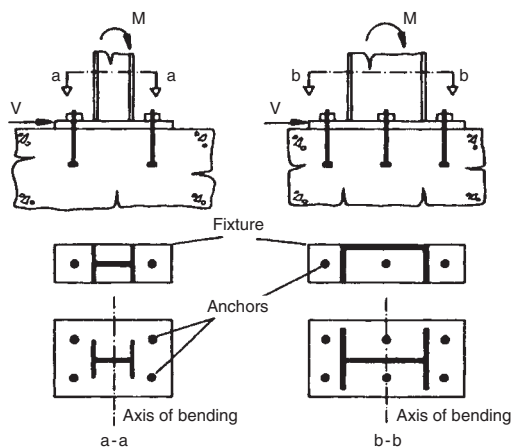


**Fig. 14.40** Fastening arrangements for which the plastic design approach may be used

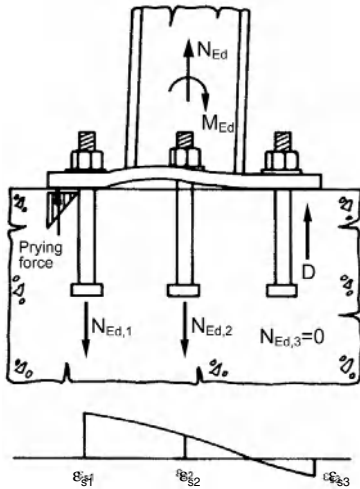


**Fig. 14.41** Example for a fastening with a flexible fixture loaded by a bending moment and a tension force

- The nominal strength of a fastener shall not exceed  $f_{uk} = 800 \text{ N/mm}^2$ , the ratio nominal steel yield strength to nominal ultimate strength shall not exceed  $f_{yk} / f_{uk} = 0.8$ , and the rupture elongation (measured over a length equal  $5 \cdot d$ ) shall be at least 12%.
- Fasteners that incorporate a reduced section should satisfy the following conditions:
  - For fasteners loaded in tension, the strength  $N_{uk}$  of the reduced section should either be greater than 1.1-times of the yield strength  $N_{yk}$  of the unreduced section or the stressed length of the reduced section should be  $\geq 5 \cdot d$  ( $d$  = fastening diameter outside reduced section).
  - For fasteners loaded in shear or which shall redistribute shear forces, the begin of the reduced section should either be  $\geq 5 \cdot d$  below the concrete surface or in the case of a threaded fastener the threaded part should extend  $\geq 2 \cdot d$  into the concrete.
  - For fasteners loaded in combined tension and shear, the two conditions given above should be met.
- The steel fixture should be embedded in the concrete or fastened to the concrete surface without an intermediate layer or with a leveling layer of mortar with a compressive strength  $\geq 30 \text{ N/mm}^2$  and a thickness  $\leq d/2$ .
- The diameter of the clearance hole in the fixture should be smaller than the values given in the relevant European Technical Approval or CEN Product Standard.

#### 14.4.14.2 Loads on fastenings

It may be assumed that all fasteners are stressed up to their design resistance without taking into account compatibility conditions. The conditions given in sections a) to e) should be met.

- For design purposes, the compressive stress between fixture and concrete may be assumed to be a rectangular stress block with  $\sigma_c = 3 \cdot f_{cd}$ .
- The location of the resultant compression force  $C_{Sd}$  shall be determined based on rigid or flexible base plate behaviour in accordance with the following:
  - Rigid base plate behaviour

For a rigid base plate behaviour the compressive force is assumed to occur at the extreme edge of the base plate as shown in Fig. 14.42. For a rigid base plate behaviour to occur, the base plate must be of sufficient thickness to prevent yielding of the fixture at the edge of the attached member on the compression side of the fixture. The minimum base plate thickness may be determined by satisfying equation (14.72).

$$M_{yd} > C_{Sd} \cdot a_4 \quad (14.72)$$

where:

$M_{yd}$  = design moment that causes yielding of the fixture calculated with

$$f_{yd} = f_{yk} / \gamma_{Ms}$$

$C_{Sd}$  = design resultant compressive force

$a_4$  = distance from the edge of attached member to the resultant compressive force

The value of  $\gamma_{Ms}$  for use in a country may be found in the National Annex to CEN Technical Specification (*European Committee for Standardisation* (2004)). The recommended value is  $\gamma_{Ms} = 1.1$ .

- Flexible base plate behaviour

In case of a flexible base plate behaviour, the

distance  $a_5$ , between the edge of the attached member and the resultant of the compressive reaction may be calculated according to equation (14.73) (see Fig. 14.43).

$$a_5 = M_{yd} / C_{Sd} \quad (14.73)$$

Conservatively, it may be assumed that the compressive reaction is located at either the

edge or centroid of the compression element of the attached member.

- c) For both cases (rigid base plate behaviour and flexible base plate behaviour) the formation of a hinge in the base plate on the tension side of the connection shall be prevented by satisfying equation (14.74) (see Fig. 14.44).

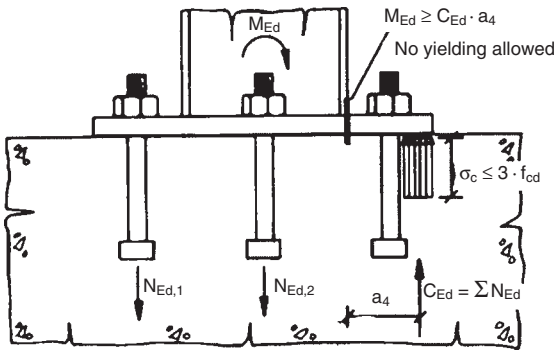


Fig. 14.42 Rigid base plate behaviour

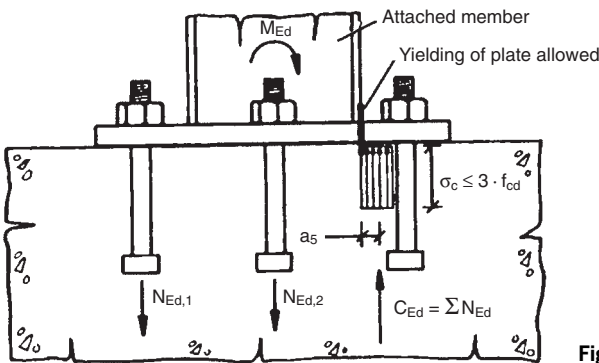


Fig. 14.43 Flexible base plate behaviour

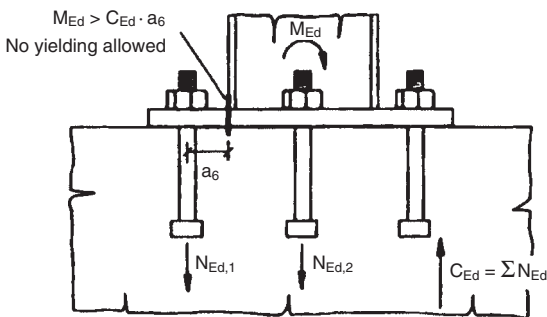
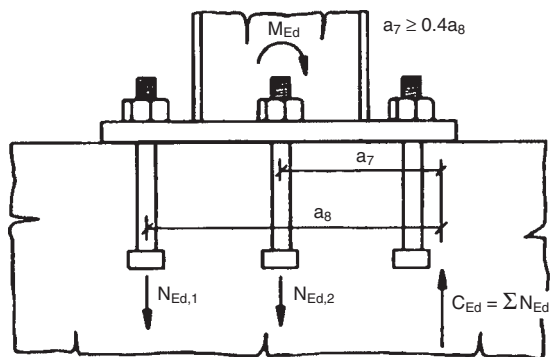


Fig. 14.44 Prevention of yielding of the fixture at the tension side of the connection



**Fig. 14.45** Condition for fasteners transferring a tension force equal to the yield force

$$M_{yd} > T_{Sd} \cdot a_6 \quad (14.74)$$

where:

$T_{Sd}$  = sum of the design tension forces of the outermost row of fastenings

- d) Only those fastenings that satisfy equation (14.75) shall be assumed to transfer a tension force (see Fig. 14.45)

$$a_7 \geq 0.4 \cdot a_8 \quad (14.75)$$

where:

$a_7$  ( $a_8$ ) = distance between the resultant compression force and the innermost (outermost) tensioned fastener

- e) It may be assumed that all fasteners or only a part of the fasteners carry shear load. The shear load taken by the individual fasteners of a group may be different. With the plastic design approach, the area of fastener steel may be reduced in comparison with an elastic design approach. However, the required anchorage depth and edge distance may be larger than for the elastic design approach, to preclude a concrete failure.

#### 14.4.14.3 Design of fastenings

In general the complete fastening is checked according to equation (14.23). Therefore the required verifications are written for the group.

##### 14.4.14.3.1 Partial safety factors

In general partial safety factors used for actions and resistances in the elastic design are also applicable for design based on plastic analysis,

except for steel failure. The partial safety factor for steel  $\gamma_{Ms,pl}$  is applied to the yield strength  $f_{yk}$ . The value of  $\gamma_{Ms,pl}$  for use in a country may be found in the National Annex to CEN Technical Specification (*European Committee for Standardisation* (2004)). The recommended value is  $\gamma_{Ms,pl} = 1.2$ .

##### 14.4.14.3.2 Resistance to tension load

###### a) Required verifications

The required verifications are summarised in Table 14.18.

**Table 14.18** Required verifications for tension loading (plastic design)

	Fastener group
Steel failure	$N_{Ed}^g \leq N_{Rk,s}^g / \gamma_{Ms,pl}$
Pull-out failure	Equation (14.77)
Concrete cone failure	Equation (14.78)
Splitting failure	See section e)

###### b) Steel failure

The characteristic resistance  $N_{Rk,s}$  of one fastener in case of steel failure may be calculated according to equation (14.76).

$$N_{Rk,s} = A_s \cdot f_{yk} \quad (14.76)$$

The characteristic resistance of a group of tensioned fasteners  $N_{Rk,s}^g$  may be taken as the sum of characteristic resistances of the fasteners loaded in tension.

**c) Pull-out failure**

The characteristic resistance  $N_{Rk,p}$  of one fastener in case of pull-out failure is given in the relevant European Technical Approval or CEN Product Standard. The pull-out resistance of all tensioned fasteners shall meet equation (14.77).

$$\frac{N_{Rk,p}}{\gamma_{Mp}} \geq 1.25 \cdot \frac{N_{Rk,s}}{\gamma_{Ms,pl}} \cdot \frac{f_{uk}}{f_{yk}} \quad (14.77)$$

**d) Concrete cone failure**

Section 14.4.6.2.1c applies without modification. The resistance in case of concrete cone failure of all tensioned fasteners shall meet equation (14.78).

$$\frac{N_{Rk,c}}{\gamma_{Mc}} \geq 1.25 \cdot \frac{N_{Rk,s}^g}{\gamma_{Ms}} \cdot \frac{f_{uk}}{f_{yk}} \quad (14.78)$$

**e) Splitting failure**

No proof of splitting failure is required if condition 1) and at least one of the conditions 2) or 3) are fulfilled.

- 1) Splitting failure is avoided by applying equation (14.78), where  $N_{Rk,c}$  is replaced by  $N_{Rk,sp}$  according to equation (14.12) for headed anchors, post-installed anchors – mechanical and chemical systems and according to equation (14.54) for anchor channels.
- 2) The edge distance in all directions is  $c \geq 1.0 \cdot c_{cr,sp}$  for single fasteners and  $c \geq 1.2 \cdot c_{cr,sp}$  for fastener groups and the member depth is  $h \geq h_{min}$  in both cases.
- 3) With fasteners for use in cracked concrete, the characteristic resistance for concrete cone failure and pull-out failure is calculated for cracked concrete and reinforcement limits the crack width to  $w_k \leq 0.3$  mm.

**14.4.14.3.3 Resistance to shear load****a) Required verifications**

The required verifications are summarised in Table 14.19.

**b) Steel failure**

The characteristic resistance  $V_{Rk,s}$  of one fastener in case of steel failure may be calculated according to equation (14.79).

$$V_{Rk,s} = 0.5 \cdot A_s \cdot f_{yk} \quad (14.79)$$

**Table 14.19** Required verifications for shear loading (plastic design)

	Fastener group
Steel failure, shear load without lever arm	$V_{Ed}^g \leq V_{Rk,s}^g / \gamma_{Ms,pl}$
Concrete pry-out failure	Equation (14.80)
Concrete edge failure	Equation (14.81)

The characteristic resistance of a group of tensioned fasteners  $V_{Rk,s}^g$  may be taken as the sum of characteristic resistances of the fasteners loaded in shear.

**c) Concrete pry-out failure**

Sections 14.4.6.2.2b (for headed fasteners and post-installed anchors – mechanical systems), section 14.4.7.2.2 (for anchor channels) and section 14.4.9.2 (for post-installed anchors – chemical systems) apply without modifications. To satisfy equation (14.72) the resistance in case of concrete pry-out failure of all sheared fasteners shall meet equation (14.80).

$$\frac{V_{Rk,cp}}{\gamma_{Mc}} \geq 1.25 \cdot \frac{V_{Rk,s}^g}{\gamma_{Ms,pl}} \cdot \frac{f_{uk}}{f_{yk}} \quad (14.80)$$

This equation is satisfied if all fasteners are anchored with an anchorage depth so that equation (14.78) is met.

**d) Concrete edge failure**

Sections 14.4.6.2.2c (for headed fasteners and post-installed fasteners – mechanical systems and chemical systems) and section 14.4.7.2.2c (for anchor channels) apply without modification. The concrete edge resistance of all sheared fasteners shall meet equation (14.81).

$$\frac{V_{Rk,c}}{\gamma_{Mc}} \geq 1.25 \cdot \frac{V_{Rk,s}^g}{\gamma_{Ms,pl}} \cdot \frac{f_{uk}}{f_{yk}} \quad (14.81)$$

**14.4.14.3.4 Resistance to combined tension and shear load**

For combined tension and shear loads the following equations shall be satisfied:

$$\beta_N \leq 1 \quad (14.82a)$$

$$\beta_V \leq 1 \quad (14.82b)$$

$$\beta_N + \beta_V \leq 1 \quad (14.82c)$$

where:

$$\beta_N = \frac{N_{Ed}}{N_{Rd}}$$

$$\beta_V = \frac{V_{Ed}}{V_{Rd}}$$

## 14.5 Design of fastenings with cast-in and post-installed metal anchors according to ACI 318-05, Appendix D

### 14.5.1 General

Appendix D of ACI 318-05 (*American Concrete Institute* (2005)) contains design provisions based on the CCD-method (CC-method) for the design of both cast-in and post-installed metal anchors. (The metric version of the 2005 edition of the ACI code is discussed here. As the final edits of the 2005 edition had not been completed at the time of publication, variations from the completed text may occur. We apologize in advance for any such errors.) The design provisions are intended to address anchors "...that transmit structural loads related to strength, stability, or life safety." Cast-in headed anchors and bolts as well as J- and L-bolts are incorporated in the provisions directly, provided that they conform to typical geometries capable of developing pull-out strengths in accordance with current experience. Post-installed anchors, metal expansion anchors and undercut anchors must be qualified in accordance with ACI 355.2-04 (*American Concrete Institute* (2001)), whereby specific values for concrete breakout, pull-out and shear capacity as well as the required material safety factors (phi factors) are established.

Appendix D of ACI 318-05 includes provisions for the design of anchors to resist seismic loads, provided the anchors are not located in a plastic hinge region where crack widths may exceed those anticipated by the design procedures. It excludes high-cycle fatigue loading and impact loads. While not specifically excluded, the design of anchors for compression loads is not addressed.

While elastic analysis is assumed for the determination of critical loads in accordance with the CCD-method, plastic analysis is permitted

where the nominal strength is controlled by ductile anchor failure provided that deformation compatibility is satisfied.

### 14.5.2 Scope

All possible configurations using cast-in headed anchors, bolts with supplementary bearing plates, J-bolts, L-bolts and post-installed metal anchors are admissible. Specialty cast-in inserts, through bolts, bonded anchors, grouted anchors and power-actuated fasteners are not included. Studs welded to embed plates are included; however, the embedded end of a group of cast-in anchors may not be joined by a common plate (as a means, for example, to increase the bearing area). The design provisions are applicable to a maximum anchor diameter of  $d_o = 50$  mm and a maximum embedment depth of  $h_{ef} = 635$  mm. Unlike the EOTA provisions (*European Organisation for Technical Approvals (EOTA)* (1997)) described in section 14.3, ACI places no limit on the number of anchors or spatial geometry associated with a group of anchors considered for analysis. From a practical standpoint, some consideration must be given to the limits of the base plate or other transmitting structure to effectively (and elastically) distribute applied loads to large anchor groups.

Appendix D of ACI 318-05 allows for other models to determine the nominal strength associated with anchors and anchor groups provided that these models are supported by "...comprehensive tests..." and that they are based on "...the 5 percent fractile of the basic individual anchor strength."

The provisions cover the use of fastenings in normal weight and light-weight concrete, whereby the value of the concrete cylinder compressive strength at 28 days ( $f'_c$ ) used for calculation purposes may not exceed  $f'_c = 69$  N/mm<sup>2</sup> (MPa) for cast-in anchors or  $f'_c = 55$  N/mm<sup>2</sup> (MPa) for post-installed anchors.

The minimum spacing and edge distance requirements in Appendix D of ACI 318-05 are intended to preclude splitting of the concrete.

The concrete in the region of the anchorage may be cracked or non-cracked. If analysis indicates no cracking of the concrete at service load lev-

els, then non-cracked concrete may be assumed. Where seismic loads are included in the design load combination, cracked concrete must be assumed for the design.

### 14.5.3 Design concept

The provisions of Appendix D of ACI 318-05 conform to the concepts of Load and Resistance Factor Design (LRFD), also commonly referred to in North America as Strength Design. Design resistances (strengths) are evaluated independently for each probable failure mode and assigned a specific capacity reduction factor ( $\phi$  factor). Design actions are established on the basis of an assessment for the controlling combination of factored loads (load combination). The basic requirement for strength as given in ACI 318 is shown in equation (14.82).

$$\text{Design Strength} \geq \text{Required Strength} \quad (14.83)$$

$$\phi(\text{Nominal Strength}) \geq U \quad (14.84)$$

where:

$\phi$  = strength reduction factor

$U$  = factored load combination

This approach bears many similarities to the partial safety factor approach used throughout Europe.

#### 14.5.3.1 Analysis for the ultimate limit state

The minimum required load combinations are defined by the applicable code, and are commonly derived from ASCE 7 (*American Society of Civil Engineers'* (2002)). Load combinations are developed on the basis of probability assessments for the likelihood that certain load types will occur and will occur in specific combinations. Therefore, the factor applied to a specific component of a load combination may change depending on the load combination being considered. Load combinations as given in Chapter 9 of ACI 318 are presented as equations (14.85) to (14.91).

$$U = 1.4 \cdot (D+F) \quad (14.85)$$

$$U = 1.2 \cdot (D+F+T) + 1.6 \cdot (L+H) + 0.5 \cdot (L_r \text{ or } S \text{ or } R) \quad (14.86)$$

$$U = 1.2 \cdot D + 1.6 \cdot (L_r \text{ or } S \text{ or } R) + (1.0 \cdot L \text{ or } 0.8 \cdot W) \quad (14.87)$$

$$U = 1.2 \cdot D + 1.6 \cdot W + 1.0 \cdot L + 0.5 \cdot (L_r \text{ or } S \text{ or } R) \quad (14.88)$$

$$U = 1.2 \cdot D + 1.0 \cdot E + 1.0 \cdot L + 0.2 \cdot S \quad (14.89)$$

$$U = 0.9 \cdot D + 1.6 \cdot W + 1.6 \cdot H \quad (14.90)$$

$$U = 0.9 \cdot D + 1.0 \cdot H + 1.6 \cdot H \quad (14.91)$$

where:

$D$  = dead loads, i.e., the weight of the building materials incorporated into the building

$L$  = live loads, i.e. loads other than environmental loads produced by the use and occupancy of the building

$L_r$  = live loads at roof level

$S$  = snow loads

$W$  = wind loads

$R$  = rain loads

$H$  = loads resulting from the weight and pressure of soil

$F$  = loads resulting from the weight and pressure of fluids with a well-defined density

$E$  = earthquake loads, i.e., load effects of seismic forces

In model building codes such as the *National Earthquake Hazard Reduction Program* (NEHRP) (2001) the probabilistic assessment of earthquake loads is made at the strength level; that is, the severity of the earthquake effects is assumed to correspond to significant levels of inelastic structure response. Correspondingly, the load factor applied to these effects is 1.0.

Load combinations must be correlated with the appropriate materials safety factors ( $\phi$  factors) in order to preserve the global factor of safety. Additional load combinations may be considered for cases not anticipated by the required combinations.

In ACI 318-05, Appendix D (*American Concrete Institute* (2005)) strength reduction factors ( $\phi$  factors) are associated with material type and failure mode, and are applied to characteristic resistances (5% fractile of resistance with a 90% confidence).

For steel failure modes, strength reduction factors are dependent on the mechanical properties



**Table 14.20** Strength reduction factors for steel failure modes

Loading type	Steel mechanical properties ASTM A307-04 assumed to qualify as ductile)	Strength reduction factor
Tension	Ductile – tensile elongation $\geq 14\%$ and reduction in area $\geq 30\%$	0.75
	Brittle – tensile elongation $< 14\%$ and/or reduction in area $< 30\%$	0.65
Shear	Ductile – tensile elongation $\geq 14\%$ and reduction in area $\geq 30\%$	0.65
	Brittle – tensile elongation $< 14\%$ and/or reduction in area $< 30\%$	0.60

**Table 14.21** Strength reduction factors for concrete breakout, side-face blow-out, pull-out or pry-out

Anchor type	Loading type	Supplementary reinforcement present?	Anchor category		
			1	2	3
Post-installed	Tension	Yes	0.75	0.65	0.55
		No	0.65	0.55	0.45
	Shear	Yes	0.75		
		No	0.70		
Cast-in	Tension	Yes	0.75		
		No	0.70		
	Shear	Yes	0.75		
		No	0.70		

of the steel element in question (see Table 14.20).

For concrete failure modes, strength reduction factors (see Table 14.21) are likewise dependent on whether the failure mode is expected to give warning of impending failure and whether failure of a single anchor will permit redistribution of load between anchors in a group. Additionally, strength reduction factors for concrete failure modes are influenced by the presence of "...supplementary reinforcement proportioned to tie the potential concrete failure prism into the structural member." Finally, the strength reduction factor for tension loads is dependent on the anchor reliability (anchor category) as determined by testing conducted according to ACI 355.2 (*American Concrete Institute* (2001)), whereby category 1 is assigned to the most reliable anchors.

Here it should be noted that while ACI 318-05, Appendix D provides no further guidance on

the type or orientation of supplementary reinforcement required to warrant the use of a larger phi factor, it is intended that this reinforcement should increase the ductility of the connection at failure. In order for this to occur, the supplementary reinforcement must satisfy displacement compatibility. In simplest terms the supplementary reinforcing should develop substantial tension forces (but remain elastic) prior to the attainment of the peak concrete fracture load. For tension loads, such reinforcement should be collinear with the anchor and designed to permit transfer of force from the anchor to the reinforcement in the manner of a reinforcing lap splice. For shear loads, hairpins placed at cover distance from the concrete surface and contacting the leading edge of the anchor at the apex of the bend are most effective. In most cases, orthogonal reinforcing oriented perpendicular to the direction of load will not be effective in substantially and consistently increasing anchorage ductility.

### 14.5.3.2 Serviceability limit state

While ACI 318-05, Appendix D does not contain specific checks for design at the serviceability limit state, Chapter 9 of the ACI code includes a general requirement that members shall "...ensure adequate performance at service load levels" whereby service loads are defined as loads determined without load factors. This may be construed as a requirement to ensure that the deformational response of the anchorage is not excessive. In addition, some safeguards on the calculated strength have been included in Appendix D in order to ensure good performance at service load levels.

### 14.5.4 Forces on anchors

ACI 318-05, Appendix D provides only nominal guidance for the establishment of anchor loads in a connection. Elastic response, whereby the anchor forces "...are considered to be proportional to the external load and its distance from the neutral axis of the anchor group", is assumed for concrete failure modes owing to the relatively small degree of load redistribution anticipated for these cases. Such an assumption can be made only if the base plate or attachment has a large flexural or shear stiffness relative to the axial stiffness of the anchors. Where significant load redistribution can be assured through the use of longer embedment depths and ductile steel, plastic design of, say, a base plate subjected to an overturning moment is accomplished through the assumption that all tension loaded anchors achieve yield.

For connections designed for regions of "...moderate or high seismic risk" or for "...structures that have been assigned to intermediate or high seismic performance or design categories", it is required that ductile yielding of the anchors controls the connection design unless it can be shown that the connection is capable of developing the yield capacity of the attachment (see section 14.5.7).

### 14.5.5 Characteristic resistances

#### 14.5.5.1 General

ACI 318-05, Appendix D requires that the following failure modes be evaluated for characteristic resistance:

- steel strength in tension
- steel strength in shear
- concrete breakout strength in tension
- concrete breakout strength in shear
- pull-out strength in tension
- concrete side-face blow-out strength in tension
- concrete pry-out strength in shear

Splitting failure is precluded through the specification of mandatory limits on edge distance, spacing and member thickness.

The requirement on resistance is given by equations (14.92) and (14.93).

$$\phi \cdot N_n \geq N_u \quad (14.92)$$

$$\phi \cdot V_n \geq V_u \quad (14.93)$$

where:

$\phi \cdot N_n$  = controlling characteristic tension strength

$\phi \cdot V_n$  = controlling characteristic shear strength

$N_u$  = factored tension load

$V_u$  = factored shear load

In addition, interaction of tension and shear must be evaluated in accordance with section 14.5.5.4.

All resistances are calculated for cracked concrete conditions but may be modified (increased) for cases where it may be assumed that cracking will not occur over the life of the anchorage.

#### 14.5.5.2 Tension resistance

Tension resistance is determined on the basis of the checks shown in Table 14.22. It may be assumed in each case that the capacity for an anchor group is based on the most critically loaded anchor.

**Table 14.22** Design checks required for tension loads

	Single anchor	Anchor group
Steel strength in tension	$\phi \cdot N_{sa} \geq N_u$	$\phi \cdot N_{sa} \geq N_u$
Pull-out strength in tension	$\phi \cdot N_{pn} \geq N_u$ ( $\phi \cdot N_p \geq N_u$ )	$\phi \cdot n \cdot N_{pn} \geq N_u$
Concrete breakout in tension	$\phi \cdot N_{cb} \geq N_u$	$\phi \cdot N_{cbg} \geq N_u$
Side-face blow-out strength in tension	$\phi \cdot N_{sb} \geq N_u$	$\phi \cdot N_{sbg} \geq N_u$

**a) Steel failure**

The characteristic axial tensile resistance of an anchor in the case of steel failure is given by equation (14.94).

$$N_{sa} = n \cdot A_{se} \cdot f_{uta} \quad (14.94)$$

In equation (14.94)  $f_{uta}$  represents the specified minimum axial tensile strength of the steel and is the tensile area of the steel component loaded in tension. In order to ensure good behaviour at service load levels, the value of  $f_{uta}$  is limited to the lesser of 190 percent of the yield value, i.e.,  $f_{uta} \leq 1.9 \cdot f_y$  or 862 N/mm<sup>2</sup> (MPa). The strength reduction factor of 0.75 for ductile fasteners is consistent with limitations on threaded fastener capacity established by the American Institute for Steel Construction.

It should be noted that in the expressions for pull-out and steel capacity, it is assumed that all anchors are uniformly loaded. In cases where the load distribution is not uniform, the critically loaded anchor should be checked as described in section 14.3.4.

**b) Pull-out/pull-through failure**

The characteristic resistance of a cast-in anchor is given by equation (14.95).

$$N_{pn} = \psi_4 \cdot N_p \quad (14.95)$$

where:

$$\begin{aligned} \psi_4 &= 1.0 \text{ for cracked concrete conditions} \\ &= 1.4 \text{ for non-cracked concrete conditions} \end{aligned}$$

The value of  $N_p$  is permitted in all cases to be determined as the 5 percent fractile of tests conducted in accordance with ACI 355.2 (*American Concrete Institute* (2001)). For cast-in headed anchors,  $N_p$  may be calculated on the basis of equation (14.96).

$$N_p = A_{brg} \cdot 8 \cdot f'_c \quad [\text{N}] \quad (14.96)$$

where:

$$\begin{aligned} A_{brg} &= \text{bearing area of the anchor head [mm}^2\text{]} \\ f'_c &= \text{specified concrete cylinder compressive strength [N/mm}^2\text{] ([MPa])} \end{aligned}$$

Note that in the CEN Technical Specification (*European Committee for Standardisation (CEN)* (2004)), the characteristic permissible bearing pressure is reduced ( $6 \cdot f_{ck,cube}$ ) in order to limit the displacement for cases where anchors are located in cracks that cycle open and closed over the life of the anchorage (see section 14.4.6.2.1 b).

For cast-in hooked bolts,  $N_p$  may be calculated on the basis of equation (14.97).

$$N_p = 0.9 \cdot f'_c \cdot e_h \cdot d_0 \quad [\text{N}] \quad (14.97)$$

where:

$$\begin{aligned} e_h &= \text{the distance as measured perpendicular to the shaft from the inner surface of the shaft of the J- or L-bolt to the outer tip of the J- or L-bolt [mm]} \\ d_0 &= \text{the diameter of the shaft [mm]} \end{aligned}$$

The characteristic resistance  $N_p$  of a post-installed anchor for a pull-out/pull-through failure depends on the design of the anchor and is derived from the results of approval tests in accordance with ACI 355.2 (*American Concrete Institute* (2001)).

**c) Concrete cone failure**

The CCD-method (see section 4.1.1.3) is used to calculate the characteristic resistance  $N_{cb}$  of a single anchor or group of anchors for concrete cone (breakout) failure. The expression for a single anchor is given as equation (14.98a).

$$N_{cb} = \frac{A_{Nc}}{A_{Nco}} \cdot \psi_{ed,N} \cdot \psi_{cp,N} \cdot \psi_{c,N} \cdot N_b \quad [\text{N}] \quad (14.98a)$$

For anchor groups, equation (14.98b) applies.

$$N_{cbg} = \frac{A_{Nc}}{A_{Nco}} \cdot \psi_{ec,N} \cdot \psi_{ed,N} \cdot \psi_{cp,N} \cdot \psi_{c,N} \cdot N_b \quad [\text{N}] \quad (14.98b)$$

The relevant terms in equations (14.98a) and (14.98b) are discussed below.

The base value  $N_b$  of the characteristic resistance of an anchor with large spacing and edge distance in cracked concrete is given by equation (14.98c):

$$N_b = k_c \cdot \sqrt{f'_c} \cdot h_{ef}^{1.5} \quad [\text{N}] \quad (14.98c)$$

where:

$f'_c$  = the specified concrete cylinder compressive strength [N/mm<sup>2</sup>] (MPa)

$h_{ef}$  = effective embedment depth [mm]

$k_c$  = coefficient for concrete breakout in cracked concrete conditions

The value of  $k_c$  is given as  $k_c = 10.0$  for headed cast-in anchors. For post-installed anchors, a minimum default of value of  $k_c = 7.0$  is provided; however, the actual values of  $k_c$  and  $\psi_{c,N}$  for a given anchor system should be derived from testing in cracked and non-cracked concrete in accordance with ACI 355.2 (*American Concrete Institute* (2001)).

The value of  $k_c = 10.0$  follows from equation (4.5b) with in the same manner as described in section 14.3.5.1c, whereby a factor of 0.75 for the conversion from mean to characteristic value is assumed, and an adjustment for the actual in situ vs. specified concrete strength is employed.

For cast-in headed anchors with an embedment depth  $280 \text{ mm} \leq h_{ef} \leq 635 \text{ mm}$ , Appendix D provides an alternate expression for  $N_b$  (see equation (14.98d)) that yields greater capacities than equation (14.98c).

$$N_b = 3.8 \cdot \sqrt{f'_c} \cdot h_{ef}^{5/3} \quad [\text{N}] \quad (14.98d)$$

The 5/3 exponent on  $h_{ef}$  is supported by tests with headed anchors at large embedment, whereby the significant degree of scatter associated with test results at large embedment requires a conservative approach.

The geometrical influence of spacings and edge distances on the characteristic resistance is taken into account by the ratio  $A_{Nc}/A_{Nco}$  in a manner identical to the EOTA Guidelines (see section 14.3.5.1), whereby  $A_{Nco}$  is the projected area of the failure surface of a single anchor remote from edges as given by equation (14.98e).

$$A_{Nco} = 9 \cdot h_{ef}^2 \quad [\text{mm}^2] \quad (14.98e)$$

$A_{Nc}$  is defined as the projected area of the failure surface for the anchor or group of anchors that may be approximated as the base of the rectangular geometrical figure that results from projecting the failure surface outward  $1.5 \cdot h_{ef}$  from the centrelines of the anchor, or in the case of a group of anchors, from a line through a row of adjacent anchors. In no case is  $A_{Nc}$  permitted to exceed  $n \cdot A_{Nc}$  where  $n$  is the number of tension loaded anchors in the group.

For cast-in headed anchors, Appendix D permits the calculation of  $A_{Nco}$  and  $A_{Nc}$  assuming a failure surface that projects horizontally  $1.5 \cdot h_{ef}$  from the effective perimeter of the head as opposed to the centreline of the anchor. For stiffness reasons, the overall effective perimeter is limited to the anchor shaft diameter plus  $2 \cdot t$  where  $t$  is the thickness of the head or bearing surface.

The factor  $\psi_{ed,N}$  takes into account the effect of proximate edges on the stress field around the anchor in a manner similar to  $\psi_{s,N}$  (see section 14.3.5.1c). For cast-in anchors, the value of the critical edge distance is assumed to be  $1.5 \cdot h_{ef}$ . Thus  $\psi_{ed,N}$  is given as per equation (14.98f).

$$\psi_{ed,N} = 0.7 + 0.3 \cdot \frac{c}{1.5 \cdot h_{ef}} \leq 1 \quad (14.98f)$$

In the case of post-installed anchors, the critical edge distance must be determined by test and the resulting value used to determine the additional modification factor for splitting given by equation (14.98g).

$$\psi_{cp,N} = \frac{c_{a,min}}{c_{ac}} \leq \frac{1.5 \cdot h_{ef}}{c_{ac}} \quad \text{if } c_{a,min} < c_{ac} \quad (14.98g)$$

The factor  $\psi_{ec,N}$  accounts for the effect of eccentric tension loads on the capacity of anchor

groups (see  $\psi_{ec,N}$  in section 14.3.5.1c) in accordance with equation (14.98h).

$$\psi_{ec,N} = \frac{1}{1 + \frac{2 \cdot e'_N}{3 \cdot h_{ef}}} \leq 1 \quad (14.98h)$$

where:

$e'_N$  = eccentricity of the resultant tensile force acting on the tension loaded anchors related to their geometrical centre of gravity

Equation (14.98h) is valid for  $e'_N \leq s/2$ .

The  $\psi_{c,N}$  term takes into account the influence of the position of an anchorage relative to cracks in the concrete:

$\psi_{c,N} = 1.00$  for anchorages in concrete that may experience cracking in the anchor vicinity over the life of the anchorage  
 $= 1.25$  for cast-in anchors in concrete that will remain non-cracked in the anchor vicinity over the life of the anchorage  
 $= 1.40$  for post-installed anchors in non-cracked concrete when  $k_c = 7$  is assumed

For post-installed anchors that have been tested in accordance with ACI 355.2 (*American Concrete Institute* (2001)), the value of  $\psi_{c,N}$  is determined by test.

For cases where the concrete breakout surface is bounded by edges in three or more orthogonal directions, evaluation of the term  $(A_{Nc}/A_{Nco})$  represents a function that has a maximum value at  $h_{ef} = c_{a,max}/1.5$ . For anchorages with three or more proximate edges the largest of which is  $c_{a,max} \leq 1.5 \cdot h_{ef}$ . Appendix D permits an adjustment to  $h_{ef}$  as follows.

For the purposes of evaluating equations (14.98c) to (14.98h),  $h_{ef}$  may be taken as the greater of  $c_{a,max}/1.5$  and  $s_{a,max}/3$  where  $s_{a,max}$  is

the maximum spacing of the tension loaded anchors in an anchor group. In general, this adjustment recognizes the inability of the  $(A_{Nc}/A_{Nco})$  term to accurately account for the edge effects in this case. It may also be thought of as providing the upper bound on the concrete breakout tension capacity for cases where splitting is more likely to control.

#### d) Side-face blow-out

ACI 318-05, Appendix D limits the tension capacity of single headed anchors located near an edge ( $c < 0.4 \cdot h_{ef}$ ) by the expression given in equation (14.99) to account for the side-face blow-out failure mode.

$$N_{sb} = 13.3 \cdot c \cdot \sqrt{A_{brg} \cdot f'_c} \quad [N] \quad (14.99a)$$

For the case of a single anchor in a corner with orthogonal edge distances  $c$  and  $c_2$  whereby  $c < c_2 < 3 \cdot c$ , the expression for  $N_{sb}$  must be further modified as shown in equation (14.99b).

$$N_{sb} = 13.3 \cdot c \cdot \sqrt{A_{brg} \cdot f'_c} \cdot \left( \frac{1 + \frac{c_2}{c}}{4} \right) \quad [N] \quad (14.99b)$$

For the case of multiple headed anchors located near an edge ( $c < 0.4 \cdot h_{ef}$ ) where the spacing between individual anchors is less than  $6 \cdot c$ , the tension capacity is limited by the expression given in equation (14.99c).

$$N_{sbg} = \left( 1 + \frac{s_o}{6 \cdot c} \right) \cdot N_{sb} \quad [N] \quad (14.99c)$$

In equation (14.99c), the term  $s_o$  represents the spacing of the outer anchors along the edge in the group, and  $N_{sb}$  is given by equation (14.99a) regardless of the proximity of other edges.

#### 14.5.5.3 Shear resistance

Shear resistance is determined on the basis of the checks shown in Table 14.23.

**Table 14.23** Design checks required for shear loads

	Single anchor	Anchor group
Steel strength in shear	$\phi \cdot V_{sa} \geq V_u$	$\phi \cdot V_{sa} \geq V_u$
Concrete breakout in shear	$\phi \cdot V_{cb} \geq V_u$	$\phi \cdot V_{cbg} \geq V_u$
Pry-out strength in shear	$\phi \cdot V_{cp} \geq V_u$	$\phi \cdot V_{cpg} \geq V_u$

### a) Steel failure

The characteristic shear resistance  $V_{sa}$  of cast-in headed anchors in the case of steel failure is given by equation (14.100a).

$$V_{sa} = n \cdot A_{se} \cdot f_{uta} \quad [\text{N}] \quad (14.100a)$$

where  $f_{uta}$  represents the specified minimum axial tensile strength of the steel and  $A_{se}$  is the tensile area of the steel component loaded in tension and is limited to the lesser of  $1.9 \cdot f_y$  or  $862 \text{ N/mm}^2$  (MPa) to ensure that the anchor stress does not exceed  $f_y$  at service load levels. It is assumed that the headed anchors are welded to a steel plate having dimensions sufficient to induce contraflexure in the stud(s) at peak load.

The nominal shear resistance of cast-in headed bolts and hooked bolts is given by equation (14.100b).

$$V_{sa} = n \cdot 0.6 \cdot A_{se} \cdot f_{uta} \quad [\text{N}] \quad (14.100b)$$

In contrast to the case of a welded headed anchor, the anchor shaft is assumed to freely rotate at the concrete surface leading to increased flexural stress.

The nominal shear resistance of post-installed anchors with a bolt of constant cross-section and without a sleeve may be calculated with equation (14.100b). For sleeve anchors, internally threaded anchors, or anchors where the anchor shaft does not have a constant cross-section, the characteristic shear resistance must be established by test.

### b) Concrete breakout failure

The characteristic resistance of a single anchor failing in shear via breakout of the concrete at the edge in the direction of shear load application is given by equation (14.101a).

$$V_{cb} = \frac{A_{Vc}}{A_{Vco}} \cdot \psi_{ed,V} \cdot \psi_{h,V} \cdot \psi_{c,V} \cdot V_b \quad [\text{N}] \quad (14.101a)$$

For anchor groups loaded in shear failing by concrete edge breakout, equation (14.101b) is relevant.

$$V_{cbg} = \frac{A_{Vc}}{A_{Vco}} \cdot \psi_{ec,V} \cdot \psi_{ed,V} \cdot \psi_{h,V} \cdot \psi_{c,V} \cdot V_b \quad [\text{N}] \quad (14.101b)$$

The term  $A_{Vc}/A_{Vco}$  accounts for group effects, near edges and member thickness in accordance with the CCD method and the EOTA Guidelines (see section 14.3.5.2d).  $A_{Vc}$  is defined as projected area of the failure surface on the side of the concrete member at its edge for a single anchor or a group of anchors. It may be taken as the base of a truncated half pyramid projected on the side face of the member where the top of the half pyramid is given by the axis of the anchor row selected as critical. The value of  $c_{al}$  is taken as the distance from this axis to the edge perpendicular to the shear force. In no case can  $A_{Vc}$  be evaluated as greater than  $n \cdot A_{Vc}$  where  $n$  is the number of anchors in the group.

$A_{Vco}$  is the projected area of a single anchor in a deep member with a distance from edges equal or greater than  $1.5 \cdot c_{al}$  in the direction perpendicular to the applied shear force. It may be taken as the area of the base of a half pyramid with a side length parallel to the edge of  $3 \cdot c_{al}$  and a depth of  $1.5 \cdot c_{al}$ , yielding the expression given in equation (14.101c).

$$A_{Vco} = 4.5 \cdot c_{al}^2 \quad [\text{mm}^2] \quad (14.101c)$$

Where a group of welded studs are arrayed at varying distances from the relevant edge, it is permitted to evaluate the group capacity based on the capacity of the anchors most distant from the edge. For other anchor groups this approach is acceptable as well; however, detailing provisions as required to prevent premature failure of the anchors nearest the edge must be employed. Otherwise, the capacity should be based on the capacity of the anchors nearest to the edge.

The basic concrete breakout strength of an anchor loaded in shear is given by equation (14.101d).

$$V_b = 0.6 \cdot \left( \frac{\ell}{d_o} \right)^{0.2} \cdot \sqrt{d_o} \cdot \sqrt{f_c'} \cdot c_{al}^{1.5} \quad [\text{N}] \quad (14.101d)$$

whereby the term  $d_o$  is the anchor diameter (at the concrete surface) and the term  $\ell$  is the anchor load-bearing length in shear, not to exceed  $8 \cdot d_o$ . For anchors with constant flexural stiffness over the full length of the embedded portion of the anchors,  $\ell \leq h_{ef}$ . For sleeve-type anchors with a discontinuous sleeve,  $\ell \leq 2 \cdot d_o$ .

For headed anchors welded to a stiff plate, the basic shear resistance is increased as shown in equation (14.101e).

$$V_b = 0.66 \cdot \left( \frac{\ell}{d_o} \right)^{0.2} \cdot \sqrt{d_o} \cdot \sqrt{f_c'} \cdot c_{a1}^{1.5} \quad [\text{N}] \quad (14.101e)$$

The factor  $\psi_{ed,V}$  takes into account the effect of proximate edges on the stress field around the anchor in a manner similar to  $\psi_{s,V}$  (see section 14.3.5.2d). For  $c_{a2} < 1.5 \cdot c_{a1}$ ,  $\psi_{ed,V}$  is given by equation (14.101f).

$$\psi_{ed,V} = 0.7 + 0.3 \cdot \frac{c_{a2}}{1.5 \cdot c_{a1}} \leq 1 \quad (14.101f)$$

For  $c_{a2} \geq 1.5 \cdot c_{a1}$ ,  $\psi_{ed,V}$  is taken as 1.0.

The factor  $\psi_{ec,V}$  is employed for anchor groups loaded in shear where, as viewed in plan, the shear resultant is eccentric to the centroid of the group. It is identical to the  $\psi_{ec,V}$  term described in section 14.3.5.2d and is given by equation (14.101g).

$$\psi_{ec,V} = \frac{1}{1 + \frac{2 \cdot e_V'}{3 \cdot c_{a1}}} \leq 1 \quad (14.101g)$$

Where the loading is such that only some of the anchors in a group are loaded in shear in the same direction, only those anchors loaded in shear in the same direction are considered when determining the eccentricity  $e_V'$ .

Where anchors loaded in shear are influenced by three or more edges and any edge distance is less than  $1.5 \cdot c_{a1}$ , the value of  $c_{a1}$  to be used in equations (14.101c) to (14.101g) may be taken as equal to or less than the greater of  $c_{a2}/1.5$ ,  $h_a/1.5$ , and one-third of the maximum anchor spacing of the anchors within the group where  $h_a$  is the member thickness. This adjustment avoids an overly conservative estimate of the shear capacity for such cases.

Additionally, for cases where the member thickness  $h_a < 1.5 \cdot c_{a1}$ , the term  $\psi_{h,V}$  as given by equation (14.101h) should be employed in order to avoid excessive conservatism in the shear resistance calculation.

$$\psi_{h,V} = \left( 1.5 \cdot \frac{c_{a1}}{h_a} \right)^{1/3} \geq 1 \quad (14.101h)$$

This term is identical to that specified in the EOTA Guidelines (section 14.5.3.2d).

The  $\psi_{c,V}$  term takes into account the influence of the position of an anchorage relative to cracks in the concrete:

$$\begin{aligned} \psi_{c,V} &= 1.00 \quad \text{for anchorages in concrete that may experience cracking in the anchor vicinity over the life of the anchorage} \\ &= 1.20 \quad \text{for anchors in cracked concrete with supplementary reinforcement having a diameter 13 mm or greater} \\ &= 1.40 \quad \text{for anchors in non-cracked concrete, i.e., where the concrete in the anchor vicinity can be assumed to remain non-cracked for the life of the anchorage, or for anchors in cracked concrete with supplementary reinforcement having a diameter 13 mm or greater that is in turn enclosed by stirrups having a spacing not greater than 100 mm} \end{aligned}$$

It should be noted that the supplementary reinforcement is assumed to be an edge bar located between the anchorage and the edge of the concrete and positioned sufficiently near the concrete fracture surface that it will engage the concrete fracture surface. The enclosure of such an edge bar with stirrups theoretically permits the development of a strut and tie mechanism between the anchor and the bar intersection points. These increases for supplementary reinforcement in the cracked concrete case should be used with caution. For effective shear resistance increase, it is recommended that hairpins located near the surface and contacting the leading face of the anchor be used.

For shear loads parallel to the edge, the resistance associated with concrete edge failure is given as twice the resistance associated with shear perpendicular to the edge with  $\psi_{ed,V} = 1.0$ . No provisions for intermediate load angles are provided; however, use of a vector approach (circular interaction) has been proposed.



**c) Concrete pry-out failure**

The resistance of a single anchor loaded in shear associated with concrete pry-out failure is given by equation (14.102).

$$V_{cp} = k_{cp} \cdot N_{cb} \quad (14.102)$$

whereby  $k_{cp}$  is a constant given as follow:

$$\begin{aligned} k_{cp} &= 1.0 \text{ for cases where } h_{ef} < 65 \text{ mm} \\ &= 2.0 \text{ for cases where } h_{ef} \geq 65 \text{ mm} \end{aligned}$$

The resistance of a group of anchors loaded in shear associated with concrete pry-out failure is given by equation (14.103).

$$V_{cpg} = k_{cp} \cdot N_{cbg} \quad (14.103)$$

These expressions provide a conservative estimate of the resistance associated with pry-out failure.

**14.5.5.4 Combined tension and shear**

For cases involving simultaneous imposition of shear and tension loads, the following conditions must be satisfied:

$$\begin{aligned} \text{if } & V_u \leq 0.2 \cdot \phi \cdot V_n \\ \text{then } & \phi \cdot N_n \leq N_u \end{aligned} \quad (14.104a)$$

$$\begin{aligned} \text{if } & N_u \leq 0.2 \cdot \phi \cdot N_n \\ \text{then } & \phi \cdot V_n \leq V_u \end{aligned} \quad (14.104b)$$

$$\begin{aligned} \text{if } & N_u > 0.2 \cdot \phi \cdot N_n \text{ and } V_u > 0.2 \cdot \phi \cdot V_n \\ \text{then } & \frac{N_u}{\phi \cdot N_n} + \frac{V_u}{\phi \cdot V_n} \leq 1.2 \end{aligned} \quad (14.104c)$$

This may be recognised as a restatement of the tri-linear interaction condition specified in the EOTA Guidelines (see section 14.3.5.3), and it represents a simplified expression of the usual 5/3 exponential function as given in equation (14.104d):

$$\left( \frac{N_u}{\phi \cdot N_n} \right)^{5/3} + \left( \frac{V_u}{\phi \cdot V_n} \right)^{5/3} \leq 1 \quad (14.104d)$$

**14.5.6 Required edge distances, spacings and member thicknesses to preclude splitting failure**

Where supplementary reinforcement is not provided to control splitting, the following minimum dimensions are required:

Minimum centre-to-centre anchor spacing:

- For cast-in anchors that remain untorqued:  $4 \cdot d_o$
- For torqued cast-in and post-installed anchors:  $6 \cdot d_o$

Minimum edge distance:

- For cast-in anchors that remain untorqued: minimum cover requirements
- For torqued cast-in anchors:  $6 \cdot d_o$
- For post-installed anchors: as determined by test, but not less than minimum cover requirements or twice the maximum aggregate size.

In lieu of testing, the following default minimum edge distances are given for post-installed anchors:

- Default for undercut anchors:  $6 \cdot d_o$
- Default for torque-controlled anchors:  $8 \cdot d_o$
- Default for displacement-controlled anchors:  $10 \cdot d_o$

For anchors that do not generate splitting forces during installation and that will remain untorqued, smaller edge distances and spacings than those given above are permitted if a fictitious anchor diameter  $d'_o$  is used for all resistance calculations, whereby  $d'_o$  is determined such that the required edge distance and spacing calculations are fulfilled.

For cases where the critical edge distance has not been established for post-installed anchors by test, the following default values are given:

- Default for undercut anchors:  $2.5 \cdot h_{ef}$
- Default for torque-controlled anchors:  $4 \cdot h_{ef}$

- Default for displacement-controlled anchors:  
 $4 \cdot h_{ef}$

The anchor embedment  $h_{ef}$  is not permitted to exceed the greater of  $(2 \cdot h_a / 3)$  or  $(h_a - 100 \text{ mm})$  where  $h_a$  is the member thickness. Note that this limit of  $h_{ef} \leq 1.5 \cdot h_a$  is substantially less than the limit of  $h_{ef} \leq 2 \cdot h_a$  established in the EOTA Guidelines. This accounts for the relatively conservative values for the critical edge distance absent test values to justify smaller values. Such tests are to be conducted in the minimum member thickness proposed for the post-installed anchor in question.

#### 14.5.7 Resistance where load cases include seismic forces

Where the design of an anchorage includes seismic forces (anchors in seismic zones classified as having moderate or high seismic risk), the following additional considerations are required:

- Anchors may not be located in so-called plastic hinge regions of reinforced concrete members. Such zones are expected to exhibit extensive fracture and spall in response to inelastic deformations of shear walls and frame members, and such conditions are not anticipated in the seismic qualification procedures for post-installed anchors, nor have they been investigated for cast-in systems.
- Post-installed anchors must be pre-qualified through a seismic simulation test regime including the effects of concrete cracking (crack opening  $\Delta w = 0.5 \text{ mm}$ ).
- Anchors are assigned a reduced capacity equal to 75% of the calculated controlling capacity, i.e.,  $0.75 \cdot \phi \cdot N_n$  and  $0.75 \cdot \phi \cdot V_n$ .
- Anchor resistance must be governed by steel failure of a ductile steel element, or the anchors must be designed to develop the yield capacity of a ductile steel attachment to which the anchors are connected. In this case, the maximum load that the anchors will experience is limited by the ductile yielding of the attachment.

It should be noted that most post-installed anchors are not suited to adaptation for ductile failure, particularly in cases where the anchors

are used in groups or with near edges. It is therefore advisable to look for yielding mechanisms that will protect the anchors from overload.

While these provisions are substantially more robust than previous codes governing the use of anchors to resist seismic forces, they cannot be expected to provide absolute protection against anchor failure in a design earthquake. They do, however, offer a guide to intelligent detailing and the conservative assignment of resistances necessary to ensure some measure of ductile response.

#### 14.5.8 Provisions of ACI 349-01 Appendix B

ACI 349-01 (*American Concrete Institute* (2001/1)) guides the proper design of concrete structures "...which form part of a nuclear power plant and which have nuclear safety-related functions..." It does not cover the design of reactor vessels and concrete containment structures. Appendix B contains the provisions for the design of cast-in and post-installed anchors in concrete. In most respects, Appendix B is identical to ACI 318-02, Appendix D (metric conversions are provided in a separate appendix). The most significant differences are discussed below.

##### 14.5.8.1 Scope

ACI 349-01 Appendix B covers the design of post-installed grouted anchorages (cementitious and polymer grouts) as well as cast-in anchors and post-installed mechanical anchors. No specific design provisions for grouted anchorages are included, however.

Concrete types other than normal weight concrete are not included.

Impact and impulse loads are included.

##### 14.5.8.2 Ductile design requirements

Regardless of seismic zone or hazard, all anchorages are required to satisfy specific requirements for ductile response as follows:

- Anchorage design is to be controlled by the strength of the anchorage steel, i.e. concrete failure modes are not permitted. This condition is assumed to be satisfied if the condi-

**Table 14.24** Design checks required for ductile anchors according to ACI 349-01, Appendix B

		Single anchor	Anchor group
Tension	A	$A_{se} \cdot f_{uta} < 0.85 \cdot \min(N_{cb}, N_{pn}, N_{sb})$	$A_{se} \cdot f_{uta} < 0.85 \cdot \min(N_{cbg}, n \cdot N_{pn}, N_{sbg})$
	B	$A_{se} \cdot f_y < 0.75 \cdot \min(\phi \cdot N_{cb}, \phi \cdot N_{pn}, \phi \cdot N_{sb})$	$A_{se} \cdot f_y < 0.75 \cdot \min(\phi \cdot N_{cbg}, \phi \cdot n \cdot N_{pn}, \phi \cdot N_{sbg})$
Shear	A	$0.65 \cdot A_{se} \cdot f_{ut} < 0.85 \cdot V_{cb}$	$0.65 \cdot A_{se} \cdot f_{ut} < 0.85 \cdot V_{cbg}$
	B	$A_{se} \cdot f_y < 0.75 \cdot \min(\phi \cdot V_{cb}, \phi \cdot V_{cp})$	$A_{se} \cdot f_y < 0.75 \cdot \min(\phi \cdot V_{cbg}, \phi \cdot V_{cpg})$

**Table 14.25** Design checks required for non-ductile anchors according to ACI 349-01, Appendix B

		Single anchor	Anchor group
Tension		$A_{se} \cdot f_y < 0.6 \cdot \min(\phi \cdot N_{cb}, \phi \cdot N_{pn}, \phi \cdot N_{sb})$	$A_{se} \cdot f_y < 0.6 \cdot \min(\phi \cdot N_{cbg}, \phi \cdot n \cdot N_{pn}, \phi \cdot N_{sbg})$
Shear		$A_{se} \cdot f_y < 0.6 \cdot \min(\phi \cdot V_{cb}, \phi \cdot V_{cp})$	$A_{se} \cdot f_y < 0.6 \cdot \min(\phi \cdot V_{cbg}, \phi \cdot V_{cpg})$

tions shown in Table 14.24 are met. Note that only one set of conditions, A or B, must be fulfilled for a given anchorage.

- Alternatively, it is permitted to design anchors as non-ductile provided that the resistances assigned to such anchors are reduced in accordance with Table 14.25.
- Ductile anchorages that incorporate a reduced plate section in the tension or shear load path must have an ultimate tensile strength at the reduced section that exceeds the yield strength of the unreduced section. For threaded anchor bolts, the length of thread in the load path must be at least two anchor diameters. These provisions are intended to encourage uniform yielding.
- Design strengths may be increased for impactive or impulsive loading in accordance with the Dynamic increase factors shown in Table 14.26, whereby plastic

response of the anchorage is permitted if the ductility requirements of Table 14.24 are satisfied.

### 14.5.8.3 Baseplate design

In ACI 349-01, Appendix B, anchors used in conjunction with built-up grout pads are assigned a resistance equal to 80 % of their nominal capacity. It is permitted, however, to include friction in the calculation of shear resistance of a baseplate connection, whereby the frictional coefficient for the baseplate-concrete interface is taken as 0.40 times the net compression normal force across the interface.

In addition, shear design may be based on the use of embedded structural (steel) shapes, fabricated shapes or shear lugs. In such cases the anchors are assumed to be fully yielded and the strength reduction factor for tension, compression, bending and all combinations thereof is taken as 0.90. For shear, the strength reduction factor is 0.55. The design of shear lugs is predicated on checking the following checks:

- The bearing resistance of the concrete or grout in contact with the shear lugs.
- The shear resistance of the concrete or grout in contact with the shear lugs, as modified by the confinement provided by adjacent tension loaded anchors.
- The concrete breakout resistance associated with nearby edges, whereby a projected area based on a 45-degree failure surface and a

**Table 14.26** Dynamic increase factors according to ACI 349-01, Appendix B

Reinforcing steel		Dynamic increase factor (DIF)
x 1000 [psi]	[MPa]	
40	275	1.20
50	345	1.15
60	414	1.10
Concrete		
Axial and flexural compression		1.25
Shear		1.10

limiting concrete stress of  $0.33 \cdot \sqrt{f'_c}$  are substituted for the CCD method. For this condition, a strength reduction factor of 0.85 is required.

The distribution of shear to individual shear lugs in an anchorage is based on the relative shear lug flexural stiffness.

Additionally, for the condition where the baseplate is embedded in the concrete (top surface flush with the concrete surface), use of the fol-

lowing friction coefficients is permitted for the shear design:

- Baseplate without shear lugs      0.9
- Baseplate with shear lugs      1.4  
(elastic design)

In such cases, the anchor resistance must be compared with both the external loads as well as the additional forces (i.e. normal forces) required to develop the frictional forces.

## References

- AISI 303 (1995): SAE/AISI Type 303, UNS S30300, SAE J1086: Numbering Metals and Alloys. Society of Automotive Engineers, Warrendale, Pennsylvania, USA, July 1995.
- AISI 304 (1995): SAE/AISI Type 304, UNS S30400, SAE J1086: Numbering Metals and Alloys. Society of Automotive Engineers, Warrendale, Pennsylvania, USA, July 1995.
- AISI 316 (1995): SAE/AISI Type 316, UNS S31600, SAE J1086: Numbering Metals and Alloys. Society of Automotive Engineers, Warrendale, Pennsylvania, USA, July 1995.
- American Concrete Institute, ACI Standard 349-90 (1990): Code Requirements for Nuclear Safety Related Concrete Structures, Appendix B – Steel Embedments, 1990.
- American Concrete Institute (2000): Provisional Test Method for Evaluating the Performance of Post-Installed Mechanical Anchors in Concrete, 2000.
- American Concrete Institute (2001): Evaluating the Performance of Post-Installed Mechanical Anchors in Concrete (ACI 355.2-04) and Commentary (ACI 355.2R-04), 2001.
- American Concrete Institute (2001/1): Code Requirements for Nuclear Safety Related Concrete Structures (ACI 349-01) and Commentary (ACI 349R-01). Appendix B – Anchorage to Concrete, 2001.
- American Concrete Institute (2005): Building Code Requirements for Structural Concrete (ACI 318-05) and Commentary (ACI 318R-05), 2005.
- American National Standards Institute (1994): ANSI B212.15-94; American National Standard for Cutting Tools – Carbide Tipped Masonry Drills and Blanks for Carbide – Tipped Masonry Drills, 1994.
- American Society for Testing Materials (1989): ASTM Standard E488-89: Standard Test Methods for Strength of Anchors in Concrete and Masonry Elements, 1989.
- American Society of Civil Engineers (2002): ASCE 7: Minimum Design Loads for Buildings and Other Structures (2002).
- Ammann, W. (1980): Static and dynamic long-term behavior of anchors. Special Publication SP 130-8, American Concrete Institute, Detroit, 1980.
- Anderson, N. S.; Meinheit, D. F. (2000): Design Criteria for Headed Stud Groups in Shear. Part 1 – Steel Capacity and Bach Edge Effects. PCI Journal, September-October 200, pp. 46–75.
- Anderson, N. S.; Meinheit, D. F. (2000/1): PCI Sponsored Headed Stud Research Program: Test Results and Comparisons to Existing Models.
- Anderson, N. S.; Meinheit, D. F. (2001): Steel Capacity of Headed Studs Loaded in Shear. In Eligehausen, R. (Editor): RILEM Proceedings PRO 21 „Connections Between Steel and Concrete“, RILEM Publications s.a.r.l. Cachan Cedex, pp. 202–211.
- Arnold, N.; Gümpel, P.; Heitz, T.; Pscheidl, P. (1997): Chloridinduzierte Korrosion von nichtrostenden Stählen in Schwimmballen-Atmosphären. Teil 1: Elektrolyt Magnesium-Chlorid (30%) (Chloride induced corrosion of stainless steel under indoor swimming pool atmospheres. Part 1: Electrolyte magnesium chloride (30 %)). Materials and Corrosion 48, pp. 679–686, 1997 (in German).
- Arnold, N.; Gümpel, P.; Heitz, T. (1998): Chloridinduzierte Korrosion von nichtrostenden Stählen in Schwimmballen-Atmosphären. Teil 2: Einfluß von Hypochloriten (Chloride induced corrosion of stainless steel under indoor swimming pool atmospheres. Part 2: Influence of hypochlorites). Materials and

- Corrosion 49, pp. 482–488, 1998 (in German).
- Arnold, N.; Gümpel, P.; Heitz, T. (1999): Chloridinduzierte Korrosion von nichtrostenden Stählen in Schwimmhallen-Atmosphären. Teil 3: Einfluß einer realen Schwimmhallen-Atmosphäre (Chloride induced corrosion of stainless steel under indoor swimming pool atmospheres. Part 3: Influence of real swimming pool atmosphere). *Materials and Corrosion* 50, pp. 140–145, 1999 (in German).
- ASTM A108-03 (2003): Standard Specification for Steel Bar, Carbon and Alloy, Cold-Finished. ASTM International, West Conshohocken, Pennsylvania, USA, 2003.
- ASTM A276-04 (2004): Standard Specification for Stainless Steel Bars and Shapes. ASTM International, West Conshohocken, Pennsylvania, USA, 2004.
- ASTM A307-04 (2004): Standard Specification for Carbon Steel Bolts and Studs, 60 000 PSI Tensile Strength. ASTM International, West Conshohocken, Pennsylvania, USA, 2004.
- ASTM A493-95 (2004): Standard Specification for Stainless Steel Wire and Wire Rods for Cold Heading and Cold Forging. ASTM International, West Conshohocken, Pennsylvania, USA, 2004.
- ASTM A510-03 (2003): Standard Specification for General Requirements for Wire Rods and Coarse Round Wire, Carbon Steel. ASTM International, West Conshohocken, Pennsylvania, USA, 2003.
- Asmus, J. (1999): Verhalten von Befestigungen bei der Versagensart Spalten des Betons (Behaviour of fasteners at concrete splitting). Doctor thesis, University of Stuttgart, 1999 (in German).
- Ballarini, R.; Shah, S. P.; Keer, L. M. (1986): Failure characteristics of short anchor bolts embedded in a brittle material. *Proceedings Royal Society London A* 404, 1986, pp. 35–54.
- Bashandy, T. R. (1996): Application of Headed Bars in Concrete Members. PhD Thesis, The University of Texas at Austin, December 1996.
- Basler, E.; Witta, E. (1967): Grundlagen für kraftschlüssige Verbindungen in der Vorfabrikation (Basis of connections in pre-fabrication). Beton-Verlag GmbH, 1967 (in German).
- Bauaufsichtliche Zulassungen (BAZ) (General approval certificates issued by DIBt). Editors: Breitschaft, G.; Reuter, F.; Wagner, O.: Erich Schmidt Verlag, Berlin, continuously published (in German).
- Bauer, C. O. (1970): Korrosionsschutz für Verbindungselemente (Corrosion protection for fasteners). *Industrie-Anzeiger*, 1970, Nos. 59 und 60 (in German).
- Bauer, C. O. (1980): Befestigungstechnik – Wettbewerb von Systemen (Fixing technology – competition of systems). *Bauingenieur* 55, 1980, No. 11, pp. 437–444 (in German).
- Bäumel, A.; Kügler, A. (1975): Meerwasserkorrosionsversuche an nichtrostenden Stählen in der Nordsee (Corrosion tests with stainless steels under seawater conditions in the North Sea). *Stahl und Eisen*, 1975, pp. 1061–1066 (in German).
- Bazant, Z. P. (1984): Size Effect in Blunt Fracture: Concrete, Rock, Metal. *Journal of Engineering Mechanics, ASCE*, 110, No. 4, April 1984, pp. 518–535.
- Bazant, Z.P.; Oh, B. (1983): Crackband theory of concrete. *Matériaux et Construction* 1983, Vol. 16, No. 93.
- Bazant, Z. P.; Ozbolt, J. (1990): Nonlocal Microplane Model for Fracture, Damage and Size Effect in Structures. *Journal of Engineering Mechanics, ASCE*, V. 116, No. 11, 1990.
- Bensimhon, J.; Lugez, J.; Combette, M. (1989): Study of the Performance of Anchor Bolts in the Tensile and Cracked Zone of Concrete. Report of Centre Scientifique et Technique du Batiment, Paris, 1989.
- Beratung Feuerverzinken (1983): Zink statt Rost (Zinc instead of corrosion). Eigenverlag der Beratung Feuerverzinken, Hagen, 1983 (in German).
- Bereiter, R. (1986): Befestigungen mit Setzbolzen (Fixings with power actuated fasteners). Lecture, given at the “Haus der Technik”, Essen, January 1986, not published (in German).
- Bergmeister, K. (1988): Stochastik in der Befestigungstechnik mit realistischen Einflußgrößen (Stochastics in fixing technology based on realistic influencing parameters). Doctor thesis, University of Innsbruck, 1988 (in German).

- Bergmeister, K. (1989): Neue Bemessung von Dübelverbindungen im Stahlbetonbau (New design of anchorages to reinforced concrete structures). Report No. 7/5–89/20 of the Institute of Construction Materials, University of Stuttgart, September 1989, not published (in German).
- Bertram, D. (1997): Stahl im Bauwesen (Steel in building construction). Beton-Kalender 1996, Part 1, pp. 149–276, Ernst & Sohn, Berlin, 1997 (in German).
- Block, K. (2001): Dübelbefestigungen unter ermüdungsrelevanten Einwirkungen (Anchors under fatigue actions). Thesis submitted for the certificate of habilitation, University of Dortmund, No. 25 der Berichte aus dem konstruktiven Ingenieurbau, July 2001 (in German).
- Block, K.; Dreier, F. (2002): Dübelbefestigungen bei ermüdungsrelevanten Einwirkungen (Anchors under fatigue actions). Mitteilungen des Deutschen Instituts für Bautechnik, pp. 98–105, Berlin, April 2002 (in German).
- Bock, H.-E.; Kügler, A.; Lennartz, G.; Michel, E. (1984): Das Verhalten von höherlegierten Stählen im Meerwasser (Behaviour of alloyed steels under sea water). Stahl und Eisen 104 (1984), No. 11, pp. 557–563 (in German).
- Bode, H.; Hanenkamp, W. (1985): Zur Tragfähigkeit von Kopfbolzen bei Zugbeanspruchung (Load-bearing capacity of headed anchors under tension loads). Bauingenieur, 1985, pp. 361–367 (in German).
- Böhni, H.; Haselmair, H.; Übeleis, A. (1992): Corrosion-resistant Materials for Fastenings in Road Tunnels - Field Tests in the Mont Blanc Tunnels. Structural Engineering International, 1992, No. 4, pp. 253–258.
- Bouwman, L. P. (1979): Fatigue of bolted connections and bolts loaded in tension. Report No. 6-79-9, Stevin Laboratory, Delft University of Technology, 1979.
- Bouwman, L. P.; Gresnigt, A. M.; Romeijn, A. (1989): Research into the Connection of Steel Base Plates to Concrete Foundations. Stevin Report 25.6.89-05/c6, 1989.
- Braestrup, M. W.; Nielsen, M. P.; Jensen, B. C.; Bach, F. (1976): Axisymmetric punching of plain and reinforced concrete. Report R. 75. Technical University of Denmark. Structural Research Laboratory, Copenhagen.
- Bruckner, M.; Eligehausen, R.; Ozbolt, J. (2001): Influence of bending compressive stresses on the concrete cone capacity. In Eligehausen, R. (Editor): Connections between Steel and Concrete. RILEM Publications s.a.r.l. Cashan Cedex, 2001.
- Burdette, E. G.; Sen, S.; Ismen, E. (1982): Effect of Abandoned Holes on Capacity of Wedge Bolts. Journal of the Structural Division, Proceedings of the American Society of Civil Engineers, Vol. 108, April 1982, pp. 743–753.
- Burdette, E. G.; Perry, T. C.; Runk, R. R. (1987): Load Relaxation Tests of Anchors in Concrete. In: Hasselwander, G. B. (Editor): Anchorage to Concrete. ACI SP-103, pp. 297–312, American Concrete Institute, Detroit.
- Cannon, R. W. (1981): Expansion Anchor Performance in Cracked Concrete. ACI-Journal, November/December 1981, pp. 471–479.
- Cannon, R. W.; Godfrey, D. A.; Moreadith, F. L. (1981): Guide to the Design of Anchor Bolts and Other Steel Embedments. Concrete International, July 1981, Vol. 3, No. 7, pp. 28–41. Discussion: Concrete International, July 1982, pp. 102–107.
- Cedolin, L.; Bazant, Z. P. (1980): Effect of Finite Element Choice in Blunt Crack Band Analysis. Computer Methods in Applied Mechanics and Engineering, 24 (1980), pp. 305–316.
- Cervenka, V.; Pukl, R.; Eligehausen, R. (1990): Computer Simulation of Anchoring Technique in Reinforced Concrete Beams. In Bicanic, N., Mang, H. (Editor): Computer Aided Analysis and Design of Concrete Structures, Pineridge Press, Swansea, 1990, pp. 1–19.
- Comité Euro-International du Béton (CEB) (1981): CEB-Manual Cracking and Deformations (Final Draft), Paris, 1981.
- Comité Euro-International du Béton (CEB) und Federation Internationale Precontrainte (FIP) (1993): CEP-FIP Model Code 1990, Thomas Telford Services Ltd, London, 1993.
- Comité Euro-International du Béton (CEB) (1994): Fastenings to Concrete and Masonry Structures: State-of-the-art report. Bulletin D'Information No. 216, Lausanne, published by Thomas Telford Services Ltd, London, 1994.



- Comité Euro-International du Béton (CEB) (1995): Design of Fastenings in Concrete. CEB Bulletin 226, pp. 1–144, Lausanne, 1995. Published by Thomas Telford Services Ltd. 1997.
- Cook, R. A. (1993): Behaviour of Chemically Bonded Anchors. Journal of Structural Engineering, American Society of Civil Engineers, V. 119, No. 9, Sept. 1993, pp. 2744–2762.
- Cook, R. A.; Klingner, R. E. (1989): Behavior and design of ductile multiple anchor steel to concrete connections. Report No. CTR 1126–3. University of Texas at Austin, 1989.
- Cook, R. A.; Doerr, G. T.; Klingner, R. E. (1993): Bond Stress Model for Design of Adhesive Anchors. ACI Structural Journal, V. 90, No. 5, 1993, pp. 514–524.
- Cook, R. A.; Fagundo, F. E.; Biller, M. H. (1993): Tensile Behaviour and Design of Adhesive Bonded Anchors and Dowels. Transportation Research Record 1392, Transportation Research Board, 1993, pp. 126–133.
- Cook, R. A.; Bishop, M. C.; Hagedoorn, H. S.; Sikes, D.; Richardson, D. S.; Adams, T. L.; De Zee, C. T. (1994): Adhesive Bonded Anchors: Bond Properties and Effects of In-Service and Installation Conditions. Report No. 94-2A, University of Florida, Department of Civil Engineering, College of Engineering, Gainesville.
- Cook, R. A.; Kunz, J.; Fuchs, W.; Konz, R. C. (1998): Behaviour and Design of Single Adhesive Anchors under Tensile Load in Uncracked Concrete. ACI Structural Journal, V. 95, No. 1, 1998, pp. 9–26.
- Cook, R. A.; Konz, R. C. (1998): Design Guidelines for Adhesive Anchors. Report for fib, Task Group 4/4 „Fastening to Concrete Structures“, 1998, not published.
- Cornelissen, H. A. W.; Reinhardt, H. W. (1984): Uni-axial tensile fatigue failure of concrete under constant amplitude and programme loading. Magazine of Concrete Research, Vol. 36, No. 129, Dec. 1989, pp. 216–226.
- Cziesielski, E.; Friedmann, M. (1983): Tragfähigkeit geschweißter Verbindungen im Betonfertigteilbau (Load-bearing capacity of welded connections in precast concrete construction). Schriftenreihe des Deutschen Ausschusses für Stahlbeton, No. 346, Ernst & Sohn, Berlin, 1983 (in German).
- Dardare, J. (1973): Etude du comportement des prédalles non armées transversalement vis à vis des efforts de cisaillement-glisement. Beton Industrial, No. 40, No. 1, 1973.
- Daschner, F. (1986): Notwendige Schubbewehrung zwischen Betonfertigteilen und Ort-beton (Required shear reinforcement between precast concrete element and in-situ concrete). Schriftenreihe des Deutschen Ausschusses für Stahlbeton, Ernst & Sohn, Berlin, 1986, No. 372, pp. 33–90 (in German).
- Deutscher Ausschuss für Stahlbeton (1981): DAST-Richtlinie 014, Empfehlungen zum Vermeiden von Terrassenbrüchen in geschweißten Konstruktionen aus Baustahl (Recommendations to avoid lamellar tearing of welded construction made from structural steel). Edition 1/1981 (in German).
- Deutscher Ausschuss für Stahlbeton (1991): Richtlinie zur Anwendung von Eurocode 2 – Planung von Stahlbeton- und Spannbeton-tragwerken, Teil 1: Grundlagen und Anwendungsregeln für den Hochbau (Guideline for the use of Eurocode 2 – Design of reinforced and prestressed concrete structures, Part 1: Basis and rules of application for building construction). Beuth Verlag, Berlin, 1991 (in German).
- Deutscher Betonverein e.V. (1991): Merkblatt „Begrenzung der Rißbildung im Stahlbeton und Spannbetonbau“ (Code of practice “Limitation of crack width in reinforced and prestressed concrete structures”). Wiesbaden, March 1991 (in German).
- Deutsches Institut für Bautechnik (1993): Bemessungsverfahren für Dübel zur Verankerung in Beton (Anhang zum Zulassungsbescheid) (Design concept for anchors in concrete (Annex for Approval Certificates)). Edition June 1993, Berlin (in German).
- Deutsches Institut für Bautechnik (1995): Bauregelliste A und Liste C – Ausgabe 95/1 (Construction Products List A and List C – Edition 95/1). Mitteilungen des Deutschen Instituts für Bautechnik, Vol. 26, Special Edition No. 10, Ernst & Sohn, Berlin, 1995 (in German).

- Deutsches Institut für Bautechnik (1998): Zulassungsbescheid Nr. Z-30.3-6 „Bauteile und Verbindungselemente aus nichtrostenden Stählen“ vom 25.9.1998 (Certificate of Approval No. Z-30.3-6 “Buildin components and fasteners made from stainless steel”, 25th September 1998). Berlin (in German).
- Deutsches Institut für Bautechnik (2003): Beurteilung von Verankerungen in Beton bei Brandbeanspruchung (Evaluation of fixings to concrete under fire). Berlin, October 2003 (in German).
- Deutsches Institut für Bautechnik (2003/1): Concrete Screw for Anchorage in Normal Weight Concrete. Common Understanding of Assessment Procedure for a European Technical Approval. Berlin, 2003.
- Deutsches Institut für Bautechnik (2003/2): Steel plate with cast-in anchor(s). Common Understanding of Assessment Procedure (CUAP) for a European Technical Approval, Berlin, 2003.
- Deutsches Institut für Bautechnik und Fachverband der Werkzeugindustrie (2002): Merkblatt über die Kennwerte, Anforderungen und Prüfungen von Mauerbohrern mit Schneidkörpern aus Hartmetall, die zur Herstellung der Bohrlöcher von Dübelverankerungen verwendet werden (Code of practice for the characteristic values, requirements and tests for masonry drill bits with carbide cutting body which are used to drill holes for anchors). Berlin, 2002 (in German).
- De Vries, R. A. (1996): Anchorage of Headed Reinforcement in Concrete. PhD-Thesis, The University of Texas at Austin, December 1996.
- Dickert, J. (1991): Einfluß der Verankerungstiefe auf das Tragverhalten von in unbewehrten Betonbauteilen eingelegten Kopfbolzenbefestigungen unter Querkzugbeanspruchung (Influence of embedment depth on the load-bearing behaviour of headed anchors under shear loading in non-reinforced concrete. Diplomarbeit, Institute of Construction Materials, University of Stuttgart, April 1991 (in German).
- Dieterle, H.; Opitz, V. (1988): Tragverhalten von nicht generell zugzonentauglichen Dübeln, Teil 1: Verhalten in Parallelrissen (Load-bearing behaviour of anchors that are not generally suitable for use in cracked concrete, Part 1: Behaviour in uni-axial cracks). Report No. 1/34–88/21, Institute of Construction Materials, University of Stuttgart, not published (in German).
- Dieterle, H.; Bozenhardt, A.; Hirth, W.; Opitz, V. (1990): Tragverhalten von Dübeln in Parallelrissen unter Schrägzugbeanspruchung (Load-bearing behaviour of anchors in uni-axial cracks under combined tension and shear loading). Report No. 1/45-89/19, Institute of Construction Materials, University of Stuttgart, February 1990, not published (in German).
- DIN V ENV 206-1990-01 (1990): Beton; Eigenschaften, Herstellung, Verarbeitung und Gütenachweis (Concrete; Characteristics, production, handling and quality assessment). Edition October 1990 (in German).
- DIN 267 Teil 11 (1980): Mechanische Verbindungselemente; Technische Lieferbedingungen mit Ergänzungen zu ISO 3506, Teile aus rost- und säurebeständigen Stählen (Mechanical fasteners; Technical terms of delivery with complements to ISO 3506, parts made from stainless and acidproof steels). Edition January 1980 (in German).
- DIN 1045 (1988): Beton und Stahlbeton, Bemessung und Ausführung (Concrete and reinforced concrete, Design and construction). Edition July 1988 (in German).
- DIN 1045-1 (2001): Tragwerke aus Beton, Stahlbeton und Spannbeton, Part 1: Bemessung und Konstruktion (Concrete, reinforced concrete and prestressed concrete structures, Part 1: Design and construction). Edition August 2001 (in German).
- DIN 1048 Teil 5 (1991): Prüfverfahren für Beton; Festbeton, gesondert hergestellte Probekörper (Test procedure for concrete; hardened concrete, seperately produced test specimen). Edition June 1991 (in German).
- DIN 1055 Teil 1 (1978): Lastannahmen für Bauten; Lagerstoffe, Baustoffe und Bauteile; Eigenlasten und Reibungswinkel (Design loads for buildings; bulk materials, building materials and building components; dead loads and angles of incline). Edition July 1978 (in German).

- DIN 1055 Teil 2 (1976): Lastannahmen für Bauten – Bodenkenngrößen; Wichte, Reibungswinkel, Kohäsion, Wandreibungswinkel (Design loads for buildings – soil characteristics; specific gravity, angles of incline, coherence, wall friction angle). Edition February 1976 (in German).
- DIN 1055 Teil 3 (1971): Lastannahmen für Bauten – Verkehrslasten (Design loads for buildings – live loads). Edition June 1971 (in German).
- DIN 1055 Teil 4 (1986): Lastannahmen für Bauten; Verkehrslasten – Windlasten bei nicht schwingungsanfälligen Bauwerken (Design loads for buildings; live loads – wind loads for buildings that react sensitive upon vibrations). Edition August 1986 (in German).
- DIN 1055 Teil 5 (1975): Lastannahmen für Bauten; Verkehrslasten, Schneelast und Eislast (Design loads for buildings; live loads, snow loads and ice loads). Edition June 1975 (in German).
- DIN 4102, Teil 4 (1994): Technische Baubestimmungen über das Brandverhalten von Baustoffen und Bauteilen, Teil 4: Zusammenstellung und Anwendung klassifizierter Baustoffe, Bauteile und Sonderbauteile (Technical building regulations for fire behaviour of building materials and building components, Part 4: List and application of classified building materials, building components and special components). Edition March 1994 (in German).
- DIN 4108, Teil 3 (1981): Wärmeschutz im Hochbau. Klimabedingter Feuchteschutz, Anforderungen und Hinweise für Planung und Ausführung (Thermal protection in building construction. Climate induced moisture protection, requirements and hints for planning and construction). Edition August 1981 (in German).
- DIN V 4108, Teil 4 (1998): Wärmeschutz und Energie-Einsparung in Gebäuden; wärme- und feuchteschutztechnische Kennwerte (Thermal protection and energy saving in buildings; characteristic values for thermal and moisture protection). Edition October 1998 (in German).
- DIN EN ISO 14 555 (1998): Schweißen – Lichtbogenschweißen von metallischen Werkstoffen (Welding – arc welding of metallic materials). Edition 1998 (in German).
- DIN 17 100 (1980): Allgemeine Baustähle; Gütenorm (General-purpose constructional steels; performance standard). Edition January 1980 (in German).
- DIN 18 168 Teil 1 (1981): Leichte Deckenbekleidungen und Unterdecken, Anforderungen für die Ausführung (Light-weight ceilings, requirements for construction). Edition October 1981 (in German).
- DIN 18 800 Teil 1 (1981): Stahlbauten; Bemessung und Konstruktion (Steel structures; Design and construction). Edition March 1981 (in German).
- DIN 18 800-1: 1990-11 (1990): Stahlbauten; Bemessung und Konstruktion (Steel structures; Design and construction). Edition November 1990 (in German).
- Eggert, H.; Kulesa, G.; Strassburg, F. W. (1975): Erläuterungen zur allgemeinen bauaufsichtlichen Zulassung nichtrostender Stähle (Commentary on the General Approval Certificate for stainless steels). Mitteilungen des Institutes für Bautechnik, Berlin, 1975, No. 1, pp. 1–9 (in German).
- Ehrenstein, G. W. (1976/1): Bauwerksdübel aus Thermoplasten, auch zugelassen als tragende Bauelemente (Anchors for building construction made from thermoplasts, also approved as load-bearing building components). *Verbindungstechnik*, 1976, No. 4, pp. 25–28 (in German).
- Ehrenstein, G. W. (1976/2): Aus Reihenuntersuchungen mit Bauwerksdübeln aus Polyamid (Research on anchors for building construction made from polyamide). *Verbindungstechnik*, 1976, No. 12, pp. 13–14 (in German).
- Ehrenstein, G. W. (1998): Tischvorlage für eine Sitzung des Sachverständigenausschusses „Verankerungen und Befestigungen“ beim Deutschen Institut für Bautechnik (Paper for discussion in a meeting of the Board of Experts “Anchorage and Fixings” at the “Deutsches Institut für Bautechnik (DIBt)”), 1998 (in German).
- Ehrenstein, G. W. (1999): Schreiben vom 5.3.1999 an Eligehausen (Letter to Eligehausen, dated 5th March 1999) (in German).

- Eibl, J.; Schürmann, U. (1982): HV-Schraubenanschlüsse für Stahlbetonkonsolen (Friction grip bolted joints for reinforced concrete brackets). *Bauingenieur* 57, 1982, pp. 61–68 (in German).
- Eibl, J.; Keintzel, E. (1989): Zur Beanspruchung von Befestigungsmitteln bei dynamischen Lasten (Loading of fastenings under dynamic loads). Universität Karlsruhe, Institut für Massivbau und Baustofftechnologie, 1989 (in German).
- Eibl, J.; Idda, K.; Lucero-Cimas, H.-N. (1997): Verbundverhalten bei Querschub (Bond behaviour under shear loading). Research Report, Universität Karlsruhe, Institut für Massivbau und Baustofftechnologie, 1997 (in German).
- Eilfgren, L.; Broms, C. E.; Johansson, H. E.; Rehnström, A. (1980): Anchor Bolts in Reinforced Concrete Foundations. Research Report, 1980: 36, University of Luleå, 1980.
- Eilfgren, L.; Broms, C.E.; Cederwall, K.; Gylltoft, K. (1982): Fatigue of Anchor Bolts in Reinforced Concrete Foundations. In: IABSE Report, Vol. 37, Fatigue of Steel and Concrete Structures. International Association for Bridges and Structural Engineering, Zürich, 1982, pp. 463–470.
- Eilfgren, L.; Ohlsson, U. (1986): Modelling of Hook Anchors, in: Fracture Mechanics of Concrete. Report TVBM-3025, Division of Building Materials, Lund Institute of Technology, Lund, 1986.
- Eilfgren, L.; Ohlsson, U.; Gylltoft, K. (1989): Anchor Bolts analysed with Fracture Mechanics. Fracture of Concrete and Rock, Editors: Shah, S., Swartz, S., Springer Verlag, New York, 1989, pp. 269–275.
- Eligehausen, R. (1979): Übergreifungsstöße zugbeanspruchter Rippenstäbe (Lapped splices of tensioned rebars). Schriftenreihe DAfStb, No. 301, Berlin, 1979.
- Eligehausen, R. (1984): Wechselbeziehungen zwischen Befestigungstechnik und Stahlbetonbauweise (Interrelations between fixing technology and reinforced concrete construction). In: Eligehausen, R.; Rußwurm, D. (Editors): Fortschritte im Konstruktiven Ingenieurbau (Progress in structural engineering), Ernst & Sohn, Berlin, 1984 (in German).
- Eligehausen, R. (1986): Vorschlag für ein Prüfprogramm für Eignungs- und Zulassungsversuche für Dübel, die in der Zugzone eingesetzt werden sollen (Proposal for a test regime for suitability and approval tests with anchors to be installed in cracked concrete). Report No. 1/16-86/2, Institut für Werkstoffe im Bauwesen, Universität Stuttgart, Februar 1986, not published (in German).
- Eligehausen, R. (1988/1): Bemessung von Befestigungen – Zukünftiges Konzept (Design of fastenings – Future concept). *Betonwerk + Fertigteil-Technik*, 1988, No. 5, pp. 88–100 (in German).
- Eligehausen, R. (1988/2): Eignung des Setzbolzen-Befestigungssystems M8 H-15-37 P8 DX-KWIK der Hilti AG für die Befestigung leichter Unterdecken an Stahlbetondecken (Suitability of Hilti power actuated fasteners M8 H-15-37 P8 DX-KWIK for the fixing of lightweight suspended ceilings to reinforced concrete slabs). Expert's opinion, Stuttgart, 1988, not published (in German).
- Eligehausen, R. (1989): Befestigungen im ungerissenen Beton (Fixing to non-cracked concrete). Report No. 1/45-89/23, Institut für Werkstoffe im Bauwesen, Universität Stuttgart, December 1989, not published (in German).
- Eligehausen, R. (1990): Bemessung von Befestigungen in Beton mit Teilsicherheitsbeiwerten (Design of fastenings to concrete with partial safety factors). *Bauingenieur* 65 (1990), pp. 295–305 (in German).
- Eligehausen, R. (1991): Behavior, design and testing of anchors in cracked concrete. In Senkiw, G. A.; Lancelot III, H.B. (Herausgeber): SP-130 "Anchors in Concrete – Design and Behavior", American Concrete Institute, Detroit, 1991, pp. 123–176.
- Eligehausen, R. (1992): Vergleich des Kappa-Verfahrens und der CC-Methode (Comparison of the Kappa-method with the CC-method). Report No. 12/16–92/7, Institut für Werkstoffe im Bauwesen, Universität Stuttgart, 1992 (in German).
- Eligehausen, R. (1995/1): Bemessung von Ankerschienen in ungerissenem und gerissenem Normalbeton. Teil 1: Ankerschienen ohne Rückhängebewehrung unter vorwiegend ruhender Belastung. Teil 2: Anker-

- schielen mit Rückhängebewehrung im ungerissenen und gerissenen Normalbeton (Design of anchor channels in non-cracked and cracked normal concrete. Part 1: Anchor channels without supplementary reinforcement under predominantly static loading. Part 2: Anchor channels with supplementary reinforcement in non-cracked and cracked normal concrete). Expert's opinion, Stuttgart, 1995, not published (in German).
- Eligehausen, R. (1995/2): Eignung von Hilti-Setzbolzen aus nichtrostendem Stahl als Befestigungselemente für Deckenabhängiger in Feuchträumen sowie für Fassadenbekleidungen (Suitability of Hilti powder actuated fasteners made from stainless steel for fixing of suspended ceilings in moist environment and for facades). Expert's opinion, Stuttgart, 1995, not published (in German).
- Eligehausen, R.; Pusill-Wachtsmuth, P. (1982): Stand der Befestigungstechnik im Stahlbetonbau (State-of-the-art: fixing technology for reinforced concrete). IVBH Report S-19/82, IVBH-Periodica 1/1982, February 1982 (in German).
- Eligehausen, R.; Clausnitzer, W. (1983): Analytisches Modell zur Beschreibung des Tragverhaltens von Befestigungselementen (Analytical model to describe the load-bearing behaviour of fixing elements). Report No. 4/1-83/3, Institut für Werkstoffe im Bauwesen, Universität Stuttgart, 1983, not published (in German).
- Eligehausen, R.; Lehmann, R. (1984): Verankerungen mit Metallspreizdübeln in der aus Lastspannungen erzeugten Zugzone von Stahlbetonbauteilen – Einflüsse auf das Tragverhalten und Vorschlag für Zulassungsversuche (Anchorage of metal expansion anchors in the tensile zone of reinforced concrete structures – Effects on the load-bearing behaviour and proposal for an approval test regime). Report No. 1/4-84/1, Institut für Werkstoffe im Bauwesen, Universität Stuttgart, 1984, not published (in German).
- Eligehausen, R.; Mällée, R.; Rehm, G. (1984): Befestigungen mit Verbundankern (Fixing with bonded anchors). Betonwerk + Fertigteil-Technik, 1984, No. 10, pp. 686–692, No. 11, pp. 781–785, No. 12, pp. 825–829 (in German).
- Eligehausen, R.; Sawade, G. (1985): Verhalten von Beton auf Zug (Behaviour of concrete under tension). Betonwerk + Fertigteil-Technik, 1985, No. 5, pp. 315–322, No. 6, pp. 389–391 (in German).
- Eligehausen, R.; Lotze, D.; Sawade, G. (1986): Untersuchungen zur Frage der Wahrscheinlichkeit, mit der Dübel in Rissen liegen (Investigation of the probability that anchors are located in cracks). Report No. 1/20-86/17, Institut für Werkstoffe im Bauwesen, Universität Stuttgart, October 1986, not published (in German).
- Eligehausen, R.; Fuchs, W.; Mayer, B. (1987): Tragverhalten von Dübelbefestigungen bei Zugbeanspruchung (Load-bearing behaviour of fastenings with anchors under tension loading). Beton + Fertigteil-Technik 1987, No. 12, pp. 826–832 and 1988, No. 1, pp. 29–35 (in German).
- Eligehausen, R.; Fuchs, W. (1988): Tragverhalten von Dübelbefestigungen unter Querkzug-, Schrägzug- und Biegezugbeanspruchung (Load-bearing behaviour of fastenings with anchors under shear, combined tension and shear and bending). Beton + Fertigteil-Technik 1988, No. 2, pp. 48–56 (in German).
- Eligehausen, R.; Bozenhardt, A. (1989): Crack widths as measured in actual structures and conclusions for the testing of fastening elements. Report No. 1/42–89/9, Institute of Construction Materials, University of Stuttgart, August 1989.
- Eligehausen, R.; Fuchs, W.; Lotze, D.; Reuter, M. (1989): Befestigungen in der Betonzugzone (Fixings in the concrete tensile zone). Beton- und Stahlbetonbau 84, 1989, No. 2, pp. 27–32, No. 3, pp. 71–74 (in German).
- Eligehausen, R.; Sawade, G. (1989): A Fracture Mechanics based Description of the Pull-Out Behaviour of headed Studs embedded in Concrete. Fracture Mechanics of Concrete Structures, From Theory to Applications. Editors: Elfgren, L., Chapman and Hall, London, New York, 1989, pp. 281–299.
- Eligehausen, R.; Fuchs, W.; Furcher, J. (1990): Sicherheit von querbelasteten Befestigungsmitteln am Bauteilrand gegen Betonausbruch (Safety of fixing elements under shear close to an edge against concrete edge failure). Report No. 10/14-90/4, Institut für



- Werkstoffe im Bauwesen, Universität Stuttgart, March 1990, not published (in German).
- Eligehausen, R.; Ozbolt, J. (1990): Size effect in anchorage behavior. Proceedings, ECF8, Fracture Behavior and Design of Materials and Structures, Turin, October 1990.
- Eligehausen, R.; Asmus, J. (1991): Zuverlässigkeitsprüfungen an Dübeln in Linienrissen (Reliability tests with anchors in uni-axial cracks). Report No. 1/49A-91/1A, Institut für Werkstoffe im Bauwesen, Universität Stuttgart, not published (in German).
- Eligehausen, R.; Ozbolt, J. (1991): Use of the Tensile Strength in Anchorage to Concrete. In: IABSE Colloquium Stuttgart 1991. In Structural Concrete. Editor IABSE, Zürich, 1991, pp. 731–736.
- Eligehausen, R.; Balogh, T.; Fuchs, W.; Breen, J. E. (1992): The CC-Method. Report No. 12/15-92/1, Institute of Construction Materials, University of Stuttgart and Ferguson Structural Engineering Laboratory; University of Texas at Austin, 1992, not published.
- Eligehausen, R.; Bouska, P.; Cervenka, V.; Pukl, R. (1992): Size Effect of the Concrete Cone Failure Load of Anchor Bolts. In: Bazant, Z. P. (Editor), Fracture Mechanics of Concrete Structures, pp. 517–525, Elsevier Applied Science, London, New York.
- Eligehausen, R.; Fuchs, W.; Ick, U.; Mällée, R.; Reuter, M.; Schimmelpfennig, K.; Schmal, B. (1992): Tragverhalten von Kopfbolzenverankerungen bei zentrischer Zugbeanspruchung (Behaviour of headed anchors under concentric tension). Bauingenieur 67, pp. 183–196 (in German).
- Eligehausen, R.; Meszaros, J. (1992): Zusammenfassender Bericht über Überprüfungen von Dübeln auf Baustellen (Report on tests of anchors on building sites). Report No. M655/08-92/32, Institut für Werkstoffe im Bauwesen, Universität Stuttgart, 1992, not published (in German).
- Eligehausen, R.; Ozbolt, J. (1992): Influence of Crack Width on the Concrete Cone Failure Load. In: Bazant, Z. P. (Editor): Fracture Mechanics of Concrete Structures. Elsevier Applied Science, London, New York, 1992, pp. 876–884.
- Eligehausen, R.; Lehr, B. (1993): Querkzugtragfähigkeit von Dübeln mit großem Randabstand (Shear capacity of anchors with large edge distance). Report No. 10/20-93/11, Institut für Werkstoffe im Bauwesen, Universität Stuttgart, 1993, not published (in German).
- Eligehausen, R.; Asmus, J.; Lehr, B.; Sippel, T. M. (1995): Use of Bonded Anchor Systems. Proceedings „Conchem“, Verlag für chemische Industrie H. Ziolkowsky GmbH, 1995.
- Eligehausen, R.; Balogh, T. (1995): Behaviour of Fasteners Loaded in Tension in Cracked Reinforced Concrete. ACI-Structural Journal, 1995, Vol. 92, No. 3, pp. 365–379.
- Eligehausen, R.; Graf, P.; Meszaros, J.; Lee, S. (1995): Setting Tests of Drop-in Anchors. Report No. 1/68-95/12, Institut für Werkstoffe im Bauwesen, Universität Stuttgart, 1995, not published.
- Eligehausen, R.; Pukl, P.; Reick, M. (1995): Behaviour of Anchors in Fire. Report No. 21/3-95/10, Institut für Werkstoffe im Bauwesen, Universität Stuttgart, 1995, not published.
- Eligehausen, R.; Varga, J. (1995): Report on Tests with Fastenings with Headed Studs. Report No. Te 696/1-95/4, Institut für Werkstoffe im Bauwesen, Universität of Stuttgart, 1995, not published.
- Eligehausen, R.; Mesureur, B.; Okelo, R. (1996): Influence of Anchor Loading on the Shear Capacity of Beams with and without Shear Reinforcement. Report No. 1/79-96/10. Institut für Werkstoffe im Bauwesen, Universität Stuttgart, 1996, not published.
- Eligehausen, R.; Meszaros, J. (1996): Influence of Installation Inaccuracies on the Behaviour of Bonded Anchors, Evaluation of the Test Results. Report No. 1/80-96/11. Institut für Werkstoffe im Bauwesen, Universität Stuttgart, 1996, not published.
- Eligehausen, R.; Okelo, R. (1996): Design of group fastenings for pull-out or pull-through failure modes of the individual anchors of a group. Report No. 18/1-96/20, Institut für Werkstoffe im Bauwesen, Universität Stuttgart, 1996, not published.
- Eligehausen, R.; Reick, M. (1996): Behaviour of Anchors in Fire. Report on Fire Tests. Report No. 21/4-96/1, Institut für Werkstoffe

- im Bauwesen, Universität Stuttgart, 1996, not published.
- Eligehausen, R.; Varga, J. (1996): Versuche mit UKA 3 M12 (EAP) bei verschiedenen Temperaturen (Tests with UKA 3 M12 (EAP) at different temperatures). Report No. 910/01-96/14, Institut für Werkstoffe im Bauwesen, Universität Stuttgart, 1996, not published (in German).
- Eligehausen, R.; Graf, P.; Fuchs, W. (1997): Verankerungen unter Querlast mit der Versagensart Betonausbruch zur lastabgewandten Seite (Anchorage under shear loading at try-out failure). Report No. 10/27-97/21, Institut für Werkstoffe im Bauwesen, Universität Stuttgart, 1997, not published (in German).
- Eligehausen, R.; Mallée, R.; Rehm, G. (1997): Befestigungstechnik (Fixing technology). Betonkalender 1997, Part II, Ernst & Sohn, 1997, pp. 609–753 (in German).
- Eligehausen, R.; Asmus, J. (1999): Nachträgliche Befestigungen in Beton (Post-installed fixings to concrete). Bundesbaublatt, No. 11, 1999, pp. 66–70 (in German).
- Eligehausen, R.; Küenzlen, J. H. R. (2002): Tragverhalten von Befestigungen mit Schraubdübeln (Load-bearing behaviour of screw anchors). Beton- und Stahlbetonbau 97, 2002, No. 2, pp. 61–68 (in German).
- Eligehausen, R.; Hofmann, J. (2003): Experimentelle und numerische Untersuchungen an Befestigungen am Bauteilrand unter Querlast (Experimental and numerical investigations on fixings under shear loading close to an edge). Report, Institut für Werkstoffe im Bauwesen, Universität Stuttgart, for the Deutsche Forschungsgemeinschaft, under preparation (in German).
- Eligehausen, R.; Fichtner, S. (2003): Einfluß des Achsabstandes auf die Betonausbruchlast von biegebeanspruchten Gruppenbefestigungen (Influence of axial spacing on the concrete failure of groups under bending). Report, Institut für Werkstoffe im Bauwesen, Universität Stuttgart, 2003, not published (in German).
- Eligehausen, R.; Hoehler, M.S. (2003): Testing of post-installed fastenings to concrete structures in seismic regions. Conference Proceedings of the fib Symposium on Concrete Structures in Seismic Regions, Athens, Greece, 2003
- Eligehausen, R.; Appl, J. J.; Lehr, B.; Meszaros, J.; Fuchs, W. (2004/1): Tragverhalten und Bemessung von Befestigungen mit Verbunddübeln unter Zugbeanspruchung. Part 1: Einzeldübel mit großem Achs- und Randabstand (Load-bearing behaviour and design of fastenings with bonded anchors under tension loading – Part 1: Single anchors with large axial and edge spacing). Beton- und Stahlbetonbau 99, 2004, No. 7, pp. 561–571 (in German).
- Eligehausen, R.; Appl, J. J.; Lehr, B.; Meszaros, J.; Fuchs, W. (2005): Tragverhalten und Bemessung von Befestigungen mit Verbunddübeln unter Zugbeanspruchung, Teil 2: Gruppen und Einzeldübel am Bauteilrand (Load-bearing behaviour of fastenings with bonded anchors under tension loading – Part 2: Anchor groups and single anchors close to an edge). Under preparation (in German).
- Eligehausen, R.; Fuchs, W.; Hofmann, J. (2004): Shear towards the free edge – an example using ACI 318-02, Appendix D. Discussion of the paper by Burdette, E. G. and Zisi, N. in Concrete International, March 2004.
- Eligehausen, R.; Pothhoff, M.; Grewin, Y.; Lotze, D. (2004): Bemessung von Ankerschienen unter Querlasten (Design of anchor channels under shear loading). Under preparation (in German).
- EN 206-1:2001-07 (2001): Concrete: Specification, performance, production and conformity. European Committee for Standardisation (CEN), Brussels, 2001.
- EN 1990: 2002 (2002): Basis of design for structural Eurocodes. European Committee for Standardisation (CEN), Brussels, 2002.
- EN 1993 Part 1-1 (2002): Eurocode 3 – Design of Steel Structures. Part 1.8: Design of Joints. Final Draft, European Committee for Standardisation (CEN), Brussels, 2002.
- EN 13501-2: Fire Classification of Construction Products and Building Elements – Part 2: Classification Using Data from Fire Resistance Tests (excluding ventilation services).
- Endo, T.; Shimizu, Y. (1985): Behavior of expansion anchor bolts. Memoirs of Faculty of Technology, Tokyo, Metropolitan University, No. 35, 1985, pp. 3607–3620.



- Ergang, R.; Rockel, M. B. (1975): Die Korrosionsbeständigkeit der nichtrostenden Stähle an der Atmosphäre – Auswertung von Versuchen bis zu 10-jähriger Auslagerung (Corrosion resistance of stainless steels under atmospheric conditions – assessment of tests with a duration of up to 10 years). *Werkstoffe und Korrosion* 26 (1975); pp. 36–41 (in German).
- Eurocode 1: EN 1990: 2002 (2002) Eurocode – Basis of structural design.
- Eurocode 2: ENV 1992-1-1: 1991 (1991): Design of concrete structures – Part 1: General rules and rules for buildings, 1991.
- Eurocode 2: EN 1992-1-1 (2003): Design of concrete structures – Part 1-1: General rules and rules for buildings. Final draft, December 2003.
- Eurocode 3: EN 1993-1-1 (2002): Design of steel structures. Part 1-1: General rules and rules for buildings, 2002.
- Eurocode 8: EN 1998-1 (2003): Design of structures for earthquake resistance. European Committee for Standardisation (CEN) (2004): Technical Specification: Design of Fastenings for Use in Concrete. Part 1: General. Part 2: Headed fasteners. Part 3: Anchor channels. Part 4: Post-installed fasteners – mechanical systems. Part 5: Post-installed fasteners – chemical systems. Final Draft, 2004.
- European Organisation for Standardization: CEN TS (2004). Design of Fastenings for Use in Concrete. Final draft, 2004. Part 1: General. Part 2: Headed Anchors. Part 3: Anchor Channels. Part 4: Post-installed Anchors – Mechanical Systems. Part 5. Post-installed Anchors – Chemical Systems.
- European Organisation for Technical Approvals (EOTA) (1997): Leitlinie für die europäische technische Zulassung für Metalleitdübel zur Verankerung in Beton. Teil 1: Dübel – Allgemeines. Teil 2: Kraftkontrolliert spreizende Dübel. Teil 3: Hinterschnittdübel. Anhang A: Einzelheiten der Versuche. Anhang B: Versuche zur Ermittlung der zulässigen Anwendungsbedingungen. Anhang C: Bemessungsverfahren für Verankerungen (Guideline for the European Technical Approval of metal anchors for use in concrete. Part 1: Anchors in general. Part 2: Torque-controlled expansion anchors. Part 3: Undercut anchors. Annex A: Details of tests. Annex B: Tests for admissible service conditions. Annex C: Design methods for anchorages). *Mitteilungen. Deutsches Institut für Bautechnik*, Vol. 28, Special edition No. 16, Berlin, December 1997 (in German).
- European Organisation for Technical Approvals (EOTA) (1998): Guideline for European Technical Approval of Metal Anchors for Use in Concrete. Part 4: Deformation-Controlled Expansion Anchors, Brussels, 1998.
- European Organisation for Technical Approvals (EOTA) (2002): Guideline for European Technical Approval of Metal Anchors for Use in Concrete. Part 5: Bonded Anchors, Brussels, 2002.
- European Organisation for Technical Approvals (EOTA) (2002): Guideline for European Technical Approval of Metal Anchors for Use in Concrete. Part 6: Anchors for Multiple Use for Non-structural Applications. Final Draft, Brussels, November 2002.
- European Organisation for Technical Approvals (EOTA) (2003): Assessment of torque-controlled bonded anchors. Technical Report No. 18, Brussels 2003.
- European Organisation for Technical Approvals (EOTA) (2004): Progress File – ETAG 001, Metal Anchors for Use in Concrete. Brussels 2004, not published.
- Farrow, C. B.; Klingner, R. E. (1995): Tensile Capacity of Anchors with Partial or Overlapping failure Surfaces: Evaluation of Existing Formulas on an LRFD Basis. *ACI Structural Journal*, Vol. 92, No. 6, November-December 1995, pp. 698–710.
- Farrow, C. B.; Frigui, I.; Klingner, R. E. (1996): Tensile Capacity of Single Anchors in Concrete: Evaluation of Existing Formulas on an LRFD Basis. *ACI Structural Journal*, Vol. 93, No. 1, January-February 1996, pp. 128–137.
- Findley, W. N. (1960): Mechanism and Mechanics of Creep of Plastics. *Society of Plastics Engineers Journal* (1960), pp. 57–65.
- Fischer, A. (1984): Befestigungen mit Hinterschnittankern (Fixing with undercut anchors). In: Eligehausen, R.; Rußwurm, D. (Editors): Fortschritte im konstruktiven Ingenieurbau (Progress in structural engineering), pp. 277–283, Ernst & Sohn, Berlin, 1984 (in German).

- Fischerwerke (1999): Dauerstandsversuche mit fischer-Rahmendübeln S10R 160 (Long-term tests with fischer frame fixings S10R 160). Report No. P 14-99, Waldachtal, 1999, not published (in German).
- Forschungs- und Materialprüfungsanstalt Baden-Württemberg (1976): Untersuchungsbericht Nr. 8/1976 vom 24.8.1976 über durchgeführte Versuche an HILTI-Verbundankern (Report No. 8/1976 dated 24.8.1976 on tests with Hilti bonded anchors). Stuttgart, 1976, not published (in German).
- Forschungs- und Materialprüfungsanstalt Baden-Württemberg (1980): Untersuchungsbericht Nr. II.4-13686 vom 28.11.1980 über Zulassungsversuche für BBT-Anker (Report No. II.4-13686 dated 28.11.1980 on approval tests with BBT-anchors). Stuttgart, 1980, not published (in German).
- Forschungs- und Materialprüfungsanstalt Baden-Württemberg (1985/1): Untersuchungsbericht Nr. II.4-14488 vom 18.4.1985 über Versuche an axialzugbeanspruchten Kopfbolzen (Serie 7) (Report No. II.4-14488 dated 18.4.1985 on tests with headed anchors (series No. 7) under axial tension). Stuttgart (1985), not published (in German).
- Forschungs- und Materialprüfungsanstalt Baden-Württemberg (1985/2): Untersuchungsbericht Nr. II.4-14562/2 vom 12.12.1985 über Versuche an Kopfbolzenbefestigungen unter Querkzugbelastung im ungerissenen Beton (Report No. II.4-14562/2 dated 12.12.1985 on tests with headed anchors under shear loading in non-cracked concrete). Stuttgart (1985), not published (in German).
- Forschungs- und Materialprüfungsanstalt Baden-Württemberg (1995/1): Untersuchungsbericht Nr. 25-10659-9 vom 16.6.1995 über Versuche zur Biegetragfähigkeit von Ankerschienen (Report No. 25-10659-9 dated 16.6.1995 on tests for determination of the bending strength of anchor channels). Stuttgart (1995), not published (in German).
- Forschungs- und Materialprüfungsanstalt Baden-Württemberg (1995/2): Untersuchungsbericht Nr. 25-18547-2 vom 18.12.1995 über Versuche mit Ankerschienen im ungerissenen und gerissenen Beton (Report No. 25-18547-2 dated 18.12.1995 on tests with anchor channels in non-cracked and cracked concrete). Stuttgart (1995), not published (in German).
- Friberg, F. (1940): Load and deflection characteristics of dowels in transverse joints of concrete pavements. Proceedings of the Highway Research Board, 20th Annual Meeting 1940, pp. 481–493.
- Fuchs, W. (1985): Tragverhalten von Dübeln unter nicht vorwiegend ruhender Belastung (Load-bearing behaviour of anchors under non predominantly static loading). Report No. 11/2-85/5, Institut für Werkstoffe im Bauwesen, Universität Stuttgart, January 1985, not published (in German).
- Fuchs, W. (1985/2): Tragverhalten von Dübelbefestigungen verankert in der Biegezugzone von stark bewehrten Betonbalken (Load-bearing behaviour of anchors in the bending tensile area of heavy reinforced concrete beams). Report No. 1/15-85/26, Institut für Werkstoffe im Bauwesen, Universität Stuttgart, December 1985, not published (in German).
- Fuchs, W. (1990): Tragverhalten von Befestigungen unter Querlast im ungerissenen Beton (Load-bearing behaviour of fastenings under shear loading in non-cracked concrete). Doctor thesis, Universität Stuttgart, 1990.
- Fuchs, W.; Eligehausen, R. (1986/1): Tragverhalten und Bemessung von Befestigungen ohne Randeinfluß unter Querkzugbelastung (Load-bearing behaviour and design of fixings without edge influence under shear loading). Report No. 10/8-86/12, Institut für Werkstoffe im Bauwesen, Universität Stuttgart, October 1986, not published (in German).
- Fuchs, W.; Eligehausen, R. (1986/2): Tragverhalten und Bemessung von auf Querkzug beanspruchten Dübelbefestigungen mit Randeinfluß im ungerissenen Beton (Load-bearing behaviour and design of fixings under shear with edge influence in non-cracked concrete). Report No. 10/9-86/13, Institut für Werkstoffe im Bauwesen, Universität Stuttgart, October 1986, not published (in German).

- Fuchs, W.; Eligehausen, R. (1988): Biegebeanspruchung von Bolzen und Schrauben bei Dübeln unter vorwiegend ruhender Belastung (Bending of bolts and screws of anchors under predominantly static loading). Report No. 10/10-88/12, Institut für Werkstoffe im Bauwesen, Universität Stuttgart, Sept. 1988, not published (in German).
- Fuchs, W.; Eligehausen, R. (1989): Tragverhalten von Befestigungsmitteln im gerissenen Beton bei Querkzugbeanspruchung (Load-bearing behaviour of fixing elements under shear loading in cracked concrete). Report No. 1/41-89/15, Institut für Werkstoffe im Bauwesen, Universität Stuttgart, July 1989, not published (in German).
- Fuchs, W.; Eligehausen, R. (1990): Bemessung von randfernen Befestigungen mit der Versagensart Stahlbruch unter Einfluß des Lochspiels (Design of fixings remote from an edge at steel failure influenced by hole clearance). Report No. 10/16-90/6, Institut für Werkstoffe im Bauwesen, Universität Stuttgart, July 1990, not published (in German).
- Fuchs, W.; Eligehausen, R. (1995): Das CC-Verfahren für die Berechnung der Betonausbruchlast von Verankerungen (CC-method for determination of the concrete failure load of fastenings). *Beton- und Stahlbetonbau*, 1995, No. 1, pp. 6–9, No. 2, pp. 38–44, No. 3, pp. 73–76 (in German).
- Fuchs, W.; Eligehausen, R.; Breen, J. E. (1995/1): Concrete Capacity Design (CCD) Approach for Fastening to Concrete. *ACI Structural Journal*, Vol. 92 (1995), No. 1, pp. 73–94.
- Fuchs, W.; Eligehausen, R.; Breen, J. E. (1995/2): Concrete Capacity Design (CCD) Approach for Fastening to Concrete, Authors' Closure to Discussions. *ACI Structural Journal*, Vol. 92 (1995), No. 6, pp. 794–802.
- Fujikake, K.; Nakayama, J.; Sato, H.; Mindess, S.; Ishibashi, T. (2003): Chemically bonded anchors subjected to rapid pullout loading. *ACI Materials Journal*, Vol. 100, No. 3, May-June, 2003, pp. 246–252.
- Furche, J. (1994): Zum Trag- und Verschiebungsverhalten von Kopfbolzen bei zentrischem Zug (Load-bearing and displacement behaviour of headed anchors under axial tension loading). Doctor thesis, Universität Stuttgart, 1994.
- Furche, J.; Dieterle, H. (1986): Ausziehversuche an Kopfbolzen mit unterschiedlichen Kopfformen bei Verankerungen in ungerissemem Beton und Parallelrisen (Pull-out tests with headed anchors with different shape of the heads, anchorage in non-cracked concrete and in uni-axial cracks). Report No. 9/1-86/9, Institut für Werkstoffe im Bauwesen, Universität Stuttgart, 1986, not published (in German).
- Furche, J.; Eligehausen, R. (1991): Lateral Blowout Failure of Headed Studs Near the Free Edge. In: Senkiw, G. A.; Lancelot, H. B. (Editor), *SP-130, Anchors in Concrete, Design and Behaviour*. American Concrete Institute, Detroit, 1991, pp. 235–252.
- Gerber, W. (1987): Theorie zum Eintreiben und Verankern von Bolzen in Beton (Theory on anchorages to concrete with bolts). *Bauingenieur* 62, 1987, pp. 213–218 (in German).
- Gollwitzer, S.; Abdo, T.; Rackwitz, R. (1989): Zuverlässigkeit von Dübelbefestigungen in Beton (Reliability of anchors in concrete). Report, Lehrstuhls für Massivbau, Technische Universität München, May 1989, not published (in German).
- Graslund, S.; Gylltoft, K.; Elfgrén, L. (1986): A Fracture Mechanics Model of Adhesive Anchors. In: *Bond and Anchorage of Reinforcement in Concrete*. Chalmers University of Technology, Division of Concrete Structures, Publication 86: 1, Göteborg, 1986, pp. 25–43.
- Grewin, Y.-C.; Potthoff, F.; Eligehausen, R. (2002): Versuche mit Ankerschienen mit Rückhängebewehrung im ungerissenen Beton (Tests with anchor channels with supplementary reinforcement in non-cracked concrete). Report No. AF 02/30-H/D 01310/11, Institut für Werkstoffe im Bauwesen, Universität Stuttgart, December 2002 (in German).
- Grewin, Y.-C.; Eligehausen, R. (2003): Verteilung der an einer Schiene angreifenden Zugkräfte auf die einzelnen Anker – Lasteinflußlänge (Distribution of single loads acting on an anchor channel on the particular anchor – load influencing length). Report, Institut für Werkstoffe im Bauwesen, Universität Stuttgart, 2003 (in German).

- Guckenberger, K. (1999): Einfluß von Druckfestigkeit, Trockenrohdichte und Feuchtegehalt des Porenbetons auf die Dübeltragfähigkeit (Influence of compressive strength, dry bulk density and moisture content of aerated concrete on the load-bearing capacity of anchors). Report: MPA Bau, Technische Universität München, 1999 (in German).
- Güth, H. (1982): Verankerungen im Mauerwerk (Fixing to masonry). Presentation given in "Haus der Technik", Essen, December 1982, not published (in German).
- Hasselwander, G.; Jirsa, J.; Breen, J. (1987): Strength and Behavior of Single Cast-in-place Anchor Bolts Subject to Tension. In: Anchorage to Concrete, SP103, American Concrete Institute, Detroit, pp. 203–233.
- Hauptverband der gewerblichen Berufsgenossenschaften (1992): Sicherheitsregeln für Transportanker und -systeme von Betonfertigteilen (Safety regulations for lifting inserts and –systems for precast concrete elements). Zentralstelle für Unfallverhütung und Arbeitsmedizin, Sankt Augustin, 1992 (in German).
- Heilmann, H.G. (1969): Beziehungen zwischen Zug- und Druckfestigkeit des Betons (Correlation between tensile and compression strength of concrete). *beton* 19, 1969, No. 2, pp. 68–70 (in German).
- Henzel, J.; Stork, J. (1990): Anchors under predominantly static shear load with alternating direction. In: Darmstadt Concrete, Vol. 5, 1990, pp. 79–86.
- Higashi, Y.; Endo, T.; Shimizu, Y.; Tomatsuri, H. (1983): Shear strength of expansion anchor bolts under reversed cyclic loading. Transactions of the Japan Concrete Institute, 1983.
- Hillerborg, A. (1983): Analysis of one single crack. Developments in Civil Engineering, Volume 7: Fracture Mechanics of Concrete. Elsevier, London 1983.
- Hilti (1985/1): Versuche mit Verbundankern M12 (EP-Patrone) bei erhöhten Temperaturen (Tests with bonded anchors M12 (EP capsule) at increased temperatures). Report No. DEV 85-152, Schaan, 1985, not published (in German).
- Hilti (1985/2): Versuche mit Verbundankern M12 (EP-Patrone) bei erhöhten Temperaturen (Tests with bonded anchors M12 (EP capsule) at increased temperatures). Report No. DEV 85-226, Schaan, 1985, not published (in German).
- Hilti (1988): Einfluß des Belastungszeitpunktes auf den Auszugversagenswert von Setzbolzen in Beton (Influence of time of loading on the pull-out load of powder actuated fasteners). Report No. XTV 50/88 dated 20.5.1988, Schaan, 1988, not published (in German).
- Hofmann, J. (2004): Tragverhalten und Bemessung von Befestigungen am Bauteilrand unter Querlasten mit beliebigem Winkel zur Bauteilkante (Load-bearing behaviour and design of fasteners close to an edge under shear loading in an arbitrary angle to the edge). Doctor thesis, Institut für Werkstoffe im Bauwesen, Universität Stuttgart, 2004 (in German).
- Hofmann, J.; Eligehausen, R. (2001): Finite-Elementberechnungen von Kopfbolzen am Bauteilrand (Finite element analysis for headed anchors close to an edge). Report No. SP3/2001, Institut für Werkstoffe im Bauwesen, Universität Stuttgart, 2001 (in German).
- Hofmann, J.; Eligehausen, R. (2002): Lokaler Betonausbruch bei randnahen Befestigungen mit Kopfbolzen (Local blow-out failure with headed anchors close to an edge). Institut für Werkstoffe im Bauwesen, Universität Stuttgart, paper presented at the meeting of fib Special Activity Group, Beijing, 2002 (in German).
- Hordijk, D. A. (1991): Local Approach to Fatigue of Concrete. Dissertation, Universität Delft, 1991.
- Hordijk, D. A.; van Mier, J.G. M.; Reinhardt, H. W. (1989): Material Properties. In: Fracture Mechanics of Concrete Structures; From theory to applications. Elfgren, L. (Editor), Chapman and Hall, pp. 67–127, 1989.
- Hunziker, P. (1983): Prüfung und Zulassung für schocksichere Befestigungen (Test and approval for shock proof fixings). VDI-Berichte No. 496, VDI-Verlag, 1983, pp. 65–70 (in German).
- Illgner, K.-H. (1985): Verhalten von Liebig Spannankern Ultraplus bei nicht vorwiegend ruhenden zentrischen Beanspruchungen

- (Behaviour of Liebig undercut anchors Ultra-plus under non predominantly static tension loads). Tagungsband, 3. Internationales Darmstädter Kolloquium "Verankern mit Dübeln", Darmstadt, November 1985 (in German).
- Illgner, K.-H.; Beelich, K. H. (1966): Einfluß überlagerter Biegung auf die Haltbarkeit von Schraubenverbindungen (Influence of superimposed bending on the durability of screwed connections). *Konstruktion*, 1966, No. 3, pp. 117–124 (in German).
- Ingraffea, A.R.; Gerstle, W.H. (1984): Nonlinear fracture model for discrete crack propagation. *Proceedings Research Workshop on Application of Fracture Mechanics to Cementitious Composites*, Evanston 1984.
- Institut für Bautechnik (1975): Prüfungen zur Beurteilung der Tragfähigkeit von zwangsweise spreizenden Dübeln aus Metall nach der Verankerung in Normalbeton  $\geq$  Bn 250 (Test and assessment of the capacity of torque-controlled metal anchors in normal concrete  $\geq$  Bn 250). Berlin, 1975, not published (in German).
- Institut für Bautechnik (1976): Zulassungsprüfungen für Dübel zur Befestigung von leichten Unterdecken an Stahlbetondecken (Approval tests for anchors for the fixing of lightweight suspended ceilings to reinforced concrete slabs). Berlin October 1976, not published (in German).
- Institut für Bautechnik (1977): Merkblatt über Kennwerte zur Gütesicherung von Hammerbohrern mit Schneidplatten aus Hartmetall (Hartmetall-Hammerbohrer), die zur Herstellung der Bohrlöcher von Dübelverbindungen verwendet werden (Code of practice for the quality assessment of hammer drills with hard metal cutting plates, that are used to drill holes for anchors). Berlin, June 1977, not published (in German).
- Institut für Bautechnik (1982): Beschlüsse des Arbeitskreises "Biegebeanspruchung von Bolzen und Schrauben bei Dübeln und Ankerschienen" des Sachverständigenausschusses "Ankerschienen und Dübel" (Decisions of the working group "Bending on bolts and screws used for anchors and anchor channels" of the Board of Experts "Anchor channels and anchors"). Berlin, June 1982, not published (in German).
- Institut für Bautechnik (1986): Grundlagen zur Beurteilung von Baustoffen, Bauteilen und Bauarten im Prüfzeichen- und Zulassungswesen (Basis for the assessment of building materials, building components and building systems for marks of conformity and approvals). Berlin, May 1986 (in German).
- Institut für Bautechnik (1989): Rahmenprogramm für Eignungs- und Zulassungsvorversuche für Dübel, die in der Betonzugzone eingesetzt werden sollen (Test regime for suitability and approval tests of anchors to be used in the concrete tensile zone). Berlin, January 1989, not published (in German).
- Institut für Bautechnik (1990): Zum Nachweis der Standsicherheit von Wärmedämm-Verbundsystemen mit Mineralfaserdämmstoffen und mineralischem Putz (Proof of stability of external thermal insulation composites with mineral fiber insulation and mineralic rendering). *Mittlungen des Instituts für Bautechnik*, No. 4, Berlin, 1990 (in German).
- ISO 834-1 (1999): Fire-resistance Tests – Elements of building construction. Part 1: General requirements.
- ISO 898-1 (1999): Mechanical properties of fasteners. Part 1: Bolts, screws and studs.
- ISO 3506-1 (1997): Mechanical properties of corrosion-resistant stainless steel fasteners. Part 1: Bolts, screws and studs.
- Jagfeld, P. (1980): Langzeituntersuchungen an epoxidharzverklebten Zementmörtelprismen (Long-term tests with cement specimen glued together with epoxy resin). *Schriftenreihe des Deutschen Ausschusses für Stahlbeton*, No. 309, Ernst & Sohn, Berlin, 1980 (in German).
- Jeng, Y.; Shah, S. (1984): Nonlinear Fracture Parameters for Cement Based Composites: Theory and Experiments. In: *Proceedings Application of Fracture Mechanics to Cementitious Composites*. Research Workshop, Evanston, 1984.
- Jiminez, R.; White, R. H.; Gergely, P. (1982): Cyclic Shear and Dowel Action Models. *Journal of the Structural Division*. *Proceedings of the American Society of Civil Engineers*, Vol. 108, No. St 5, May 1982, pp. 1106–1123.
- Johnson, M. K.; Lew, H. S. (1990): Experimental Study of Post-Installed Anchors under



- Combined Shear and Tension Loading. Report No. NISTIR 90-4274, National Institut of Standards and Technology, Gaithersburg, March 1990.
- Kani, G .N. J. (1966): Basic Facts Concerning Shear Failure. ACI-Journal, Vol. 63, No. 6, pp. 675–692, 1966.
- Keintzel, F. (1990): Dübel unter dynamischer Beanspruchung (Anchors under dynamic loading). Presentation at the 24<sup>th</sup> symposium of the DafStb in Karlsruhe, Karlsruhe, 1990 (in German).
- Kellermann, R.; Klein, H. (1955): Untersuchungen über den Einfluß der Reibung auf Cor-spannung und Anzugsmoment bei Schraubenverbindungen (Investigation of the influence of friction on the tightening torque of screws). Konstruktion, 1955, No. 7, pp. 54–68 (in German).
- Kessler, E. (1979): Schocksichere Dübelbefestigungen in Zivilschutzbauten (Shock proof fixings with anchors in civil defense buildings). Schweizer Ingenieur und Architekt, 1979, No. 45 (in German).
- Klausen, D. (1978): Festigkeit und Schädigung des Betons bei häufig wiederholter Beanspruchung (Strength and deterioration of concrete due to frequently repeated loads). Doctor thesis, Technische Hochschule Darmstadt, 1978 (in German).
- Klingner, R. E. (2001): Probabilistic Calibration of Design Methods. In Eligehausen, R. (Editor): RILEM Proceedings PRO 21 „Connections Between Steel and Concrete“, RILEM Publications s.a.r.l. Cachan Cedex, pp. 699–707.
- Klingner, R. E. (2002): Design of Anchorage to Concrete. A Look Back, a Look Around, and a Look Ahead. In: Befestigungstechnik, Bewehrungstechnik...ibidem-Verlag 2002, pp. 167–181.
- Klingner, R. E.; Mendonca, J. A.; Malik, J. B. (1982/1): Effect of Reinforcing Details on the Shear Resistance of Anchor Bolts Under Reversed Cyclic Loading. ACI Journal, Vol. 79, No. 1, January/February 1982, pp. 3–12.
- Klingner, R. E.; Mendonca, J. A. (1982/2): Tensile Capacity of Short Anchor Bolts and Welded Studs: A Literature Review. ACI-Journal, July/August 1982, pp. 270–279.
- Klingner, R. E.; Mendonca, J. A. (1982/3): Shear Capacity of Short Anchor Bolts and Welded Studs: A Literature Review. ACI-Journal, September/October 1982, pp. 339–349.
- Klingner, R. E.; Hollowell, J. M.; Lotze, D.; Park, H.-G.; Rodriguez, M.; Zhang, Y.-G.(1998): Anchor Bolt Behaviour and Strength During Earthquakes. Report No. NUREC/CR-5434. The University of Texas at Austin, August 1998.
- Klingner, R. E.; Muratli, H.; Shirvane, M. (1998): A Technical Basis for Revision to Anchorage Criteria. Report No. NUREC/CR-5563. The University of Texas at Austin, 1998.
- Klöcker, W. (1977): Auf Reaktionsharzbasis spreizdruckfrei verankern (Anchoring expansion free with resin). Verbindungstechnik, 1977, No. 9, pp. 37–42, No. 11, pp. 35–40 (in German).
- Kobarg, J. (1982): Verbundfestigkeit von nachträglich reaktionsharzvermörtelten Betonstählen in Beton (Bond strength of post-installed resin bonded rebars in concrete). Research Report, Institut für Beton- und Stahlbetonbau, Universität Karlsruhe, June 1982, not published (in German).
- König, G.; Scheidler, D.; Fehling, E. (1986): Grundlagen zur Traglastermittlung unbewehrter Betonbauteile unter Zugbeanspruchung (Basis for determining the capacity of non-reinforced concrete elements under tension). Beton- und Stahlbetonbau, 1986, No. 11, pp. 292–296, No. 12, pp. 325–329 (in German).
- Kordina, K.; Meyer-Ottens, C. (1981): Beton-Brandschutz-Handbuch (Handbook for concrete fire protection). Beton-Verlag, Düsseldorf, 1981 (in German).
- Kordina, K.; Meyer-Ottens, C. (1999): Beton-Brandschutz-Handbuch (2. Auflage) (Handbook for concrete fire protection (2nd Edition)).Verlag Bau+Technik, 1999 (in German).
- Kordina, K.; Blume, F. (1985): Empirische Zusammenhänge zur Ermittlung der Schubtragfähigkeit stabförmiger Stahlbetonelemente (Empirical correlations for determination of the shear capacity of bar-shaped reinforced concrete elements). DAfStb, No. 364, Ernst & Sohn, Berlin, 1985 (in German).

- Kraus, Josef (2003): Tragverhalten und Bemessung von Ankerschienen unter zentrischer Zugbelastung (Load-bearing behaviour and design of anchor channels under axial tension). Doctor thesis, Universität Stuttgart, 2003 (in German).
- Küenzlen, J. H. R. (2004): Tragverhalten von Schraubdübeln unter zentrischer Zugbeanspruchung (Load-bearing behaviour of screw anchors under axial tension). Doctor thesis, Universität Stuttgart, 2004 (in German).
- Küenzlen, J. H. R.; Sippel, T. M. (2001): Behaviour and design of fastenings with concrete screws. In: RILEM Proceedings PRO 21 „Symposium on Connections between Steel and Concrete“. Cachan Cedex, 2001, pp. 919–929.
- Küenzlen, J. H. R.; Eligehausen, R. (2002): Load Bearing Behaviour of Fastenings with Concrete Screws. *Otto-Graf-Journal* Vol. 13, 2002.
- Kummerow, A. (1996): Tragverhalten von unter Querzug beanspruchten Verbundankern mit geringem Randabstand (Load-bearing behaviour of bonded anchors close to an edge under shear loading). Institut für Werkstoffe im Bauwesen, Universität Stuttgart, 1996 (in German).
- Kunz, J. (2003): Chemical Fastenings for Fatigue Loads. In: *Joining Techniques in the Building Construction Industry*. Internationales Klebetechnik-Symposium, Munich, 2003.
- Kunz, J.; Cook, R. A.; Fuchs, W.; Spieth, H. (1998): Tragverhalten und Bemessung von chemischen Befestigungen (Load-bearing behaviour and design of chemical fixings). *Beton- und Stahlbetonbau*, 93 (1998), No. 1, pp. 15–19, No. 2, pp. 44–49 (in German).
- Labes, M. (1983): Definition der dynamischen Tragfähigkeit von Dübelbefestigungen bei Schockbelastung (Definition for the dynamic load-bearing capacity of anchors under shock loading). VDI-Report No. 496, VDI-Verlag, 1983, pp. 61–64 (in German).
- Lacher, G. (1986): Zeit- und Dauerfestigkeit von schwarzen und feuerverzinkten hochfesten Schrauben M20 der Festigkeitsklasse 10.9 unter axialer Beanspruchung (Fatigue strength for finite life and fatigue strength of uncoated and hot-dip galvanized high-strength screws M20 of the strength class 10.9 under axial tension). *Bauingenieur* 61, 1986, pp. 227–233 (in German).
- Lang, G. (1979): Festigkeitseigenschaften von Verbundanker-Systemen (Mechanical properties of bonded anchors). *Bauingenieur*, 1979, pp. 41–46 (in German).
- Latenser, K. (1993): Safety in Case of Fire – Test results. Document 59 of the EOTA Working Group 06.01/03 “Anchors”, 1993, not published.
- Latenser, K. (2000): Dübel mit allgemeiner bauaufsichtlicher Zulassung und mit europäischer technischer Zulassung (Anchors with German and European Technical Approval). *Mauerwerk-Kalender 2000*, Verlag Ernst & Sohn, Berlin, 2000, pp. 387–401 (in German).
- Lehmann, R. (1993): Tragverhalten von Metallspreizdübeln in ungerissenem und gerissenem Beton bei der Versagensart Herausziehen (Load-bearing behaviour of metal expansion anchors in non-cracked and cracked concrete for pull-out). Doctor thesis, Universität Stuttgart, 1993 (in German).
- Lehr, B. (2003): Tragverhalten von Verbunddübeln unter zentrischer Belastung im ungerissenen Beton – Gruppenbefestigungen und Befestigungen am Bauteilrand (Load-bearing behaviour of bonded anchors under axial tension in non-cracked concrete – Anchor groups and anchors close to an edge). Doctor thesis, Universität Stuttgart, 2003 (in German).
- Lehr, B.; Eligehausen, R. (1998): Vorschlag eines Bemessungskonzeptes für Verbundanker (Proposal for a design concept for bonded anchors). Report No. 20/25-98/6, Institut für Werkstoffe im Bauwesen, Universität Stuttgart, 1998, not published (in German).
- Lehrke, H.-P.; Flade, D.; Steinweder, F. (1983): Mehraxiale Simulation stoßartiger Belastungen an Rohrkomponenten und Vergleich mit Rechenergebnissen (Multiple axial simulation of shock loads on pipes and comparison with calculations). VDI-Report No. 496, VDI-Verlag, 1983, pp. 71–78 (in German).
- Lewandowski, R. (1969): Beurteilung von Bauwerksfestigkeiten an Hand von Betongüewürfeln und -bohrproben, Beitrag zur Abschätzung der Festigkeitsverteilung in



- Bauwerken (Evaluation of building strength by means of concrete cubes and specimen taken from the building, comment on the distribution of strengths in the building). Doctor thesis, Technische Universität Braunschweig, 1969 (in German).
- Li, L., Eligehausen, R. (1994): Load-Bearing Behaviour of Multiple Anchorfastenings subjected to Combined Tension and Shear Load and Bending Moment. Report No. 19/2-94/17, Institute of Construction Materials, University of Stuttgart, August 1993, not published.
- Li, Y.-J.; Eligehausen, R. (2001): Numerical Analysis of Group Effect in Bonded Anchors with Different Bond Strengths. In Eligehausen, R. (Editor): RILEM Proceedings PRO 21 „Connections Between Steel and Concrete“, RILEM Publications s.a.r.l. Cachan Cedex, pp. 699–707.
- Li, Y.-J.; Eligehausen, R.; Ozbolt, J.; Lehr, B. (2002): 3D Numerical Analysis of Quadruple Fastenings with Bonded Anchors. *ACI Structural Journal*, March-April 2002, pp. 149–156.
- Lieberum, K. H. (1986): Dübelverankerungen in Bereichen maximaler Momente und erhöhter Hauptzugspannungen (Anchorage in the area of maximum bending moments and increased main tension stresses). 18. Forschungskolloquium des Deutschen Ausschusses für Stahlbeton in Darmstadt, Ernst & Sohn, Berlin, 1986, pp. 99–104 (in German).
- Lieberum, K. H. (1987): Das Tragverhalten von Beton bei extremer Teilflächenbelastung (Load-bearing behaviour of concrete under extreme local stresses). Doctor thesis, Technische Hochschule Darmstadt, 1987 (in German).
- Lieberum, K. H.; Reinhardt, H. W.; Walraven, J. C. (1987): Lasteinleitung über Dübel in der Schubzone von Beton-Plattenstreifen (Introduction of load into the shear area of reinforced concrete slabs by anchors). *Beton + Fertigteile-Technik* 10 (1987), pp. 708–715 (in German).
- Liersch, K. W. (1981): Belüftete Dach- und Wandkonstruktionen (Ventilated roof- and wall construction). Bauverlag, Wiesbaden, Berlin, 1981 (in German).
- Lotze, D. (1987/1): Ermüdungsfestigkeit des Betonausbruchs (Fatigue strength of concrete failure). Report No. 11/4-87/12, Institut für Werkstoffe im Bauwesen, Universität Stuttgart, 1987, not published (in German).
- Lotze, D. (1987/2): Untersuchungen zur Frage der Wahrscheinlichkeit, mit der Dübel in Rissen liegen – Einfluß der Querbewehrung (Investigation on the probability that anchors are located in cracks – influence of a transverse reinforcement). Report No. 1/24-87/6, Institut für Werkstoffe im Bauwesen, Universität Stuttgart, 1987, not published (in German).
- Lotze, D. (1989/1): Tragverhalten von Dübeln unter nicht ruhender Belastung – Stand der Kenntnisse und mögliche Perspektiven (Load-bearing behaviour of anchors under non predominantly static loading – State-of-the-art and outlook). Report No. 11/7-89/14, Institut für Werkstoffe im Bauwesen, Universität Stuttgart, July 1989, not published (in German).
- Lotze, D. (1989/2): Beeinflussung der Trag- und Gebrauchsfähigkeit von Stahlbetonbauteilen durch Spaltkräfte von Befestigungen (Influence of splitting forces caused by fixings on the load-bearing capacity and serviceability of reinforced concrete structures). *Werkstoff und Konstruktion II*, pp. 169-178, Institut für Werkstoffe im Bauwesen, Universität Stuttgart und Forschungs- und Materialprüfungsanstalt Baden-Württemberg, 1989 (in German).
- Lotze, D. (1993): Tragverhalten und Anwendung von Dübeln unter oftmals wiederholter Belastung (Load-bearing behaviour and application of anchors under frequently repeated loading). Doctor thesis, Universität Stuttgart, 1993 (in German).
- Lotze, D. (1998): Letter to Eligehausen, 1998 (in German).
- Lotze, D.; Klingner, R. E. (1997): Behaviour of Multiple-Anchor Connections to Concrete From the Perspective of Plastic Theory. PMFSEL Report No. 96-4. The University of Texas at Austin, March 1997.
- Mallée, R. (2001): Behaviour and Design of Anchors Close to an Edge under Torsion. In Eligehausen, R. (Editor): RILEM Proceedings PRO 21 „Connections Between Steel

- and Concrete“, RILEM Publications s.a.r.l. Cachan Cedex, pp. 178–185.
- Mallée, R. (2002): Dübelgruppen am Bauteilrand unter Torsionsbeanspruchung (Anchor groups close to an edge under torsion). *Beton- und Stahlbetonbau*, 2002, No. 2, pp. 69–77 (in German).
- Mallée, R.; Burkhardt, F. (1999): Befestigungen von Ankerplatten mit Dübeln (Fixings of steel plates with anchors). *Beton- und Stahlbetonbau*, 1999, No. 12, pp. 502–511 (in German).
- Manleitner, S.; Stichel, W. (1986): Zur Korrosion von Bauteilen aus nichtrostendem Stahl in Schwimmbadhallenatmosphäre (Corrosion of building components made from stainless steel under indoor swimming pool atmospheres). *Mitteilungen des Institutes für Bautechnik*, Berlin, 1986, No. 5, pp. 145–148 (in German).
- Mayer, R. (1988): Wahrscheinlichkeit, mit der Dübel in Rissen liegen (Probability that anchors are located in a crack). Report No. 1/35-88/22, Institut für Werkstoffe im Bauwesen, Universität Stuttgart 1988, not published (in German).
- Mayer, B. (1990): Funktionsersatzprüfung für die Beurteilung der Eignung von kraftkontrolliert spreizenden Dübeln (Function simulation tests for evaluation of suitability of torque-controlled expansion anchors). Doctor thesis, Universität Stuttgart, 1990 (in German).
- Mayer, B.; Eligehausen, R. (1984): Ankergruppen mit Dübeln in der Betonzugzone (Groups of anchors in the concrete tensile zone). In: *Werkstoffe und Konstruktion*. Institut für Werkstoffe im Bauwesen, Universität Stuttgart and Forschungs- und Materialprüfungsanstalt Baden-Württemberg, October 1984, pp. 167–180 (in German).
- Mc Mackin, P. J.; Slutter, R. G.; Fisher, J. W. (1973): Headed Steel Anchors Under Combined Loading. *AISC Engineering Journal*, 2nd Quarter, 1973, pp. 43–52.
- Meinheit, D. F.; Heidbrink, F. D. (1985): Behavior of Drilled-In Expansion Anchors. *Concrete International*, April 1985, pp. 62–66.
- Menzel, K. (1985): Korrosion von Befestigungselementen hinter vorgehängten Fassaden (Corrosion of fixing elements behind curtain walls). Report No. 5/7-85/17, Institut für Werkstoffe im Bauwesen, Universität Stuttgart, November 1985, not published (in German).
- Menzel, K. (1992): Zur Korrosion von verzinktem Stahl in Kontakt mit Beton (Corrosion of galvanised steel in contact with concrete). Doctor thesis, Universität Stuttgart, 1992 (in German).
- Mesureur, B. (1995): Study of the Pryout Failure Mode, Fastenings Placed Near an Edge in Non-Cracked Concrete. Research Report No. 94095/3, Centre Scientifique Et Technique Du Batiment, Paris, 1995.
- Mesureur, B. (1995/1): Fatigue Loading Acting on the Concrete Member Serving as an Anchoring Base. Report No. 1/67-95/5, Centre Scientifique Et Technique Du Batiment, Paris, 1994.
- Meszaros, J. (1999): Tragverhalten von Verbunddübeln im ungerissenen und gerissenen Beton (Load-bearing behaviour of bonded anchors in non-cracked and cracked concrete). Doctor thesis, Universität Stuttgart, 1999 (in German).
- Meszaros, J.; Eligehausen, R. (1992): Zentrische Zugversuche mit Einschlagdübeln M12 mit verschiedenen Verspreizungszuständen im gerissenen und ungerissenen Beton (Axial tension tests with displacement-controlled expansion anchors (drop-in anchors) M12 with different expansion conditions in cracked and non-cracked concrete). Report No. 1/54-92/25, Institut für Werkstoffe im Bauwesen, Universität Stuttgart. 1992, not published (in German).
- Meszaros, J.; Eligehausen, R. (1996/1): Ausziehversuche mit Verbunddübeln, die in gereinigte und nicht gereinigte Bohrlöcher gesetzt wurden (Pull-out tests with bonded anchors installed in cleaned and uncleaned holes). Report No. 1/81-96/14, Institut für Werkstoffe im Bauwesen, Universität Stuttgart, 1996, not published (in German).
- Meszaros, J.; Eligehausen, R. (1996/2): Ausziehversuche mit Verbunddübeln, die in feuchten Beton gesetzt wurden (Pull-out tests with bonded anchors installed in humid concrete). Report No. 1/86-96/23, Institut für Werkstoffe im Bauwesen, Universität Stuttgart, 1996, not published (in German).

- Meszaros, J.; Eligehausen, R. (1998): Einfluß der Bohrlochreinigung und von feuchtem Beton auf das Tragverhalten von Injektionsdübeln (Influence of hole cleaning and of humid concrete on the load-bearing behaviour of injection anchors). Report No. 98/2-2/2, Institut für Werkstoffe im Bauwesen, Universität Stuttgart, 1998, not published (in German).
- Moe, J. (1961): Shearing Strength of Reinforced Concrete Slabs and Footings under concentrated Loads. Bulletin D 47, Portland Cement Association, Research and Development Laboratories, Skokie, Illinois, 1961.
- Naithani, K. C.; Gupta, V. K.; Gudh, A. D. (1988): Behavior of Shear Connection Under Dynamic Loads. *Material und Construction*, 1988, 21, pp. 359–363.
- National Earthquake Hazard Reduction Program (NEHRP) (2001): Recommended Provisions for Seismic Regulations for New Buildings and Other Structures, 2000 Edition. Building Seismic Safety Council, Washington, D.C., 2001.
- Nürnbergger, U. (1995): Korrosion und Korrosionsschutz im Bauwesen (Band 1 und 2) (Corrosion and corrosion protection in the building industry (Vol. 1 and 2)). Bauverlag GmbH, Wiesbaden und Berlin, 1995 (in German).
- Okada, T.; Icki, M. (1984): Nonlinear earthquake response of equipment system anchored on reinforced concrete building floor. Proceedings, 8 WCEE, San Francisco, 1984.
- Ollgaard, J. G.; Slutter, R. G.; Fisher, J. W. (1971): Shear Strength of Stud Connectors in Lightweight and Normal-Weight Concrete. *AISC Engineering Journal*, Vol. 8, No. 2, April 1971, pp. 55–64.
- Oluokon, F. A.; Burdette, E. G. (1993): Behavior of Channel Anchors in Thin Slabs under Combined Shear and Tension (Pullout) Loads. *ACI Structural Journal*, July-August 1993, pp. 407–413.
- Opitz, V.; Eligehausen, R. (1989): Auswertung der zentrischen Zugversuche mit dem Verbunddübel UKA 3 M12 (Evaluation of results of tests with bonded anchors UKA 3 M12 under axial tension). Report No. 1/39-89/12, Institut für Werkstoffe im Bauwesen, Universität Stuttgart, 1989, not published (in German).
- Ottosen, N. S. (1981): Non-linear Finite-Element-Analysis of Pull-Out-Tests. *Journal of Structural Division*, Vol. 107, No. St4, April 1981, pp. 591–603.
- Ozbolt, J. (1995): Maßstabeffekt und Duktilität von Beton- und Stahlbetonkonstruktionen (Size effect and ductility of concrete and reinforced concrete structures). Thesis submitted for the certificate of habilitation, Universität Stuttgart, 1995, published in: *Mitteilungen des IWB*, No. 1995/2 (in German).
- Ozbolt, J. (1998): MASA – Finite Element Program for Nonlinear Analysis of Concrete and Reinforced Concrete Structures. Institut für Werkstoffe im Bauwesen, Universität Stuttgart, 1998.
- Ozbolt, J.; Eligehausen, R. (1990): Numerical Analysis of headed studs embedded in large plain concrete blocks. In: Bicanic, N.; Mang, H. (Herausgeber): *Computer Aided Analysis and Design of Concrete Structures*. Pineridge Press, London, 1990.
- Paschen, H.; Schönhoff, T. (1983): Untersuchungen über in Beton eingelassene Scherbolzen aus Betonstahl (Investigation on shear bolts in concrete made from concrete steel). *Schriftenreihe des Deutschen Ausschusses für Stahlbeton*, No. 346, Ernst & Sohn, Berlin, 1983 (in German).
- Paterson, W. S. (1978): Indicative fire tests on fixings. CIRIA, Technical Note 92, London, 1978.
- Patzak, M. (1979): Zur Frage der Sicherheit von Setzbolzenbefestigungen in Betonbauteilen (Safety of fixings with powder actuated fasteners in concrete elements). *Betonwerk + Fertigteile-Technik*, 1979, No. 5, pp. 308–314 (in German).
- Peier, W. H. (1983): Model for Pull-Out Strength of Anchors in Concrete. *Journal of Structural Engineering*, Vol. 109 (1983), No. 5, pp. 1155–1173.
- Plank, A. (1977): Bautechnische Einflüsse auf die Tragfähigkeit von Kunststoffdübeln in Mauerwerk (Influences on the load-bearing capacity of plastic anchors in masonry). *Baumaschine-Bautechnik*, 1977, No. 6, pp. 406–416 (in German).
- Powell, J. B.; Burdette, E. G.; Oluokun, F. A. (1991): Prediction of Pullout Capacity of

- Channel Anchors. *ACI Structural Journal*, September – October 1991, pp. 624–630.
- Powell, J. B.; Burdette, E. G.; Oluokun, F. A. (1992): Prediction of Shear Capacity of Anchors in Thin Slabs. *ACI Structural Journal*, September – October 1992, pp. 564–568.
- Pregartner, T. (2003): Tragverhalten von Kunststoffdübeln im ungerissenen und gerissenen Beton (Load-bearing behaviour of plastic anchors in non-cracked and cracked concrete). Doctor thesis, Universität Stuttgart, 2003.
- Primavera, E. J.; Pinelli, J.-P.; Kalajian, E. H. (1997): Tensile Behaviour of Cast-in-Place and Undercut Anchors in High-Strength Concrete. *ACI Structural Journal*, V. 94, No. 5, September-October 1997, pp. 583–593.
- Pukl, R.; Ozbolt, J.; Schlottke, B.; Eligehausen, R. (1993): Splitting of Concrete. Part 3: Computer Simulation of Concrete Members Under Combined Load. Report No. 16/6-93/13, Institute of Construction Materials, University of Stuttgart, 1993, not published.
- Pukl, R.; Ozbolt, J.; Eligehausen, R. (1998): Load-Carrying Behavior of Bonded Anchors Based on FEM-Analysis. Report No. 98/3-2/3, Institute of Construction Materials, University of Stuttgart, 1998, not published.
- Pusill-Wachtsmuth, P. (1982): Tragverhalten von Metallspreizdübeln unter zentrischer Zugbeanspruchung bei den Versagensarten Betonausbruch und Spalten des Betons (Load-bearing behaviour of metal expansion anchors under axial tension for concrete and splitting failure). Doctor thesis, Universität Stuttgart, 1982 (in German).
- Pusill-Wachtsmuth, P. (1999): Die Europäische Technische Zulassung für Dübel (European approvals for anchors). *Beton- und Stahlbetonbau* 94 (1999), No. 12, pp. 496–501 (in German).
- Ramm, W. (1993): Gutachten zur Bemessung von Kopfbolzenverankerungen mit Rückhängebewehrung (Expert's opinion: Design of headed anchors with supplementary reinforcement). Kaiserslautern, 1993 (in German).
- Ramm, W.; Greiner, U. (1991): Verankerungen mit Kopfbolzen – Randnahe Verankerungen unter Querzugbeanspruchung und randferne Verankerungen unter zentrischer Zugbeanspruchung – Untersuchung des Einflusses von speziellen Rückhängebewehrungen (Anchorage with headed anchors – anchors close to an edge under shear loading and anchors remote from an edge under axial tension loading – Investigation of the influence of special supplementary reinforcement). Research Report, Universität Kaiserslautern, Fachgebiet Massivbau und Baukonstruktion, 1991 (in German).
- Rankweil (1989): Tragfähigkeit von Setzbolzen bei dynamischer Zuglast (Load-bearing capacity of powder actuated fasteners under dynamic tension loading). Report No. 126/89 of HTL Rankweil dated 6.6.1989, Rankweil, 1989, not published (in German).
- Rasmussen, B. H. (1963): The Carrying Capacity of Transversely Loaded Bolts and Dowels Embedded in Concrete. *Bygningstiske Meddelelser*, Copenhagen, 1963.
- Rehm, G. (1978): Langzeitverhalten von HILTI-Verbundankern HVA (Long-term behaviour of Hilti bonded anchors HVA). Expert's opinion dated 23.6.1978, not published (in German).
- Rehm, G. (1985/1): Zur Frage des Langzeitverhaltens von HILTI-Verbundankern (HVA) (Long-term behaviour of Hilti bonded anchors (HVA)). Expert's opinion No. 22/07.85 dated 1.10.1985, not published (in German).
- Rehm, G. (1985/2): Zur Frage der Eignung von HILTI-Verbundankern auf Basis eines EP-Acrylatharzes für tragende Konstruktionen (Suitability of Hilti bonded anchors based on EP-acrylate resin for load-bearing structures). Expert's opinion No. 31/12.85 dated 16.12.1985, not published (in German).
- Rehm, G. (1986): Zur Frage des Langzeitverhaltens von UPAT-Verbundankern UKA 3 (Long-term behaviour of Upat bonded anchors UKA 3). Expert's opinion No. 43/07.86 dated 1.7.1986, not published (in German).
- Rehm, G. (1987): Gutachtliche Stellungnahme vom 27.10.1987 (Expert's opinion dated 27.10.1987). München, not published (in German).
- Rehm, G. (1988): Zur Frage der Eignung von Upat-Verbunddübeln auf der Basis eines

- Epoxy-Acrylatharzes für tragende Konstruktionen (Suitability of Upat bonded anchors based on EP-acrylate resin for load-bearing structures). Expert's opinion dated 5.5.1988, not published (in German).
- Rehm, G.; Eligehausen, R. (1977): Einfluß einer nicht ruhenden Belastung auf das Verbundverhalten von Rippenstählen (Influence of a non predominantly static load on the bond behaviour of ribbed rebars). *Betonwerk + Fertigteil-Technik*, 1977, No. 6, pp. 295–299 (in German).
- Rehm, G.; Franke, L. (1978): Verankerungen von Betonrippenstählen in Kunstharzmörtel und Kunstharzbeton (Anchorage of ribbed rebars in resin mortar and resin concrete). *Bauingenieur* 53, 1978 (in German).
- Rehm, G.; Pusill-Wachsmuth, P. (1978): Sicherheitsbetrachtungen bei Dübelverbindungen (Safety aspects with anchors). Research Report, Lehrstuhl für Werkstoffe im Bauwesen, Universität Stuttgart, January 1978, not published (in German).
- Rehm, G.; Pusill-Wachsmuth, P. (1979): Einfluß der Bewehrung auf das Tragverhalten von Dübelverbindungen (Influence of reinforcement on the load-bearing behaviour of anchors). Research Report, Lehrstuhl für Werkstoffe im Bauwesen, Universität Stuttgart, November 1979, not published (in German).
- Rehm, G.; Eligehausen, R. (1979): Bond of Ribbed Bars under High Cycle Repeated Loads. *ACI Journal*, February 1979, pp. 297–309, 1979.
- Rehm, G.; Eligehausen, R.; Paul, F. (1980): Verbundbewehrung in Fugen von Platten ohne Schubbewehrung (Bond reinforcement in joints of slabs without shear reinforcement). Research Report, Institut für Werkstoffe im Bauwesen, Universität Stuttgart, January 1980, not published (in German).
- Rehm, G.; Franke, L.; Zeus, K. (1980): Kunstharzmörtel und Kunstharzbetone unter Kurzzeit- und Dauerstandbelastung (Resin mortars and resin concrete under short- and long-term loading). Schriftenreihe des Deutschen Ausschusses für Stahlbeton, No. 309, Ernst & Sohn, Berlin, 1980 (in German).
- Rehm, G.; Lehmann, R.; Nürnberger, U. (1980): Korrosion der Befestigungselemente bei vorgehängten Fassaden (Corrosion of fixing elements behind curtain walls). Research Report, Forschungs- und Materialprüfungsanstalt Baden-Württemberg, Stuttgart, March 1980, not published (in German).
- Rehm, G.; Franke, L. (1982): Kleben im konstruktiven Ingenieurbau (Bonding in structural engineering). Schriftenreihe des Deutschen Ausschusses für Stahlbeton, No. 321, Ernst & Sohn, Berlin, 1982.
- Rehm, G.; Lehmann, R. (1982): Untersuchungen mit Metallspreizdübeln in der gerissenen Zugzone von Stahlbetonbauteilen (Investigation on metal expansion anchors in the cracked tensile zone of reinforced concrete elements). Research Report, Forschungs- und Materialprüfungsanstalt Baden-Württemberg, Stuttgart, July 1982, not published (in German).
- Rehm, G.; Eligehausen, R. (1984): Auswirkungen der modernen Befestigungstechnik auf die konstruktive Gestaltung im Stahlbetonbau (Effect of modern fixing technology on the construction of reinforced concrete elements). *Betonwerk + Fertigteil-Technik*, 1984, No. 6, pp. 388–392 (in German).
- Rehm, G.; Schlaich, J.; Schäfer, K.; Eligehausen, R. (1985): Fritz-Leonhardt-Kolloquium 1984 – 15. Forschungskolloquium des Deutschen Ausschusses für Stahlbeton. *Beton- und Stahlbetonbau*, 1985, No. 6, pp. 156–161 and No. 7, pp. 190–194 (in German).
- Rehm, G.; Eligehausen, R.; Mallée, R. (1988): Befestigungstechnik (Fixing technology). *Betonkalender 1988, Part II*, Ernst & Sohn, Berlin, 1988, pp. 569–663 (in German).
- Rehm, G.; Eligehausen, R.; Mallée, R. (1992): Befestigungstechnik (Fixing technology). *Betonkalender 1992, Part II*, Ernst & Sohn, Berlin, 1992, pp. 597–715 (in German).
- Reick, M. (1998/1): Brandverhalten von Befestigungen in Beton bei zentrischer Zugbeanspruchung: Auswertung der Versuche mit Stahlversagen (Behaviour of fixings under fire and axial tension: Assessment of tests with steel failure). Report No. 21/8-98/1, Institut für Werkstoffe im Bauwesen, Universität Stuttgart, 1998, not published (in German).



- Reick, M. (1998/2): Brandverhalten von Befestigungen; Befestigungen mit der Versagensart Herausziehen (Behaviour of fixings under fire; Pull-out failure). Report No. 98/9-4/1, Institut für Werkstoffe im Bauwesen, Universität Stuttgart, 1998, not published (in German).
- Reick, M. (2001): Brandverhalten von Befestigungen mit großem Randabstand in Beton bei zentrischer Zugbeanspruchung (Behaviour of fixings remote from an edge in concrete under axial tension). Doctor thesis, Universität Stuttgart, IWB Mitteilungen 2001/4, 2001 (in German).
- Reick, M.; Eligehausen, R. (2003): Befestigungen unter Brandbeanspruchung (Fixings under fire). Beton- und Stahlbetonbau 98, 2003, No. 6, pp. 317–325 (in German).
- Reinhardt, H.-W. (1984): Fracture Mechanics of an Elastic Softening Material like Concrete. HERON, 1984, Vol. 29, No. 2.
- Reinhardt, H.-W. (1997): Werkstoffe des Bauwesens (Building materials). In: Der Ingenieurbau, Editor: Mehlhorn, G., Ernst & Sohn, Berlin, 1997, pp. 1–163 (in German).
- Rommel, G. (1994): Zum Zug- und Schubtragverhalten von Bauteilen aus hochfestem Beton (Tension and shear behaviour of building components made from high-strength concrete). Deutscher Ausschluß für Stahlbeton, No. 444, Beuth Verlag (1994) (in German).
- Reuter, M.; Eligehausen, R. (1986): Zulässiger Anteil der durch Befestigungselemente in die Zugzone einleitbaren Lasten an der Gesamtbelastung von Stahlbetonbauteilen ohne Schubbewehrung (Permissible ratio of the load transmitted to reinforced concrete elements without shear reinforcement by fixings to the total load). Report No. 1/17a-86/18, Institut für Werkstoffe im Bauwesen, Universität Stuttgart, November 1986, not published (in German).
- Reuter, M.; Eligehausen, R. (1992): Einfluß der Lasteinleitung durch Befestigungen auf die Tragfähigkeit von Stahlbetonbauteilen (Influence of load transmission by fixings on the load-bearing capacity of reinforced concrete elements). Bauingenieur 67, 1992, pp. 461–474 (in German).
- Rieche, G.; Weißmann, U.; Wehrle, S. (1998): Galvanisch verzinkte Stahlschrauben in Kunststoffdübeln zur Verankerung der Unterkonstruktion für Fassadenbekleidungen in Porenbeton (Galvanised steel screws in plastic anchors for fixings of substructures of claddings to aerated concrete). Materials and Corrosion 49, 1998, pp. 585–590 (in German).
- Riemann, H. (1981): Schreiben vom 25.11.1981 und 8.12.1981 an das Institut für Bautechnik, Berlin (Letters to the “Institut für Bautechnik”, Berlin, dated 25.11.1981 and 8.12.1981) (in German).
- Riemann, H. (1985): Das “erweiterte  $\kappa$ -Verfahren” für Befestigungsmittel, Bemessung an Beispielen von Kopfbolzenverankerungen (The expanded  $\kappa$ -method for fixings, design examples for headed anchors). Betonwerk + Fertigteil-Technik, 1985, No. 12, pp. 808–815 (in German).
- Riemann, H. (1987): Zugbeanspruchte randnahe Verankerungen – Nachweis gegen Betonversagen mit einem verbesserten  $\kappa_r$ -Wert (Fastenings close to an edge under tension loading – Proof for concrete cone failure using an improved  $\kappa_r$ -value). Betonwerk + Fertigteil-Technik, No. 6, 1987, pp. 437–442 (in German).
- Riemann, H. (1990): Schreiben vom 20.9.1990 an das Institut für Bautechnik, Berlin (Letter to “Institut für Bautechnik”, Berlin, dated 20.9.1990) (in German).
- Roeder, K. (1984): Tragverhalten von Kunststoffdübeln (Load-bearing behaviour of plastic anchors). Kunststoffe im Bau, 1984, No. 1, pp. 15–18 (in German).
- Roik, K. (1982): Verbundkonstruktion (Composite construction). Stahlbau-Handbuch, Vol. 1, Stahlbau-Verlags-GmbH, Köln, 1982, pp. 627–672 (in German).
- Sawade, G. (1994): Ein energetisches Materialmodell zur Berechnung des Tragverhaltens von zugbeanspruchtem Beton (Energetic material model to describe the load-bearing behaviour of concrete under tension). Doctor thesis, Universität Stuttgart, 1994 (in German).
- Scheer, J.; Peil, U.; Nölle, P. (1987): Schrauben mit planmäßiger Biegebeanspruchung (Screws under planned bending). Report

- No. 6079, Institut für Stahlbau, TU Braunschweig, 1987 (in German).
- Schießl, P. (1986): Einfluß von Rissen auf die Dauerhaftigkeit von Stahlbeton- und Spannbetonbauteilen (Crack influence on the durability of reinforced and prestressed concrete components). Schriftenreihe des Deutschen Ausschusses für Stahlbeton, No. 370, Ernst & Sohn, Berlin, 1986 (in German).
- Schießl, P. (1989): Erläuterung von DIN 1045, Ausgabe 07.88, Abschnitt 17.6 "Beschränkung der Rißbreite unter Gebrauchslast" (Comments on DIN 1045, Edition 07.88, section 17.6 "Limitation of crack width under service load"). Schriftenreihe des Deutschen Ausschusses für Stahlbeton, No. 400, Berlin, 1989, pp. 84–92 (in German).
- Schlaich, J.; Schäfer, K. (1989): Konstruieren im Stahlbetonbau (Reinforced concrete construction). Betonkalender 1989, Part II, Ernst & Sohn, Berlin, 1989, pp. 563–715 (in German).
- Schmidt, H.; Knoblauch, M. (1988): Schrauben unter reiner Scherbeanspruchung und kombinierter Scher-Zugbeanspruchung (Screws under shear and under combined shear-tension loading). Stahlbau 57 (1988), No. 6, pp. 169–174 (in German).
- Schou, A.; Christiansen, M. W.; Andersen, R. (1998): Fracture Analysis of bonded Anchors. Master Thesis in Civil Engineering, Aalborg University, 1998.
- Schuler, D.; Erdin, B. (1998): Einflüsse auf das Tragverhalten schockbeanspruchter Metallspreizdübel im gerissenen Beton (Effects on the load-bearing behaviour of metal expansion anchors in cracked concrete under shock loading). AC-Laboratorium Spiez, 1998 (in German).
- Schweizerischer Ingenieur- und Architektenverein (1979): SIA 161, Stahlbauten (SIA 161, Steel construction). Zürich, 1979 (in German).
- Schweizerischer Ingenieur- und Architektenverein (1993): SIA 162, Betonbauten (SIA 162, Concrete construction). Zürich, 1993 (in German).
- Schweizerischer Ingenieur- und Architektenverein (1998): SIA 179, Befestigungen in Beton und Mauerwerk (SIA 179, Fixings to concrete and masonry). Zürich, 1998 (in German).
- Seghezzi, H. D. (1983): Wirtschaftliche und sichere Befestigungssysteme für die Baupraxis (Economic and safe fixing systems for buildings). Betonwerk + Fertigteil-Technik, 1983, No. 1, pp. 41–45, No. 2, pp. 117–123 (in German).
- Seghezzi, H. D. (1984): Befestigungsverfahren im Bauwesen mit besonderer Berücksichtigung des Bolzensetzens (Fixing systems for the building industry with special emphasis on powder actuated fasteners). In: Eligehausen, R.; Rußwurm, D. (Editors): Fortschritte im konstruktiven Ingenieurbau, Ernst & Sohn, Berlin, 1984, pp. 285–295.
- Seghezzi, H. D. (1985): Wechselbeziehungen zwischen Prüftechnik und Entwicklung von Befestigungselementen (Interactions between testing technology and development of fastening elements), Lecture held on January 15th, 1985 at the University of Stuttgart, not published (in German).
- Seghezzi, H. D. (1986): Einflüsse der Belastungsgeschichte und der Umgebung (Effects of load history and environment). Manuskript der Vorlesungsreihe Befestigungstechnik an der ETH Zürich, Sommersemester 1986, pp. 8.1–8.10, not published (in German).
- Seiler, H. F.; Kupfer, H.; Manleitner, S. (1989): Stahlbetonfertigteile, Geschloßdecken, Dachdecken und vergleichbare Bauteile mit Fertigteilen (Precast reinforced concrete members, ceilings, roofs and comparable precast building components). Schriftenreihe des Deutschen Ausschusses für Stahlbeton, No. 400, Beuth-Verlag, Berlin/Köln, 1989, pp. 125–128 (in German).
- Sell, R. (1973/1): Festigkeit und Verformung mit Reaktionsharmörtelpatronen versetzter Anker (Capacity and displacement of bonded capsule anchors). Verbindungstechnik, 1973, No. 8, pp. 11–16 (in German).
- Sell, R. (1973/2): Tragfähigkeit von mit Reaktionsharmörtel versetzten Betonankern und deren Berechnung (Load-bearing capacity and design of bonded anchors). Die Bautechnik, 1973, No. 10, pp. 333–339 (in German).



- Shaikh, A. F.; Whayong, Y. (1985): In-Place Strength of Welded Headed Studs. *Journal of the Prestressed Concrete Institute*, March/April 1985, pp. 56–81.
- Sippel, T. M.; Asmus, J.; Eligehausen, R. (2001): Safety concepts for fastenings in nuclear power plants. In Eligehausen, R. (Editor): *RILEM Proceedings PRO 21 "Connections Between Steel and Concrete"*, RILEM Publications s.a.r.l. Cachan Cedex, pp. 564–575.
- Sippel, T.; Eligehausen, R. (2003): Einfluß einer Rückhängebewehrung auf die Tragfähigkeit von Befestigungen am Bauteilrand bei Belastung durch eine Querlast zum Rand (Influence of supplementary reinforcement on the load-bearing capacity of fixings close to an edge loaded by a shear load perpendicular to the edge). Report, Ingenieurbüro Eligehausen & Sippel, Stuttgart (in German).
- Slutter, R. G.; Fisher, J. W. (1966): *Fatigue Strength of Shear Connectors*. Report No. 147, Highway Research Board, Washington, 1966.
- Spieth, H. A. (2002): *Tragverhalten und Bemessung von eingemörtelten Bewehrungsstäben (Load-bearing behaviour and design of post-installed reinforcement)*. Doctor thesis, Universität Stuttgart, 2002 (in German).
- Spieth, H. A.; Eligehausen, R. (2000): Prüfbericht über Zulassungsversuche mit eingemörtelten Bewehrungsstäben mit Hilti HIT-HY 150 unter nichtruhender Belastung (Report on approval tests with post-installed rebars using Hilti HIT-HY 150 under non predominantly static loading). Institut für Werkstoffe im Bauwesen, Universität Stuttgart, November 2000, not published (in German).
- Spieth, H. A.; Eligehausen, R. (2002): *Bewehrungsanschlüsse mit nachträglich eingemörtelten Bewehrungsstäben (Starter bars with post-installed rebars)*. *Beton- und Stahlbetonbau* 97, No. 9, pp. 445–459, Berlin, 2002 (in German).
- Stampfer, S.; Ehrenstein, G. W. (1995): Einfluß des Molekulargewichts und des Glasfasergehalts auf das Kriechen von Thermoplasten (Effect of molecular weight and of glass fibre content on the creep behaviour of thermoplasts). *GAK* 6/1995, pp. 372–378 (in German).
- Stichel, W. (1986): *Beurteilung des Korrosionsverhaltens von Metallen und Korrosionsschutzmaßnahmen in Hallenbädern (Assessment of corrosion behaviour of metals and corrosion protection in indoor swimming pools)*. Research Report No. 126, Bundesanstalt für Materialforschung und -prüfung, Berlin, Verlag für neue Wissenschaft GmbH, Bremerhaven, 1986 (in German).
- Stichting Bouwresearch (1971): *Uit beton stekende ankers*. Report of the Studienkommission B 7, No. 29, 1971.
- Storck, J. (1990): *Nicht vorwiegend ruhende Belastung – Anwendungsbeispiele mit dem Liebig Einspananker Ultraplus M12 (Non predominantly static loading – Applications using Liebig Einspananker Ultraplus M12)*. Darmstädter Massivbau Seminar, Vol. 5, pp. XIII 1–16, 1990 (in German).
- Theiler, F. (1993): *Umweltbedingungen und Schäden an Befestigungen im Hochbau (Environmental conditions and damages to fixings in building constructions)*. *Befestigungstechnik im Hochbau*, 3rd annual set, August 1993, pp. 25–30 (in German).
- Thomala, W. (1978): *Beitrag zur Dauerhaltbarkeit von Schraubenverbindungen (Durability of screwed connections)*. Doctor thesis, TH Darmstadt, 1978 (in German).
- Uéda, T.; Stitmannathum, B.; Matupagout, S. (1991): *Experimental Investigation on Shear Strength of Bolt Anchorage Groups*. *ACI Structural Journal*, May-June 1991, pp. 292–300.
- Union Européene Pour L'Agrément Technique Dans La Construction (1986): *UEAtc Directives for Assessment of Anchor Bolt*. M.O.A.T. No. 42:1986, British Board of Agrément, Watford, December 1986.
- Union Européene Pour L'Agrément Technique Dans La Construction (1992): *UEAtc Technical Guide on Anchors for Use in Cracked and Non-cracked Concrete*. M.O.A.T. No. 49:1992, British Board of Agrément, Watford, June 1992.
- Upat (1989): *Zugversuche mit UKA 3 M12 – K27, UKA 3 M12 – EAP und Hilti HEA M12 im Beton bei verschiedenen Temperaturen (Tensile tests with UKA3 M12 – K27, UKA3 M12 – EAP and Hilti HEA M12 in*

- concrete at different temperatures). Report No. 1451, Emmendingen, 1989 (in German).
- Usami, S.; Abe, Y.; Matsuzaki, Y. (1980/1): Experimental Research on the Tensile Fatigue Strength of 19 mm Headed Studs. Proceedings of the Annual Meeting of Kanton Branch of Architectural Institute of Japan, Tokio, 1980.
- Usami, S.; Abe, Y.; Matsuzaki, Y. (1980/2): Experimental study of the strength of headed anchor bolts under alternate shear load and combined shear load. Proceedings of the Annual Meeting of Kanton Branch of Architectural Institute of Japan, Tokio, 1980.
- Usami, S.; Abe, Y.; Matsuzaki, Y. (1983): Studies on the Fatigue Strength of Anchors for Supporting Equipment and Piping. Tensile Fatigue Strength against Cone-shaped Concrete Failure. Proceedings of the Annual Meeting of Kanton Branch of Architectural Institute of Japan, Tokio, 1983.
- Usami, S.; Abe, Y.; Nagano, T.; Kowada, A.; Kobayashi, J.; Kodama, J.; Koike, K. (1988): Supporting Capacity of Anchorage for Pipe and Equipment of Shear Walls in Nuclear Power Plants. Proceedings of the Annual Meeting of Kanton Branch of Architectural Institute of Japan, Tokio, 1988.
- U.S. Occupational Safety and Health Administration (OSHA) (1989): Requirements for Precast Concrete-1926.704, October 1989.
- Utescher, G. (1978): Beurteilungsgrundlagen für Fassadenverankerungen (Assessment of facade fixings). Ernst & Sohn, Berlin 1978 (in German).
- Valtinat, G. (1982): Schraubverbindungen (Screwed connections). Stahlbau-Handbuch, Vol. 1, Stahlbau-Verlags-GmbH, Köln, 1982, pp. 402–425.
- Varga, J.; Eligehausen, R. (1994): Bending of Anchors. Report No. 10/24-94/22, Institut für Werkstoffe im Bauwesen, Universität Stuttgart, not published.
- Varga, J.; Eligehausen, R. (1995): Test Program for Fastenings with Headed Studs, Part 1. Report No. Te 696/1 – 95/4, Institut für Werkstoffe im Bauwesen, Universität Stuttgart, not published.
- Varga, J.; Eligehausen, R. (1996): Test Program for Fastenings with Headed Studs, Part 2. Report No. Te 696/03 – 96/05, Institute of Construction Materials, University of Stuttgart, not published.
- Verein deutscher Ingenieure (VDI) (1983): Systematische Berechnung hochbeanspruchter Schraubverbindungen (Systematical design of highly loaded bolt connections). VDI-Richtlinie 2230, Beuth Verlag, Berlin, 1983 (in German).
- Vintzeleou, E.; Tassios, T. P. (1987): Behavior of dowels under cyclic deformations. ACI-Journal, January/February 1987, pp. 18–30.
- Vintzeleou, E.; Eligehausen, R. (1991): Behavior of fasteners under monotonic or cyclic shear displacements. In: Senkiw, G.A.; Lancelot, H.B. (Editor): SP-130 “Anchors in Concrete – Design and Behaviour”. American Concrete Institute, Detroit, 1991, pp. 181–204.
- Wälti, P.; Thürlimann, B. (1981): Probabilistic Safety Model for the Design of Fastening Systems. Proceedings of Iccosar, 81, 1981, pp. 359–370.
- Wagner-Grey, U. (1977/1): Experimentelle und theoretische Untersuchungen zum Tragverhalten von Spreizdübeln im Beton (Experimental and theoretical research on the load-bearing behaviour of metal expansion anchors in concrete). Doctor thesis, Technische Universität München, 1977 (in German).
- Wagner-Grey, U. (1977/2): Einflüsse auf die Tragfähigkeit von Spreizdübeln im Beton (Influences on the load-bearing behaviour of metal expansion anchors in concrete). Verbindungstechnik, 1977, No. 4, pp. 27–30 (in German).
- Wagner-Grey, U. (1978): Nachträglich eingesetzte Dübel für tragende Verbindungen (Post-installed anchors for load-bearing connections). Bauingenieur 53, 1978, pp. 57–62 (in German).
- Weigler, H.; Fischer, R.; Dettling, H. (1964): Verhalten von Beton bei hohen Temperaturen (Behaviour of concrete at high temperatures). Schriftenreihe des Deutschen Ausschusses für Stahlbeton, No. 164, Ernst & Sohn, Berlin, 1964 (in German).
- Weigler, H.; Lieberum, K. H. (1984): Belastungsprüfungen an Liebig-Einspannankern Ultraplus M16, verankert in kreuzartig gerissenen Betonprobekörpern bei stoßartiger und

- statischer Belastung (Load tests on Liebig undercut anchors Ultraplus M16, anchored in concrete specimens with intersecting cracks under impact and static loads), Research Report, Technische Hochschule Darmstadt, Institut für Massivbau, 1984 (in German).
- Wellinger, K.; Dietmann, H. (1968): Festigkeitsberechnung (Strength determination). Alfred Körner Verlag, 1968 (in German).
- Wesche, K. (1993): Baustoffe für tragende Bauteile, Band 2: Beton, Mauerwerk (Building materials for load-bearing components, Vol. 2: Concrete, masonry). Bauverlag GmbH, Wiesbaden und Berlin, 1993 (in German).
- Weyerhäuser, C.-C. (1977): Befestigungen mit Spreizdübeln in Beton – Berechnungsverfahren für Dübelverbindungen (Fastenings with expansion anchors to concrete – design method for anchors). Mitteilungen des Instituts für Massivbau der Technischen Hochschule Darmstadt, 1977 (in German).
- Weyerhäuser, C.-C. (1984): Ein Verfahren zur Berechnung von dickwandigen, unbewehrten Betonringen unter zentrischer innerer rotationssymmetrischer Radial- und Tangentialbeanspruchung mit Hilfe der Finite-Element-Methode (Method for the design of thick, non reinforced concrete rings under concentric internal radial and tangential loads using the Finite Element method. Doctor thesis, Darmstadt, 1984 (in German).
- Wiedenroth, M. (1971): Einspanntiefe und zulässige Belastung eines in einem Betonkörper eingespannten Stabes (Length of restraint and permissible load of a rod clamped to a concrete member). Die Bautechnik, 1971, No. 12, pp. 426–436 (in German).
- Wiegand, H. (1974): Die Schraubenverbindung – Beispiel einer Gemeinschaftsaufgabe für Konstruktion, Fertigung und Werkstofftechnik (Bolt connections – Construction, production and material technology). VDI-Reports No. 220, VDI-Verlag, 1974, pp. 5–10 (in German).
- Wiegand, H.; Illgner, K.-H. (1962): Berechnung und Gestaltung von Schraubverbindungen (Design and construction of bolt connections), 3rd Edition, Springer-Verlag, Berlin, 1962 (in German).
- Wohlfahrt, R. (1996): Tragverhalten von Ankerschienen ohne Rückhängebewehrung (Behaviour of anchor channels without supplementary reinforcement). Doctor thesis, Universität Stuttgart, 1996 (in German).
- Wolinski, S.; Hordijk, D. A.; Reinhardt, H.W.; Cornelissen, H.A.W. (1987): Influence of Aggregate Size on Fracture Mechanics Parameters of Concrete. International Journal Cement Composites and Lightweight Concrete, 1987, 9 (2), pp. 95–103.
- Wong, T. L.; Donahey, R. C.; Lloyd, J. P. (1988): Stud groups loaded in shear near a free edge. Research Report. School of Civil Engineering, Oklahoma State University, 1988.
- Wüstner, J. (2002): Tragverhalten von Ankerschienen (Load-bearing behaviour of anchor channels). Diplomarbeit, Institut für Werkstoffe im Bauwesen, Universität Stuttgart, 2002 (in German).
- Zeitler, R.; Wörner, J.-D. (1995): Tragverhalten von Dübelverankerungen in hochfestem Beton (Behaviour of anchors in high strength concrete). Beton- und Stahlbetonbau 90, 1995, No. 9, pp. 241–244 (in German).
- Zhang, Y.-G. (1997): Dynamic Behavior of Multiple-Anchor Connections in Cracked Concrete. Doctor thesis, The University of Texas at Austin, Austin, 1997.
- Zhang, Y.-G.; Klingner, R. E.; Graves III, H. L. (2001): Seismic Response of Multiple-Anchor Connections to Concrete. ACI Structural Journal, November/December 2001, pp. 811–822.
- Zhao, G. (1993): Tragverhalten von randfernen Kopfbolzenverankerungen bei Betonbruch (Behaviour of headed anchors remote to an edge at concrete failure). Doctor thesis, Universität Stuttgart, 1993 (in German).
- Zhao, G.; Fuchs, W.; Eligehausen, R. (1989): Einfluß der Bauteildicke auf das Tragverhalten von Dübelbefestigungen im ungerissenen Beton unter Querkzugbeanspruchung (Influence of component thickness on the load-bearing behaviour of anchors in non-cracked concrete under shear loading). Report No. 10/12A-89/5, Institut für Werkstoffe im Bauwesen, Universität Stuttgart, March 1989, not published (in German).
- Zhao, G.; Eligehausen, R. (1992/1): Tragfähigkeit von Befestigungen unter kombinierter

- Zug- und Querlast (Load-bearing capacity of fastenings under combined tension and shear loading). Report No. 10/17-92/2, Institut für Werkstoffe im Bauwesen, Universität Stuttgart, 1992, not published (in German).
- Zhao, G.; Eligehausen, R. (1992/2): Vorschläge zur Modifikation des CC-Verfahrens (Proposals for modification of the CC method). Report No. 12/20-92/11, Institut für Werkstoffe im Bauwesen, Universität Stuttgart, 1992, not published (in German).
- Zhao, G.; Eligehausen, R. (1992/3): Betontragfähigkeit randferner Kopfbolzenverankerungen bei Querkzugbeanspruchung (Concrete capacity of headed anchors remote to an edge under shear loading). Report No. 12/22-92/15, Institut für Werkstoffe im Bauwesen, Universität Stuttgart, 1992, not published (in German).

## Subject Index

- actions on fasteners 2, 4, 238
- anchor diameter, influence on plastic anchor 212
- anchor spacing
  - shear load 114–122, 170
  - tension load 76–88, 152, 163, 193
- anchors for autoclaved aerated concrete 33
- base plate 55, 137, 153
- bending of the base plate 137, 138
- bond 5
- bonded anchors
  - description 19–25
  - failure load
    - – borehole cleaning 23, 187–189
    - – combined tension and shear 200, 207
    - – concrete breakout 200, 207
    - – concrete breakout/pull-out failure 184–200
    - – concrete edge breakout 200
    - – environmental factors 202
    - – fatigue strength 201
    - – influence of temperature 190
    - – load-displacement behaviour 183–189, 204
    - – pry-out failure 200
    - – pull-out failure 205
    - – splitting of the concrete 200, 206
    - – steel failure 184, 200, 205
  - failure modes 181, 200
- bonded anchors for crack concrete
  - bonded expansion anchors 29, 208
  - bonded undercut anchors 23, 208
- bonded expansion anchors 208
- bonded undercut anchors 23, 208
- borehole cleaning 187–189
- cable loop 6
- cantilever bending of anchors 107–109
- capacity of components in which anchors are installed
  - flexural capacity 263
  - overlap splice 262
  - precast concrete girders and cast in-situ concrete 261
  - serviceability 263
  - slab without shear reinforcement 260
- capsule anchor systems 19–21
- carbonated concrete 255
- cast-in channel
  - description 7–8
  - failure load
    - – combined tension and shear 178
    - – concrete cone breakout 165
    - – concrete edge failure 170–178
    - – concrete side blow-out failure 168
    - – fatigue strength 179
    - – load-displacement behaviour 163
    - – pry-out failure 170
    - – pull-out failure 168
    - – splitting 169
    - – steel failure 164, 170
  - failure modes 163, 170
- cast-in-place installation 1, 10
- cast in-situ concrete layer 261
- CC-method 70–137, 146–162
- ceiling hanger 25, 26
- clamping force 55
- combined tension and shear 128, 159
  - failure loads
    - – bonded anchors 200, 208, 210
    - – cast-in channels 178
    - – headed studs 132–137, 159
    - – mechanical expansion anchors 132–137, 159
    - – plastic anchors 215, 222
    - – power actuated fasteners 224, 226
    - – undercut anchors 132–137, 159

- failure modes 128, 159, 178, 215
- load displacement behaviour 128–132, 159
- concrete
  - behaviour of concrete in tension 34–37
  - crack process zone 37
  - cracked concrete 51–54
  - fracture energy 36–41
  - tensile strength 35, 38, 41, 259
- concrete cone breakout under tension
  - characteristic of concrete failure cone 46, 49, 69, 76, 81
  - crack characteristics 41, 42, 44–48
  - failure load, cracked concrete 146–154, 179, 206, 234
  - failure load, uncracked concrete 45–50, 165, 184, 200, 232
  - influence of bending moment 86–88
  - influence of concrete strength 71–76, 232
  - influence of cracks 141–154, 179, 208, 234
  - influence of eccentric tension loading 83–86
  - influence of edge distance 81–83, 167
  - influence of embedment depth 71, 73–75, 166, 232
  - influence of reinforcement 88, 90, 153, 154, 168
  - influence of spacing 76–81, 166–167, 193, 233
  - load-displacement behaviour 66, 67, 143–145, 234
- concrete edge breakout
  - failure load, cracked concrete 158, 179, 210
  - failure load, uncracked concrete 112–128, 170–178, 200, 233
  - influence of bending moment 121
  - influence of concrete strength 112, 113
  - influence of cracks 157, 158, 179, 210
  - influence of different angles between shear load and edge 125–128
  - influence of eccentric shear load 120
  - influence of edge distance 112, 116, 117, 120, 171
  - influence of embedment depth 112
  - influence of hanger reinforcement 122–125
  - influence of load transfer length 112
  - influence of member thickness 119, 120, 172
  - influence of spacing 114–118, 170
  - load-displacement behaviour 117
- concrete failure cone 46, 49, 69, 76, 81, 231
- concrete strength 71–76, 112, 113
- corrosion of anchors 255–258
- corrosion protection class 257
- crack
  - crack width, causes of cracking, crack types, crack appearance 51–53, 142
  - influence on failure load
    - – bonded anchors 202–210
    - – cast-in channels 179
    - – headed studs 146–156, 158–160
    - – mechanical expansion anchors 146–156, 158–160
    - – plastic anchors 220
    - – power actuated fastener 225
    - – screw anchors 234
    - – undercut anchors 146–156, 158–160
  - influence on load-displacement behaviour
    - – bonded anchors 204
    - – headed studs 143–146, 157
    - – mechanical expansion anchors 143–146, 157
    - – plastic anchors 220
    - – screw anchors 234
    - – undercut anchors 143–146, 157
- crack process zone 37
- cracked concrete
  - crack width, cause of cracking, crack type, crack appearance 51–53, 142
  - influence on failure load
    - – bonded anchors 204–210
    - – cast-in channels 179
    - – headed studs 146–162
    - – mechanical expansion anchors 146–162
    - – plastic anchors 220
    - – power actuated fasteners 225
    - – screw anchors 234
    - – undercut anchors 146–162
  - influence on load-displacement behaviour
    - – bonded anchors 208
    - – headed studs 143–146, 157
    - – mechanical expansion anchors 143–146, 157
    - – plastic anchors 220
    - – screw anchors 234
    - – undercut anchors 143–146, 157
- crevice corrosion 258

- degree of rotational fixity 109
- design of fastenings
  - ACI 318-05 (American Concrete Institute) 330–342
  - cast-in channels (CEN, European Committee for Standardisation) 302–313
  - fatigue loads 317–320
  - fire 323–325
  - forces on anchors 271–274
  - headed fasteners 289–300
    - – CC-method (EOTA) 267–283
    - – CEN, European Committee for Standardisation 289–300
  - plastic design
    - – headed fasteners 325–330
    - – post-installed fasteners 325–330
  - post-installed fasteners – chemical systems
    - – CEN, European Committee for Standardisation 315–317
  - post-installed fasteners – mechanical systems
    - – CEN, European Committee for Standardisation 313–315
  - seismic loads 320–323
  - undercut anchors
    - – CC-method (EOTA) 267–283
    - – CEN, European Committee for Standardisation 283–300
  - verification of suitability 266–271
- diamond core drill 10
- drill techniques
  - diamond core drilling 10, 189
  - rotary-impact drilling 10
- drilled-in systems 10
  
- eccentricity 83–86, 120
- edge distance
  - shear load 112, 116, 118, 120, 171
  - tension load 81–83, 166
- elastic theory 57–61
- embedment depth
  - cast-in channels 166
  - headed studs 71–76, 89, 148
  - mechanical expansion anchors 71–76, 89, 148
  - plastic anchors 213
  - screw anchors 232
  - undercut anchors 71–76, 89, 148
- environmental factors, bonded anchors 202
- expansion force 13
- externally applied moment 87, 121
  
- fastening systems
  - bonded Anchors 19–25, 181–210
  - bonded expansion anchors 24, 208
  - bonded undercut anchors 23, 208
  - cast-in channels 7, 8, 163–179
  - ceiling hangers 25, 26
  - headed studs 9, 65–162
  - mechanical expansion anchors 11–16, 65–162
  - plastic anchors 27–29, 211–222
  - power-actuated fasteners 30, 31, 223–226
  - screw anchors 25, 227–236
  - threaded sleeves 6, 9
  - undercut anchors 16–19, 65–162
- failure load
  - bonded anchors
    - – combined tension and shear 200, 207
    - – concrete breakout 200, 206
    - – concrete breakout/pull-out failure 184–200
    - – concrete edge breakout 200
    - – pry-out failure 200
    - – pull-out failure 205
    - – splitting of the concrete 200, 206
    - – steel failure 184, 200
  - cast-in channels
    - – combined tension and shear 178
    - – concrete cone breakout 165
    - – concrete edge failure 170–178
    - – concrete side blow-out failure 168
    - – fatigue strength 179
    - – pry-out failure 170
    - – pull-out failure 168
    - – splitting 169
    - – steel failure 164, 170
  - headed studs
    - – combined tension and shear, cracked concrete 159
    - – combined tension and shear, uncracked concrete 132–137
    - – concrete cone breakout 69–93, 146–154
    - – concrete edge breakout 112–128
    - – local concrete side blow-out failure 93–97, 154
    - – pry-out failure 109–112, 158
    - – pull-out and pull-through failure 97–100, 155–157
    - – shear load, cracked concrete 158
    - – shear load, uncracked concrete 10–128
    - – shear load with lever arm 107–109



- - splitting 100–103, 157
  - - steel failure 68, 105–109, 157
  - - tension load, cracked concrete 146–157
  - - tension load, uncracked concrete 68–103
  - mechanical expansion anchors
    - - combined tension and shear, cracked concrete 159
    - - combined tension and shear, uncracked concrete 132–137
    - - concrete cone breakout 69–93, 146–154
    - - concrete edge breakout 112–128
    - - pry-out failure 109–112, 158
    - - pull-out and pull-through failure 97–100, 155–157
    - - shear load, cracked concrete 158
    - - shear load, uncracked concrete 10–128
    - - shear load with lever arm 107–109
    - - splitting 100–103, 157
    - - steel failure 68, 105–109, 157
    - - tension load, cracked concrete 146–157
    - - tension load, uncracked concrete 68–103
  - plastic anchors
    - - shear and combined tension and shear 215, 221
    - - tension load 211, 220
  - power actuated fasteners
    - - shear and combined tension and shear 224, 226
    - - tension load 223, 225
  - screw anchors
    - - concrete edge breakout 233
    - - pry-out failure 233
    - - shear load 233
    - - steel failure 233
    - - tension load 231, 234
  - undercut anchors
    - - combined shear and tension, cracked concrete 159
    - - combined shear and tension, uncracked concrete 132–137
    - - concrete cone breakout 69–93, 146–154
    - - concrete edge breakout 112–128
    - - pry-out failure 109–112, 158
    - - pull-out and pull-through failure 97–100, 155–157
    - - shear load, cracked concrete 158
    - - shear load, uncracked concrete 10–128
  - - shear load with lever arm 107–109
  - - splitting 100–103, 157
  - - steel failure 68, 105–109, 157
  - - tension load, cracked concrete 146–157
  - - tension load, uncracked concrete 68–103
- failure mechanisms of fastenings
- experimental studies 45–50
  - theoretical studies 37–45
- failure modes
- combined tension and shear 128, 159, 178
  - shear load 103–105, 157–159, 170, 200
  - tension load 65–69, 143, 163, 181
  - - bonded anchors 181
  - - cast-in channels 163
  - - headed studs 65–69, 138–141
  - - mechanical expansion anchors 65–69, 138–141
  - - screw anchors 231
  - - undercut anchors 65–69, 138–141
- fatigue loading
- bonded anchors 200, 208
  - headed studs 139–142, 162
  - mechanical expansion anchors 139–142, 162
  - screw anchors 234
  - undercut anchors 139–142, 162
- fatigue strength
- bonded anchors 200
  - cast-in channels 179
  - headed studs 139
  - mechanical expansion anchors 139
  - screw anchors 234
  - undercut anchors 139
- findley approach 217
- finite element method (FEM) 37–45
- fire 249–254
- characteristic tension strength 252
  - failure load 250
  - - concrete cone breakout 253
  - - steel failure 251
  - standard time-temperature curve 249
- fire resistance 249
- flexural capacity of a reinforced concrete member 263
- follow-up expansion 14, 144, 148, 210
- fracture energy 36–41
- friction 5
- galvanic corrosion 258
- galvanised steel 255

- hanger reinforcement
  - shear load 122–125, 177
  - tension load 90, 97, 103, 168
- headed studs
  - description 9
  - failure load
    - – combined shear and tension, cracked concrete 159
    - – combined shear and tension, uncracked concrete 132–137
    - – concrete cone breakout 69–93, 146–154
    - – concrete edge breakout 112–128
    - – fatigue strength 140
    - – local concrete side blow-out failure 93–97, 154
    - – pry-out failure 109–112, 158
    - – pull-out and pull-through failure 97–100, 155–157
    - – shear load, cracked concrete 158
    - – shear load, uncracked concrete 10–128
    - – shear load with lever arm 107–109
    - – splitting 100–103, 157
    - – steel failure 68, 105–109, 157
    - – tension load, cracked concrete 146–157
    - – tension load, uncracked concrete 68–103
  - failure modes
    - – combined shear and tension 128, 159
    - – shear load 103–105, 157–159
    - – tension load 65–69, 146
  - load-displacement behaviour
    - – combined shear and tension 128–132, 159
    - – shear load 103, 157
    - – sustained load 138, 160
    - – tension load 66, 143–146
- in-place installation 10
- installation configurations
  - cast-in-place technique 2, 5
  - direct installation 29
  - drilled-in systems 10
  - post-installed 10
  - pre-positioned 10
  - stand-off 10, 11
- internal forces
  - elastic theory 57–61
  - forces acting on a fixture 57
  - forces acting on an anchor 57
  - non-linear method 57–61
- load angle to the edge 126
- load-displacement behaviour under combined tension and shear 128–132, 159
- load-displacement behaviour under shear 103, 157, 170
- load-displacement behaviour under tension
  - bonded anchors 183–189, 204
  - cast-in channels 163
  - headed studs 65, 143–146
  - metal expansion anchors 65, 143–146
  - numerical investigation 42
  - plastic anchors 211, 221
  - screw anchors 234
  - undercut anchors 65, 143–146
- load transfer mechanism
  - bond 5
  - friction 5
  - mechanical interlock 5
- loads on anchors
  - elastic theory 57–61
  - non-linear method 61
- local concrete side blow-out failure 66, 93–97, 154, 168
- long-term behaviour, bonded anchors 203
- mechanical expansion anchors
  - description 11–16
  - failure load
    - – combined shear and tension, cracked concrete 159
    - – combined shear and tension, uncracked concrete 132–137
    - – concrete cone breakout 69–93, 146–154
    - – concrete edge breakout 112–128
    - – fatigue strength 139–142, 162, 179
    - – pry-out failure 109–112, 158
    - – pull-out and pull-through failure 97–100, 155–157
    - – shear load, cracked concrete 158
    - – shear load, uncracked concrete 10–128
    - – shear load with lever arm 107–109
    - – splitting 100–103, 157
    - – steel failure 68, 105–109, 157
    - – tension load, cracked concrete 146–157
    - – tension load, uncracked concrete 68–103
  - failure modes
    - – combined shear and tension 128, 159
    - – shear load 103–105, 157–159
    - – tension load 65–69, 146

- load-displacement behaviour
  - – combined shear and tension 128–132, 159
  - – shear load 103, 157
  - – sustained load 138, 160
  - – tension load 66, 143–146
- mechanical interlock 5
- member thickness 119, 120
- minimum spacing and edge distance 100, 101
- moisture content of plastic sleeve 214
  
- non-linear methods 61
- numerical investigations 37–54
  
- overlap splices 262
  
- plastic anchors
  - autoclaved aerated concrete 28
  - description 27–29
  - failure load
    - – influence of cracks 220
    - – influence of embedment depth 213
    - – influence of hole diameter 213
    - – influence of moisture content of plastic sleeve 214
    - – influence of screw insertion depth 212
    - – influence of temperature 214
    - – influence of the diameter of the drill bit 213
    - – long-term behaviour 215–220
    - – pull-out 211–215
  - failure modes 211, 215
  - load-displacement behaviour
    - – concrete breakout failure 211, 221
  - profiled nail 28
  - screw 27
- plastic anchors with profiled nails 28
- post-installed 10
- power actuated fasteners
  - description 30–31
  - failure load
    - – shear and combined tension and shear 224, 226
    - – tension load 223, 225
  - pilot-hole 31
- precast components with site-cast topping slab 261
- pre-positioned installation 10
- prestressing force 55–57
- pry-out failure 105, 109–112, 158, 170, 200, 233
  
- pull-out
  - failure load
    - – bonded anchors 184–200, 205
    - – bonded expansion anchors 208
    - – bonded undercut anchors 208
    - – cast-in channels 168
    - – headed studs 97–100, 155–157
    - – mechanical expansion anchors 97–100, 155–157
    - – plastic anchors 211–215, 220
    - – screw anchors 231
    - – undercut anchors 97–100, 155–157
  - load-displacement behaviour
    - – bonded anchors 183–190
    - – bonded expansion anchors 208
    - – bonded undercut anchors 208
    - – headed studs 65, 66, 143
    - – mechanical expansion anchors 65, 66, 143
    - – plastic anchors 211, 220
    - – undercut anchors 65, 66, 143
- pull-through
  - failure load 97–100, 155–157
  - load-displacement behaviour 65–66, 143
  
- reinforcement
  - near the surface of the concrete 88, 103
  - shear load 122–125, 177
  - tension load 88, 90, 97, 99, 103, 154, 168
- re-torquing of anchors 56, 57
- rotary-impact drilling 10
  
- screw anchors 25, 227–235
- screw anchors
  - description 25, 227–235
  - failure load
    - – influence of embedment depth 232
    - – influence of spacing 233
  - failure modes 231, 233
  - installation 227–231
- screw insertion
  - influence on plastic anchor 213
- seismic loading
  - behaviour of anchors 240–248
    - – combined tension and shear 245
    - – crack cycling 247
    - – load cycle sequence 246
    - – loading rate 245
    - – shear cycling 242
    - – tension cycling 241

- condition of the concrete 239
- seismic actions 238
- type of force 239
- shear load 101, 157, 170, 200, 207
  - failure loads
    - – bonded anchors 200, 207, 210
    - – cast-in channels 170–178
    - – headed studs 105–128, 158
    - – influence of edge distance 112, 116, 117, 120, 171
    - – influence of reinforcement 122–125, 177
    - – influence of spacing 114, 118, 170
    - – mechanical expansion anchors 105–128, 158
    - – power actuated fasteners 224
    - – screw anchors 233
    - – undercut anchors 105–128, 158
  - failure modes 103–105, 157–159, 170, 215
  - load-displacement behaviour 103, 157, 170
- shear load lever arm 108
- shear load with lever arm 107–109
- size effect 45, 71, 112
- slab without shear reinforcement 260
- special mark for drill bits 10
- stand-off installation 10, 11
- steel failure
  - fatigue loading 139, 179
  - shear load 105–109, 157, 170, 233
  - tension load 67, 68, 146, 164, 184, 205, 231
- strain gradient 35
- sustained loads 138, 160, 179, 215, 224
- splitting force 100, 200, 263
- splitting of the concrete 67, 100–103, 157, 169, 200, 206
- stress corrosion 258
  
- T-headed bolt 8
- temperature
  - bonded anchors 190
  - plastic anchors 214
- tensile strength of concrete 35, 38, 41, 259
- tension load
  - failure load
    - – bonded anchors 184–200, 204
    - – cast-in channels 164–170
    - – headed studs 68–103, 105–108, 146–156
    - – influence of edge distance 81–83, 167
    - – influence of hangar reinforcement 90, 97, 103
    - – influence of reinforcement 88, 90, 97, 103, 154, 168
    - – influence of spacing 76–81, 151, 166, 193
    - – plastic anchors 211–215, 220
    - – power actuated fasteners 223, 225
    - – screw anchors 232
    - – undercut anchors 68–103, 105–108, 146–156
  - failure modes 65–69, 143
  - failure modes
    - – bonded anchors 181
    - – cast-in channels 163, 170
    - – headed studs 65–68, 146
    - – mechanical expansion anchors 65–68, 146
    - – plastic anchors 211
    - – screw anchors 231, 233
    - – undercut anchors 65–68, 146
  - load-displacement behaviour
    - – bonded anchors 183–189, 204
    - – cast-in channels 163
    - – headed studs 65, 143–146
    - – mechanical expansion anchors 65, 143–146
    - – numerical investigations 42
    - – plastic anchors 211, 220
    - – screw anchors 234
    - – undercut anchors 65, 143–146
- threaded sleeves 6, 9
- torque moment 228–230
- torsional stress 120
- transport anchor 6
  
- undercut anchors
  - description 16–19
  - failure load
    - – combined shear and tension, cracked concrete 159
    - – combined shear and tension, uncracked concrete 132–137
    - – concrete cone breakout 69–93, 146–154
    - – concrete edge breakout 112–128
    - – fatigue strength 139–142, 162
    - – pull-out and pull-through failure 97–100, 155–157
    - – pry-out failure 109–112, 158

- - shear load, cracked concrete 158
- - shear load, uncracked concrete 10–128
- - shear load with lever arm 107–109
- - splitting 100–103, 157
- - steel failure 68, 105–109, 157
- - tension load, cracked concrete 146–157
- - tension load, uncracked concrete 68–103
- failure modes
  - - combined shear and tension 128, 159
  - - shear load 103–105, 157–159
  - - tension load 65–69, 146
  - load-displacement behaviour 65, 66, 103, 128–132, 143–146, 157
- white rust 255
- zink coating 255